2000

METAL BIOGEOCHEMISTRY OF A MINE CONTAMINATED EsTUARiNE-CoASTAL SYSTEM IN SW SPAIN

BRAUNGARDT, CHARLOTTE BARBARA

METAL BIOGEOCHEMISTRY OF A MINE CONTAMINATED ESTUARINE COASTAL SYSTEM IN SW SPAIN

C. B. BRAUNGARDT

Ph. D. 2000

METAL BIOGEOCHEMISTRY OF A MINE CONTAMINATED ESTUARINE-COASTAL SYSTEM IN SW SPAIN

by

CHARLOTTE BARBARA BRAUNGARDT

A thesis submitted to the University of Plymouth
in partial fulfilment of the degree of

DOCTOR OF PHILOSOPHY

Department of Environmental Sciences
Faculty of Science

March 2000

Metal biogeochemistry of a mine contaminated estuarine-coastal system in SW Spain

Charlotte Barbara Braungardt

Abstract

The aim of this project was to investigate the biogeochemistry and transport of metals in a river/estuarine system contaminated by acid mine drainage. The Rio Tinto and Rio Odiel drain a metalliferous mining area in the Iberian Pyrite Belt in the south-west of Spain. The pH values in the rivers were low (≤ 3) and dissolved metal concentrations were extremely high, up to 2.6 mM Zn, 860 µM Cu, 6.0 µM Cd and 72 nM U. The seasonal cycle of low precipitation and flash floods was identified as an important factor in generating the more severe contamination of the rivers with Fe, Al, Mn, Zn, Cu, Ni, Co and Cd observed during autumn and winter, compared to spring and summer.

The estuarine behaviour of dissolved Fe, Mn, Zn, Cu, Ni, Co and Cd was primarily controlled by pH. Apart from an addition of these metals from the sediment in the upper Tinto estuary, conservative mixing was observed up to pH $\approx$ 5 (at S $\approx$ 30), above which Fe, Mn, Zn, Cu, Ni and Co were removed from solution. Voltammetric speciation studies showed that Cu complexing organic ligands ($\log K'_{CuL} \approx 11.5$, C_L = 32 - 199 nM) in the estuary were saturated, and thermodynamic calculations indicated that the concentration of Cu^{2+} reached values ($pCu^{2+} < 9$) that are toxic to some marine and estuarine organisms.

The estimation of fluxes indicated that the dissolved metal export from this system to the coastal zone averages 10 t d^{-1} Zn, 2.3 t d^{-1} Cu, 180 kg d^{-1} Ni and 236 kg d^{-1} Co, with higher contributions during wet, compared to the dry seasons. On-line measurements of Zn, Cu and Ni in the Gulf of Cádiz revealed metal plumes associated with the Tinto/Odiel system and the Guadiana and Guadalquivir rivers. As a result of entrainment by the Atlantic Ocean surface current flowing into the Mediterranean Sea, the metal contamination in waters of the Gulf of Cádiz is transported south and eastward.

Table of Contents

List of Figures

List of Tables

Acknowledgement

I would like to thank Eric Achterberg for the invaluable support with this research, especially during fieldwork. I am grateful to Eric and Malcolm Nimmo for their comments on the manuscripts.

Many colleagues have contributed to this thesis by sharing their knowledge with me and making fieldwork a pleasurable experience. For this I am particularly indebted to Eric and Malcolm, Françoise Elbaz-Poulichet (University of Montpellier II), Nick Morley (University of Southampton) and Antonio Cruzado (C.E.A.B. Blanes). I appreciate Chris Bowler's introduction to the Geology of the Iberian Pyrite Belt.

I would like to thank Françoise for the organisation of the four TOROS surveys, and Juan-Antonio Morales-Gonzales and José Borrego (University of Huelva) for the provision of logistics and laboratory space during surveys. I am grateful to Nick Morley for the filtration of many sea water samples. I would like to thank Veronique Herzl for the filtration of samples the during tidal cycle studies at Huelva Bridge and for the analysis of alkalinity/acidity in estuarine samples, and Mercedes López for the analysis of major ions and assistance in the field. The assistance of the cruise technicians Arturo Castllón, Ánchel Cristóbal, Philippe Nomérange, Susanna Plá and Ljiljana Simic and the crew of the *B/O Garcia del Cid* during the TOROS 2 and 4 cruises is greatly appreciated.

I would like to thank Françoise (estuarine trace metals), Nick (marine trace metals), Antonio (nutrients) and Zoila R. Velásquez (C.E.A.B. Blanes, phytoplankton and chlorophyll) for allowing me to use their unpublished data. I acknowledge preliminary information on particulate metal studies received from Veronique Herzl.

I am grateful to the 5th floor technicians, especially Ian Doidge, Andy Arnold and Derek Henon for their helpfulness, patience and efficiency. Derek deserves special thanks

for his support during the preparation of surveys and in their aftermath. I also would like to thank the technical departments for the construction of KIPPER-1 and the manufacturing of electronic equipment, without which successful on-line metal measurements would have been impossible. Thanks also to Rockrun for the donation of metal-free epoxy paint and its application to the KIPPER-1 at short notice.

I would like to thank Georgina Spyres for a crash-course in sampling for and analysis of dissolved organic carbon, and to Kevin Soleman in the Geography department for providing and operating the Shimadzu HTCO instrument. Special thanks to Andy Fisher and Les Pitts for an introducing to the secrets of ICP-MS, assistance with the analysis and provision of materials. I would like to thank Graham Carter in the Institute of Marine Sciences for carrying out the salinity measurements.

Long hours in the laboratory were bearable and even fun thanks to sharing them with many great characters over the years. Special thanks go to Manuela Martino for many sessions of shared problem solving.

A special 'cheers' to the chandlers of Sutton Harbour Marina, for lending us a portable GPS for the TOROS 3 cruise free of charge, and to Derek and Mary Scofield for the use of their scanner.

I am indebted to my parents Erika and Karl-Heinz for their long-lasting trust and support of most of my endeavours. Finally, I would like to thank David for the tremendous support he has given me in all aspects of life and for taking me sailing in 'times of need'. He made this work an 'easier read' through his linguistic advice and the surely tedious (after all, this is not about S, D and R&R) proof-reading of the manuscripts.

The funding of this research by the European Commission is gratefully acknowledged.

Author's Declaration

At no time during the registration for the degree of Doctor of Philosophy has the author been registered for any other University award.

This study was financed by the European Commission (DGXII) within the Environment and Climate Program (ELOISE No. 011), under contract TOROS (ENV4-CT96-0217).

Relevant scientific seminars and conferences were regularly attended at which work was often presented; external institutions were visited for consultation and meeting purposes and several papers were prepared for publications.

Publications:

Achterberg, E.P., Braungardt, C. and Whitworth, D.J. Electrochemical monitor for near real-time determination of dissolved trace metals in marine waters. *Chemical sensors in oceanography*, pp. 227-247, **in press.**

Achterberg, E.P. and Braungardt, C. (1999a) Stripping voltammetry for the determination of trace metal speciation and in-situ measurements of trace metal distributions in marine waters. *Anal.Chim.Acta* **400**, 381-397.

Achterberg, E.P., Braungardt, C., Morley, N.H., Elbaz-Poulichet, F. and Leblanc, M. (1999b) Impact of Los Frailes mine spill on riverine, estuarine and coastal waters in southern Spain. *Water.Research* **33**, 3387-3394.

Braungardt, C., Achterberg, E.P. and Nimmo, M. (1998) On-line voltammetric monitoring of dissolved Cu and Ni in the Gulf of Cádiz, south-west Spain. *Anal.Chim.Acta* **377**, 205-215.

Elbaz-Poulichet, F., Dupuy, C., Cruzado, A., Velasquez, Z., Achterberg, E.P. and Braungardt, C.B. (2000) Influence of sorption processes by Fe oxides and algal uptake on arsenic and phosphate cycle in an acidic estuary (Tinto river, Spain). *Water Research,* **in press.**

Elbaz-Poulichet, F., Morley, N.H., Cruzado, A., Velasquez, Z., Green, D., Achterberg, E.P. and Braungardt, C.B. (1999) Trace metal and nutrient distribution in an extremely low pH (2.5) river-estuarine system, the Ria of Huelva (south-west Spain). *The Science of the Total Environment* **227**, 73-83.

Presentations and Conferences and Meetings Attended:

October 1998: Oral Presentation at the Second Annual Scientific ELOISE Conference in Huelva, Spain.
Charlotte Braungardt, Eric Achterberg & Malcolm Nimmo:
The speciation of dissolved Cu and Ni in the Huelva estuary, SW Spain.

September 1998: Oral Presentation at the UK Oceanography Conference in Southampton.
Charlotte Braungardt, Eric Achterberg & Malcolm Nimmo:
Behaviour of dissolved Cu and Ni in the Huelva estuary, SW Spain: A voltammetric speciation study in a river-ocean system affected by acid mine drainage.

September 1998: Poster Presentation at the Goldsmith Conference in Toulouse, France.
Charlotte Braungardt, Eric Achterberg & Malcolm Nimmo:
Dissolved trace metal behaviour in a highly contaminated estuarine system in the south-west of Spain.

November 1997: Oral Presentation at the Marc'hmore Meeting in Brest, France.
Charlotte Braungardt, Eric Achterberg, Malcolm Nimmo & Nick Morley:
Ship-board monitoring of dissolved trace metals in the Gulf of Cadiz.

September 1997: Poster Presentation at the Progress in Chemical Oceanography Meeting in Southampton
Charlotte B. Braungardt, Eric P. Achterberg, Malcolm Nimmo & Françoise Elbaz-Poulichet:
High resolution on-line monitoring of dissolved metals in the Gulf of Cadiz, south-west Spain.

May 1997: Poster Presentation at the First Annual Scientific ELOISE Conference in Arcachon, France.
Charlotte Braungardt, Eric Achterberg & Malcolm Nimmo:
Automated High Resolution Voltammetric Instrumentation for On-board Ship Dissolved Metal Determination in Marine Systems.

External Contacts:
Françoise Elbaz-Poulichet, University of Montpellier II, France;
Juan-Antonio Morales-Gonzales, University of Huelva, Spain;
Maria Jesus Gutierrez de la Camara, INTA Madrid, Spain;
Mario Chica-Olmo, University of Grenada, Spain;
Nick Morley, University of Southampton, United Kingdom;
Jean-Marie Beckers, University of Liege, Belgium;
Antonio Cruzado, CSIC/CEAB Blanes, Spain.

Signed C. Braungardt

Date 22. May 2000

Chapter 1

Introduction

Coastal systems are the interface between fluvial/terrestrial and oceanic environments in which the fate of a chemical constituent is determined by a complex system of interactions and feedback loops between physical, biological and chemical processes. Coastal seas are important habitats and serve as breeding grounds for a multitude of oceanic species. Many coastal land regions are densely populated, and in some areas, coastal development, land erosion, over-fishing, municipal and industrial effluents and waste dumping has been detrimental to aquatic ecosystems.

The European Land Ocean Interaction Studies (ELOISE) project is a recognition of the importance of the coastal seas to the health of the ocean, and the consequences of change for the global climate. ELOISE is jointly implemented by the European Union Marine Science and Technology (MAST) and Environment & Climate programmes and represents a co-ordinated European input into the international Land Ocean Interactions in the Coastal Zone (LOICZ) project. The objectives of ELOISE reflect the multidisciplinary character of coastal research:

- To determine the role of coastal seas in land ocean interactions in the perspective of global change;
- To determine the regional and global consequences of human impact through pollution, eutrophication and physical disturbance on land-ocean interactions in the coastal zone;

- To formulate a strategic approach to the management of sustainable coastal zone research use and development, and to investigate information, policy and market failures that hamper sustainable coastal resources management;
- To promote the development of a European scientific infrastructure for coastal zone research that can optimise both national and regional research and the benefits accruing from it.

The work presented in this thesis was carried out as part of the Tinto Odiel River Ocean Study (TOROS), a research project funded by the European Union in the framework of ELOISE. TOROS gave a unique opportunity to study the intricate connections between geographical and geological setting of a river/estuarine system, the exploitation of this position and its natural resources, the contamination of terrestrial and aquatic systems and its impact on the ecosystem (e.g. adaptation and biodiversity), and contaminant transport.

The Rio Tinto and Rio Odiel rise in the Iberian Pyrite Belt in the Spanish province of Andalucía, southwest Spain. The Iberian Pyrite Belt is one of the most important metal sulphide deposits in the world and has been mined continuously for Cu, Zn and precious metals for thousands of years. Weathering of natural deposits and waste material introduce metal-rich acidic effluent into the two rivers, which meet in a common estuary at the highly industrialised city of Huelva. The aims of TOROS were:

- To quantify metal fluxes from the Rio Tinto and Rio Odiel into the Gulf of Cádiz;
- To identify biogeochemical processes that determine metal behaviour in the estuary, where extreme changes in physico-chemical parameters (e.g. pH 2 - 8) occur;
- To investigate the fate of metals in the Gulf of Cádiz in relation to early diagenesis, hydrodynamics and biological activity;

- To record effects of human activity through historical times, from ancient (pre-Phoenician) to more recent mining activities, and industrial inputs;
- To assess the possibility of reclamation and assist local policy makers in decisions regarding water resource management.

The various aspects of the investigation were covered by eight research partners:

- Françoise Elbaz-Poulichet, University of Montpellier II, France:

  Project co-ordination, metal mineralisation, fate of metals in the estuary (dissolved, particulate and sedimentary phases), isotopic signature of Pb;

- Juan-Antonio Morales-Gonzales, University of Huelva, Spain:

  Local logistics during field campaigns, master variables and major ion analysis in dissolved phase, sedimentology and sedimentary record;

- Maria Jesus Gutierrez de la Camara, INTA Madrid, Spain:

  Investigation of physical mixing and transport processes and chlorophyll distributions via remote sensing techniques, satellite image processing and aircraft based multispectral scanner;

- Mario Chica-Olmo, University of Grenada, Spain:

  Geostatistics, remote sensing and geographical information systems, management of the TOROS database;

- Nick Morley, University of Southampton, United Kingdom:

  Dissolved and particulate trace metals in offshore regions, metal fluxes, sediment-water exchange, development of a near bottom water sampler;

- Eric Achterberg, University of Plymouth, United Kingdom:

  Biogeochemical behaviour of metals in the rivers and estuary using electrochemical speciation techniques (Cu and Ni), on-line high resolution metal monitoring (Zn, Cu, Ni and Co) in the estuary and coastal sea;

- Jean-Marie Beckers, University of Liege, Belgium:

  Development of a 3D linear model for the Gulf of Cádiz, comprising of a hydro-dynamic model, a tracer model for metals and advective fluxes and a coupled biological model;

- Antonio Cruzado, CSIC/CEAB Blanes, Spain:

  Phytoplankton species and nutrient analysis in fresh, estuarine and coastal waters, including depth profiles.

The long-term legacy of large scale mining operations has become the focus of an increasing number of scientific investigations. Such studies commonly aim at the quantification of the contamination resulting from mining, ore processing and waste deposits, the biogeochemical fate, transport pathways and fluxes of pollutants in soil, water, air and biota, and possible remediation strategies. The release of metals in toxic quantities from mining activities in the Iberian Pyrite Belt had visible effects on the appearance of the rivers receiving the acid mine drainage, and on the community structure and biodiversity of the riverine and estuarine ecosystem. The possible contamination of fresh water resources is of concern for agriculture and public health in the arid southwest of Spain. The Rio Tinto and Rio Odiel represent the main transport system of mining-related contaminants and because of the short distance between source and sea, the marine ecosystem and food-chains are particularly affected. These issues are discussed in more detail in the introductions to each of the following chapters.

The research presented in this thesis was carried out for TOROS. The main aims were to determine the magnitude and seasonal variability of dissolved metal fluxes (Zn, Cu, Ni, Co, Cd, Pb, Mn and U) from the Rio Tinto and Rio Odiel, and to identify the processes that influence the biogeochemical behaviour of metals in the estuary. Furthermore, the dissolved fluxes from the estuary into the coastal sea were to be estimated and the transport of metals in the Gulf of Cádiz to be investigated.

Voltammetric techniques were found particularly suitable for the investigation of metal biogeochemistry in this system, because the linear range of the method can be extended from pico-molar to micro-molar metal concentrations by choice of analytical parameters. Furthermore, anodic stripping voltammetry (ASV) and adsorptive cathodic stripping voltammetry (AdCSV) can be used for speciation studies, with a minimum of sample treatment. These voltammetric techniques are discussed in Chapter 2.

The analytical instrumentation used for voltammetry is portable, can be readily automated and has been used for on-line measurements of total dissolved Zn, Cu, Ni and Co in the Huelva estuary and Gulf of Cádiz. The fresh water discharge from the estuary is very low, and as a consequence its salinity signal in the coastal sea is weak. Under these circumstances, it is of particular importance to study the development and dispersal of metal plumes with high spatial resolution and during different stages of the tidal cycle. The method and scope of applications of automated metal monitors during this research is described in Chapter 3.

The following chapters are organised in an order that arises from the pursuit of the project's aims. Four surveys at all seasons were carried out, during which water samples were taken from the riverine end-members, the estuary over the whole salinity range and the coastal sea.

In Chapter 4, results from the analysis of total dissolved metal concentrations in the rivers and estuary are presented. These, together with master variables determined *in-situ*, data contributed by other research partners and published work, are used to elucidate the metal geochemistry, suggest mechanisms causing seasonal variability and calculate fluxes of dissolved metals in this estuarine system.

Results from high resolution on-line measurements of total dissolved Zn, Cu and Ni in surface waters of the Gulf of Cádiz are presented in Chapter 5. The dispersal and transport of the metal signals from the major river systems are discussed by taking prevailing water circulation patterns into account.

In Chapter 6 the distribution of dissolved metals in the rivers, estuary and shelf sea is revisited from the perspective of metal speciation. The highly acidic and metal-rich waters of the rivers were not suitable for voltammetric speciation studies, and had a low content of dissolved organic material. Thermodynamic equilibrium calculations were carried out in order to gain an insight into metal geochemistry of the rivers and upper estuaries. Results from voltammetric speciation studies were used to assess how the relative importance of organic and inorganic ligands for the speciation of Cu changed between highly contaminated estuarine and more pristine coastal waters.

Chapter 7 combines the conclusions from individual chapters to present an overall integrated description of the Tinto/Odiel river ocean system. Several questions remain unanswered, and these are listed as subjects that need further research.

Chapter 2

Voltammetric Methods

2.1 Abstract

Trace metal concentrations (pico to nano mol l^{-1}) commonly found in sea water present marine scientists with great challenges. These include the minimisation of contamination of samples during collection and processing, and the development of methods with suitably low detection limits, which may require the removal of interfering matrix constituents. Stripping voltammetry offers several solutions to these challenges. High sensitivity can be achieved without the necessity of sample preconcentration or matrix removal. Portability of the instrumentation enables *in-situ* applications, and techniques for the study of metal complexation are available.

This chapter reviews the basic functionality of voltammetric instrumentation and describes stripping voltammetry methods for total dissolved trace metal (Zn, Cu, Ni and Co) analysis. The theory of speciation studies and ligand titrations is presented. The voltammetric methods used in the study of metal biogeochemistry in Huelva Ría and the Gulf of Cádiz are discussed, including analytical and instrumental parameters and analytical performance.

2.2 INTRODUCTION

Sea water concentrations of many trace metals are low (< 10^{-8} M, e.g. Cu, Ni, Zn, Co, Fe), while major ions (e.g. Ca^{2+}, Cl^-, Mg^{2+} and Na^+) are present at concentrations (up to 0.5 M) that cause interferences with several analytical methods used for trace metal analysis (e.g. ICP-AES and ICP-MS: Inductively Coupled Plasma - Atomic Emission Spectroscopy and Mass Spectroscopy, respectively and GFAAS: Graphite Furnace Atomic Absorption Spectroscopy). Preconcentration and matrix removal procedures have been developed to remove major ion interferences and to lower the limit of detection for these analytical techniques. For example, in preparation for sea water analysis using GFAAS, samples may be subjected to the complexation of the analyte with DDDC/APCD (dipyrrolidine dithiocarbamate/ammonium pyrrolidine dithiocarbamate), followed by the extraction of the metal complex into chloroform, and back extraction into nitric acid. In this way, trace metals may be concentrated several hundred fold (Bruland *et al.* 1985). Solid-phase preconcentration techniques are also commonly used prior to GFAAS analysis, for example using Chelex columns (Bruland *et al.* 1985; Sunda, 1984). More recently, ICP-AES and ICP-MS techniques have been used with flow injection solid phase extraction for determinations of trace metals in sea water (Bloxham *et al.* 1994; Lan and Yang, 1994). The advantages of flow injection techniques with ICP-AES or ICP-MS detection lie in their high sensitivity, multi-element capability and reduced sample handling. Established methods have been used successfully for the analysis of trace metals at sea water concentrations, however, the necessary preconcentration/matrix removal steps increase the risk of contamination and the instrumental requirements preclude *in-situ* and ship-board deployment.

Since the 1960s, modifications of classical voltammetric techniques and advances in electronic signal amplification promoted the development of sensitive and selective voltammetric methods for the determination of trace metals in solution. Stripping voltammetry is particularly suited for trace metal analysis, because a preconcentration step is an integral part of the measuring cycle. The advantages include reduced sample handling and high sensitivity.

Voltammetry is based on the measurement of a current response as a function of a variable potential applied to an electrochemical cell. Stripping voltammetric techniques have been developed for more than 20 metals (van den Berg, 1989), some of which can be detected at extremely low concentrations (10^{-10} to 10^{-12} M). Some metals can be determined in a multi-elemental mode (Colombo and van den Berg, 1997a; van den Berg, 1986b). Stripping voltammetry is suitable for speciation studies (van den Berg, 1991; van den Berg, 1989; van den Berg, 1988; Buffle, 1988), and the instrumentation is portable and can be automated, which enables ship-board or *in-situ* deployment (Achterberg and Braungardt, 1999; Colombo *et al.* 1997b; Tercier and Buffle, 1996; Achterberg and van den Berg, 1994a).

Versatility and speciation capabilities were the reasons for choosing stripping voltammetry as the main analytical tool for investigations of metal biogeochemistry in the Huelva estuary and the associated coastal sea. Stripping voltammetric techniques were used for the analysis of total dissolved Zn, Cu, Ni and Co in discrete samples (Chapter 4), and speciation studies were undertaken for dissolved Cu (Chapter 6). Voltammetric instrumentation was integrated into a fully automated system for high-resolution on-line ship-board trace metal determinations (Chapters 3 and 5).

2.3 STRIPPING VOLTAMMETRY

2.3.1 INSTRUMENTATION

The principal components of a voltammetric analyser are a three-electrode cell, voltage generator, voltmeter, current meter and recorder. The working, reference and counter electrodes (WE, RE and CE, respectively) are immersed in the sample containing the analyte and a supporting electrolyte. The voltage generator controls the potential of the WE during the preconcentration step (deposition) and measuring cycle (potential scan). The potential of the RE remains constant. The CE serves to conduct current from the source to the WE. During the potential scan, this current is measured and recorded as a function of the potential difference between WE and RE.

In the most basic case, the voltage is changed linearly at a fixed rate (mV s^{-1}) during the potential scan. Other waveforms, for example square wave (SW) and differential pulse (DP), have been developed to improve the separation between capacitative and faradaic components in the current signal. The faradaic current is proportional to the concentration of the analyte in solution, while the capacitative component is the undesired result of the electrical double layer, formed at the electrode surface (van den Berg, 1988). Other advantages of these waveforms are increased speed and sensitivity of the analysis, improved peak separation between analytes and reduced interferences caused by surface active compounds in solution. The characteristics of these wave forms are well documented elsewhere (van den Berg, 1988; Buffle, 1988).

Commonly used working electrodes for trace metal determinations in natural waters are the hanging mercury drop electrode (HMDE) and the mercury film electrode (MFE). Different kinds of MFEs are available and they can be formed by the deposition of Hg on various substrates (e.g. graphite, gold, semi-conductors), or by *in-situ* plating of Hg on glassy carbon. MFEs have a high surface area to volume ratio and excellent sensitivity

as a result of the high analyte enrichment factor during the preconcentration step (Mota and Correia dos Santos, 1995). Recent improvements of microelectrodes (size < 10 μm) allow trace metal analysis at subnanomolar levels. Materials used for microelectrodes include gold, Hg plated carbon fibre and Hg plated iridium (Wang *et al.* 1995; Amez del Pozo *et al.* 1994; de Vitre *et al.* 1991).

Voltammetric signals depend on the dimensions of the electrode, which must therefore be constant. Here lies the disadvantage of solid state electrodes, as they are prone to fouling (e.g. by surfactants), which alters the effective surface area. Semi-permeable protective membranes have recently been introduced, in order to prevent the migration of potentially interfering compounds to the electrode surface (Tercier and Buffle, 1996; Wang *et al.* 1987). The surface of the HMDE is a Hg drop, which is formed on the end of a glass capillary. A new electrode surface is produced for each measurement, which contributes greatly to the reproducibility and reliability of the HMDE.

2.3.2 Adsorptive Cathodic Stripping Voltammetry (AdCSV)

Adsorptive cathodic stripping voltammetry (AdCSV) is based on the adsorption onto the Hg surface of a complex formed between the metal (M) and an added, specific ligand (AL) (Equations 2.1 and 2.2). Any element that forms a chelate that will adsorb onto the electrode surface and that is reducible can be determined by this method. AdCSV methods employ specific ligands for each metal, or groups of metals, determined simultaneously. The formation of the MAL complex is pH-dependent, and therefore samples are buffered at a suitable pH. Table 2.1 shows some AdCSV ligand/buffer combinations for metals commonly analysed in natural waters at concentrations in the pM and nM range.

Table 2.1 - Commonly employed ligands and buffers for the determination of trace metals in sea water using AdCSV (Campos and van den Berg, 1994; van den Berg, 1991; van den Berg, 1988; Donat and Bruland, 1988).

Ligand	Metal(s)	pH range	Buffer (pH)
Oxine	Cd	7.5 - 8.5	HEPES (7.8)
DMG	Co	7.5 - 10	HEPES (7.8) or Borate (8.5)
Nioxime	Co	6.8 - 7.8	HEPES (7.8)
DTPA	Cr	6.0 - 6.8	acetate (6.2)
Oxine	Cu	6.0 - 9.0	HEPES (7.8) or Borate (8.5)
Tropolone	Cu	6.0 - 9.0	HEPES (7.8) or Borate (8.5)
Catechol	Cu	6.0 - 9.0	Borate (8.5)
SA	Cu	8.0 - 8.4	Borate (8.35)
Nioxime	Ni	6.8 - 7.8	HEPES (7.8)
DMG	Ni	7.0 - 10	HEPES (7.8) or Borate (8.5)
Oxine	Pb	7.0 - 8.5	HEPES (7.8)
Oxine	U	6.5 - 7.1	PIPES (6.8)
Catechol	V	6.6 - 7.2	PIPES (6.8)
APDC	Zn	6.2 - 8.5	BES (7.3) or HEPES (7.8)
NN	Fe	6.8 - 8.0	PIPES (6.9) or HEPES (8.0)
Oxine	Cu and Zn		HEPES (7.8)
Oxine	Cu and Cd		HEPES (7.8)
DMG	Ni and Co		HEPES (7.8) or Borate (8.5)

APDC - ammonium pyrrolidine dithiocarbamate
BES - *N,N*-bis(*2*-hydroxyethyl)-*2*-aminoethanesulphonic acid
DMG - dimethylglyoxime
DTPA - diethylenetriamine pentaacetic acid
NN - 1-nitroso-2-napthol
HEPES - *N*-hydroxyethylpiperazine-*N'-2'*-ethanesulphonic acid
Nioxime - cyclohexane-*1,2*-dione dioxime
Oxine - hydroxy quinoline
PIPES - piperazine-*N,N'*-bis-*2*-ethanesulphonic acid
SA - salicylaldoxime

The analytical sequence for AdCSV is illustrated in Figure 2.1. Dissolved oxygen is removed from the sample by purging with an inert gas (N_2, Ar, 100 - 200 s). This precludes possible interferences from redox reactions involving oxygen. During the following preconcentration step a constant potential is applied, usually under conditions of forced convection (stirring). The deposition potential is slightly more positive (by ≥ 0.1V) than the reduction potential of the analyte. During deposition, a minute fraction of the MAL complex forms a mono-molecular layer on the Hg surface (van den Berg, 1989). The preconcentration efficiency is influenced by the deposition potential. AdCSV ligands either contain aromatic or other ring structures (e.g. 8-hydroxyquinoline (Oxine), 2-hydroxy-2,4,6-cyclo-heptatrienone (Tropolone) or ammonium pyrrolidine dithiocarbamate (APDC)), or form ring structures upon chelating with the analyte (dimethylglyoxime (DMG)/Ni^{2+}). Therefore electrostatic and π-orbital interactions are considered important factors in the adsorption process of the MAL complex onto the Hg surface (van den Berg, 1989). After a resting period (equilibration time), a potential scan to more negative voltages is carried out in the quiescent solution. At a potential specific to the analyte-ligand complex, the adsorbed metal is reduced (Equation 2.3) and stripped from the Hg surface. In some cases reduction of a group on AL occurs (e.g. when using the ligand Mordant blue 9 for the analysis of uranium, van den Berg, 1989). The recorded reduction current is measured as the height or area of the peak above the baseline. It is proportional to the metal concentration in the cell.

$$yM^{n+} + zAL^{m-} \leftrightarrow M_y(AL)_z^{(yn-zm)} \qquad (2.1),$$

$$M_y(AL)_z^{(yn-zm)} \leftrightarrow M_y(AL)_z^{(yn-zm)}{}_{(adsorbed)} \qquad (2.2),$$

$$M_y(AL)_z^{(yn-zm)}{}_{(adsorbed)} + e^- \leftrightarrow yM^{(n-1)+} + zAL^{m-} \qquad (2.3).$$

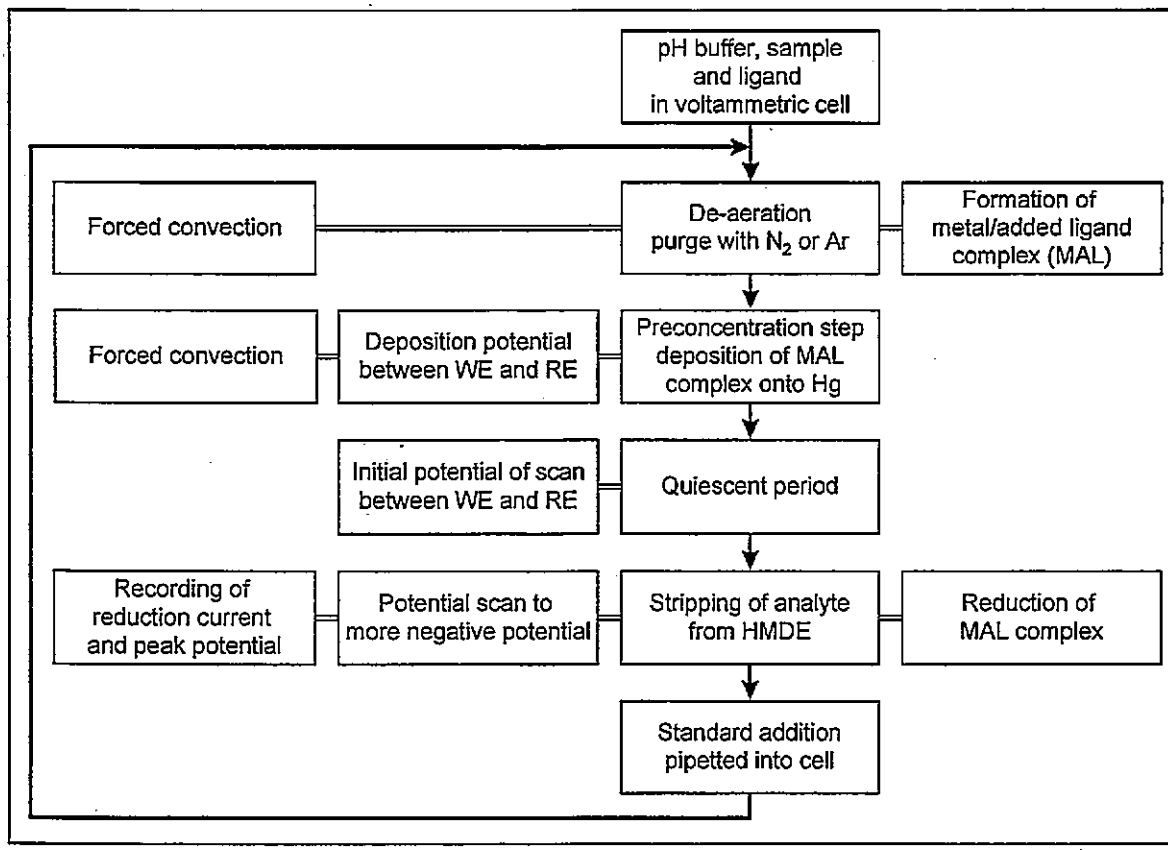

Figure 2.1 - Sequence of steps carried out during a typical AdCSV analysis of trace metals. Usually, two standard additions, each increasing the initial current response by 100 %, are carried out.

The measuring cycle is repeated after standard additions, which serve to calibrate the measurement (Equations 2.4 - 2.6). The standard additions should be of a concentration that increases the current response by at least 100%. This increase in current response is calculated to:

$$\Delta i_p = i_{p1} - i_{p0} \qquad (2.4),$$

where i_{p0} and i_{p1} are the current responses measured in the sample before and after the standard addition, respectively. The sensitivity of the method is:

$$S = \frac{\Delta i_p}{\Delta M} \qquad (2.5),$$

where ΔM is the concentration increase in the sample due to the standard addition. The analyte concentration C_M can be calculated:

$$C_M = \frac{i_{p0}}{S} \qquad (2.6).$$

2.3.3 Anodic Stripping Voltammetry (ASV)

ASV is limited to metals that form an amalgam with mercury (are soluble in Hg) and can be reduced to the metallic state at potentials between 0 and -1.5 V (within the stability boundaries of Hg and H_2O). Although these criteria apply to many metals, ASV measurements in sea water have been successful mainly for Cu, Pb, Cd and Zn. For other elements (e.g. In, Tl) ASV methods are not sensitive enough or hampered by interferences (van den Berg, 1991; van den Berg, 1988).

In order to maintain the sensitivity during ASV analysis, the sample is buffered at a suitable pH. ASV measurements may be conducted in acidified samples (pH 2). Also commonly used is acetate buffer (pH 4), which allows the simultaneous determination of

Zn, Cu, Pb and Cd concentrations in one sample aliquot. After de-aeration, a deposition potential is applied, which is usually more negative (by 0.3 - 0.4 V) than the oxidation potential of the analyte. During deposition the analyte is reduced to the metallic state and collected into the HMDE or MFE by amalgamation with the Hg (forward direction in Equation 2.7).

$$M^{n+} + ne^- + Hg \leftrightarrow M(Hg) \qquad (2.7)$$

The potential scan starts at a value more negative than the oxidation potential of the metal and proceeds towards more positive values. At a specific potential the metal is oxidised and stripped from the Hg (reverse direction in Equation 2.7). The resulting oxidation current is measured and recorded. Standard additions and calculations are carried out as described in Section 2.3.2.

The fundamental difference between AdCSV and ASV is that the former is based on the adsorption of a MAL complex onto the electrode surface, while the latter depends on the dissolution of the metal in its elemental state in the Hg. During the stripping step in AdCSV the mono-molecular layer of MAL on the electrode surface is fully accessible to reduction, this allows fast potential scanning (e.g. with square wave modulation) and results in high sensitivity. By comparison, in ASV the speed of the stripping step is limited by the oxidation and diffusion kinetics of analyte contained within the Hg (van den Berg, 1991).

2.3.4 Interferences

Metal complexing organic ligands (natural or anthropogenic) and surface-active compounds in the sample may interfere with stripping voltammetric techniques in various ways. Organic material may form strong complexes with trace metals (e.g. Zn, Co, Ni, Cu

and Fe) in solution. AdCSV and ASV detect only the electrochemically reactive fraction of the dissolved metals in the sample, so a reduced signal can be caused by competition for the analyte by metal complexing ligands in the sample (van den Berg, 1991; van den Berg, 1988).

Competitive adsorption of organic compounds at the electrode surface can lower the sensitivity of AdCSV methods. Organic compounds may produce a current peak during the stripping step, which may overlap with the analyte peak. At high concentrations, surface-active compounds may present a physical barrier to the adsorption or diffusion of the analyte onto or into the Hg electrode during AdCSV or ASV analysis, respectively (van den Berg, 1991; Buffle, 1988). In solutions containing surfactants the potential of the reduction or oxidation peak tends to shift to more positive values, or the current peak may split, producing several sub-peaks (Neeb, 1989), from which the analyte peak is not easily separated and quantified.

For total metal determinations, interference caused by organic compounds can be eliminated by acidification followed by UV-irradiation. The UV photo-digestion destroys most surfactants and organic complexing material, thus releasing metals as electro-chemically reactive species (Yokoi *et al.* 1995; Achterberg and van den Berg, 1994b). Sample acidification releases metal ions complexed by inorganic ligands. In addition, acidification reduces the loss of analyte to the walls of the quartz tubes, which are used for the irradiation step (van den Berg, 1988).

Interference during stripping voltammetry can arise from the formation of inter-metallic compounds, either between the analyte and mercury electrode surface or other metals in solution present at high concentrations. The magnitude of this interference depends on the stability constant of these compounds (Neeb, 1989).

Competitive adsorption of complexes formed between the added ligand with metals, other than the analyte, can cause interference. This can be alleviated by adding an excess of ligand to the sample.

2.4 Electrochemical Speciation Studies

In natural waters, dissolved metals may be present as free hydrated ions, inorganically complexed species and chelates with natural or anthropogenic organic ligands. The knowledge of total dissolved metal concentrations does not provide sufficient information about the toxicity, biological availability and geochemical behaviour of metals in natural waters. A large number of trace metals are micro-nutrients, and are essential for the metabolism of aquatic organisms at low levels (e.g. Co, Cu, Fe and Zn). However, at higher concentrations these metals may have toxic effects. For some metals (e.g. Cu, Zn, Cd and Ni) the free ionic species have been found to be the most biologically available form, because of their ability to pass through cell membranes of organisms, such as phytoplankton and macro algae (Campbell, 1995). The presence of organic ligands reduces the biological availability of metals, because they reduce the free metal ion concentration. In addition, metal-organic complexes are commonly large and/or hydrophilic and thus unable to diffuse across cell membranes (Pettine *et al.* 1999; Campbell, 1995; Zhou and Wangersky, 1989; Buffle, 1988).

The organic species involved in metal complexation reactions are thought to consist of a continuous spectrum of ligands of varying origin, structure, molecular weight and complexing properties, ranging from 1:1 co-ordination sites to polyfunctional chelators (Gerringa *et al.* 1995). The sources of organic metal complexing matter in sea water include humic and fulvic acids, as well as phytoplankton and bacterial exudates and organic break down products of these organisms.

Only a few analytical techniques (including stripping voltammetry and chemiluminescence, Sunda and Huntsman, 1991) have the sensitivity required for the direct determination of free and labile trace metal concentrations in natural waters. Stripping voltammetry methods have been employed to determine metal redox speciation (Cr, As, Fe), the fraction of strongly (typically organically) complexed metals (e.g. Zn, Cu, Ni, Co, Cd, Pb), and the concentration of metal complexing (organic) ligands naturally present in water samples (e.g. Cu, Ni, Fe) (Aldrich and van den Berg, 1998; Achterberg and van den Berg, 1997; Ruzic, 1996; Gledhill and van den Berg, 1995; Campos and van den Berg, 1994; Donat and van den Berg, 1992; van den Berg *et al.* 1990; Nimmo *et al.* 1989; van den Berg and Nimmo, 1987; van den Berg, 1986a).

In the following, the term 'dissolved metal speciation' will be used with respect to the operationally defined partitioning of metals in solution between electrochemically labile and non-labile dissolved metals. The labile fraction consists of the proportion of dissolved metal that is detected by the AdCSV or ASV method employed. It includes inorganic metal species and may include weak metal-organic complexes. The non-labile metal fraction is calculated from the difference between the measured total dissolved and labile concentrations. For reasons of simplicity, the term 'organic' is used for ligands that form strong complexes with the metal and make up the non-labile fraction, however, this fraction does not necessarily include all organically complexed metals.

Metal complexing organic matter in natural waters may be present in dissolved or colloidal form, or coating on particles. Thus, the operational definition of speciation measurements begins with the filtration. The dissolved metal concentration in this study is defined as the concentration measured in a sample after filtration using acid-cleaned WCN membrane filters with 0.45 μm pore size (cellulose nitrate, Whatman, 47 mm diameter) or 0.4 μm pore size (polycarbonate, Nuclepore, 125 mm diameter). This cut-off point is

thought to include the fraction that is available to algae (Gledhill *et al.* 1997). However, it does not allow for distinguishing between 'truly dissolved' trace metals and those associated with the fraction of the colloidal phase that is not retained by the filter.

2.4.1 Speciation Studies with AdCSV

AdCSV speciation studies are based on the competitive equilibrium between the added ligand (AL) and the naturally present metal complexing ligands (L) in the sample. The amount of analyte complexed with AL after equilibration represents the 'labile' metal concentration ([MAL] = [M_{lab}]) measured in the sample (van den Berg, 1988). The operational competition conditions, or detection window, of the speciation method can be controlled by selecting a certain AdCSV ligand AL with a known conditional stability constant for the analyte, at a certain concentration (Miller and Bruland, 1997; van den Berg and Donat, 1992). For example, Cu speciation has been studied using various AdCSV ligands, including (in order of increasing strength of Cu complexes) Tropolone (Donat and van den Berg, 1992), Benzoylacetone (Moffett, 1995), Catechol (Donat and van den Berg, 1992), Salicylaldoxime (Campos and van den Berg, 1994) and Oxine (van den Berg, 1986a).

The theoretical relationships between the labile and total metal concentrations, the stability constants of the complexes involved, and their α-coefficients have been widely discussed in literature (Donat and van den Berg, 1992; Zhang *et al.* 1990; van den Berg, 1984), and are summarised in Figure 2.2 (Equations 2.8 - 2.19). M^{n+} is the n-valent metal of interest, and C_M is its total dissolved and [M'] is its sum concentration of inorganc complexes (Equations 2.8 and 2.9). L_j and L_x are inorganic and natural organic ligands, respectively, in the sample. The α-coefficients are a measure of the degree of complexation of the metal with a particular ligand, and are the proportion of the complexed relative to

the free metal concentration (Equation 2.11). α_{MLx} and α_{MAL} are the α-coefficients for the complex formation of the metal with L_x and AL, respectively (Equations 2.13 - 2.16). The coefficient α_{MAL} defines the analytical competition strength of the complex formed between M^{n+} and the added ligand, and its value is the centre of the detection window. In Equation 2.14 the presence of one ligand (L_x) is assumed. For several organic ligands $\alpha_{MLxi} = \Sigma(K'_{MLxi}C_{Lxi})$.

The stability constant describing the formation of a 1:1 complex ML is defined by Equation 2.18. The equilibrium between metal ions and organic ligands in solution is affected by inorganic complexation of M^{n+} with anions (e.g. CO_3^{2-}, OH^-, SO_4^{2-} and Cl^-) and by the association of organic ligands with major cations (e.g. Ca^{2+} and Mg^{2+}) and with H^+ (Coale and Bruland, 1988). The conditional stability constant (K') takes side reactions of reactants and products into consideration. The relationship between the conditional stability constant (K') and the side reaction coefficients (α) is given in Equation 2.19 (Ringbom and Harju, 1972a). The α-coefficient for the inorganic side reactions of M ($\alpha_{M'}$) is given in Equation 2.12, whereby K_{MLj} are the stepwise ionic-strength corrected stability constants for the respective ML_j complexes. $\beta'_{M(AL)i}$ is the conditional stability constant for the complex of M with i AL ions (Equation 2.13). K'_{MLx} and K'_{MLj} are the conditional stability constants for the complex ML_x and the complex ML_j, respectively.

C_{AL}, C_{Lj} and C_{Lx} are the concentrations of the added ligand, the natural inorganic ligands and organic ligands, respectively. C'_{AL} and C'_{Lx} are the concentrations of the respective ligands not complexed with the metal of interest, whereby usually $C_{AL} >> C_M$, so the assumption $C'_{AL} = C_{AL}$ can be made.

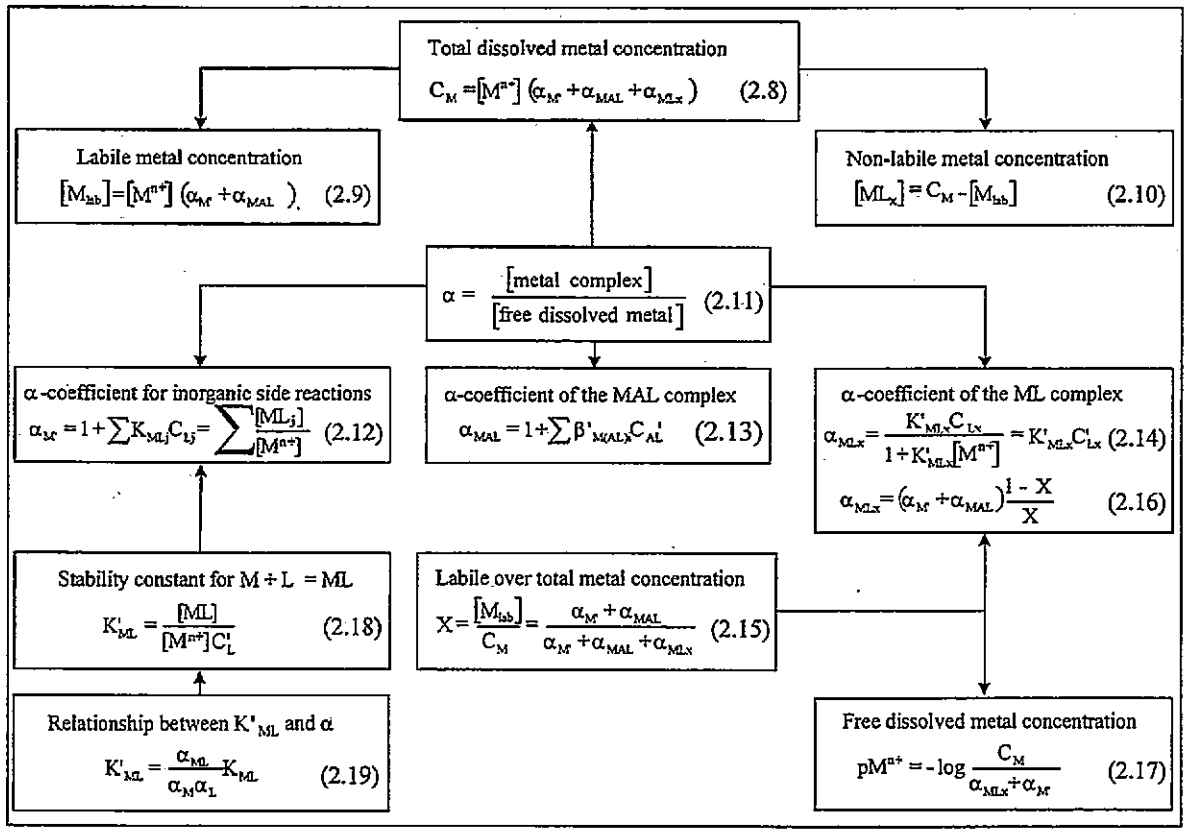

Figure 2.2 - Definition of labile and non-labile concentrations measured by AdCSV (Donat and van den Berg, 1992; Zhang *et al.* 1990; van den Berg, 1988; van den Berg, 1984).

$[M_{lab}]$ and C_M are measured by AdCSV, and the ratio (X) of labile over total metal concentration can be calculated (Equation 2.15). Titrations of samples with the metal of interest enables the calculation of C_{Lx}, K'_{MLx} and $[M^{n+}]$ (see Section 2.4.4). Values for $\alpha_{M'}$ and α_{MAL} are obtained by correcting literature values for the ionic strength, pH and temperature of the sample, using methods described in literature (e.g. Donat and van den Berg, 1992; Dickson and Whitfield, 1981; Ringbom and Still, 1972b). Values for $\beta'_{M(AL)i}$ can be determined by titration against EDTA (Donat and van den Berg, 1992; Zhang *et al.* 1990).

2.4.2 Speciation Studies with ASV

ASV speciation methods directly measure the equilibrium concentration of free metal ions and labile metal complexes that dissociate to free metal ions during the preconcentration time at the deposition potential applied. The method relies on the kinetic stability of the non-labile metal fraction during analysis (Campos and van den Berg, 1994). The detection window of the method depends on the thickness of the electrode's diffusion layer, which determines the residence time of a chemical species on the electrode surface. The relationship of this residence time with the dissociation rate constants of the Cu complexes shows whether a complex will dissociate or not (Kozelka and Bruland, 1998; Mota and Correia dos Santos, 1995; van den Berg, 1991). Kinetically labile complexes include inorganic metal species (e.g. carbonate, sulfate, chloro and free hydrated species) and may include a fraction of relatively labile organic complexes. The ASV-non-labile fraction consists of strong complexes (i.e. irreversible during ASV), which are formed between the metal and organic ligands. The choice of the deposition potential and sample pH is critical (Plavsic *et al.* 1982), the former operationally defines the metal species labile to the method, and the latter influences the chemical equilibrium in the sample.

Theoretical aspects of the measurement of ASV-labile metal concentrations are similar to those of AdCSV, with the exception that there is no competition from an added ligand. Hence, with $\alpha_{MAL} = 0$, Equations 2.8 and 2.9 (Figure 2.2) become:

$$C_M = [M^{n+}](\alpha_{M'} + \alpha_{ML}) \qquad (2.20),$$

$$[M_{lab}] = [M^{n+}]\alpha_{M'} \qquad (2.21).$$

Coale and Bruland (1988) assumed that ASV techniques measure predominantly the inorganic concentration of the analyte in sea water and suggested that the approximation $[M_{lab}] \cong [M']$ can be made. From this the analytical competition strength of ASV methods can be estimated to approximate the inorganic side reaction coefficient of the analyte ($\alpha_{M'}$, Equation 2.12).

2.4.3 Comparison of AdCSV and ASV Speciation Methods

There are advantages using AdCSV over using ASV for speciation studies. The complexation between the metal of interest and the added AdCSV ligand is well characterised by its α-coefficients and conditional stability constants. Therefore, the competition between the added and the natural ligands is accurately known. During the measuring step the equilibrium between the metal ions and all ligands in the sample is not altered (Zhang *et al.* 1990). Furthermore, compared to ASV using a HMDE, the sensitivity of AdCSV is higher. Consequently, deposition times can be shorter with AdCSV, so that surface-active substances are less likely to be adsorbed onto the electrode surface and cause analytical interferences.

The ASV-labile fraction depends on the stability of metal complexes and their dissociation kinetics. Thus, complexes with a fast dissociation velocity may not be

detected, because the dissociated metal is deposited at the electrode and is measured as part of the labile concentration. This phenomenon is emphasised at low metal concentrations, as the required long deposition time gives more opportunity for the dissociation of natural organic metal complexes to take place (Gerringa *et al.* 1995).

In ASV, the analytical competition strength is not accurately known, but under ideal conditions, it is approximately equal to the side reaction coefficient for the metal ($\alpha_{M'}$). Therefore, the detection window of ASV methods covers a lower range of stability constants, compared to AdCSV methods (see Sections 2.5.4.1 and 2.5.4.2). Analytical detection windows of voltammetric techniques are narrow in contrast to the wide range of complexation strengths of organic ligands present in natural water samples. It follows that labile metal concentrations measured with ASV and AdCSV are not directly comparable. For example the centre of the detection window for the tropolone method (AdCSV) in sea water is in the range of $\log\alpha_{CuTrop}$ = 2.5 - 4.5 (Campos and van den Berg, 1994; Donat and van den Berg, 1992), while α-coefficients for ASV-labile Cu determinations can be expected in the range of $\log\alpha_{Cu'}$ = 1.1 - 1.3 at pH 7.5 - 8.2 (Coale and Bruland, 1988; Byrne *et al.* 1988).

2.4.4 Ligand Titrations with AdCSV

Several studies have shown that the toxicity of Cu in sea water is not related to its total, but to its free ionic concentration (Cu^{2+}) (Gledhill *et al.* 1997; Moffett and Brand, 1996; Simkiss and Taylor, 1995; Anderson and Morel, 1978). It is therefore desirable to quantify the free cupric ion concentration, estimate the system's capacity to complex additional Cu inputs and to determine the strength of the complexes involved (Sunda and Huntsman, 1991). This can be achieved by titration of a sample with the metal of interest.

In preparation of an AdCSV metal titration, the sample is divided into several aliquots (typically 10), to which an AdCSV ligand and buffer are added at suitable concentrations. To each aliquot (except one) a different concentration of the titration metal is added. After equilibration (typically 12 - 24 hours), the AdCSV-labile metal concentration is measured in each aliquot. The total dissolved metal concentration in the original sample is determined separately after UV-digestion of the acidified sample (pH 2).

The calculation of the free metal ion concentration ($[M^{n+}]$), the concentration of ligand(s) (C_{Lx}) that form non-labile complexes with the metal and their conditional stability constants (K'_{MLx}) require mathematical transformation of the titration data. A variety of methods have been suggested, including linear regression methods (e.g. van den Berg/Ruzic linearisation, Zhang *et al.* 1990; van den Berg, 1984) and non-linear regression of the Langmuir equation (Gerringa *et al.* 1995; Zhang *et al.* 1990; van den Berg, 1984). Data transformation using non-linear regression is preferable because it allows the calculation of asymptotic standard errors for the estimates of C_L and K'_{ML}, while for the linear regression method, a method for statistically meaningful error calculations is not available (Gerringa *et al.* 1995). The majority of titration data in this study show ligand saturation and hence are linear functions. Therefore the data was not suitable for non-linear regression analysis, and the linear data transformation, utilising the van den Berg/Ruzic plot, was used.

The linearisation after van den Berg/Ruzic is based on the linear relationship between the free metal ion concentration ($[M^{n+}]$) and the concentration of M complexed by L_x ($[ML_x]$), assuming that only one group of natural metal complexing organic ligand L_x is present:

$$C_{Lx} = C'_{Lx} + [ML_x] \qquad (2.22),$$

where C'_{Lx} is the concentration of L_x not complexed with M (symbols explained in Section 2.4.1). The conditional stability constant for the formation of the complex ML_x (K'_{MLx}) is defined by:

$$K'_{MLx} = \frac{[ML_x]}{[M^{n+}]\, C'_{Lx}} \qquad (2.23).$$

Substitution of C'_{Lx} in Equation 2.22 with Equation 2.23 gives the linear relationship:

$$\frac{[M^{n+}]}{[ML_x]} = \frac{[M^{n+}]}{C_{Lx}} + \frac{1}{K'_{MLx}\, C_{Lx}} \qquad (2.24).$$

The titration of a sample with the metal of interest (M), and in the presence of an AdCSV ligand (AL), yields a series of labile concentrations, $[M_{lab}]$. The concentrations of the ML_x complex in each aliquot $[ML_x]$ is calculated from the mass balance:

$$[ML_x] = C_M - [M_{lab}] \qquad (2.25),$$

where C_M is the total dissolved metal concentration in the respective aliquot, which is calculated from the total dissolved metal concentration in the original sample plus the added metal concentration during the titration. In the presence of AL, C_M is given by:

$$C_M = [M'] + \sum [M(AL)_i] + \sum [ML_x] \qquad (2.26),$$

where [M'] is the inorganic metal concentration, and $[M(AL)_i]$ and $[ML_x]$ are the fractions of the metal complexed with AL and the natural ligands L_x, respectively (see Section 2.4.1). The measured labile concentration $[M_{lab}]$ is the metal concentration that equilibrates with AL:

$$[M_{lab}] = [M'] + [M(AL)_i] \qquad (2.27),$$

whereby the inorganic metal fraction is included, because a small constant fraction of the added metal is not complexed, but remains as free ions in solution (Zhang *et al.* 1990). The relationship between the current response (i_p) of the AdCSV measurement and the labile metal concentration is:

$$i_p = S[M_{lab}] \qquad (2.28),$$

where S is the sensitivity of the analytical method employed. S is calibrated by standard additions of M to titration aliquots in which the natural organic ligands have been saturated with a concentration of M greater than C_{Lx}. In this case, S is equal to the slope of a plot of I_p as a function of C_M. The free metal ion concentration $[M^{n+}]$ is related to the labile concentration via Equations 2.9 - 2.13 (see Figure 2.2). The conditional stability constant for the formation of $M(AL)_i$ ($\beta'_{M(AL)i}$) is:

$$\beta'_{M(AL)i} = \frac{[M(AL)_i]}{[M^{n+}][AL']^i} \qquad (2.29).$$

Substitution of $[M^{n+}]$ in Equation 2.24 with Equation 2.9 (Figure 2.2) gives:

$$\frac{[M_{lab}]}{[ML_x]} = \frac{[M_{lab}]}{C_{Lx}} + \frac{\alpha_{M'} + \alpha_{MAL}}{C_{Lx}\, K'_{MLx}} \qquad (2.30),$$

whereby the overall α-coefficient of M^{n+}, excluding complexation by L_x, is:

$$\alpha' = \alpha_{M'} + \alpha_{MAL} \qquad (2.31).$$

The total ligand concentration (C_{Lx}) detected (within the detection window of the titration method applied) can be calculated as follows. Equation 2.30 implies that a plot of $[M_{lab}]/[ML_x]$ as a function of $[M_{lab}]$ is linear (van den Berg/Ruzic plot). In this case, linear least-squares regression can be applied to calculate the total ligand concentration from the slope of the graph (C_{Lx} = 1/slope), and the conditional stability constant from the y-

intercept of the graph ($K'_{MLx} = \alpha'/(\text{intercept} \times C_{Lx})$, van den Berg, 1984). The free ion concentration can be calculated using Equation 2.9. In practice the free cupric ion concentration was calculated using the thermodynamic equilibrium program MINEQL+ (Schecher and McAvoy, 1994; see Chapter 6). The α-coefficient of the complex ML_x (α_{MLx}) can be calculated using Equation 2.14, whereby the concentration of L_x not complexed by M ($C_{Lx'}$) can be determined using the Cu speciation model suggested by van den Berg and Donat (1992).

Many titrations of natural samples produce a linear van den Berg/Ruzic plot, suggesting the presence of only one group of ligands, while a curvature would indicate the presence of more than one class of complexing sites (Zhang *et al.* 1990; van den Berg, 1984). However, it must be considered that the titration covers a limited range of metal concentrations, and that the range of detectable ligands is restricted by the detection window of the method applied (Donat and van den Berg, 1992; Apte *et al.* 1990).

The detection window of the titration depends on the detection limit of the analytical method and its sensitivity to determine a small decrease in the current response caused by the complexation of the added metal with the natural ligand (L_x), rather than with the added ligand (AL) (Zhang *et al.* 1990; van den Berg, 1988). Therefore, the detection window is set by the relative magnitudes of α_{MAL} and α_{MLx}. It has been suggested that approximately two decades on either side of α_{MAL} delimits the detection window for the accurate determination of α_{MLx} (Donat and van den Berg, 1992).

Natural organic metal complexing material consists of a variable mixture of organic molecules with relative molecular weights between a few hundreds and several thousands. Smaller organic molecules in natural waters have been isolated (e.g. amino acids), but the large groups of humic and fulvic acids, which contain a wide range of molecular sizes and structures, remain largely unidentified (Turner, 1995). Experiments indicated that the

properties of organic ligands describe a continuum of binding sites, rather than have boundaries which separate them into distinct classes (Campos and van den Berg, 1994; Donat and van den Berg, 1992; van den Berg and Donat, 1992; van den Berg *et al.* 1990). Hence, different ligands (e.g. L_{x1} and L_{x2}) identified from titration results are representative of operationally defined groupings of ligands with similar metal binding characteristics, which fall into the same detection window of the titration method employed (Miller and Bruland, 1997).

2.5 Voltammetric Methods Employed in this Study

2.5.1 Reagents and Equipment

MQ water was obtained from an ultra-clean water purification system, which consists of a reverse osmosis set-up (Milli-RO), followed by a deionisation stage (Milli-Q, resistancy R ≥18 MΩ cm^{-1}, both Millipore). Hydrochloric acid (HCl), nitric acid (HNO_3) and methanol of AnalaR grade (Merck) were purified by distillation in a sub-boiling quartz still. Ammonia (NH_3) (AnalaR, Merck) was purified by isothermal distillation. Unless otherwise stated, these purified reagents were used throughout.

Oxine solutions (0.1 M and 0.01 M) were prepared from 8-hydroxyquinoline (99%, Merck) in MQ water. Tropolone stock solution (0.1 M) was prepared from 2-hydroxy-2,4,6-cycloheptatrienone (98%, Aldrich) in methanol. DMG solutions (0.1 M and 0.01 M) were prepared from dimethylglyoxime (99+%, Aldrich) in methanol. APDC stock solution (0.1 M) was prepared from ammonium pyrrolidine dithiocarbamate (99%, Sigma) in MQ water. EDTA stock solution (0.092M) was prepared from ethylene-dinitrilotetraacetic acid (AnalaR, Merck) in MQ water. The pH value of EDTA solution was adjusted to pH 7.8 using NH_3, and dilutions (5 mM and 1 mM EDTA) were prepared with MQ.

An aqueous HEPES pH buffer stock solution (1 M) was prepared from *N*-hydroxyethylpiperazine-*N'-2'*-ethanesulphonic acid (Biochemical grade, Merck) in MQ water. The pH value of HEPES was adjusted with NH_3 to give pH 7.8 in sea water (with 0.01M HEPES). Contamination of HEPES with Zn and Cu was reduced by adding an excess of the metal complexing ligand Oxine (50 μM) to the HEPES stock and passing the solution through a Sep-Pak C18 cartridge (pre-packed column of octadecyl carbon units chemically bonded to a silica gel support, Waters Corporation) (flow rate ca. 1 ml min^{-1}). The Oxine and Oxine-metal chelates were retained on the C18 resin, thus removing metals from the HEPES solution. Prior to buffer cleaning the C18 cartridge was conditioned by passing through HCl (0.1 M, 20 ml), MQ water (50 ml), methanol (10 ml), followed by MQ water (50 ml). The cleaning procedure of the buffer reduced the contribution of HEPES (0.01 M, final concentration) to the analysed metal concentration in the sample from ca. 2 nM Zn and 0.8 nM Cu to ≤ 0.2 nM Zn and ≤ 0.15 nM Cu. The contribution of HEPES (0.01 M) to the Ni concentration was typically 0.1 nM Ni.

A Borate pH buffer stock solution (1 M) was prepared from ortho boric acid (Aristar, Merck). The pH value was adjusted with NH_3 to give pH 8.4 in sea water (0.01 M Borate, final concentration). Contamination of Borate with Ni was reduced by adding the metal complexing ligand DMG (50 μM) to the Borate stock and passing it through a Sep-Pak C18 cartridge, which had been conditioned as described in the previous paragraph. Organic contaminants, including remaining traces of DMG, were removed from the Borate buffer by UV-irradiation (4 h, 400 W medium pressure Hg lamp, Photochemical Reactors). The cleaning procedure reduced the concentration of Ni contributed by Borate (0.01 M, final conc.) from ca. 0.7 nM Ni to typically 0.04 nM Ni.

For the calibration of voltammetric measurements, aqueous metal standards for Zn, Cu, Ni, Co and mixed standards (Cu/Zn and Ni/Co) in a range of concentrations (10^{-4}, 10^{-5}, 10^{-6} M) were prepared by dilution of Spectrosol Stock Solutions (Merck) in HCl (0.01 M).

The preparation of reagents and standards, as well as the handling of samples in the laboratory, were carried out in a laminar-flow unit (Class 100, Model 56, Bassaire, Southampton). Cleaning procedures for sampling bottles, filter holders and other equipment are described in Chapter 3.

2.5.2 INSTRUMENTATION

Voltammetric studies were carried out using a hanging mercury drop electrode (HMDE, VA 663 Stand, drop surface area A = 0.52 mm^2, Metrohm), which was connected to a μAutolab voltammeter (EcoChemie) via the interface for the mercury electrode (IME, EcoChemie). On occasions, a PAR 303A HMDE, with electromagnetic stirrer (PAR model 305) and Teflon® coated stirrer bar, was used together with an Autolab voltammeter (EcoChemie) and IME. The reference electrode was Ag/AgCl, filled with KCl (3.5 M), and all potentials given are with respect to this reference potential. The respective voltammeter was connected to a personal computer (PC), which controlled the analysis using specialised software (GPES, EcoChemie). The software provided an interface for the input of analytical conditions, such as the wave form (e.g. square wave or differential pulse) and their parameters (step potential and amplitude, scan frequency or modulation frequency and interval time), the initial and final values for the potential scan, deposition potential and time etc. Another function enabled the semi-automatic calculation of the height or area of the current peak.

2.5.3 Total Dissolved Trace Metal Analysis

Sample preparations for total dissolved metal analysis included filtration (see Chapters 3, 4 and 5), acidification (HCl, pH 2) and UV-irradiation. For UV-digestion, the acidified sample was transferred to acid-washed quartz glass tubes (30 ml volume, loosely covered with a Teflon® screw cap). Hydrogen peroxide (0.05% H_2O_2, final concentration) was added to aid the destruction of organic matter and maintain oxic conditions during the irradiation period. The samples were irradiated in a home-built UV unit (capacity 24 tubes) for three hours using a 400 W medium pressure Hg lamp (Photochemical Reactors). The sample temperature in the UV unit was maintained at ca. 70°C with a fan. Each quartz tube was marked to monitor evaporation loss, which in most cases was negligible. However, high or persistent organic compounds in some estuarine samples required prolonged irradiation times (up to 8 hours), and evaporation in these samples was compensated for by addition of MQ water.

For analysis, sample aliquots (10 ml) were pipetted from the UV-tubes into the voltammetric cell (borosilicate glass, Metrohm), to which the appropriate buffer, NH_3 and AdCSV ligand had been added. The NH_3 was used to neutralise the acidified sample. Table 2.2 lists ligands and buffers used for AdCSV in this study.

The analytical sequence (see Section 2.3.2) was carried out and, at each stage (before and after standard additions), the deposition/stripping/measurement cycle was repeated until the peak current remained constant (standard deviation of ca. 5% between measurements). In order to eliminate random errors and check analytical linearity, a minimum of two aliquots were analysed for each sample, and two standard additions (each doubling the initial peak height) were made in at least one of the sample aliquots.

Table 2.2 - Ligands and buffers used in AdCSV analysis of trace metals. All final concentrations in the voltammetric cell. HEPES: pH 7.8, Borate: pH 8.5, reduction potentials are approximate.

Voltammetric Parameter	Zn	total Cu	labile Cu	total Ni/Co
AdCSV ligand	APDC	Oxine	Tropolone	DMG
Ligand concentration	200 μM	20 μM	200 μM	200 μM
pH buffer	HEPES	HEPES	HEPES	HEPES/Borate
Buffer concentration	0.01 μM	0.01 μM	0.01 μM	0.01 μM
Deposition potential (V)	-1.2	-1	-0.13	-0.9
Reduction potential (V)	-1.05	-0.43	-0.21	-0.93/-1.08

Square wave modulation was used throughout the study. Other voltammetric parameters - scanning frequency, step potential and amplitude, deposition potential and time, initial and final scan potential and stirring rate - were selected depending on the metal(s) of interest, their concentration (see Chapter 3), and the nature of the sample matrix.

2.5.4 Speciation Studies

For labile trace metal determinations, samples were filtered shortly after collection, filled into acid-cleaned HDPE bottles (250 or 500 ml) and stored in the dark and at low temperature (4°C). Analysis (AdCSV or ASV) was carried out onboard ship within a few hours, or in a laboratory ashore within a maximum of 48 hours after collection.

Zero second deposition measurements were carried out for all speciation studies, in order to determine the baseline for the analysis and check whether interfering peaks resulting from organic matter in the sample were present. Organic interference occurred in some samples, and could be usually eliminated through changes made to the analytical parameters (e.g. deposition time). Otherwise, such samples were taken out of the speciation series. The stirring rate and deposition times were adjusted according to the encountered metal concentrations.

2.5.4.1 Cu Speciation Studies with Tropolone

Tropolone forms Cu complexes with a low stability constant compared to other AdCSV ligands (Donat and van den Berg, 1992). Therefore, the detection window of the Tropolone method allows the determination of relatively weak Cu complexing organic ligands, which are generally present at high concentrations in sea water (Miller and

Bruland, 1997; Donat and van den Berg, 1992; van den Berg *et al.* 1990). Previous studies have shown that the complexation of dissolved Cu is controlled by strong organic ligands, which are present in sea water at concentrations comparable to that of Cu. Weaker organic ligands become important for the complexation of Cu when the stronger ligands are saturated (Moffett *et al.* 1997). The latter was expected to be the case in the study area where high inputs of trace metals enter estuarine and coastal waters. Therefore, speciation studies in this work were focussed on the weaker ligands with the selection of Tropolone as AdCSV ligand.

For the determination of AdCSV-labile Cu, HEPES (0.01 M, pH 7.8) and Tropolone (200 μM, final concentrations) were added to the voltammetric cell before adding the sample aliquot (10 ml), which was analysed immediately. The deposition was carried out at a potential of -0.13 V for 5 to 120 s (depending on sample) and with a stirring rate between zero and maximum (position 6). The potential scan (-0.13 V to -0.45 V, step potential 2.44 mV, amplitude 25 mV) was carried out with a frequency of 50 Hz.

The analytical competition strength of the AdCSV method is defined as the α-coefficient of the Cu-Tropolone complex. Tropolone forms two complexes with Cu, $Cu(Trop)^+$ and $Cu(Trop)_2$, so that:

$$\alpha_{CuTrop} = 1 + K'_{CuTrop+}[Trop'] + \beta'_{CuTrop2}[Trop']^2 \qquad (2.32),$$

whereby the detection window typically spans one to two decades either side of α_{CuTrop} (Miller and Bruland, 1997; Campos and van den Berg, 1994).

Values for $K'_{CuTrop+}$ at the appropriate salinity and pH 7.8 were calculated from the thermodynamic stability constant ($K_{CuTrop+}$ = 8.35 at 25°C and I = 0.1; Martell and Smith, 1977) as follows. The inorganic side reaction coefficient for Tropolone ($\alpha_{Trop'}$) was calculated according to:

$$\alpha_{Trop'} = 1 + [Mg^{2+}]K_{MgTrop} + [Ca^{2+}]K_{CaTrop} + [Sr^{2+}]K_{SrTrop} + [H^{+}]K_{a1} \qquad (2.33).$$

The stability constants for complexes of Tropolone with Mg^{2+}, Ca^{2+}, Sr^{2+} and the acidity constant were taken from Martell and Smith (1977) and corrected for ionic strength using the Davie's equation:

$$\log K^{*} = \log K + S\Delta z^{2}\left(\frac{\sqrt{I_e}}{1+\sqrt{I_e}} - 0.3I_e\right) \qquad (2.34),$$

whereby logK is the stability constant for the equilibrium M + L = ML, and $logK^{*}$ is log K corrected for ionic strength, S is the Debye-Hückel slope (0.511 $mol^{-1/2}$ $l^{1/2}$ at 25°C and 1 atm), z stands for ionic charge ($\Delta z^2 = \Sigma z^2$(products) - Σz^2(reactants)) and I_e is the effective ionic strength. The effective ionic strength and free major ion concentrations were calculated for the required salinities using an ion pairing model by van den Berg (based on Dickson and Whitfield, 1981). Using corrected stability constants and major ion concentrations, $\alpha_{Trop'}$ was calculated for different salinities using Equation 2.33.

The conditional stability constant, $logK'_{CuTrop+}$, was calculated using:

$$\log K'_{CuTrop+} = \log K^{*}_{CuTrop+} - \log \alpha_{Trop'} \qquad (2.35),$$

where $logK^{*}_{CuTrop+}$ is the thermodynamic stability constant for the Cu-Tropolone complex, corrected for the required ionic strength.

Values for $\beta'_{CuTrop2}$ at the pH value used in this study (pH 7.8) are not available from literature. Therefore, α_{CuTrop} was calibrated in sea water of various salinities at pH 7.8, using ligand competition against a known ligand (EDTA). For the calibration a titration with EDTA as detailed in literature (Donat and van den Berg, 1992; van den Berg and Nimmo, 1987) was carried out. Filtered (WCN, 47 mm diameter, 0.45 µm pore size, Whatman) and UV-irradiated sea water (collected west of the Straits of Gibraltar, depth 76

m) of accurately known salinity (S = 36.13) was diluted with MQ, so that (taking the added reagent volume into account) salinities of 35.6 and 25.0 were used for the titrations.

The procedure for preparing the titration series for this calibration and the equipment used has been described in detail for ligand titrations below (Section 2.6.5). Aliquots of the sea water containing Tropolone (300 μM, final concentration) and HEPES buffer (0.01 M, final concentration, pH 7.8) and approximately 30 nM Cu were allowed to equilibrate with EDTA (pH 7.8, ca. 23 °C, ≥ 36 hours) at a range of concentrations between zero (in triplicate) and 15 μM EDTA. Labile Cu concentrations were determined in all aliquots, using a deposition potential and time of -0.13 V and 150 s, respectively and the potential scan (-0.13 V to -0.45 V, step potential 2.44 mV, amplitude 25 mV) was carried out with a frequency of 50 Hz.

In presence of Tropolone and HEPES and in absence of EDTA, the Cu reduction current is:

$$i_{p0} = \frac{S\alpha_{CuTrop}C_{Cu}}{\alpha_{Cu} + \alpha_{CuTrop} - 1} \qquad (2.36),$$

where S is the sensitivity of the method. In the presence of Tropolone, HEPES and EDTA, the Cu reduction current is:

$$i_{p} = \frac{S\alpha_{CuTrop}C_{Cu}}{\alpha_{Cu} + \alpha_{CuTrop} + \alpha_{CuEDTA} - 2} \qquad (2.37).$$

The α-coefficient for the Cu-EDTA complex is:

$$\alpha'_{CuEDTA} = 1 + K'_{CuEDTA}[EDTA'] \qquad (2.38),$$

where [EDTA'] is the concentration of EDTA not complexed by Cu and can be approximates to equal [EDTA]. The stability constants for the complex $CuEDTA^{2-}$

(K_{CuEDTA}) and $M^{n+}EDTA^{4-n}$ (for Ca^{2+}, Mg^{2+}, Sr^{2+}, K^{+}, Na^{+} and H^{+}) were taken from Martell and Smith (1977). Corrections for the inorganic side reaction coefficient of EDTA and for ionic strength were carried out in the same way as described above for $\log K^{*}_{CuTrop+}$. The ratio of the current response in the presence over that in the absence of EDTA is:

$$X = \frac{i_p}{i_{p0}} = \frac{\alpha_{Cu} + \alpha_{CuTrop} - 1}{\alpha_{Cu} + \alpha_{CuTrop} + \alpha_{CuEDTA} - 2} \qquad (2.39).$$

Equation 2.39 was rearranged to enable the calculation of α_{CuTrop} at the respective Tropolone concentration and salinity by using the values for X obtained from the titrations:

$$\alpha_{CuTroop} = \frac{\alpha_{Cu} - X(\alpha_{Cu} + \alpha_{CuEDTA} - 2) - 1}{X - 1} \qquad (2.40).$$

From the calibrated values of α_{CuTrop}, values for $\beta'_{CuTrop2}$ were calculated for different salinities (Table 2.3) using the rearranged Equation 2.32. The obtained values for $\log\beta'_{CuTrop2}$ at pH 7.8 were somewhat higher than those reported by Donat and van den Berg (1992) for pH 8.3 (e.g. S = 34.8: $\beta'_{CuTrop2}$ = 10.00±0.12), although the conditional stability constant of a complex is expected to decrease with decreasing pH value. However, within the analytical error (ca. 5%) and the uncertainty of the method (unknown) there is no difference between the values for $\log\beta'_{CuTrop2}$ obtained here and by Donat and van den Berg. The calculation of $\beta'_{CuTrop2}$ at the desired salinities was based on a function ($\log\beta'_{CuTrop2} = 12.402 \times S^{-0.063}$) found describing the relationship between the values for $\log\beta'_{CuTrop2}$ and salinity given in Donat and van den Berg (1992).

With the use of salinity-adjusted $K'_{CuTrop+}$ values and calculated $\beta'_{CuTrop2}$ values, α_{CuTrop} was calculated (Table 2.4) for the appropriate concentrations of tropolone used in speciation studies (0.2 mM) or ligand titrations (0.3 mM).

Table 2.3 - Values for α_{CuTrop}, and $\beta_{CuTrop2}$ obtained by calibration against EDTA at S = 35.6 and 25.

Salinity	[Tropolone]	log K'_{CuEDTA}	log$K'_{CuTrop+}$	log $\beta_{CuTrop2}$	logα_{CuTrop}
35.6	0.3 mM	10.16	5.83	10.18	3.20
25.0	0.3 mM	10.31	5.98	10.27	3.30

Table 2.4 - Values calculated for α_{CuTrop}, at different salinities and Tropolone concentrations for labile Cu determinations using 0.2 mM Tropolone and for ligand titrations using 0.3 mM Tropolone (pH 7.8).

Salinity	[Tropolone]	logα_{CuTrop}	Salinity	[Tropolone]	logα_{CuTrop}
1.5	0.2 mM	5.06	33.5	0.3 mM	3.00
5	0.2 mM	3.87	35.8	0.3 mM	2.96
10	0.2 mM	3.74	36.0	0.3 mM	2.96
15	0.2 mM	3.17	36.1	0.3 mM	2.95
20	0.2 mM	2.99	36.3	0.3 mM	2.95
25	0.2 mM	2.87			
30	0.2 mM	2.76			
37	0.2 mM	2.64			

2.5.4.2 Cu Speciation Studies with ASV

For some estuarine water containing very high metal concentrations (μM), ASV was used for Cu speciation studies. ASV-labile Cu was determined in aliquots of 10 ml, to which HEPES buffer (pH 7.8, 0.01 M) had been added. The deposition was carried out at a potential of -0.65 V for 5 to 30 s with a low stirring rate (0 - 2). The potential was scanned at 50 Hz between -0.65 V and -0.25 V (step potential 2.44 mV, amplitude 25 mV).

In an attempt to estimate the detection window of the ASV speciation method, the inorganic side reaction coefficient for Cu (α'_{Cu}) was calculated for different salinities and the alkalinity determined in the estuary during the second survey (June 1996, Chapter 4). For this, an ion pairing model by van den Berg was used, which utilises the extended Debye-Hückel equation (2.41) with stability constants and values for B, C and D given in Turner and Whitfield *et al.* (1981) for the correction of ionic strength. The calculations were carried out for the sample pH during analysis (7.8, buffered by HEPES).

$$\log\beta_j^* = \log\beta_j^0 + S\Delta z^2 \frac{\sqrt{I_e}}{1+B\sqrt{I_e}} + CI_e + D\sqrt[3]{I_e} \qquad (2.41),$$

where S and Δz^2 are as described for the Davie's Equation (2.34). At salinity ranges of S = 36 - 36.5, S = 33 - 35 and S < 32, the corresponding coefficients were $\log\alpha_{Cu'}$ = 1.16 - 1.20, $\log\alpha_{Cu'}$ = 0.77 - 1.06 and $\log\alpha_{Cu'}$ < 0.55. The detection window depends on method-specific parameters, which influence the dissociation kinetics of metal-organic complexes at the electrode (see Section 2.4.2). Therefore, the side-reaction coefficient may underestimate the value for the centre of the detection window.

2.5.5 LIGAND TITRATIONS

Ligand titrations were carried out in order to estimate the concentration of Cu complexing organic ligands (C_{CuLx}), their conditional stability constant (K'_{CuLx}), and calculate the free cupric ion concentration, [Cu^{2+}]. For reasons given above (Section 2.5.4), Tropolone was selected as AdCSV ligand for the titrations. The calculation of the inorganic side reaction coefficient for Cu (α'_{Cu}) has been given in Section 2.5.4.2. For the titration calculations, it is insignificant in magnitude, compared to α'_{CuTrop}, which was calculated for the Tropolone concentration used in the titrations (0.3 mM) following the method described in Section 2.5.4.1.

For the equilibration of samples with added Cu and Tropolone, non-expanded polystyrene portion cups (60 ml/2 oz, with lids, Sweetheart, USA) were used. Leaching experiments with MQ water and with HCl (pH 2) overnight showed no detectable contribution of Cu resulting from the cups. The adsorption behaviour of the cups was assessed by equilibrating overnight buffered MQ water (pH 7.8, HEPES) spiked with Cu (5 and 50 nM) and one of two AdCSV ligands (Tropolone, 0.3 mM or Oxine, 20 µM). The maximum adsorption was observed in aliquots containing 50 nM Cu and Tropolone, and concentrations of 44.5 ± 0.33 nM Cu (n = 3) were measured after 24 hours. In order to reduce Cu adsorption, the cups were equilibrated overnight with sea water, which had been prepared in the same way as the planned titration (see below). After conditioning, the cups were rinsed with MQ water and dried in a laminar flow unit. The cups were conditioned only once, and the titrations were carried out in order of increasing total Cu concentrations. The cups were re-used after rinsing with MQ water and drying. Possible carry-over from previous ligand titrations was assessed by equilibrating cups, previously used for high concentrations (300 nM Cu), with MQ water (with HEPES, pH 7.8 and Oxine, 20 µM) overnight. An increase of 0.6 ± 0.07 nM Cu was observed in the MQ water (n = 3), which was deemed negligible.

For ligand titrations, sub-samples were taken from the filtrate for speciation studies into acid-cleaned HDPE bottles (500 ml). The samples were placed into a deep freezer in Spain as soon as possible, and maintained frozen with dry ice during transport to the UK where they were stored in a freezer (-20°C). At the University of Plymouth, all ligand titrations were carried out over a period of ten days, in order to maintain consistency of conditions and technique. Samples were placed into a fridge to defrost slowly (ca. 22 hours, 4°C), and prepared within hours after defrosting for titration.

The defrosted sample was accurately weighed (250 ml, taking the density of sea water at 4°C into account) into a conditioned HDPE bottle. Buffer (HEPES, pH 7.8, 0.01 M) and Tropolone (0.3 mM, final concentrations) were added and the sample was mixed carefully. The sample was pipetted into 11 polystyrene cups (cup 0: 40 ml, cups 1 - 10: 20 ml each). To cups 1 - 10, increasing concentrations of Cu standard were added and mixed. The maximum Cu concentration added was one to six times its total dissolved Cu concentration, which previously had been determined in acidified and UV-irradiated sub-samples (see Section 2.5.3). The cups were covered with lids and left to equilibrate at room temperature (ca. 21°C) for ca. 15 hours in a laminar flow unit. Suitable deposition times and stirrer rates, which enabled the last titration step to be measured within the linear range, were established in spiked sea water samples ahead of the titration series. A complete list of concentrations and titration conditions is given in Table 2.5.

After equilibration, aliquots (10 ml) were pipetted into the voltammetric cell and the reduction current was measured, using the parameters listed in Table 2.5. Decreasing current responses during the measurement of the first two aliquots without added Cu indicated the conditioning of the cell and results were discarded. Subsequent aliquots were measured in the order of increasing concentrations.

Table 2.5 - Parameters used for ligand titrations. Deposition potential was -0.13 V, scan frequency was 50 Hz, and the scan was from -0.05 V to -0.35V. C_{Cu}: total dissolved Cu concentration in original sample (nM), C_0 - C_{10}: added Cu concentration (nM) for each titration step.

Sample, April 1998	MZ4	MZ7	MZ10	MZ21	MZ21	MZ16
C_{Cu} (nM)	104	177	220	38.3	38.3	107
Deposition time (s)	2	2	1	45	70	1
Stirrer setting (0…6)	1	1	1	5	5	1
Equilibration time (s)	3	4	2	8	8	2
Step potential (mV)	4.88	4.88	4.88	2.44	4.88	4.88
Step amplitude (mV)	18	18	18	21	18	18
Sensitivity (nA nM^{-1})	0.101	0.103	0.070	0.719	0.824	0.081
C_0	0	0	0	0	0	0
C_1	10	10	10	5	2.5	10
C_2	20	20	20	10	5	20
C_3	30	30	30	15	8	30
C_4	40	40	40	20	12	40
C_5	60	60	60	25	16	60
C_6	80	80	80	40	20	80
C_7	100	100	100	50	25	100
C_8	150	150	150	60	30	130
C_9	200	200	200	70	40	160
C_{10}	250	250	250	80	50	200
Sample, Oct. 1998	MZ3	MZ7	HR9	A1	E5	F7
C_{Cu} (nM)	56.9	10.7	289	3.57	5.07	8.04
Deposition time (s)	12	45	1	80	40	20
Stirrer setting (0…6)	4	5	0	5	5	5
Equilibration time (s)	8	8	0	8	8	8
Step potential (mV)	4.88	2.44	4.88	4.88	4.88	4.88
Step amplitude (mV)	18	21	18	18	18	18
Sensitivity (nA nM^{-1})	0.294	0.801	0.044	1.06	0.626	0.286
C_0	0	0	0	0	0	0
C_1	5	2	20	1	1	1
C_2	10	4	40	2	2	2
C_3	15	6	60	3	3	3
C_4	20	8	80	4	4	4
C_5	30	10	120	6	6	6
C_6	40	12	160	8	8	8
C_7	50	16	200	10	10	10
C_8	60	20	300	12	12	12
C_9	80	25	400	16	16	16
C_{10}	100	32	500	20	20	20

In order to determine the sensitivity, standard additions were made to several aliquots, for which ligand saturation had been indicated with a linear relationship between current response and added Cu concentration.

The organic ligand concentration, its conditional stability constant for Cu complexes, and the free cupric ion concentration were calculated as detailed in Section 2.4.4, and the results are presented in Chapter 6.

Test-titrations were carried out on three fresh samples in a laboratory of the University of Huelva. The titrations were repeated under equal conditions on defrosted samples at Plymouth, in order to assess the changes effected by the freezing process. The titration of the sample T3 MZ 21 was carried out in triplicate to determine the reproducibility of the titration method in defrosted samples.

2.5.6 Analytical Performance

The accuracy of the stripping voltammetry methods employed was assessed for each series of experiments. Before each survey, new reagents and metal standards were prepared, and these were used to analyse certified reference materials (CRM). CRMs for river water (SLRS-2), estuarine water (SLEW-2) and coastal sea water (CASS-3, all National Research Council of Canada) were UV- irradiated in acid-leached quartz tubes. Total dissolved analysis of Zn, Cu, Ni and Co were carried out using appropriate buffers and AdCSV-ligands according to the methods detailed in Section 2.5.3. The analysis was carried out repeatedly for each metal, and good agreement with the certified values was achieved throughout. Typical results are summarised in Table 2.6.

A large batch (ca. 9 litres) of aged Irish Sea water (IRSW) was prepared as an internal reference material. The water was filtered and UV-irradiated on-line, following the

method described for the sample preparation during on-line voltammetric metal analysis in Chapter 3. IRSW was acidified (HCl, pH 1.6) and stored in an acid-cleaned HDPE container in the dark. Total dissolved metal concentrations (Zn, Cu, Ni, Co, Cd) were determined against CRM-verified AdCSV and ASV methods. IRSW was used routinely for intra-laboratory calibrations and to verify the quality of standards and methods of analysis (Table 2.6). Typical values for reagent blanks, limits of detection and linear ranges of AdCSV methods are given in Chapter 3.

The upper part of Table 2.7 compares results from ligand titrations on fresh samples with those on frozen, stored and defrosted samples. For both samples the concentration of Cu complexing ligands determined in defrosted samples was higher (factor 1.2 and 1.3 for M 4 and M 6, respectively) compared to that in fresh samples. Differences in the calculated conditional stability constant for the CuL complex ($\log K'_{CuL}$) and the alpha coefficient ($\log \alpha_{CuL}$) between fresh and frozen samples were small when the uncertainty (not quantified) of the method is taken into account. Changes leading to the different results may include the de-naturalisation of organic material in the sample, resulting in alterations in its complexing capacity for Cu. Moreover, the loss of labile Cu to the walls of the container would lead to an over-estimation of the ligand concentration in the defrosted sample.

For the calculations it was assumed that the difference in the labile Cu concentration in fresh and defrosted samples was lost from the total Cu concentration.

It can be concluded that the preservation of the sample introduced a high degree of error (20 - 30%) into the method, and considering other sources of uncertainty (e.g. analytical errors) it is possible that the error for the calculated ligand concentrations exceeds 30%.

Table 2.6 - Typical results from analysis certified reference materials CASS-3 (coastal sea water), SLEW-2 (estuarine water) and SLRS-2 (river water) by AdCSV in batches of 10 ml. Confidence intervals refer to ± 2 SD of the sample mean of n analysis. 'Overall mean' for IRSW refers to all contributing analysts and all methods (incl. ASV for Zn and Cu, and AdCSV with nioxime for Co).

CRM	Ligand/Buffer	n	AdCSV (nM)	certified (nM)	recovery (%)
CASS-3					
Zn	APDC/HEPES	8	17.7 ± 2.58	19.0 ± 3.82	93
Cu	Oxine/HEPES	4	8.17 ± 1.05	8.14 ± 0.98	100
Ni	DMG/HEPES	6	6.48 ± 0.40	6.58 ± 1.06	99
Co	DMG/HEPES	5	0.53 ± 0.06	0.70 ± 0.15	76
SLEW-2					
Zn	Oxine/HEPES	5	15.8 ± 1.59	16.8 ± 2.10	94
Cu	Oxine/HEPES	4	22.2 ± 2.54	25.5 ± 1.73	87
Ni	DMG/Borate	3	12.7 ± 1.05	12.1 ± 0.92	105
Co	DMG/Borate	5	0.82 ± 0.09	0.93 ± 0.14	88
SLRS-2					
Zn	APDC/HEPES	5	16.2 ± 0.77	15.9 ± 1.40	102

IRSW	Ligand/Buffer	n	AdCSV (nM)	IRSW mean (nM)	n	recovery (%)
Zn	APDC/HEPES	8	29.2 ± 2.1	28.1 ± 2.0	14	104
Cu	Oxine/HEPES	6	11.7 ± 1.1	11.0 ± 1.0	19	106
Cu	Tropolone/HEPES	3	10.8 ± 0.8	11.0 ± 1.0	19	98
Ni	DMG/Borate	5	5.8 ± 0.5	5.7 ± 0.6	15	101
Co	DMG/Borate	4	0.34 ± 0.01	0.35 ± 0.02	11	100

Table 2.7 - Comparison of two ligand titrations (M 4 and M 6) carried out with fresh (F) and with defrosted (D) samples after several months of storage, using equal methods and conditions. Comparison of three ligand titrations carried out with defrosted sample MZ 21. The Tropolone concentration was 0.3 mM, the pH was buffered at 7.8. Cu_T and Cu_L - total dissolved and AdCSV labile Cu concentration, respectively, Cu_L % - proportion of labile Cu in percent, CL - concentration of Cu complexing organic ligands fomring Cu complexes with the conditional stability constant $logK'_{CuL}$, $log\alpha_{CuL}$ - alpha coefficient of the CuL complex.

Sample	S	pH field	Cu_T nM	Cu_L nM	Cu_L %	Method	CL nM	$logK'_{CuL}$	$log\alpha_{CuL}$
M 4	35.7	8.04	193	88.7	78	F	87	11.7	4.7
			171	66.7	39	D	103	11.9	4.9
M 6	36.1	8.07	126	64.2	69	F	51	12.1	4.8
			130	68.0	52	D	65	11.8	4.6
MZ 21	36.0	8.30	36.6	1.59	4.3	D	35	12.7	5.2
						D	38	12.0	4.7
						D	41	13.0	5.6

However, freezing did not affect the estimation of the stability constant beyond the uncertainty inherent in the titration method. With respect to ligand concentrations the results contradict Apte and Gardner *et al.* (1990), who reported that freezing as a technique for sample preservation for ligand titrations showed good results.

The reproducibility of the titrations was assessed by calculating the standard error for the results from three titrations on the same sample (Table 2.7, MZ 21). The errors remained below 10% for the ligand concentration (C_L = 38±2.8 nM, n = 3). The errors for the stability constant and the alpha coefficient of the CuL complex were half log units ($\log K'_{CuL}$ = 12.6±0.5 and $\log\alpha_{CuL}$ = 5.2±0.5, both n = 3).

2.6 Conclusions

Stripping voltammetry techniques have been chosen as the main analytical tool for the work presented here because of its sensitivity, speciation capability, portability and adaptability to a wide range of concentrations. The high sensitivity of stripping voltammetry methods enabled direct determination of trace metals at sea water concentrations without preconcentration steps. High sensitivity and portability enabled speciation studies to be carried out within hours of sample collection, and with minimal disturbance of the natural chemical equilibrium.

Stripping voltammetry methods have limitations. The labile trace metal fractions and ligand concentrations, which are determined by voltammetric speciation studies and ligand titrations, are operationally defined. This limits the comparability of speciation results acquired using different methods, and inter-comparison between different metals. Specific to this study, Cu speciation results from ASV and AdCSV studies were carried out at different detection windows, and therefore results are not directly comparable. Ideally,

samples for ligand titrations should be analysed directly after collection, as the alteration of samples during storage may lead to speciation changes. Voltammetry has only limited multi-element capabilities, compared to ICP-AES and ICP-MS methods.

Overall, the stripping voltammetric methods employed proved to be very suitable for this study. Good analytical performance was achieved.

2.7 REFERENCES

Achterberg, E.P. and Braungardt, C. (1999) Stripping voltammetry for the determination of trace metal speciation and in-situ measurements of trace metal distributions in marine waters. *Anal.Chim.Acta* **400**, 381-397.

Achterberg, E.P. and van den Berg, C.M.G. (1994a) Automated voltammetric system for shipboard determination of metal speciation in sea water. *Anal.Chim.Acta* **284**, 463-471.

Achterberg, E.P. and van den Berg, C.M.G. (1994b) In-line ultraviolet-digestion of natural water samples for trace metal determination using an automated voltammetric system. *Anal.Chim.Acta* **291**, 213-232.

Achterberg, E.P. and van den Berg, C.M.G. (1997) Chemical speciation of chromium and nickel in the western Mediterranean. *Deep-Sea Research Part Ii-Topical Studies In Oceanography* **44**, 693-720.

Aldrich, A. and van den Berg, C.M.G. (1998) Determination of iron and its redox speciation in seawater using catalytic cathodic stripping voltammetry. *Electroanalysis* **10**, 369-373.

Amez del Pozo, J., Costa-Garcia, A. and Tuñón-Blanco, P. (1994) Novel mercury-coated carbon fibre voltammetric detector for use in adsorptive stripping flow analysis. *Anal.Chim.Acta* **289**, 169-176.

Anderson, D.M. and Morel, F.M. (1978) Copper sensitivity of Gonyaulax tamarensis. *Limnology and Oceanography* **23**, 283-295.

Apte, S.C., Gardner, M.J., Ravenscroft, J.E. and Turrell, J.A. (1990) Examination of the range of copper complexing ligands in natural waters using a combination of cathodic stripping voltammetry and computer simulation. *Anal.Chim.Acta* **235**, 287-297.

Bloxham, M.J., Hill, S.J. and Worsfold, P.J. (1994) Determination of trace metals in sea-water and the on-line removal of matrix interferences by flow injection with inductively coupled plasma mass spectrometric detection. *Journal of Analytical Atomic Spectrometry* **9**, 935-938.

Bruland, K.W., Coale, K.H. and Mart, L. (1985) Analysis of seawater for dissolved cadmium, copper and lead: an intercomparison of voltammetric and atomic absorption. *Mar.Chem.* **17**, 285-300.

Buffle, J. (1988) *Complexation Reactions in Aquatic Systems*, Chichester: Ellis Horwood Ltd.

Byrne, R.H., Kump, L.R. and Cantrell, K.J. (1988) The influence of temperature and pH on trace metal speciation in seawater. *Mar.Chem.* **25**, 163-181.

Campbell, P.G.C. (1995) Interactions between trace metals and aquatic organisms: A critique of the free-ion activity model. In: Tessier, A. and Turner, D.R., (Eds.) *Metal speciation and bioavailability in aquatic systems*, pp. 45-102. Chichester: John Wiley & Sons Ltd.

Campos, M.L.A.M. and van den Berg, C.M.G. (1994) Determination of Cu complexation in sea water by CSV and ligand competition with salicylaldoxime. *Anal.Chim.Acta* **284**, 481-496.

Coale, K.H. and Bruland, K.W. (1988) Copper complexation in the northeast Pacific. *Limnology and Oceanography* **33**, 1084-1101.

Colombo, C. and van den Berg, C.M.G. (1997a) Simultaneous determination of several trace metals in seawater using cathodic stripping voltammetry with mixed ligands. *Anal.Chim.Acta* **337**, 29-40.

Colombo, C., van den Berg, C.M.G. and Daniel, A. (1997b) A flow cell for on-line monitoring of metals in natural waters by voltammetry with a mercury drop electrode. *Anal.Chim.Acta* **346**, 111

de Vitre, R.R., Tercier, M.-L., Tsacopoulos, M. and Buffle, J. (1991) Preparation and properties of a mercury-plated iridium-based microelectrode. *Anal.Chim.Acta* **249**, 419-425.

Dickson, A.G. and Whitfield, M. (1981) An ion-association model for estimating acidity constants (at 25°C and 1 atm total pressure) in electrolyte mixtures related to seawater (ionic strength <1 mol kg^{-1} H2O). *Mar.Chem.* **10**, 315-333.

Donat, J.R. and Bruland, K.W. (1988) Direct determination of dissolved cobalt and nickel in seawater by differential pulse cathodic stripping voltammetry preceded by adsorptive collection of cyclohexane-1,2-dione dioxime complexes. *Analytical Chemistry* **60** , 240-244.

Donat, J.R. and van den Berg, C.M.G. (1992) A new cathodic stripping voltammetric method for determining organic copper complexation in seawater. *Mar.Chem.* **38**, 69-90.

Gerringa, L.J.A., Herman, P.M.J. and Poortvliet, T.C.W. (1995) Comparison of the linear Van den Berg/Ruzic transformation and a non-linear fit of the Langmuir isotherm applied to Cu speciation data in the estuarine environment. *Mar.Chem.* **48**, 131-142.

Gledhill, M., Nimmo, M., Hill, S. and Brown, M. (1997) The toxicity of copper (II) species to marine algae, with particular reference to macroalgae. *Journal of Phycology* **33**, 2-11.

Gledhill, M. and van den Berg, C.M.G. (1995) Measurement of the redox speciation of iron in seawater by catalytic cathodic stripping voltammetry. *Mar.Chem.* **50**, 51-61.

Kozelka, P.B. and Bruland, K.W. (1998) Chemical speciation of dissolved Cu, Zn, Cd, Pb in Narragansett Bay, Rhode Island. *Mar.Chem.* **60**, 267-282.

Lan, C.R. and Yang, M.H. (1994) Synthesis, properties and applications of silica-immobilized 8-quinolinol. Part 2. *Anal.Chim.Acta* **287**, 111

Martell, A.E. and Smith, R.M. (1977) *Critical Stability Constants*, Vol. 3. 3 edn. New York: Plenum Press.

Miller, L.A. and Bruland, K.W. (1997) Competitive equilibration techniques for determining transition metal speciation in natural waters: evaluation using model data. *Anal.Chim.Acta* **343**, 161-181.

Moffett, J.W. (1995) Temporal and spatial variability of copper complexation by strong chelators in the Sargasso Sea. *Deep-Sea Research I* **42**, 1273-1373.

Moffett, J.W. and Brand, L.E. (1996) Production of strong, extracellular Cu chelators by marine cyanobacteria in response to Cu stress. *Limnology and Oceanography* **41**, 388-395.

Moffett, J.W., Brand, L.E., Croot, P.L. and Barbeau, K.A. (1997) Cu speciation and cyanobacterial distribution in harbors subject to anthropogenic Cu inputs. *Limnology and Oceanography* **42**, 789-799.

Mota, A.M. and Correia dos Santos, M.M. (1995) Trace metal speciation of labile chemical species in natural waters: electrochemical methods. In: Tessier, A. and Turner, D.R., (Eds.) *Metal speciation and bioavailability in aquatic systems*, pp. 205-258. Chichester: John Wiley & Sons Ltd.

Neeb, P.D.R. (1989) *Stripping Voltammetry*, Herisau: Metrohm AG.

Nimmo, M., van den Berg, C.M.G. and Brown, J. (1989) The chemical speciation of dissolved Nickel, Copper, Vanadium and Iron in Liverpool Bay, Irish Sea. *Estuarine, Coastal and Shelf Science* **29**, 57-74.

Pettine, M., Patrolecco, L., Manganelli, M., Capri, S. and Farrace, M.G. (1999) Seasonal variations of dissolved organic matter in the northern Adriatic Sea. *Mar.Chem.* **64**, 153-169.

Plavsic, M., Krznaric, D. and Branica, M. (1982) Determination of the apparent copper complexing capacity of seawater by anodic stripping voltammetry. *Mar.Chem.* **11**, 17-31.

Ringbom, A. and Harju, L. (1972a) Determination of stability constants of chelate complexes. Part 1. Theory. *Anal.Chim.Acta* **59**, 33-47.

Ringbom, A. and Still, E. (1972b) The calculation and use of α coefficients. *Anal.Chim.Acta* **59**, 143-146.

Ruzic, I. (1996) Trace metal complexation at heterogeneous binding sites in aquatic systems. *Mar.Chem.* **53**, 1-15.

Schecher, W.D. and McAvoy, D.C. (1994) *MINEQL+, user's manual*, Hallowell, ME: Environmental Software.

Simkiss, K. and Taylor, M.G. (1995) Transport of metals across membranes. In: Tessier, A. and Turner, D.R., (Eds.) *Metal speciation and bioavailability in aquatic systems*, pp. 1-45. Chichester: John Wiley & Sons Ltd.

Sunda, W.G. (1984) Measurement of manganese, zinc and cadmium complexation in seawater using chelex ion exchange equilibria. *Mar.Chem.* **14**, 365-378.

Sunda, W.G. and Huntsman, S.A. (1991) The use of chemiluminescence and ligand competition with EDTA to measure copper concentration and speciation in seawater. *Mar.Chem.* **36**, 137-163.

Tercier, M.-L. and Buffle, J. (1996) Antifouling membrane-covered voltammetric microsensor for in-situ measurements in natural waters. *Analytical Chemistry* **68**, 3670-3678.

Turner, D.R. (1995) Problems in trace metal speciation modeling. In: Tessier, A. and Turner, D.R., (Eds.) *Metal speciation and bioavailability in aquatic systems*, pp. 149-204. Chichester: John Wiley & Sons Ltd.

Turner, D.R., Whitfield, M. and Dickson, A.G. (1981) The equilibrium speciation of dissolved components in freshwater and seawater at 25C and 1 atm pressure. *Geochimica et Cosmochimica Acta* **45**, 855-881.

van den Berg, C.M.G. (1984) Determination of the complexing capacity and conditional stability constants of complexes of copper(II) with natural organic ligands in seawater by cathodic stripping voltammetry of copper-catechol complex ions. *Mar.Chem.* **15**, 1-18.

van den Berg, C.M.G. (1986a) Determination of copper, cadmium and lead in seawater by cathodic stripping voltammetry of complexes with 8- hydroxyquinoline. *Journal of Electroanalytical Chemistry* **215**, 111-121.

van den Berg, C.M.G. (1986b) The determination of trace metals in sea-water using cathodic stripping voltammetry. *The Science of the Total Environment* **49**, 89-99.

van den Berg, C.M.G. (1988) Electroanalytical chemistry of sea-water. In: Riley, J.P. and Chester, R., (Eds.) *Chemical Oceanography*, 9 edn. pp. 197-245. New York: Academic Press, Ltd.

van den Berg, C.M.G. (1989) Adsorptive cathodic stripping voltammetry of trace elements in sea water. *Analyst* **114**, 1527-1530.

van den Berg, C.M.G. (1991) Potentials and potentialities of cathodic stripping voltammetry of trace elements in natural waters. *Anal.Chim.Acta* **250**, 165-276.

van den Berg, C.M.G. and Donat, J.R. (1992) Determination and data evaluation of Cu complexation by organic ligands in sea water using CSV at varying detection windows. *Anal.Chim.Acta* **257**, 281-291.

van den Berg, C.M.G. and Nimmo, M. (1987) Determination of interactions of nickel with dissolved organic material in sea water using cathodic stripping voltammetry. *The Science of the Total Environment* **60**, 185-195.

van den Berg, C.M.G., Nimmo, M., Daly, P. and Turner, D.R. (1990) Effects of the detection window on the determination of organic copper speciation in estuarine waters. *Anal.Chim.Acta* **232**, 149-159.

Wang, J., Bonakdar, M. and Pack, M.M. (1987) Glassy carbon electrodes coated with cellulose acetate for adsorptive stripping voltammetry. *Anal.Chim.Acta* **192**, 215-223.

Wang, J., Foster, N., Armalis, S., Larson, D., Zirino, A. and Olsen, K. (1995) Remote stripping electrode for in situ monitoring of labile copper in the marine environment. *Anal.Chim.Acta* **310**, 223-231.

Yokoi, K., Tomisaki, T., Koide, T. and van den Berg, C.M.G. (1995) Effective UV photolytic decomposition of organic compounds with a low-pressure mercury lamp as pretreatment for voltammetric analysis of trace metals. *Fresenius Journal of Analytical Chemistry* **352**, 547-549.

Zhang, H., van den Berg, C.M.G. and Wollast, R. (1990) The determination of interactions of cobalt(II) with organic compounds in seawater using cathodic stripping voltammetry. *Mar.Chem.* **28**, 285-300.

Zhou, M. and Wangersky, P.J. (1989) Study of copper-complexing organic ligands: isolation by a Sep- pak C18 column extraction technique and characterization by chromarod thin-layer chromatography. *Mar.Chem.* **26**, 21-40.

Chapter 3

On-line Monitoring of Dissolved Cu, Zn, Ni and Co in Huelva Ría and the Gulf of Cádiz

3.1 Abstract

Geochemical processes in estuarine and coastal waters have an important temporal and spatial variability, resulting in changes in metal speciation and dissolved element concentrations. Therefore, surveys that are aimed to improve our understanding of metal behaviour in such systems benefit from high-resolution, interactive sampling campaigns.

This chapter discusses a high-resolution approach to coastal monitoring and the application of an automated voltammetric metal analyser for on-line measurements of dissolved trace metals in the Huelva estuary and Gulf of Cádiz, southwest Spain.

The fully automated, PC-controlled metal monitor consisted of the analytical voltammetric system, a sample and reagent transport system, and a syringe pump for metal standard additions. The system provided calibrated measurements of total dissolved Cu, Zn, Ni and Co with a frequency of about 15 - 20 min. Surface samples (3 - 4 m depth) were obtained using a continuous pumping system. The sample was filtered and UV-digested on-line. Adjustment of voltammetric parameters enabled the application of this system in highly contaminated estuarine and relatively pristine offshore coastal waters.

Steep gradients and strong tidal variability were observed in the dissolved metal plume extending from the Huelva estuary into the Gulf of Cádiz. Total dissolved metal concentrations measured on-line in the Gulf of Cádiz ranged from less than 5 nM Cu (< 3 nM Ni) ca. 50 km off-shore to 60 - 90 nM Cu (5 - 13 nM Ni) in the vicinity of the Huelva

estuary. During tidal cycle studies in the estuary, dissolved Zn and Cu ranged from nM to μM concentrations.

The chosen examples demonstrated the adaptability of the metal monitor to a wide range of environmental conditions in the dynamic waters of estuaries and coastal seas. The near real time acquisition of dissolved metal concentrations at high resolution provided the information necessary for investigating small scale geochemical processes and enabled an interactive sampling campaign. This chapter is an adaptation of a published paper (Braungardt *et al.* 1998).

3.2 INTRODUCTION

The growth of environmental awareness, the introduction of new environmental laws and the efficient management of coastal zones has presented science with a challenge that requires competence in many disciplines, including the understanding of biogeo-chemical processes that affect pollutant behaviour in estuaries and coastal waters. As a result, an increased effort is made to monitor physical and chemical parameters in marine systems.

Coastal waters are highly dynamic and complex systems, which are often characterised by steep physical and chemical gradients, both on temporal and spatial scales. Pollutants can be carried into coastal waters by several pathways, including riverine and atmospheric sources, and industrial discharges. A number of processes act upon the chemical speciation of pollutants and, consequently, their relative associations with dissolved, colloidal and particulate phases in the water column. For example, important factors influencing dissolved trace metal concentrations in estuarine and coastal waters

include fresh water inputs, pH, redox conditions, tidal mixing and resuspension of sediment, colloid formation and coagulation, precipitation, sorption, biological cycling and organic complexation (e.g. Muller, 1996; Stumm and Morgan, 1996; Morris *et al.* 1986; Foerstner, 1983).

The dynamic nature of coastal waters requires monitoring activities of trace metal distributions with a frequency and spatial resolution similar to those at which processes occur that affect metal behaviour (Achterberg *et al.* 1999). In the marine analytical field, *in-situ* monitoring techniques are becoming more widely used, as such methods allow the analysis of constituents at a higher frequency than traditional discrete sampling strategies (Andrew *et al.* 1994; Johnson *et al.* 1985). Additional advantages of *in-situ* methods are a reduced risk of contamination and loss of analyte, as sample handling is kept to a minimum. Sample preservation, transport, storage and land-based analysis become unnecessary, and speciation studies can be carried out with minimal disturbance of the chemical equilibrium.

In-situ analysis of physical properties of bodies of water (e.g. temperature, pressure, conductivity) have a long tradition, and the measurement of fluorescence, turbidity, dissolved oxygen with instrumentation mounted on CTD systems during oceanographic surveys has become common practice (Klinkhammer *et al.* 1997; Bearman, 1995; Riley *et al.* 1975). The development of automated instrumentation utilising segmented continuous-flow analysis (CFA) in the 1960s allowed ship-board on-line analysis of nitrate, nitrite, phosphate, silicate and amino acids in sea water (Johnson *et al.* 1985; Riley *et al.* 1975). More recently, flow-injection analysis (FIA) has been used *in-situ* in combination with a variety of detection methods including spectrophotometry (Fe(II), Fe(III) and nutrients) and chemiluminescence (Fe, Cu and Mn) (Bowie *et al.* 1998; Bowie *et al.* 1995; Andrew *et al.* 1994; Coale *et al.* 1992; Elrod *et al.* 1991).

Latest developments of ship-board trace metal monitoring techniques include fully automated on-line voltammetric analysers, which are robust, reliable and relatively cheap. Electrochemical methods, especially stripping voltammetry, are particularly suited for biogeochemical trace metal studies because of their capability to detect a wide variety of metals directly in differing sample matrices, and their applicability to (operationally defined) dissolved metal speciation (see Chapter 2). Successful applications of stripping voltammetry in open ocean (Achterberg and van den Berg, 1994a), coastal (Achterberg *et al.* 1999; Braungardt *et al.* 1998; Achterberg and van den Berg, 1996; van den Berg and Achterberg, 1994; Tercier and Buffle, 1993) and estuarine waters (Whitworth *et al.* 1998; Braungardt *et al.* 1998) confirmed the suitability of this method for on-line surveys.

This chapter discusses the application of an automated on-line metal monitor in the Huelva estuary and the Gulf of Cádiz, southwest Spain. This coastal system receives metal-rich water from rivers, which rise in an important mining area and flow through industrial zones. As a consequence of the enhanced metal inputs and tidal water movements, high spatial and temporal variability of dissolved metal concentrations occur. The aim of the study was to gain a better understanding of the complex physical and biogeochemical processes that affect the behaviour and variability of dissolved metal concentrations. Therefore, a high resolution *in-situ* on-line monitoring strategy was the preferred option over discrete sample collection followed by land-based laboratory analysis of the trace metals.

Stripping voltammetry methods were chosen because they enabled the use of a single analytical technique for dissolved trace metal determinations at concentrations ranging from pico to micro moles per litre in samples with a wide salinity range. A modification of the fully automated on-line voltammetric metal monitoring system

described by Achterberg and van den Berg (1996 and 1994a) was used for the near real time high resolution analysis of surface waters from the river bank and onboard ship.

The automated application of Adsorptive Cathodic Stripping Voltammetry (AdCSV) methods allowed the direct determination of dissolved Zn, Cu, Ni and Co in natural water samples. The use of stripping voltammetry precludes laboratory-based pre-concentration or matrix removal steps, which are required before analysis of saline samples using Inductively Coupled Plasma - Mass Spectroscopy (ICP-MS) or Graphite Furnace Atomic Absorption Spectroscopy (GFAAS).

3.3 The Huelva Estuarine and Coastal System

An important objective of TOROS was to investigate the distribution and transport of trace metal from the Tinto/Odiel estuarine system into the Gulf of Cádiz (Figure 3.1). Shelf waters and sediments in the Gulf of Cádiz have been reported to be enriched with trace metals, especially Cu, Zn and Cd (Palanques *et al.* 1995; Van Geen *et al.* 1991). Published research suggested the Tinto and Odiel rivers as a possible source for metals to this sea area (Van Geen *et al.* 1997; Leblanc *et al.* 1995; Palanques *et al.* 1995; Nelson and Lamothe, 1993). Surface waters in the Gulf of Cádiz move in a south-easterly direction, following the coast line, and are entrained by the flow of Atlantic water through the Straits of Gibraltar (Ochoa and Bray, 1991). This has raised concerns about a possible enrichment of the western Mediterranean Sea with trace metals originating in the Gulf of Cádiz (Van Geen *et al.* 1991; Van Geen *et al.* 1988).

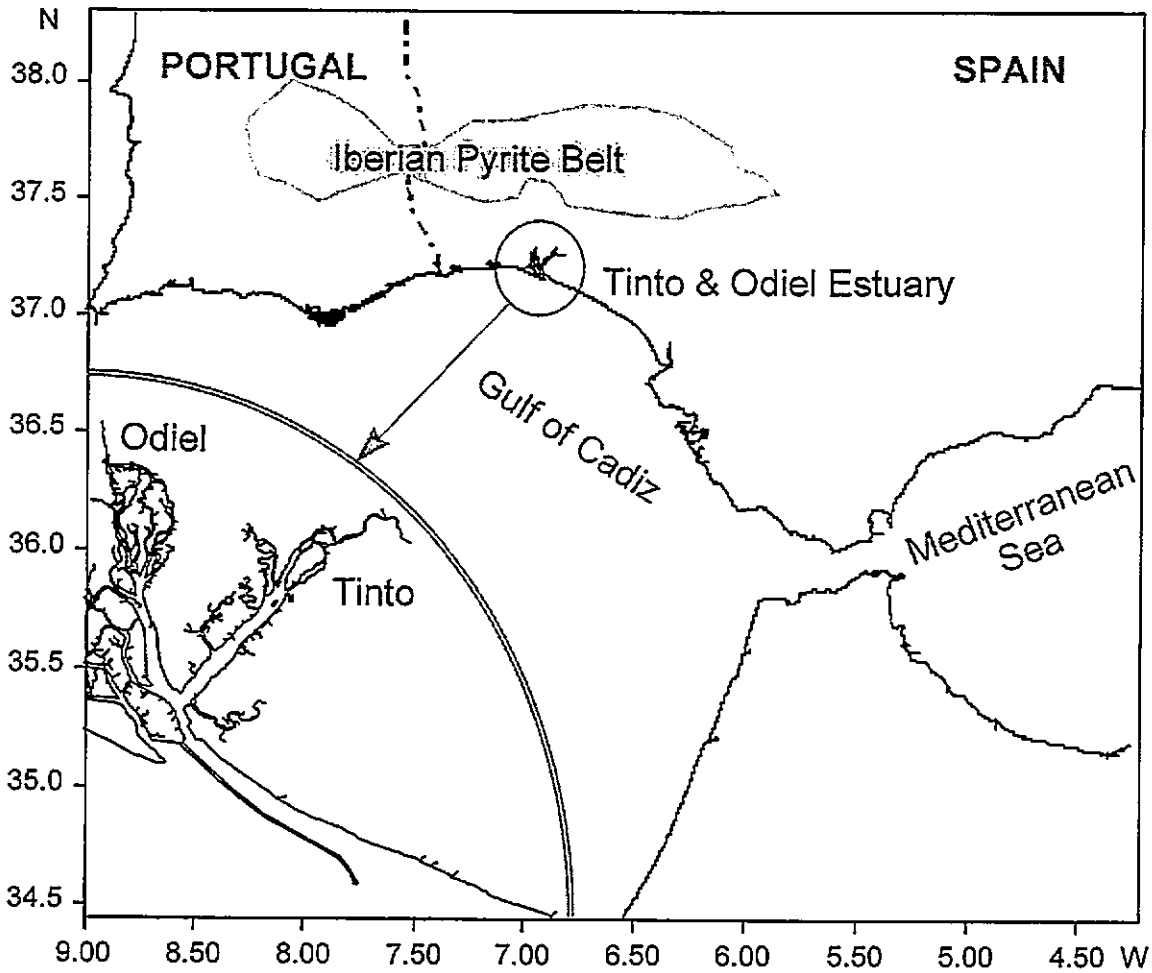

Figure 3.1 - Location of the Gulf of Cádiz, major rivers and the sulphide bearing Iberian Pyrite Belt in the southwest of the Iberian Peninsular. The inset shows the confluence of the Tinto and Odiel estuaries to form Huelva Ría.

Only the main characteristics of the study area are summarised here; a more detailed account is given in Chapter 4. The Rio Tinto and Rio Odiel are two small rivers, which originate in a heavily reworked area of metalliferous mining in the Iberian Pyrite Belt (Leblanc *et al.* 1995) (Figure 3.1). The massive sulphide ore bodies in the Pyrite Belt are rich in metals, especially Zn, Pb and Cu, with traces of Cd, Ag and Au. A long history of mining (Thornburn, 1990) has left a legacy of large quantities of mine tailings, slag and processed ore within the catchments of the Rio Tinto and Rio Odiel.

The two rivers have low average discharge volumes (annual mean: 3 m^3 s^{-1} and 15 m^3 s^{-1}, respectively), with a large seasonal variation (Borrego-Flores, 1992). As a result of the oxidation of sulphides (see Chapter 4) in the catchment, the fresh water of the Tinto and Odiel rivers is extremely low in pH (pH 2.2 - 3.5) and high in metal concentrations (e.g. Rio Tinto: 0.3 - 2.6 mM Zn, 121 - 856 μM Cu, 1.2 - 16.7 μM Ni and 0.78 - 6.0 μM Cd, see Chapter 4). The two rivers join in a common estuary (inset in Figure 3.1) at the city of Huelva, an important industrial centre in the southwest of Spain. Among the industries which discharge effluents into the estuary are paper and fertiliser plants, ore roasting facilities, titanium dioxide and copper production plants, oil refineries and sewage works.

3.4 METHODS

3.4.1 REAGENTS

The quality, preparation and purification of de-ionised water (MQ), reagents (HCl, HNO_3, NH_3, methanol, Oxine, DMG, APDC, Borate, HEPES) and metal standard solutions have been described in Chapter 2.

Mixed reagents for the on-line voltammetric analysis were prepared on a daily basis from the appropriate stock solutions of HEPES, Borate, Oxine and DMG. Total dissolved

Cu and Zn were determined simultaneously in the presence of Oxine (2×10^{-5} M, final conc.) and HEPES (pH 7.8, 0.01 M). Total dissolved Ni and Co analysis was carried out in the presence of DMG (2×10^{-4} M) and HEPES (0.01 M) during the first two TOROS surveys (November 1996, and June 1997). For the surveys in April 1998, and October 1998, Ni and Co was determined in the presence of DMG (2×10^{-4} M) and Borate (pH 8.4, 0.01 M) (all final concentrations). The substitution of Borate for HEPES resulted in a better separation of the Ni and Co peaks, probably as a result of the different pH. Addition of 250 µl of mixed reagent to 10 ml samples in the voltammetric cell gave the required AdCSV ligand concentrations and pH values (method adapted from Achterberg and van den Berg, 1994b).

Mixed standards for ICP-MS and ICP-AES were prepared from Spectrosol Stock Solutions (Al, As, Cd, Co, Cu, Fe, In, Mn, Ni, Pb, U and Zn, Merck) in HNO_3 (0.015 M).

For field work, several batches of each reagent and standard were packed separately in sealed plastic bags, in order to have a clean reserve should a bottle of reagent get spilled or contaminated.

3.4.2 Cleaning Procedures for Equipment

Sampling containers for dissolved trace metal analysis were made from high density polyethylene (HDPE, Nalgene). Sample bottles were cleaned by soaking in detergent (Pyroneg, one week), followed by a rinse with distilled water. Subsequently the bottles were immersed in HCl (50%, Analar, one week), rinsed in MQ, immersed in HNO_3 (2 M, Analar, one week) and finally rinsed with copious amounts of MQ. The cleaned bottles were filled with HCl (0.01 M, quartz distilled) and stored in two layers of sealable plastic bags. PTFE (Teflon®) containers, filter holders and other equipment were soaked in

detergent (Pyroneg), rinsed with distilled water and immersed in HCl (1 M, Analar), followed by a rinse with MQ.

Membrane filters (WCN: cellulose nitrate, 47 mm, pore size 0.45 µm, Whatman) were soaked in HCl (0.01 M, one day), rinsed and stored in MQ.

Tubing for underway sampling was made from polyvinylchloride (PVC, braided, 12 mm inner diameter, ID). Tubing for peristaltic pumps was made from high-strength silicone (Altesil™, Altech) or Santoprene®. This tubing was cleaned by pumping detergent (Pyroneg) through, followed by deionised water, HCl (1 M, Analar, left in the tubing several days), and MQ. All other tubing in contact with sample or reagents during on-line analysis was made from PTFE. PTFE tubing was cleaned by pumping HCl (0.1 M) through, followed by MQ.

3.4.3 Instrumentation

3.4.3.1 Field Instrumentation

During the coastal survey on board the Spanish oceanographic vessel *B/O Garcia del Cid*, a MARK III CTD package (Neil-Brown) was mounted on a 24 bottle rosette (General Oceanics). The CTD package included sensors for transmittance, fluorescence and dissolved oxygen. In addition, conductivity and temperature were measured continuously (every 5 - 30 s) by a T/S system (SeaBird). The T/S sensors were mounted close to the sea water inlet of the conduit (PVC), which supplied the ship's laboratories. Salinity was calculated from both conductivity sensors and compared with calibrated measurements in discrete surface samples, taken from rosette-mounted bottles.

During land-based surveys and estuarine transects with small boats, conductivity measurements were carried out with a combination Conductivity-Temperature-pH (CTpH,

purpose-built) meter and conductivity field instruments (model 52E, pHOX). For conversion to salinity, the instruments were calibrated against a series of standards of known salinity (S = 0 - 35.6). Measurements of pH were carried out with the CTpH meter, combined with a pH glass electrode (Merck) and reference electrode (double junction Ag/AgCl, Merck), and with digital instruments (model HI 9025, HANNA) with combination electrodes (HANNA). The pH meters were calibrated on a daily basis with buffers for pH 4.0 ± 0.02 and pH 7.0 ± 0.02 (Merck). The redox potential (Eh) was measured using digital field instruments (model HI 9025, HANNA) with a Combination Redox electrode. Each Eh measurement was compared with a ZoBell standard (theoretical Eh = 0.430 V against standard hydrogen electrode), and corrected accordingly. No corrections were made for temperature, as the error this introduces was deemed negligible within the accuracy of the method (Nordstrom, 1977). Dissolved oxygen was measured with a digital field instrument (model YSI 55, Yellow Spring Industries, USA), which also provided temperature measurements.

3.4.3.2 ICP-MS

Total dissolved metal concentrations in samples from the Rio Tinto, Rio Odiel, and the upper Tinto and Odiel estuaries were analysed by ICP-MS. The instrument used was a PlasmaQuad PQ2+ Turbo (VG Elemental), fitted with a double pass spray chamber (Scott) and a nebuliser for high solids (Galan). The analysis was carried out with the forward power set to 1350 W, and with the following gas flow rates: coolant gas 16 l min^{-1}, auxiliary gas 1.0 l min^{-1}, and nebuliser gas 0.85 l min^{-1}.

3.4.3.3 Voltammetric Equipment

The determination of dissolved concentrations of Zn, Cu, Ni and Co in discrete samples taken in the Huelva estuary and Gulf of Cádiz was carried out with two near identical systems, each consisting of a hanging drop mercury electrode (HMDE, VA 663 Stand, Metrohm) connected to a μAutolab voltammeter (EcoChemie) and interface for the mercury electrode (IME, EcoChemie). Samples were analysed in batches (10 ml) under the control of specialised software ('GPES', EcoChemie), running on a PC. For details regarding voltammetry see Chapter 2.

3.4.3.4 On-line Voltammetric Monitor

The continuous underway sampling with a torpedo-shaped fish (KIPPER-1) is illustrated in Figure 3.2. KIPPER-1 was designed and constructed specifically for this task from mild steel at the University of Plymouth. A braided tube (ID: 16 mm, PVC) was inserted into a bore that lead from the front of KIPPER-1, through its centre and out in front of the holding ring. The braided tube contained the sample pick-up tube (ID: 12 mm, PVC), leading to the peristaltic sample pump, which was positioned in the ship's laboratory. The design and weight (ca. 40 kg) of KIPPER-1 ensured that the sampling hose pointed forward and was kept at a constant depth (ca. 4 m) at speeds between one and 12 knots. KIPPER-1 was coated with metal-free epoxy-based paint (International Paint Ltd.). It was deployed from a winch on a strong wire about 3 m away from the side and about 4 m below the hull of the ship, which reduced the risk of sample contamination from the ship's hull. The braided tubing was attached to the lower part of the winch cable, which was covered with water resistant tape to reduce the risk of metal contamination. Continuous pumping (peristaltic pump, Watson-Marlow with Santoprene® pump tubing,

ID: 15 mm) of large volumes of sea water (1 - 2 l min^{-1}) flushed the pick-up tubing and allowed equilibration of the material (PVC) with the metal levels in the sampled water (van den Berg and Achterberg, 1994).

A schematic diagram of the automated metal monitoring system is shown in Figure 3.3. From the peristaltic sampling pump, PTFE tubing (ID: 0.6 mm) lead to the continuous on-line sample pre-treatment in two steps (filtration and UV-digestion) and to the automated metal monitor. On-line filtration was carried out with a tangential flow filtration unit made from an adapted Swinnex filter holder and fitted with a membrane filter (WCN, 47 mm, pore size 0.45 μm). The blocking of filter pores by particles was minimised by a high volume cross-flow (0.5 - 1 l min^{-1}). Filter changes were necessary approximately every four hours in estuarine waters and once daily in coastal waters.

Filtration was followed by on-line UV-digestion of dissolved organic matter. This step was necessary to break down surfactants and natural metal-complexing organic ligands, which may interfere with the voltammetric analysis of total dissolved metals (Achterberg and van den Berg, 1994b). The UV-digestion unit contained a medium pressure mercury vapour lamp (400 W, Photochemical Reactors) surrounded by a quartz glass coil (ID: 1.0 mm, length ca. 3.5 m). A fan attached to the UV unit ensured that the sample temperature remained around 70°C. The sample cooled to ambient temperature during its transfer from the UV-digestion unit to the voltammetric cell.

The two voltammetric systems described in Section 3.4.3.3 were converted into fully automated trace metal monitors for on-line analysis. Each metal monitor included a voltammeter, IME, electrode (HMDE), sample and reagent transport system (SRTS) and syringe pump (Cavro), all of which were controlled using a portable PC.

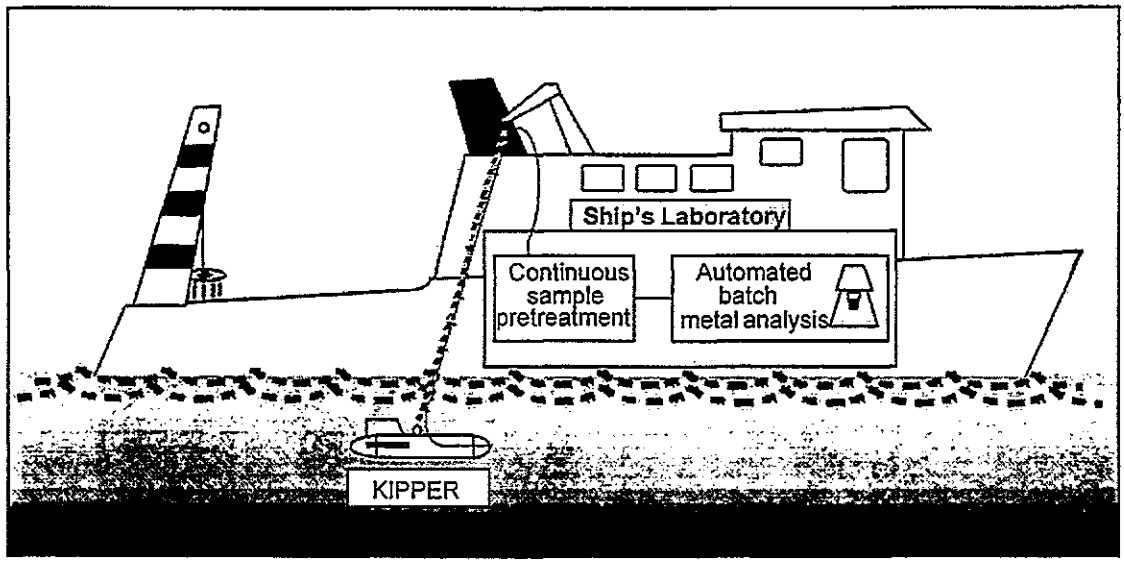

Figure 3.2 - Set-up for continuous underway sampling with KIPPER-1 for high resolution automated ship-board analysis of dissolved trace metals in surface waters.

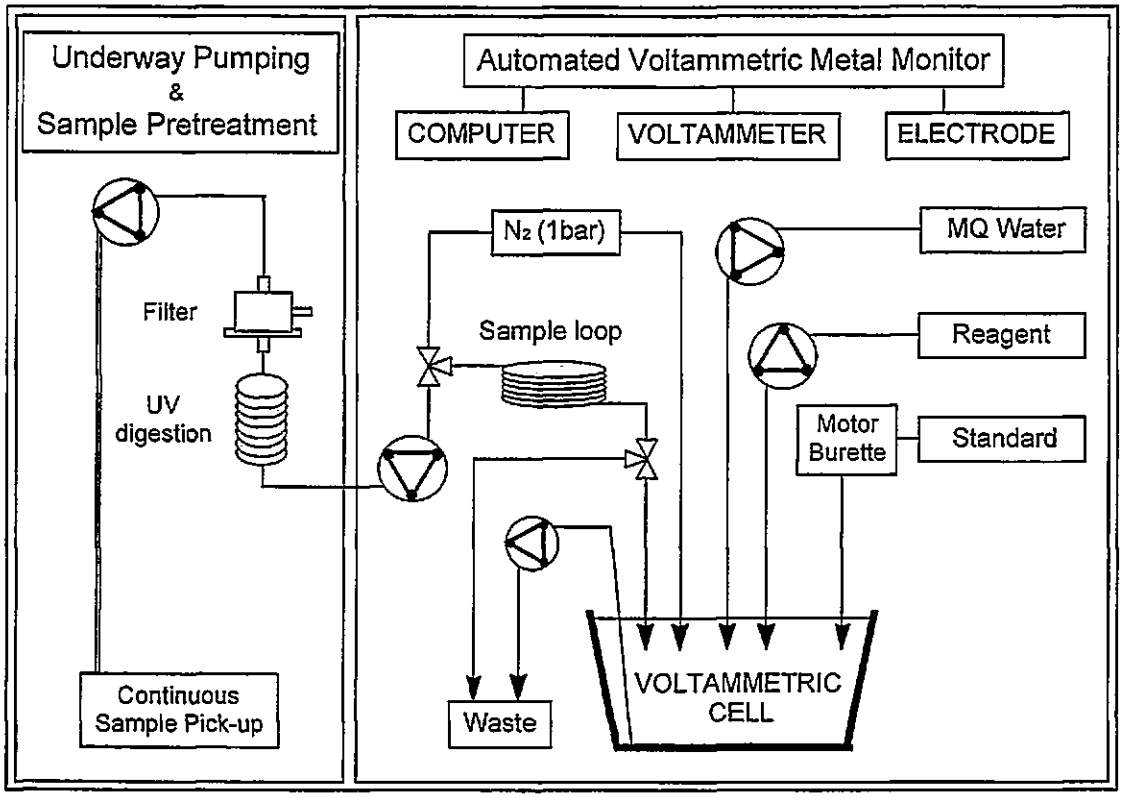

Figure 3.3 - Schematic representation of the automated metal monitor. The continuous underway pumping system and sample pre-treatment (left box) is linked to the fully automated, computer controlled voltammetric metal monitor (right box), which operates in batch mode.

The monitors were identical, with the exception of the SRTS, which in system I was a commercially available unit (EcoChemie). The SRTS for system II was purpose-built at the University of Plymouth for the TOROS project and provided identical functions to those of the EcoChemie unit. The automated analysis was carried out under the control of the 'EAS' software (EcoChemie), which had been modified to control the SRTS, the syringe pump, and to perform data quality verification and storage (see below).

The path of the sample to and within the SRTS is illustrated in Figure 3.3. A peristaltic pump conveyed the pre-treated sample to the sample loop (system I: 10.00 ± 0.01 ml, system II: 9.90 ± 0.01 ml; n = 8), which was enclosed by two inert three-way valves (coated with PTFE, Cole-Parmer). The valves were set in a position that allowed the flushing of the loop with sample water (ca. 15 ml). In this way, the wall of the tubing was equilibrated with the metal concentration in the sample. After flushing, the valves were actuated to empty the water contained in the sample loop into the voltammetric cell by means of nitrogen gas (oxygen free N_2, 1 bar). Subsequently a peristaltic reagent pump delivered mixed reagent (250 µl, PC-timed) to the voltammetric cell. After de-aeration of the sample (oxygen free N_2) the measuring cycle was carried out. A syringe pump received signals from the PC software (RS 232 interface) specifying the volume of metal standard to be dispensed to the voltammetric cell for the internal calibration of each measurement. After completion of the analysis, two more peristaltic pumps were activated, one to discard the sample, the other to carry out a rinsing cycle with MQ (3 x 12 ml, PC-timed). This prepared the cell for the next sample. PTFE tubing was used throughout the monitor, with the exception of the pump tubing, which was high strength silicone (AlteSil™, Altech) or Santoprene®.

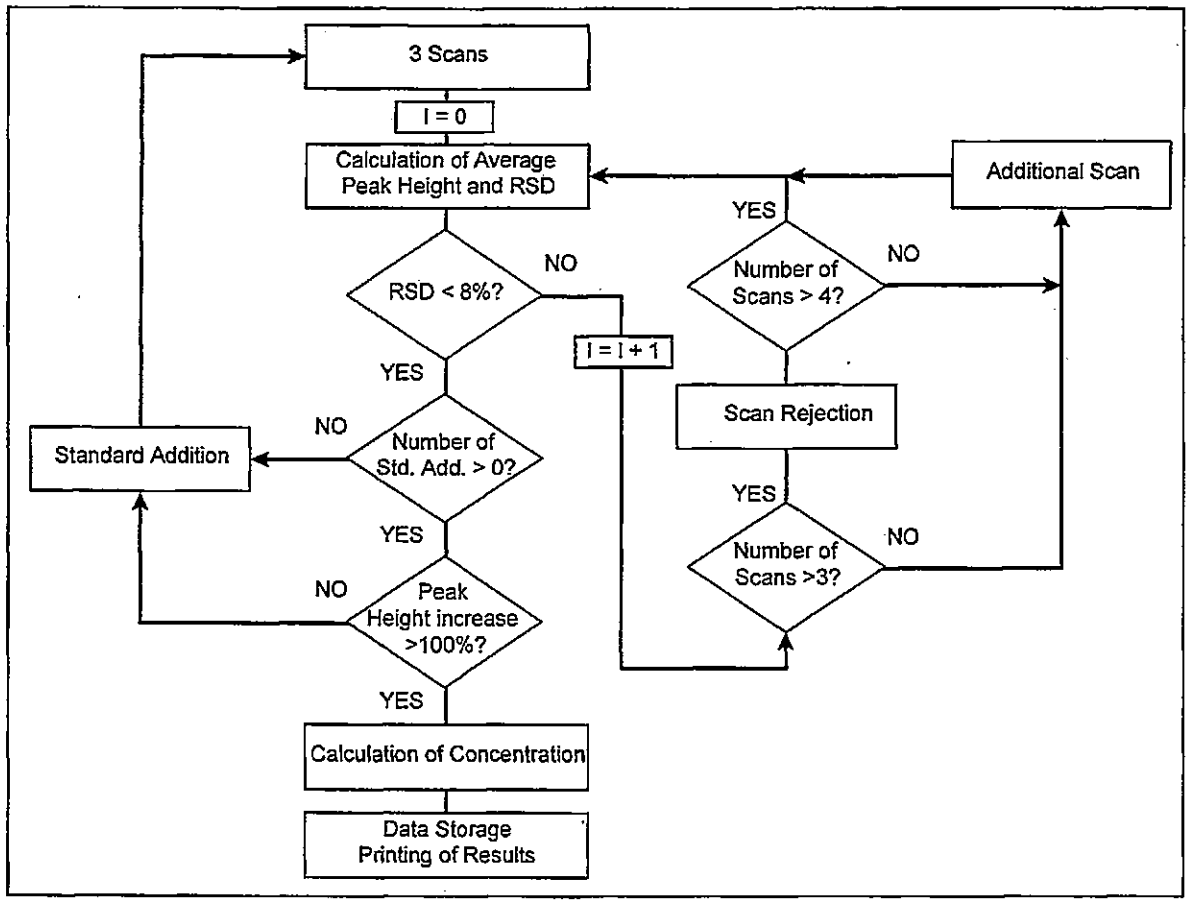

Figure 3.4 - Flow diagram of software-controlled analytical cycle during automated analysis with the voltammetric metal monitor. The cycle starts with three voltammetric scans and ends with data storage and printing of results. Details see text. Adapted from Achterberg (1993).

A flow diagram of the sample analysis cycle is presented in Figure 3.4. After three voltammetric scans (see Chapter 2), the average peak height (i_{p0}) and relative standard deviation (RSD) was calculated. If the RSD was below a pre-set value (e.g. 8%), a standard addition was made. Three voltammetric scans were followed by the calculation of average peak height (i_{p1}) and RSD. The RSD test was repeated and if passed the ratio i_{p1} : i_{p0} was calculated to test the increase in peak height. In case of $ip_1 : i_{p0} \geq 2$, the sensitivity (S) was calculated by dividing the increase in peak height (Δi_p) by the concentration of added standard (ΔC). The analyte concentration in the sample aliquot was calculated as $C = i_{p0}/S$. Data storage and printing of the results conclude the measuring cycle.

However, in case of a failed RSD test, a fourth scan was carried out. If the RSD test for the four scans failed, the scan that differed by more than the pre-set criterion from the mean was discarded and a fifth scan was carried out. If the RSD test failed again, another scan was rejected, no additional scan was initiated and the RSD test following the calculation of the average peak height was ignored. If the standard addition was insufficient to increase the peak height two-fold, another standard addition was carried out, the volume of which was estimated from the increase in peak height following the first standard addition.

3.4.4 Sampling and Analysis

3.4.4.1 On-line Monitoring of dissolved Cu, Zn, Ni and Co

In June 1997, and October 1998, on-line metal monitoring was carried out almost continuously for eight days and seven days, respectively, onboard the *B/O Garcia del Cid.* High resolution on-line measurements of dissolved metals were performed along estuarine transects and in the coastal sea, using two automated voltammetric metal monitors for the simultaneous analysis of Zn and Cu (system I), and Ni and Co (system II).

On-line metal analyses were carried out during tidal cycle (TC) studies in the Huelva estuary. During TCs, the monitoring instrumentation was deployed at one geographical point over a 13-hour period to record a time series of the tidal variability of physico-chemical parameters and metal concentrations. In the upper and mid-estuary, TCs were carried out from a mobile laboratory (Ford Transit van) positioned on the bank of the estuary (Figure 3.5). A petrol generator (240V, 2.5 kW) was used to supply the power. A continuous sample pick-up was made up from a braided PVC hose (ca. 50 m length, ID: 12 mm), the end of which was anchored some distance (typically 10 - 30 m) from the shore. The inlet was held ca. 50 cm below the surface by a PVC-covered lead doughnut and a float, which were fastened to the hose and the anchor with nylon rope. During the survey in October 1998, a TC was performed from the *B/O Garcia del Cid*, which was anchored close to the mouth of the estuary. The KIPPER-1 was used as sample pick-up in the same way as described for underway monitoring.

During the TC studies, discrete samples were taken at hourly intervals, either from the shore or with the facilities available onboard ship (see Section 3.4.4.2). These samples were used for inter-comparison with results from the automated on-line analysis.

On-line trace metal analysis was carried out using square wave adsorptive cathodic stripping voltammetry (AdCSV, see Chapter 2). Before the analysis, the sample was purged for 120 and 200 s (Zn/Cu and Ni/Co, respectively) with oxygen free N_2 (Air Liquide). In-between cathodic scans, the purge was repeated for a short time (15 s). The wide range of dissolved metal concentrations in the Huelva estuary and Gulf of Cádiz required the adaptation of analytical parameters used. Typical parameters for the analysis of relatively pristine water in the outer Gulf of Cádiz and highly polluted estuarine water are given in Table 3.1.

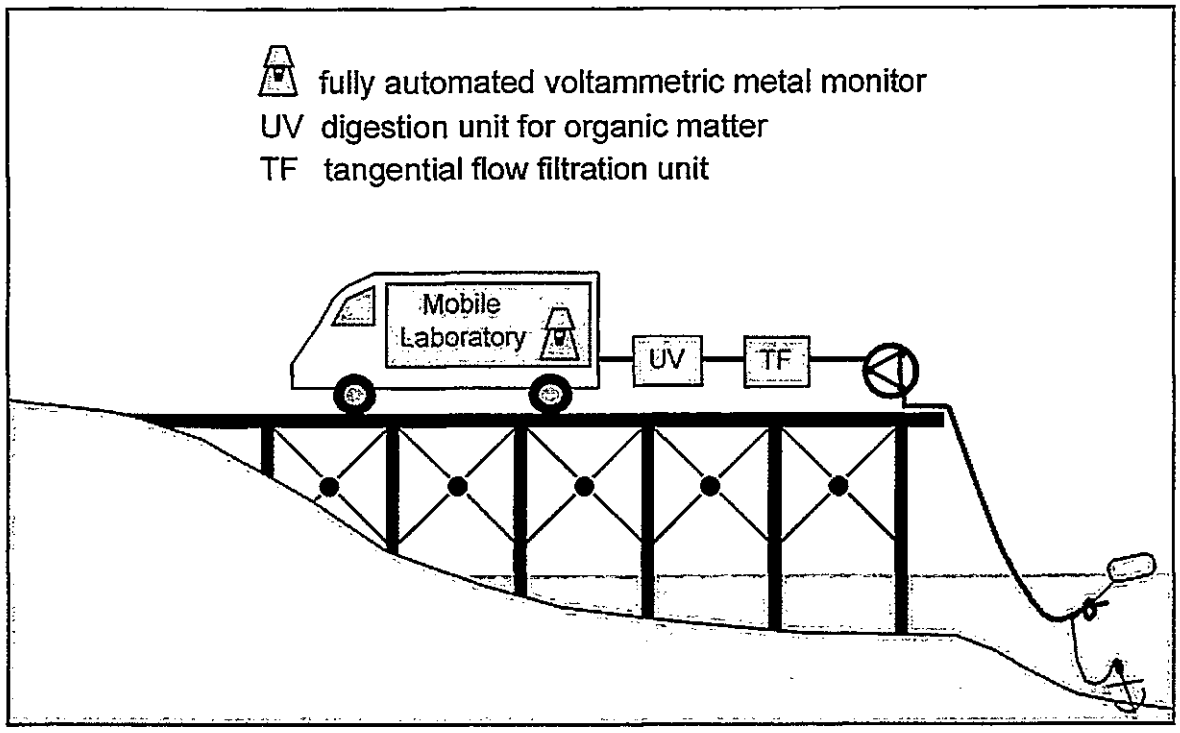

Figure 3.5 - Set-up for continuous sampling with an anchor and float, with the mobile laboratory stationed on the bank of the estuary. Sample is pumped through filter and UV-digestion unit into the automated metal monitor.

Table 3.1 - Typical parameters for square wave cathodic stripping voltammetry during ship-board analysis of total dissolved Cu and Ni in surface waters of the Gulf of Cádiz (nM range) and in the mid-Odiel estuary (low µM range). Values in brackets refer to the simultaneously analysed metal (i.e. Zn with Cu, and Co with Ni). nd - not determined.

Voltammetric Parameter Concentration Range	Cu (Zn) nM	Ni (Co) nM	Cu (Zn) low µM	Ni (Co) low µM
Deposition potential (V)	-0.5	-0.8	-0.5	-0.97
Deposition time (s)	40	40	0	2
Stirrer setting (max. 6)	5	5	0	1
Scan Frequency (Hz)	100	100	50	50
Initial potential (V)	-0.2	-0.8	-0.2	-0.8
Final potential (V)	-1.3	-1.2	-1.3	-1.2
Step potential (mV)	2.4	2.4	4.9	4.9
Modulation ampl. (mV)	25	25	10	10
Reduction potential (V)	-0.45 (-1.02)	-0.97 (-1.04)	-0.45 (-1.02)	-0.97 (-1.04)
LOD (nM)	0.48 (0.81)	0.21 (0.24)	nd	nd
Linear range	25 (35) nM	20 (25) nM	4 (7) µM	1 (2) µM

The calculation of the dissolved metal concentration was based on one standard addition only. The linear range of certain sets of parameters (deposition time, stirring rate) was tested in the laboratory. Parameters were set at the beginning of an on-line survey according to the range of metal concentrations expected. Regular checks (on screen or print outs) were carried out in order to detect any calculated metal concentrations outside the linear range of the set parameters, or the initiation of multiple standard additions by the program (see Figure 3.4) in combination with non-linear current responses. When necessary, analytical parameters were adjusted when passing through areas of higher (or lower) concentrations during on-line surveys. The preconcentration efficiency could be adjusted (factor 2 - 4) by changing the stirrer rate without interrupting the on-line analysis.

3.4.4.2 Discrete Samples

During TC studies in the upper estuary, discrete surface samples were taken from the shore. Water was collected with a bucket (attached to a nylon rope) which was thrown into the water from the shore. The bucket was rinsed three times before it was used to rinse and fill an acid-cleaned container (10 l) with sample. Filtration (WCN, pore size 0.45 μm) was carried out within two hours of collection. For trace metal determinations, acid cleaned Nalgene filter holders (500 ml) and vacuum hand-pumps were used in a 'clean space' set up in the mobile laboratory. Between samples, the filter holder was rinsed with MQ. The first batch of filtrate (100 - 150 ml) was used to rinse filter paper and filter holder with the sample. Filtration blanks (MQ) were filtered before the first sample and between two samples at some stage during the TC, and analysed with the discrete samples in Plymouth. The filtered samples were acidified (HNO_3, pH 2) in a laboratory at the University of Huelva. Analysis of total dissolved Zn, Cu, Ni and Co, among other metals, was carried out by ICP-MS. For the analysis the samples were diluted ($\geq$ 50 times) in

HNO_3 (0.015 M), in order to reduce interference from the saline matrix. Indium (10 μg l^{-1}, Spectrosol, Merck) was used as internal standard in all samples, blanks and standards to compensate for instrumental drift during analysis. Certified reference material (SLRS-2) was used to verify the analytical performance.

During the TC at the mouth of Huelva estuary, discrete samples were taken from Niskin bottles, which were deployed on the CTD rosette of the *B/O Garcia del Cid* and fired at a depth of seven to eight metres. Trace metal clean Niskin bottles (NERC, Southampton Oceanography Centre, SOC), that had been modified for open ocean trace metal work and contained no internal metal parts were used throughout the survey (Morley *et al.* 1993). Samples were filtered (WCN, pore size 0.45 μm) within two hours of collection in a laminar flow hood set up in the ship's wet laboratory following the procedure described above. Samples were acidified with HCl (pH 2) onboard and analysed with voltammetric methods at the University of Plymouth. For voltammetric analysis of total dissolved Zn, Cu, Ni and Co samples were subjected to UV-irradiation (see Chapter 2). Square wave AdCSV was carried out in batches of 10 ml: Zn in the presence of 200 μM APDC and 0.01 M HEPES, Cu in the presence of 20 μM Oxine and 0.01 M HEPES, Ni and Co simultaneously in the presence of 200 μM DMG and 0.01 M Borate. The scanning frequency was 50 Hz, and typical values were 2.44 mV for step potential and 25 mV for step amplitude. The deposition time ranged between 5 s and 60 s, depending on the metal concentration encountered.

MQ blanks were analysed on a daily basis and before the analysis of discrete samples. To 10 ml of MQ the appropriate reagents were added at the same concentration as for sample analysis (see previous paragraph). Voltammetric parameters were set as for sample analysis, with the exception of an extended deposition period of 60 s (Zn, Cu, and Ni) or 120 s (Co, Cd), and a scanning frequency of 10 Hz.

3.5 Results and Discussion

3.5.1 Analytical Performance

Typical values of MQ blanks gave concentrations of 0.35 - 0.5 nM Zn, 0.25 - 0.35 nM Cu, 0.05 - 0.1 nM Ni. Blank concentrations of Co and Cd were below the limit of detection (see following paragraphs). The metal concentrations found in MQ blanks were the combined result of metals in MQ (typically 0.2 nM Zn, 0.2 nM Cu), and contamination in pH buffer (HEPES, Borate) and AdCSV ligand (Oxine, DMG, APDC). Though care was taken to work as clean during field work, as under normal laboratory conditions, experience showed that metal concentrations in blanks during surveys were more variable and sometimes higher than in the laboratory in Plymouth (e.g. June survey: maximum concentration in reagent blank was 0.46 ± 0.16 nM Cu). Contamination introduced during handling of the aliquot in field situations may have been the cause for this. For metal concentrations in filter blanks see Chapter 4.

For the determination of the limits of detection (LOD), sea water from the Gulf of Cádiz was analysed in batches using multi-elemental determinations with AdCSV and conditions as for on-line analysis and with the voltammetric parameters for the concentration range < 20 nM (Table 3.1). The sea water concentrations were 3.8 ± 0.27 nM (LOD_{Zn} = 0.81 nM) for Zn (n = 4), 2.61 ± 0.16 nM (LOD_{Cu} = 0.48 nM) for Cu (n = 5), 2.88 ± 0.07 nM (LOD_{Ni} = 0.21 nM) for Ni (n = 4), 0.49 ± 0.11 nM (LOD_{Co} = 0.33 nM) for Co (Table 1). The LOD was calculated as three times the standard deviation.

For single element determinations in discrete samples, the LOD was lowered to LOD_{Zn} = 0.27 nM, LOD_{Cu} = 0.21 nM, LOD_{Ni} = 0.21 nM and LOD_{Co} = 0.28 nM, by

optimising voltammetric parameters for individual metals, and using APDC instead of Oxine as AdCSV ligand for Zn (Table 3.2).

The linear range of the AdCSV method was determined in laboratory experiments, using the on-line parameters listed in Table 3.1. With parameters used for the 'nM' range, the linear range was 35 nM Zn, 25 nM Cu, 20 nM Ni and 25 nM Co. By lowering the stirring rate during deposition, decreasing the deposition time, and altering the scanning parameters and deposition potential, the linear range for direct analysis without sample dilution was extended to 7 μM Zn, 4 μM Cu, 1 μM Ni and 2 μM Co (parameters as for 'low μM' range in Table 3.1).

The accuracy of the analytical methods, including calibration, was verified by the analysis of certified reference materials. For stripping AdCSV techniques, estuarine water (SLEW-2) and coastal sea water (CASS-3) were UV- irradiated and several batches were analysed after neutralisation with quartz distilled NH_3 for total dissolved Zn, Cu, Ni and Co. During each ICP-MS run five aliquots of river water (SLRS-2), were analysed using the same instrument parameters as for blanks, standards and samples. Good agreement of analytical with certified values was achieved (see Chapter 2 for AdCSV, Chapter 4 for ICP-MS).

The reproducibility of on-line analysis with the automated metal monitor was determined using filtered, UV-irradiated and acidified (HCl, pH 2) sea water, which was sampled in the vicinity of Plymouth. This sea water contained Zn, Cu, Ni and Co values at concentrations similar to levels observed in the coastal waters of the Gulf of Cádiz. Several aliquots of this water were analysed in automated on-line mode for Zn with Cu and Ni with Co in multi-elemental mode. In order to adjust the pH of the acidified aliquots, NH_3 was added to the voltammetric cell with the mixed reagent.

Table 3.2 - Parameters and reagents for the determination of limits of detection in sea water samples. LOD calculated as three times standard deviation of the mean. HEPES - pH 7.8, Borate - pH 8.4.

Voltammetric Parameter	Zn	Cu	Ni	Co
AdCSV ligand	APDC	Oxine	DMG	DMG
pH buffer	HEPES	HEPES	Borate	Borate
Deposition potential (V)	-1.2	-1	-0.9	-0.95
Deposition time (s)	60	60	60	120
Stirrer setting (max. 6)	5	5	5	5
Scan Frequency (Hz)	100	50	50	50
Initial potential (V)	-0.8	-0.2	-0.8	-0.8
Final potential (V)	-1.3	-0.6	-1.2	-1.2
Step potential (mV)	2.4	2.4	2.4	2.4
Modulation ampl. (mV)	25	25	25	25
Reduction potential (V)	-1.05	-0.43	-0.93	-1.08
LOD (nM)	0.27	0.21	0.21	0.28

The relative standard deviation in this experiment was 6.3 % for Zn (44.8 ± 2.82 nM, n = 15), 5.9% for Cu (23.2 ± 1.38 nM, n = 16), 7.4% for Ni (10.4 ± 0.77 nM, n = 13) and 6.1% for Co (1.9 ± 0.12 nM, n = 13). Values determined during batch analysis (n = 3) of this sample were in good agreement with the on-line analysis (42.9 ± 2.3 nM Zn, 22.4 ± 0.78 nM Cu, 9.89 ± 0.52 nM Ni and 2.0 ± 0.13 nM Co). Errors given represent one standard deviation of the mean concentration.

3.5.2 Environmental Data

Two tidal cycle studies and a coastal survey are used to illustrate the suitability of the metal monitor for the extreme fluctuations of physico-chemical parameters and metal concentrations in the highly contaminated Huelva estuary and the adjacent coastal sea.

3.5.2.1 Tidal Cycle Study at Huelva Bridge

The TC at Huelva Bridge was carried out in June 1997. Huelva Bridge crosses the estuary downstream from where the narrow and highly branched Ría del Odiel becomes wider to form the Huelva estuary (Figure 3.6). The location was chosen to monitor the water with the lowest possible salinity at a point that was accessible with the mobile laboratory.

The extreme conditions with respect to metal concentrations and sample matrices encountered during this TC made the semi-automated dilution (x 100) of samples during parts of the automated on-line analysis necessary.

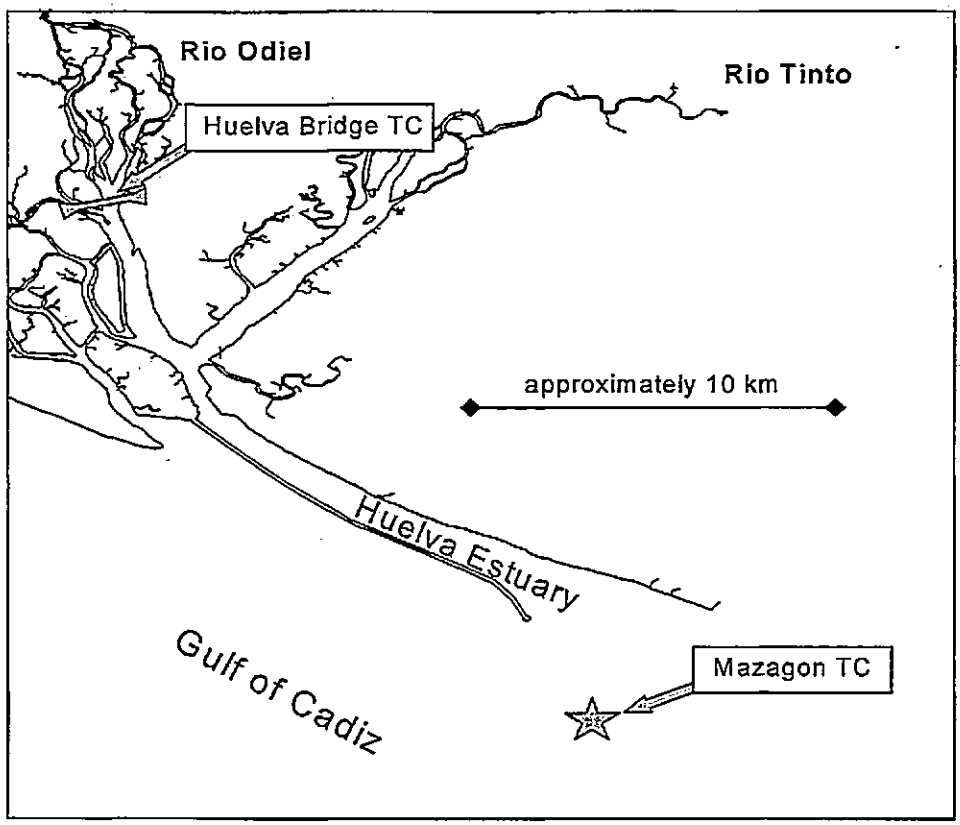

Figure 3.6 - Locations of tidal cycle studies at Huelva Bridge and off the mouth of the Huelva estuary.

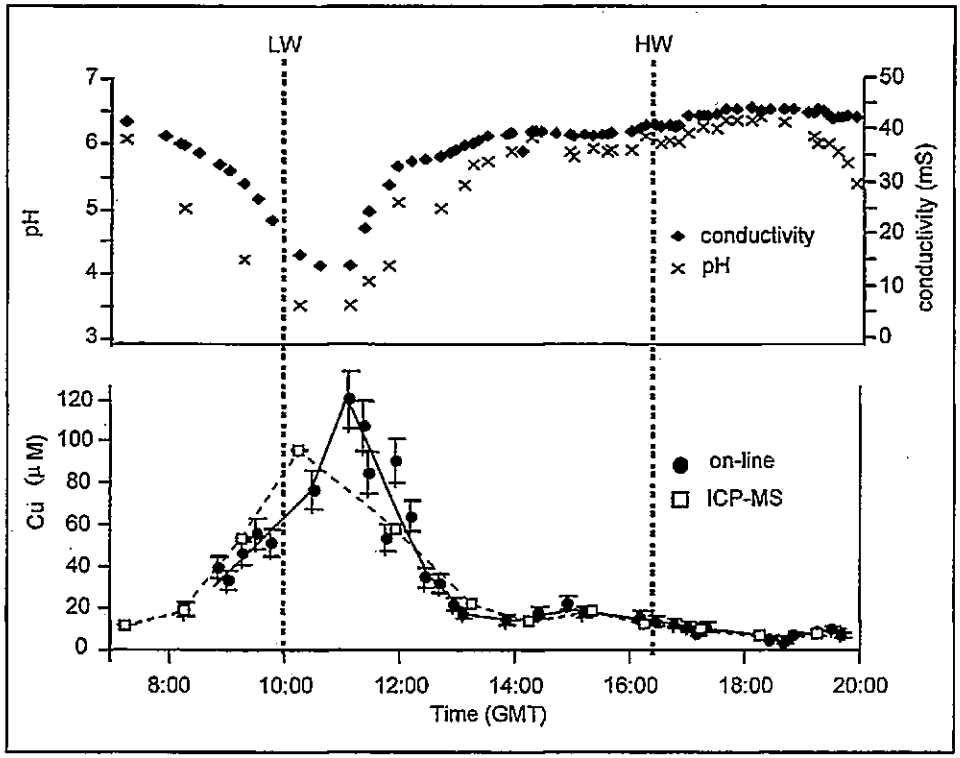

Figure 3.7 - Time series of conductivity, pH and dissolved Cu over a full tidal cycle at Huelva Bridge in June, 1997. The lower part shows on-line voltammetric measurements of Cu from the river bank and results from ICP-MS analysis of discrete samples, taken parallel at hourly intervals. Error bars refer to the maximum error of ± 8 % between repeated scans during on-line analysis (AdCSV), and to standard deviation of sample replicates during discrete analysis (ICP-MS). LW and HW: low and high water at Mazagón harbour (situated at the mouth of Huelva estuary).

Figure 3.7 shows the time series recorded at Huelva Bridge. Conductivity and pH minima indicated that at this location low water occurred approximately one hour later (ca. 11:00 h) than at the mouth of the estuary (vertical dashed line marked 'LW'). The salinity, calculated from conductivity, varied between S = 9.0 and S = 34.8. Results from the on-line monitoring (closed circles in Figure 3.7) during the TC show that total dissolved Cu concentrations increased steeply during the ebb tide and reached a maximum of 121 μM, which coincided with the minimum conductivity and pH.

Discrete samples were analysed by ICP-MS, and results for total dissolved Cu (squares in Figure 3.7) compared well with the on-line trend. Similar observations were made for Zn, Ni and Co (data not presented). It is apparent from the comparison of the two sets of data that on-line high resolution monitoring provided the time and concentration of the Cu maximum, while the discrete sample analysis failed to fully resolve the tidal variability during the monitored period.

From the close agreement between discrete and on-line data it follows that contamination from carry-over between samples during on-line measurements was minimal. Because the two sets of data resulted from the analysis of different samples, and not sub-samples of one another, no direct statistical comparison was made. Small differences in the results for Cu between the on-line and discrete samples are likely to have been genuine differences in the samples, which were taken with a spatial distance of a few metres from each other by the sample-pick up and from the shore, respectively. This inter-comparison of samples and analytical methods showed that the on-line monitoring produced good quality data in extreme sampling matrices and over a wide range of metal concentrations.

3.5.2.2 Ship-board Tidal Cycle at Mazagón

In October 1998, a TC was carried out on board the *B/O Garcia del Cid*, which was anchored about three kilometres off the mouth of the Huelva estuary (Figure 3.6). The strong marine influence on water composition at this location was reflected in the small salinity range encountered during the TC (S = 36.33 - 36.35, Figure 3.8), and the salinity time series did not yield information related to flood and ebb tides.

Total dissolved Zn was analysed on-line by AdCSV and the ligand Oxine (multi-elemental determination of Zn with Cu), while discrete samples were analysed by AdCSV using the ligand APDC (single-elemental determination of Zn). The Zn concentration in discrete samples agreed well with the results from on-line analysis. The slightly lower concentrations in some discrete samples could be the result of differences in sampling position. Discrete samples were taken at a depth of seven to eight metres, compared to on-line analysis for which the water was pumped from a depth of three to four metres, using KIPPER-1. During a ship-board TC, the contamination risk from the ship while anchored is higher than during steaming. Tidal movement is slow and, therefore, the sampled water may have been in contact with the ship's hull for a sufficient time to pick up contamination, and surrounding water may have been mixed with cooling water from the ship's engine. However, the vessel was allowed to swing on anchor and the sample pick-up was deployed from a winch off the side of the ship. Therefore, except during slack water, it is likely that KIPPER-1 was under less influence from these sources of contamination than the Niskin bottles deployed from the stern of the ship. Under these circumstances, it is difficult to judge whether or not contamination from the vessel influenced either or both sets of data, and its possible magnitude.

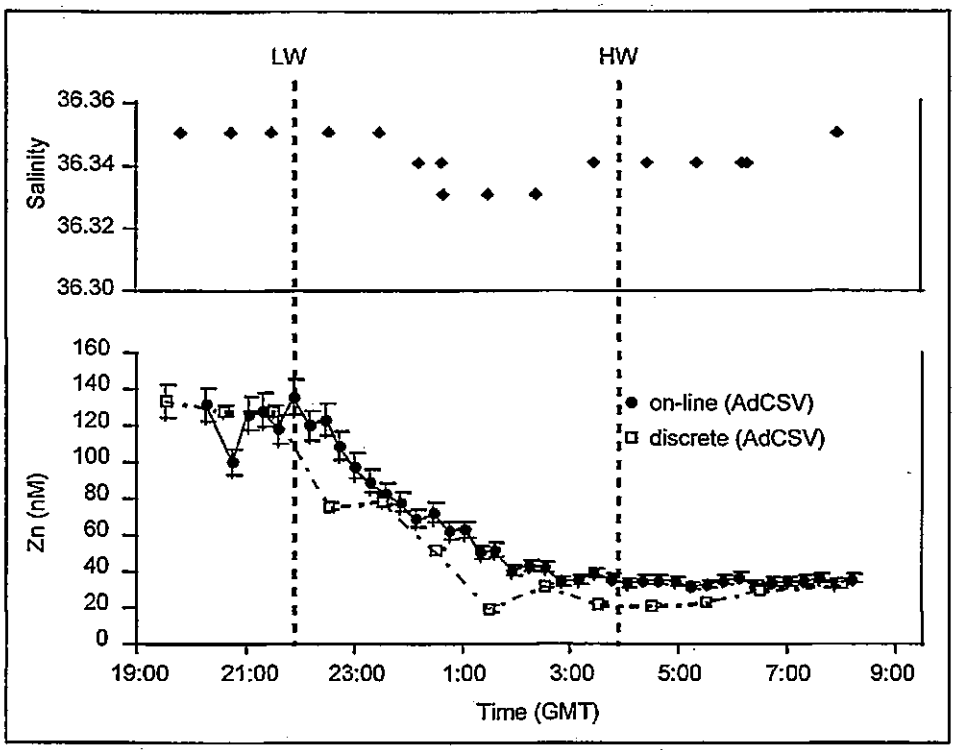

Figure 3.8 - Time series of conductivity and dissolved Zn over a full tidal cycle off the mouth of Huelva estuary, October, 1998. The lower part shows ship-board on-line voltammetric measurements of Zn and results from AdCSV analysis of discrete samples, taken parallel at hourly intervals. Error bars refer to the maximum error of ± 8 % between repeated scans during on-line analysis (AdCSV), and the standard deviation of sample replicates during discrete analysis. LW and HW: low and high water at Mazagón harbour.

A broad peak of total dissolved Zn (100 - 136 nM) was observed around the time of low water. A gradual decrease of the Zn concentration followed, reaching a plateau of 31 - 38 nM, which represented the background concentration in nearshore waters of the Gulf of Cádiz. The high number of data points (n = 41) from on-line analysis gives a clearer picture of the trend in dissolved Zn concentrations, compared to the discrete samples (n = 13). Furthermore, high-resolution time-series can be used with greater confidence for the calculation of metal fluxes across the mouth of an estuary, compared to results from a single sample collected at the mouth of an estuary during conventional transects.

3.5.2.3 On-line Monitoring in the Gulf of Cádiz

During the first part of the coastal survey, the *B/O Garcia del Cid* cruised for four days between the coast line and the 500 m depth contour in the Gulf of Cádiz. During this period, a total of 52 separate discrete depth profiles were obtained, for which the vessel stopped at each sampling station. Continuous underway sampling was carried out in parallel and the voltammetric metal monitor operated almost continuously onboard ship. Interruptions of on-line analysis (10 - 30 minutes) were necessary occasionally to retrieve data for safe storage. About 250 on-line measurements were completed with each of the monitoring systems during steaming and while the vessel was on station. Figure 3.9 illustrates the high spatial resolution attainable with the automated monitoring approach (3.5 - 4.5 km between measurements along the cruise track), compared with the spacing of discrete sampling stations (ca. 10 - 15 km).

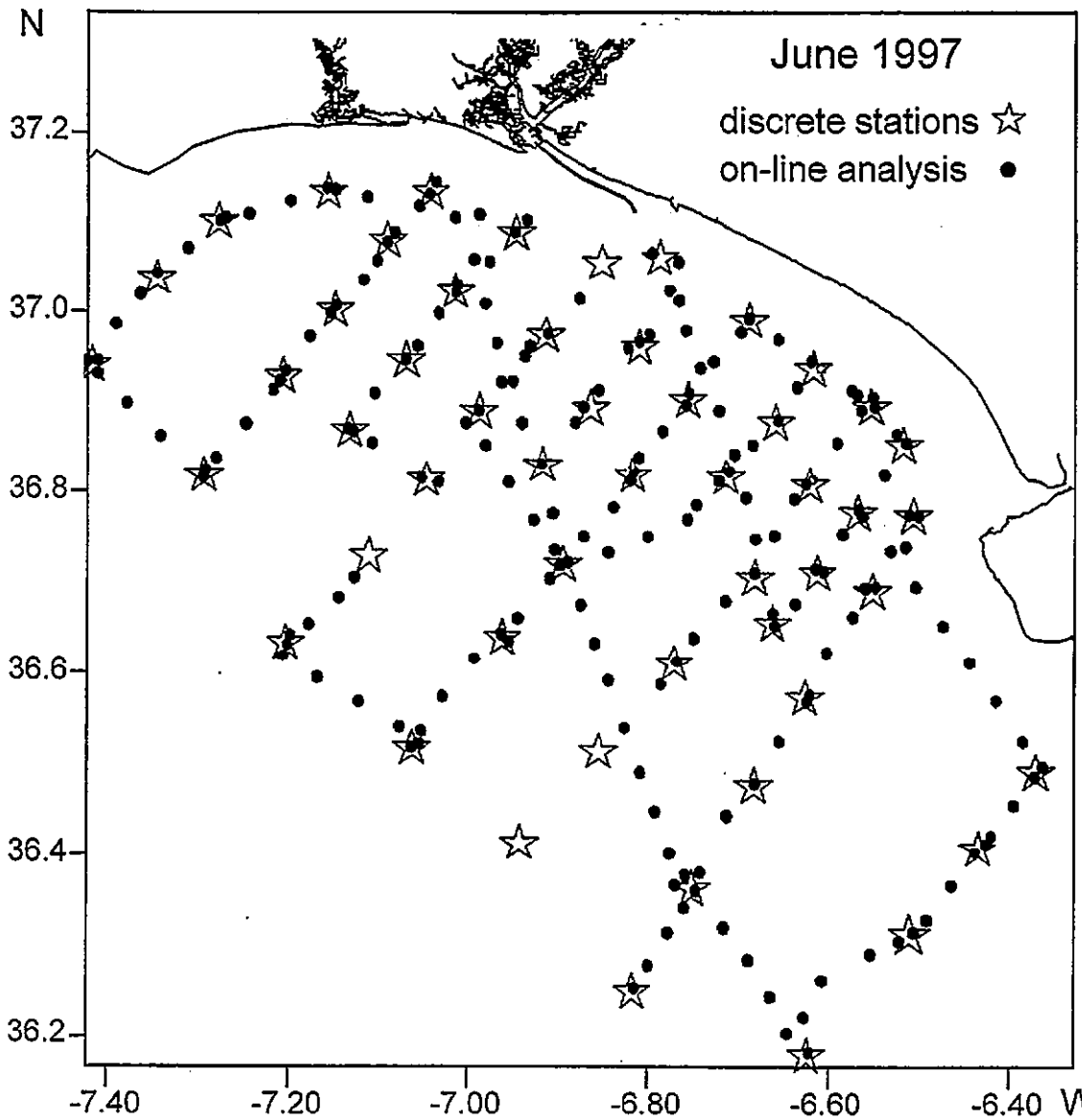

Figure 3.9 - Comparison between the resolution of discrete sampling stations (stars) and on-line automated measurements (circles) of Cu in the Gulf of Cádiz, June, 1997.

Contour plots of total dissolved Cu and Ni concentrations in surface waters of the Gulf of Cádiz are shown in Figure 3.10 and Figure 3.11, respectively. The gridding method used to create the contour plots is described in Chapter 5. Enhanced metal levels were observed around the mouths of the Huelva (15 nM Cu, 5 nM Ni) and the Guadalquivir (20 nM Cu, 15 nM Ni) estuaries. Metal concentrations decreased with increasing distance from the coast to levels below 5 nM Cu and 3 nM Ni at the seaward limit of the sampling area. This decrease can be explained by the mixing of metal-polluted estuarine with more pristine North Atlantic waters (see Chapter 5). Dissolved metal concentrations measured during this survey are comparable to those published by van Geen *et al.* (1991), who reported typical dissolved metal concentrations over the Spanish shelf of 6.6 nmol kg^{-1} Cu and 3.4 nmol kg^{-1} Ni, and levels of 8 - 21 nmol kg^{-1} Cu and 3 - 6 nmol kg^{-1} Ni some 40 km to the southwest of the Guadalquivir estuary.

The waters of the Guadalquivir river and estuary have been reported to have a lower metal concentration (9.5 - 16 nmol kg^{-1} Cu and 21 - 79 nmol kg^{-1} Ni, (Van Geen *et al.* 1991); 27 - 86 nM Cu and 20 - 48 nM Ni, this study), compared to levels observed at the mouth of the Huelva estuary (50 - 600 nM Cu and 7.5 - 290 nM Ni, this study, see Chapter 4). However, the metal signal from the Guadalquivir river at the time of sampling extended farther into the Gulf of Cádiz than the Huelva river plume (Figure 3.10 and Figure 3.11). The more distinct Guadalquivir metal plume, compared with that from the Huelva, was related to the higher discharge volume of the Guadalquivir (annual mean: Guadalquivir 164 m^3 s^{-1}, Huelva 18 m^3 s^{-1}, Palanques *et al.* 1995; Borrego-Flores, 1992). Moreover, the state of the tide at the time of the ship's passage can have an important influence on the trace metal concentrations encountered, as will be discussed in Section 3.5.2.4. The distribution of dissolved metals and salinity in the Gulf of Cádiz this will be discussed in detail in Chapter 5.

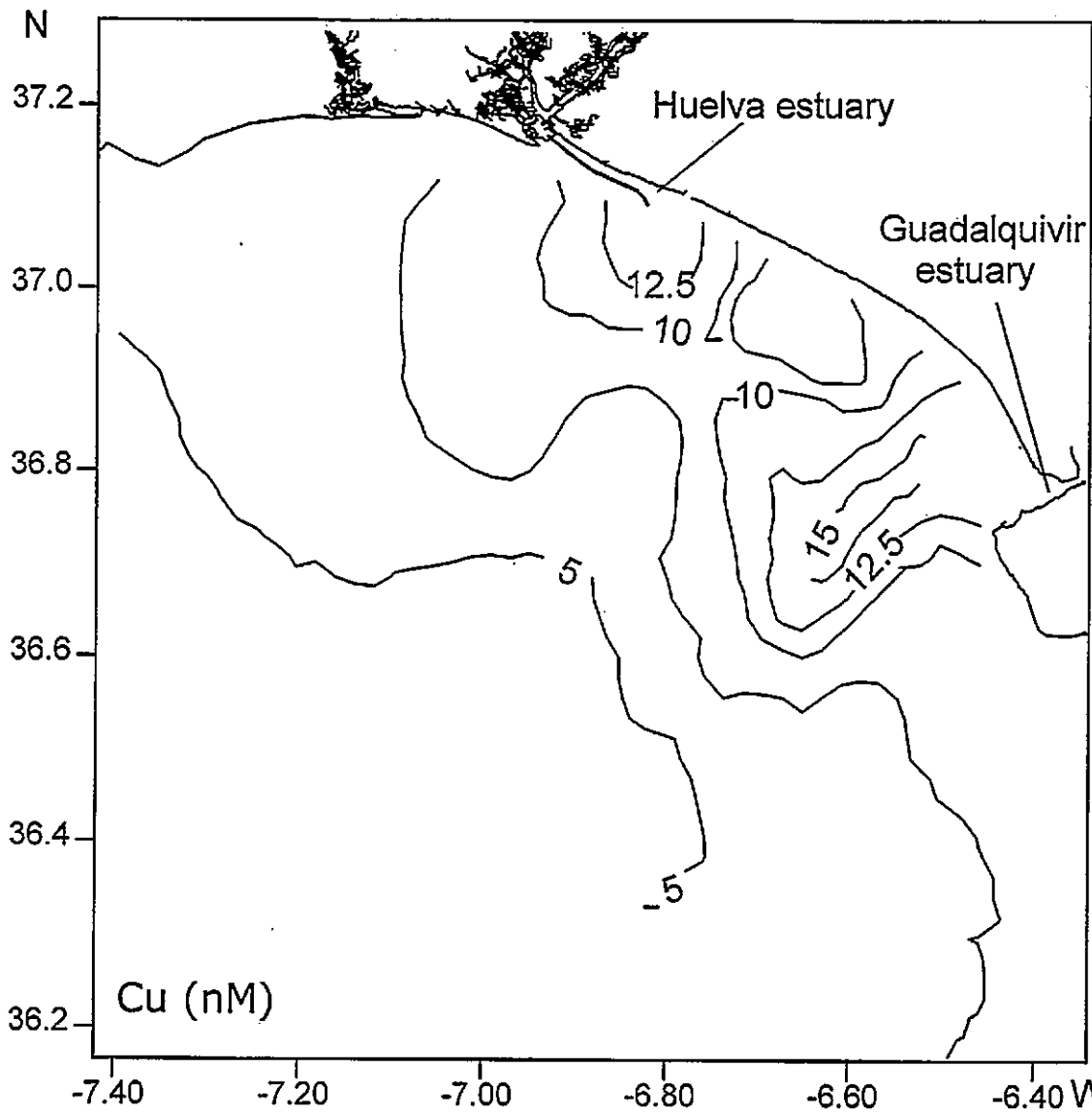

Figure 3.10 - Total dissolved Cu (nM) distribution in the Gulf of Cádiz, June, 1997. The contour plots were created from ca. 250 on-line measurements, performed on-line during four days of steaming onboard *B/O Garcia del Cid*.

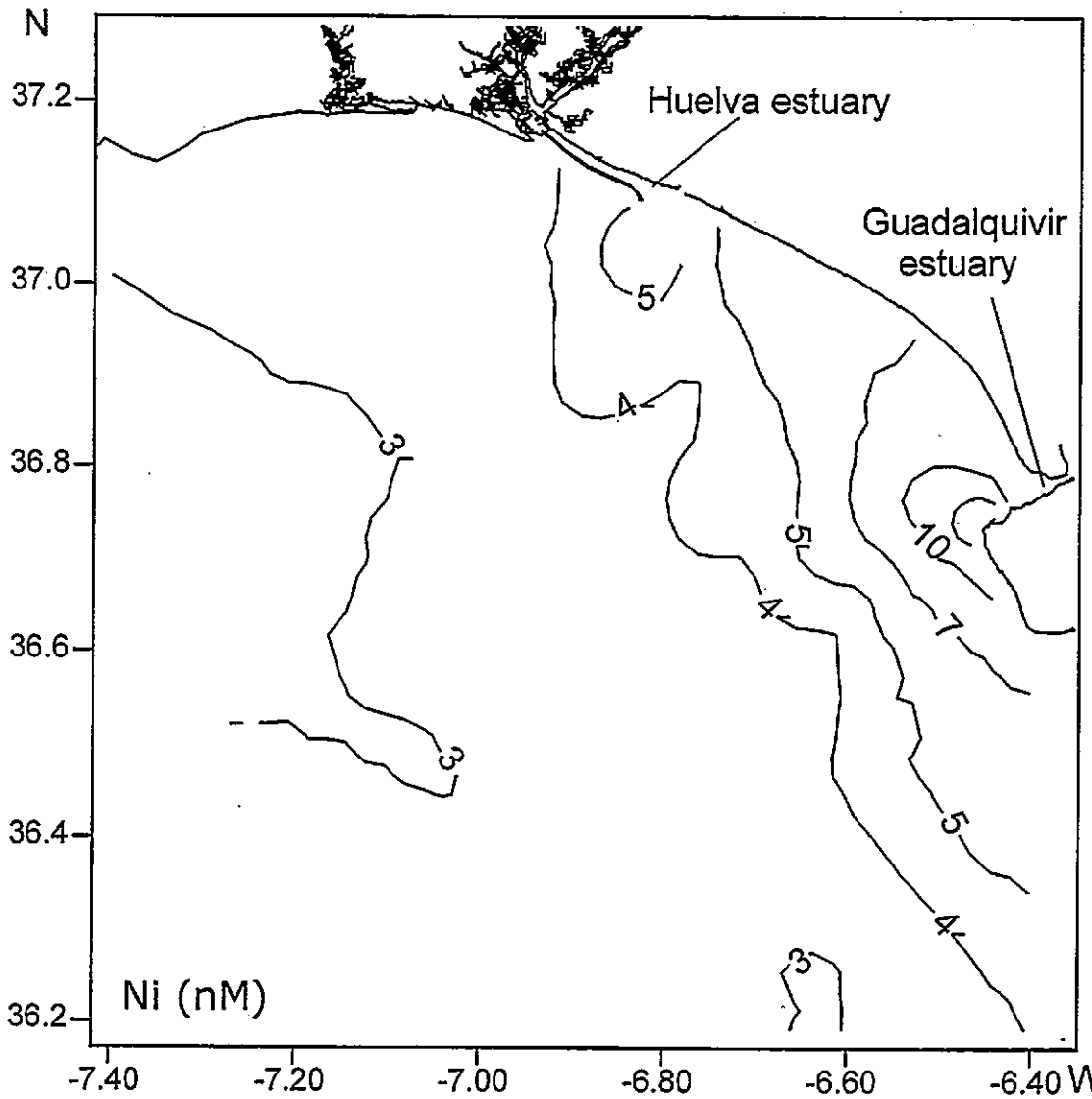

Figure 3.11 - Total dissolved Ni (nM) distribution in the Gulf of Cádiz, June, 1997. The contour plots were created from ca. 250 on-line measurements, performed on-line during four days of steaming onboard *B/O Garcia del Cid*.

3.5.2.4 Tidal Variability of the Huelva Estuary Plume

The second part of the coastal survey in June was dedicated to the investigation of development and the tidal variability of the Huelva estuary metal plume. During this part of the survey, a spatial resolution of 1.5 - 2 km for the on-line metal measurements was achieved by reducing the cruise speed from eight to four knots, and the ship steamed continuously without stopping for discrete sampling. Figure 3.12 shows dissolved Cu concentrations along a cruise track, which was followed twice. On day 15, 2.5 hours after low water (LW), concentrations of 60 - 80 nM Cu were measured to the southeast of the Huelva estuary. One day later, concentrations were considerably lower (13 - 14 nM Cu) when the same area was sampled around the time of high water (HW). On both days, Cu concentrations increased steeply upon returning to the estuary, whereby Cu levels were higher on day 15 at LW (> 500 nM), than on day 16, when the vessel returned two hours ahead of LW (> 200 nM).

The observed variations in metal concentrations illustrate the importance of tidal movement for the timing of nearshore coastal surveys, and the value of a sampling regime with high spatial resolution. Observed metal concentrations off the Huelva Ría during the first part of the survey (Figure 3.10 and Figure 3.11) and on day 16 suggested this estuary to be a minor contributor of Cu and Ni to the Gulf of Cádiz. However, the analysis during day 15 showed that highly contaminated water is discharged from Huelva Ría with the ebb tide. The combination of the low fresh water volume with high metal concentrations caused small salinity changes in the vicinity of the Huelva Ría to be accompanied by marked tidal gradients in dissolved metal concentrations. Monitoring exercises performed during different states of the tide are therefore required for the investigation of estuarine plumes, especially where low water discharges are combined with high contaminant concentrations.

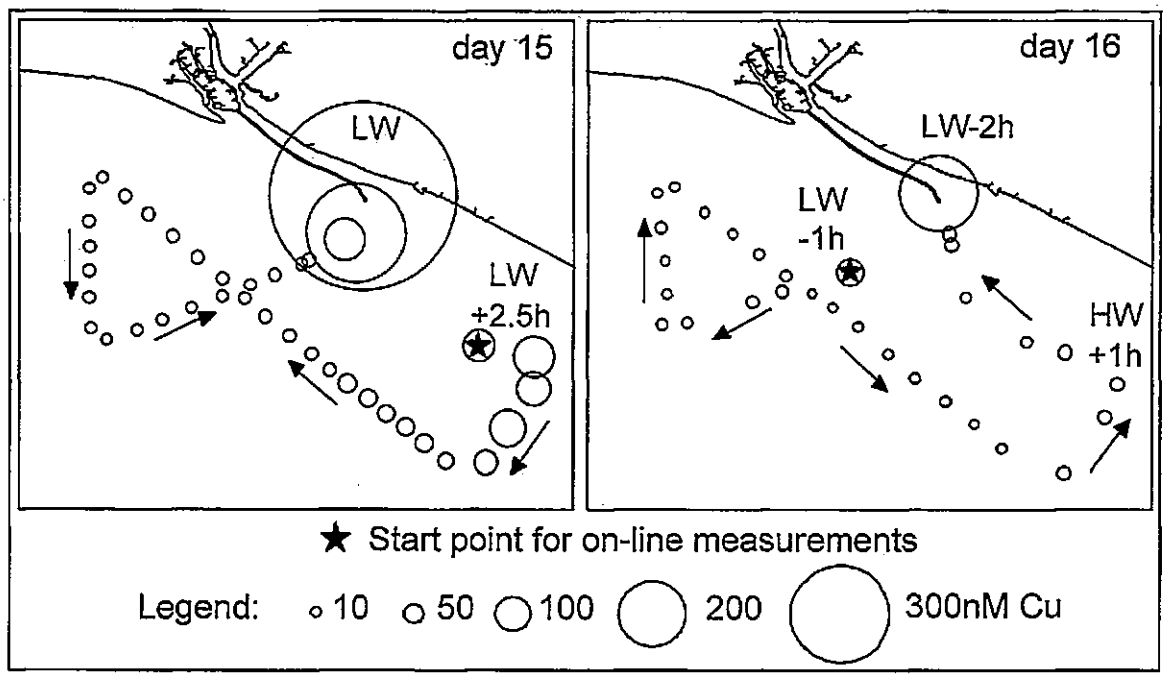

Figure 3.12 - On-line ship-board measurements of total dissolved Cu in the plume of the Huelva estuary during two consecutive days. The size of circles relates to the concentration; the cruise direction is indicated by arrows. The star denotes the first measurement of each day. On day 15 (16) the survey began 2.5 hours after LW (1 hour before LW) and took 10 hours (12.5 hours). LW, HW - low and high water at Mazagón harbour.

3.6 CONCLUSIONS

On-line analysis of total dissolved Zn, Cu, Ni and Co was carried out with two fully automated voltammetric metal monitors in the Huelva estuary and Gulf of Cádiz. The *in-situ* application of automated AdCSV methods in waters with a wide range of salinities (S = 9 - 36.7) and metal concentrations (nM - μM) was possible because analytical parameters were adapted to the sample matrix and the metal level encountered, and each measurement was calibrated by standard additions.

Comparisons between on-line and discrete samples confirmed the high quality of the acquired data, during laboratory experiments and during tidal cycle studies in the field. Careful planning of the sampling succession and intermediate acid-cleaning of the under-way sampling system was important in order to reduce the risk of cross-contamination and enable to move from areas of high to those of low dissolved metal concentrations.

On-line data was acquired at a rate of four to five measurements an hour, providing information about the timing and magnitude of dissolved metal maxima during tidal cycle studies. By comparison, the full resolution of small-scale features was left to chance by discrete sampling at hourly intervals from the shore. Therefore, high-resolution monitoring exercises in estuaries are a valuable tool for geochemical studies, as the resulting data can be used with a higher level of confidence, than data gathered at lower resolution.

In the Gulf of Cádiz, the on-line analysis revealed clearly defined areas of elevated dissolved metal concentrations associated with discharges from the Huelva and Guadalquivir estuaries. Near real time metal analysis enabled the close investigation of tidal variations in the Huelva estuary plume and facilitated an interactive sampling campaign, which was of particular value in this system, which is characterised by small salinity changes and strong metal concentration gradients. The data collected during on-

line analysis highlighted the importance of a high-resolution approach to contaminant monitoring at different states of the tide. Especially in highly dynamic coastal systems, the undertaking of a single survey would only provide a snap-shot of the state of the coastal environment and may therefore result in erroneous conclusions to be drawn.

3.7 REFERENCES

Achterberg, E.P. (1993) Trace metal speciation in natural waters. University of Liverpool, PhD Thesis, p. 13.

Achterberg, E.P., Colombo, C. and van den Berg, C.M.G. (1999) The distribution of dissolved Cu, Zn, Ni, Co and Cr in English coastal surface waters. *Continental Shelf.Research* **19**, 537-558.

Achterberg, E.P. and van den Berg, C.M.G. (1994a) Automated Voltammetric System for Shipboard Determination of Metal Speciation in Sea Water. *Analytica et Chimica Acta* **284**, 463-471.

Achterberg, E.P. and van den Berg, C.M.G. (1994b) In-line ultraviolet-digestion of natural water samples for trace metal determination using an automated voltammetric system. *Analytica et Chimica Acta* **291**, 213-232.

Achterberg, E.P. and van den Berg, C.M.G. (1996) Automated monitoring of Ni, Cu and Zn in the Irish Sea. *Marine Pollution Bulletin.* **32**, 471-479.

Andrew, K.N., Blundell, N.J., Price, D. and Worsfold, P.J. (1994) Flow injection techniques for water monitoring. *Analytical Chemistry* **66**, 916A-922A.

Bearman, G. (1995) In: Bearman, G., (Ed.). *Seawater, its Composition, properties and Behaviour.* Milton Keynes: Pergamon in association with Open University

Borrego-Flores, J. (1992) *Sedimentologia del estuario del Rio Odiel* (Huelva, S.O. Espana). University of Sevilla, PhD Thesis.

Bowie, A.R., Achterberg, E.P., Mantoura, R.F.C. and Worsfold, P.J. (1998) Determination of sub-nanamolar levels of iron in seawater using flow injection with chemiluminescence detection. *Analytica et Chimica Acta* **361**, 189-200.

Bowie, A.R., Fielden, P.R., Lowe, R.D. and Snook, R.D. (1995) Sensitive determination of manganese using flow injection and chemiluminescence detection. *Analyst* **20**, 2119-2127.

Braungardt, C., Achterberg, E.P. and Nimmo, M. (1998) On-line voltammetric monitoring of dissolved Cu and Ni in the Gulf of Cádiz, southwest Spain. *Analytica et Chimica Acta* **377**, 205-215.

Coale, K.H., Johnson, K.S., Stout, P.M. and Sakamoto, C.M. (1992) Determination of copper in sea water using a flow-injection method with chemiluminescence detection. *Analytica et Chimica Acta* **266**, 345-351.

Elrod, V.A., Johnson, K.S. and Coale, K.H. (1991) Determination of subnanomolar levels of iron(II) and total dissolved iron in sea water by flow injection analysis with chemiluminescence detection. *Analytical Chemistry* **63**, 893-898.

Förstner, U. (1983) Metal pollution in rivers and estuaries. In: Thornton, I., (Ed.) *Applied Environmental Geochemistry*, pp. 408-411. London: Academic Press

Johnson, K.S., Petty, R.L. and Thomsen, J. (1985) Flow-injection analysis for seawater micronutrients. In: Zirino, A., (Ed.) *Mapping strategies in chemical oceanography*, pp. 7-30. Washington, D.C.: American Chemistry Society

Klinkhammer, G.P., Chin, C.S., Wilson, C., Rudnicki, M.D. and German, C.R. (1997) Distributions of dissolved manganese and flourescent dissolved organic matter in the Columbia River estuary and plume as determined by in situ measurement. *Marine Chemistry* **56**, 1-14.

Leblanc, M., Benothman, D., Elbaz-Poulichet, F., Luck, J.M., Carvajal, D., Gonzalez-Martinez, A.J., Grande-Gil, J.A., Ruiz de Almodovar, G. and Saez-Ramos, R. (1995) Rio Tinto (Spain), an acidic river from the oldest and most important mining areas of Western Europe: Preliminary data on metal fluxes. In: Pasava, Kribek and Zak, (Eds.) *Mineral Deposits*, pp. 669-670. Rotterdam: Balkema.

Morley, N.H., Statham, P.J. and Burton, J.D. (1993) Dissolved trace metals in the southwestern Indian Ocean. *Deep-Sea Research I* **40**, 1043-1062.

Morris, A.W., Bale, A.J., Howland, R.J.M., Millward, G.E., Ackroyd, D.R., Loring, D.H. and Rantala, R.T.T. (1986) Sediment mobility and its contribution to trace metal cycling and retention in a macrotidal estuary. *Water Science and Technology* **18**, 111-119.

Muller, F.L.L. (1996) Interactions of copper, lead and cadmium with the dissolved, colloidal and particulate components of estuarine and coastal waters. *Marine Chemistry* **52**, 245-268.

Nelson, C.H. and Lamothe, P.J. (1993) Heavy metal anomalies in the Tinto and Odiel river and estuary system, Spain. *Estuaries* **16**, 496-511.

Nordstrom, D.K. (1977) Thermochemical redox equilibria of ZoBell's solution. *Geochimica et Cosmochimica Acta* **41**, 1835-1841.

Ochoa, J. and Bray, N.A. (1991) Water mass exchange in the Gulf of Cadiz. *Deep-Sea Research* **38**, S465-S503

Palanques, A., Diaz, J.I. and Farran, M. (1995) Contamination of heavy metals in the suspended and surface sediment of the Gulf of Cadiz (Spain): the role of sources, currents, pathways and sinks. *Oceanologica Acta* **18**, 469-477.

Riley, J.P., Skirrow, G. and *et al.* (1975) Chemical oceanography, 2 edn. New York: Academic Press.

Stumm, W. and Morgan, J.J. (1996) Aquatic chemistry - chemical equilibria and rates in natural waters, 3 edn. New York: John Wiley & Sons.

Tercier, M.-L. and Buffle, J. (1993) In situ voltammetric measurements in natural waters: Future prospects and challenges. *Electroanalysis* **5**, 187-200.

Thornburn, J.A. (1990) The industrial archaeology of Rio Tinto and the Iberian Pyrite Belt. Bulletin of the Peak District Mines Historical Society **11**, 97-108.

van den Berg, C.M.G. and Achterberg, E.P. (1994) Automated in-line sampling and analysis of trace elements in surface waters with voltammetric detection. *Trends in Analytical Chemistry* **13**, 348-353.

Van Geen, A., Adkins, J.F., Boyle, E.A., Nelson, C.H. and Palanques, A. (1997) A 120 yr record of widespread contamination from mining of the Iberian pyrite belt. *Geology* **25**, 291-294.

Van Geen, A., Boyle, E.A. and Moore, W.S. (1991) Trace metal enrichments in waters of the Gulf of Cadiz, Spain. *Geochimica et Cosmochimica Acta* **55**, 2173-2191.

Van Geen, A., Rosener, P. and Boyle, E.A. (1988) Entrainment of trace metal-enriched Atlantic shelf-water in the inflow to the Mediterranean Sea. *Nature* **331**, 423-426.

Whitworth, D.J., Achterberg, E.P., Nimmo, M. and Worsfold, P.J. (1998) Validation and in situ application of an automated dissolved nickel monitor for estuarine studies. *Analytica et Chimica Acta* **371**, 235-246.

Chapter 4

Dissolved Trace Metals in Rio Tinto, Rio Odiel and their Common Estuary

4.1 Abstract

This chapter introduces the geographic and geologic setting of the Rio Tinto and Rio Odiel and outlines the natural and industrial processes that lead to the high level of contamination found in the rivers and their common estuary.

Observed dissolved metal concentrations in the lower reaches of the rivers were extremely high, resulting in a combined mean daily flux of ca. 27 t Zn, 13 t Mn, 9.3 t Cu, 210 kg Ni, 480 kg Co, 93 kg Cd, 180 kg Pb and 5.2 kg U into the estuary. The main source of this metal contamination was the discharge of acid mine drainage generated in the metalliferous mining area of the Iberian Pyrite Belt. Variability in riverine metal load is discussed, and it is postulated that a seasonal cycle dependent on rainfall may have been an important factor in influencing this variability. The observed removal of metals from solution at low pH values (< 2.5) may be explained by redox-cycling induced by micro-organisms.

The estuarine behaviour of dissolved Fe, Mn, Zn, Cu, Ni, Co and Cd was congruent in the upper reaches of both estuarine branches. In the Ría del Tinto an initial increase in dissolved metal concentrations was attributed to remobilisation from the sediment, whereby reductive dissolution, acid-leaching and injection of metal-rich interstitial waters may have been important processes. Downstream of this dissolved metal maximum, the behaviour of Fe, Mn, Zn, Cu, Ni, Co and Cd was broadly conservative during all surveys.

A similar behaviour was observed in the Ría del Odiel. In the upper estuarine regions, the low pH value was the controlling factor for the metal behaviour. Removal of Zn, Cu, Ni and Co from solution was observed at near-sea water salinities ($S \geq 30$) and pH values above five, and this process was largely complete for Zn, Cu, Ni and Co at $pH \approx 7.0$. Cadmium remained conservative throughout the estuary. Lead exhibited strong removal in the low salinity region because of its high particle affinity. The distribution of U was dominated by strong industrial sources within the estuary.

Estuarine metal fluxes to the Gulf of Cádiz were estimated using a simple extrapolation method. Results showed that the annual dissolved export of Zn (3700 t), Cu (850 t), Ni (68 t) and Co (86 t) from Huelva Ría is several times higher than that reported in literature for some of the most polluted European rivers, including the Humber and Rhone.

4.2 Introduction

The utilisation of metals has a long history. Records of mining-related dispersion of metals in the environment during Phoenician and Roman periods have been found in fluvial sediment cores (Morales, 1999a) and in ice cores (Rosman *et al.* 1997). The intensification of metal extraction from the 18th century on has left a legacy of dereliction and contamination in mining areas. Soil, air and water pollution are ubiquitous around active mines, and in many cases metal contamination has entered ground water resources or the food chain (Featherstone and O'Grady, 1997; Van Geen *et al.* 1997; Miller *et al.* 1996; Jordao *et al.* 1996; Gao and Bradshaw, 1995; Bowell and Bruce, 1995). Abandoned mines and tailings are potentially long-term sources of contamination, and the remediation

of water and soil quality is often expensive (Thornton, 1996). A thorough understanding of the (bio)geochemistry of metal pollution in each particular case is needed in order to be able to assess the impact on the environment and biota and develop an effective remediation strategy.

The biogeochemistry of metals released by mining activity is complex, and the impact of the pollution created depends largely on the geochemical character and neutralisation capacity of the receiving environment. In areas of sulphide mineralisation the production of acid mine drainage (AMD) is a central process. Natural weathering, microbial activity and mining-related processes lead to the oxidation of sulphides, releasing metal-rich acid drainage (Bonnissel-Gissinger *et al.* 1998; Krauskopf and Bird, 1995). The presence of acidophilic bacteria and UV light enhances redox cycling of sulphur, iron and other metals in acidic waters (Kirby and Elder Brady, 1998; Ehrlich, 1996). Neutralisation of AMD upon mixing with alkaline river or sea water leads to the precipitation of iron and other metals and the formation of ochres and metal-rich coatings on particles in the sediment (McCarty *et al.* 1998). Although the solubility and biological availability of metals to aquatic life is thus reduced, environmental hazards can arise from the remobilisation of metal enriched sediments caused by changes in physical or chemical conditions, for example pH, redox potential and river flow.

Estuarine systems exhibit very different characteristics, depending on the chemistry and morphology of the river catchment, geographic location (climate), biological productivity and anthropogenic influences. As a result, the metal/salinity relationships in estuaries may be conservative or deviate from the theoretical dilution line. In any study of estuarine metal biogeochemistry, it is desirable to understand the solute/particle and colloidal interactions, sediment characteristics and transport, nutrient status, biological activity, metal speciation as well as chemical and physical master variables of the system.

Although many of these points were addressed within the TOROS programme, limitations in time and funding prohibited a comprehensive investigation of all aspects of the estuarine chemistry and biology.

Interactions between dissolved and particulate phases have been considered important control mechanisms for the behaviour of metals in estuarine systems for a number of decades (Stumm and Morgan, 1996; Sholkovitz, 1978; Turekian, 1977). Benoit *et al.* (1994) suggested that the dissolved concentration of metals in shallow estuaries is mainly controlled by re-suspension of colloidal and particulate matter from bottom sediments, and by the establishment of a steady-state kinetic or an equilibrium partitioning of metals between the dissolved and solid phases. Gibbs (1986) highlighted the importance of riverine particles as carriers of trace metals to estuaries. Experiments showed that differential coagulation (related to composition and size) of mineral particles upon the initial stages of estuarine mixing (salinity $S < 1$) resulted in a segregation of settling flocs containing different proportions of adsorbed trace metals. Moreover, the chemical behaviour of elements determine their dissolved speciation, which in turn influences their estuarine behaviour. For example, flocculation of humic acids during estuarine mixing generally has a more pronounced effect on the removal of Cu, than of Zn or Cd from solution, because the speciation of the former is dominated by organic and of the latter by inorganic complexation (Zwolsman *et al.* 1997 and references therein). However, Benoit *et al.*(1994) found in six Texan estuaries that the colloidal fraction of Cu, as determined by ultrafiltration in filtrate (0.4 μm) using a 10 k Dalton filter, is small compared to that in the truly dissolved phase.

The behaviour of each metal varies between estuaries and differences have been observed in some cases within estuaries. Hereby, seasonal differences in fluvial discharges and primary productivity, leading to changes in the redox conditions and the concen-

trations of metal complexing organic ligands can be of particular importance (Zwolsman *et al.* 1997). Conservative mixing with sea water has been observed for a variety of metals, including Cu (Elbaz-Poulichet *et al.* 1996; Shiller and Boyle, 1991), Ni (Paucot and Wollast, 1997; Shiller and Boyle, 1991; Windom *et al.* 1988) and Pb (Elbaz-Poulichet *et al.* 1996). At near-neutral pH the non-reactive dilution of river with sea water has been explained with the short residence time of water in estuaries of large rivers (e.g. Amazon, Mississippi), or with the complexation of dissolved metals (e.g. Cu) by organic ligands. The time necessary to reach equilibrium in adsorption/desorption processes may be in the order of days or weeks (Comber *et al.* 1996).

Conversely, the rapid formation of colloids (Fe, Mn, organic material), their flocculation and settling has been well documented for the initial stages of estuarine mixing. At near-neutral pH values the scavenging of trace metals by freshly formed solids and the adsorption onto particles resulted in a pronounced removal of trace metals from solution in many estuaries (Zwolsman and Van Eck, 1993; Johnson and Thornton, 1987; Ackroyd *et al.* 1986; Duinker, 1980).

The phenomenon of dissolved metal maxima at low or mid-salinities is well known for Cd (Zwolsman *et al.* 1997; Kraepiel *et al.* 1997; Shiller and Boyle, 1991; Elbaz-Poulichet *et al.* 1987). Experimental data suggests that desorption of Cd from particles in estuaries takes place as a result of increasing ionic strength and the formation of stable chloride complexes (Comans and van Dijk, 1988). The addition of Mn, Zn, Cu, Cd, Co and/or Ni to the dissolved phase during estuarine mixing has been observed, and in some estuaries this occurred after an initial decrease in dissolved concentrations in the low salinity zone (Simpson *et al.* 1998; Chiffoleau *et al.* 1994; Zwolsman *et al.* 1993; Zwolsman and Van Eck, 1993; Windom *et al.* 1988; Ackroyd *et al.* 1986; Morris *et al.* 1986; Morris *et al.* 1982 and references therein). Where anthropogenic inputs were

excluded, the mobilisation of metals from the solid phase was attributed to: (a) desorption from riverine or re-suspended particles in the high turbidity zone, (b) infusion of pore waters, (c) reductive dissolution from oxidised sediment layers in concurrence with the re-mineralisation of organic matter, (d) exposure of sediments and oxidative dissolution of sulphides from deeper sediment layers, (e) localised acidification due to the oxidation of iron sulphides and organic matter, and/or (f) cyclical shifts between oxidising and reducing conditions during inundation.

Hereby, metals exhibit differential behaviour. For example, the distribution of Ni and Co in salt-marsh sediments of the Scheldt estuary has been exclusively linked to the redox cycle of Mn, while Cd, Cu, Pb and Zn were associated with Fe and Mn oxyhydroxides and their cycling at the oxic/suboxic boundary (Zwolsman *et al.* 1993). The degree of net mobilisation from sediments depends not only on oxidation or reduction rates of the mineral phases involved, but also on the processes acting upon the metal once dissolved. Of particular importance are metal solubility, organic (e.g. Cu, Ni) or inorganic (e.g. Cd) complexation of the dissolved species, sorption, precipitation or co-precipitation with newly forming solid phases in the oxic water column (Simpson *et al.* 1998; Millward and Turner, 1995; Zwolsman *et al.* 1993; Yeats and Loring, 1991).

This chapter discusses the geochemical behaviour of dissolved trace metals in the Rio Tinto and Rio Odiel, which rise in one of the world's most important sulphide mineralisations, the Iberian Pyrite Belt. The Tinto/Odiel river-ocean system is unusual in its character. The rivers originate ca. 100 km from the sea in the arid southwest of Spain and carry low water volumes (combined mean $\approx$ 18 m s^{-1}), which are highly influenced by AMD. The observed low pH values are slowly neutralised in the estuarine mixing zone, where industrial discharges complicate the pollution chemistry. Elevated trace metal concentrations are carried into the coastal sea, where dispersal, complexation, biological

uptake, as well as colloid and particle interactions may act upon the distribution of metals and their partitioning.

The socio-economic and ecological interest of the Tinto/Odiel system is apparent from its location. The city of Huelva is an important port, industrial base and population centre, where 250,000 inhabitants are exposed to air, water and soil pollution and the consumption of local sea food is traditional. The tourism resort of Punta Umbria is located to the west of the Huelva estuary. An important ecosystem, the Marismas del Odiel, a Nature Park with European Union status as a Special Area for the Protection of Birds and a UNESCO Biosphere Reserve is formed by salt marshes and barrier islands on the western boundary of the estuary. In the east, a string of beaches, camping grounds and hotels separate the Huelva estuary from the Doñana National Park, a wetland located in the delta of the Guadalquivir and Guadiamar estuaries.

The aims of the research presented in this chapter were:

- to establish the sources and quantitative variation of metal contamination in the Tinto/Odiel system,
- to define and understand the geochemical behaviour of dissolved trace metals in the estuary, and
- to evaluate the contribution of the Tinto/Odiel system to the metal load in the Gulf of Cádiz.

The objectives in the pursuit of these aims were:

- to carry out surveys of the rivers, estuary and coastal sea during different seasons,
- to measure master variables during the surveys, e.g. pH, conductivity, temperature, dissolved oxygen concentration and redox potential,

- to take samples for laboratory analysis of total dissolved trace metal and dissolved organic carbon concentrations, and
- to estimate trace metal fluxes from the estuary into the coastal zone.

In order to gain a broad understanding of the riverine water composition a range of trace metals were investigated. Iron, Mn and Al were chosen because of their geochemical importance and redox sensitivity (Fe and Mn), and Zn, Cu, Pb and Cd as indicators specific to the mineralisation in the mining area. Cobalt, Ni and U were studied because these metals are not strongly enriched in the Iberian Pyrite Belt, and U was interesting because of its additional anthropogenic sources in the estuary. The investigations focussed on Zn, Cu, Ni and Co for estuarine and sea water studies, because of their biogeochemical importance and toxicity (Förstner, 1980) and the different concentration factors in the local geology.

4.3 Environmental Setting

The study area is situated in Huelva Province, southwest Spain. The area is hot and arid, with a high solar irradiation (1800 kWh m^2 a^{-1}) and low annual precipitation (390 mm a^{-1}) (Izquierdo *et al.* 1997). The studied water courses drain parts of the Sierra de Aracena, on the western foothills of the Sierra de Moreno, and flow to the Spanish southern Atlantic coast, the Gulf of Cádiz.

4.3.1 METAL MINING IN THE IBERIAN PYRITE BELT

The Iberian Pyrite Belt covers an area of about 250 km × 40 km, reaching from near the Portuguese Atlantic coast to the Guadalquivir river valley in the east (Figure 4.1). More than 80 known deposits contained ca. 1700 Mt of sulphide ore (mined and reserves), and therefore, the Iberian Pyrite Belt is considered one of the most important sulphide mineralisations in the world (Leistel *et al.* 1998b).

It is postulated that the ore deposits in the Iberian Pyrite Belt were formed during the Devonian period, by precipitation from hydrothermal fluids during a time of intense submarine volcanism. At their base associated stockwork formed, which is rich in pyrite (FeS_2), chalcopyrite ($CuFeS_2$) and other Cu ores. The outer and upper parts of the ore bodies contain typically 50% S, 42% Fe, 2 - 8% Cu and 1 - 5 g t^{-1} Au, and Pb-Zn-Ag enrichment is commonly found (Pons and Morales, 1998; Leistel *et al.* 1998a). The sulphide deposits formed were buried by marine sediments, generating a volcano-sedimentary series, which was folded into steeply dipping ore bodies in the late Carboniferous period (Thornburn, 1990). Exposure and intense weathering of exposed sulphide ores resulted in the formation of metal enriched gossans with jarosite ores ((H, Na, K, NH_4)$Fe_3(SO_4)_2(OH)_6$) at their base (Leistel *et al.* 1998b).

The gossans and surrounding mineralisations of the Iberian Pyrite Belt usually contain high concentrations in Fe, Zn, Cu, Pb, Ag, As, Sb, Bi, Au and Sn, and low values in Mn and Ni, while Co was found to be variable (Leistel *et al.* 1998b; Strauss *et al.* 1977). Calculations carried out by Van Geen *et al.* (1997) illustrated the extreme enrichment of the ores in the mining area with S (Enrichment Factor, EF = 1900), Pb, Zn and Cu (EF = 630, 190 and 120, respectively) and moderate enrichment with Fe and Co (EF < 10) with respect to average crustal element concentrations after Taylor (1964). The enrichment factors of Al, Mn and Ni (EF < 0.5) showed a slight depletion of these metals in the area.

Secondary minerals (especially gossans) were worked for Cu, Ag and Au by Phoenicians and Romans and possibly even earlier cultures (Leblanc *et al.* 1995; Thornburn, 1990). More recently, mining activities in the Iberian Pyrite Belt intensified in the 16th century and again in the 19th century, when the Cu mines of the Rio Tinto were developed (Thornburn, 1990). The location of important mines, mostly abandoned now, in the central mining area of the Iberian Pyrite Belt are presented in Figure 4.2.

Underground mining, practised since Roman times, was relatively inefficient, leaving ca 85% of the ore *in-situ*. It was not until the introduction of open cast mining and new methods of underground mining in the late 19th century that efficiency increased, but so did the volume of overburden. At the same time, metallurgical processes were improved, enabling the treatment of low-grade ores and old mine tailings.

In addition to smelting, hydro-metallurgical processing became important, a system that produced a copper-rich liquor, which was subsequently precipitated onto iron surfaces, for example rail tracks, was developed (Thornburn, 1990). The processing of ore accelerated the natural enrichment of water courses with metals and created air pollution, causing health problems and impoverished the vegetation in the mining district (Pons and Morales, 1998). In recent decades, ore was extracted predominantly for the production of sulphuric acid with sidelines in the production of Cu concentrate (20%) from low grade ore and overburden, and the processing of gossans (cyanidation) to manufacture bullions containing 80% Ag and 10% Au (Morales, 1998a). Today, the industrial landscape of the mining district is shaped by processing facilities, opencast pits, overburden material, slag, processed ore and dams, which collect leachate before it is discharged into local water courses.

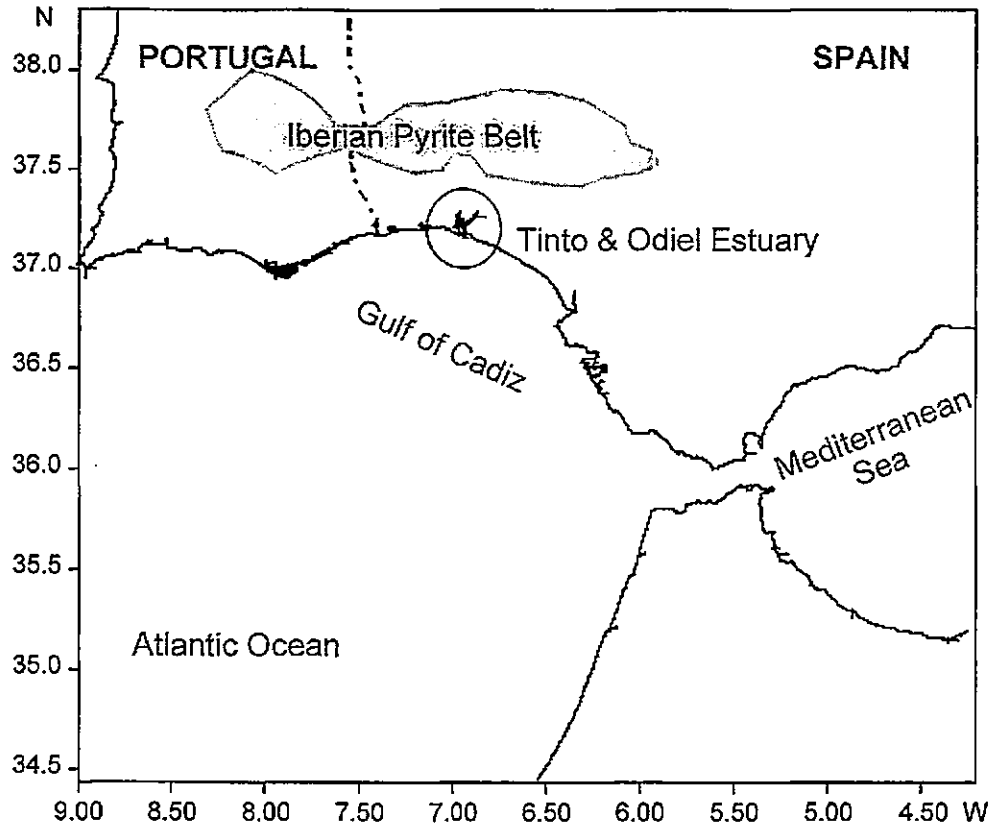

Figure 4.1 - The location of the Iberian Pyrite Belt and Gulf of Cádiz on the southern Iberian Peninsular.

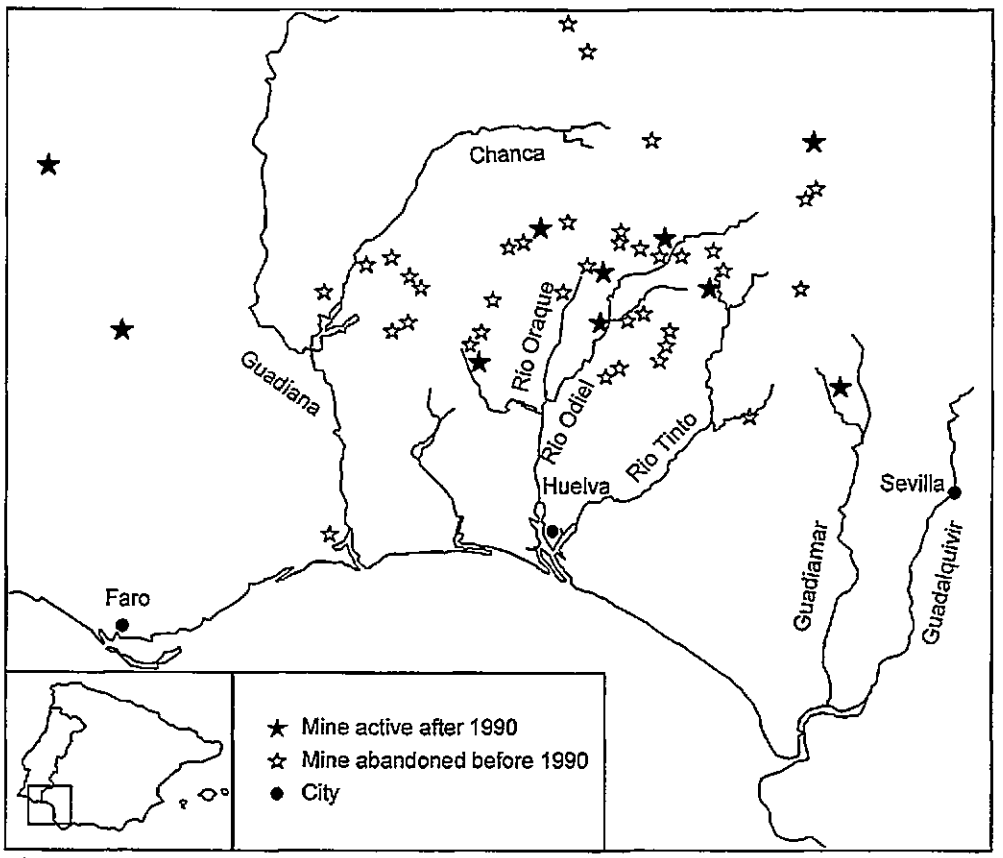

Figure 4.2 - Locations of important mines and affected river systems in the main mining area of the Iberian Pyrite Belt. Adapted from Achterberg *et al.* (1999) and Bowler (1995).

4.3.2 Rio Tinto and Rio Odiel

The area around the Minas de Rio Tinto forms the centre of sulphide mining in the Iberian Pyrite Belt. It is located within a drainage basin covering 3352 km^2, which is shared almost equally between the Rio Tinto and the Rio Odiel. Several small tributaries to the Guadiana and Guadalquivir (Figure 4.2) arise at the fringes of this mining area (Palanques *et al.* 1995).

The Rio Tinto and Rio Odiel are 83 and 126 km in length, respectively and have an annual mean water discharge of approximately 3 $m^3 s^{-1}$ and 15 $m^3 s^{-1}$, respectively. Located in the arid southwest of Spain, river flow is directly related to rainfall (Borrego *et al.* 1997), which is highly variable. During the summer the Rio Tinto may dry completely, while a high proportion (typically > 90 %) of the annual discharge occurs during a few days of winter floods between October and March (Borrego-Flores, 1992). Long-term records from a gauging station in the Rio Tinto at Niebla (Morales, 1998b) show a cyclical pattern in the mean annual water discharge (Figure 4.3), which appears to be related to the North Atlantic Oscillation (Rodwell and Folland, 1999). Monthly long-term averages in water discharge indicate a distinct division into a wet autumn/winter and a dry spring/summer season.

The Rio Tinto and Rio Odiel have the potential for considerable environmental impact, because of the high proportion of AMD in their upper reaches and their proximity to the sea. Central in the production of AMD is the oxidation of sulphides of the form MeS_2 (e.g. pyrite), which releases metals, sulphate and protons into aquatic systems:

$$FeS_{2\,(s)} + H_2O + {}^7/_2O_2 \leftrightarrows Fe^{2+} + 2SO_4^{2-} + 2H^+ \qquad (4.1),$$

$$Fe^{2+} + {}^1/_4O_2 + H^+ \leftrightarrows Fe^{3+} + {}^1/_2H_2O \qquad (4.2),$$

$$Fe^{3+} + 3H_2O \leftrightarrows Fe(OH)_{3\,(s)} + 3H^+ \qquad (4.3),$$

$$Fe^{3+} + 2½\ H_2O + ¼O_2 \leftrightarrows Fe(OH)_{3\,(s)} + 2H^+ \quad (4.4),$$

and, at low pH values (pH < 3.5):

$$FeS_{2\,(s)} + 8H_2O + 14Fe^{3+} \leftrightarrows 15Fe^{2+} + 2SO_4^{2-} + 16H^+ \quad (4.5).$$

The oxidation of pyrite (Reaction 4.1) occurs abiotically or by direct bacterial oxidation. Reaction (4.4) is predominantly abiotic at pH > 4.5 and slows down as the pH decreases. Below pH 4.5 the rate of this process is determined by bacterial activity. At lower pH values, reaction (4.2) is solely dependent on bacterial oxidation, and its rate determines the rate of the chemical reaction (4.5). The processes described in equations (4.1) and (4.3) - (4.5) contribute to the progressive lowering of pH (Krauskopf and Bird, 1995; Salomons, 1995; Banks *et al.* 1997).

In the Rio Tinto and the upper Rio Odiel, ochre deposits can be found in the river beds, on boulders and along the banks. Hudson-Edwards *et al.*(1999) identified purple-red alluvium derived from the mine tailings, pyrite-rich and orange-laminated alluvium, Fe-rich cement, as well as sands and silts in the bed and overbank sediments of the Rio Tinto.

Both rivers rise near each other and are similar in appearance in their upper reaches. The strong AMD character of the rivers is maintained with low pH and high metal concentrations to the fresh water limit at Niebla and Gibraleón, respectively (Figure 4.4). Copper and iron sulphates crystallise naturally in the hot climate along the bank of the Rio Tinto and historically these were collected as raw materials for medicines and dye-stuffs (Thornburn, 1990). The precipitation of ochre is regarded as a major removal mechanism of iron from solution in AMD affected streams (McCarty *et al.* 1998; Webster *et al.* 1998; Boult *et al.* 1994). At low pH ochre formation may be accelerated by bacterial activity (Kirby and Elder Brady, 1998 and references therein; Ehrlich, 1996; Miller *et al.* 1996).

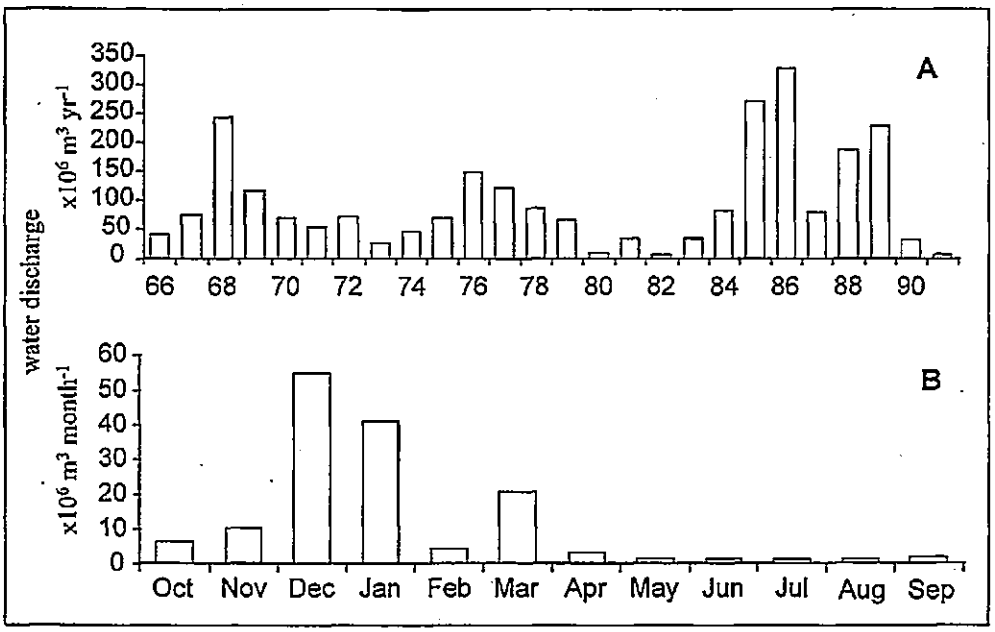

Figure 4.3 - Mean annual (A) and mean monthly (B) water discharges at a gauging station in the Rio Tinto at Niebla, from observations during the hydrological years of 1966/67 to 1991/92. The station has been out of service since 1996. Prepared from Morales (1998).

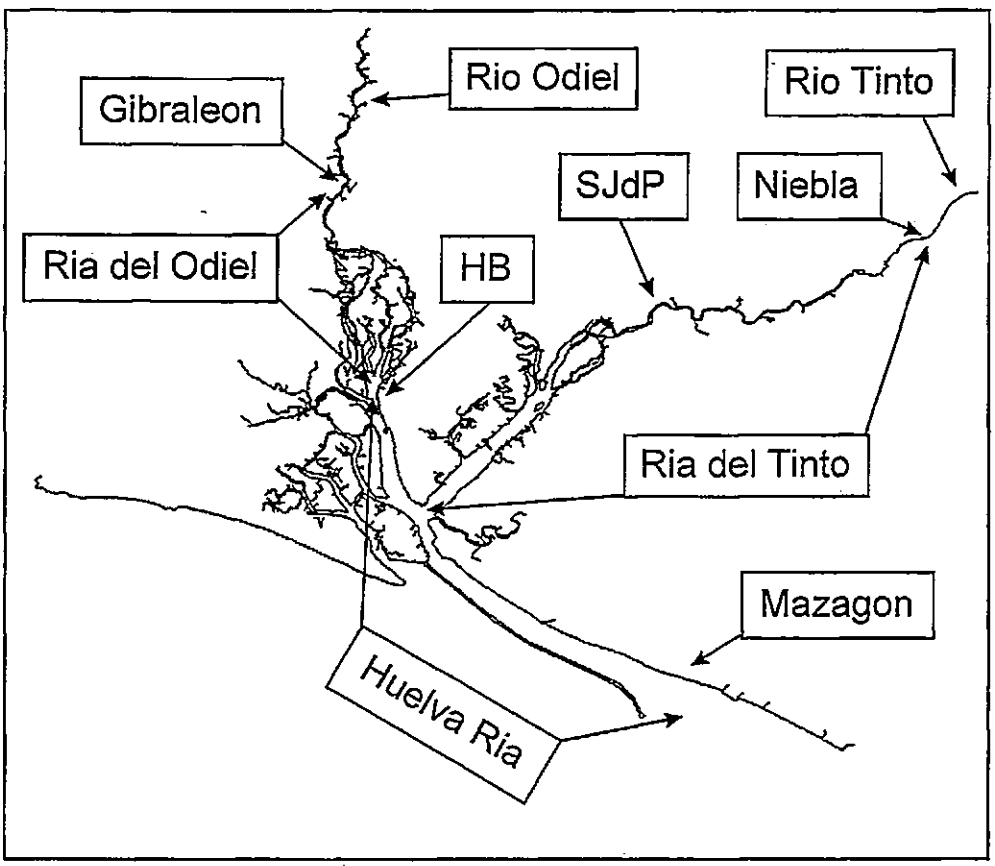

Figure 4.4 - The Tinto/Odiel estuarine system. SJdP - San Juan del Puerto, HB - Huelva Bridge.

Solids formed from AMD may be well defined crystalline minerals or amorphous metal hydroxides and poorly crystallised oxyhydroxides. It has been shown that sulphate is an important constituent in some AMD-derived solids (Kirby and Elder Brady, 1998; Ehrlich, 1996; Winland *et al.* 1991; Bigham *et al.* 1990).

Mining activity in the catchment of the Rio Odiel is less intense compared to that in the Rio Tinto, and a dam in the upper reaches of the Rio Odiel retains some of the metal-rich suspended load (Nelson and Lamothe, 1993). As a result, the conditions in the lower Rio Odiel are less extreme with respect to dissolved concentrations of AMD-typical constituent (SO_4^{2-}, Fe, Zn, Cu, Co, Cd, Al and pH), compared to those in the Rio Tinto. At the fresh water limit of the Rio Odiel at Gibraleón, the river bed is formed by coarse sand, pebbles and boulders. The appearance of the river varies. Filamentous green algae growing on boulders have been observed in clear water, and on other occasions, the river bed was smothered with ochre deposits.

Amils *et al.* (1998) found that algae and bacterial slimes in the Rio Tinto were associated with ochre layers and iron oxide concretions in the river bed, an occurrence also observed in other mine adits and AMD affected rivers (Chapman *et al.* 1996). A complex microbial community has been reported to thrive in the Rio Tinto, and its biodiversity has been compared to that in rivers of 'normal' pH (Amils *et al.* 1998). Amils *et al.* observed a micro organism population that consisted of 95% bacteria, 4% algae and 1% fungi (averaged over the seasons and length of river). Identified primary producers were mainly photosynthetic algae (65% of biomass) and prokaryotic chemolithotrophs (10^7 cells ml^{-1}), which derive their energy from sulphides. Diatoms appeared in dense blooms at several points in the river. Heterotrophic bacteria, filamentous fungi and yeasts were also identified in biofilms on boulders, and in the river bed some predatory species were found.

Amils *et al.* suggested that this community of acidophiles takes part in the creation and maintenance of the unique conditions found in the Rio Tinto.

4.3.3 Ría del Tinto, Ría del Odiel and Huelva Ría

The Tinto/Odiel estuarine system can be divided into two shallow upper estuarine sections (Ría del Tinto and Ría del Odiel) and the navigable lower section (Huelva Ría) (Figure 4.4). It is located along a tide-dominated mixed-energy mesotidal coast with a mean tidal amplitude of 2.5 m (1.15 m and 2.8 m, at neap and spring tides, respectively). More extreme values may occur at equinox neaps and springs, with tidal ranges between 0.5 and 4 m, respectively. Huelva Ría is a well mixed estuary with a tendency to become partially mixed during spring tides.

The upper tidal limit of the Ría del Tinto is located at a low weir, ca. 50 metres upstream from a Roman bridge at Niebla. Between Niebla and San Juan del Puerto (SJdP, Figure 4.4), the upper estuary remains a narrow (10 - 30 m) and shallow (up to a few metres) channel. This fluvial part of the Ría del Tinto is similar to the Rio Tinto in appearance, and probably rarely experiences saline intrusion. Approximately one kilometre upstream of the road bridge at San Juan del Puerto, the estuary opens into a wide (several hundred meters) and shallow mudflat and salt marsh, which extends some distance downstream of the bridge. The abundance of fine sediment and mineral phases (jarosite and other hydrated sulphates, Borrego-Flores, 1992) identifies this area as the upper mixing zone. Downstream of the bridge, the Ría del Tinto is navigable with a rigid inflatable boat (RIB) at high water. The main channel meanders through vegetated marsh and mudflats and deepens and widens after two to three kilometres into the lower Ría del Tinto. In this section, discharges from a cellulose factory and sewage works enter the estuary (Figure 4.5). The salt marshes on the northern bank of the lower Ría del Tinto have

been used to deposit pyrite ash from the ore processing industry (now grassed over) and are still used to stockpile phosphogypsum, which is a by-product of phosphate fertiliser industry (Martinez-Aguirre and Garcia-Leon, 1997). Leachate from the phosphogypsum lagoons (4 - 6 m depth, ca. 4×10^6 m^2, Elbaz-Poulichet *et al.* 1999) containing trace elements (e.g. PO_4, As, Pb and F), radioactive elements (e.g. U and Th) (Elbaz-Poulichet *et al.* 2000; Martinez-Aguirre and Garcia-Leon, 1996), entered the estuary until a closed water cycle was constructed in spring 1998 (Morales, 1999a).

The limit of tidal influence in the Ría del Odiel is not restricted by a physical barrier. It is located somewhere between a narrow tidal channel (Caño del Fraile) and the village of Gibraleón. The Caño del Fraile is the main channel of the highly branched upper estuary. It leads through a densely vegetated salt marsh, and is partially navigable with a RIB at high water. The estuary widens some 100 metres upstream of Huelva Bridge, which forms the (arbitrary) boundary with the Huelva Ría.

The upper part of the Huelva Ría, between the Ría del Odiel and the confluence with the Ría del Tinto, is characterised by the industrial zone of Huelva on the eastern bank, and the Marismas del Odiel on the western bank (Figure 4.5). In the 1960s and early 1970s, an industrial centre was developed between the city of Huelva and the bank of Huelva Ría. The industries include plants producing titanium dioxide from Australian black beach sand (ilmenite), fertiliser from North African phosphate rock, copper concentrate and sulphuric acid from local ores, and other metallurgic industries under the umbrella of the Association of Chemical and Base Industries from Huelva (AIQB). In addition there is a ship yard, salinas for the production of industrial salt and a power station. Effluents from various industrial plants were discharged untreated until 1985, when some control of industrial water disposal was introduced (Borrego-Flores and Morales, 1998).

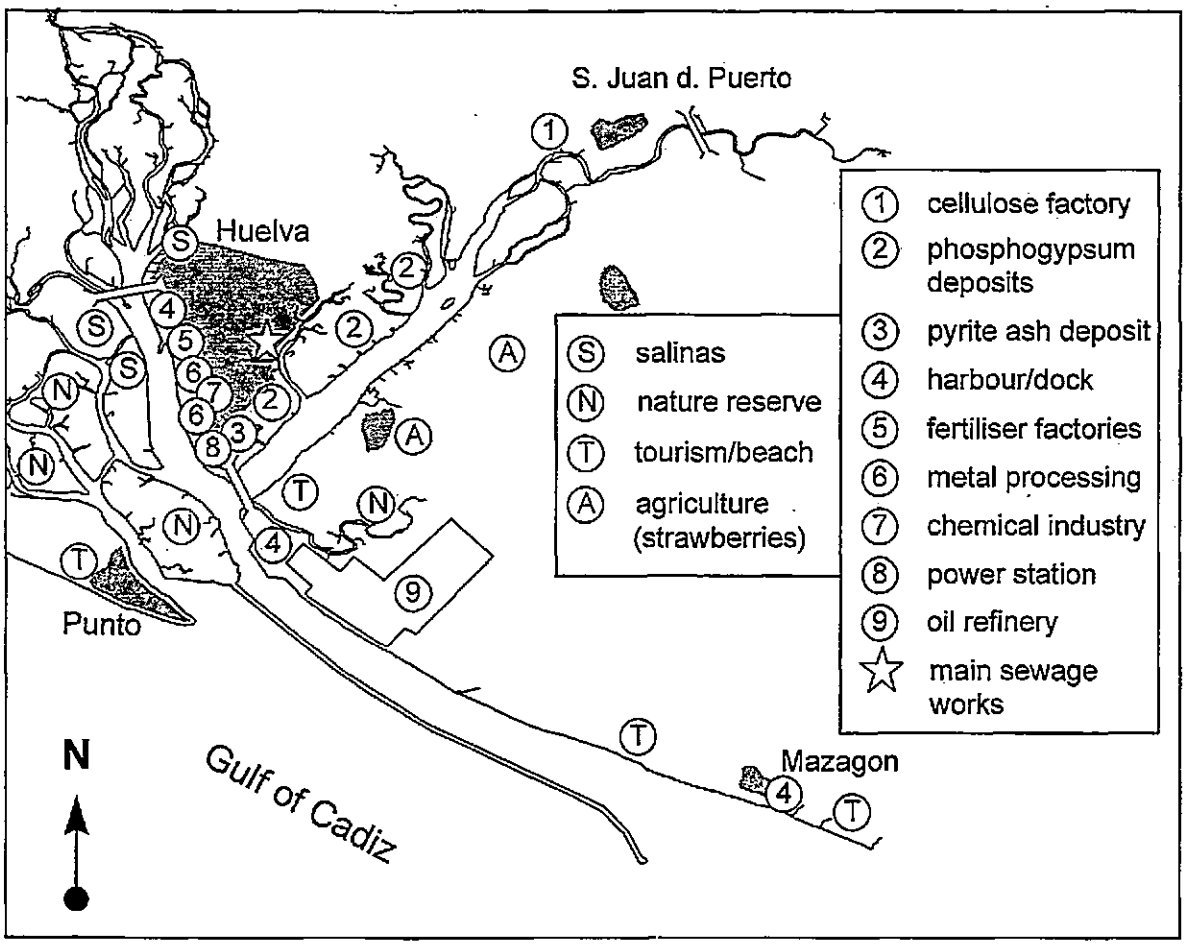

Figure 4.5 - The Tinto/Odiel estuarine system, showing the urban and industrial developments of Huelva in the context of agricultural land and nature reserves. The Marismas del Odiel, a Natural Park and UNESCO Biosphere Reserve are located to the west of Huelva Ría, and the reserve of the Estero Domingo Rubio is located between the lower Ría del Tinto and oil refineries.

However, direct discharges have been reported since then, including the continued release of dissolved and particulate Pb, U, Th and Ra-isotopes and phosphate from the fertiliser industry (Perianez *et al.* 1996; Martinez-Aguirre and Garcia-Leon, 1996; Martinez-Aguirre *et al.* 1994b).

The Marismas del Odiel on the western bank of the estuary are to some extent protected from the influence of industrial and mining pollution by a circulation pattern that allows sea water from the Gulf of Cádiz to enter the salt marshes directly. However, a study of halophytes (e.g. *Zostera noltii, Spartina ssp.*) in the Odiel salt marshes showed elevated concentrations of Fe, Zn, Mn, Cu, Ti, Pb, As, Ni and Cr, especially in specimens from the lower marsh. The concentrations of Cu, Pb and Zn in the plants were considerably higher than levels inducing toxic effects in plants from non-polluted sites, indicating adaptations to long-term metal contamination (Luque *et al.* 1999).

The lower Huelva Ría has been extended to the town of Mazagón by the construction of a breakwater, which is several kilometres long. The main sea port is situated below the confluence with the Ría del Tinto. Oil refineries are located between the harbour and the natural reserve of the tidal creek Estero Domingo Rubio. The main channel of Huelva Ría is dredged to ca. 12 meters, with its deepest point at the sea port (> 20 m).

4.4 Methods

4.4.1 Reagents and Equipment

The quality, preparation and purification of de-ionised water (MQ), reagents (HCl, HNO_3, NH_3, methanol, Oxine, DMG, APDC, Borate, HEPES) and metal standard solutions for voltammetric methods have been given in Chapter 2, and for ICP methods

have been given in Chapter 3. Cleaning procedures for sampling bottles, filter holders and other equipment have been described in Chapter 3.

For the determination of suspended particulate matter (SPM) concentrations, filter membranes (WCN, 47 mm diameter, 0.45 μm pore size) were dried to constant weight (50°C) and weighed.

Filter holders (glass), sampling bottles (brown glass), tweezers (metal) and filters (GFF, 47 mm diameter, 0.7 μm pore size, Whatman) in contact with samples for dissolved organic carbon analysis (DOC) were ashed (450°C, > 4 hours) and wrapped into ashed aluminium foil for storage and transport. Special glass vials (10 ml), fitting into the sample changer of the DOC analyser, were also ashed.

4.4.2 INSTRUMENTATION

4.4.2.1 Field Instrumentation

Field instrumentation used during surveys onboard the Spanish *B/O Garcia del Cid* and portable instruments for field measurements of conductivity, pH, temperature (T), dissolved oxygen (DO) and redox-potential (Eh), together with appropriate calibration procedures, have been detailed in Chapter 3.

4.4.2.2 Instrumentation for Trace Metal Analysis

Two near identical voltammetric systems were used for trace metal analysis. The instrumentation used for discrete samples has been described in Chapter 2, and the automated voltammetric metal monitor for on-line trace metal analysis has been described in Chapter 3. The total dissolved metal analysis in discrete samples using ICP-MS was

carried out as detailed in Chapter 3. For ICP-AES analysis of discrete samples a Varian Liberty 200 instrument was used.

4.4.2.3 Dissolved Organic Carbon

The analysis of dissolved organic carbon was carried out with the high temperature catalytic oxidation method (HTCO) using a Shimadzu TOC-5000 analyser and sample changer (78 positions). The oxidation column was a quartz tube filled with Shimadzu catalyst (0.5% Pt on Al_2O_3).

4.4.3 Sampling Protocol

The following sections give a detailed account of the discrete samples taken during the four scientific surveys, carried out within the TOROS programme:

TOROS 1: 18 - 28 November 1996,

TOROS 2: 4 -21 June 1997,

TOROS 3: 10 - 29 April 1998,

TOROS 4: 4 - 21 October 1998.

The discrete samples taken during the surveys are given in chronological order in Table 4.1, and the sample locations are given in Figure 4.6 to Figure 4.12. Also mentioned in Table 4.1 are the times when on-line trace metal measurements were carried out, typically at a frequency of three to four analysis per hour for Cu, Zn, Ni and Co.

Table 4.1 - Discrete samples obtained and on-line trace metal monitoring activities during the river and estuarine studies of the four TOROS surveys. FW - fresh water, SR - sample at San Juan del Puerto, TR - samples in Rio Tinto or Ría del Tinto, OR - samples in Rio Odiel, HR - Huelva Ría. TC - tidal cycle study, OL - on-line metal determination. GdC - *B/O Garcia del Cid*, RIB - rigid inflatable boat. CN - Club Nautico, HB - Huelva Bridge, MZ - Mazagón.

TOROS 1, Nov '96	Day	Sample ID: TOR-96-11-	Method	Remark
FW, Rio Tinto	19	1	river bank	
FW, Rio Odiel	19	2	river bank	
Transect Ría del Tinto	19	3 - 12	RIB	
Transect Ría del Odiel	20	18 - 24	RIB	parallel to 13 - 17
Transect Huelva Ría	20	13 - 17	small craft	parallel to 18 - 24
Transect Huelva Ría	20	25 - 33	small craft	following 24
Transect Huelva Ría	25	44 - 50	*Popeye*	CN to HB, OL Cu, Zn, Ni, Co
Transect Huelva Ría	25	50 - 64	*Popeye*	HB to MZ, OL Cu, Zn, Ni, Co

TOROS 2, Jun '97	Day	Sample ID: TOR-97-06-	Method	Remark
TC, La Rábida	6	7 - 19	jetty	OL Cu, Zn, Ni, Co
TC, Huelva Bridge	8	20 - 32	estuary bank	OL Cu, Zn, Ni, Co
Transect Huelva Ría	15	HR1 - HR13, G47bis	GdC	OL Cu, Zn, Ni, Co
Transect Ría del Odiel	16	OR1 - OR7	RIB	
Transect Ría del Tinto	17	SR1, TR1 - TR10	RIB	
Transect Huelva Ría	18	HR1bis - HR13bis, G47tris	GdC	OL Cu, Zn, Ni, Co
FW, Rio Odiel	20	G1	river bank	
FW, Rio Tinto	20	N1	river bank	

Table 4.1 - continued.

TOROS 3, Apr '98	Day	Sample ID: TOR-98-04-	Method	Remark
FW, Rio Tinto	11	N1	river bank	
FW, Rio Odiel	11	G1	river bank	
TC, Mazagón harbour	12	M 1 - M 12	estuary bank	OL Cu, Zn, Ni, Co
TC, Club Nautico	16	CN1 - CN13	jetty	OL Cu, Ni, Co
TC, Huelva Bridge	18	TC13 - TC25	estuary bank	OL Cu, Zn
TC, Mazagón	21	MZ1 - MZ12	*Cirry Tres*	OL Cu, Zn, Ni, Co
Transect Huelva Ría	24	HR1 - HR10	*Cirry Tres*	
Transect Ría del Tinto	25	TR1 - TR10, TR2-2, TR7-7	RIB	
Transect Ría del Odiel	27	OR0 - OR7	RIB	

TOROS 4, Oct. '98	Day	Sample ID: TOR-98-10-	Method	Remark
FW, Rio Tinto	4	Rio Tinto E1	river bank	mining area
FW, Rio Tinto	6	RT E2 - 4	river bank	between Niebla and mining area
FW, Rio Odiel	6	RO E1, E2, E2a, E3	river bank	between Gibraleón and mining area
TC, Huelva Bridge	8	TC01 - TC13	estuary bank	OL Cu, Zn, Ni, Co
Transect Ría del Tinto	15	TR 1 - 10	RIB	day
Transect Huelva Ría	16	HR13 - HR7, HR3 - HR1	GdC	
Confluence	16	G48/96, G48/97	GdC	
SJ, Ría del Tinto	17	SJ	bridge	
FW, Rio Tinto	18	N1	river bank	
FW, Rio Odiel	18	G1	river bank	
Transect Ría del Odiel	18	OR 1 - 7	RIB	
TC, Mazagón	19/20	G47/MZ 1 - 13	GdC	OL Cu, Zn, Ni, Co

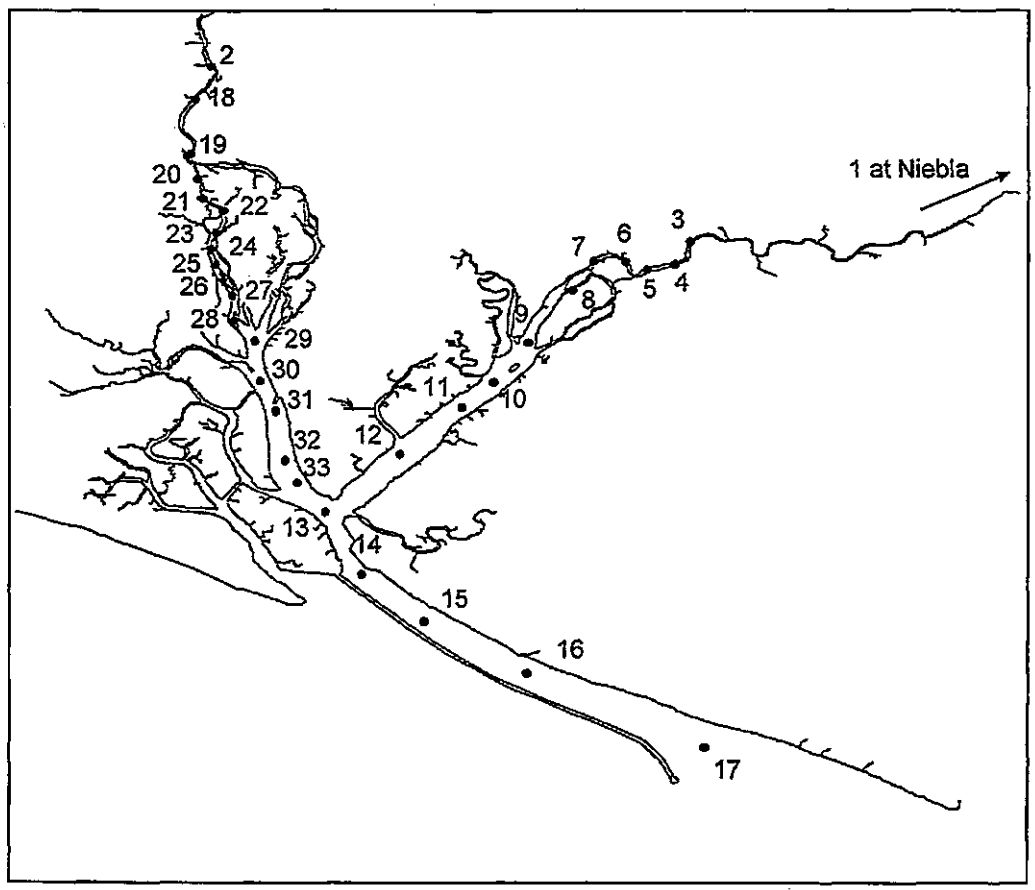

Figure 4.6 - TOROS 1: Sampling positions in Ría del Tinto, Ría del Odiel and Huelva Ría, 19 and 20 November 1996.

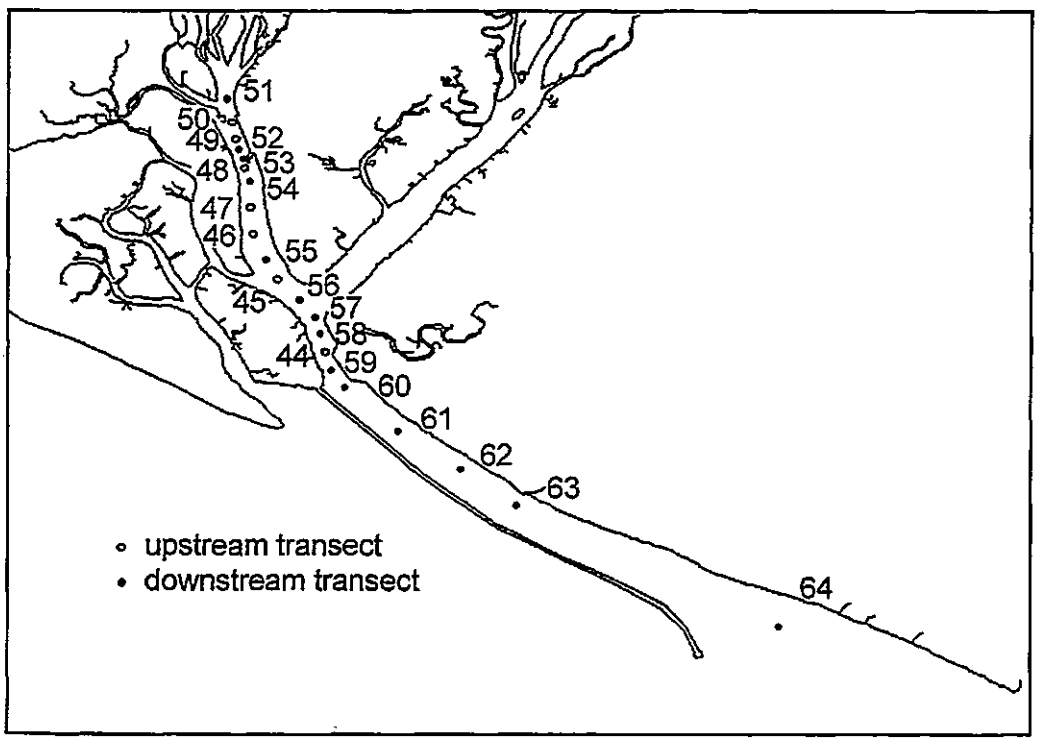

Figure 4.7 - TOROS 1: Sampling positions in Huelva Ría , 25 November 1996.

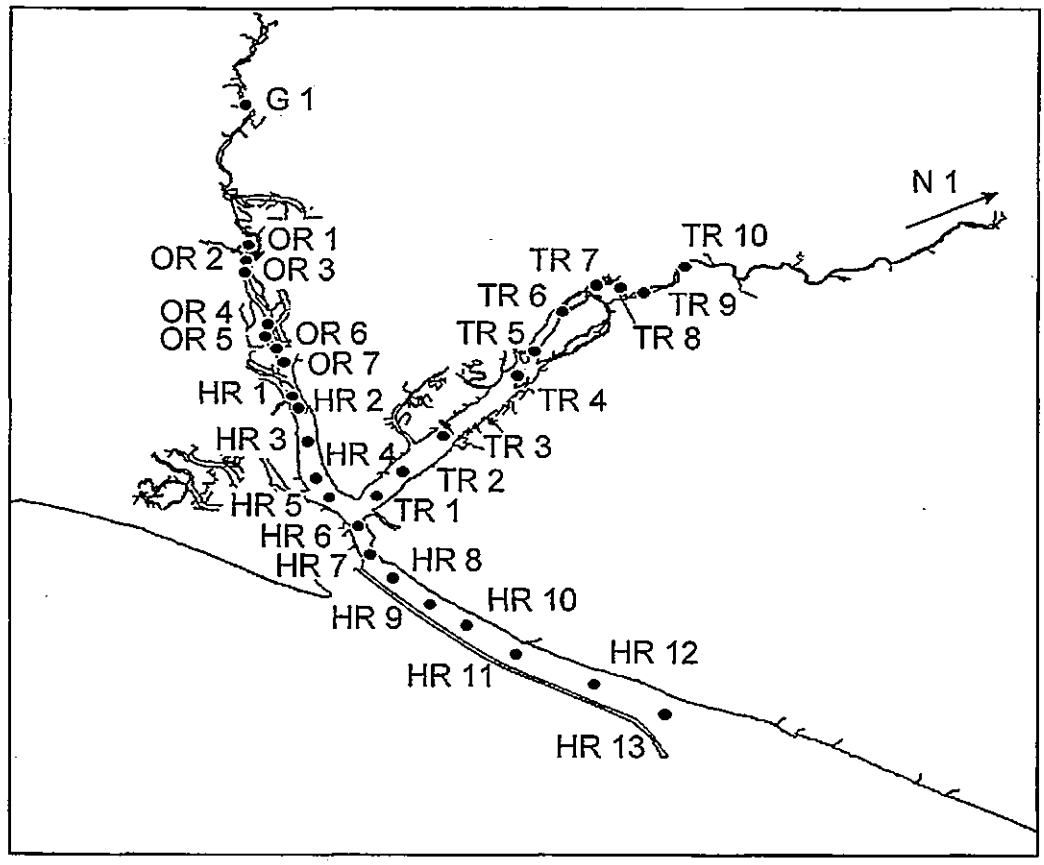

Figure 4.8 - TOROS 2: Sampling positions in the Ría del Tinto (TR) and Ría del Odiel (OR), and Huelva Ría (HR) in June 1997. The transect in Huelva Ría was repeated during the same survey, revisiting the sampling positions (HR bis).

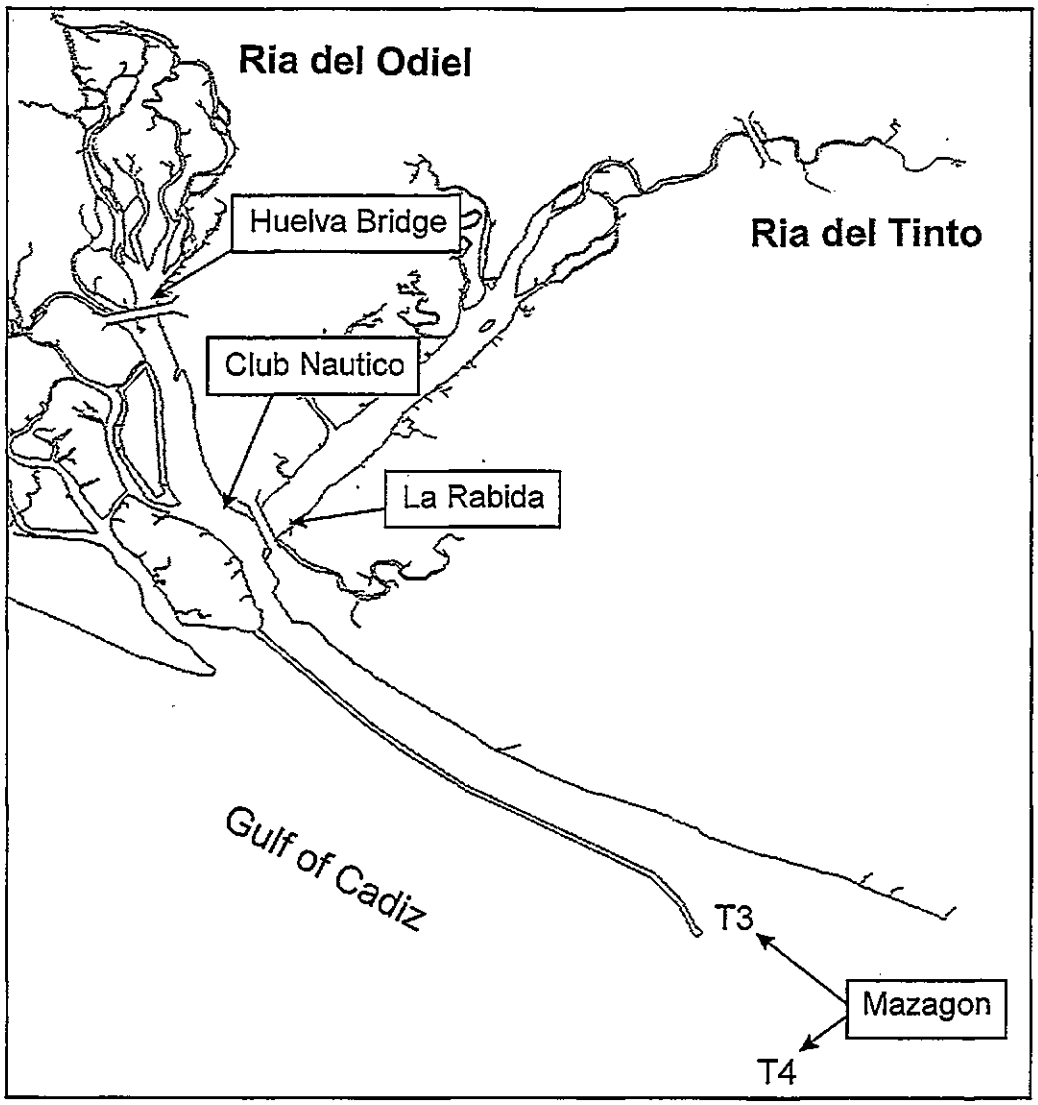

Figure 4.9 - Positions of tidal cycle studies, carried out during TOROS 2, 3 and 4 surveys in the Huelva Ría. June, 1997: La Rábida and Huelva Bridge; April 1998: Huelva Bridge, Club Nautico, and Mazagón, position 'T3'; October 1998: Huelva Bridge and Mazagón, position 'T4'.

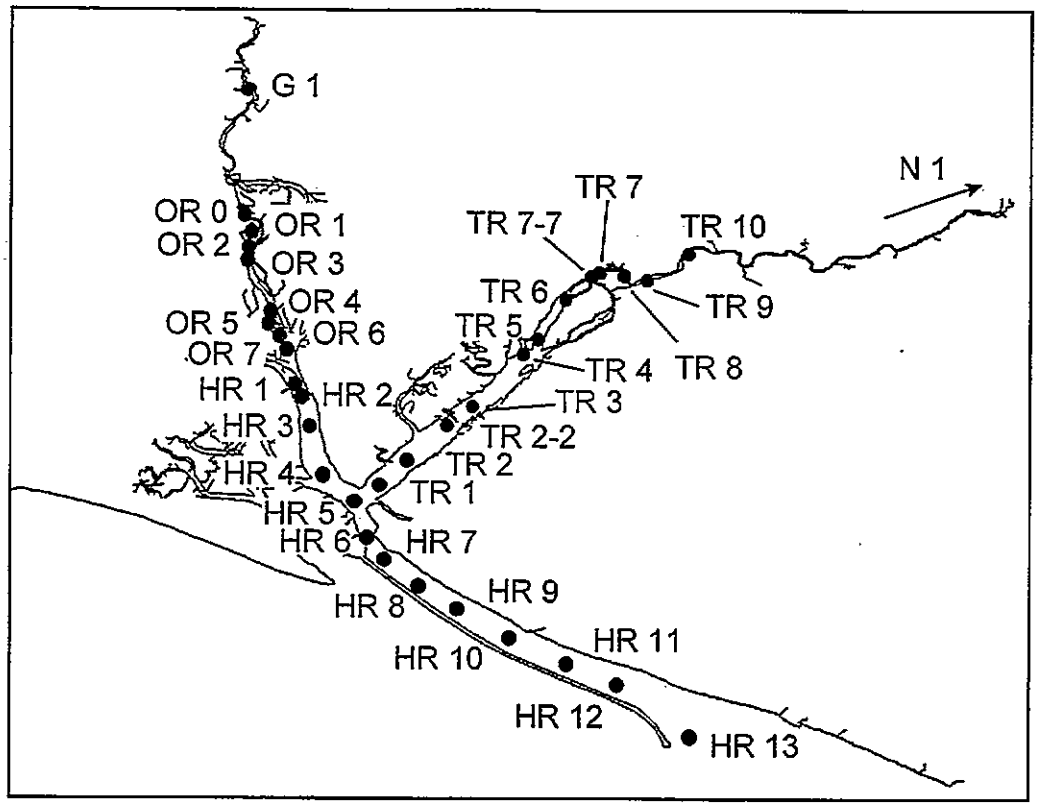

Figure 4.10 - TOROS 3: Sampling positions in the Ría del Tinto, Ría del Odiel, and Huelva Ría, April 1998.

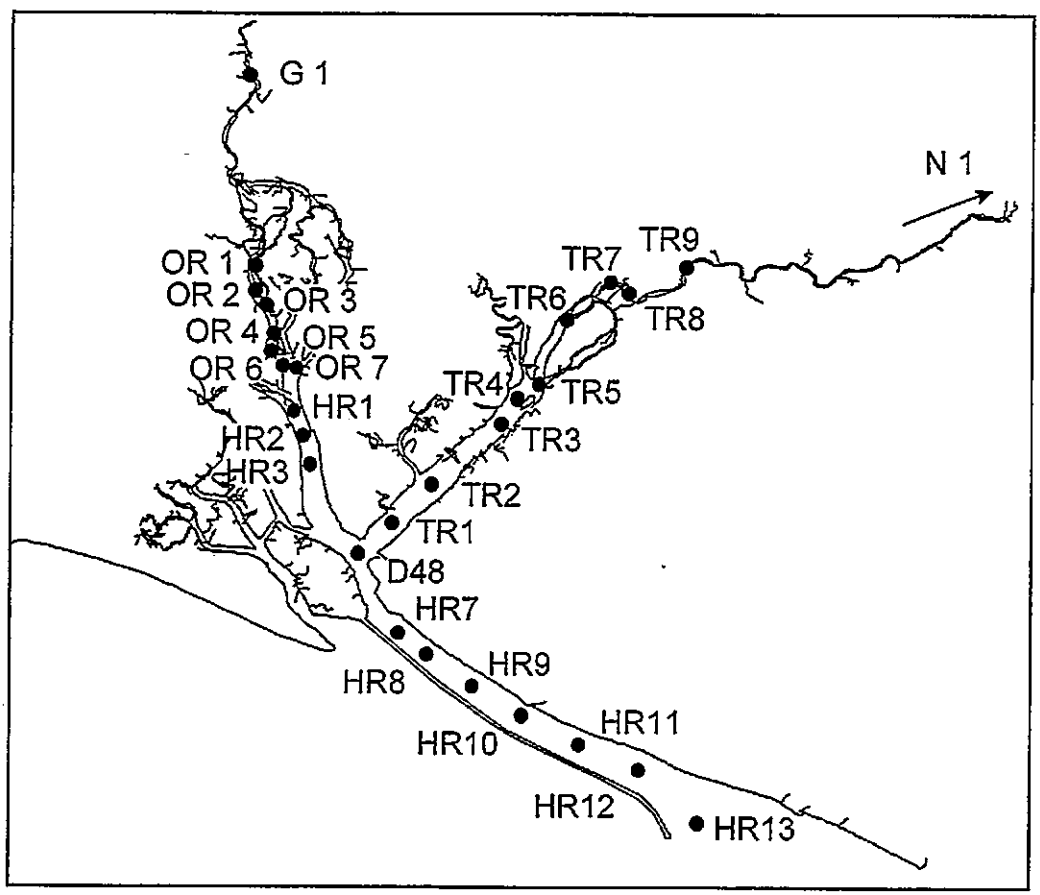

Figure 4.11 - TOROS 4: Sampling positions in the Ría del Tinto, Ría del Odiel and Huelva Ría, October 1998.

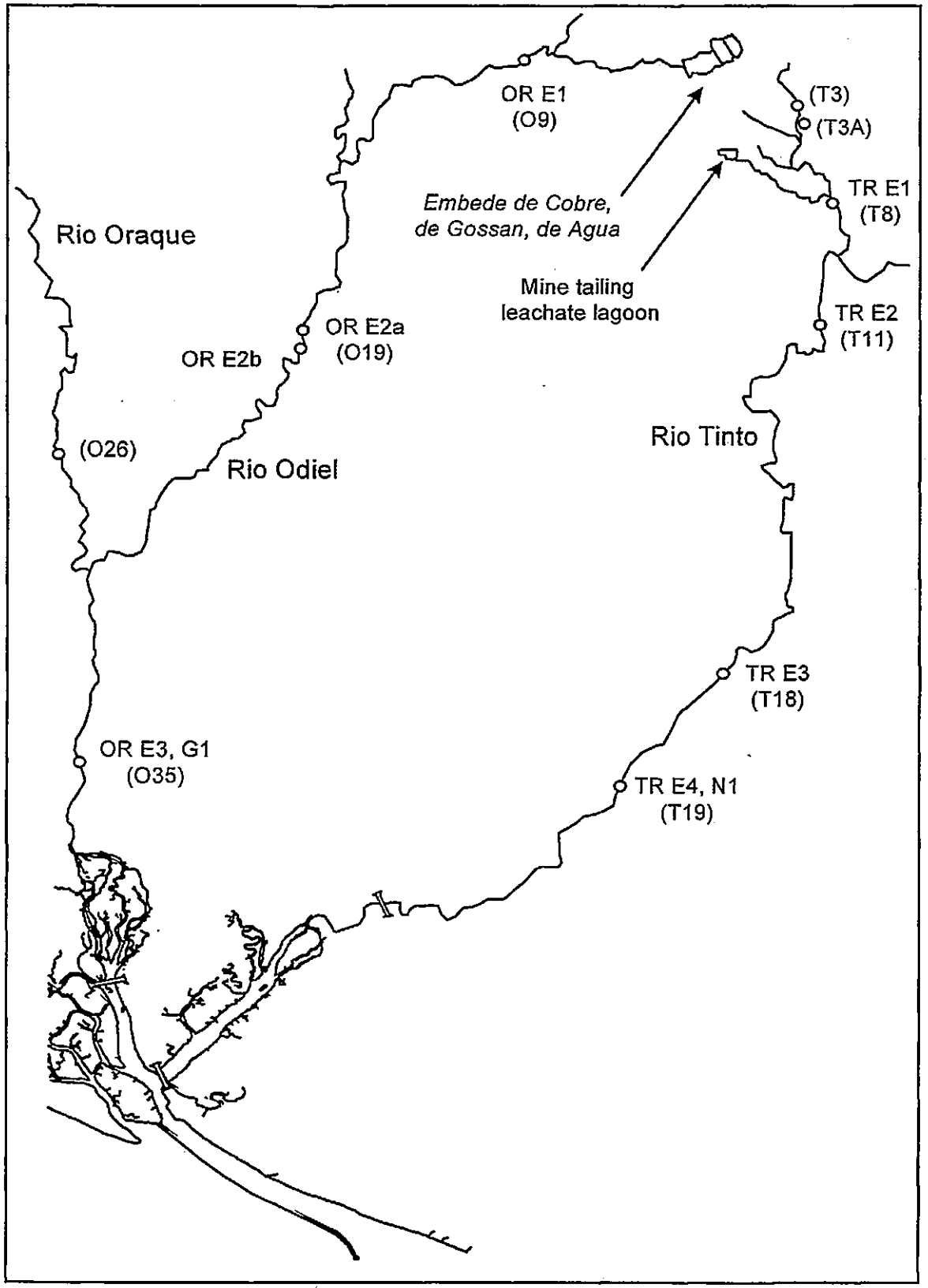

Figure 4.12 - TOROS 4: Sampling positions in the Rio Tinto and Rio Odiel, between the fresh water end-member stations (Niebla, N1 and Gibraleón, G1, respectively) and the upper reaches in the mining district of the Iberian Pyrite Belt. *Embede de Cobre, Emb. de Gossan and Emb. de Agua* are alkaline impoundments in which effluent from cyanidation processes is collected.

All bulk containers and sample bottles were acid washed as described in Chapter 3. Buckets (PVC) used for sample collection were acid washed initially and rinsed thoroughly with sample water ahead of each use. Between individual parts of the sampling campaign buckets were soaked overnight with HCl (10% v/v). All other containers used for sample collection were rinsed twice with sample water before the sample was taken. Filled sample bottles were packed in a double layer of re-sealable plastic bags and stored in large plastic containers. Bulk containers were protected from contamination with large plastic bags.

During estuarine surveys measurements of conductivity, pH, temperature, dissolved oxygen, and during TOROS 2, 3 and 4, redox potential were carried out with suitable field instruments (see Chapter 3).

Fresh water samples were collected from the river banks. Sample bottles (HDPE, see Chapter 3) were dipped directly into the water, rinsed, filled, and packed. Sample locations for the fresh water end-members were at Niebla in the Rio Tinto and at Gibraleón in the Rio Odiel. During TOROS 4, additional river samples were taken at sample locations between the source of the rivers in the mining area and Niebla and Gibraleón. The additional stations were selected from sites that are visited regularly by the local environment agency, the Junta de Medio Ambiente de Andalucia (Medio Ambiente, 1998).

In the upper estuaries sampling was restricted by accessibility. In the Ría del Tinto, the most upstream sampling station was the road bridge at San Juan del Puerto, from which a bulk sampling container (10 l) was filled with a bucket on a rope. In the Ría del Odiel, the most upstream sampling station was located in the channel Caño del Fraile, the exact position of which depended on the navigability during the survey (Figure 4.6, Figure 4.8, Figure 4.10 and Figure 4.11).

In the shallow upper parts of the estuaries, sample collection along transects was carried out using a RIB. When possible, sampling was started at high water at the most

upstream point navigable. Sampling criteria were conductivity changes and important discharge locations within the estuary, for example effluent from the cellulose factory and sewage works in the Ría del Tinto.

In the lower Ría del Tinto, a small craft (ca. 5 m, glass fibre) was used for sample collection. Bulk containers (2, 5, or 10 l) were dipped into the water over the side of the boat. In Huelva Ría, a variety of vessels were used for sample collection. During the TOROS1 survey, a small vessel (*Popeye*, ca. 12 m, glass fibre) was used for three axial transects (Figure 4.6 and Figure 4.7). Bulk containers were filled using a purpose-built, hand-operated vacuum pump and siphon arrangement (Morley, University of Southampton). During TOROS 2 and 4 surveys, Huelva Ría samples were collected onboard *B/O Garcia del Cid*, using 'clean' Niskin bottles (Chaper 3) mounted on the ship's CTD rosette (Figure 4.8 and Figure 4.11, respectively). During the TOROS 3 survey, *Popeye*'s sister-vessel (*Cirry Tres*) was used for estuarine sample collection (Figure 4.10). Surface samples were collected with a custom-made PTFE sampler (2 × 0.5 l bottles), deployed from a hydrographic wire (Kevlar™) and activated with a messenger (IFREMER, France). Depth samples were collected directly into sample bottles with a bottom-weighed acid washed PVC hose and peristaltic pump (Watson & Marlow).

For land-based tidal cycle studies (TCs) a mobile laboratory was parked on the bank of the estuary for the deployment of two automated voltammetric metal monitors and for filtration work (Chapter 3). TCs were carried out in the lower Ría del Odiel from the estuary bank at Huelva Bridge (TOROS 2, 3 and 4), at the confluence from a jetty at Club Nautico (TOROS 3) and from a jetty at La Rábida (Figure 4.9). Discrete samples were taken at hourly intervals from the estuary bank or jetty, using a bucket and bulk container (10 l). During the TOROS 3 and 4 surveys, TCs were performed onboard ship (*Cirry Tres* and *B/O Garcia del Cid*, respectively), while the vessels were anchored off Mazagón at the

mouth of the estuary. Onboard *Cirry Tres*, the continuous sample pick-up was made from a short length (ca. 5 m) of bottom-weighed PVC hose, which was lowered into the water off the side of the vessel, to a depth of ca. two metres. On bord *B/O Garcia del Cid*, KIPPER-1 was used as sample pick-up. Discrete samples were taken at hourly intervals with means available on the vessels, as described in the previous paragraph. The on-line analysis of Cu, Zn, Ni and Co was carried out as described for river bank and ship-board deployment of the metal monitor in Chapter 3.

Conductivity and temperature measurements were taken using field instruments on *Popeye* and *Cirry Tres*, and ship-board equipment on the *B/O Garcia del Cid* (Chapter 3). In Huelva Ría sub-samples were taken in glass bottles for salinity measurements by accurately calibrated salinometers (Portasal 8410, Guildline, Canada) at the Institute of Marine Sciences (IMS at University of Plymouth) or at the Southampton Oceanography Centre.

Sub-samples for the analysis of dissolved organic carbon (DOC) were taken during the TOROS 2, 3 and 4 surveys for all riverine and estuarine samples (see Table 4.1). Different methods were applied for the preservation and storage of the samples, as described in Section 4.4.4.

4.4.4 Treatment of Discrete Samples

Bulk containers were commonly used for initial sample collection, so that sub-samples could be distributed between different groups within the TOROS project. Sub-samples were taken for filtration in a protected environment (class 100 laminar flow) after agitation. Samples collected from the river bank or from aboard small vessels were filtered on return to the laboratory at the University of Huelva, within 24 hours of sample collection. Discrete samples taken onboard *B/O Garcia del Cid* were filtered in the ship's

laboratory immediately after collection. During land-based TC studies, filtration was carried out within a maximum of two hours after collection in a protected space constructed in the mobile laboratory.

River and estuarine samples for trace metal analysis were filtered using acid leached cellulose nitrate membrane filters (WCN, 47 mm diameter, 0.45 μm pore size, Whatman), fitted into acid-washed Nalgene filter holders (500 ml, polycarbonate). Vacuum was drawn with hand pumps. Between samples, the filter holder was rinsed with MQ. The first batch of filtrate (100 - 150 ml) was discarded. Filtration blanks (MQ) were obtained before the first sample in a filtration series, and between two samples at some stage during the filtration. During two estuarine surveys and TCs at Huelva Bridge (TOROS 2 and 3), samples were pressure filtered (N_2, oxygen-free, 1 - 2 bar) by a colleague (Herzl, University of Plymouth), using acid-washed polycarbonate filters (125 mm diameter, 0.4 μm pore size, Nuclepore) fitted into an acid-washed home-built Teflon® filter holder. Filter holders and tweezers for filter membrane handling were acid-washed overnight (0.1 M HCl and 0.01 M HCl, respectively) between filtration series.

Samples from the Ría del Tinto and Ría del Odiel were acidified with HNO_3 (pH < 2) in preparation for ICP-MS or ICP-AES analysis. Samples from the lower estuary were acidified with HCl (pH 2) for total dissolved trace metal analysis using stripping voltammetry. Fresh water samples from the Rio Tinto and Rio Odiel were diluted (× 100) in HNO_3 (0.015 M HNO_3) immediately after filtration. This was done to prevent the precipitation of Fe solids during storage.

Sub-samples for the determination of SPM concentrations were filtered separately, using dried and pre-weighed filters. Filtration was carried out using a dedicated filter holder (Nalgene, 250 ml) and a vacuum hand pump. When polycarbonate filters were used for trace metal filtration, SPM filtration was carried out on separate filter papers using the

same filtration method as for the dissolved phase. The filter membranes containing the retained SPM were rinsed free of sea salt with MQ and sucked dry under vacuum, then folded and stored in individual Petri dishes.

During the TOROS 2 survey, sub-samples from the usual filtration procedure were taken for dissolved organic carbon (DOC) determinations. The samples were poured directly from the filter unit into polystyrene containers (Sterilin, 30 ml) and acidified to pH < 2 by the addition of 180 µl phosphoric acid (50% v/v, Aristar, Merck) to 30 ml sample. Care was taken to exclude air when closing vials (polyethylene cap). During TOROS 3, DOC samples were collected separately in ashed glass bottles (250 ml). The samples were vacuum filtered (hand pump), using an ashed glass filtration unit and filters (GFF, 0.7 µm pore size, 47 mm diameter, Whatman). The initial 100 - 150 ml of filtrate was used to rinse the filter and filtration unit and was discarded. The filtered samples were transferred into glass ampoules (25 ml), which had been cracked open just prior to use. The samples were acidified as described above and the ampoules were sealed immediately using a blow-torch. Between samples, the filtration unit was rinsed with MQ. During TOROS 4, sub-samples from the usual filtration procedure (see above) were filled into glass ampoules and treated as described for the TOROS 3 survey. Filter banks (MQ) were taken during all surveys. DOC samples were stored in the dark and refrigerated (4°C) ahead of analysis. During transport to the UK the samples were stored in cool boxes with ice packs.

4.4.5 Analytical Methods

A summary of analytical methods applied to discrete samples is given in Table 4.2.

Table 4.2 - Analytical methods applied to discrete samples collected during TOROS surveys. For sample IDs and sampling methods refer to Table 4.1. FW - fresh water of Rio Tinto and Rio Odiel. Trace metal analysis refers to total dissolved concentrations. nd - not determined.

TOROS 1, Nov '96	Cu, Zn, Ni, Co	Fe, Al	Mn, U, Pb	DOC
FW	ICP-MS	ICP-AES	ICP-MS	nd
Transect Ría del Tinto	ICP-MS	ICP-AES	ICP-MS	nd
Transect Ría del Odiel	ICP-MS	ICP-AES	ICP-MS	nd
Transect Huelva Ría	AdCSV	<LOD	<LOD	nd

TOROS 2, Jun '97	Cu, Zn, Ni, Co	Fe, Al	Mn, U, Pb	DOC
FW	ICP-MS	nd	ICP-MS	HTCO
Transect Ría del Tinto	ICP-MS	nd	ICP-MS	HTCO
Transect Ría del Odiel	ICP-MS	nd	ICP-MS	HTCO
Transect Huelva Ría	AdCSV	nd	<LOD	HTCO
TC, La Rábida	ICP-MS	nd	ICP-MS	HTCO
TC, Huelva Bridge	ICP-MS	nd	ICP-MS	HTCO

TOROS 3, Apr '98	Cu, Zn, Ni, Co	Fe, Al	Mn, U, Pb	DOC
FW	ICP-MS	nd	ICP-MS	HTCO
Transect Ría del Tinto	ICP-MS	nd	ICP-MS	HTCO
Transect Ría del Odiel	ICP-MS	nd	ICP-MS	HTCO
Transect Huelva Ría	AdCSV	nd	<LOD	HTCO
TC, Mazagón harbour	AdCSV	nd	<LOD	HTCO
TC, Club Nautico[#]	ICP-MS	nd	ICP-MS	HTCO
TC, Huelva Bridge	ICP-MS	nd	ICP-MS	HTCO
TC, Mazagón[#]	AdCSV	nd	<LOD	HTCO

TOROS 4, Oct. '98	Cu, Zn, Ni, Co	Fe, Al	Mn, U, Pb	DOC
FW	ICP-MS	nd	ICP-MS	HTCO
Transect Ría del Tinto	ICP-MS	nd	ICP-MS	HTCO
Transect Ría del Odiel	ICP-MS	nd	ICP-MS	HTCO
Transect Huelva Ría	AdCSV	nd	<LOD	HTCO
Confluence	AdCSV	nd	<LOD	HTCO
TC, Huelva Bridge	ICP-MS	nd	ICP-MS	HTCO
TC, Mazagón[#]	AdCSV	nd	<LOD	HTCO

[#] Data from these tidal cycle studies is not presented here, but used in Chapter 6.

4.4.5.1 Voltammetry

Stripping voltammetry was used for the determination of total dissolved concentrations of Zn, Cu, Ni and Co in samples collected in Huelva Ría (Table 4.2). Filtered and acidified samples were UV-digested and analysed at the University of Plymouth using AdCSV methods, as described in Chapter 2.

4.4.5.2 ICP-MS

Total dissolved Zn, Cu, Ni, Co, Cd, U, Pb and Mn in riverine and estuarine samples (Table 4.2) were analysed using ICP-MS, because trace metal concentrations in these samples was too high for stripping voltammetric methods. The analysis was carried out in diluted (≥ 50 times, 0.015 M HNO_3) samples, as described in Chapter 3.

4.4.5.3 ICP-AES

Total dissolved Fe and Al were determined for the first survey in samples from the upper estuaries (Table 4.2) using ICP-AES. In order to reduce matrix effects, samples were diluted (≥ 50 times, 0.015 M HNO_3). The analysis was carried out with the following instrumental parameters: Photo multiplier tube voltage: 650 V, power: 1 kW, plasma gas flow: 15 l min^{-1}, and auxiliary gas flow: 1.5 l min^{-1}, viewing height 2 mm.

4.4.5.4 Dissolved Organic Carbon (DOC)

The HTCO instrument for DOC analysis was calibrated using standard solutions of Na_2CO_3 and $NaHCO_3$ for inorganic carbon (0 - 20 mg C l^{-1}), and potassium hydrogen phthalate for total carbon analysis (0 - 20 mg C l^{-1}).

The ashed glass vials for the sample changer were rinsed three times with the sample before they were finally filled with the sample and placed into the automatic sample changer. The first four positions (1 - 4) and last four positions (75 - 78) were occupied by procedure blanks and check samples (Na_2CO_3, $NaHCO_3$ and potassium hydrogen phthalate, 12 mg C l^{-1}), followed by three analytical blanks, which were prepared from MQ and phosphoric acid (Aristar, pH 2). The remaining positions were filled with filter blanks and samples. A dust cover was placed onto the sample changer and the automated analysis was initiated.

Principle steps in the automated measuring cycle were the injection of sample through a stainless steel tube and glass syringe pump into the oxidation column, which was located in the furnace (680°C). The injection volume was 200 µl. In the oxidation column the dissolved carbon was converted to CO_2 by the HTCO process. The combustion products (CO_2, H_2O, etc.) passed with a carrier gas (ultra-pure O_2) through a halogen scrubber before it entered the non-dispersive infrared (IR) detector. The CO_2 signal was recorded and the total carbon concentration (C_{TC}) was calculated using an integration system (peak area) and the calibration curve determined earlier. For the analysis of inorganic carbon the sample was injected into the reaction vessel for inorganic carbon (IC), where it was allowed to react with H_3PO_4 (25% v/v., Aristar, Merck). This converted IC (carbonate, bicarbonate, magnesium carbonate etc.) to CO_2, which was transported with the carrier gas to the IR detector. The inorganic carbon signal was recorded and treated as described for total carbon. The concentration of DOC was calculated by subtracting C_{IC} from C_{TC}. All calculations were carried out by software integrated into the HTCO analyser.

In order to rinse and condition the instrument for each sample, three injections of MQ were followed by three injections of sample before each sample analysis. The analysis for both TC and IC was repeated three times.

The HTCO method for DOC analysis with the Shimadzu TOC 5000 instrument and associated analytical challenges have been discussed widely (Cauwet, 1994; Benner and Strom, 1993; Chen and Wangersky, 1993; Sugimura and Suzuki, 1988).

4.4.5.5 Salinity

In the upper part of the Tinto and Odiel estuaries, the use of salinity to describe the degree of mixing with sea water is erroneous, because of the high concentration of ions derived from the mining area. Different methods were used to measure the influence of sea water. In order to be consistent, salinity was chosen for all data representations, although chlorinity would have been more appropriate for estuarine data.

For tidal cycle studies, salinity was calculated from calibrated conductivity measurements. For estuarine transects the salinity was calculated from chlorinity measurements supplied by the research partner F. Elbaz-Poulichet (University of Montpellier II). For samples taken from aboard *B/O Garcia del Cid* in June, salinity was determined using calibrated data from the ship's underway conductivity instruments and CTD supplied by A. Cruzado *et al.* (1999; 1998).

4.5 RESULTS

4.5.1 ANALYTICAL PERFORMANCE

4.5.1.1 Voltammetry

Methods and typical analytical performance for the analysis of certified reference materials, using stripping voltammetry, have been discussed in Chapter 2. Typical values for reagent blanks, limits of detection and linear ranges of AdCSV analysis have been given in Chapter 3.

Filtration blanks, taken during the filtration of samples from Huelva Ría and tidal cycle studies (TCs) were analysed using voltammetric methods as described for MQ blank determinations in Chapter 3. Blanks taken at the start of a filtration series, i.e. with acid washed filter holders under field-conditions, typically contained 0.5 - 0.6 nM Zn, 0.3 - 0.5 nM Cu and 0.1 nM Ni (this includes the reagent blank). Values for Co were below the detection limit of the method applied (LOD_{Co} = 0.28 nM, see Chapter 3). Filtration blanks taken between two samples during a filtration series contained less than 2% of the Zn, Cu, Ni and Co concentrations of the sample, which was filtered prior to the blank.

4.5.1.2 ICP-MS

With each ICP-MS analysis session of riverine and estuarine samples, several aliquots (n = 4) of undiluted riverine CRM (SLRS-2, National Research Council of Canada) were analysed. Generally, the results of this analysis (Figure 4.13) agreed well with the certified values for Zn, Cu, Ni, Co, Mn, Cd, Pb and U. Some results have a high uncertainty, including Zn, Cu, Ni, Cd and Pb (TOROS 1), Pb (TOROS 2) and U (TOROS 4).

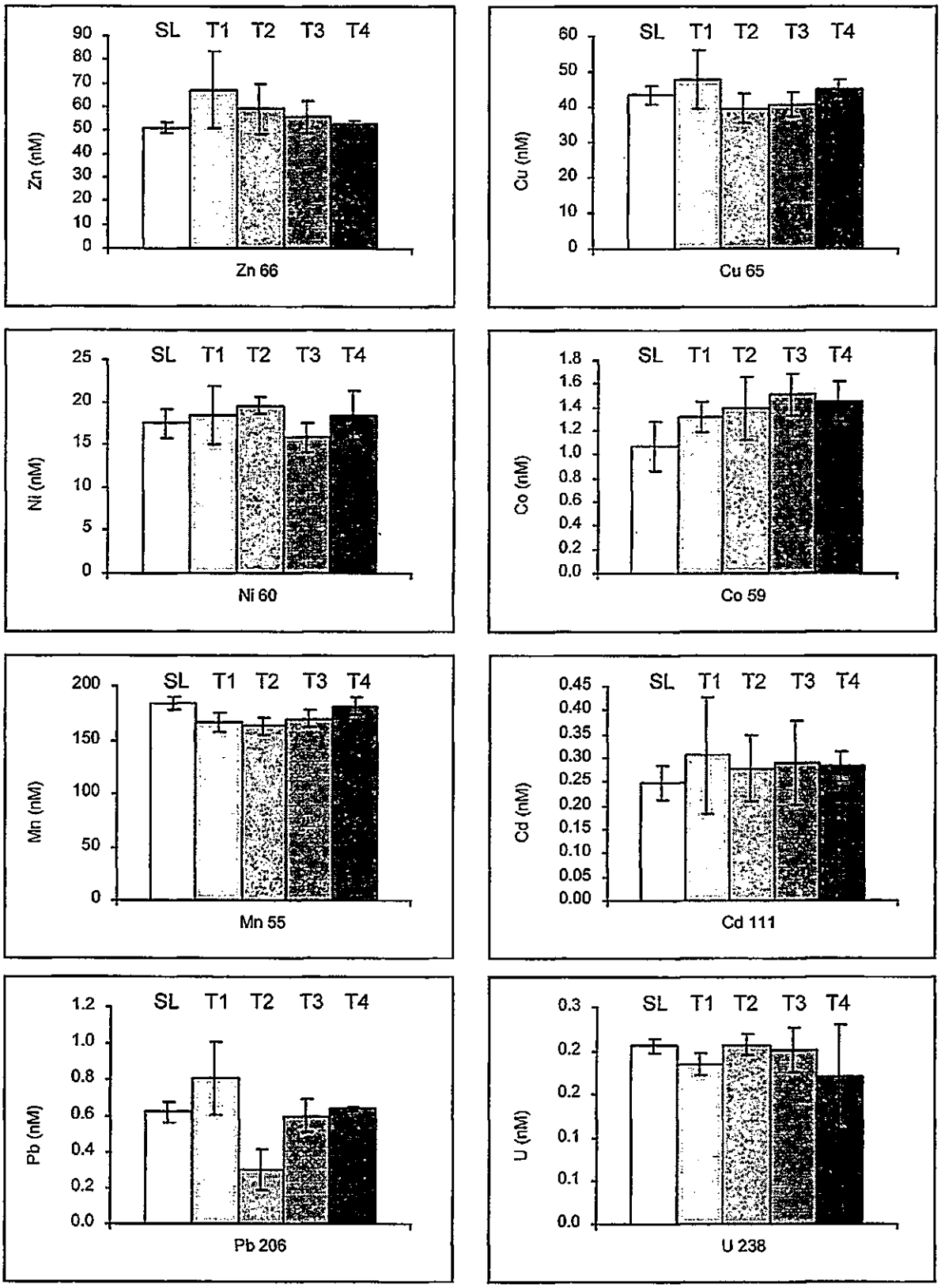

Figure 4.13 - Analysis of certified reference material for river water (SLRS-2) using ICP-MS. The white bar represents the certified values in SLRS-2, the bars marked T1- T4 stand for analysis for TOROS 1 - 4 surveys. Error bars denote two standard deviations of the mean (n = 4). Results of the lead analysis in TOROS 2 samples were not used.

Dissolved metal concentrations analysed by Elbaz-Poulichet (University of Montpellier II, ICP-MS analysis) in riverine and estuarine samples agreed within 10 - 15% with the results from this study. Therefore the results for metals that carry high errors in CRM analysis can still be used with some confidence. Samples processed by Elbaz-Poulichet were filtered using membranes with 0.2 µM pore size, which retain bacteria such as *Thiobacillus ferrooxidans* (Kirby and Elder Brady, 1998). The agreement between the two sets of data indicates that the sample treatment (acidification) in this study inhibited bacterial activity that could influence dissolved trace metal concentrations during storage.

Fourteen aliquots of the blank (0.015 M HNO_3 in MQ) were analysed by ICP-MS. The mean of the blank ± standard deviation were: Mn 55: 0.63 ± 0.15 nM (0.45), Ni 60: 2.88 ± 0.05 nM (0.16), Co 59: 0.85 ± 0.02 nM (0.08), Zn 66: 1.08 ± 0.14 nM (0.42), Cu 65: 0.71 ± 0.15 nM (0.46), Cd 111: 0.75 ± 0.04 nM (0.13), Pb 206: 0.35 ± 0.03 nM (0.09), and U238: 0.009 ± 0.002 nM (0.005). The limit of detection (LOD), given in brackets in nM, was calculated as three times the standard deviation of the mean.

4.5.1.3 ICP-AES

For the ICP-AES analysis no certified material was analysed to verify the analytical accuracy of the method. However, an inter-laboratory and inter-method comparison was carried out with the results of Elbaz-Poulichet (University of Montpellier II, ICP-MS analysis) and Morley (Southampton Oceanography Centre, GFAAS analysis). The results for Fe and Al in samples from the Ría del Tinto and Ría del Odiel between the three laboratories involved agreed within 10 - 15% for most samples.

4.5.1.4 High Temperature Catalytic Oxidation (HTCO)

The Shimadzu TOC 5000 was calibrated in automatic mode overnight ahead of sample analysis. At the time of analysis no certified reference materials for DOC analysis were available. In order to evaluate the stability and analytical performance of the instrument, check samples of known composition (KHP, Na_2CO_3 and $NaHCO_3$) and instrument/reagent blanks were analysed with each series of sample analysis. Maintenance (change of reagents, cleaning etc.) and re-calibration were carried out if the analysis of check samples for KHP showed a deviation larger than 10% from the specified value, or if the blanks were high in organic carbon.

Some KHP check samples appeared to have a small concentration (ca. 0.3 mg l^{-1} C) of IC present. Comparison between this unexpected IC concentration with IC in the mean instrument/reagent blank values (0.47 mg l^{-1} C) indicated that a similar level of IC was present in the MQ, or that the IC signal resulted from instrumental background. Because of the instrumental set-up of the available TOC analyser no sparge was carried out to remove carbon dioxide present in the acidified samples. As a result, the signal for total and inorganic carbon included any dissolved CO_2 present in the sample, and this lead to an over-estimation of the carbon concentrations. Ideally, the results for DOC should have been largely independent (within the analytical precision) from this artefact because the dissolved CO_2 concentration in the sample was subtracted as part of C_{IC} from C_{TC} to yield C_{DOC}. However, current literature recommends the removal of CO_2 before sample analysis (Williams *et al.* 1993) and therefore, while the results of this study are a good indication of trends, they should be treated with caution with respect to their accuracy.

The instrument/reagent blank for the analysis was prepared from acidified MQ (H_3PO_4, Aristar, Merck, ca. pH 2). The DOC values (33 - 45 µM C, mean 39 ± 9 µM C) were high compared to those reported in the literature for platinised quartz catalysts

(5 μM C, Cauwet, 1994; 6 μM C, Benner and Strom, 1993), but were within the range reported for platinised alumina catalysts (10 - 50 μM C, Hedges *et al.* 1993). Blanks prepared with acidified deionised water (H_3PO_4, Aristar, Merck, ca. pH 2) had similar carbon concentrations (45 ± 6 μM C, n = 5) as the MQ blanks. Potential sources of carbon in the blank were the water used to prepare it, the reagent acid and components within the instrument (Sugimura and Suzuki, 1988). It has been suggested that the platinised alumina catalyst is the largest contributor to DOC in blanks. This has been attributed to the adsorption of CO_2 onto the catalyst's carrier material (Al_2O_3), and subsequent desorption and transport of CO_2 with the carrier gas stream leading to the detector (Cauwet, 1994; Benner and Strom, 1993).

Both, calibration and sample analysis were affected by the instrumental contribution to DOC and therefore, the blank value was subtracted from the measurements. Estuarine samples analysed in this study contained medium to high DOC concentrations (0.12 - 6.6 mM C). The carbon concentration measured in blanks introduced a high level of uncertainty to results for samples with low DOC concentrations.

Dissolved organic carbon concentrations in blanks taken before a filtration series and between samples of low carbon concentrations were similar to the instrument/reagent blank values (43 ± 3.3 μM C). Slightly higher DOC concentrations were observed in blanks filtered within a series of samples from the upper estuarine areas (57 ± 6.8 μM C), where DOC concentrations reached low mM levels.

The DOC concentrations determined in MQ filtered through acid leached cellulose nitrite membrane filters (WCN, 0.45 μm pore size) fitted into Nalgene filter holders (500 ml, polycarbonate) were not elevated, compared to DOC concentrations in MQ filtered through ashed GFF filters (0.7 μm pore size). Any contribution in DOC from the WCN membranes was probably masked by the high background value for DOC in the

instrument/reagent blank, which resulted mainly from the catalyst. When comparing the results from the two filtration methods the differences in pore size and membrane characteristics have to be considered, because it is likely that the fraction of organic material (particulate organic matter, colloids, bacteria, viruses) in the filtrate varied between the two methods (Lee and Henrichs, 1993).

The reproducibility of the DOC analysis was assessed with a series of samples of different concentrations (0.15 - 1.6 mM C). The relative standard deviation (RSD) was determined for the analysis of: (a) three injections automatically carried out within the analytical protocol of the instrument, (b) aliquots in several sample changer vials (n = 4) filled from one sample ampoule and (c) aliquots from several sample ampoules containing sub-samples of each other (n = 5). In experiment (a) and (b), RSD values ranged from 0.25 - 3.3%. In experiment (c), values of RSD = 0.1 - 8.9% were determined (mean 2.8%), whereby the highest uncertainty (RSD = 8.9%) was attached to the sample with the lowest concentration (0.15 mM C).

In addition to the constraints mentioned above the preservation for DOC samples from the TOROS 2 survey may have lead to the desorption or loss of organic matter from or to the container walls, and/or an exchange of gases through the walls of the container or lid. The method of storing DOC samples in heat-sealed ampoules has been shown not to induce storage effects (Hedges *et al.* 1993).

4.5.2 TOROS 1 - AUTUMN/WINTER SURVEY

Dissolved metal concentrations, salinity, pH, temperature, total sulphate and dissolved oxygen (DO) concentrations in the Rio Tinto at Niebla and Rio Odiel at Gibraleon are given in Table 4.3. The salinity was calculated from sample chlorinity determined by Elbaz-Poulichet using capillary ion analysis. Sulphate concentrations were supplied by Elbaz-Poulichet (Elbaz-Poulichet *et al.* 1999). Dissolved oxygen (field instrument) was provided by M. López (Morales *et al.* 1999c).

Total dissolved concentrations of Fe, Mn, Al, Zn, Cu, Ni, Co, Cd, Pb and U, pH and sulphate concentrations observed during the TOROS 1 survey were plotted versus salinity for transects in the Ría del Tinto (Figure 4.14), the Ría del Odiel (Figure 4.15) and the Huelva Ría (Figure 4.16). For the Huelva Ría, plots of metal/salinity relationships include the most downstream samples from the Ría del Odiel (Figure 4.16, also Figure 4.19, Figure 4.24 and Figure 4.28 below). Sulphate concentrations were supplied by Elbaz-Poulichet. The concentrations of Fe, Al and Pb in the Huelva Ría were below the detection limit of the method.

Table 4.3 - TOROS 1: Master variables and total dissolved metal concentrations in the fresh water end-members of the Rio Tinto (N 1) and Rio Odiel (G 2) in November 1996. The error given represents one standard deviation of the mean (three measurements during ICP-MS or ICP-AES analysis).

TOR-96-11-	Niebla, N 1	Gibraleon, G 2
Salinity[1]	0.086	0.075
pH	2.47	2.84
T (°C)	19.3	18.0
SO_4 (mM)[1]	27.1	12.5
Q_i ($l\ s^{-1}$)[3]	100	400
Zn (μM)	612 ± 2	356 ± 1
Cu (μM)	460 ± 2	136 ± 1
Ni (μM)	4.70 ± 0.12	4.65 ± 0.11
Co (μM)	9.56 ± 0.06	7.61 ± 0.05
Cd (nM)	1382 ± 12	602 ± 16
Fe (mM)	10.9 ± 0.1	0.91 ± 0.01
Al (mM)	3.55 ± 0.02	2.34 ± 0.01
Mn (μM)	172 ± 1	202 ± 1
Pb (μM)	3.06 ± 0.20	0.23 ± 0.02
U (nM)	30.3 ± 1.5	25.3 ± 0.5

[1] From chlorinity supplied by F. Elbaz-Poulichet, Univ. Montpellier II.
[2] From M. López, University of Huelva.
[3] Estimated from data supplied by J. A. Morales, University of Huelva.

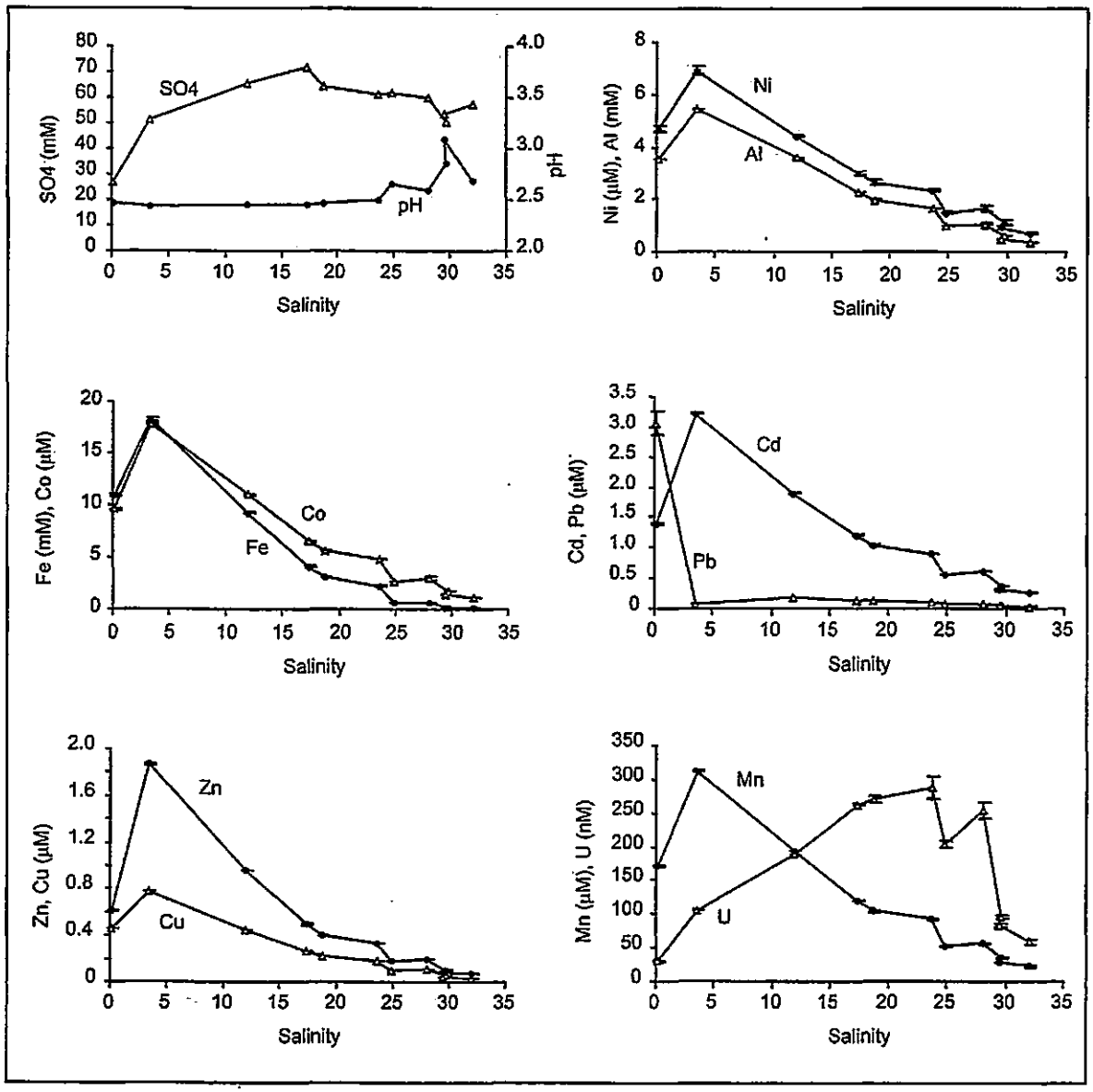

Figure 4.14 - TOROS 1: Sulphate, pH and total dissolved metal concentrations plotted versus salinity in the Ría del Tinto between Niebla and the confluence with Huelva Ría (samples 1, 3 - 12, November 1996). Error bars represent the analytical error (± 1σ) for three scans during ICP-MS or ICP-AES analysis. SO_4^{2-} concentrations are from F. Elbaz-Poulichet, University of Montpellier II.

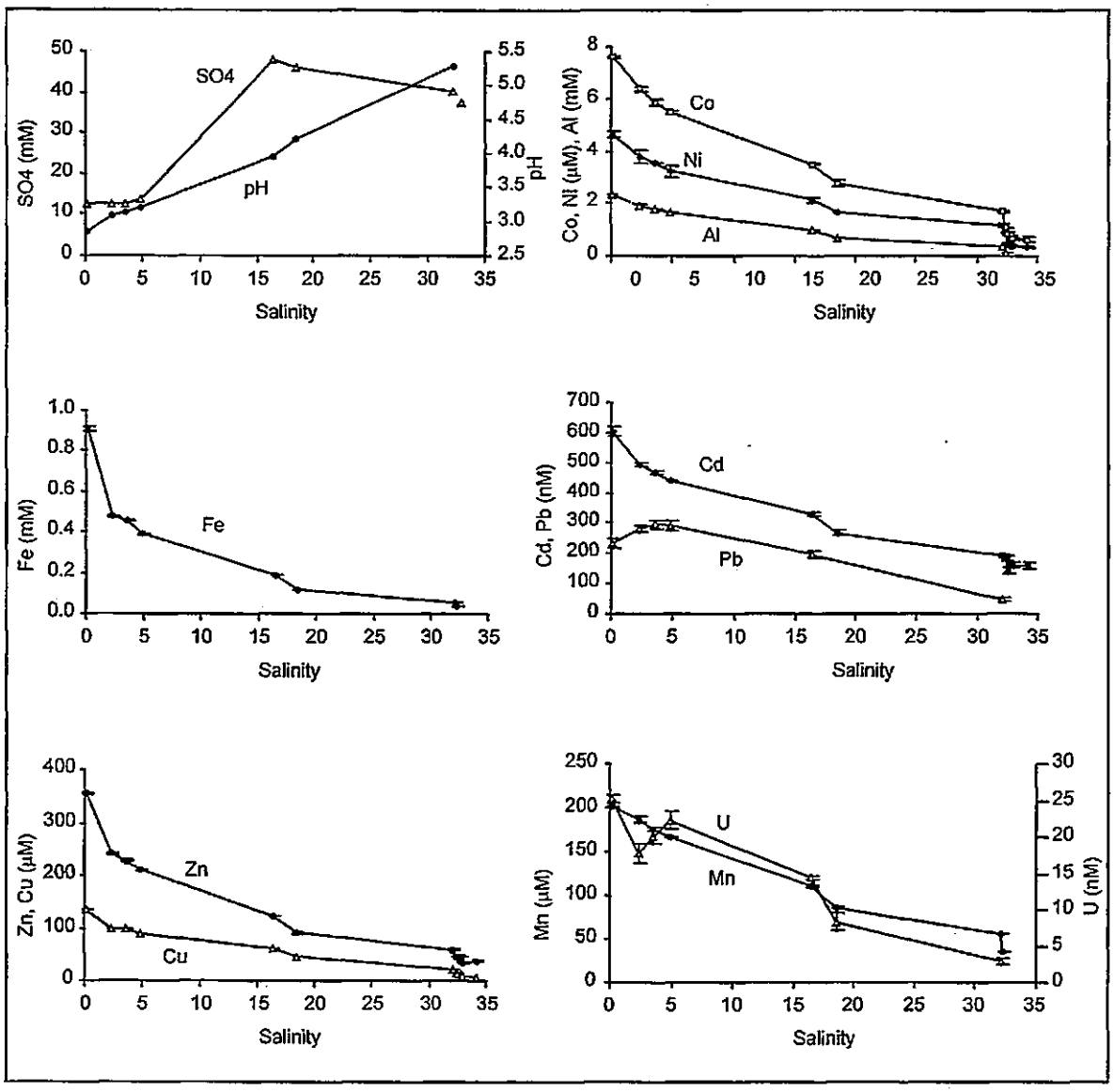

Figure 4.15 - TOROS 1: Sulphate, pH and total dissolved metal concentrations plotted versus salinity in the Ría del Odiel between Gibraleón and Huelva Bridge (samples 2, 18 - 29, November 1996). Error bars and SO_4^{2-} concentrations as for Figure 4.14.

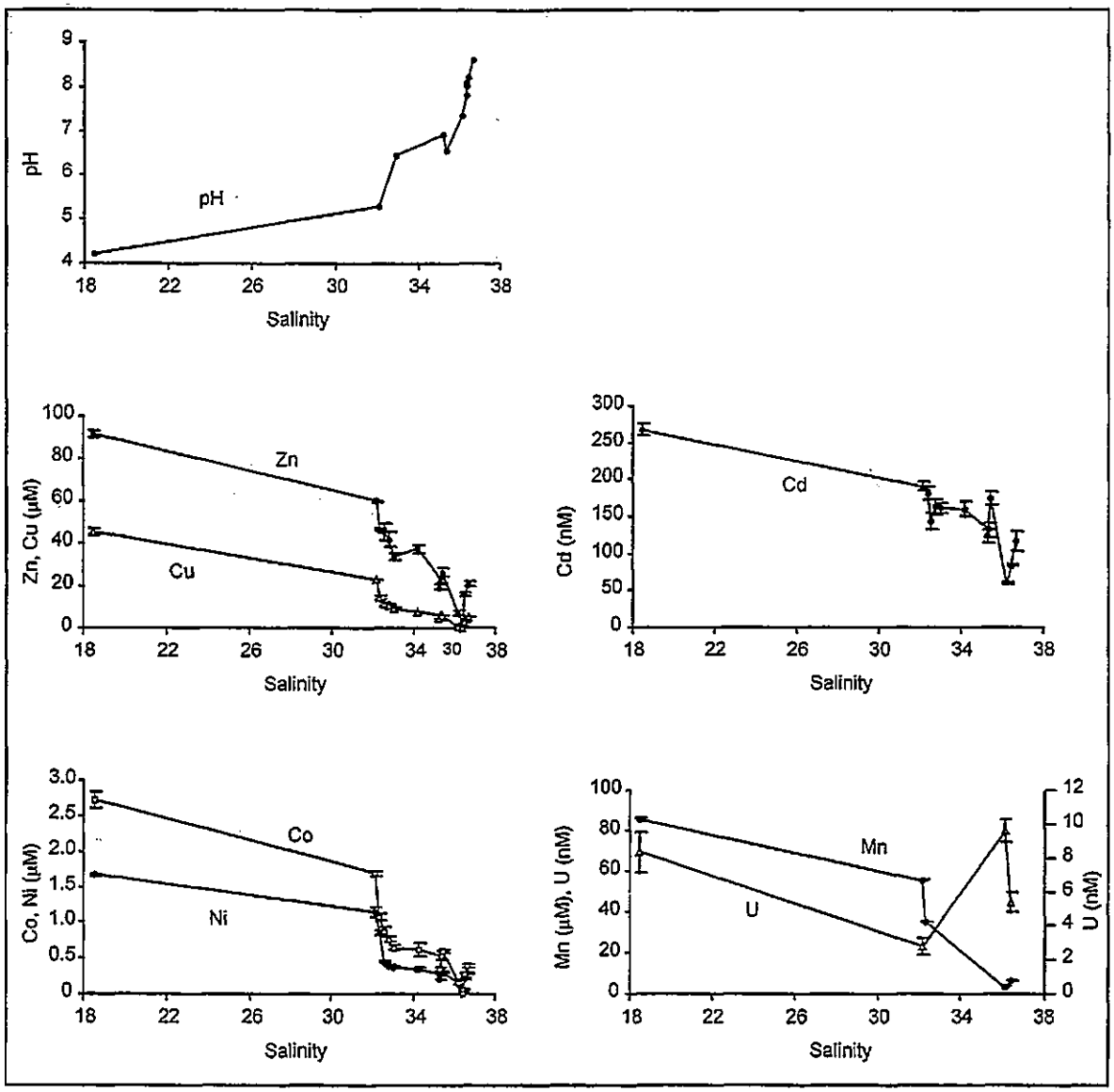

Figure 4.16 - TOROS 1: pH and total dissolved metal concentrations plotted versus salinity in the Huelva Ría (samples 22 - 29, 30 - 33, 13 - 17 November 1996). Samples 22 - 29 were included to visualise the connection between the Ría del Odiel and Huelva Ría. Error bars represent the analytical error (± 1σ) calculated from three scans for ICP-MS analysis and repeat aliquots for voltammetric methods, respectively.

4.5.3 TOROS 2 - SUMMER SURVEY

Dissolved metal concentrations, salinity, pH, temperature, total sulphate and suspended particulate matter (SPM) concentrations in the Rio Tinto at Niebla and Rio Odiel at Gibraleon are given in Table 4.4. The salinity was calculated from chlorinity, which was supplied by Elbaz-Poulichet, as were sulphate concentrations (Elbaz-Poulichet, 1999a). SPM concentrations were provided by Herzl..

Estuarine master variables (pH, alkalinity, acidity, Eh, temperature, SPM), DOC, SO_4 and total dissolved metal concentrations were plotted versus salinity for transects taken in the Ría del Tinto (Figure 4.17), the Ría del Odiel (Figure 4.18) and in Huelva Ría (Figure 4.19). Iron measurements were supplied by Morley. Sulphate concentrations were supplied by Elbaz-Poulichet. Alkalinity, acidity, Eh and SPM were determined by Herzl. Lines linking data points in the Huelva Ría plots were omitted in order to increase clarity.

Estuarine master variables and total dissolved metal concentrations measured during tidal cycle studies are plotted versus time (GMT). The positions of all TC studies are given in Figure 4.9. Figure 4.20 shows results from on-line measurements of total dissolved Zn, Cu, Ni and Co acquired during a TC under Huelva Bridge. Minima in salinity and pH coincided with maxima in dissolved metal concentrations, and this occurred a short time ahead of low water at the mouth of the estuary. In Figure 4.21 metal concentrations measured in the discrete samples collected over a 12-hour period from the jetty at La Rábida are presented in order to illustrate the differential behaviour of Zn, Cu and Cd, compared to U and Pb. Dissolved maxima of Cd, Zn and Cu coincided with low water, but the pattern of salinity variations did not agree with the tidal stage. This was possibly the result of disturbed water circulation patterns close to the confluence of three estuarine systems (Huelva Ría, Ría del Tinto and Estero Domingo Rubio).

Table 4.4 - TOROS 2: Master variables and total dissolved metal concentrations in the fresh water end-members of the Rio Tinto (N 1) and Rio Odiel (G 1) in June 1997. The error given represents one standard deviation of the mean.

TOR-97-06-	Niebla, N 1	Gibraleon, G 1
Salinity[1]	0.07	0.03
pH	2.21	3.00
T (°C)	19.5	18
SO_4 (mM)[1]	8.64	5.52
O_2 (mg l^{-1})[2]	13.4	10.7
SPM (mg l^{-1})[2]	21.4	-
Q_i ($l \cdot s^{-1}$)[3]	80	300
Zn (µM)	295 ± 42	141 ± 2
Cu (µM)	121 ± 11	51.4 ± 0.7
Ni (µM)	1.78 ± 0.44	1.47 ± 0.07
Co (µM)	3.71 ± 0.22	2.44 ± 0.08
Cd (nM)	782 ± 80	430 ± 102
Fe (mM)[4]	1.69	0.039
Al (mM)	2.35 ± 0.02	0.765 ± 0.011
Mn (µM)	112 ± 2	72 ± 1
Pb (µM)	4.13 ± 0.15	0.277 ± 0.041
U (nM)	28.7 ± 3.3	17.7 ± 5.3

[1] From chlorinity supplied by F. Elbaz-Poulichet, Univ. Montpellier II.
[2] From V. Herzl, University of Plymouth, sample at G1 did not yield enough SPM to be measured.
[3] Estimated from data supplied by J. A. Morales, University of Huelva.
[4] From N Morley, Southampton Oceanography Centre.

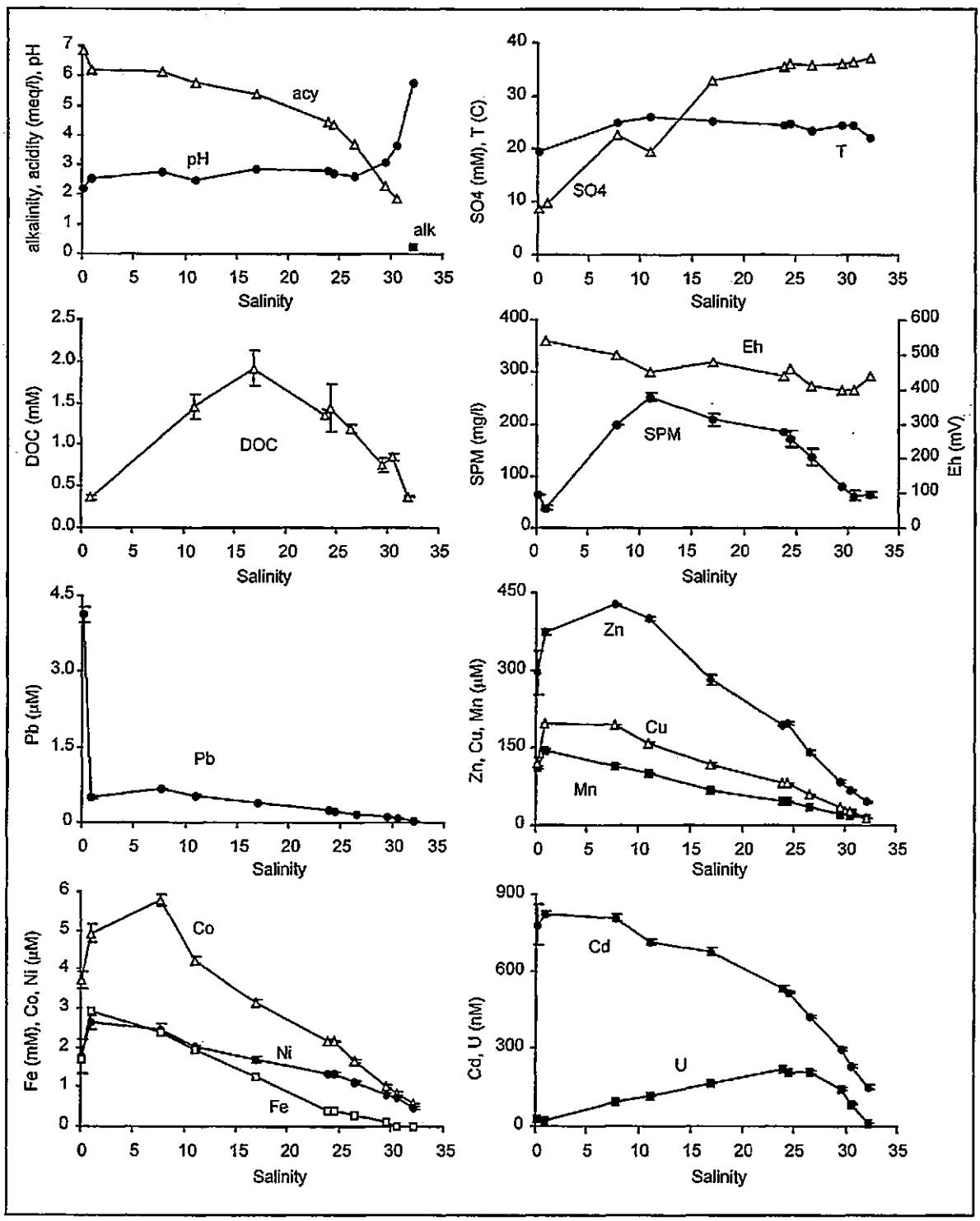

Figure 4.17 - TOROS 2: Sulphate, pH, alkalinity, acidity, Eh, temperature, SPM, DOC and total dissolved metal concentrations plotted versus salinity in the Ría del Tinto between Niebla and the confluence with Huelva Ría (samples TR 1-10, N1, June 1997). Error bars represent the analytical error (± 1σ) for three scans during ICP-MS or ICP-AES analysis.

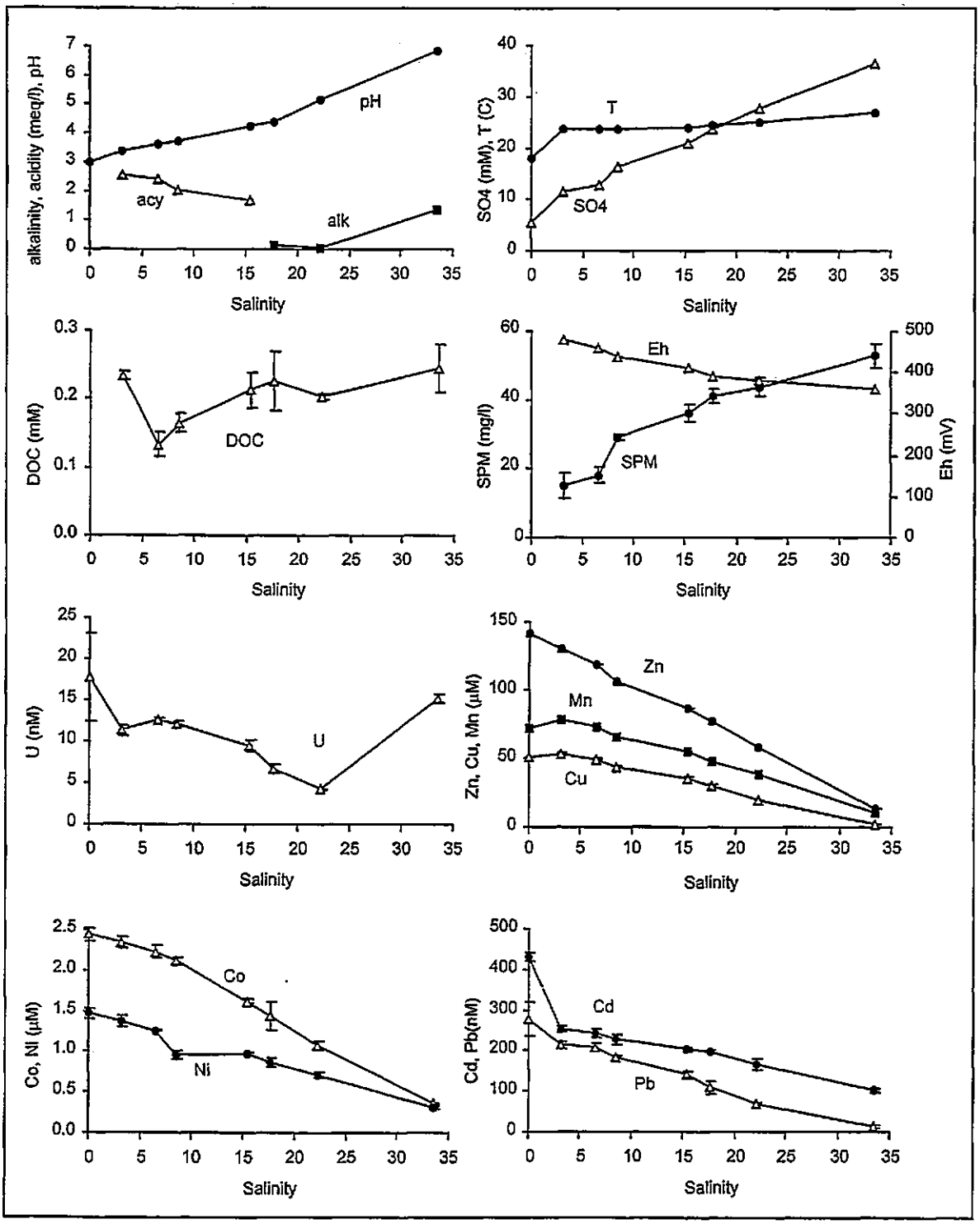

Figure 4.18 - TOROS 2: Sulphate, pH, alkalinity, acidity, Eh, temperature, SPM, DOC and total dissolved metal concentrations plotted versus salinity in the Ría del Odiel between Gibraleón and Huelva Bridge (samples OR 1-7, G1, June 1997). Error bars as for Figure 4.17.

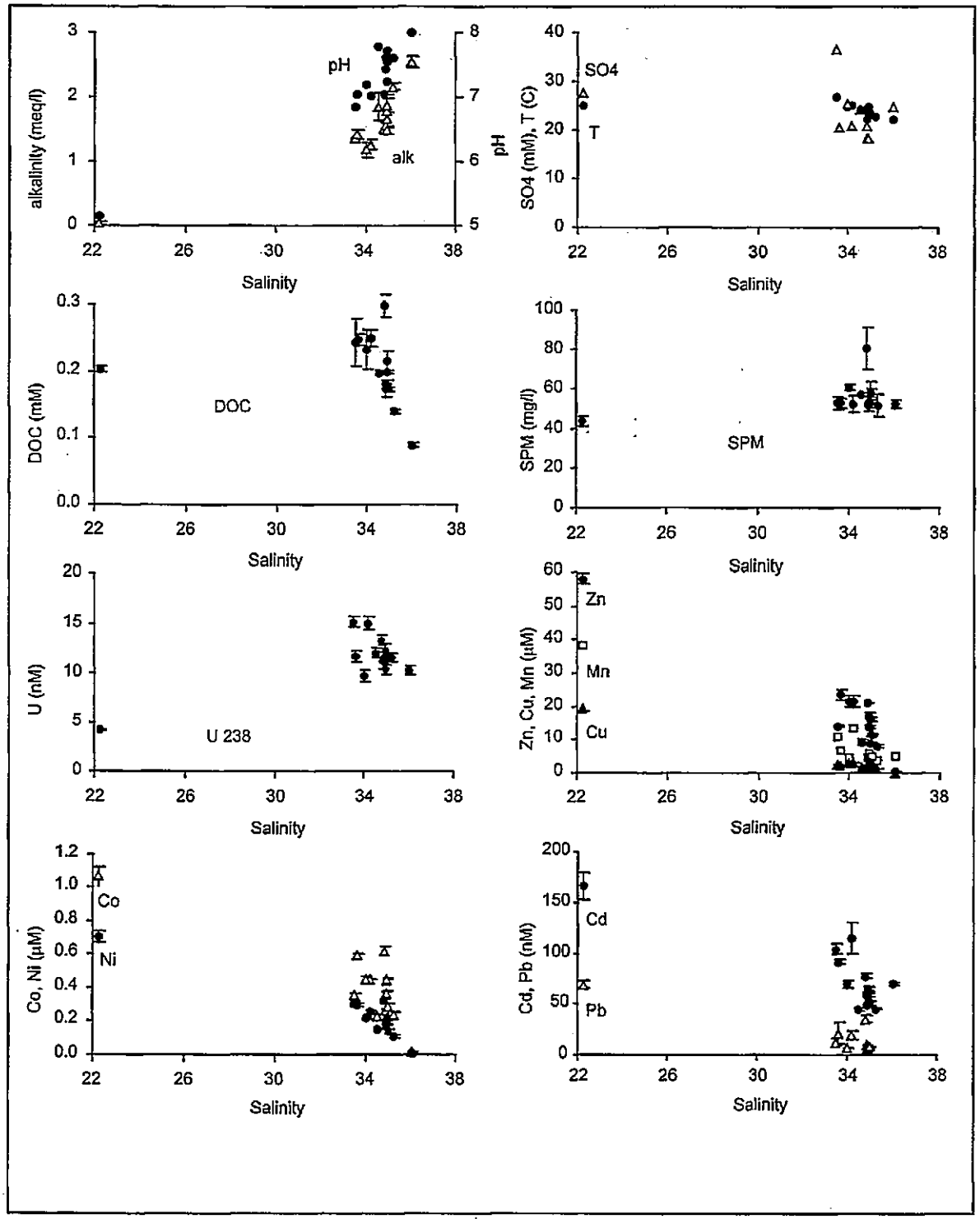

Figure 4.19 - TOROS 2: Sulphate, pH, alkalinity, acidity, temperature, SPM, DOC and total dissolved metal concentrations plotted versus salinity in the Huelva Ría (samples HR 1-13, OR 6-7, June 1997). Samples OR 6-7 were included to visualise the connection between the Ría del Odiel and Huelva Ría. Error bars represent the analytical error (± 1σ) calculated from three scans for ICP-MS analysis and repeat aliquots for voltammetric methods, respectively.

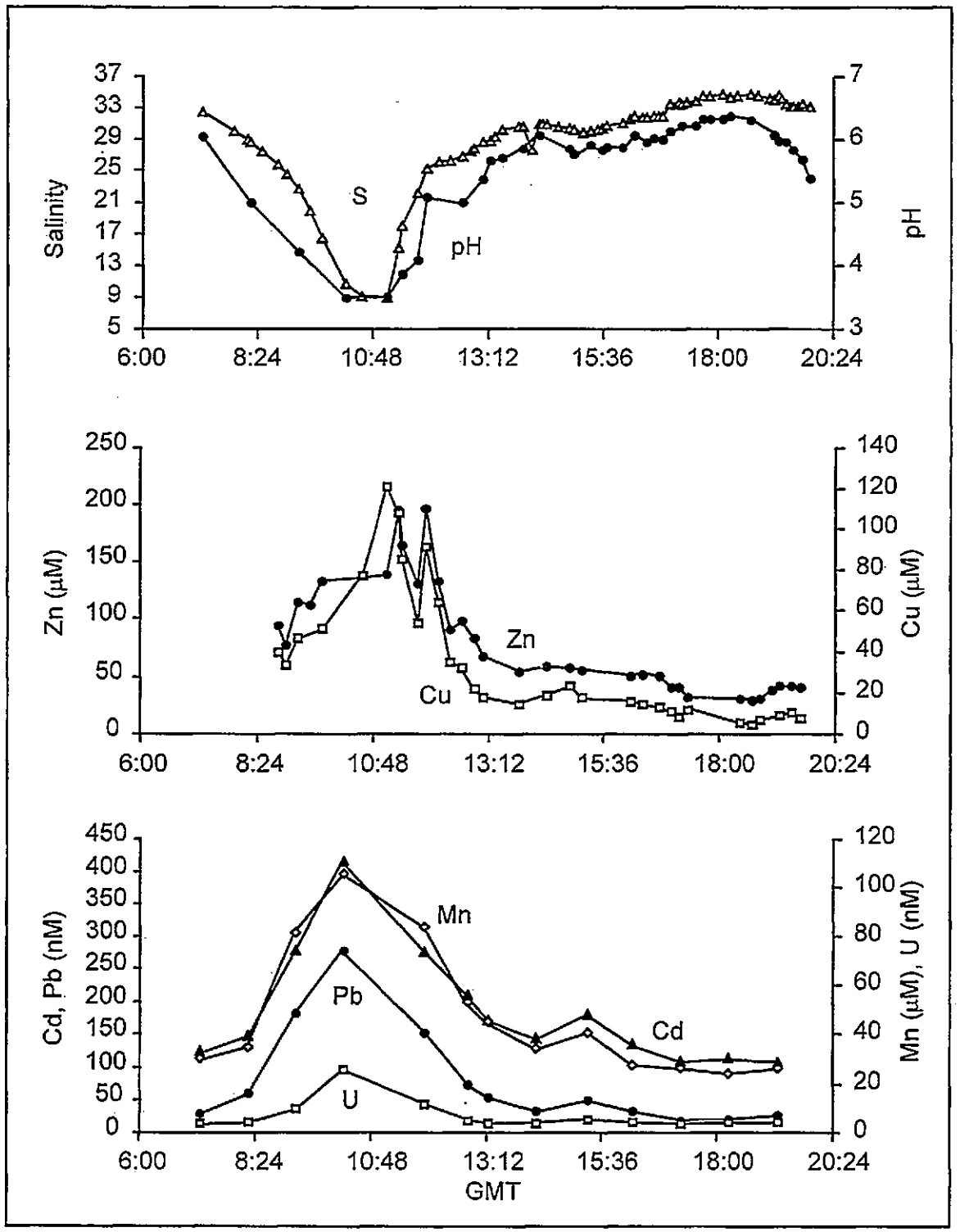

Figure 4.20 - TOROS 2: Tidal cycle study at Huelva Bridge between the Ría del Odiel and Huelva Ría. Salinity was calculated from conductivity measurements. Total dissolved Zn and Cu was measured on-line, Mn, Cd, Pb and U concentrations were determined in discrete samples. The analytical standard deviation were typically < 10% and were omitted to enhance the clarity of the graph. At Mazagón, high water was at 16:16 h and low water at 9:57 h and 22:23 h GMT.

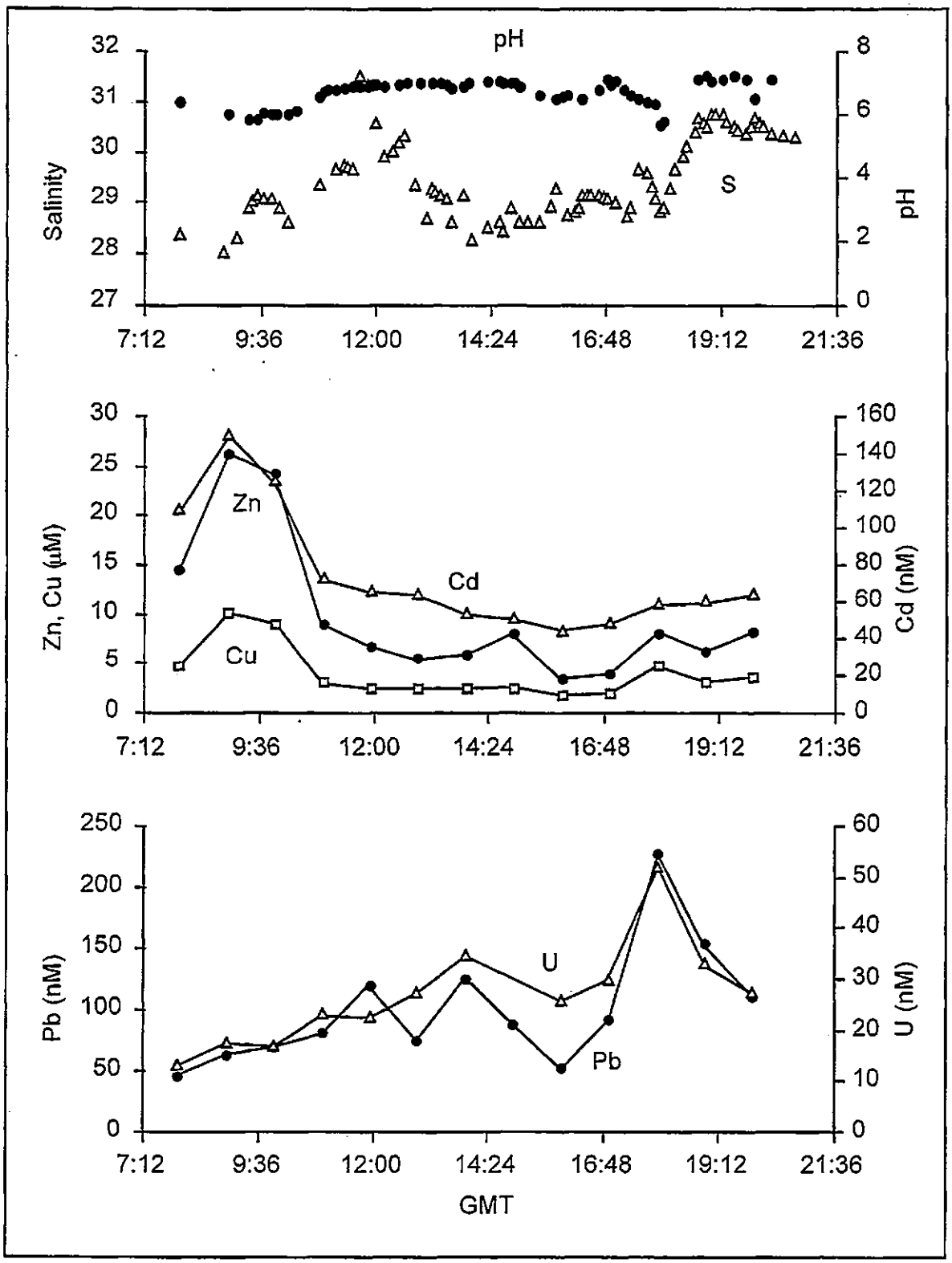

Figure 4.21 - TOROS 2: Tidal cycle study at La Rábida in the lower Ría del Tinto. Conductivity and pH measurements were carried out in 5 - 10 min intervals. The presented total dissolved concentrations of Zn, Cu, Cd, Pb and U were measured in discrete samples. The analytical standard deviation were typically < 10% and were omitted to enhance the clarity of the graph. At Mazagón, high water was at 14:59 h and low water at 8:43 h and 21:10 h GMT.

4.5.4 TOROS 3 - SPRING SURVEY

Dissolved metal concentrations, salinity, pH, Eh, temperature, total sulphate, DO and SPM concentrations in the Rio Tinto at Niebla and Rio Odiel at Gibraleon are given in Table 4.5. The salinity was calculated from chlorinity, which was supplied by Elbaz-Poulichet, as were sulphate concentrations (Elbaz-Poulichet, 1999a). Eh and DO were measured by Herzl (with field instrument and by Winkler titration, respectively, unpublished data). SPM was provided by López (Morales *et al.* 1999c).

Estuarine master variables (pH, alkalinity, acidity, Eh, temperature, SPM), DOC, SO_4 and total dissolved metal concentrations were plotted versus salinity for transects taken in the Ría del Tinto (Figure 4.22), the Ría del Odiel (Figure 4.23) and in Huelva Ría (Figure 4.24). Sulphate concentrations were supplied by Elbaz-Poulichet. Alkalinity, acidity, Eh and SPM were determined by Herzl.

Figure 4.25 shows results from on-line measurements of total dissolved Zn and Cu, and concentrations of Mn, Cd, Pb and U measured in discrete samples taken during a tidal cycle study at hourly intervals at Huelva Bridge. Salinity calculated from conductivity measurements, pH, DOC and SPM concentrations are also shown. Maxima in dissolved Zn, Cu, Ni and Co concentrations coincided with minima in salinity and pH, which occurred a short time ahead of low water at the mouth of the estuary. In contrast, the dissolved U minimum coincided with minima in pH and salinity, indicating the transport of U from a source downstream of Huelva Bridge during the flood tide.

Table 4.5 - TOROS 3: master variables and total dissolved metal concentrations in the fresh water end-members of the Rio Tinto (N 1) and Rio Odiel (G 1) in April 1998. The error given represents one standard deviation of the mean.

TOR-98-04-	Niebla, N1	Gibraleon, G1
Salinity[1]	0.03	0.01
pH	2.56	3.20
Eh (mV)[2]	551	552
T (°C)	15.3	15.7
SO_4 (mM)[1]	23.2	6.14
O_2 (mg l^{-1})[2]	20.3	8.06
SPM (mg l^{-1})[3]	15.5	-
Q_i (l s^{-1})[4]	80	380
Zn (µM)	355 ± 3	192 ± 10
Cu (µM)	175 ± 5	72.2 ± 2.2
Ni (µM)	1.15 ± 0.02	2.05 ± 0.03
Co (µM)	6.42 ± 0.68	4.66 ± 0.25
Cd (nM)	796 ± 8	424 ± 48
Mn (µM)	72.7 ± 2.6	130 ± 4
Pb (µM)	0.496 ± 0.016	1.3 ± 0.1
U (nM)	10.9 ± 0.3	18.2 ± 1.2

[1] From F. Elbaz-Poulichet, Univ. Montpellier II.
[2] From V. Herzl, University of Plymouth.
[3] From M. López, University of Huelva, sample at G1 did not yield enough SPM to be measured.
[4] Estimated from data supplied by J. A. Morales, University of Huelva.

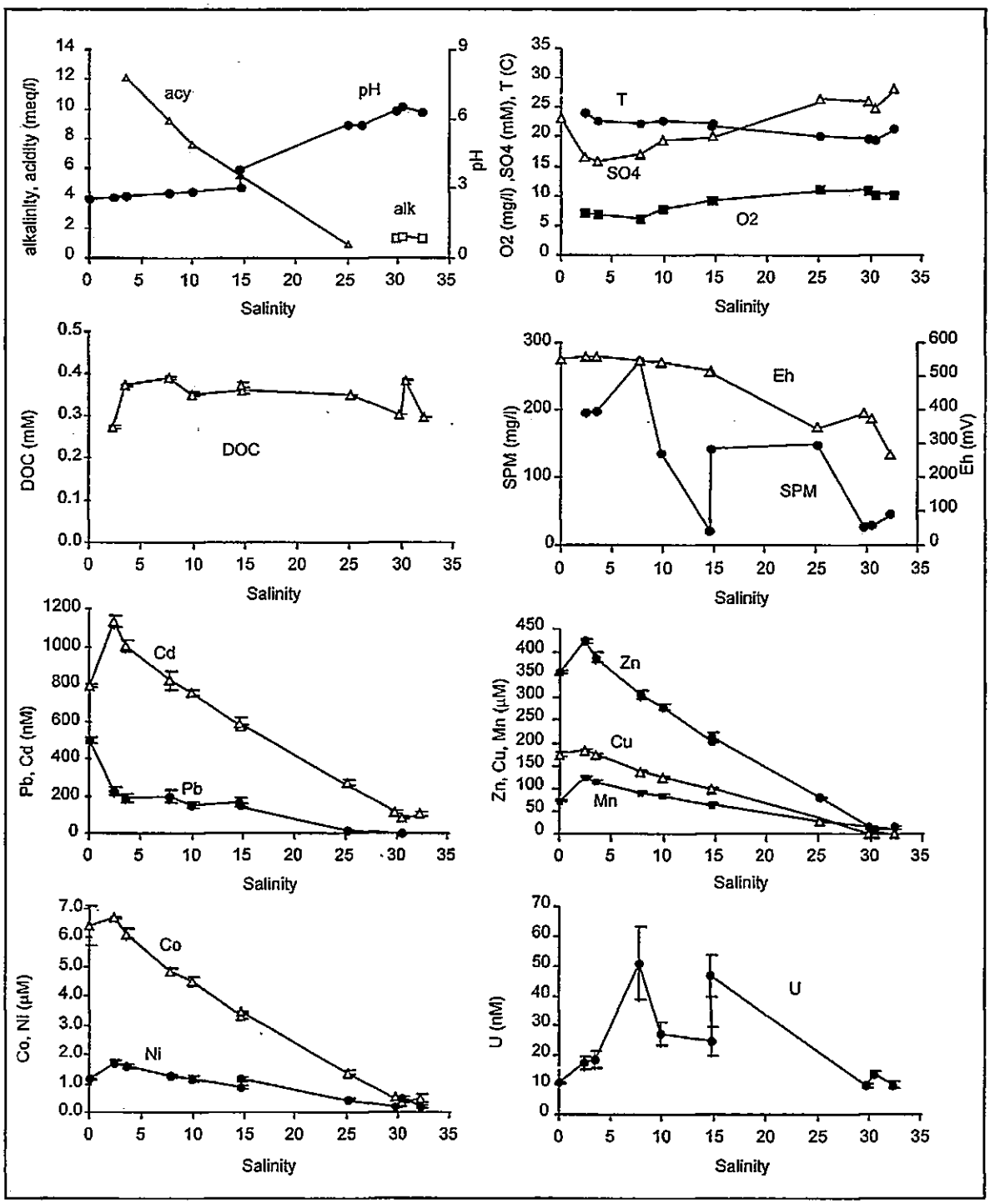

Figure 4.22 - TOROS 3: Sulphate, pH, alkalinity, acidity, Eh, temperature, SPM, DOC and total dissolved metal concentrations plotted versus salinity in the Ría del Tinto between Niebla and the confluence with Huelva Ría (samples TR 1-10, N1, April 1998). Error bars represent the analytical error (± 1σ) for three scans during ICP-MS analysis.

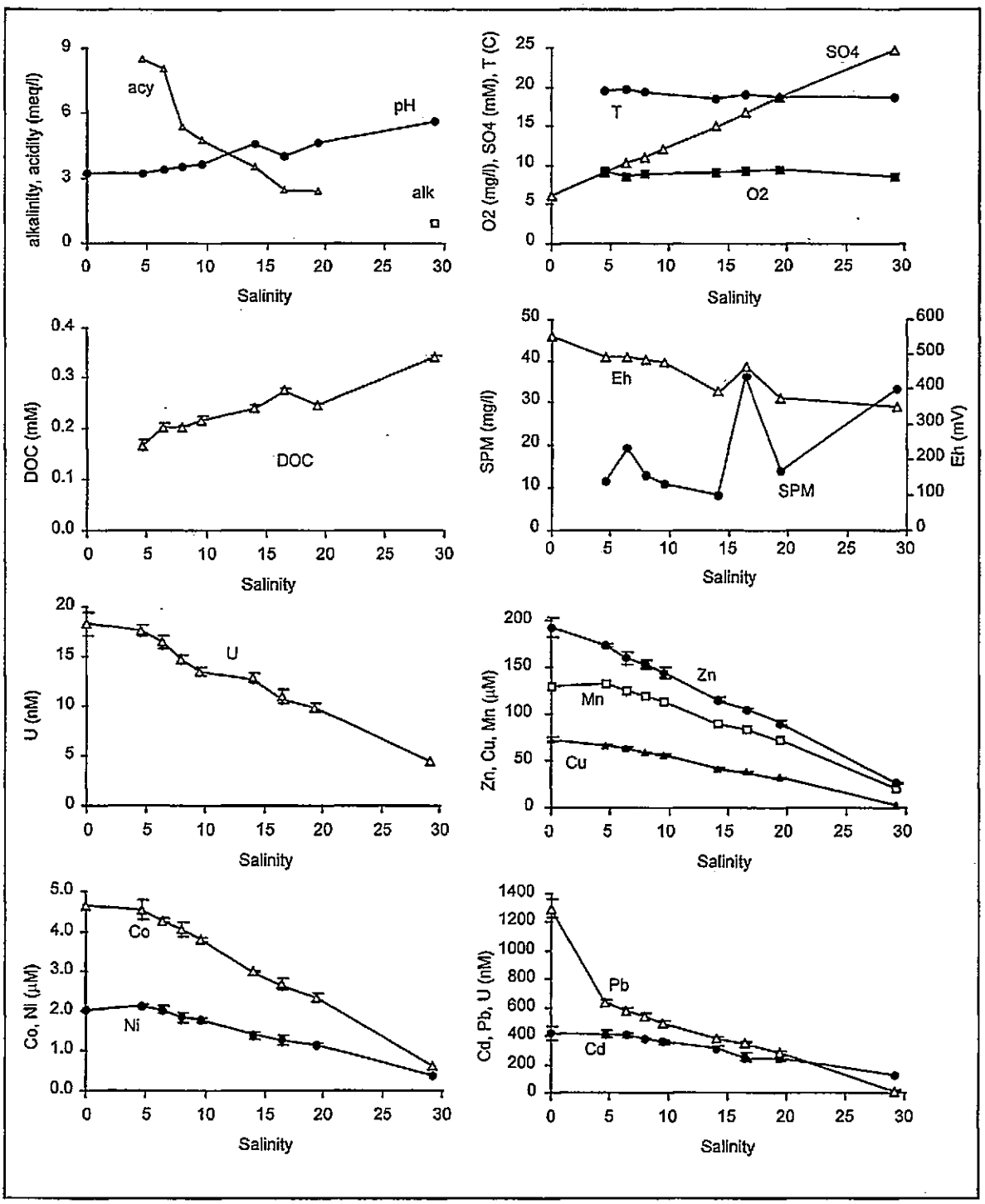

Figure 4.23 - TOROS 3: Sulphate, pH, alkalinity, acidity, Eh, temperature, SPM, DOC and total dissolved metal concentrations plotted versus salinity in the Ría del Odiel between Gibraleón and Huelva Bridge (samples OR 0-7, G1, April 1998). Error bars as for Figure 4.22.

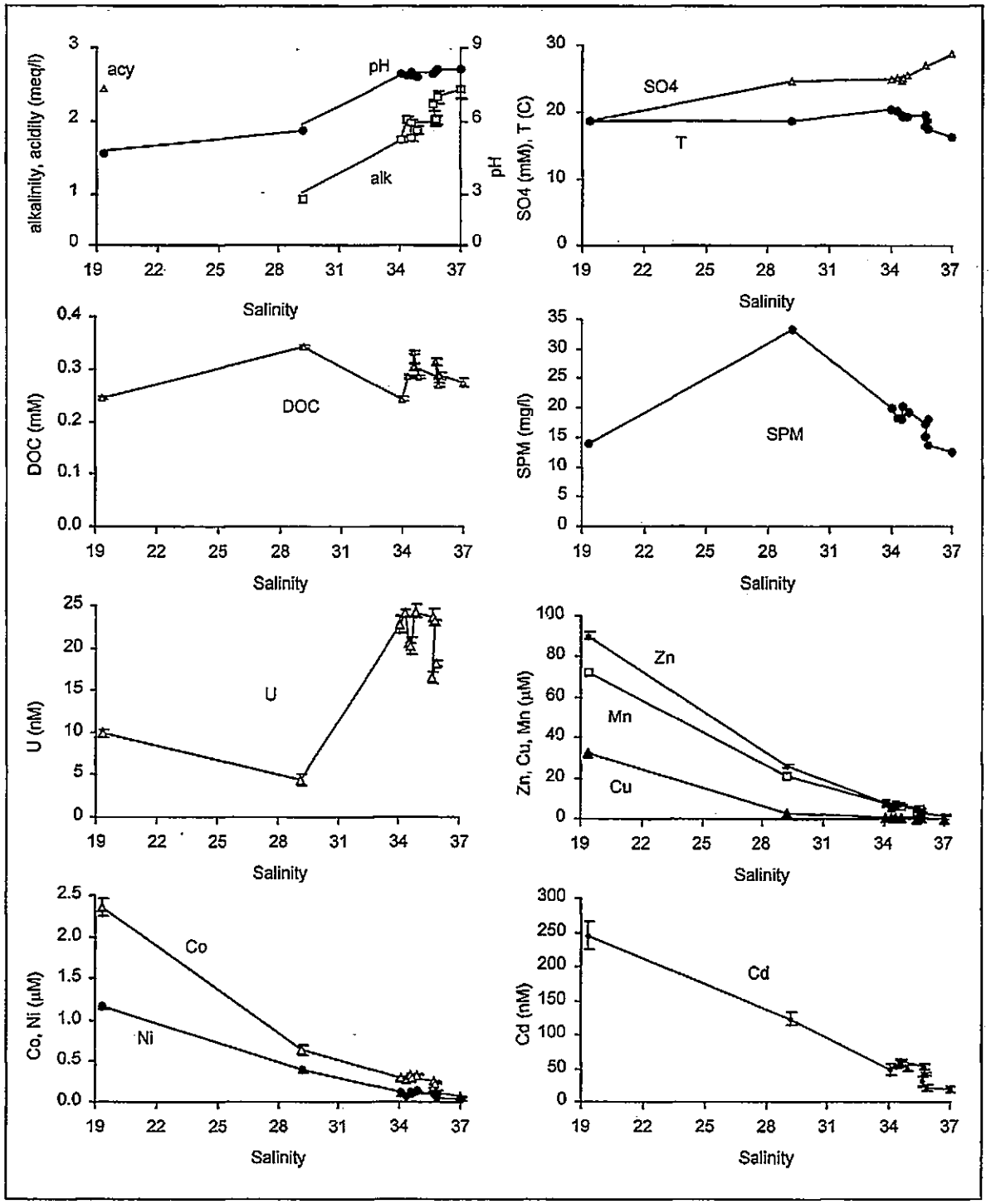

Figure 4.24 - TOROS 3: Sulphate, pH, alkalinity, acidity, temperature, SPM, DOC and total dissolved metal concentrations plotted versus salinity in Huelva Ría between Huelva Bridge and Mazagón (samples HR 1-13, April 1998). Error bars represent the analytical error (± 1σ) calculated from three scans for ICP-MS analysis and repeat aliquots for voltammetric methods, respectively.

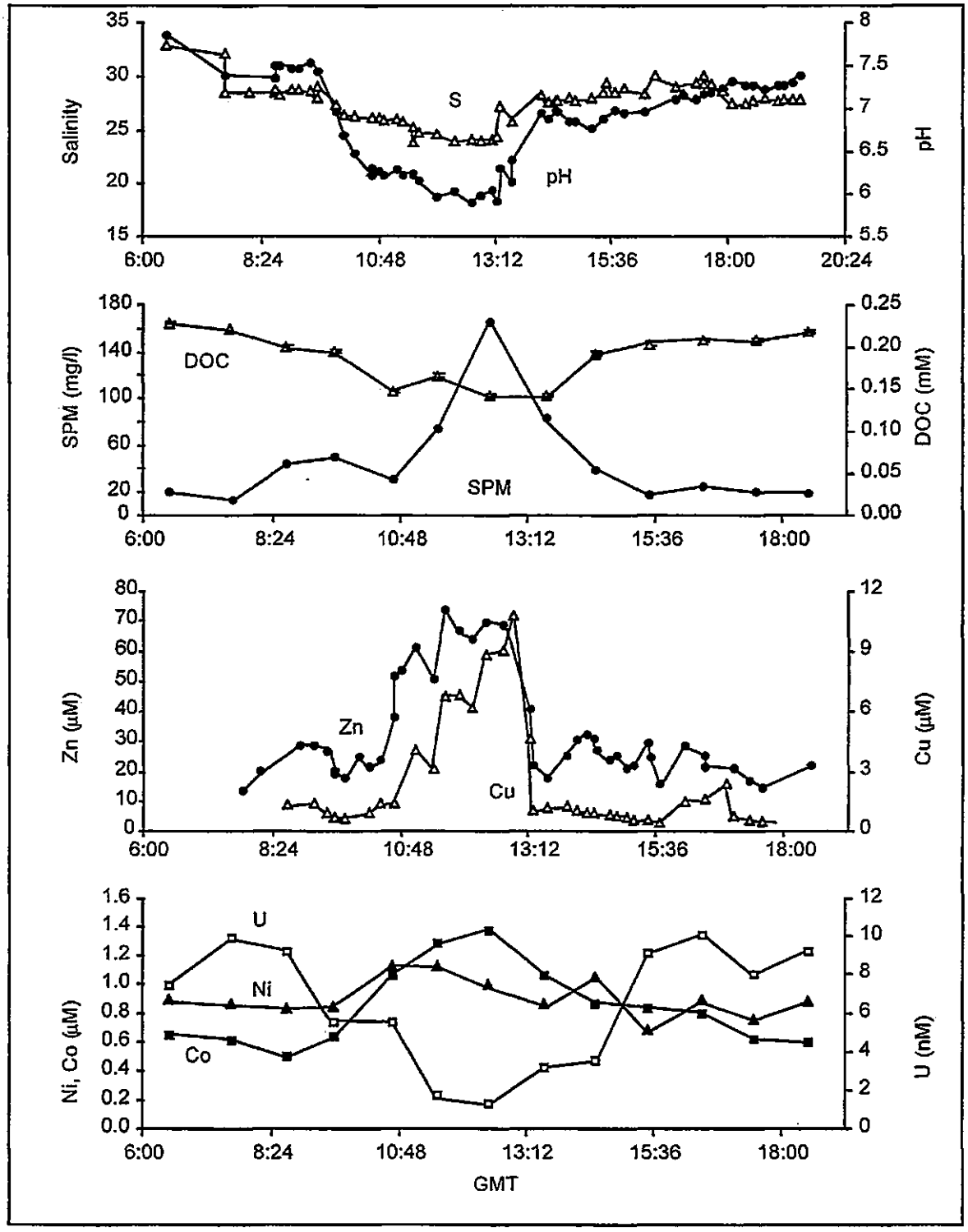

Figure 4.25 - TOROS 3: Tidal cycle at Huelva Bridge. Cu and Zn concentrations were measured on-line and total dissolved Mn, Cd, Pb and U concentrations were measured in discrete samples. The analytical standard deviation were typically < 10% and were omitted to enhance the clarity of the graph. At Mazagón high water was at 7:51 h and low water was at 13:58 h GMT.

4.5.5 TOROS 4 - AUTUMN SURVEY

Dissolved metal concentrations, salinity, pH, Eh, temperature, total sulphate, DO and SPM concentrations in the Rio Tinto at Niebla and Rio Odiel at Gibraleon are given in Table 4.6. The salinity was calculated from conductivity measurements. Table 4.7 gives the dissolved metal concentrations in samples taken from both rivers between their upper reaches in the Iberian Pyrite Belt and the respective fresh water end-members (Niebla and Gibraleón, Figure 4.12).

Estuarine master variables (pH, Eh, temperature and SPM) and total dissolved concentrations were plotted versus salinity for transects taken in the Ría del Tinto (Figure 4.26), the Ría del Odiel (Figure 4.27) and in Huelva Ría (Figure 4.28).

Figure 4.29 shows results from on-line measurements of total dissolved Zn and Cu, and concentrations of Mn, Cd, Pb and U measured in discrete samples taken at hourly intervals during a tidal cycle study at Huelva Bridge. Also shown are the development of salinity, pH, DOC and SPM concentrations over time. Maxima in dissolved concentrations of Zn, Cu, Cd, and Mn coincided with a minimum in pH, indicating low water. A second maximum in the Cu concentration was observed at mid-tide. The variability in salinity was low and did not reflect tidal stage, possibly because the water was not homogeneously mixed throughout the estuary, and the sampling location close to the bank of the estuary did not allow for a representative sample to be taken.

Table 4.6 - TOROS 4: master variables and total dissolved metal concentrations in the fresh water end-members of the Rio Tinto (N1) and Rio Odiel (G1) in October 1998. The error given represents one standard deviation of the mean.

TOR-98-10-	Niebla, N 1	Gibraleon, G 1
Salinity[1]	0.96	1.81
pH	2.26	2.83
Eh (mV)	606	482
SPM (mg l^{-1})	14.5	1.6
DOC (mM)	0.69 ± 0.02	0.15 ± 0.01
Q_i (l s^{-1})[2]	100	400
Zn (µM)	2590 ± 143	425 ± 6
Cu (µM)	856 ± 11	74.4 ± 1.8
Ni (µM)	16.8 ± 2.2	3.59 ± 1.22
Co (µM)	38.8 ± 0.9	8.53 ± 0.12
Cd (nM)	6007 ± 500	674 ± 48
Mn (µM)	775 ± 19	400 ± 3.09
Pb (µM)	0.635 ± 0.063	0.931 ± 0.061
U (nM)	71.7 ± 5.2	22.8 ± 3.0

[1] From conductivity measurements.
[3] Estimated from data supplied by J. A. Morales, University of Huelva.

Table 4.7 - TOROS 4: pH, Eh, temperature and total dissolved metal concentrations in the Rio Tinto (TR) and Rio Odiel (OR) between their source in the mining area and the estuary in October 1998. The error represents one standard deviation of the mean. nd - not determined, nr - not reliable.

Rio Tinto	TR E 1	TR E 2	TR E 3	TR E 4
Salinity	0.04	0.06	0.06	0.03
pH	2.60	2.42	2.27	2.35
Eh (mV)	nd	433	569	575
T(C)	nd	20.5	20.8	21.0
Zn (µM)	4098 ± 32	3351 ± 73	4861 ± 36	1555 ± 45
Cu (µM)	1505 ± 20	1339 ± 19	1481 ± 12	526 ± 5
Ni (µM)	18.9 ± 0.5	19.0 ± 1.5	21.8 ± 2.4	9.42 ± 0.77
Co (µM)	63.0 ± 1.0	53.2 ± 0.4	67.6 ± 0.4	23.4 ± 0.1
Cd (nM)	8915 ± 649	7572 ± 440	10840 ± 245	3280 ± 295
Mn (µM)	1034 ± 14	890 ± 5	1240 ± 12	460 ± 8
Pb (nM)	2604 ± 204	2252 ± 268	518 ± 30	603 ± 763
U (nM)	108 ± 13	93.4 ± 6.6	127 ± 5	43.3 ± 3.9
Rio Odiel	OR E 1	OR E 2	OR E 2 a	OR E 3
Salinity	0.02	0.03	0.03	0.02
pH	2.98	2.60	2.58	2.76
Eh (mV)	492	429	478	503
T(C)	20.7	22.8	21.3	20.6
Zn (µM)	590 ± 13	620 ± 13	780 ± 14	510 ± 4
Cu (µM)	356 ± 6	264 ± 7	312 ± 7	77 ± 0.4
Ni (µM)	7.24 ± 1.03	20.5 ± 0.4	13.5 ± 4.7	3.84 ± 0.48
Co (µM)	19.0 ± 0.7	18.6 ± 0.8	21.0 ± 0.4	8.58 ± 0.13
Cd (nM)	2064 ± 278	1808 ± 101	2224 ± 186	811 ± 245
Mn (µM)	610 ± 13	694 ± 13	797 ± 3	440 ± 13
Pb (nM)	nr	1265 ± 109	1480 ± 94	1111 ± 79
U (nM)	69.3 ± 4.5	70.0 ± 5.3	76.8 ± 16.0	18.0 ± 1.3

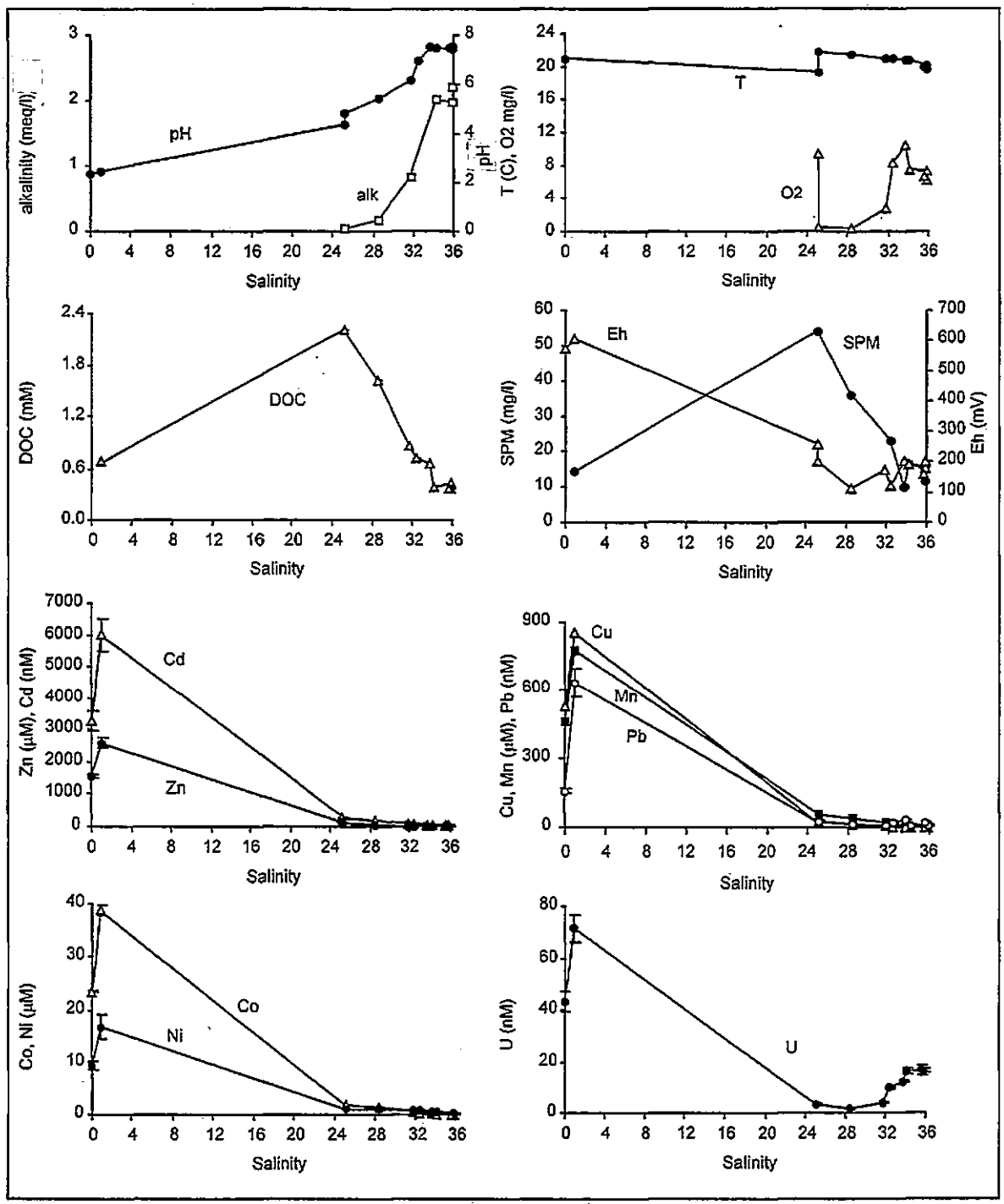

Figure 4.26 - TOROS 4 : pH, alkalinity, acidity, Eh, temperature, SPM, DOC and total dissolved metal concentrations plotted versus salinity in the Ría del Tinto between Niebla and the confluence with Huelva Ría (samples TR 1-10, N1, October 1998). Error bars represent the analytical error (± 1σ) for three scans during ICP-MS analysis.

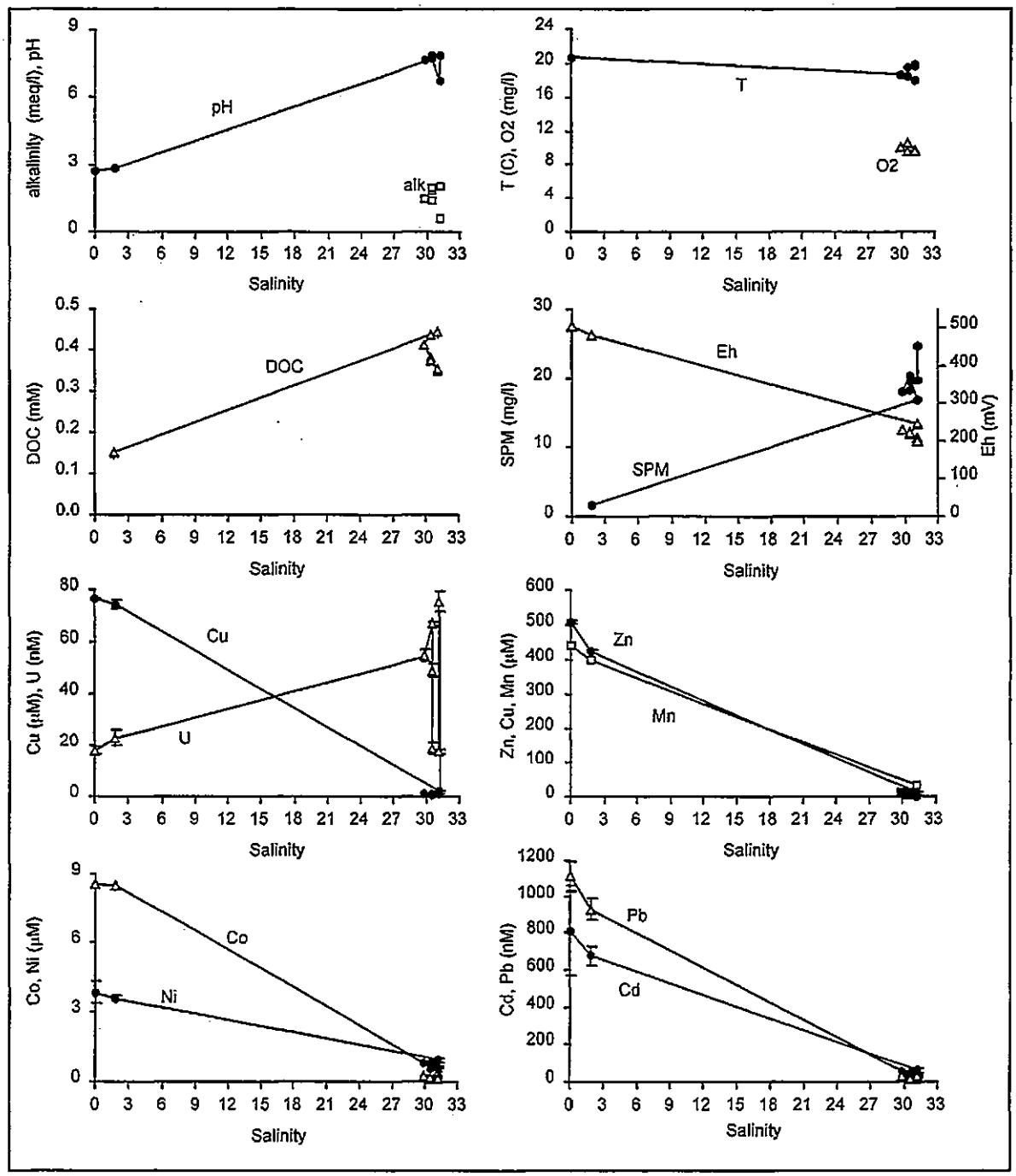

Figure 4.27 - TOROS 4: pH, alkalinity, acidity, Eh, temperature, SPM, DOC and total dissolved metal concentrations plotted versus salinity in the Ría del Odiel between Gibraleón and Huelva Bridge (samples TR 1-7, G1, October 1998). Error bars and alkalinity/acidity as for Figure 4.26.

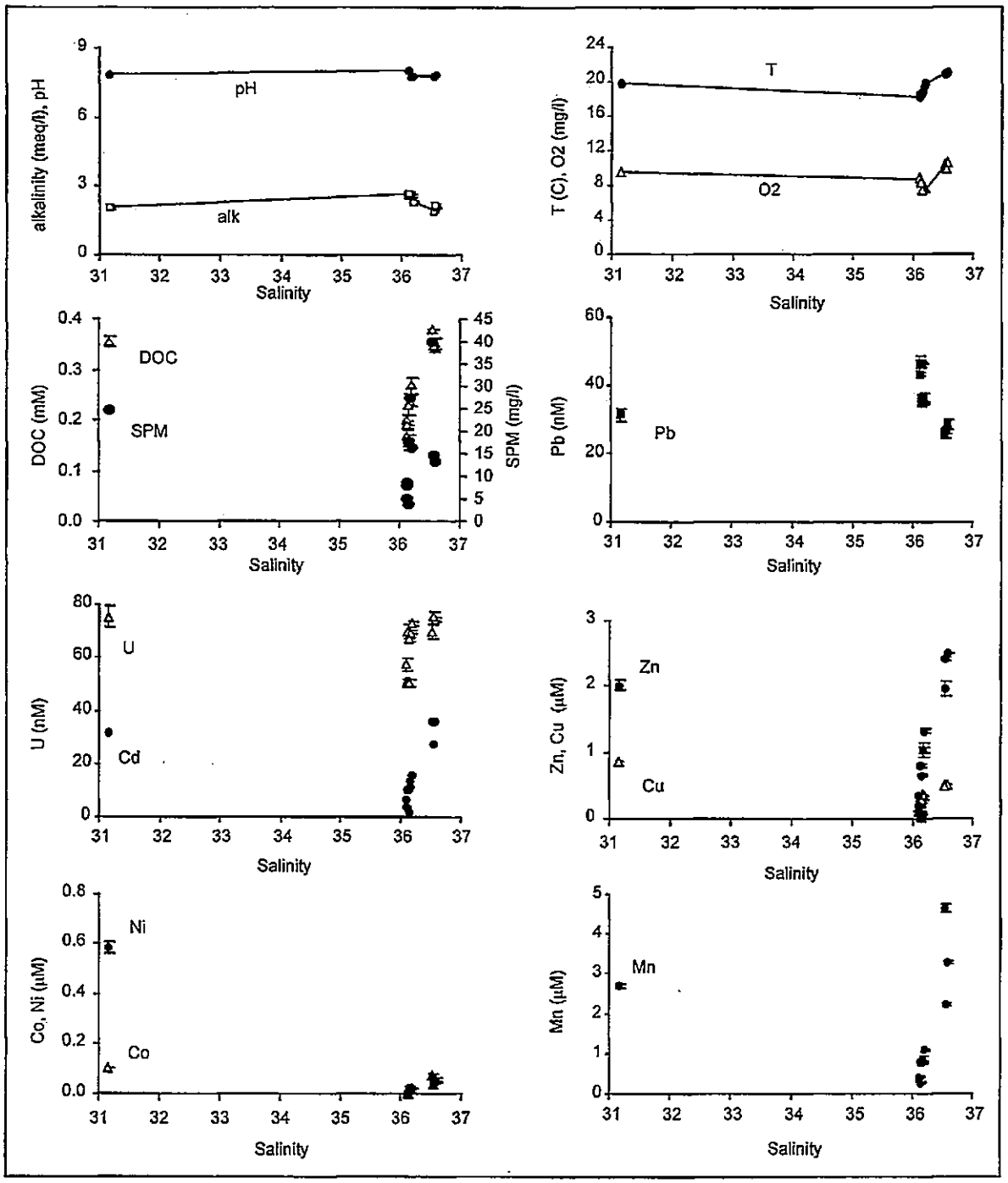

Figure 4.28 - TOROS 4: pH, alkalinity, acidity, temperature, SPM, DOC and total dissolved metal concentrations plotted versus salinity in Huelva Ría between Huelva Bridge and Mazagón (samples HR 1-3, 7-13, G48, October 1998). Error bars represent the analytical error (± 1σ) calculated from three scans for ICP-MS analysis and repeat aliquots for voltammetric methods, respectively.

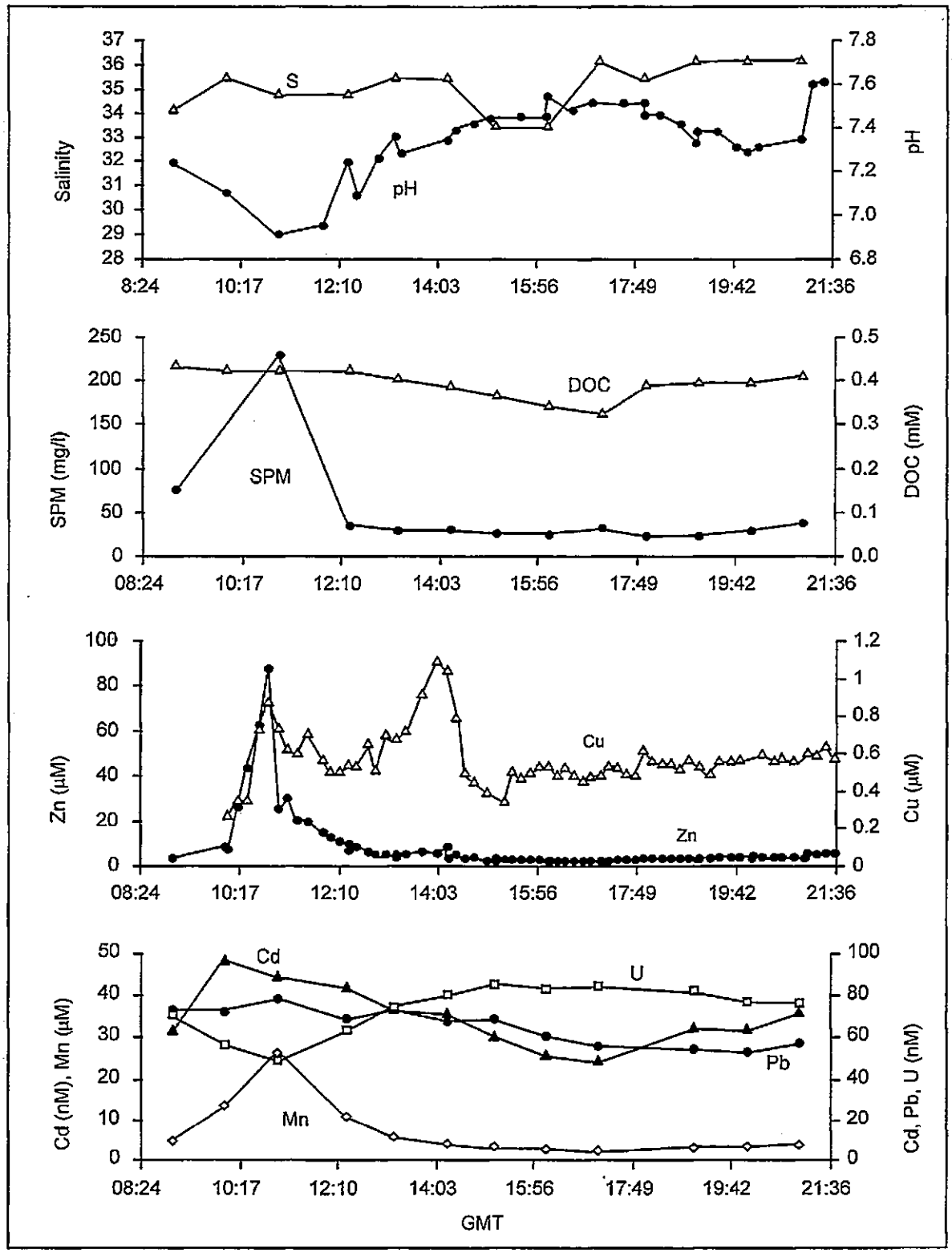

Figure 4.29 - TOROS 4: Tidal cycle at Huelva Bridge. Salinity was determined from conductivity measurements. Total dissolved Zn and Cu were measured on-line, Mn, Pb, Cd and U were determined in discrete samples. The analytical standard deviation were typically < 10% and were omitted to enhance the clarity of the graph. At Mazagón low water was at 11:34 h and high water was at 17:52 h and GMT.

4.6 Discussion

4.6.1 Fresh Water End-members

4.6.1.1 Source and Magnitude of Contamination in the Rivers

The fresh water end-members showed the typical characteristics of small rivers strongly affected by acid mine drainage (AMD). The low pH values in the Rio Tinto and Rio Odiel (pH 2.21 - 2.56 and pH 2.83 - 3.20, respectively, Table 4.3 - Table 4.6) correspond to the range commonly reported for AMD (pH 2.0 - 3.5) (Bigham *et al.* 1990). Sulphate was the dominant anion in the rivers (Rio Tinto: 8.6 - 27.1 mM; Rio Odiel: 5.5 - 12.5 mM). The pH values, metal and sulphate concentrations in the rivers were comparable to other strongly polluted water courses and other mine drainage systems (Table 4.8).

Dissolved concentrations of Al, Pb, Mn, Fe, Zn, Cu, Ni, Co and Cd resembled previous observations in the Rio Tinto and Rio Odiel (Table 4.8 and van Geen *et al.* (1997): 3.2 mM Al, 240 μM Mn, 19 μM Co and 0.43 μM Pb).

Reported activity of U isotopes illustrated that levels in the Rio Tinto and Rio Odiel exceeded those in unperturbed river systems (Martinez-Aguirre *et al.* 1994b). More than 99% of the total ^{238}U and ^{234}U were present in the dissolved phase, which was the result of the dissolution of U solids at the low pH values encountered in the Tinto/Odiel system (Martinez-Aguirre *et al.* 1994b). At low pH values and under oxidising conditions U is present as U(VI) and forms soluble cationic species, e.g. uranyl ion, UO_2^{2+} (Sandino and Bruno, 1992). In comparison to other rivers, the dissolved U concentrations in the Rio Tinto and Rio Odiel were more than one order of magnitude higher (11 - 72 nM U in fresh water end-members) than the average of value found in river water world-wide (ca. 1 nM U, Martin and Whitfield, 1983).

Table 4.8 - Total dissolved metal concentrations and pH values in various AMD affected waters. 'nr' - not reported. 'ca.' - values estimated from graphs. Values marked with * refer to concentrations given in mmol kg^{-1} for Fe and SO_4, and in µmol kg^{-1} for Zn, Cu, Cd in the source.

Location	pH	Fe (mM)	Zn (µM)	Cu (µM)	Cd (µM)	SO_4 (mM)
Rio Tinto[1]	1.5 - 2.1	nr	770 - 1500	530 - 950	3 - 5	nr
Rio Tinto[2]	2.6	8.8*	920*	390*	2*	30*
Rio Tinto[3]	2.7	3.0	520	222	1.3	nr
Guadiamar[4]	< 3	ca. 0.02 - 11	1700	255	nr	nr
Afon Goch[5]	< 3	0.7 - 4.6	241 - 645	71 - 949	0.09 - 17	nr
Berkeley Pit[6]	2.8	6.9	4300	2500	nr	60
Parc Mine[7]	nr	nr	41	nr	2.4	nr
Daylight Creek[8]	ca. 2.7	ca. 4	ca. 1300	ca. 130	ca. 7	ca. 11
Deep Adit[9]	3.3 - 3.8	1.5 - 4.4	887 - 1575	16 - 160	1.7 - 5.3	13 - 19
Levant Mine[10]	2.1 - 4.4	0.02 - 6.5	nr	nr	nr	25 - 117
Carnon[11]	3.1 - 5.6	0.11 - 0.52	109 - 184	4.1 - 1.75	nr	nr
Aitik Cu Mine[12]	3.8	0.04	89	299	nr	14
King River[13] (max)	4.6	0.152	nr	110	nr	nr

[1] River water (Leblanc *et al.* 1995).
[2] River water (van Geen *et al.* 1997).
[3] River water, mean of four surveys in 1997/98 (Medio Ambiente, 1998).
[4] River water, upper reaches, Spain (Albaiges *et al.* 1987).
[5] River water, Wales, UK (Boult *et al.* 1994).
[6] Mining pit lake, Montana, USA (Miller *et al.* 1996).
[7] Mine tailings leachate, Wales, UK (Gao and Bradshaw, 1995).
[8] Mine tailings leachate, New South Wales, Australia (Chapman *et al.* 1996).
[9] Copper and sulphur mine adit, Avoca mining area, Republic of Ireland (Gray, 1998).
[10] Mine drainage, Cornwall, UK (Bowell and Bruce, 1995).
[11] River Carnon, Cornwall, UK (Johnson, 1986).
[12] Mine tailings leachate, Sweden (Stromberg and Banwart, 1994).
[13] River water, affected by AMD form Mt Lyell Cu mine, Tasmania, Australia (Featherstone and O'Grady, 1997).

The low pH and high sulphate and dissolved metal concentrations in the two rivers can be attributed to metal sulphide oxidation in the mining district of the Iberian Pyrite Belt. Conditions that favoured sulphide oxidation in this region include the warm arid climate, resulting in the under-saturation of mine tailings with water and the availability of oxygen therein (Stromberg and Banwart, 1999; Miller *et al.* 1996). In addition, the large amount of mine tailings within the river catchments provide a high surface area. Although redox conditions and dissolved oxygen in the rivers were not measured during all surveys, there was no evidence for anaerobic/reducing conditions in the waters at any time.

The pH of AMD is partially controlled by the weathering of minerals that co-exist with the sulphides, and which may consume or produce hydrogen ions upon dissolution. The high Al concentration in rivers with low pH values can be attributed to the weathering of aluminosilicates (sandstones, clays, slates or silicious ore) in waste rocks (Banks *et al.* 1997). Compared to metal sulphides, the weathering rate of silicates is slow (Stromberg and Banwart, 1994), and the exposure of carbonates to weathering was probably low in the catchments of the Rio Tinto and Rio Odiel. Therefore, alkalinity generation from the dissolution of silicates and carbonates in this AMD system was limited.

Strong sources for Zn, Cu, Pb, Co, Cd, Mn and U were evident in the upper reaches of the Rio Tinto and Rio Odiel during the TOROS 4 survey (Table 4.7). This was also evident in published data (Hudson-Edwards *et al.* 1999; Nelson and Lamothe, 1993) and quarterly surveys of water quality conducted by the local environment agency (Medio Ambiente, 1998). An example is given in Figure 4.30, which shows high metal concentrations in two channels (Stations T3 and T3A, locations see Figure 4.12) that supply tailings leachate (pH 1.6 - 2.3) to the upper Rio Tinto (data from Medio Ambiente, 1998).

Dissolved levels of Fe Zn, Cu, Co, Cd and sulphate were consistently higher and pH values lower in the Rio Tinto, compared to the Rio Odiel. This may be explained by the less intense mining in the catchment of the Rio Odiel and a dam in the upper reaches of the Rio Odiel that partially retains eroded material (Nelson and Lamothe, 1993). In addition, overflow from an alkaline mine tailings pond (*Embede de Gossan*, pH 9 - 10) enters the headwaters of the Rio Odiel (Figure 4.12). This input is comparatively depleted in metals and will result in the dilution of the metal rich waters from the upper Odiel and a slight increase in pH, which may lower the solubility of metals.

Fluctuations of dissolved Zn, Cu, Cd, Ni, Co and Mn concentrations along the length of both rivers were observed in October 1998 (Table 4.7) and are evident in Figure 4.30. The lowest metal levels were observed farthest downstream, at Niebla and Gibraleón. The highest concentrations of Zn, Cu, Cd and Pb in river sediments (Table 4.9) have been reported for the headwaters of the Rio Tinto and Rio Odiel (Hudson-Edwards *et al.* 1999; Medio Ambiente, 1998; Nelson and Lamothe, 1993). Hudson-Edwards *et al.* showed that primary minerals derived from mine tailings (purple-red alluvium) contained higher concentrations of Zn, Cu, Pb and Mn, compared to secondary minerals formed in the stream bed. The down stream trend of decreasing dissolved and sediment metal concentrations could be the combined effect of a limited transfer of dissolved metals into solid phases, the mixing with less polluted water (seepage or tributaries), the leaching of metals from sediment and the progressive mixing of contaminated with less contaminated sediment with increasing distance from the mining area.

Mid-river increases of dissolved trace metal levels may be attributable to the in-stream oxidation of metal sulphide grains and a flux of metal rich fluids from suboxic or anoxic sediments in the Rio Tinto, and/or to the contribution of dissolved metals from AMD-polluted tributaries in the Rio Odiel (e.g. via the Rio Oraque, Figure 4.2 and Figure

4.12). Similar fluctuations have been observed by Nelson and Lamothe (1993) and the Medio Ambiente (1998).

Dissolved Ni was found to be less enriched in the upper reaches of the rivers compared to the other trace metals studied. This is consistent with the relatively low Ni content in the mineralisation of the river catchments. Nickel concentrations in the dissolved phase (Table 4.7) and in the sediments (Table 4.9) (Medio Ambiente, 1998) of the two rivers were lower in the headwaters, compared to downstream sites. This suggests inputs of Ni to the system from additional sources, possibly surrounding soils (Van Geen *et al.* 1997) or the dissolution of river bed rock at low pH (Elbaz-Poulichet *et al.* 1999). The relatively constant concentrations of Mn in the dissolved phase and sediments (Medio Ambiente, 1998) and its low concentration in secondary minerals in the alluvium (Hudson-Edwards *et al.* 1999) suggests that the main source of this metal may be the bed rock, rather than the mining area and that it is not removed from solution within the river.

The high sediment concentrations of Pb reported in Table 4.9 (Hudson-Edwards *et al.* 1999; Medio Ambiente, 1998; Nelson and Lamothe, 1993) and the continuously decreasing dissolved concentrations (Table 4.7) of this metal in the rivers reflect the low mobility of Pb sulphides, the low solubility of oxidised Pb species (Gray, 1998) and the affinity of Pb for solid phases.

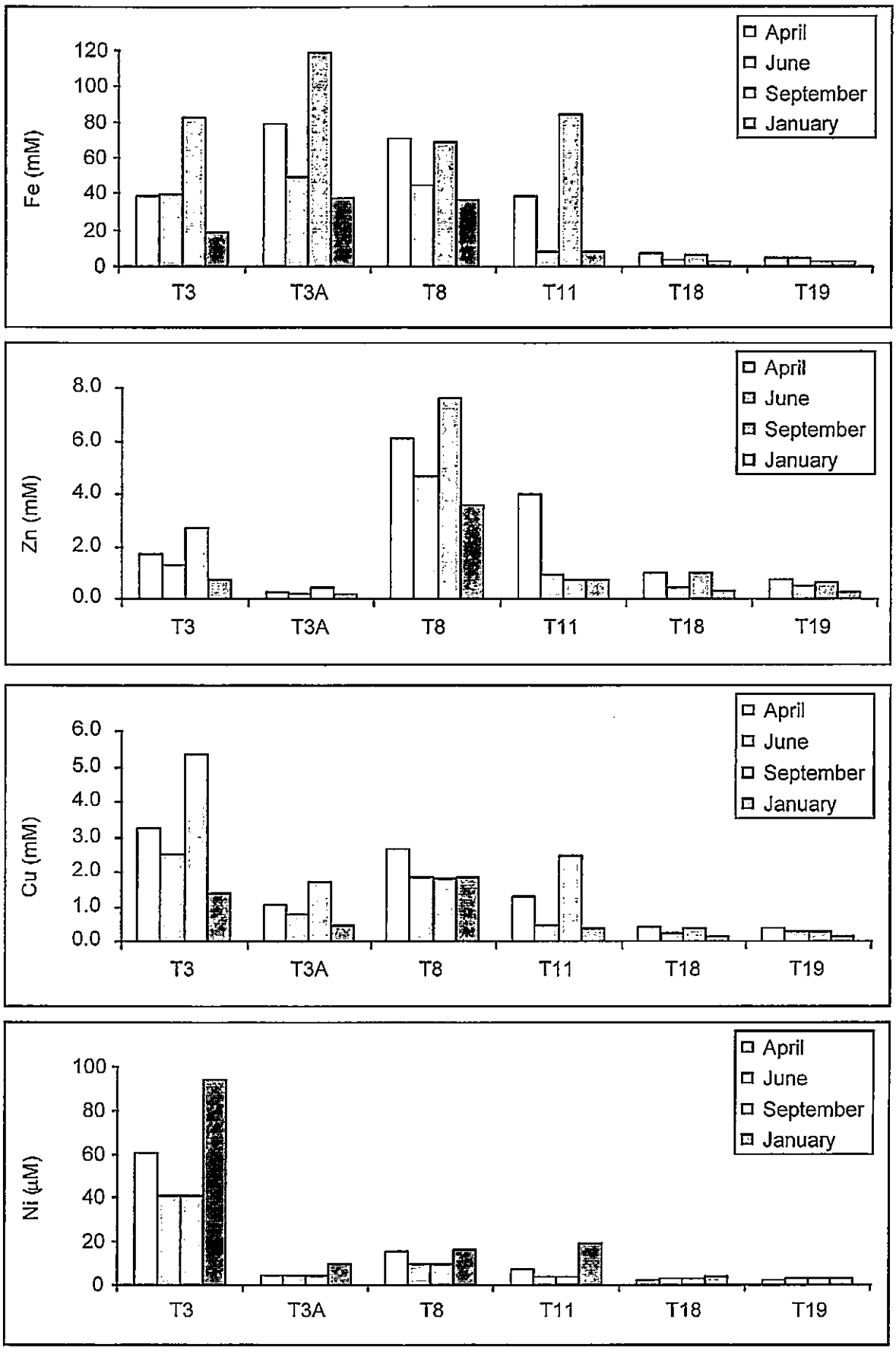

Figure 4.30 - Graphs prepared from data given in the annual survey report for 1997 by the Medio Ambiente (Medio Ambiente, 1998). Dissolved Fe, Zn, Cu and Ni in the Rio Tinto (stations T8, T11, T18 and T19), and two AMD drainage channels (stations T3 and T3A) for April, June and September 1997 and January 1998. The location of the sampling stations are marked on the map in Figure 4.12.

Table 4.9 - Metal concentrations in sediments (< 63 μM) of the Rio Tinto (T..) and Rio Odiel (O..) reported for the year 1997 analysed by atomic absorption spectroscopy (Medio Ambiente, 1998). Locations of the sampling sites are given in Figure 4.12. All concentrations are given in mg kg^{-1} sediment.

Medio Ambiente	Mn	Zn	Cu	Cd	Pb	Ni
T 3	129	510	1080	3.2	1110	3
T 8	95	1480	977	4.4	13400	9
T 11	140	843	731	2.5	7140	10
T 18	166	547	647	1.7	3000	12
T 19	168	340	352	2.3	462	6
O 9	442	424	911	0.9	712	9
O 19	306	531	1200	0.6	1940	12
O 35	387	323	397	< LOD	632	24
O 26 *	363	392	436	< LOD	210	18
Nelson *et al.*[1]	Mn	Zn	Cu	Cd	Pb	Ni
Rio Tinto	150 - 300	< 200 - 3000	150 - 1500	0.1 - 7	100 - 2000	< 5 - 15
Rio Odiel	150 - 1500	< 200 - 1500	150 - 1500	0.1 - 7	100 - 2000	7 - 150
H.-E. *et al.*[2]	Mn	Zn	Cu	As	Pb	Fe
Fe cement	35	480	320	230	1400	94000
Orange	26	27	84	750	3100	68000
Purple	36 - 140	60 - 1200	200 - 1500	160 - 250	1200 - 7600	5300 - 47000

* O 26 was taken in Rio Oraque, a tributary to the Rio Odiel (between station O19 and O35).
[1] Metal concentrations in river sediment were analysed with semiquantitative spectrographic analysis. '<' indicates values below the lower limit of detection (Nelson and Lamothe, 1993).
[2] Metal concentrations in alluvium of the Rio Tinto. Analysis were carried out in Fe-rich cement from the upper reaches, orange laminated and tailings-derived purple-red alluvium from the lower Rio Tinto (Hudson-Edwards *et al.* 1999).

4.6.1.2 River Flow and Seasonal Variability

River discharge in Huelva Province is directly related to rainfall (Morales, 1998b), which varies considerably between the seasons and between years (Figure 4.3). Therefore, the volume of AMD and 'clean' water entering from tributaries and hence the composition of the Rio Tinto and Rio Odiel will be influenced by precipitation. However, meteorological data (Morales, 1999b) indicated that all surveys were carried out after periods of low or no rainfall, which was evident in similar low river flows encountered during all surveys.

Dissolved trace metal concentrations in the fresh water end-members were higher and more variable in autumn and winter (e.g. Rio Tinto: 0.61 - 2.59 mM Zn, 1.38 - 6.01 μM Cd), compared to spring and summer surveys (e.g. Rio Tinto: 295 - 355 μM Zn, 782 - 796 nM Cd). Additional data from a limited sampling campaign during high river flow in February 1998 was provided by Morley and Elbaz-Poulichet (unpublished data, Table 4.10). The February survey showed that with increased river flow the observed pH values for both rivers were higher and the total dissolved concentrations of Mn, Cu, Ni, Cd and U below those of the autumn/winter TOROS surveys, but largely comparable with values observed during the spring/summer surveys. A survey of the Rio Tinto carried out by Garcia-Vargas *et al.* (1980, reported in: Nelson and Lamothe, 1993) showed higher dissolved Cu, Zn, Fe and Mn concentrations in dry seasons, compared to wet seasons. However, the paper does not indicate whether the survey was carried out at the beginning (autumn) or end (late winter) of the wet season. Dissolved Fe, Zn, Co and Ni concentrations in the rivers during the hydrological year 1997/98 (Figure 4.30, Medio Ambiente, 1998) were highest in September and lowest in January.

Table 4.10 - pH and total dissolved total dissolved metal concentrations in the Rio Tinto at Niebla and Rio Odiel at Gibraleón in February 1998. The samples were collected by N. Morley, the analysis carried out by F. Elbaz-Poulichet.

February 1998	Niebla	Gibraleon
pH	2.94	3.63
Cu (μM)	130	70
Ni (μM)	0.76	1.57
Cd (nM)	590	290
Mn (μM)	48.1	80.6
U (nM)	13.7	11.3

The presented evidence suggests a seasonal cycle. At the height of the dry, warm season a shortage of moisture within mine tailings prevented the formation of leachate at sufficient quantities to reach the rivers. As a consequence, lower dissolved metal concentrations were observed in the rivers. At the beginning of the rainy season the amount of AMD entering the rivers increased, as highly concentrated leachate in tailing ponds and ditches collected during dryer periods was washed into the rivers, lowering the water pH. The higher water velocity carried more eroded material from the mining area into the rivers and led to the re-suspension of bed sediments. It is likely that metal desorption, acid leaching and dissolution from suspended particles added to the dissolved metal load. The disturbance of sediment may have released metal-rich interstitial waters and exposed deeper anoxic sediment zones to oxidising conditions in the water column. Prolonged intense precipitation resulted in the gradual reduction of dissolved and suspended metal concentrations in the rivers. This occurred because dilution took effect and river sediments would have been scoured from the river bed and transported out of the system. As a result, comparatively low dissolved metal concentration and rivers devoid of ochre precipitates would be observed at the end of the wet season. With lower precipitation during spring, dissolved metal concentrations increased towards summer and the more quiescent river flow allowed the accretion of ochre in the river bed.

Similar cycles of river-flow related fluctuations of dissolved metal loads have been observed in the Rhone river (Elbaz-Poulichet *et al.* 1996), in acidic woodland streams in New Jersey (Sherrell and Ross, 1999) and a number of AMD-affected systems. For example, the mobilisation of ochre from the river bed has been observed during periods of high river flow in the Guadiamar (Figure 4.2), which drains the mining area of Aznalcóllar to the east of the Rio Tinto (Albaiges *et al.* 1987). Dissolved Fe concentrations in the upper Guadiamar were low in January, increased throughout spring, declined in summer and increased rapidly at the beginning of the wet autumn season. In the King River, Tasmania,

the increase of dissolved trace metal concentrations during flood events was attributed to the release of acidic interstitial water, which had been generated during the *in-situ* oxidation of sulphides settled under conditions of low river flow (Featherstone and O'Grady, 1997 and references therein).

4.6.1.3 Geochemistry and Microbiology of AMD

A mineralogical study of Rio Tinto sediments (Hudson-Edwards *et al.* 1999) concluded that sedimentation of Fe and sulphate bearing minerals from the river water takes place. The contamination of the alluvium with Ag, As, Cu, Pb and Zn was most pronounced in primary minerals eroded from mine tailings, but important concentrations of these metals were also associated with various secondary mineral phases. However, no mechanism that could be responsible for the reduction in dissolved metal concentrations in acid (pH 1.5) waters of the lower Rio Tinto was elucidated.

The answer may lie in microbial processes, the importance of which is illustrated in Figure 4.31 for the iron cycle. Under acidic conditions (pH < 4) abiotic iron oxidation is slow (Chapman *et al.* 1996; Pronk and Johnson, 1992). Comparisons of iron oxidation rates obtained from field studies with those from abiotic laboratory experiments indicated that oxidation mediated by acidophilic bacteria may outweigh the abiotic rate by several orders of magnitude (Kirby and Elder Brady, 1998). Rapid formation of Fe(III) solids as hydroxides, oxides, oxyhydroxides, phosphates or sulphates has been found to follow bacterial oxidation in aerobic systems (Ehrlich, 1996; Bowell and Bruce, 1995; Tuovinen *et al.* 1994; Carlson and Lindstrom, 1992). In addition, the variability in water chemistry may be related to seasonal fluctuations in temperature, as temperature influences the kinetics of abiotic and biotic AMD generation and metal solid/solution interactions (Miller *et al.* 1996; Krauskopf and Bird, 1995).

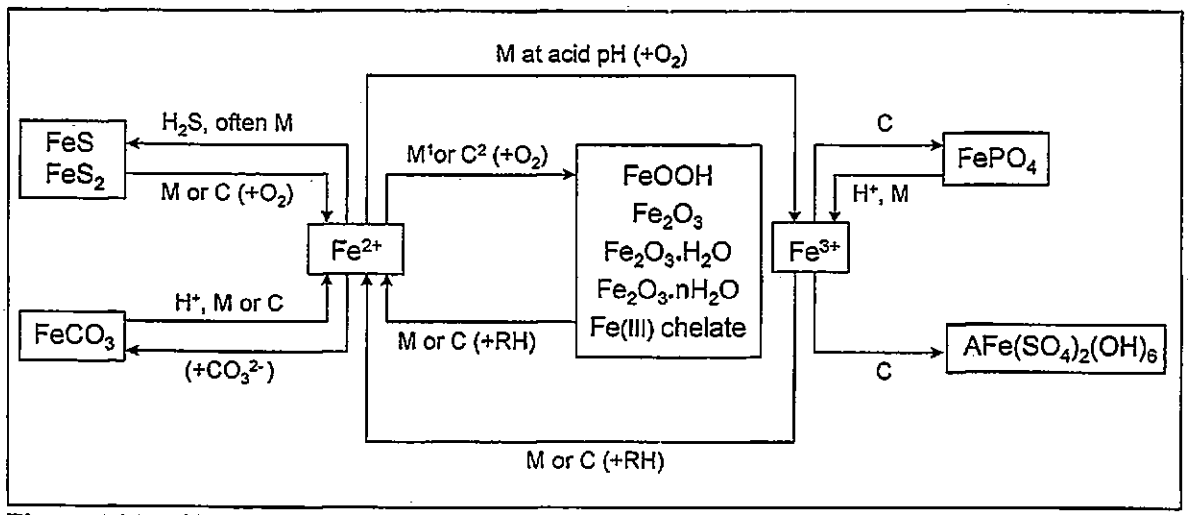

Figure 4.31 - Chemical and biological pathways in the iron cycle. M - microbially mediated, C - chemically mediated, M^1 - microbial at neutral pH, C^2 - chemical at neutral pH when O_2 tension is high, RH - organic molecules (as reducing agents), A - any one of the cations (Na^+, K^+, NH_4^+ or H_3O^+) involved in the formation of jarosite. After Ehrlich, 1996.

The microbes involved in the iron cycle are acidophiles, some of which derive their energy and reducing power from the oxidation of ferrous iron, reduced sulphur species (H_2S, S^0, $S_2O_3^{2-}$) and metal sulphides (among others). Commonly studied is the mesophilic (with respect to temperature) *Thiobacillus ferrooxidans*, which oxidises ferrous iron around pH 2 and, depending on the strain observed, growth occurs at a pH range between 1.5 and 6.0 (Webster *et al.* 1998; Ehrlich, 1996). The temperature range of *T. ferrooxidans* is 15 - 45 °C, with maximum activity and growth at 30 - 35 °C (Ehrlich, 1996; Noike *et al.* 1983). Other examples of sulphide oxidising bacteria are the halo-tolerant *T. prosperus*, *Leptospirillum ferrooxidans* (optimum growth at pH 1.5 - 2) and the acid-tolerant *Metallogenium* (pH 3.5 - 6.8, optimum at pH 4.1) (Ehrlich, 1996; Pronk and Johnson, 1992). According to Amils *et al.*(1998) mesophilic acidophilic microbes occur in the Rio Tinto.

Thermophilic bacteria identified in the Rio Tinto (e.g. *Sufolobales*, Amils *et al.* 1998) probably originated in the mine tailing heaps, where temperatures are elevated above ambient levels by the heat released during sulphide mineral oxidation (Niemela *et al.* 1994). Various acidophilic organisms (including some fungi) are able to oxidise sulphide ores of a multitude of metals (e.g. Fe, Mn, Cr, Zn, Cu, As, Ni, Sb, Ga, Cd, Pb and Mo). In addition, the ferric iron released into solution during this process acts as a further oxidant on metal sulphides ($MS + 2Fe^{3+} \rightarrow M^{2+} + S^{\circ} + 2Fe^{2+}$) (Miller *et al.* 1996; Ehrlich, 1996 and references therein; Tuovinen *et al.* 1994).

The immediate precipitation of ferric iron produced by iron oxidising bacteria has been observed at pH > 1.6 (Ehrlich, 1996 and references therein). The formed ochres, which are mainly poorly crystallised (amorphous) iron (oxy)hydroxides, may contain a significant amount of sulphate (e.g. schwertmannite: $Fe_8O_8(OH)_6SO_4$ and jarosite: $(H,Na,K)Fe_3(SO_4)_2(OH)_6$) (Bigham *et al.* 1996; Bigham *et al.* 1990) and have high surface

reactivity for the scavenging of other trace metals in solution. Hudson-Edwards (1999) reported the presence of secondary minerals, including Fe oxides, hydroxides, oxyhydroxides and oxyhydroxysulphates in the sediment of the Rio Tinto. While primary iron minerals contained higher concentrations of Zn, Cu, Pb and As, compared to secondary mineral phases, a certain degree of metal scavenging during the formation of secondary Fe minerals was evident.

Co-precipitation and adsorption of cations onto Fe oxyhydroxides is known to be important in systems with pH > 5. In more acidic waters (pH < 4), co-removal of trace metals with iron has been found to be less pronounced (McCarty *et al.* 1998). This has been attributed to the electrostatic repulsion generated by the presence of positive charges on mineral and particle surfaces, either in form of cationic species (e.g. Fe^{3+}, $FeOH^{2+}$ and $Fe(OH)_2^+$) or due to the protonation of adsorption sites at low pH (Bonnissel-Gissinger *et al.* 1998; Krauskopf and Bird, 1995; Bowell and Bruce, 1995; Groot *et al.* 1987). Electrophoretic mobility experiments carried out in October 1998 by a colleague (Herzl, personal communication) showed that suspended particles from the Tinto and Odiel rivers and their upper estuaries carried an overall positive charge, which decreased at higher pH and salinity values. This phenomenon has resulted in the absence of a strong removal of dissolved Fe and other metals in the rivers and the low salinity zone of the Tinto and Odiel estuaries (see Section 4.6.2), and this is in contrast to metal behaviour commonly observed in estuaries not affected by AMD.

The presence of *T. ferrooxidans* has been found to enhance trace metal adsorption to oxides formed from AMD, and this was associated with the supply of adsorptive surfaces in the form of cell membranes, or to a change in the mechanism of oxide precipitation (Webster *et al.* 1998). Microbal precipitation of Fe and Mn may be effected by enzymatic or non-enzymatic processes, whereby ferrous or ferric iron is either

deposited within the organism or passively accumulated on its cell surface (e.g. in *Metallogenium*) (Ehrlich, 1996 and references therein; Pronk and Johnson, 1992).

No evidence was found for the formation of colloids in the rivers (pH ≤ 3.2), neither visual (the water was clear at all times) nor from an ultra-filtration experiments carried out during the TOROS 2 survey by a colleague (Herzl, personal communication). Colloidal matter has been found to be low or absent in other AMD affected river systems, for example the Carnon in southwest England (Johnson, 1986 and references therein). Furthermore, thermodynamic equilibrium speciation modelling of the fresh water system indicated that none of the considered dissolved species had reached saturation concentrations (see Chapter 6). Therefore, microbal precipitation of Fe and Mn and scavenging of trace metals by these freshly precipitated phases may be of particular importance in the studied system.

Once solid phases exist, concretion (i.e. growth of solid metal phases on existing sediments or particles) may accelerate the removal of metals from solution. Concretion has been shown to be an abiotic mechanism of trace metal removal from solution at low pH (< 3) in AMD polluted streams (Chapman *et al.* 1996). Such deposits (Fe-rich cements, jarosites and schwertmannite as overgrowths on pyrite) have been found in the Rio Tinto (Hudson-Edwards *et al.* 1999). Some of these phases contained anomalous amounts of Cu and relatively low concentrations of Pb, Zn and As. High concentrations of As, Cu and Zn have been reported for yellow and white precipitates (gypsum: $CaSO_4 \cdot 2H_2O$, alunogen: $Al_2(SO_4)_3 \cdot 17H_2O$ and Fe oxyhydroxysulphates), which form on pyrite-rich surfaces.

T. thiooxidans and other mesophilic heterotrophic acidophiles are able to utilise Fe for respiration (Pronk and Johnson, 1992). The mentioned strain is capable of aerobic Fe(III) reduction at pH values around 2.5, because the Fe(II) produced by the organism does not readily auto-oxidise at pH < 5 (Ehrlich, 1996). Via this pathway, amorphous ferric

hydroxides, hydrous ferric oxides (e.g. lepidocrocite: γ-FeOOH and goethite: α-FeOOH) and crystalline compounds (schwertmannite, jarosite) can be reduced, depending on the bacterial strain involved (Pronk and Johnson, 1992). Furthermore, anaerobic bio-reduction of Fe(III) and Mn(IV) can be important in sub-surface sediments (Ehrlich, 1996).

An important aspect in the iron redox cycle occurring in shallow rivers may be photo-induced reduction and dissolution of Fe(III) (hydr)oxides (e.g. lepidocrocite, goethite and hematite: α-Fe_2O_3) under acid and aerobic conditions. Experiments (Sulzberger and Laubscher, 1995; Miles and Brezonik, 1981) showed that dissolved organic matter (oxalate, formate, humic or fulvic material) acted as reducing agent during the photo-reduction of Fe(III), which was followed by re-oxidation of Fe(II) to Fe (III).

In summary, the higher temperatures and increased light incidence in summer, compared to winter, is likely to accelerate redox-cycling (biotic and abiotic) in the river systems. In the shallow, aerobic Rio Tinto and Rio Odiel, photo-reduction, dissolution and re-oxidation of iron may be mechanisms of transferring Fe from thermodynamically stable mineral phases into more soluble species. These processes influence the redox behaviour of other metals (e.g. Fe(II) can reduce Mn(III, IV) oxides, Stumm and Morgan, 1996) and the dissolution/desorption and co-precipitation/adsorption of trace metals associated with Fe oxyhydroxides and Fe oxyhydroxysulphides. Enhanced microbial activity may lead to enhanced sulphide oxidation rates and enable the precipitation and accretion of solid Fe phases at low pH values. Without further investigations (e.g. *in-situ* study of microbial oxidation and reduction rates, trace metals associated with precipitated mineral phases) the effects of the above mentioned metal dissolution-precipitation and redox processes on seasonal variability cannot be ascertained. It appears that the amount of moisture available for AMD generation and transport and the influence of acidophilic micro-organisms could play a major role in regulating the metal chemistry of the Rio Tinto and Rio Odiel.

4.6.2 GEOCHEMISTRY IN THE ESTUARY

Although the range of metal concentrations observed in the riverine end-members were similar to AMD affected systems in many locations, the estuarine system of the Rio Tinto and Rio Odiel is relatively unique. The proximity of the AMD source to the coast, its intensity and industrial waste discharges into the mixing zone created estuarine conditions that are rarely encountered or studied.

The tidal ranges during the surveys were 2.07 m (TOROS 1), 1.54 m (TOROS 2), 2.91 m (TOROS 3) and 1.86 m (TOROS 4). However, the sea water intrusion at the time of sampling not only depends on tidal ranges, but also on wind force, atmospheric pressure, fresh water discharges and the timing of the survey. Figure 4.32 shows the spatial extent of the tidal intrusion as a plot of pH and salinity versus distance. In both upper estuaries, the sea water intrusion reached farthest upstream during the TOROS 4 surveys (T4), compared to the other surveys. During TOROS 4 the low salinity mixing zone could not be sampled because of the limited navigability of the upper tidal channels.

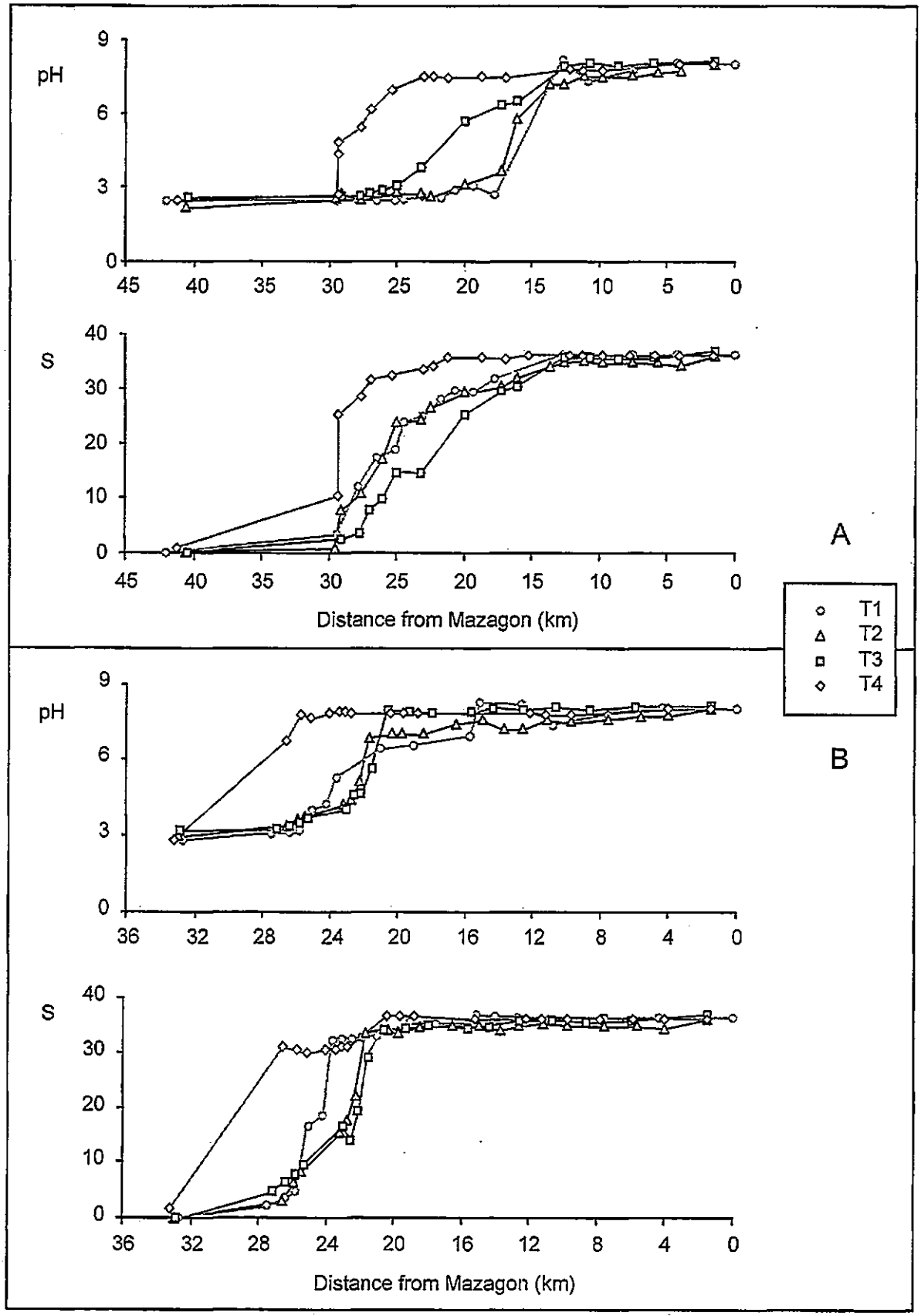

Figure 4.32 - Salinity and pH of four transects (TOROS 1, 2, 3 and 4) plotted over distance from the estuary's mouth at Mazagón. A: Ría del Tinto from the fresh water end-member at Niebla to the confluence and from there to Mazagón. B: Ría del Odiel from the fresh water end-member at Gibraleón to Huelva Bridge and to Mazagón.

4.6.2.1 pH, Acidity, Alkalinity and Sulphate

During the TOROS 1 and 2 surveys, low pH values (2.4 - 3.7) were maintained throughout the Ría del Tinto. Steep pH gradients were observed only near the confluence with Huelva Ría, where the salinity reached values above 30 (Figure 4.14 and Figure 4.17). The low pH in the upper estuary resulted from the strong riverine source of AMD. In the lower Ría del Tinto phosphoric acid, sulphuric acid and fluoride are released from phosphogypsum deposits (Elbaz-Poulichet *et al.* 1999) located at the northern bank (Figure 4.5), and HF is formed in the estuary. In the vicinity of the deposits, evidence for the acidic discharge (pH 1.5) was given by elevated sulphate concentrations (Figure 4.14 and Figure 4.17), high phosphate concentrations (TOROS 2: $PO_4 > 270$ µM, Cruzado *et al.* 1998) and high fluoride levels (1997: F = 6.8 - 11 mg l^{-1} at low water; Medio Ambiente, 1998), compared to those found in the upper mixing zone (TOROS 2: $PO_4 = 44.7$ µM, Cruzado *et al.* 1998, 1997: F ≤ 1.8 mg l^{-1} at low water; Medio Ambiente, 1998).

In April and October 1998 the neutralisation of the pH started farther upstream (Figure 4.32) and at lower salinities (Figure 4.22 and Figure 4.26), compared with earlier surveys. This indicates that less acid entered the Ría del Tinto during TOROS 3 and 4 from the phosphogypsum deposits, than during TOROS 1 and 2. According to Morales (1999a), the construction of a closed water cycle for the phosphogypsum deposits began to take effect in spring 1998, with a reduction of acidic effluent entering the lower Ría del Tinto, which then stopped completely later that year. The observed decrease in phosphate levels between June 1997 and October 1998 (TOROS 4: PO_4 = 17.6 - 26.2 µM, Cruzado *et al.* 1999) was indicative of the effects of the closed water cycle. The nutrient decrease was not the result of depletion through primary production, as total chlorophyll concentrations in this part of the estuary were approximately 10 times lower in October compared to June (Cruzado *et al.* 1999; 1998).

The pH values in the Ría del Odiel increased steadily with increasing salinity during all surveys and neutral pH values were reached in the upper Huelva Ría (Figure 4.15, Figure 4.18, Figure 4.23, Figure 4.27 and Figure 4.32). At salinities above 30 the pH values observed in the Ría del Odiel were between 5.2 and 7.8, with lowest values in autumn/winter and spring. The high salinity (S >36) values observed in the lower Huelva Ría reflected the mixing of a small volume of river water with high-salinity coastal sea water, in which surface-salinities between 35.9 and 36.5 were observed during TOROS surveys (see Chapter 5).

The high level of sulphate observed during the TOROS 1 survey (November 1996) may be partially explained by the high concentrations of this anion in the fresh water end-members of the Rio Tinto and Rio Odiel and the discharges from phosphogypsum deposits in the lower Ría del Tinto. In addition, effluent from fertiliser factories in the upper Huelva Ría may have contributed to maintaining elevated SO_4 concentrations (SO_4 = 40 mM at S = 35) throughout the estuary. These discharges were traceable in June 1997, when elevated phosphate concentrations were observed in the upper Huelva Ría (stations HR 1 and HR 2: PO_4 = 51 - 60 μM, compared to station HR 11: PO_4 = 5.6 μM; Cruzado *et al.* 1998).

Sulphate concentrations during the subsequent surveys (TOROS 2 and 3) remained below 40 mM in the Ría del Tinto and below 30 mM in the Ría del Odiel, where a conservative mixing of the anion was observed. The discharge from the phosphogypsum deposits during the dry summer period (June 1997, TOROS 2) were probably low and, in April 1998, discharges had been reduced. During these two surveys estuarine sulphate concentrations in Huelva Ría were around the sea water level (28 mM, Stumm and Morgan, 1996) at salinities above 35.

The total acidity decreased with increasing salinity in both upper estuaries (Figure 4.17 and Figure 4.18). Before the acid discharges from the phosphogypsum ceased in the

Ría del Tinto, carbonate alkalinity was detected only in an advanced stage of mixing ($S \geq 32.2$, $pH \geq 5.8$, TOROS 2). In contrast to this, the acidity of the Ría del Odiel was lower throughout and alkalinity was detected at mid-salinities and lower pH values ($S > 17.5$, $pH > 4.4$, TOROS 2). In accordance with conservative mixing, the carbonate alkalinity increased from zero to values typical for sea water (2.3 - 2.6 meq l^{-1}, Stumm and Morgan, 1996) at salinities above 36.

4.6.2.2 Suspended Particulate Matter

The turbidity maximum zone (TMZ) in the Ría del Tinto was located between the bridge at San Juan del Puerto and the cellulose factory (Figure 4.5). SPM concentrations reached maxima around $S = 11$ (253 mg l^{-1}) and $S = 8$ (272 mg l^{-1}) during the TOROS 2 and 3 surveys, respectively. In October 1998, no samples were taken for SPM between the fresh water end-member and estuarine water of $S = 25.1$, so that the presence of a TMZ and its magnitude remained uncertain. In the Ría del Odiel, no distinct TMZ was observed in any of the transects. In April 1998 (Figure 4.23), a sample with elevated SPM concentration was taken in the mid-Odiel (OR 4, $S = 16.5$, Figure 4.10), however, this could have been an artefact of sampling in the shallow waters. The SPM concentration in the Ría del Odiel increased with the salinity to a level between 20 and 60 mg l^{-1}, which was approximately the range of SPM concentrations found in Huelva Ría. This SPM concentration range appears to be typical for Huelva Ría and has been used for SPM modelling by Perianez *et al.* (1996).

4.6.2.3 Eh, DOC and Dissolved Oxygen

The redox potential (Eh) in the fully oxygenated fresh water end-members was between 480 and 600 mV during TOROS 2, 3 and 4 surveys. In the upper estuaries a gradual decline in Eh values was concurrent with the increase in pH, and levels between 270 and 400 mV were reached in the lower Ría del Tinto and Ría del Odiel during the TOROS 2 and 3 surveys. Eh expressed as pε is the hypothetical activity of electrons and it is inversely related with pH as a result of several redox equilibria (mainly involving species of C, O, N, Fe, Mn and S) that occur in natural waters (Stumm and Morgan, 1996).

During TOROS 4 a more rapid decrease to 110 and 200 mV was observed in the Ría del Tinto and Ría del Odiel, respectively. The low Eh values in the mid-Tinto estuary coincided with a minimum in dissolved oxygen and high DOC concentrations in the vicinity of the cellulose factory (S = 24 - 28, Figure 4.26). Samples containing an important proportion of effluent from this plant during TOROS 2 and 3 surveys had higher pH values (7.9), lower Eh values (170 - 220 mV) and higher temperatures (24 - 29 °C) and DOC concentrations (6.6 mM), compared to the main stream estuarine water. The localised oxygen and Eh minimum can therefore be attributed to an increased biochemical oxygen demand (resulting from the degradation of organic matter) and elevated temperatures associated with the factory's effluent.

Dissolved organic carbon concentrations in the Ría del Tinto during the spring survey (April 1998: 0.27 - 0.39 mM) were comparable to levels generally found in the Ría del Odiel and Huelva Ría. Levels were similar to those found in other populated and industrialised estuaries, for example the Severn (0.08 - 0.58 mM C, Mantoura and Woodward, 1983), but higher than levels found in coastal surface waters of the Mediterranean Sea in March (ca. 0.08 mM) and July (0.08 - 0.2 mM) (Cauwet *et al.* 1997). High DOC concentrations were associated with effluent from the cellulose factory in the

Ría del Tinto during in June 1997 and October 1998 (6.6 and 2.2 mM C, respectively), and DOC levels values declined towards the confluence where concentrations around 0.37 mM were reached. In June 1997, maxima of chlorophyll-a (chl-a = 342 μg l^{-1} Cruzado *et al.* 1998) and DOC coincided, suggesting a contribution of organic matter from primary producers. In April and October 1998, chl-a levels were lower (maxima 90 μg l^{-1} and 38 μg l^{-1}, respectively Cruzado *et al.* 1999; Elbaz-Poulichet *et al.* 1999b) than in June 1997 and it appears that variations in factory effluents determined DOC levels in the Ría del Tinto.

DOC concentrations in the Ría del Odiel (0.13 - 0.44 mM C) and Huelva Ría (0.1 - 0.38 mM C) were lower and less variable compared to those in the Ría del Tinto. Minima in DOC levels were generally found in the upper Ría del Odiel and towards the sea water end-member. The higher DOC values occurred in the upper Huelva Ría, possibly as a result of effluent from a raw sewage channel and enhanced productivity supported by nutrient-rich effluent from fertiliser factories. Generally, DOC is thought to behave conservatively in estuaries (Mantoura and Woodward, 1983), but in the Tinto/Odiel system additional sources of DOC within the estuary and effluent from the fertiliser industry, promoting primary productivity, masked such behaviour.

4.6.2.4 Geochemistry of Fe, Al, Mn, Zn, Cu, Ni, Co and Cd

Ría del Tinto and Ría del Odiel

In the upper Ría del Tinto and Ría del Odiel the dissolved concentrations of Fe, Al, Mn, Zn, Cu, Ni, Co and Cd reflected the variability of their riverine sources, with higher concentrations in autumn/winter (TOROS 1 and 4), compared to spring/summer (TOROS 2 and 3). The concentration gap between wet and dry seasons was more pronounced in the Rio Tinto than the Rio Odiel, and this was mirrored in metal levels found in the upper mixing zone of their estuaries.

Zinc, Cu and Cd are particularly enriched in the Iberian Pyrite Belt and may be viewed as tracers of the fate of AMD-related discharges. The comparison of their estuarine distribution with that of Fe, Al, Mn, Ni and Co affirms their common riverine source and similar geochemical behaviour in the estuary (Figure 4.14, Figure 4.15, Figure 4.17, Figure 4.18, Figure 4.22, Figure 4.23 and Figure 4.26 - Figure 4.28). Multivariable correlation calculations indicated strong positive correlation ($R^2 > 0.90$) between Fe, Al, Mn, Zn, Cu, Ni, Co and Cd in the Ría del Tinto and Ría del Odiel/Huelva Ría for all four surveys. A strong negative correlation was found between these metals and salinity ($R^2 > 0.85$), indicating that the behaviour of dissolved Fe, Al, Mn, Zn, Cu, Ni, Co and Cd in the estuary was broadly conservative. Deviations from the conservative behaviour are discussed in the following paragraphs.

In the Ría del Tinto, the early stages of mixing were characterised by an increase in total dissolved concentrations of Fe, Al, Mn, Zn, Cu, Ni, Co and Cd to levels above those in the fresh water end-members (Figure 4.14, Figure 4.17, Figure 4.22 and Figure 4.26). The maxima occurred at different salinities (S = 0.93 - 7.7), but within a narrow range of pH values (pH = 2.43 - 2.61). On plots of dissolved Mn, Zn, Cu, Ni, Co or Cd versus pH (Figure 4.33, Co and Mn not shown), the profiles of all four surveys overlap closely. This indicates an important influence of pH on the metal geochemistry in the Ría del Tinto and to a lesser extent in the Ría del Odiel.

During the TOROS 1, 2 and 3 surveys the distribution of dissolved Fe, Mn, Zn, Cu, Ni, Co and Cd between the maxima and the confluence of the Ría del Tinto with Huelva Ría (S = 30.4 - 32.2, pH = 2.7 - 6.6) was governed by conservative dilution with sea water (Figure 4.14, Figure 4.17 and Figure 4.22).

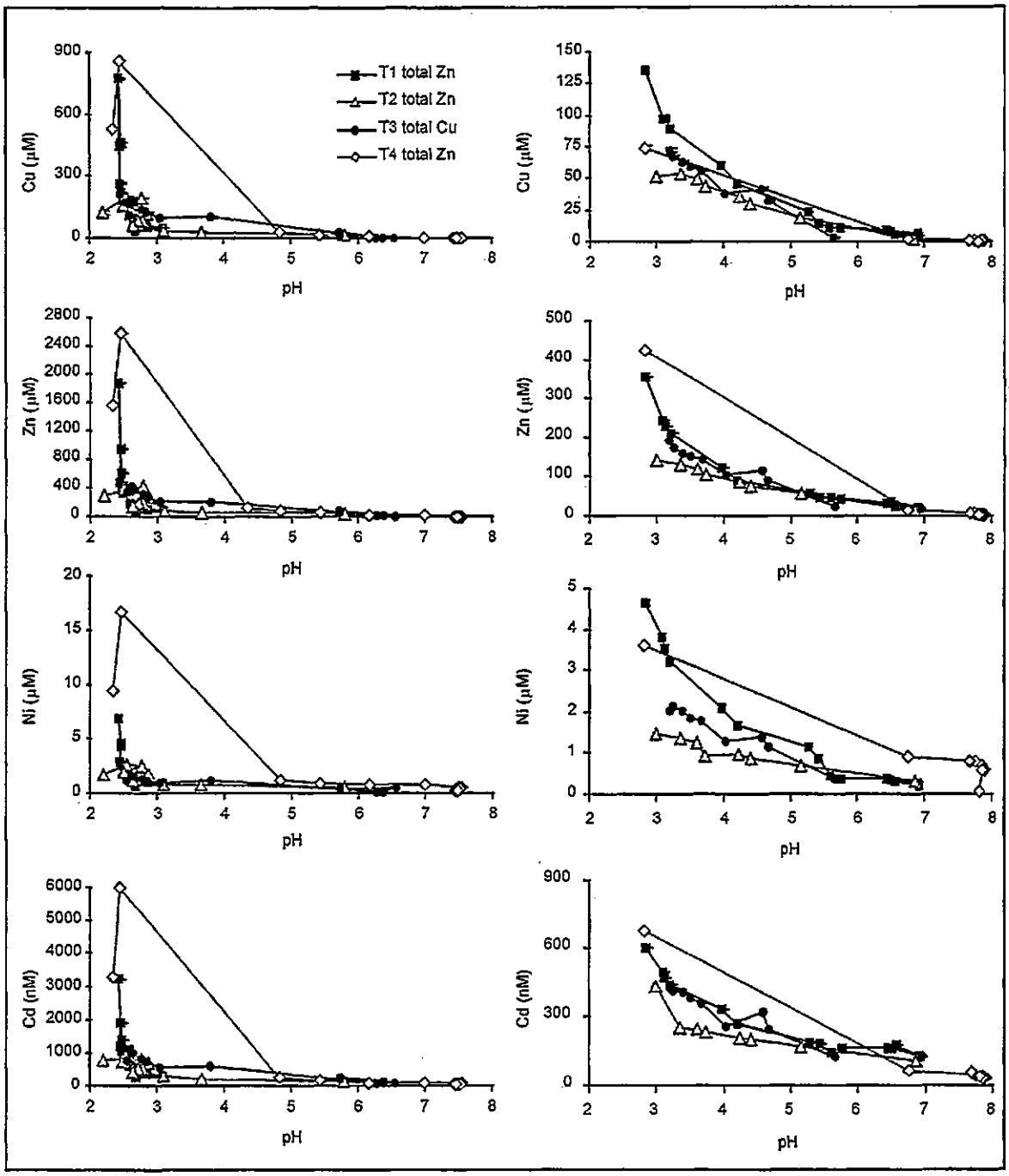

Figure 4.33 - Comparison of total dissolved Zn, Cu, Ni, Co, Mn and Cd concentrations observed during TOROS surveys 1, 2, 3 and 4 in the Ría del Tinto and Ría del Odiel (left and right colunn, respectively) plotted versus pH.

In October 1998 (TOROS 4), a removal of Fe, Mn, Zn, Cu, Ni, Co and Cd from solution in the upper region of the Ría del Tinto at mid-salinities (S < 25, pH < 4.4) can be inferred from the metal/salinity profiles. The lack of data points in this region does not allow a more detailed discussion. However, it is likely that the somewhat higher pH and salinity encountered during this survey shifted the zone of metal removal upstream, compared to preceding surveys.

In the Ría del Odiel estuarine mixing of dissolved Fe, Al, Mn, Zn, Cu, Ni, Co and Cd appeared to be broadly conservative up to salinity and pH values around 31 and 6.2, respectively (Figure 4.15, Figure 4.18, Figure 4.23 and Figure 4.27). Slight removal during the early stages of mixing may have occurred during the TOROS 1 survey, and slight addition was indicated during TOROS 2 for Mn, Cu and Al and during TOROS 3 for Mn and Co. However, the curvature in the metal profiles from the latter surveys may be an artefact of variability in concentration, because the river end-members were not collected on the same day as estuarine samples. The behaviour of trace metals during TOROS 4 in the Ría del Odiel cannot be inferred because of the lack of samples from the mixing zone.

During the TOROS 1 survey, re-suspension of bed sediment in the shallow upper Ría del Tinto (close to San Juan del Puerto) was observed during sampling. In samples from the TOROS 2 transect, maxima in dissolved Fe, Al, Mn, Zn, Cu, Ni, Co and Cd coincided with a SPM concentration peak in the low salinity zone. In April 1998 (TOROS 3) high SPM concentrations (≈ 200 mg l^{-1}) coincided with the dissolved metal maxima, but the SPM peak (270 mg l^{-1}) occurred in the sample directly downstream from the metal maxima. Assuming the absence of an external source in the upper Ría del Tinto, the observed increase in dissolved metals must have resulted from a reworking of the sediments.

Published work affirmed the estuarine sediment as strong potential source for the (re)mobilisation of dissolved metals. High concentrations of Fe, Mn, Zn, Cu, Ni, Cd, Pb and U in surface sediments have been observed in the Ría del Tinto, Ría del Odiel and the Odiel salt marshes (Medio Ambiente, 1998; Izquierdo *et al.* 1997; Albaiges *et al.* 1987; Stenner and Nickless, 1975). Borrego *et al.* (1997) and Izquierdo *et al.* (1997) reported the presence of pyrite grains and metal sulphides associated with remains of microorganisms and foraminifera in the salt marshes of the estuary. Generally, reported sediment Zn, Cu and Cd levels in the Tinto and Odiel estuaries were comparable with those in other AMD affected systems (e.g. Restronguet Creek, Dulas Bay, Table 4.11), but very much higher than those reported for other estuaries and coastal salt marshes of the Gulf of Cádiz (e.g. Guadiamar, Guadiana, Bay of Cadiz) and in other estuaries affected by general industrial wastes (e.g. Humber, Mersey).

Elbaz-Poulichet *et al.* (1999b) suggested that organic material originating from the cellulose factory in the upper Ría del Tinto may have acted as reducing agent, resulting in the dissolution of metal oxides from surface sediment. The lack of a metal maximum in the low salinity zone of the Ría del Odiel supports this argument. In the Ría del Odiel there was no strong source of organic matter and this was reflected in the lower DOC levels, compared to the upper Ría del Tinto. In addition, the morphology of the upper Ría del Odiel (narrow channels, reed-beds) indicates a more quiescent, less reactive environment, compared to the open and sparsely vegetated mudflats of the Ría del Tinto. This would differentially influence another proposed metal mobilisation mechanism, the disturbance of deeper, anoxic sediment layers at times of high river flow or other high-energy situations (wind/wave action, tidal advance). Sub- or anoxia in sub-surface sediment layers was indicated by the black colour of the mud and presence of partially decomposed organic debris in sub-surface sediment layers of the lower Ría del Tinto mud-flats (Morley, personal communication). According to Borrego *et al.* (1997), the C/S ratio in sediments of

sub-tidal channels and salt-marshes (3.4 - 7.0) of the estuary was indicative of favourable conditions for sulphur reduction. Similar observations have been made in other AMD affected estuaries, where reducing conditions were indicated by the presence of metal sulphides and H_2S and evidence for (bacterial) SO_4^{2-} reduction (Parkman *et al.* 1996).

Moreover, the infusion of metal-rich interstitial waters into the water column and the dissolution and leaching of metals from mineral phases freshly exposed to low pH values (< 2.7) may have contributed to the observed increase in dissolved Fe, Mn, Zn, Cu, Ni, Co and Cd in the upper Ría del Tinto. During the TOROS 2 and 3 surveys, Elbaz-Poulichet (1999b) observed a decrease in particulate Fe concentrations coinciding with the dissolved metal maxima in the upper Ría del Tinto mixing zone. Once released, the metals were probably maintained in solution by the effects of the low pH at S < 30, and by complexation with inorganic (e.g. chloride, sulphate) and organic ligands present in the water column (Zwolsman and Van Eck, 1993).

The deposition of metals in the sediments of the Ría del Tinto is evident from the high concentrations reported in literature (Table 4.11). Sediment concentrations of Mn, Zn, Cu and Cd reported for the upper Ría del Tinto mixing zone (Table 4.11, San Juan del Puerto, location see Figure 4.4) were lower than the concentrations of these metals found in the lower Ría del Tinto, the lower Ría del Odiel and the Odiel salt marshes. This supports the suggestion that the deposition of metals in the sediment was more important in the lower estuary, compared to the upper Ría del Tinto and/or that sediments in the upper Ría del Tinto were re-worked and mobilised metals transported downstream as dissolved and/or particulate species. In addition, industrial inputs may have contributed to the sediment load of metals in the mid-estuary.

Table 4.11 - Total metal concentrations (μg g^{-1}) in sediments of the Tinto/Odiel estuarine system, control sites in south-west Spain and estuaries receiving metal contamination. 'nr' - not reported. Some values were rounded to significant figures.

Location	Mn	Zn	Cu	Cd	Pb	Fe
San Juan[1]	87	340	550	1.8	670	nr
Odiel HB[1]	320	310	1360	4.4	470	nr
Odiel SM[2]	560	1000	220	9	120	40200
La Rábida[3]	nr	3100	1400	4.1	1600	nr
Mazagón[3]	nr	42	6.5	0.9	6.0	nr
Cadiz SM[4]	530	98	31	0.3	26	7500
Cadiz Bay[5]	nr	6	2	1.1	6	nr
Guadiamar[6]	nr	59	26	nr	11	nr
Ayamonte[7]	nr	148	30	1.1	26	nr
Dulas Bay[8]	nr	3800	6600	nr	nr	46000
LV 08[9]	11900	620	120	<30	<200	nr
LV 16[9]	34200	2550	760	30	470	nr
Restronguet[10]	485	2820	2400	1.5	340	49100
Mersey[10]	1170	380	84	1.2	120	27300
Humber[10]	1020	250	54	0.48	110	35200
Axe[10]	250	76	12	0.17	26	14000

[1] San Juan del Puerto, location of extended mud flats in the upper Ría del Tinto. Huelva Bridge is located between the lower Ría del Odiel and Huelva Ría (Medio Ambiente, 1998).
[2] Bacuta saltmarsh of the Ría del Odiel (Izquierdo *et al.* 1997).
[3] La Rábida is located on the lower Ría del Tinto, Mazagón at the mouth of Huelva Ría (Stenner and Nickless, 1975).
[4] San Carlos saltmarsh, Bay of Cadiz, south-west Spain (Izquierdo *et al.* 1997),.
[5] Inner Bay of Cadiz, south-west Spain (Stenner and Nickless, 1975).
[6] Guadiamar saltmarsh and estuary (mean), south-west Spain (Albaiges *et al.* 1987).
[7] Lower Guadiana estuary, south-west Spain (Stenner and Nickless, 1975).
[8] Ochre sample from the Afon Goch estuary, Wales, UK (Parkman *et al.* 1996).
[9] Ochre and limonites from Levant Mine, Cornwall, UK. LV 08: water pH 2.1, LV 16: water pH 5.8 due to salt water mixing (Bowell and Bruce, 1995).
[10] Restronguet Creek in the Fal estuarine system, Cornwall, received AMD from abandoned Sn mine. Mersey and Humber estuaries (UK) are affected by industrial discharges. The Axe can be seen as UK background (Bryan and Langston, 1992).

The near-conservative behaviour observed for dissolved Fe, Mn, Zn, Cu, Ni, Co and Cd in the Ría del Tinto between the metal maxima and the confluence, and in the upper Ría del Odiel (S < 30) is not uncommon in estuaries affected by acid discharges. In estuarine waters with moderately acid pH (< 5) the observed conservative mixing of Fe and Mn has been attributed to the slow oxidation of Fe(II) to Fe(III) and of Mn(II) to Mn(IV) (Millward and Marsh, 1986). Experiments in sea water showed that adsorption of Zn, Cu, Cd and Pb to goethiite occurred at pH values above 5.5, 4.0, 6.0 and 4.0, respectively (Balistrieri and Murray, 1982). In the Tinto/Odiel system, removal by adsorption may have been hampered by electrostatic repulsion due to the protonation of particle surfaces at the prevailing low pH (see Section 4.6.1.3).

Huelva Ría

Tidal cycle studies at Huelva Bridge during TOROS 2, 3 and 4 studies indicated a steep increase of total dissolved Zn, Cu, Ni, Co and Cd concentrations at low water (Figure 4.20, Figure 4.25 and Figure 4.29). Coinciding with this increase were minima in pH, clearly indicating the riverine origin of the enhanced metal concentrations. The dissolved metal/salinity relationship at Huelva Bridge was linear during TOROS 2 and 3 surveys (Cu: $R^2 = 0.82$ and 0.72; Zn: $R^2 = 0.73$ and 0.81, respectively, significant at 1% confidence level), indicating conservative mixing at this point of the estuary over wide salinity and pH ranges (TOROS 2: S = 11 - 35, pH = 3.5 - 6.4; TOROS 3: S = 35.0 - 36.6, pH = 8.2 - 8.3).

During TOROS 1, the removal of Zn, Cu, Ni, Co and Mn from solution observed in the lower Ría del Odiel (at S > 32, pH > 5.3) continued in samples from the Huelva Ría transect. Less pronounced was the removal of these metals during the spring (TOROS 2: at S > 33.5, pH > 6.85) and summer (TOROS 3: at S > 29, pH > 5.7) surveys. The possibility that complexation of dissolved metals (especially Cu) by strong organic ligands may

maintain metals in solution at times of high primary productivity is discussed in Chapter 6. Cadmium behaved largely conservatively during all four surveys, and this may be explained with the formation of soluble complexes with chloride (Chapter 6). The overall conservative behaviour of dissolved Cd and the removal of Zn and Cu in the Tinto/Odiel estuarine system has been reported previously (Van Geen *et al.* 1997).

The observed removal from solution of Fe, Mn, Zn, Cu, Ni and Co in this estuary at near-sea water salinity may be explained by dissolved/solid interactions, which were impeded by the low pH values encountered in the low salinity regions, but occurred upon neutralisation of pH in the mid-estuary. Thermodynamic speciation calculations (Chapter 6) indicated that the formation and flocculation or precipitation of Fe, Al and Mn oxyhydroxides may play an important role in the removal of Fe and Mn and co-removal of other metals in Huelva Ría. Other possible removal processes include the adsorption of metals onto particles or organic coatings on particles, the flocculation of organic matter and the scavenging of metals with newly formed solids. Palanques *et al.* (1995) reported the enrichment of fine sediment in the central Gulf of Cádiz with Fe, Zn, Cu, Ni, Co, Cr and Pb, but not Cd. Their conclusion suggested that metal-contaminated flocs and particles were transported from Huelva Ría into the Gulf of Cádiz, where they settled as fine sediment on the shelf and slope.

Samples taken just below the surface during rapid transects of Huelva Ría (TOROS 1 and 3) show a steady increase of salinity with distance from the river end-member. Compared to this, samples taken with Niskin bottles at 5 - 10 m depth (TOROS 2 and 4) over several hours had a more erratic salinity distribution. As a result metal/salinity profiles of Huelva Ría from these surveys are difficult to compare and interpret. When plotted versus distance an overall downstream decrease in dissolved Cu, Zn, Ni, Co and Cd concentrations becomes apparent (Figure 4.34 - Figure 4.37).

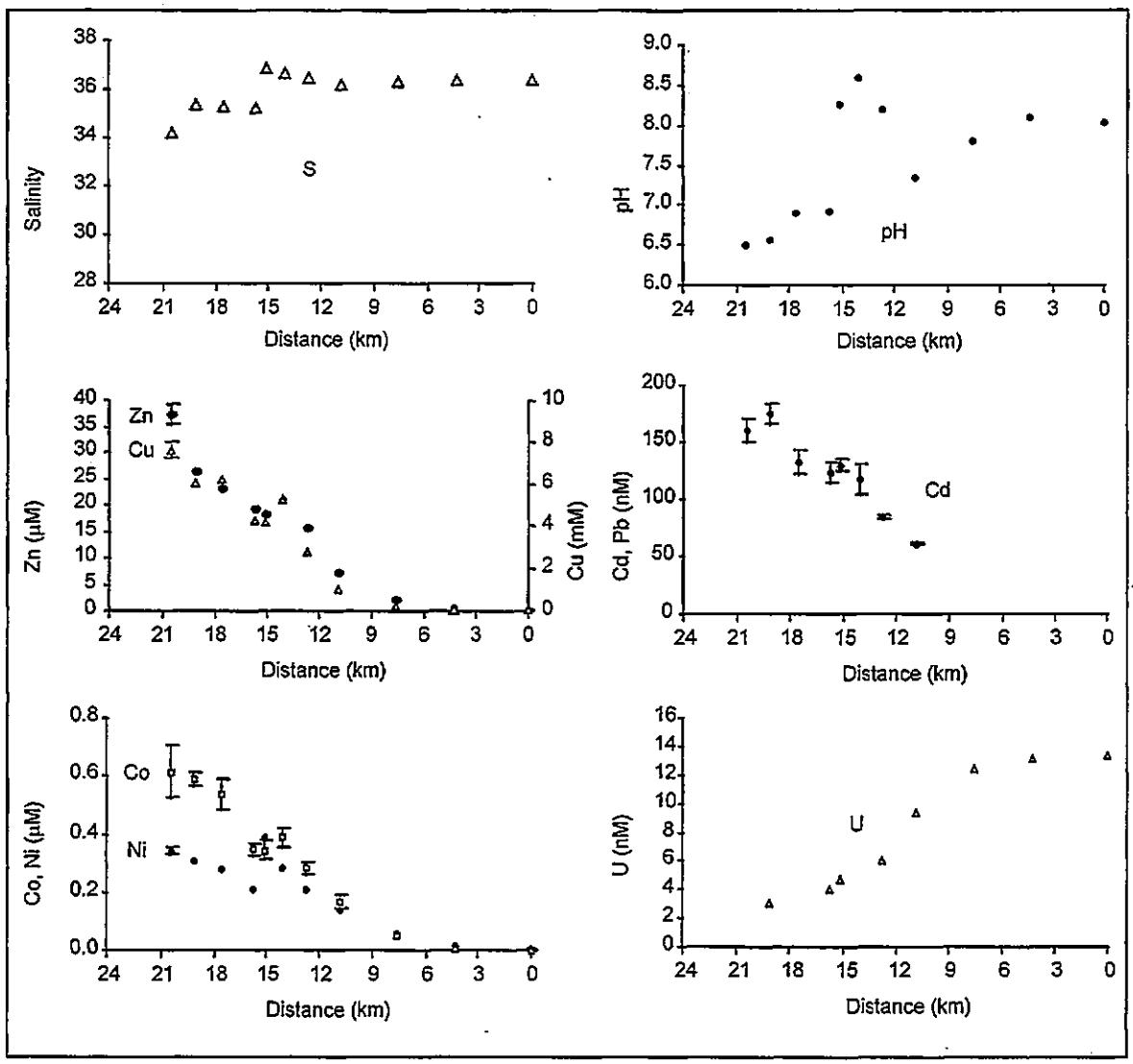

Figure 4.34 - TOROS 1: Salinity, pH and total dissolved metal concentrations in Huelva Ría plotted versus the distance from the mouth of the estuary at Mazagón. For clarity, the error bars for Zn, Cu and Ni were omitted, except for the most upstream value. Zn: ●, Cu: △, Co: □ and Ni: ●.

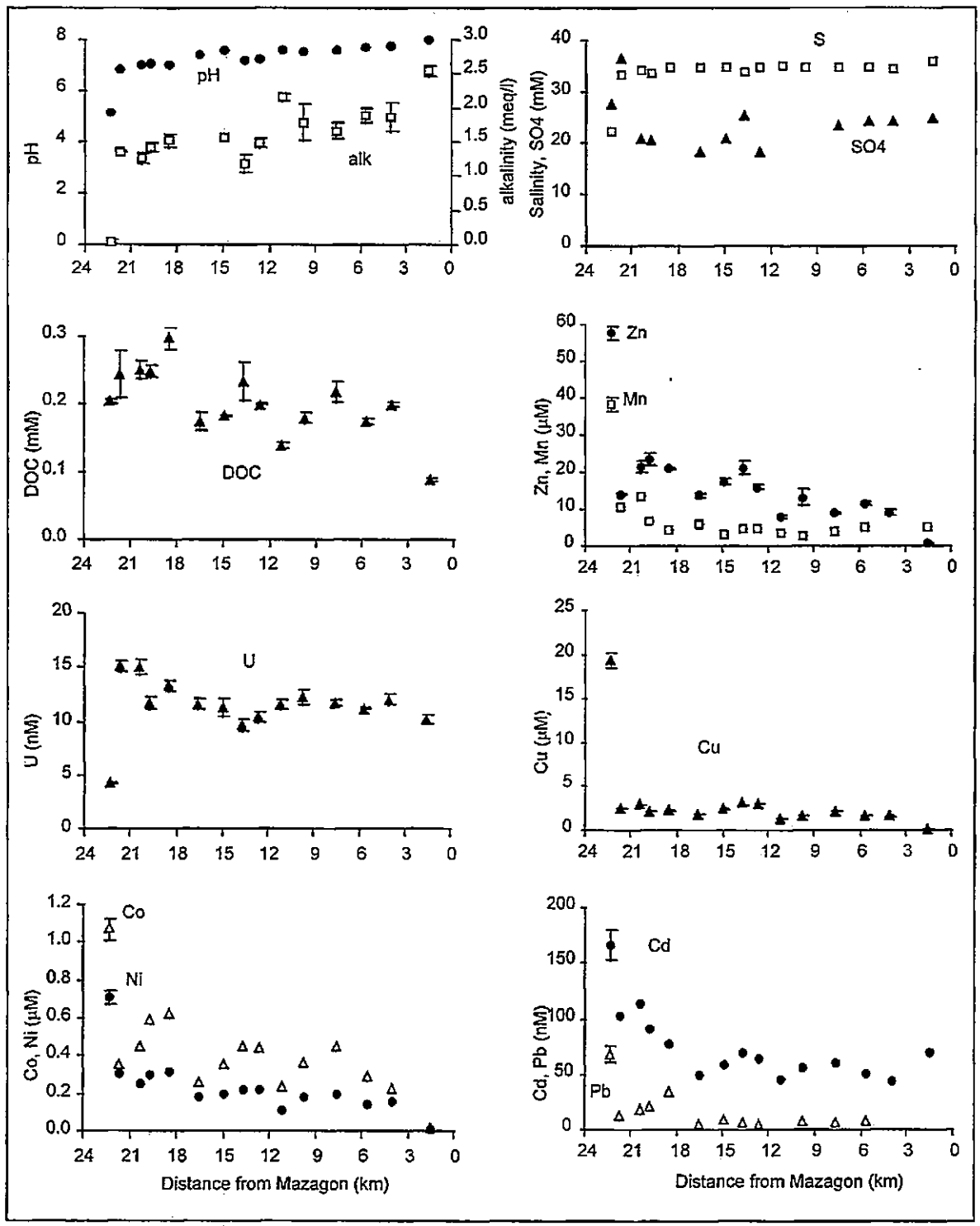

Figure 4.35 - TOROS 2: Salinity, pH, SPM, DOC and total dissolved metal concentrations in Huelva Ría plotted versus the distance from the mouth of the estuary at Mazagón. For clarity, the error bars for Mn, Co, Ni, Cd and Pb were omitted, except for the most upstream value. Zn: ●, Mn: □, Co: △, Ni: ●, Cd: ● and Pb: △.

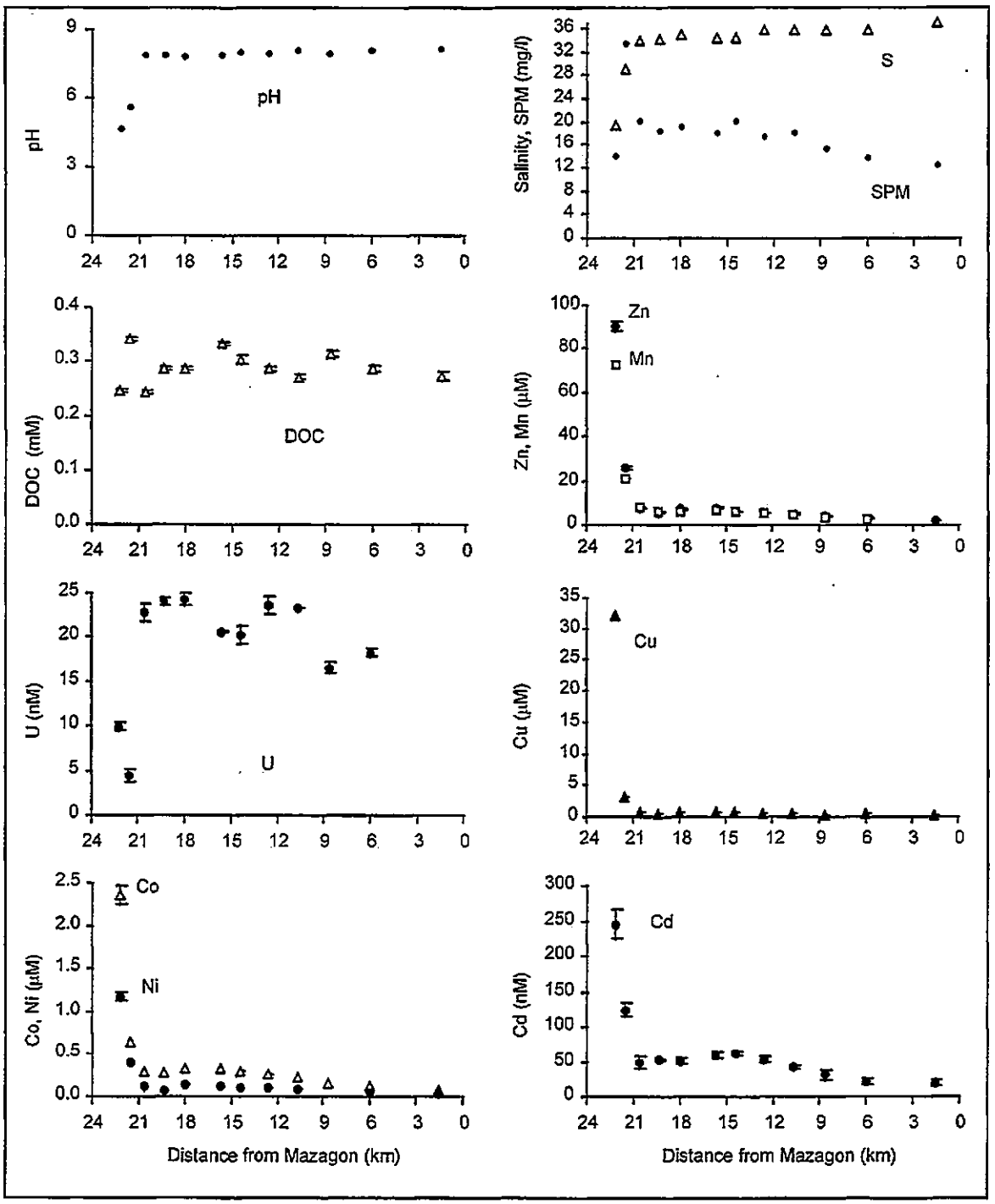

Figure 4.36 - TOROS 3: Salinity, pH, SPM, DOC and total dissolved metal concentrations in Huelva Ría plotted versus the distance from the mouth of the estuary at Mazagón. For clarity, the error bars for Co and Ni were omitted, except for the most upstream value. Zn: ●, Mn: □, Co: △ and Ni: ●.

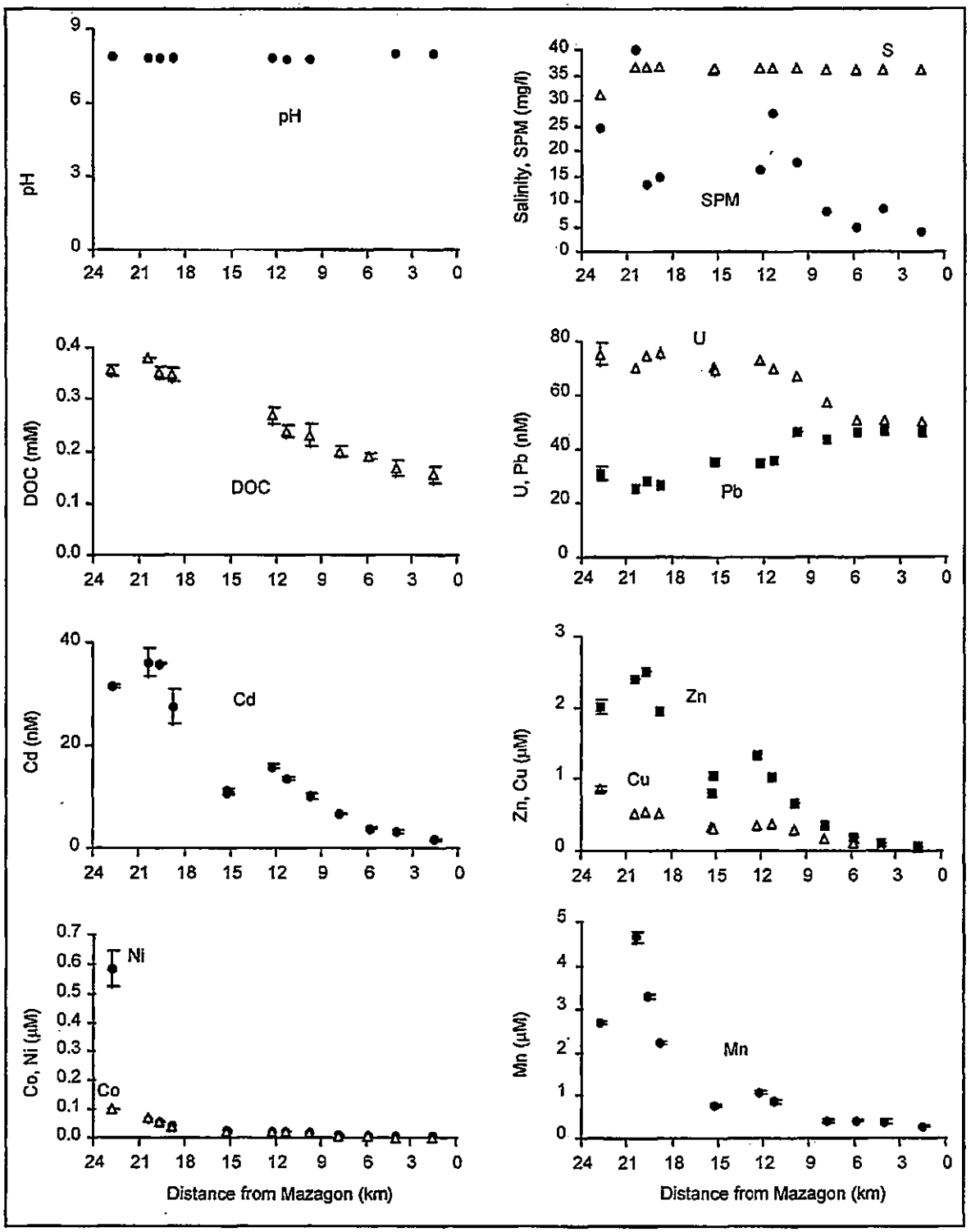

Figure 4.37 - TOROS 4: Salinity, pH, SPM, DOC and total dissolved metal concentrations in Huelva Ría plotted versus the distance from the mouth of the estuary at Mazagón. For clarity, the error bars for U, Pb, Zn, Cu, Co and Ni were omitted, except for the most upstream value. U: △, Pb: ■, Cu: △, Co: △ and Ni: ●.

During TOROS 3, the metal removal coincided with a peak in SPM concentrations, suggesting that adsorption onto particles took place. In October 1998 (TOROS 4), maxima in the SPM concentration in the upper Huelva Ría (between 15 and 20 km from Mazagón) coincided with additions of Zn, Mn and Cd to estuarine waters, while Ni and Co showed no concurrent increase in concentration. It is likely that industrial discharges from metal processing facilities and fertiliser factories in the upper Huelva Ría may have contributed to the increase in both SPM and metal concentrations.

The increase in dissolved metal concentrations at a distance of 12 to 15 km from Mazagón has been observed during TOROS 1 (Zn, Cu, Ni, Co and possibly Cd), TOROS 2 (Zn and lesser so Cu, Mn, Ni, Co, Cd) and TOROS 3 and 4 (Mn, Zn, Cu, Ni, Co and Cd). These mid-estuarine metal peaks occur at the confluence between the Ría del Tinto and the Huelva Ría and are probably the result of the mixing of Ría del Tinto water containing higher dissolved metal concentrations (factor 1.3 - 3.3 for Mn, 1.8 - 4.4 for Zn, 1.2 - 11.8 for Cu, 2.1 - 9.2 for Ni, 1.3 - 3.9 for Co and 1.5 - 3 for Cd) with that of the Huelva Ría.

Comparison with other AMD-affected systems

No system was found that could be directly compared with the low pH range and high dissolved metal concentrations in the Ría del Tinto. However, conditions observed in the lower Ría del Odiel and Huelva Ría were comparable to other AMD-affected estuaries, such as the Fal (Cornwall). In this system only a small proportion of the riverine AMD input of Co, Cd, Mn, Ni and Zn into the Restronguet Creek was retained within this branch of the estuary, but removal of dissolved metals was observed in the main estuary at near-sea water salinity (Bryan and Gibbs, 1983). Contrary to the Ría del Tinto, and a result of the higher pH values in Restronguet Creek, most of the riverine Cu, Pb and As was

removed from solution in the upper Restronguet Creek with flocculating iron oxides and humic substances (Bryan and Langston, 1992; Bryan and Gibbs, 1983).

Similar observations were made in other AMD-affected estuaries. The King River, Tasmania, receives drainage from the Mt Lyell Cu mine and enters a semi-enclosed coastal bay (Macquarie Harbour) via a small delta. In an experiment inducing a sudden increase in river flow, the removal of dissolved Fe and Cu (maximum riverine concentrations: 150 μM Fe and 110 μM Cu, see Table 4.8) upon mixing with sea water was observed at $S < 10$ (Featherstone and O'Grady, 1997). Mixing experiments showed that particle interactions played a minor role in dissolved Cu behaviour. The loss of Cu from solution was attributed to the co-removal of Cu with newly formed Fe(III) oxyhydroxides and existing Fe colloids, which flocculated upon the rapid increase in pH during estuarine mixing. Metal removal was also evident from sequential leaching experiments on sediments collected in the Afon Goch estuary (Dulas Bay, Wales, total metal concentrations see Table 4.8 and Table 4.11) (Parkman *et al.* 1996). This study indicated that an important proportion of Zn and Cu was adsorbed onto reducible Fe phases (e.g. Fe oxyhydroxides and oxyhydroxysulphates) in the ochre. In black mud, Cu was predominantly extracted during the oxidising step, suggesting the association with organic matter or acid-stable sulphide minerals in sub-oxic or anoxic sediment layers (Parkman *et al.* 1996). Luther *et al.* (1996) attributed the precipitation of dissolved Fe from acidic ($pH < 3$) salt marsh pore waters to the precipitation of Fe-humic complexes.

Summary

Overall, the accumulated evidence leads to the suggestion that the aggregation of metal rich sediment in the upper Ría del Tinto mixing zone predominantly occurred during quiescent periods (e.g. low water) through the deposition of eroded material, microbial

activity and concretion processes similar to those discussed for the fresh water end-member (see Section 4.6.1.3). The presence of high DOC concentrations in the upper Ría del Tinto could have resulted in the reductive dissolution of metals from the sediment, but also in the precipitation of acid-insoluble Fe-organic complexes. The sediments in the upper Ría del Tinto were reworked by the advancing tide, resulting in the release of metals into the water column, which were transported downstream and, as a result of the low pH values, dissolved metals were subjected to conservative mixing with sea water (before October 1998). Remobilisation of metals was not observed in the Ría del Odiel, probably because this branch of the estuary is a lower energy environment, has no strong inputs of organic matter and less microbial activity, compared to the Ría del Tinto. Removal of dissolved metals in the estuary occurred at salinities greater than 30 and pH values above five. The surveys indicated that this process is largely completed in the lower Huelva Ría ($S > 36$, $pH \approx 7.0$). In the Ría del Tinto, metal profiles from the last survey showed a decrease in dissolved metal concentrations at mid-salinity, indicating that the closure of the phosphogypsum drainage water cycle had an important impact on the metal geochemistry in the Ría del Tinto.

4.6.2.5 Geochemistry of Lead

The dissolved distributions of U and Pb in the Tinto/Odiel system were in contrast to those of Fe, Al, Mn, Zn, Cu, Ni, Co and Cd during the first three TOROS surveys. In the Ría del Tinto, Pb was rapidly removed from solution at low salinity (< 3.5), from 3060 nM to 80 nM, 4130 nM to 510 nM and 500 nM to 230 nM Pb during TOROS 1,2 and 3, respectively (Figure 4.14, Figure 4.17 and Figure 4.22). During TOROS 1 and 2 a slight increase in the dissolved concentration was observed at S = 12 and 7.7, respectively. Lead concentrations in the remainder of the Ría del Tinto declined gradually to levels around 50

nM Pb at S ≈ 30 and pH = 2.9 - 3.7 (TOROS 1 and 2) and below 10 nM at S ≈ 30 and pH ≈ 6.3 during TOROS 3 and 4 (Figure 4.26). The tidal cycle at La Rábida in June 1997 (Figure 4.21) clearly showed the contrasting behaviour of U and Pb, compared to Zn, Cu and Cd. Dissolved U and Pb maxima occurred at mid-ebb tide, indicating that the dominant source of these metals was different (phosphogypsum) from that of Zn, Cu and Cd (fluvial).

In upper mixing zone of the Ría del Odiel, a slight addition of dissolved Pb was observed during the first survey and some removal during TOROS 2 and 3. Lead mixed conservatively between S = 5 and approximately S = 30, whereby concentrations below 10 nM Pb and 20 - 50 nM Pb were reached in Huelva Ría during TOROS 2 and 4, respectively (Figure 4.15, Figure 4.18, Figure 4.23 and Figure 4.27). Additions of dissolved and particulate Pb in the upper Huelva Ría have been attributed to discharges from the fertiliser industry (Martinez-Aguirre and Garcia-Leon, 1996). However, the tidal cycle in June 1997 (TOROS 2) showed a strong riverine source of U and Pb at the boundary between Ría del Odiel and Huelva Ría (Huelva Bridge, Figure 4.20).

The concurrence of Pb removal and mobilisation of Fe, Al, Mn, Zn, Cu, Ni, Co and Cd in the upper Ría del Tinto mixing zone suggests that the reworking of sediment (see Section 4.6.2.4) favoured both phenomena. Lead is known to have a high affinity for the particulate phase (Balistrieri and Murray, 1984) and humic substances (Yu *et al.* 1996), however, experiments usually focused on media with near-neutral pH values. Simpson *et al.* (1998) demonstrated the low solubility of PbS during a HCl (1 M) leaching experiment and its resistance to oxidation upon resuspension into an oxic water column. This could account for the immunity of Pb for mobilisation in the upper estuary. In an acidic (pH 4.4 - 6.3) woodland stream in New Jersey, Sherrell and Ross (1999) observed lower particulate fractions of Pb (76%), Al (43%), Cu (30%), Zn (5%) and Cd (< 7%) than commonly found

in U.S. East Coast rivers. The metal concentration in the > 0.45 μm fraction exceeded the dissolved concentration only for Pb. Adsorption of Pb onto goethite has been observed at low pH values (< 5) in marine environments by Balistiery and Murray (1982), who also showed that the sorption of Pb to goethite in sea water occurs at lower pH values, compared to that of Cu, Zn or Cd. In the Whagaehu River, New Zealand, which receives metal-rich acid (pH 0.6 - 1.2) overflow from a volcanic lake, Pb was found to be adsorbed to the surface fine grained sediments at low pH (< 3), while Cu, Zn and Mn were associated with mineral lattices of larger grains (Deely and Sheppard, 1996). Therefore, it is possible that Pb is scavenged out of solution by Fe and Mn oxyhydroxides and Fe-humic complexes in the upper mixing zone, while other trace metals are released upon the tidal reworking of the sediment. The less pronounced decrease in dissolved Pb concentrations in the upper Ría del Odiel may then be related to the generally lower reactivity in this part of the estuary.

4.6.2.6 Geochemistry of Uranium

In contrast to Fe, Mn, Zn, Cu, Ni, Co and Cd the dissolved distribution of U was dominated by inputs within the estuary. During the TOROS 1, 2 and 3 surveys, dissolved U concentrations increased from 32.2 nM, 28.7 nM and 10.9 nM in the riverine end-member to 288 nM, 220 nM and 50.9 nM, respectively in the lower Ría del Tinto. The dissolved U maxima were located between the phosphogypsum deposits and the cellulose factory (Figure 4.5). There is unequivocal evidence that the fertiliser industry located at Huelva Ría and its wastes in the form of phosphogypsum deposits on the bank of the lower Ría del Tinto are sources of phosphate, U, ^{210}Pb and other radio-isotopes to this estuarine system (Elbaz-Poulichet *et al.* 1999 and 1999b; Martinez-Aguirre and Garcia-Leon, 1997 and 1996). Phosphate ores contain up to 300 μg g^{-1} U (Martinez-Aguirre and Garcia-Leon,

1997). Concentrations of 11 μg g^{-1} U (dry weight) were found in a sample from the phosphogypsum deposits at the lower Ría del Tinto (Elbaz-Poulichet *et al.* 1999). The low pH values in the estuary favoured the dissolution of solid U phases. Phosphate distributions, which are indicative of phosphogypsum discharges, exhibited similar profiles to that of dissolved U during TOROS surveys (Elbaz-Poulichet *et al.* 1999; Cruzado *et al.* 1998), indicating that a plug of water containing phosphogypsum effluent had been relocated by the rising tide to a position upstream of its source. The decline in U concentrations between the maximum and the confluence may have been the result of dilution and sorption processes at near to sea water salinities and pH values.

The mixing behaviour of dissolved U was broadly conservative in the Ría del Odiel, where concentrations decreased from 17 to 25 nM U in the riverine end-member to concentrations below 4.5 nM U at near to sea water salinities (TOROS 1, 2 and 3). The conservative mixing in this part of the estuary may be explained by the presence of soluble U(VI) complexes under the oxidising conditions and low pH (< 3) (Sandino and Bruno, 1992). These conditions prevented the formation of solid U phases and limited the precipitation of Fe (oxy)hydroxides and thus effective scavenging of U.

In the upper Huelva Ría, effluent from the fertiliser industry has been identified as source of U (Martinez-Aguirre and Garcia-Leon, 1997 and 1996; Martinez-Aguirre *et al.* 1994a), and elevated concentrations in the vicinity of these factories have been observed during the TOROS 3 and 4 surveys. The tidal cycle studies carried out under Huelva Bridge during TOROS 3 and 4 surveys (Figure 4.25 and Figure 4.29) showed that dissolved U was transported into the lower Ría del Odiel with the rising tide.

Conservative behaviour of U, as well as removal from solution has been observed in other estuaries (Church *et al.* 1996; Maeda and Windom, 1982). In the Huelva Ría, U from strong riverine and estuarine sources are stored in marsh sediments with such

efficiency that water with near-neutral pH in Huelva Ría contained lower U concentrations compared to average sea water (ca. 13.5 nM, Martin and Whitfield, 1983). Martinez-Aguirre *et al.* (1994a) has attributed this to the co-precipitation U with amorphous ferromanganese oxyhydroxides and deposition in the Odiel salt marshes. A major removal mechanism of U from sea water is the diffusion of dissolved U into suboxic sediments, where it is reduced to less soluble species (Klinkhammer and Palmer, 1991).

In the lower estuary, dissolved U concentrations were similar to typical levels in sea-water, except during TOROS 4, when unusually high concentrations were maintained throughout Huelva Ría (50 - 76 nM U). It is not likely that an extreme increase in industrial discharges was the cause of the high U levels, as they were fairly evenly distributed throughout the estuary, and there was no evidence for enhanced phosphate concentrations related to the factories. Therefore, the source of the additional U during the TOROS 4 survey remains uncertain. During the same survey, lower U concentrations were observed in the Ría del Tinto, compared to previous surveys, and this was attributed to the introduction of a closed water cycle for phosphogypsum deposits. The slight increase in dissolved U close to the confluence is probably the result of mixing with Huelva Ría water.

Generally, the distribution of U in the Tinto/Odiel system verifies earlier suggestions that little or none of the U that enters the estuary in the dissolved phase is exported to the coastal zone (Elbaz-Poulichet *et al.* 1999). However, the last survey suggested that exceptions exist. Experiments in other estuaries (Amazon shelf, Long Island Sound) suggested that the oxidised U(VI) is adsorbed onto newly formed Fe (oxy)hydroxides, and both metals are re-mobilised under more reducing conditions (Barnes and Cochran, 1993). Several studies found a correlation between solid/dissolved U partitioning and the redox cycle of sulphur species, which indicated that microbes are important in the diagenesis of U (Church *et al.* 1996; Barnes and Cochran, 1993;

Klinkhammer and Palmer, 1991). In the Tinto/Odiel system, it is possible that important amounts of U may be eroded from the sediment and transported out of the estuary during flood events and winter storms, and during the dredging of harbour sediments.

4.6.3 Dissolved Metal Fluxes

4.6.3.1 Riverine Metal Flux to the Estuary

The water discharge conditions in the Rio Tinto and Rio Odiel were similar during the four TOROS surveys. However, the river water flow varies greatly between seasons and between years (see Figure 4.3). Therefore, the flow conditions and metal concentrations observed during the four surveys were not representative for all possible scenarios in this system. For example, more than 90% of the annual rainfall may occur during a few days in winter (Borrego-Flores, 1992), and the ochre layer covering the bed of the rivers has been found to be removed during the resulting floods (Morales, personal communication). It is likely that the majority of the annual sediment transport occurs during winter flood events, for which the volume and metal content of SPM carried from the estuary into the coastal sea is unknown. The storage of contaminants in estuarine sediment and release during times of extreme flow has been observed in other systems, for example the Mississippi (Shiller and Boyle, 1991) and the River Eel (California) (Wollast and Duinker, 1982). From a long-term study (21 years) of the River Eel, Wollast and Duinker estimated that 90% of the sediment discharge occurs within 10% of the time. Dilution and re-suspension of bed sediment during floods will lead to a reduction in the dissolved and an increase in the suspended particulate metal load carried by the rivers. Particulate metal concentrations were analysed by colleagues, but not for all surveys, and detailed data was not available in time to be included in the flux calculations. However, SPM concentrations were low in the fresh water end-members and preliminary particulate

metal data (TOROS 4: sequential extraction of particulate Zn; Herzl, unpublished data) indicated that the metal flux was predominantly carried in the dissolved phase. The error introduced by not considering particulate metal fluxes during winter floods may be very large and the calculated flux will be an estimation for 'normal' flow conditions only.

Mean annual gross metal fluxes from the Rio Tinto and Rio Odiel were calculated in order to estimate the magnitude of contamination entering the estuary. The calculations of fluxes from very limited hydrological data required a number of simplifications and assumptions. Calculations were based on the long-term average monthly river water discharge for the Rio Tinto for the period between 1966 and 1992 (Figure 4.3). River discharge is directly related to rainfall and therefore the ratio between the flow rates of the two rivers can be assumed to be constant. From sporadic flow rate measurements (Morales, 1999b) the Odiel:Tinto flow rate ratio was calculated to 4.6 ± 0.6, and this value was used to estimate the long-term average monthly river water discharge for the Rio Odiel from the data available for the Rio Tinto.

Following from the discussion in Section 4.6.1.2 the presence of a seasonal link to variability in river water composition will be assumed for the calculations of mean annual metal fluxes. The chosen procedure gives discharge-weighted gross metal fluxes and emphasises seasonal variability in metal concentrations and river water flow rates:

$$F_{GA} = K \sum_{i=1}^{n} C_i \overline{Q}_s \qquad (4.6).$$

The mean seasonal river water flow rates (Q_a) were calculated by averaging the long-term monthly river flow rates for March - May (spring), June - August (summer), September - November (autumn) and December - February (winter). The mean seasonal water flow rates were 196 and 900×10^3 m^3 d^{-1} (autumn), 263 and 1224×10^3 m^3 d^{-1} (spring) and 10 and 48×10^3 m^3 d^{-1} (summer) for the Rio Tinto and Rio Odiel, respectively. No

complete data set of metal concentrations was available for the winter season. Mean seasonal dissolved metal fluxes were calculated by multiplying the instantaneous metal concentrations by the respective mean seasonal water flow rate (l d^{-1}). The results were added and corrected for the time factor and units to gain the mean annual dissolved gross metal flux for the Rio Tinto and Rio Odiel. The results are presented in Table 4.12.

Because of the linear relationship between river flow and rainfall and the assumed constant factor between the water flow rate of the two rivers, the magnitude of dissolved metal flux followed the pattern of the metal concentrations. With the exception of the last survey (TOROS 4) the contribution of the Rio Odiel to the dissolved flux of Zn, Cu, Ni, Co, Cd and U to the estuary was higher than that of the Rio Tinto. The input of Fe from the Rio Tinto to the estuary was substantially larger than that from the Rio Odiel during all surveys, while Pb did not exhibit a distinct pattern.

A large uncertainty is attached to the results. The variability in the long-term river flow data was ca. 90%, the variability of the dissolved metal data was between 80 and 130% for the Rio Tinto and 30 - 80% for the Rio Odiel (depending on the metals considered), and for the analytical error 10% was assumed. Error propagation carried out for the calculation of the total gross dissolved flux from the Rio Tinto and Rio Odiel resulted in relative standard deviations between 70% and 150% for Mn, U, Ni, Co, Pb, Zn, Cu and Cd. Furthermore, the accuracy of the flux calculation depends on whether the instantaneous metal concentrations were representative for mean seasonal conditions. From the cyclical nature of annual and inter-annual river flow it can be inferred that a reliable flux estimation for this system would require at least monthly sampling for about 10 years. At best, the fluxes calculated for the Rio Tinto and Rio Odiel offer an approximation for comparisons with other AMD affected systems, for which published fluxes are often estimates of a similar nature and accuracy.

Table 4.12 - Gross riverine metal flux from Rio Tinto and Rio Odiel to their estuaries calculated as explained in text. Global riverine fluxes of metals were taken from estimates of rivers of low or no pollution by Martin and Meybeck (1979), 'global p' - global riverine particulate metal flux, 'global d' - global riverine dissolved metal flux, 'fraction' - the percentage of the combined Tinto and Odiel dissolved metal flux with respect to the global riverine dissolved flux. * From Chester (1990), dissolved flux up-scaled from net fluvial fluxes of the US eastern seaboard by Kremling (1985).

($t\ a^{-1}$)	Rio Tinto	Rio Odiel	Total	Global P	Global D	Fraction D (%)
Zn	4300	5600	9900	5400000	1100000	0.90
Cu	1800	1600	3400	1550000	370000	0.92
Ni	24	53	77	2325000	82280	0.94
Co	66	110	180	310000	7480	2.3
Cd	17	17	34	-	4600*	0.74
Mn	1000	3500	4500	162750000	306680	1.5
Pb	17	50	67	2325000	37400	0.18
U	0.5	1.4	1.9	2635000	1496	0.13

Compared to the Tinto/Odiel system, the mean flux of Cu and Zn from the Carnon river, Cornwall (1992: 20 and 360 t a^{-1}, respectively) was lower by several factors (Bryan and Langston, 1992). Dissolved metal fluxes of similar magnitude, but different composition compared to the Tinto/Odiel system were reported for discharge from an acidic crater lake in New Zealand (Deely and Sheppard, 1996), with values of: 20 - 25 t a^{-1} Cu and Cd, 400 - 500 t a^{-1} Pb and Ni, 1000 - 3000 t a^{-1} Zn and 20000 - 2000000 t a^{-1} Al, Fe and Mn. The last example illustrates the great uncertainties associated with flux calculations.

The comparison with the annual global metal fluxes compiled by Martin and Meybeck (1979) and Chester (1990) for major rivers (Table 4.12) shows that the combined flux of the Rio Tinto and Rio Odiel is of importance on a global scale, even when considering that Martin and Meybeck's global gross flux estimates were based on rivers with low or no pollution. According to these estimates the contribution of the Tinto/Odiel rivers to global riverine metal fluxes would be 2.3% Co, 1.5% Mn, 0.9 - 0.94% Zn, Cu and Ni, 0.74% Cd, 0.18% Pb and 0.13% U.

4.6.3.2 Estuarine Dissolved Metal Flux

Recent publications (Regnier and Steefel, 1999; Jarvie *et al.* 1997; Dyer, 1997; Webb *et al.* 1997; Lane *et al.* 1997; Millward *et al.* 1996; Morris and Allen, 1993) offer a variety of approaches for the calculation of estuarine metal, nutrient and particle fluxes into coastal zones. Most of the applied models require a detailed knowledge of hydrodynamics and bathimetry, as well as metal concentrations and water flow data of high temporal resolution. This information is not available at present for the Huelva Ría. Therefore, fluxes from Huelva Ría to the Gulf of Cádiz were estimated following a model suggested by Boyle *et al.* (1974). The calculations were based on the assumption that a given

dissolved metal concentration behaves conservatively at high salinity. The extrapolation of the linear metal/salinity relationship at high salinity to zero salinity, the theoretical net riverine end-member metal concentration of the system can be found. The annual net dissolved fluxes of Zn, Cu, Ni and Co from Huelva Ría were calculated by multiplying the net riverine dissolved metal concentration with the combined mean seasonal flow rates of the Rio Tinto and Rio Odiel (see Section 4.6.3).

Zinc, Cu, Ni and Co were removed from solution in the lower Huelva Ría and at $S > 30$ and $pH > 5.0$. Metal/salinity relationships in the lower Huelva Ría (see Section 4.6.2.4) and in discrete samples form the Gulf of Cádiz analysed by a colleague (Morley, personal communication) were broadly conservative. Close examination of the data indicated that the removal of Zn, Cu, Ni and Co during the four surveys was largely complete at pH values above 6.5 during the TOROS 1 survey and above 7.5 during the remaining surveys. In order to find the zero-salinity metal concentration, the metal-salinity relationships in samples taken downstream from the confluence in Huelva Ría that had pH values greater that those given above were calculated. A sea water end-member representative for the Gulf of Cádiz outside the Huelva metal plume (20 nM Zn, 5 nM Cu, 3 nM Ni and 0.8 nM Co) was included. Linear relationships for Zn, Cu, Ni and Co are given in Table 4.13, whereby the intercept with the y-axis signifies the extrapolated net metal concentrations in the zero-salinity end-member. The presence of a relatively large extrapolation error cannot be excluded.

This simple extrapolation approach to flux calculations has serious limitations. It is based on the hypothesis that the system is one dimensional and at a steady state, which is not necessarily correct for the dynamic Huelva Ría. Furthermore, seasonally changing geochemical or biogeochemical processes that affect the metal concentration in the water are not described in any way and are only taken account of indirectly by the observations

used for the calculations. Only instantaneous fluxes are considered and therefore, the end-member approach cannot be used as a predictive tool. In spite of these limitations, the zero-end-member approach is still being used (Webb *et al.* 1997; Chiffoleau *et al.* 1994). In addition, the uncertainties arising from the question of representativeness of the metal data and the variability of the river flow apply as discussed in Section 4.6.3.

The results (Table 4.14) indicate that a high proportion of Cu and Zn (75 and 63%, respectively) and about half of Co (49%) was removed from solution within the estuary, while Ni remained largely in the dissolved phase (22% removal). The removal from solution was most pronounced in the autumn/winter surveys and lowest during summer. High metal levels reported for sediments of the lower estuary (Table 4.9) indicate that a proportion of the metals lost from solution are at least temporarily retained within the estuary. The export of particulate metals from the estuary at times of average river flow probably constitutes only a minor fraction of the total flux (ca. 10% for Zn, Morley, personal communication). However, particulate material mobilised and flushed out of the estuary under flood conditions could be a major source of metal contamination to the coastal sea. The accumulation of metal rich sediment originating in Huelva Ría on the shelf and slope of the Gulf of Cádiz has been reported by Palanques *et al.* (1995).

High-resolution monitoring of dissolved Cu and Ni in the Gulf of Cádiz (Chapter 5) covered the Guadalquivir plume area during TOROS 2 and 4 surveys. Significant linear relationships between salinity and dissolved Cu and Ni concentrations were observed in surface waters, while Zn was removed from solution in the river plume area. From the linear relationships, the zero-salinity end-member for Cu and Ni in the Guadalquivir river was calculated as described above (410 nM and 210 nM Cu, 135 nM and 220 nM Ni for TOROS 2 and 4, respectively).

Table 4.13 - Metal/salinity relationships in the lower Huelva Ría and to an sea water end-member of 20 nM Zn, 5 nM Cu, 3 nM Ni and 0.8 nM Co. The intercept with the y-axis is the extrapolated net metal concentration (μM) in the zero-salinity end-member.

Survey	Zn	Cu	Ni	Co
TOROS 1	-11S + 390	-2.7S + 100	-0.084S + 3.2	-0.19S + 7.2
TOROS 2	-5.0S + 180	-1.4S + 51	-0.099S + 3.6	-0.19S + 6.8
TOROS 3	-2.1S + 80	-0.22S + 8.2	-0.036S + 1.4	-0.099S + 3.7
TOROS 4	-1.6S + 59	-0.55S + 20	-0.18S + 6.4	-0.054 + 2.0

Table 4.14 - Annual combined gross fluxes from the Rio Tinto and Rio Odiel to the estuary and annual net dissolved fluxes of Zn, Cu, Ni and Co from Huelva Ría to the Gulf of Cádiz. The estimation procedure is described in the text.

	Gross Flux (t a^{-1})	Net Flux (t a^{-1})	Removal (%)
Zn	9900	3700	63
Cu	3400	850	75
Ni	77	68	22
Co	180	86	49

Table 4.15 - Net dissolved metal fluxes from European estuaries.

(t a^{-1})	Zn (t a^{-1})	Cu (t a^{-1})	Ni (t a^{-1})	Co (t a^{-1})
Seine, low discharge[1]	91 - 128	15 - 22	18 - 22	0.73 - 1.5
Humber estuary[2]	11 - 46	4.0 - 14	6.2 - 20	0.37 - 1.1
Irish Sea[3]	-	38 - 51	-	-
Rhone estuary[4]	-	107	74	4

[1] Seine estuary, English Channel (Chiffoleau *et al.* 1994).
[2] Humber (North Sea), winter, spring and summer surveys (Morris and Allen, 1993).
[3] Irish Sea, total riverine input (Williams *et al.* 1998 and references therein).
[4] Rhone input to the Gulf of Lion, Western Mediterranean Sea (Guieu *et al.* 1991 and references therein).

Using the mean annual river discharge (164 m^3 s^{-1}), a very rough estimate of the metal discharge from the Guadalquivir estuary was made. The results (65 - 130 t a^{-1} Cu and 41 - 67 t a^{-1} Ni) show that the Guadalquivir is a minor contributor to the dissolved Cu load of the Gulf of Cádiz, compared with the Huelva system, while the input of Ni from both rivers are of a similar magnitude. Comparisons with other estuaries (Table 4.15) show that the Huelva system is a major source of dissolved metals to European coastal waters.

4.7 Conclusions

Total dissolved metal concentrations and estuarine master variables, which had been collated during four surveys in the Rio Tinto, Rio Odiel and their estuary, as well as work published about comparable systems were examined in order to define and understand the metal geochemistry in the Tinto/Odiel system. Dissolved concentrations of Fe, Al, Mn, Zn, Cu, Ni, Co, Cd, Pb and U in the Rio Tinto and Rio Odiel reached levels comparable to the most polluted natural water courses reported in the literature. The main source of these metals (except U) was acid mine drainage, which was generated in the metalliferous mining area of the Iberian Pyrite Belt. The process of metal sulphide oxidation also resulted in high sulphate concentrations and low pH values in the rivers, which maintained metals in solution and encouraged acidophilic micro-organisms to thrive and possibly be an important driving force in the redox cycles of iron, manganese and sulphur.

The seasonal differences in riverine pollution load were tentatively linked with the cycle of dry summers (accretion of metal-rich sediments and solution), wet autumns (enhanced leaching and flushing of AMD into rivers) and winter floods (dilution of AMD and removal of accumulated ochre from the river bed). However, the kinetic effect of seasonal changes in light intensity and temperature changes on abiotic and biotic redox

cycling cannot be excluded as factors for seasonal variability, and this would be an interesting area of further investigation in this system.

In the estuary of the Rio Tinto, very low pH values were maintained by acidic industrial discharges until the second half of 1998. The combination of sediment re-suspension, low pH and high levels of organic matter derived from a cellulose factory created conditions that favoured the remobilisation of metals from solid phases during the early stages of mixing with sea water. Otherwise, the behaviour of Fe, Mn, Zn, Cu, Ni, Co and Cd in the Ría del Tinto and Ría del Odiel was found to be largely conservative up to mid- or high salinities. Removal of trace metals from solution occurred in Huelva Ría only when pH values reached 4 to 5. The behaviour of dissolved metals was dominated by pH in this system.

The estuarine distribution of Pb and U was in contrast to that of Fe, Mn, Zn, Cu, Ni, Co and Cd. Dissolved Pb concentrations decreased rapidly in the upper Ría del Tinto, which was attributed to its limited solubility and high affinity for the particulate phase. The estuarine distribution of U and to a lesser extent of Pb was dominated by wastes from the fertiliser industry, with dissolved and particulate U and Pb inputs entering the upper Huelva Ría, and leachate and erosion of phosphogypsum entered the lower Ría del Tinto. Both metals appeared to be trapped within the estuary, so that under average discharge conditions a comparatively small fraction of U and Pb will be exported to the coastal zone.

Rough approximations of dissolved Zn, Cu, Ni and Co fluxes from the river to the estuary and from the estuary to the Gulf of Cádiz were calculated, however, the necessary assumptions introduced a high uncertainty to the results. Nevertheless, the comparison with annual global riverine metal fluxes after Martin and Meybeck (1979) indicated that the Rio Tinto and Rio Odiel carry metal loads of local and global importance. Estuarine flux estimations showed that a considerable proportion of dissolved Zn and Cu, but less Ni

and Co were removed from solution within the estuary. The dissolved metal discharge from Huelva Ría was found to be high, compared to some of the major estuarine sources of Zn, Cu, Ni and Co to European coastal waters. The deposition of metal-rich fine sediment from the Huelva system on the shelf and slope of the Gulf of Cádiz suggest that particulate metals are only temporarily retained. The particulate metal export from Huelva Ría could be an important source of contamination to the coastal zone, especially during winter flood conditions.

4.8 REFERENCES

Achterberg, E.P., Braungardt, C., Morley, N.H., Elbaz-Poulichet, F. and Leblanc, M. (1999) Impact of Los Frailes mine spill on riverine, estuarine and coastal waters in southern Spain. *Water Research* **33**, 3387-3394.

Ackroyd, D.R., Bale, A.J., Howland, R.J.M., Knox, S., Millward, G.E. and Morris, A.W. (1986) Distributions and Behaviour of Dissolved Cu, Zn and Mn in the Tamar Estuary. *Estuarine, Coastal and Shelf Science* **23**, 621-640.

Albaiges, J., Algaba, J., Arambarri, P., Carrera, F., Baluja, G., Hernandez, L.M. and Castroviejo, J. (1987) Budget of organic and inorganic pollutants in the Donana National Park (Spain). *Science of the Total Environment* **63**, 13-28.

Amils, R., López-Archilla, A., González, E., Durán, C. and Marín, I. Morales, J.A. and Borrego-Flores, J., (Eds.) (1998) The Tinto river life: Microbial characterisation of the Tinto river, a 90 km chemolithotrophic reactor in the pyritic belt of Huelva. pp.15-18. Huelva: Universidad de Huelva.

Balistrieri, L.S. and Murray, J.W. (1982) The adsorption of Cu, Pb, Zn, and Cd on goethite from major ion seawater. *Geochimica et Cosmochimica Acta* **46**, 1253-1265.

Balistrieri, L.S. and Murray, J.W. (1984) Marine scavenging: trace metal adsorption by interfacial sediment from MANOP site H. *Geochimica et Cosmochimica Acta* **48**, 921-929.

Banks, D., Younger, P.L., Arnesen, R.-T., Iversen, E.R. and Banks, S.B. (1997) Mine-water chemistry: the good, the bad and the ugly. *Environmental Geology* **32**, 157-174.

Barnes, C.E. and Cochran, J.K. (1993) Uranium geochemistry in estuarine sediments: controls on removal and release processes. *Geochimica et Cosmochimica Acta* **57**, 555-569.

Benner, R. and Strom, M. (1993) A critical evaluation of the analytical blank associated with DOC measurements by high-temperature catalytic oxidation. *Mar.Chem.* **41**, 153-160.

Benoit, G., Oktay-Marshall, S.D., Cantu, A., II, Hood, E.M., Colemen, C.H., Corapcioglu, M.O. and Santschi, P.H. (1994) Partitioning of Cu, Pb, Ag, Zn, Fe, Al, and Mn between filter-retained particles, colloids, and solution in six Texas estuaries. *Mar.Chem.* **45**, 307-336.

Bigham, J.M., Schwertmann, U., Carlson, L. and Murad, E. (1990) A poorly crystallized oxyhydroxysulfate of iron formed by bacterial oxidation of Fe(II) in acid mine waters. *Geochimica et Cosmochimica Acta* **54**, 2743-2758.

Bigham, J.M., Schwertmann, U. and Pfab, G. (1996) Influence of pH on mineral speciation in a bioreactor simulating acid mine drainage. *Appl.Geochem.* **11**, 849

Bonnissel-Gissinger, P., Alnot, M., Ehrhardt, J.-J. and Behra, P. (1998) Surface Oxidation of Pyrite as a Function of pH. *Environmental Science & Technology* **32**, 2839-2845.

Borrego-Flores, J. (1992) Sedimentologia del estuario del Rio Odiel (Huelva, S.O. Espana). University of Sevilla. PhD Thesis.

Borrego-Flores, J. and Morales, J.-A. (Eds.) (1998) The estuary, interaction between the river and sea. pp.18-26. Huelva: Universidad de Huelva.

Borrego, J., Lopez, M., Pendon, J.G. and Morales, J.A. (1997) C/S ratios in estuarine sediments of the Odiel river mouth, S.W. Spain. *Journal of Coastal Research* **14**, 32-39.

Boult, S., Collins, D.N., White, K.N. and Curtis, C.D. (1994) Metal transport in a stream polluted by acid mine drainage - the Afon Goch, Anglesey, UK. *Environmental Pollution* **84**, 279-284.

Bowell, R.J. and Bruce, I. (1995) Geochemistry of iron ochres and mine waters from Levant Mine, Cornwall. *Appl.Geochem.* **10**, 237-250.

Bowler, C. (1995) The Iberian Pyrite Belt, active and abandoned mines. Visual aid for geology lecture series, University of Plymouth.

Boyle, E., Collier, R., Dengler, A.T., Edmond, J.M., Ng, A.C. and Stallard, R.F. (1974) On the chemical mass-balance in estuaries. *Geochimica et Cosmochimica Acta* **38**, 1719-1728.

Bryan, G.W. and Gibbs, P.E. (1983) Heavy Metals in the Fal Estuary. *Marine Biological Association of the United Kingdom, Occasional Publication* **Number 2.**

Bryan, G.W. and Langston, W.J. (1992) Bioavailability, accumulation and effects of heavy metals in sediments with special reference to United Kingdom estuaries: a review. *Environmental Pollution* **76**, 89-131.

Carlson, L. and Lindstrom, E.B. (1992) Solid-phase products of bacterial oxidation of arsenical pyrite. *Applied and Environmental Microbiology* **58**, 1046-1049.

Cauwet, G. (1994) HTCO method for dissolved organic carbon analysis in seawater: influence of catalyst on blank estimation. *Mar.Chem.* **47**, 55-64.

Cauwet, G., Miller, A., Brasse, S., Fengler, G., Mantoura, R.F.C. and Spitzy, A. (1997) Dissolved and particulate organic carbon in the western Mediterranean Sea. *Deep-Sea Research II* **44**, 769-779.

Chapman, B.M., Jones, D.R. and Jung, R.F. (1996) Processes controlling metal ion attenuation in acid mine drainage streams. *Pure and Applied Chemistry* **68**, 1639-1656.

Chen, W. and Wangersky, P.J. (1993) A high-temperature catalytic oxidation method for the determination of marine dissolved organic carbon and its comparison with the UV photo-oxidation method. *Mar.Chem.* **42**, 95-106.

Chester, R. (1990) Marine Geochemistry. Cambridge: The University Press.

Chiffoleau, J.-F., Cossa, D., Auger, D. and Truquet, I. (1994) Trace metal distribution, partition and fluxes in the Seine Estuary (France) in low discharge regime. *Mar.Chem.* **47**, 145-158.

Church, T.M., Sarin, M.M., Fleisher, M.Q. and Ferdelman, T.G. (1996) Salt marshes: An important coastal sink for dissolved uranium. *Geochimica et Cosmochimica Acta* **60**, 3879-3887.

Comans, R.N.J. and van Dijk, C.P.J. (1988) Role of complexation processes in cadmium mobilization during estuarine mixing. *Nature* **336**, 151-154.

Comber, S.D.W., Gardner, M.J., Gunn, A.M. and Whalley, C. (1996) Kinetics of trace metal sorption to estuarine suspended particulate matter. *Chemosphere* **33**, 1027-1040.

Cruzado, A., Velasquez, Z., Garcia, H.E., Bahamon, N., Perez, M.d.C., Grimaldo, N.S., Pla, S. and Simic, L. (1998) TOROS, 2nd Field Experiment, 10 - 21 June 1997. TOROS II, Blanes, Spain: CEAB, Centro de Estudios Avanzados de Blanes.

Cruzado, A., Velasquez, Z., Ridolfi, F., Bahamon, N., Grimaldo, N.S., Simic, L. and Pla, S. (1999) TOROS, 4nd Field Experiment, 1 - 20 October 1998. TOROS IV, Blanes, Spain: CEAB, Centro de Estudios Avanzados de Blanes.

Deely, J.M. and Sheppard, D.S. (1996) Whangaehu River, New Zealand: Geochemistry of a river discharging from an active crater lake. *Appl.Geochem.* **11**, 447-460.

Duinker, J.C. (1980) Suspended matter in estuaries: adsorption and desorption processes. In: Olausson, E. and Cato, I., (Eds.) *Chemistry and biogeochemistry of estuaries*, pp. 121-152. Chichester: John Wiley & Sons.

Dyer, K.R. (1997) *Estuaries: a physical introduction*, 2 edn. Chichester: John Wiley & Sons Ltd.

Ehrlich, H.L. (1996) *Geomicrobiology*, 3 edn. New York: Marcel Dekker, Inc.

Elbaz-Poulichet, F., Dupuy, C., Cruzado, A., Velasquez, Z., Achterberg, E.P. and Braungardt, C.B. (2000) Influence of sorption processes by Fe oxides and algal uptake on arsenic and phosphate cycle in an acidic estuary (Tinto river, Spain). *Water Research* **in press**.

Elbaz-Poulichet, F. Cruise reports and data from TOROS field experiments. (1999) Internet Communication: http://carpanta.ugr.es/toros/.

Elbaz-Poulichet, F., Garnier, J.-M., Guan, D.M., Martin, J.-M. and Thomas, A.J. (1996) The Conservative Behaviour of Trace Metals (Cd, Cu, Ni and Pb) and As in the Surface Plume of Stratified Estuaries: Example of the Rhone River (France). *Estuarine, Coastal and Shelf Science* **42**, 289-310.

Elbaz-Poulichet, F., Martin, J.-M., Huang, W.W. and Zhu, J.X. (1987) Dissolved Cd behaviour in some selected french and chinese estuaries. Consequences on Cd supply to the ocean. *Mar.Chem.* **22**, 125-136.

Elbaz-Poulichet, F., Morley, N.H., Cruzado, A., Velasquez, Z., Green, D., Achterberg, E.P. and Braungardt, C.B. (1999) Trace metal and nutrient distribution in an extremely low pH (2.5) river-estuarine system, the Ria of Huelva (south-west Spain). *The Science of the Total Environment* **227**, 73-83.

Featherstone, A.M. and O'Grady, B.V. (1997) Removal of dissolved copper and iron at the freshwater-saltwater interface of an acid mine stream. *Mar.Poll.Bull.* **34**, 332-337.

Förstner, U. (1980) Inorganic pollutants, particularly heavy metals in estuaries. In: Olausson, E. and Cato, I., (Eds.) *Chemistry and biogeochemistry of estuaries*, pp. 307-348. Chichester: John Wiley & Sons]

Gao, Y. and Bradshaw, A.D. (1995) The Containment of Toxic Wastes: II. Metal Movement in Leachate and Drainage at Parc Lead-Zinc Mine, North Wales. *Environmental Pollution* **90**, 3-3.

Gibbs, R.J. (1986) Segregation of metals by coagulation in estuaries. *Mar.Chem.* **18**, 149-159.

Gray, N.F. (1998) Acid mine drainage composition and the implications for its impact on lotic systems. *Water Research* **32**, 2122-2134.

Groot, W.T.d., Jong, F.M.W.d. and Berg, M.M.H.E.E. (1987) Population dynamics of duckweed cover in polder ditches. *Arch.Hydrobiol.* **109**, 601-618.

Guieu, C., Martin, J.-M., Thomas, B. and Elbaz-Poulichet, F. (1991) Atmospheric versus river inputs of metals to the Gulf of Lions. *Mar.Poll.Bull.* **22**, 176-183.

Hedges, J.I., Bergamaschi, B.A. and Benner, R. (1993) Comparative analyses of DOC and DON in natural waters. *Mar.Chem.* **41**, 121-134.

Hudson-Edwards, K.A., Schell, C. and Macklin, M.G. (1999) Mineralogy and geochemistry of alluvium contaminated by metal mining in the Rio Tinto area, southwest Spain. *Appl.Geochem.* **14**, 1015-1030.

Izquierdo, C., Usero, J. and Gracia, I. (1997) Speciation of heavy metals in sediments from salt marshes on the southern Atlantic coast of Spain. *Mar.Poll.Bull.* **34**, 123-128.

Jarvie, H.P., Neal, C. and Tappin, A.D. (1997) European land-based pollutant loads to the North Sea: An analysis of the Paris Commission data and review of monitoring strategies. *Sci.Total.Environ.* **194-195**, 39-58.

Johnson, C.A. (1986) The regulation of trace element concentrations in rivers and estuarine waters contaminated with acid mine drainage: The adsorption of Cu and Zn on amorphous Fe oxyhydroxides. *Geochimica et Cosmochimica Acta* **50**, 2433-2438.

Johnson, C.A. and Thornton, I. (1987) Hydrological and chemical factors controlling the concentrations of Fe, Cu, Zn and As in a river system contaminated by acid mine drainage. *Water Research* **21**, 358-365.

Jordao, C.P., Pereira, J.C., Brune, W., Pereira, J.L. and Braathen, P.C. (1996) Heavy metal dispersion from industrial wastes in the Vale do Aco, Minas Gerais, Brazil. *Environ.Technol.* **17**, 489-500.

Kirby, C.S. and Elder Brady, J.A. (1998) Field determination of Fe^{2+} oxidation rates in acid mine drainage using a continuously-stirred tank reactor. *Appl.Geochem.* **13**, 509-520.

Klinkhammer, G.P. and Palmer, M.R. (1991) Uranium in the oceans: where it goes and why. *Geochimica et Cosmochimica Acta* **55**, 1799-1806.

Kraepiel, A.M.L., Chiffoleau, J.-F., Martin, J.-F. and Morel, F.M.M. (1997) Geochemistry of trace metals in the Gironde estuary. *Geochimica et Cosmochimica Acta* **61**, 1421-1436.

Krauskopf, K.B. and Bird, D.K. (1995) *Introduction to geochemistry*, 3 edn. New York: McGraw-Hill, Inc.

Kremling, K. (1985) The distribution of cadmium, nickel, manganese and aluminium in surface waters of the open Atlantic and European shelf area. *Deep Sea Res.* **32**, 531-555.

Lane, A., Prandle, D., Harrison, A.J., Jones, P.D. and Jarvis, C.J. (1997) Measuring fluxes in tidal estuaries: sensitivity to instrumental and associated data analyses. *Estuarine, Coastal and Shelf Science* **45**, 433-451.

Leblanc, M., Benothman, D., Elbaz-Poulichet, F., Luck, J.M., Carvajal, D., Gonzalez-Martinez, A.J., Grande-Gil, J.A., Ruiz de Almodovar, G. and Saez-Ramos, R. (1995) Rio Tinto (Spain), an acidic river from the oldest and most important mining areas of Western Europe: Preliminary data on metal fluxes. In: Pasava, Kribek and Zak, (Eds.) *Mineral Deposits*, pp. 669-670. Rotterdam: Balkema.

Lee, C. and Henrichs, S.M. (1993) How the nature of dissolved organic matter might affect the analsis of dissolved organic carbon. *Mar.Chem.* **41**, 105-120.

Leistel, J.M., Marcoux, E., Deschamps, Y. and Joubert, M. (1998a) Antithetic behaviour of gold in the volcanogenic massive sulphide deposits of the Iberian Pyrite Belt. *Mineralium Deposita* **33**, 82-97.

Leistel, J.M., Marcoux, E., Thiéblemont, D., Quesada, C., Sánchez, A., Almodóvar, G.R., Pascual, E. and Sáez, R. (1998b) The volcanic-hosted massive sulphide deposits of the Iberian Pyrite Belt. *Mineralium Deposita* **33**, 2 - 30

Luque, C.J., Castellanos, E.M., Castillo, J.M., Gonzalez, M., Gonzales-Vilches, C. and Figueroa, M.E. (1999) Metals in Halophytes of a Contaminated Estuary (Odiel Saltmarshes, SW Spain). *Mar.Poll.Bull.* **38**, 49-51.

Luther, G.W., III, Shellenbarger, P.A. and Brendel, P.J. (1996) Dissolved organic Fe(III) and Fe(II) complexes in salt marsh porewaters. *Geochimica et Cosmochimica Acta* **60**, 951-960.

Maeda, M. and Windom, H.L. (1982) Behaviour of uranium in two estuaries of the south-eastern United States. *Mar.Chem.* **11**, 427-436.

Mantoura, R.F.C. and Woodward, E.M.S. (1983) Conservative behaviour of riverine dissolved organic carbon in the Severn Estuary: chemical and geochemical implications. *Geochimica et Cosmochimica Acta* **47**, 1293-1309.

Martin, J.-M. and Meybeck, M. (1979) Elemental Mass-Balance of Material Carried by Major World Rivers. *Mar.Chem.* 7, 173-206.

Martin, J.-M. and Whitfield, M. (1983) The significance of the river input of chemical elements to the ocean. In: Wong, C.S., Boyle, E., Bruland, K.W., Burton, J.D. and Goldberg, E.D., (Eds.) *Trace metals in sea water*, pp. 265-269. New York: Plenum Press, Ltd.

Martinez-Aguirre, A. and Garcia-Leon, M. (1996) 210Pb Distribution in Riverwaters and Sediments near Phosphate Fertilizer Factories. *Applied Radiation and Isotopes* **47**, 599-602.

Martinez-Aguirre, A. and Garcia-Leon, M. (1997) Radioactive Impact of Phosphate Ore Processing in a Wet Marshland in Southwestern Spain. *Journal of Environment and Radioactivity* **34**, 45-57.

Martinez-Aguirre, A., Garcia-Leon, M. and Ivanovich, M. (1994a) Identification and Effects of Anthropogenic Emissions of U and Th on the Composition of Sediments in a River/Estuarine System in Southern Spain. *Journal of Environment and Radioactivity* **23**, 231-248.

Martinez-Aguirre, A., Garcia-Leon, M. and Ivanovich, M. (1994b) U and Th Distribution in Solution and Suspended Matter from Rivers Affected by the Phosphate Rock Processing in Southwestern Spain. *Nuclear Instruments andMethods in Physics Research* **A 339**, 287-293.

McCarty, D.K., Moore, J.N. and Marcus, W.A. (1998) Mineralogy and trace element association in an acid mine drainage iron oxide precipitate; comparison of selective extractions. *Appl.Geochem.* **13**, 165-176.

Medio Ambiente Seccion de Medio Ambiente, (Ed.) (1998) Ejecucion del plan de policia de aguas del litoral Andaluz. Informe del año 1997, Sevilla: E.S.I.I. de Sevilla. Dpto. Ingen. Química y Ambiental.

Miles, C.J. and Brezonik, P.L. (1981) Oxygen consumption in humic-colored waters by a photochemical ferrous-ferric catalytic cycle. *Environmental Science & Technology* **15**, 1089-1094.

Miller, G.C., Lyons, W.B. and Davis, A. (1996) Understanding the water quality of pit lakes. *Environmental Science & Technology/News* **30**, 118A-123A.

Millward, G.E., Allen, J.I., Morris, A.W. and Turner, A. (1996) Distributions and fluxes of non-detrital particulate Fe, Mn, Cu, Zn in the Humber coastal zone, U.K. *Cont.Shelf.Res.* **16**, 967-993.

Millward, G.E. and Marsh, J.G. (1986) Dissolved Arsenic Behaviour in Estuaries Receiving Acid Mine Wastes. In: Lester, J.N.e.a., (Ed.) *Proceedings of the International Conference on Chemicals in the Environment*, pp. 470-476. London: Selper Ltd.

Millward, G.E. and Turner, A. (1995) Trace metals in estuaries. In: Salbu, B. and Steinnes, E., (Eds.) *Trace elements in natural waters*, pp. 223-245. London: CRC Press.

Morales, J.A. (1998a). Excursion to the mining area of Riotinto during the 2nd annual ELOISE Scientific Conference, October 1998, Huelva, Spain.

Morales, J.A. Morales, J.A. and Borrego-Flores, J., (Eds.) (1998b) General characteristics of the Tinto river. pp.4-6. Huelva: Universidad de Huelva.

Morales, J.A. (1999a). 5th scientific TOROS meeting, April 1999, Grenada, Spain.

Morales, J. A. Hydrology of the Tinto and Odiel rivers and Huelva estuary, south-west Spain. (1999) Internet Communication.

Morales, J. A., Borrego-Flores, J., Lopez, M., and Gonzalez Martinez, A. Cruise reports and data from TOROS field experiments. (1999) Internet Communication.

Morris, A.W. and Allen, I. (1993) Behaviour and flux of contaminant metals in the north sea. Contract No PECD7/7/362, Plymouth Marine Laboratories.

Morris, A.W., Bale, A.J. and Howland, R.J.M. (1982) The dynamics of estuarine manganese cycling. *Estuarine, Coastal and Shelf Science* **14**, 175-192.

Morris, A.W., Bale, A.J., Howland, R.J.M., Millward, G.E., Ackroyd, D.R., Loring, D.H. and Rantala, R.T.T. (1986) Sediment mobility and its contribution to trace metal cycling and retention in a macrotidal estuary. *Water Science and Technology* **18**, 111-119.

Nelson, C.H. and Lamothe, P.J. (1993) Heavy Metal Anomalies in the Tinto and Odiel River and Estuary System, Spain. *Estuaries* **16**, 496-511.

Niemela, S.I., Sivela, C., Luoma, T. and Tuovinen, O.H. (1994) Maximum temperature limits for acidophilic, mesophilic bacteria in biological leaching systems. *Applied and Environmental Microbiology* **60**, 3444-3446.

Noike, T., Nakamura, K. and Matsumoto, J. (1983) Oxidation of ferrous iron by acidophilic iron-oxidizing bacteria from a stream receiving acid mine drainage. *Water Research* **17**, 21-27.

Palanques, A., Diaz, J.I. and Farran, M. (1995) Contamination of Heavy Metals in the Suspended and Surface Sediment of the Gulf of Cadiz (Spain): the Role of Sources, Currents, Pathways and Sinks. *Oceanologica Acta* **18**, 469-477.

Parkman, R.H., Curtis, C.D. and Vaughan, D.J. (1996) Metal fixation and mobilisation in the sediments of the Afon Goch estuary - Dulas Bay, Anglesey. *Applied Geochemistry*, **11**, 203 - 210.

Paucot, H. and Wollast, R. (1997) Transport and transformation of trace metals in the Scheldt estuary. *Mar.Chem.* **58**, 229-244.

Perianez, R., Abril, J.M. and Garcia-Leon, M. (1996) Modelling the Suspended Matter Distribution in an Estuarine System. Application to the Odiel River in Southwest Spain. *Ecological Modelling* **87**, 169-179.

Pons, J.M. and Morales, J.A. Morales, J.A. and Borrego-Flores, J., (Eds.) (1998) The source zone. Rio Tinto mines in the setting of the Iberian Pyrite Belt. pp.7-14. Huelva: Universidad de Huelva.

Pronk, J.T. and Johnson, B.D. (1992) Oxidation and reduction of iron by acidophilic bacteria. *Geomicrobiology Journal* **10**, 153-171.

Regnier, P. and Steefel, C.I. (1999) A high resolution estimate of the inorganic nitrogen flux from the Scheldt estuary to the coastal North Sea during a nitrogen-limited algal bloom, spring 1995. *Geochimica et Cosmochimica Acta* **63**, 1359-1374.

Rodwell, M.J. and Folland, C.K. (1999) Oceanic forcing of the wintertime North Atlantic Oscillation and European climate. *Nature* **398**, 320-323.

Rosman, K.J.R., Chisholm, W., Hong, S., Candelone, J.-P. and Boutron, C.F. (1997) Lead from Carthaginian and Roman Spanish mines isotopically identified in Greenland ice dated from 600 B.C. to 300 A.D. *Environmental Science & Technology* **31**, 3413-3416.

Salomons, W. (1995) Environmental impact of metals derived from mining activities: processes, predictions, prevention. *Journal of Geochemical Exploration* **52**, 5-23.

Sandino, A. and Bruno, J. (1992) The solubility of (UO2)3(PO4)2.4H2O(s) and the formation of U(VI) phosphate complexes: their influence in uranium speciation in natural waters. *Geochimica et Cosmochimica Acta* **56**, 4135-4145.

Sherrell, R.M. and Ross, J.M. (1999) Temporal variability of trace metals in New Jersey Pinelands streams: Relationships to discharge and pH. *Geochimica et Cosmochimica Acta* **63**, 3321-3336.

Shiller, A.M. and Boyle, E.A. (1991) Trace elements in the Mississippi River Delta outflow region: Behavior at high discharge. *Geochimica et Cosmochimica Acta* **55**, 3241-3251.

Sholkovitz, E.R. (1978) The flocculation of dissolved Fe, Mn, Al, Cu, Ni, Co and Cd during estuarine mixing. *Earth and Planetary Science Letters* **41**, 77-86.

Simpson, S.L., Apte, S.C. and Batley, G.E. (1998) Effect of short-term resuspension events on trace metal speciation in polluted anoxic sediments. *Environmental Science & Technology* **32**, 620-625.

Stenner, R.D. and Nickless, G. (1975) Heavy metals in organisms of the Atlantic coast of S.W. Spain and Portugal. *Mar.Poll.Bull.* **6**, 89-92.

Strauss, G.K., Madel, J. and Alonso, F.F. (1977) Exploration practice for strata-bound volcanogenic sulphide deposits in the Spanish-Portuguese pyrite belt. In: Klemm and Scheinder, H.J., (Eds.) *Time- and strata-bound ore deposits*, pp. 55-93. Berlin: Springer Verlag.

Stromberg, B. and Banwart, S. (1994) Kinetic modelling of geochemical processes at the Aitik ining waste rock site in northern Sweden. *Appl.Geochem.* **9**, 595

Stromberg, B. and Banwart, S.A. (1999) Experimental study of acidity-consuming processes in mining waste rock: some influences of mineralogy and particle size. *Appl.Geochem.* **14**, 1-16.

Stumm, W. and Morgan, J.J. (1996) *Aquatic Chemistry-Chemical equilibria and rates in natural waters*, 3 edn. New York: John Wiley & Sons.

Sugimura, Y. and Suzuki, Y. (1988) A high-temperature catalytic oxidation method for the determination of non-volatile dissolved organic carbon in seawater by direct injection of a liquid sample. *Mar.Chem.* **24**, 105-131.

Sulzberger, B. and Laubscher, H. (1995) Reactivity of Various Types of Iron(III) (hydr)oxides Towards Light-induced Dissolution. *Mar.Chem.* **50**, 103-115.

Taylor, S.R. (1964) The abundance of chemical elements in the continental crust. *Geochimica et Cosmochimica Acta* **28**, 1273-1285.

Thornburn, J.A. (1990) The Industrial Archaeology of Rio Tinto and the Iberian Pyrite Belt. *Bulletin of the Peak District Mines Historical Society* **11**, 97-108.

Thornton, I. (1996) Impacts of mining on the environment; some local, regional and global issues. *Appl.Geochem.* **11**, 355-361.

Tuovinen, O.H., Bhatti, T.M., Bigham, J.M. and Hallberg, K.B. (1994) Oxidative dissolution of arsenopyrite by mesophilic and moderately thermophilic acidophiles. *Applied and Environmental Microbiology* **60**, 3268-3274.

Turekian, K.K. (1977) The fate of metals in the ocean. *Geochimica et Cosmochimica Acta* **41**, 1139-1144.

Van Geen, A., Adkins, J.F., Boyle, E.A., Nelson, C.H. and Palanques, A. (1997) A 120 yr record of widespread contamination from mining of the Iberian pyrite belt. *Geology* **25**, 291-294.

Webb, B.W., Phillips, J.M., Walling, D.E., Littlewod, I.G., Watts, C.D. and Leeks, G.J.L. (1997) Load estimation methodologies for British rivers and their relevance to the LOIS RACS(R) programme. *The Science of the Total Environment* **194/195**, 379-389.

Webster, J.G., Swedlund, P.J. and Webster, K.S. (1998) Trace metal adsorption onto an acid mine drainage iron (III) oxy hydroxy sulfate. *Environmental Science & Technology* **32**, 1361-1368.

Williams, M.R., Millward, G.E., Nimmo, M. and Fones, G. (1998) Fluxes of Cu, Pb and Mn to the north-eastern Irish Sea: the importance of sedimental and atmospheric inputs. *Mar.Poll.Bull.* **36**, 366-375.

Williams, P.J.l.B., Bauer, J., Benner, R., Hegeman, J., Ittekkot, V., Miller, A., Norrman, B., Suzuki, Y., Wangersky, P.J. and McCarthy, M. (1993) DOC subgroup report. *Mar.Chem.* **41**, 11-21.

Windom, H., Smith Jr, R., Rawlinson, C., Hungspreugs, M., Dharmvanij, S. and Wattayakorn, G. (1988) Trace metal transport in a tropical estuary. *Mar.Chem.* **24**, 293-305.

Winland, R.L., Traina, S.J. and Bigham, J.M. (1991) Chemical composition of ochreous precipitates from Ohio coal mine drainage. *Journal of Environmental Quality* **20**, 460.

Wollast,R. and Duinker,J.C. (1982) General methodology and sampling strategy for studies on the behaviour of chemicals in estuaries. *Thalassia Jugosl.* **18**, 471-491.

Yeats, P.A. and Loring, D.H. (1991) Dissolved and particulate metal distributions in the St. Lawrence estuary. *Canadian Journal of Earth Sciences* **28**, 729-742.

Yu, Y.S., Bailey, G.W. and Xianchan, J. (1996) Application of a lumped, nonlinear kinetics model to metal sorption on humic substances. *Journal of Environmental Quality* **25**, 552-561.

Zwolsman, J.J.G., Berger, G.W. and Van Eck, G.T.M. (1993) Sediment accumulation rates, historical input, postdepositional mobility and retention of major elements and trace metals in salt marsh sediments of the Scheldt estuary, SW Netherlands. *Mar.Chem.* **44**, 73-94.

Zwolsman, J.J.G., Van Eck, B.T.M. and Van der Weijden, C.H. (1997) Geochemistry of dissolved trace metals (cadmium, copper, zinc) in the Scheldt estuary, southwestern Netherlands: impact of seasonal variability. *Geochimica et Cosmochimica Acta* **61**, 1635-1652.

Zwolsman, J.J.G. and Van Eck, G.T.M. (1993) Dissolved and particulate trace metal geochemistry in the Scheldt estuary, S.W. Netherlands (water column and sediments). *Netherlands Journal of Aquatic Ecology* **27**, 287-300.

Chapter 5

Dissolved Zn, Cu, Ni and Co in the Gulf of Cadiz

5.1 Abstract

Continental shelf seas are often enriched with trace metals, compared to the open ocean. In the Gulf of Cádiz, the enrichment of the water column and shelf sediment with Zn, Cu and other metals has been mainly attributed to inputs from mining activities and industrial discharges. The circulation patterns of surface water masses west of Gibraltar give rise to the transport of metal contamination from the Gulf of Cádiz into the Mediterranean Sea (van Geen *et al.* 1997). In this chapter, the sources, distribution and transport of dissolved Zn, Cu, Ni and Co in the Gulf of Cádiz are discussed.

On-line measurements of total dissolved Zn, Cu and Ni in surface waters of the Gulf of Cádiz during TOROS surveys provided an extensive data set with a high spatial resolution. Detailed surveys of the plume areas of the Huelva and Guadalquivir estuaries revealed the intensity, variability and dispersion of the metal contamination. In the Huelva Ría plume, concentrations of 19 - 800 nM Zn, 15 - 330 nM Cu and 2 - 31 nM Ni were measured, compared to 22 - 150 nM Zn, 7.5 - 71 nM Cu and 2.3 - 18 nM Ni off the Guadalquivir estuary. Additional sources of Zn, Cu and Ni in the north-western Gulf of Cádiz were attributed to the Guadiana estuary or to metal inputs along the southern Portuguese coast. Metal contamination from the Guadiana, Huelva and Guadalquivir estuaries was entrained and transported south-easterly, most probably into the Mediterranean Sea. Compared to North Atlantic surface water, the outer area of the Gulf of Cádiz was enriched with Zn (factor 3.6 - 14), Cu (factor 2.5 - 6.5) and Co (factor 1.8 - 8.8), while Ni varied from enriched in June 1997 (factor 2.3) to depleted in October 1998 (factor 0.51 - 0.8).

5.2 INTRODUCTION

Coastal seas are important transition zones between oceanic and terrestrial environments, where the concentration and physico-chemical form of trace metals may undergo modification by biogeochemical processes. When compared to the open ocean, shelf waters are usually enriched with dissolved trace metals. For example on the European Shelf around the British Isles, Al, Cd, Co, Cu, Mn and Ni concentrations are enhanced largely as a result of anthropogenic activities (Hydes and Kremling, 1993). Mechanisms of metal input into the ocean margins include the upwelling of deep oceanic water (e.g. Cd and Ni, Sanudo-Wilhelmy and Flegal, 1996), the remobilisation from shelf sediment (e.g. Cu and Co, Sanudo-Wilhelmy and Flegal, 1996; Cu and Pb, Williams *et al.* 1998; Fe and Mn, Tappin *et al.* 1993), aeolian deposition (e.g. Al, Cd, Co, Cr, Cu, Fe, Mn, Ni, Pb and Zn, Guieu *et al.* 1997), the dumping of waste and fluvial discharges (e.g. Jarvie *et al.* 1997; Laslett, 1995; Martin and Whitfield, 1983).

Like estuaries, coastal zones are important ecosystems and highly productive, whereby the uptake by primary producers and regeneration in the water column may play important roles in the behaviour and cycling of metals (e.g. Cu, Zn, Ni, Cd and Pb, Tappin *et al.* 1993, and references therein). The adsorption onto fine particles and subsequent formation and deposition of particle aggregates is a major removal mechanism for metals from the water column in estuarine and coastal mixing zones (Jackson and Burger, 1998; Gibbs, 1986; Salomons and Förstner, 1983; Turekian, 1977). Hereby, the supply of fresh particles in coastal waters enhances the surface area available for sorption processes. The partitioning of a metal between the solid and solute phase may vary widely with seasonal differences in the character of suspended particulate matter, especially with respect to the proportion of biogenic material (Tappin *et al.* 1995). In addition to the magnitude of the

supply and biogeochemical processes, local circulation patterns are important in determining the distribution of dissolved metals in the coastal zone.

A detailed understanding of biogeochemical processes and transport mechanisms, which affect the distribution of pollutants in coastal waters, sediment and biota, is desirable, not least because of the ecological and socio-economic importance of estuaries and shelf seas. The enrichment of the Gulf of Cádiz with trace metals has implications reaching beyond the local scale, as water from the Spanish Shelf is entrained in the Atlantic influx to the Mediterranean Sea (van Geen *et al.* 1988). Within the TOROS project, high resolution measurements of dissolved concentrations of Zn, Cu and Ni were carried out with the aim to investigate the spatial development and dispersal of the main estuarine metal plumes. The surveys were carried out at different tidal stages and seasons, in order to assess the temporal variability of metal concentrations in the Gulf of Cádiz.

5.3 The Gulf of Cádiz

The Gulf of Cádiz encompasses the sea area between the Portuguese coast at Faro and the entrance to the Strait of Gibraltar (Figure 5.1). The shelf slopes gently from the coast to a depth of approximately 100 m, and the continental slope is formed by a rapid increase in water depth to more than 500 m. Canyons cut across the slope in north-east to south-westerly direction. With a mean tidal amplitude of 2.5 m, the Gulf of Cádiz is a mesotidal coastal sea. The tidal wave progresses from east to west (Borrego *et al.* 1997), while surface currents flow in the opposite direction (Brown *et al.* 1995).

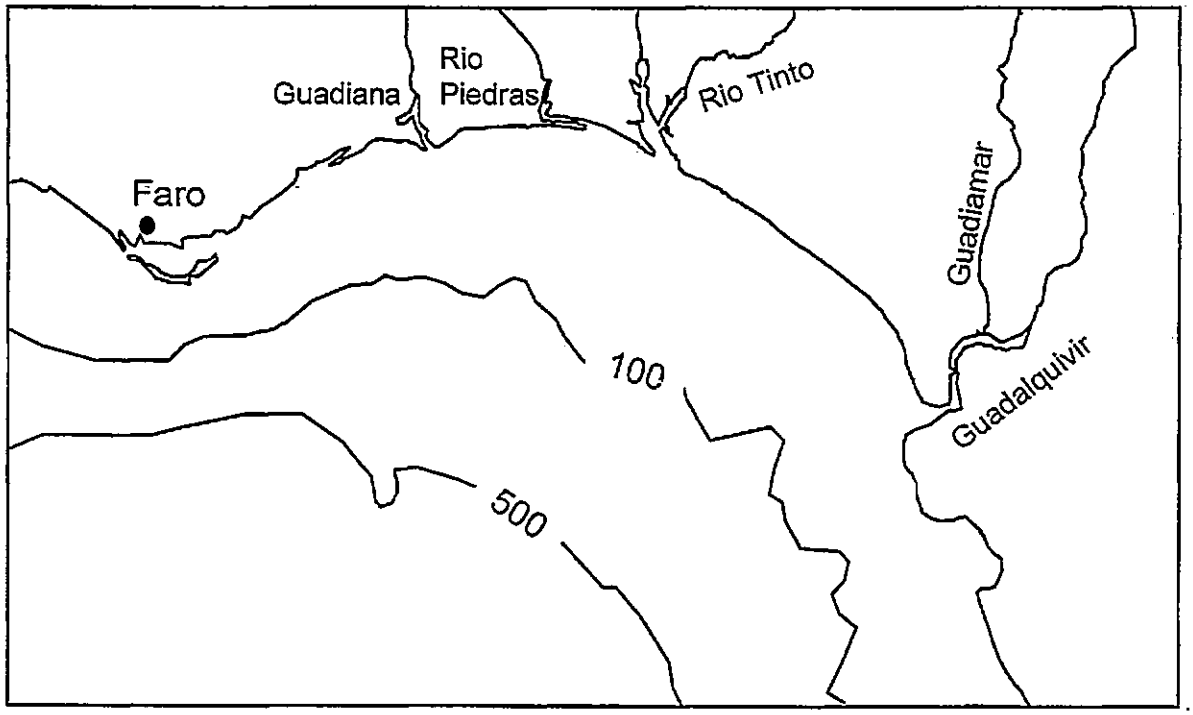

Figure 5.1 - The main rivers draining into the Gulf of Cádiz are the Guadiana and Guadalquivir with respect to water discharge volume, and the Rio Tinto and Rio Odiel and with respect to metal fluxes. Isobaths are drawn at 100 m and 500 m depth (after Palanques *et al.* 1995 and Ochoa and Bray, 1991).

Evaporation exceeds precipitation in the Mediterranean basin. As a result, there is a transport of surface water from the Atlantic Ocean (S ≈ 36.2) into the Mediterranean Sea through the Strait of Gibraltar. It has been suggested that the Atlantic influx consists of a mixture of North Atlantic Surface Water (NASW), North Atlantic Central Water (NACW) and Gulf of Cádiz Water (GCW, 15 - 55%) (Palanques *et al.* 1995 and references therein; van Geen *et al.* 1991). The Mediterranean outflow of deep water (S ≈ 37.7) is a current driven by the density gradient between the Mediterranean and Atlantic deep water masses. It crosses a sill (ca. 300 m depth) at Gibraltar, is redirected to the north by a ridge, follows the continental slope of the Gulf of Cádiz to the west and can be detected at a depth of 1200 m at Cape St. Vincent on the south-western corner of the Iberian Peninsular (Ochoa and Bray, 1991 and references therein).

The Atlantic surface and Mediterranean deep currents and upwelling of NACW at the shelf determine the water circulation and influence the sediment dynamic on the shelf and slope of the Gulf of Cádiz (Palanques *et al.* 1995; van Geen and Boyle, 1990). Van Geen *et al.* (1988) identified the Gulf of Cádiz as a source for dissolved Zn, Cu and Cd to surface waters of the Alboran Sea, east of the Gibraltar, by investigating the transport of contaminants. Subsequent studies have shown that the Tinto and Odiel rivers, which are affected by acid mine drainage and industrial discharges into their estuary, were major contributors to the concentrations of dissolved Zn, Cu and Cd (Leblanc *et al.* 1995) and particulate Fe, Mn, Ni, Co, Pb, Ti and Cr (Palanques *et al.* 1995; Nelson and Lamothe, 1993) to the Gulf of Cádiz.

Palanques *et al.* (1995) found that estuarine suspended particulate matter (SPM) entering the Gulf of Cádiz is deposited partially in form of aggregates, while lighter particles are entrained by the south-eastern Atlantic surface current. Settling of such particles may result in their re-orientation and dispersion by the Mediterranean outflow

towards the north-western slope. In a comparison between metal concentrations in suspended particulate matter (SPM) in the plume zones of the Guadiana, Huelva and Guadalquivir estuaries, Nelson and Lamothe (1993) found the highest SPM levels of Cu (470 - 620 mg kg^{-1}), Pb (910 - 1050 mg kg^{-1}), Cr (250 - 300 mg kg^{-1}), Co (45 - 78 mg kg^{-1}), Fe (4.8 - 4.6%) and Mn (2080 - 2530 mg kg^{-1}) associated with the Huelva system. Particulate Zn concentrations (257 - 370 mg kg^{-1}) were similar on the shelf outside the Huelva and Guadalquivir estuaries.

The distribution of particulate metals in the Gulf of Cádiz corresponded to the east-ward transport of contaminants with the prevailing current. Metal-enriched silt and clay deposits of estuarine origin have been found on the shelf between the 30 m and 100 m isobath, and in calmer zones of the submarine canyons along the continental slope (Palanques *et al.* 1995). Enrichments of Fe (4.3%), Co (19 mg kg^{-1}), Ni (36.6 mg kg^{-1}) and Cr (30 mg kg^{-1}) were highest on the continental slope (factor 8.6, 6.1, 7.0 and 5.3 for Fe, Co, Ni and Cr, respectively), compared to offshore locations. This was attributed to advective and diffusive transport of contaminated SPM from estuaries and the dumping of industrial wastes from metal processing facilities in the Huelva industrial zone. Exceptions were Pb (154 mg kg^{-1}) and Cu (158 mg kg^{-1}), which were most enriched (factor 4.1 for Pb and 12.3 for Cu) in the fine sediment outside the Huelva and Guadiana estuaries, respectively (Palanques *et al.* 1995). The data indicated that the Guadalquivir and Guadiana rivers may contribute noticeably to the metal load in this coastal area. The highly contaminated sediments of the Gulf of Cádiz are a potential secondary source of metal pollution to the overlying water column.

5.4 METHODS

5.4.1 REAGENTS AND EQUIPMENT

The quality, preparation and purification of de-ionised water (MQ), reagents (HCl, HNO_3, NH_3, methanol, Oxine, DMG, APDC, Borate, HEPES) and metal standard solutions have been described in Chapter 2.

Mixed reagents and metal standards (Zn, Cu, Ni and Co) for the on-line voltammetric analysis were prepared on a daily basis from the appropriate stock solutions of HEPES, Borate, Oxine and DMG and metal stock solutions as described in Chapter 3.

Materials and cleaning procedures applied to tubing, containers and filter membranes used for sampling, filtration and storage of water samples from the Gulf of Cádiz have been described in Chapter 3.

5.4.2 INSTRUMENTATION

The instrumentation used for the measurement of physico-chemical parameters (conductivity, temperature and pH) during coastal surveys onboard the small vessels *Popeye* and *Cirry Tres* (TOROS 1 and 3, respectively) and the Spanish oceanographic vessel *B/O Garcia del Cid* (TOROS 2 and 4) has been described in Chapter 3.

A detailed account of the fully automated voltammetric metal analyser used onboard ship for the on-line determinations of dissolved Zn, Cu, Ni and Co concentrations in surface waters was given in Chapter 3. Voltammetry as a method of metal analysis has been discussed in Chapter 2.

5.4.3 Sampling Protocol

The dates, vessels used and metals analysed on-line during the four TOROS surveys are given in Table 5.1.

On-line trace metal analysis was carried out using square wave adsorptive cathodic stripping voltammetry (AdCSV) for the simultaneous determination of Zn and Cu (System I) and Ni and Co (System II) as described in Chapter 3. Discrete samples were taken for speciation studies (Chapter 6), but were also used to compare analytical results with total metal concentrations analysed using on-line methods. Methods of sampling and sample treatment and analysis for on-line and discrete methods have been detailed in Chapter 3.

During the ship-board tidal cycle studies (TCs) at anchor stations in or off the mouth of Huelva Ría, discrete samples were taken at hourly intervals, using the same methods of sampling and sample processing as during coastal surveys.

The survey area in the Gulf of Cádiz was restricted to an area encompassed by a radius of between 20 and 40 km off Mazagón during TOROS 1 and 3 surveys, when small vessels (*Popeye* and *Cirry Tres*) were used. Surveys carried out onboard *B/O Garcia del Cid* (TOROS 2 and 4) covered the shelf and slope area in the Gulf of Cádiz between the Guadalquivir in the east and the Guadiana in the west. Figure 5.2 - Figure 5.5 show the locations of samples taken using on-line methods for the analysis of Cu and Zn, and stations where discrete samples were taken for comparisons with on-line analysis.

Table 5.1 - Details of on-line determination of total dissolved Zn, Cu, Ni and Co and discrete samples taken at the mouth of Huelva Ría (Mazagón) and in the Gulf of Cádiz. TC - tidal cycle study, GdC - *B/O Garcia del Cid.* (Me) - metal was below limit of detection for simultaneous analysis during parts of the survey. The locations of sampling stations in the Gulf of Cádiz are given in Figure 5.2 - Figure 5.5, locations of TCs are given in Chapter 4, Figure 4.9.

TOROS 1, Nov '96	Day	Sample ID: TOR-96-11-	Vessel	Remark
Coastal Survey	21	34 - 38	*Popeye*	Zn, Cu, Ni, (Co)
Coastal Survey	24	39 - 43	*Popeye*	Zn, Cu, Ni, (Co)
Coastal Survey	25	65 - 68	*Popeye*	Zn, Cu, Ni, (Co)
TOROS 2, Jun '97	Day	Sample ID: TOR-97-06-	Vessel	Remark
Coastal Survey	10	E23	GdC	Cu, (Zn), Ni
Coastal Survey	11	D19, C11	GdC	Cu, (Zn), Ni
Coastal Survey	12	C16, B7, B9, G41	GdC	Cu, (Zn), Ni
Coastal Survey	13		GdC	Cu, (Zn), Ni
Coastal Survey	14		GdC	Cu, (Zn), Ni
Coastal Survey	16		GdC	Cu, (Zn), Ni, (Co)
Coastal Survey	17		GdC	Cu, (Zn), Ni, (Co)
TOROS 3, Apr '98	Day	Sample ID: TOR-98-04-	Vessel	Remark
TC, Mazagón	21	MZ1 - MZ12	*Chirry Tres*	Cu, Zn, Ni, Co
Coastal Survey	22	MZ13 - MZ17	*Chirry Tres*	Cu, Zn, Ni, Co
Coastal Survey	23	MZ18 - MZ23	*Chirry Tres*	Cu, Zn, Ni, Co
TOROS 4, Oct. '98	Day	Sample ID: TOR-98-10-	Vessel	Remark
Coastal Survey	11	A1-A4	GdC	Cu, Zn, Ni
Coastal Survey	12	A5, C4 - C6, D7	GdC	Cu, Zn, Ni
Coastal Survey	13	D6 - D5, E5 - E7, F8 - F6	GdC	Cu, Zn, Ni
Coastal Survey	14	G6	GdC	Cu, Zn, Ni
Coastal Survey	15		GdC	Cu, Zn, Ni
Coastal Survey	15		GdC	Cu, Zn, Ni
TC, Mazagón	19/20	G47/MZ 1 - 13	GdC	Cu, Zn, Ni, Co

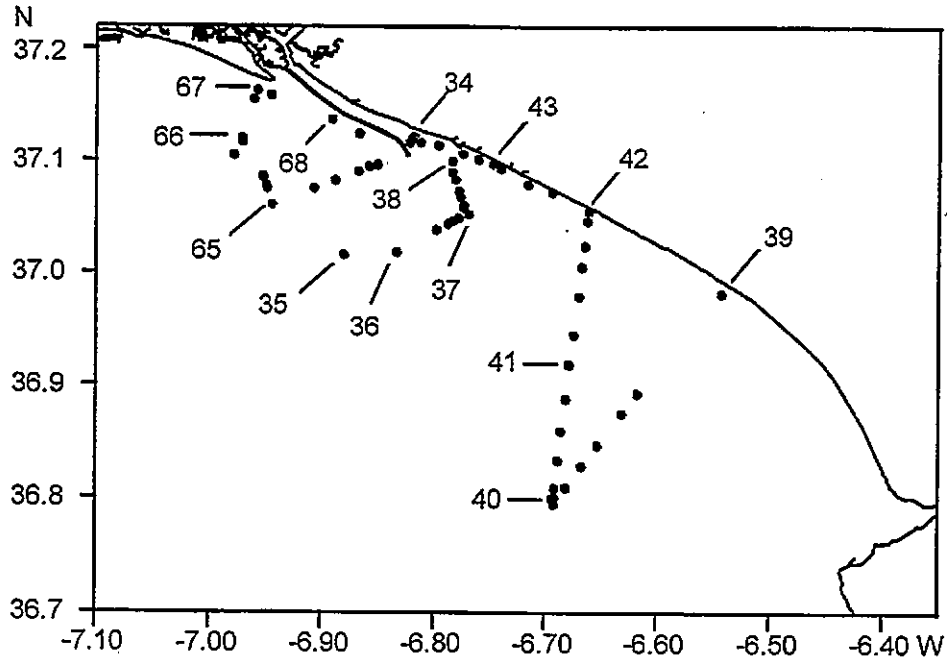

Figure 5.2 - TOROS 1: Locations of on-line (•) and discrete samples (number) in the Gulf of Cádiz in November 1996.

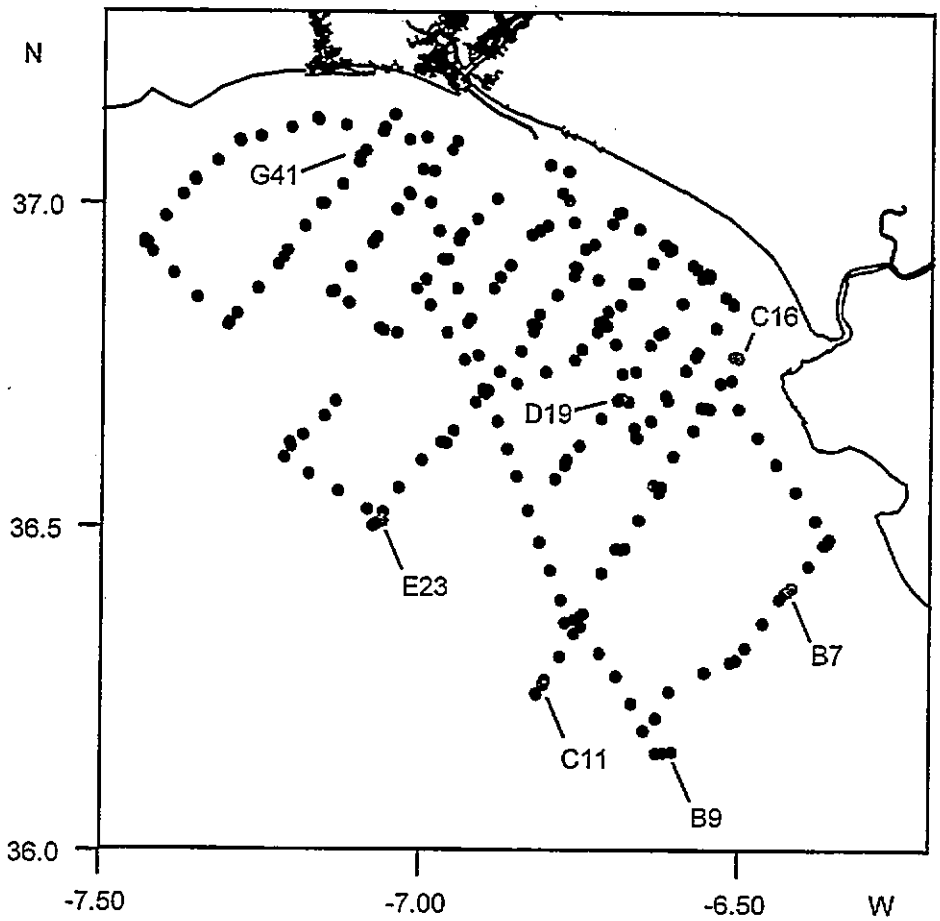

Figure 5.3 - TOROS 2: Locations of on-line (•) and discrete samples (number) in the Gulf of Cádiz between 10 and 14 June 1997.

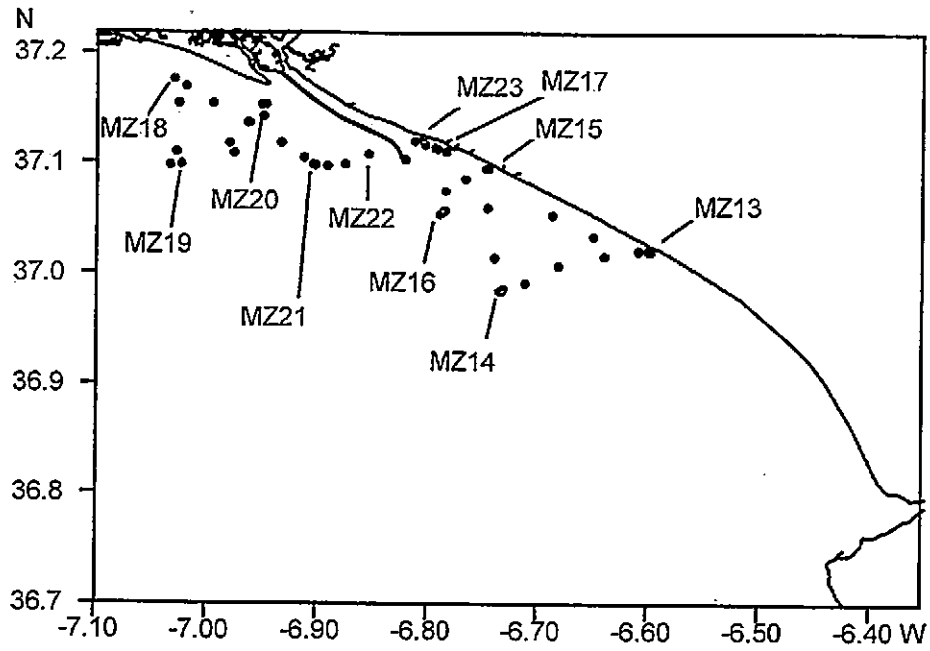

Figure 5.4 - TOROS 3: Locations of on-line (•) and discrete samples (number) in the Gulf of Cádiz in April 1998.

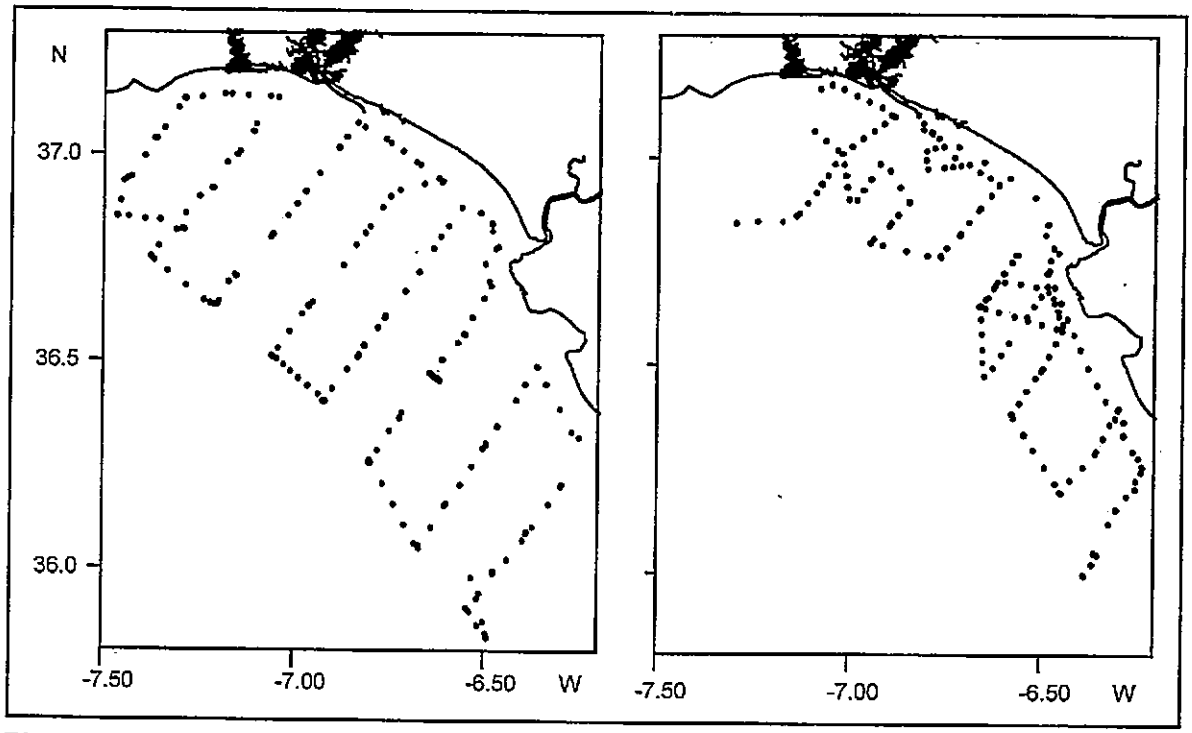

Figure 5.5 - TOROS 4: Locations of on-line samples between 10 and 14 October (left) and 15 and 19 October 1998 (right) in the Gulf of Cádiz.

5.4.4 Data Treatment

In order to generate surface contour plots from high spatial resolution on-line measurements of salinity, temperature and dissolved metal concentrations, the PC-based surface mapping system Surfer(Win32) (Version 6.01, Golden Software, Inc.) was used. The interpolation between data points was carried out with Kriging as the gridding method. A linear variogram model was selected without anisotropic radius. The error variance was set at 1% of the semivariance (given in Surfer by default scale C), and this allowed the smoothing of contours and alleviated the nugget effect. This treatment of the data is a simplification which was deemed acceptable, as the generated contour plots are intended only to aid the visualisation of the data. The author is aware that a more rigorous data treatment is necessary if the interpolated data is used for predictions and modelling purposes. The techniques necessary to generate an experimental variogram in order to determine the suitable variogram model for geostatistical data treatment are discussed in specific textbooks (e.g. Burrough and McDonnel, 1998; Isaaks and Srivastavia, 1989).

5.5 Results

Results from on-line and discrete measurements of metals in the Gulf of Cádiz were not corrected for tidal excursion, which has to be considered when interpreting the contour plots. With the exception of estuarine metal plume areas, the dissolved concentration of Co in the Gulf of Cádiz was close to the limit of detection for the automated combined determination of Ni and Co (LOD_{Ni} = 0.21 nM and LOD_{Co} = 0.33 nM, see Chapter 3). Because of the patchy coverage of Co data in the Gulf of Cádiz, results for this metal are not presented in the form of contour plots, with the exception of the first survey.

5.5.1 TOROS 1: NOVEMBER 1996

Figure 5.6 shows the distributions of salinity and total dissolved Zn, Cu, Ni and Co concentrations in the Gulf of Cádiz in November 1996. The salinity contour plot was generated from calibrated conductivity measurements in discrete samples. The area to the south of Huelva Ría (from station 34 to 38, Figure 5.2) was covered on 21 November 1996, and the eastern (from station 39 to 43) and western (from station 65 to 68) areas were surveyed on the 24 and 25 November, respectively.

Compared to the salinity in the centre of the Gulf of Cádiz ($S \geq 36.0$) the salinity distribution shows areas of lower salinity associated with the Huelva Ría system ($S \leq 35.0$) and the Guadalquivir estuary ($S \leq 34.6$) in the eastern corner of the surveyed area.

Total dissolved metal concentrations in the proximity of Huelva Ría were 130 - 800 nM Zn, 44 - 330 nM Cu, 5.4 - 31 nM Ni and 4.7 - 8.2 nM Co. Higher concentrations of Ni (up to 43 nM) were measured to the west of the low salinity area. The metal concentrations in the salinity minimum at the eastern boundary of the surveyed area were 150 nM Zn, 71 nM Cu, 18 nM Ni and 1.3 nM Co. The lowest dissolved concentrations were observed around the discrete sampling stations 40, 41 and 35 (Figure 5.2, < 25 nM Zn, < 15 nM Cu, < 4.5 nM Ni and < 0.50 nM Co), whereas the contour calculations gave the lowest concentrations in the centre of the survey area, where the salinity was highest.

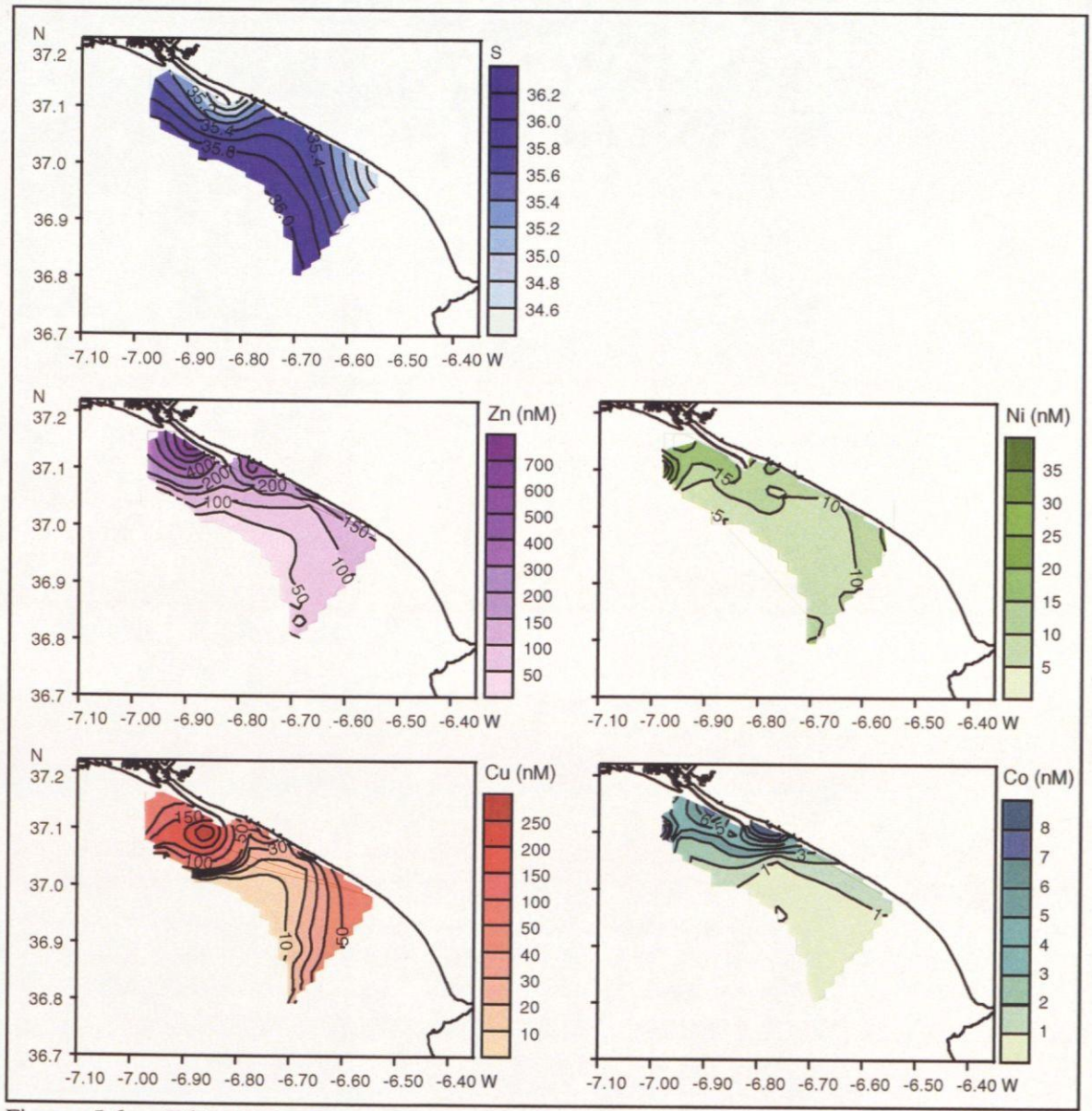

Figure 5.6 - TOROS 1: Contour plot of salinity and total dissolved Zn, Cu, Ni and Co concentrations in surface water of the Gulf of Cádiz close to the mouth of Huelva Ría during November 1996. Plots of Zn, Cu and Ni were generated from on-line measurements, and Co from concentrations in discrete samples.

5.5.2 TOROS 2: JUNE 1997

The surface distributions of salinity and total dissolved Zn, Cu and Ni in the Gulf of Cádiz between 10 and 14 June 1997 are given in Figure 5.7. The survey started in the southeast and meandered between coast and offshore boundaries to the north-west of the surveyed area. The salinity contour plot was generated from high resolution measurements (5 - 30 s intervals) by the ship's conductivity system, whereby one value every five minutes was used.

Low salinity regions were observed in the north ($S \leq 36.0$) and east ($S \leq 35.2$) of the survey area, and these were probably associated with the estuaries of the Guadiana in the northwest, the Huelva system in the north and the Guadalquivir in the east. In the centre and towards the offshore margin of the Gulf of Cádiz the salinity was above 36.2 (maximum: 36.5).

The surface distribution contours of Cu and Ni were generated from ca. 250 on-line voltammetric measurements. For technical reasons, on-line Zn measurements were patchy and restricted to the first three days of the survey (130 data points). On-line measurements of Zn failed in the area around the mouth of Huelva Ría and the north-western region of the surveyed area, and therefore, the boundary for the interpolation calculation was restricted (Figure 5.7).

A tongue of elevated dissolved metal concentrations ($\geq$ 30 nM Zn, $\geq$ 20 nM Cu and $\geq$ 10 nM Ni) extended from the Guadalquivir estuary. Less pronounced were Cu and Ni in the plumes associated with the Huelva estuary ($\geq$ 15 nM Cu and $\geq$ 4 nM Ni). However, on subsequent surveys designed to assess the tidal variability of the Huelva metal plume, up to 80 nM Cu (but only 5 nM Ni) were measured ca. 12 km southeast of the estuary's mouth (see Chapter 3).

The surface concentration of Zn in the north of the surveyed area was above 20 nM. Zinc concentrations in discrete samples taken at 10 m depth by Morley (unpublished data) to the north of the area covered by on-line measurements for Zn showed concentrations between 45 - 125 nM in the plume of Huelva Ría and more than 30 nM Zn in the northwest.

Dissolved metal concentrations decreased towards the Atlantic margin of the Gulf of Cádiz, where levels below 3 nM Zn, 4 nM Cu and 3 nM Ni were reached, and concentrations below 0.2 nM Co were measured in discrete samples.

5.5.3 TOROS 3: APRIL 1998

Salinity contours for the April survey (Figure 5.8) were generated from calibrated conductivity measurements, which were taken at approximately five minutes intervals in the discard water from the tangential filtration system. The area to the east of Huelva Ría was covered on 22 April 1998 and the area to the west on the following day. Areas of low salinity were observed to the southeast ($S < 34.2$) and to the west ($S < 34.4$) of Huelva Ría, and an additional pocket ($S < 34.2$) was located at the western fringe of the survey area.

The surface distribution plots for dissolved metal concentrations were generated from on-line measurements of Zn and Cu (ca. 50) and Ni (ca. 30) taken during the two-day survey. Metal concentrations were elevated in the Huelva Ría plume to the southeast of the estuary's mouth ($\leq$ 300 nM Zn, $\leq$ 30 nM Cu and $\leq$ 10 nM Ni, and up to 22 nM Co in discrete samples) and in the north-western corner of the surveyed area (108 nM Zn, 25 nM Cu and 5.1 nM Ni). The lowest metal concentrations observed during this survey were 9.4 nM Zn, 4.4 nM Cu and 2.3 nM Ni, and 0.23 nM in the discrete sample MZ 14 (Figure 5.4).

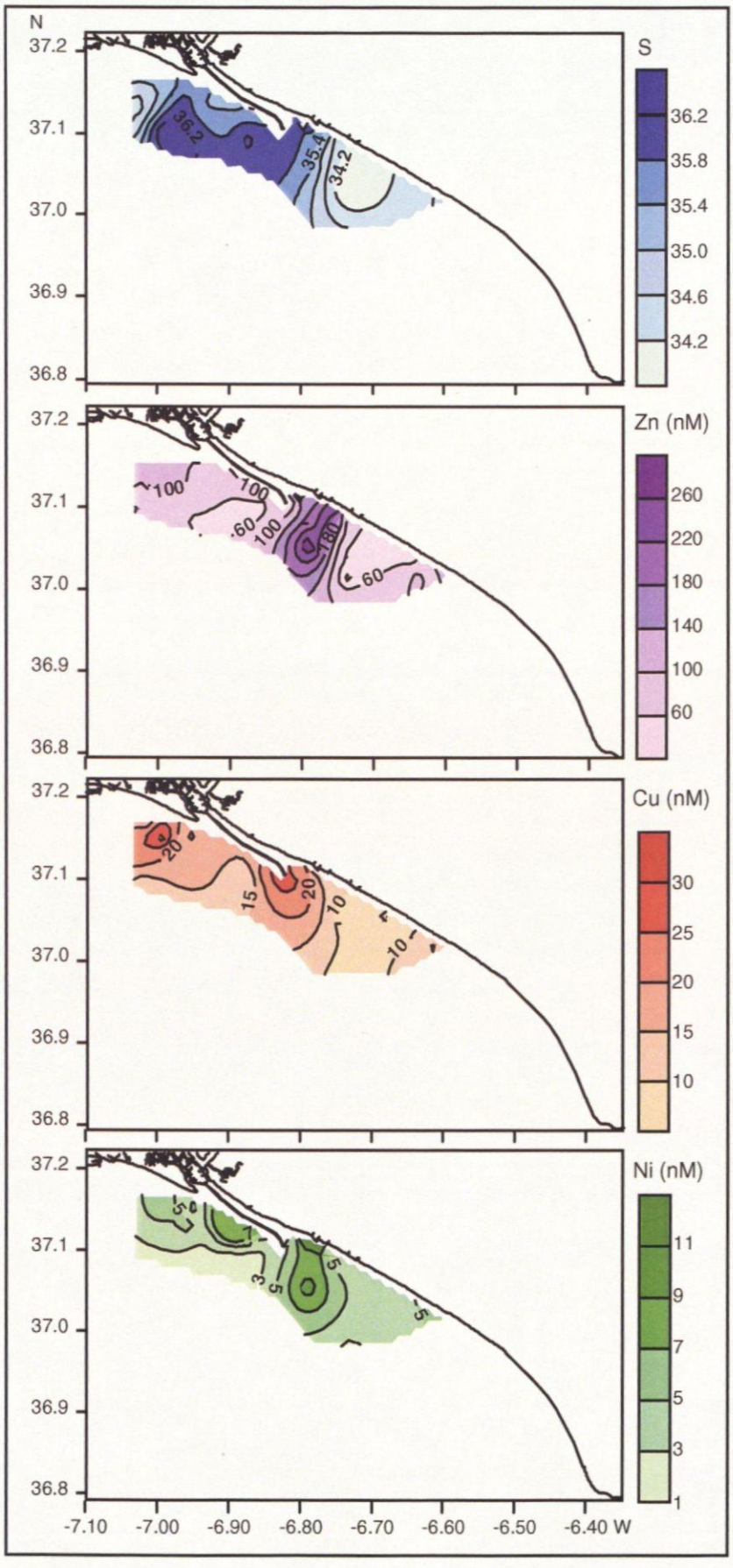

Figure 5.8 - TOROS 3: Contour plot of salinity and total dissolved Zn, Cu and Ni concentrations in surface water of the Gulf of Cádiz close to the mouth of Huelva Ría in April 1998.

5.5.4 TOROS 4: OCTOBER 1998

The surface distributions of salinity and total dissolved Zn, Cu and Ni concentrations in the Gulf of Cádiz between 11 and 15 October 1998 (plots on the left) and between 15 and 19 October (plots on the right), are given in Figure 5.9. The first part of the survey started in the southeast and meandered between the coast and offshore boundaries to the northwest of the surveyed area (Figure 5.5, left plot). The second part began in the west and followed an irregular pattern, whereby the focus was on the metal plumes of Huelva Ría and the Guadalquivir and the inshore area between the two estuaries (Figure 5.5, right plot). The salinity contour plot was generated as described for the TOROS 2 survey. Dissolved metal contours were based on high resolution on-line measurements of Zn and Cu (ca. 220 and 190 data points for first and second part, respectively) and Ni (ca. 320 and 270 data points).

Areas of low salinity ($\leq$ 36.0) associated with the Guadiana in the west, Huelva Ría in the north and the Guadalquivir in the east of the Gulf of Cádiz were observed during both parts of the October survey. In surface waters of the central and offshore areas of the Gulf of Cádiz the salinity was greater than 36.2, with maxima above 36.6.

A distinct tongue of elevated Zn and Cu concentrations (22 - 50 nM Zn, 7.5 - 11 nM Cu and 2.3 - 3.3 nM Ni) extending from the Guadalquivir was observed during the first part of the survey, when a smaller plume of similar intensity (19 - 57 nM Zn, 6.3 - 9.4 nM Cu and 1.9 - 2.5 nM Ni) was associated with the Huelva system. During a tidal cycle study from an anchor point approximately 4 km outside Huelva Ría (data see Appendix 2) not shown) dissolved concentrations of 21 - 140 nM Zn, 11 - 69 nM Cu, 1.8 - 4.0 nM Ni and 0.8 - 4.4 nM Co were measured on-line over a period of 13 hours.

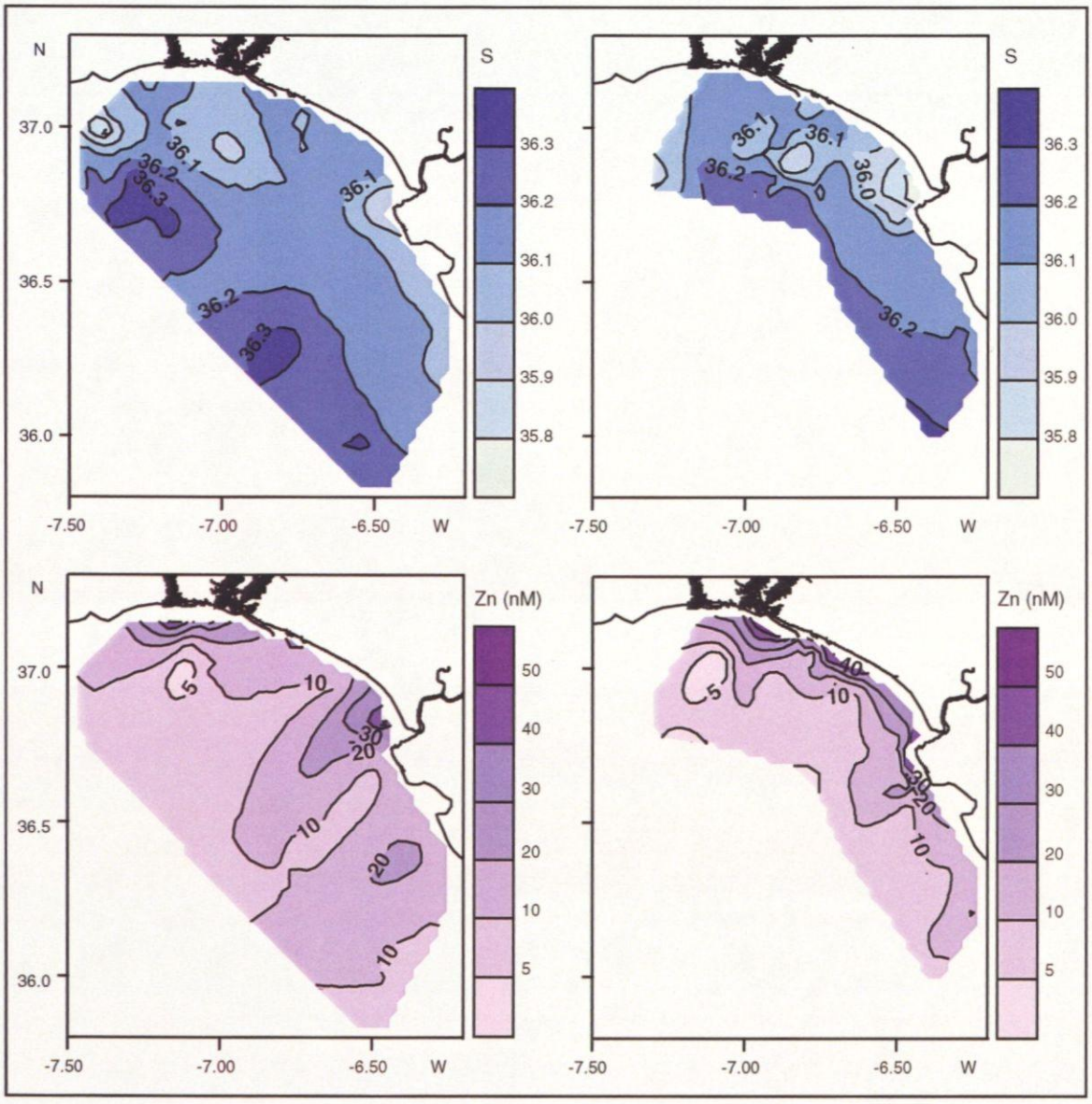

Figure 5.9 - TOROS 4: Contour plot of salinity and total dissolved Zn, Cu and Ni concentrations in surface water of the Gulf of Cádiz. The left and right plot of each pair was created from on-line measurements between 11 and 14, and 15 and 19 October 1998, respectively. Sampling points are given in Figure 5.5. Note the different scales for the two Cu plots.

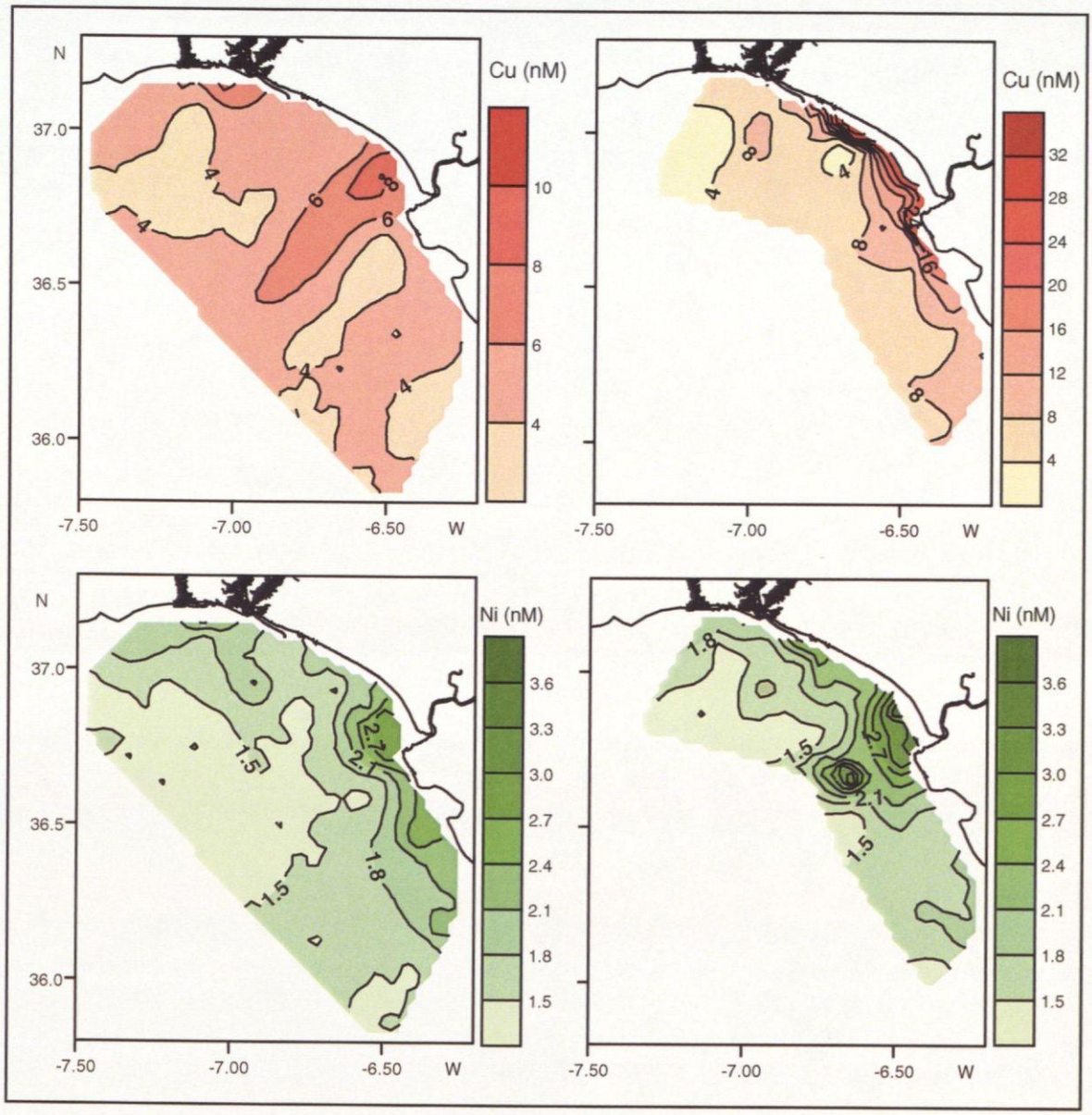

Figure 5.9 - continued.

The second part of the survey took the cruise track closer inshore (minimum depth 10 m). High concentrations of Zn (18 - 90 nM) and Cu (6.3 - 48 nM) and elevated Ni levels (2.0 - 6.0 nM) were measured along the shoreline throughout the second part, resulting in the steep concentration gradient between Huelva Ría and the Guadalquivir plume on the contour plots. Concentrations at offshore locations in the Gulf of Cádiz were ≤ 11 nM Zn, ≤ 6.5 nM Cu and ≤ 2.0 nM Ni, and Co concentrations in discrete samples were below 0.1 nM.

5.5.5 Comparison of On-line with Discrete Measurements

Table 5.2 compares on-line measurements of dissolved Zn, Cu and Ni in surface waters with results from the analysis of discrete samples using voltammetric methods. Considerable discrepancies are apparent, especially for measurements taken in the estuarine metal plume.

Table 5.2 - Comparison of results from on-line and discrete measurements of total dissolved Zn, Cu and Ni for samples from the Gulf of Cádiz. At some stations samples from different depths were analysed to illustrate the highly variable nature of the Huelva Ría metal plume. OL - on-line measurements; D - metal analysis in discrete samples; all values in nM; standard deviation of on-line analysis ≤ 10%; sample stations see Figure 5.2 - Figure 5.4.

TOR-96-11-	OL Zn	D Zn	OL Cu	D Cu	OL Ni	D Ni
40 0.5 m	33.1	45.7 ± 3.84	26.2	29.8 ± 1.24	2.76	8.29 ± 0.54
10 m		23.0 ± 1.22		24.4 ± 2.18		9.26 ± 0.59
28 m		24.2 ± 1.13		7.84 ± 0.42		10.5 ± 0.32
41 0.5 m	70.1	163 ± 6.60	22.4	23.8 ± 1.35	7.32	7.60 ± 0.27
10 m		63.4 ± 7.50		30.9 ± 2.01		8.39 ± 0.55
22 m		74.1 ± 2.55		29.9 ± 0.55		8.54 ± 0.38
37	128	137 ± 5.52	25.2	37.0 ± 1.71	7.45	5.38 ± 0.46
38	732	374 ± 27.0	57.9	89.3 ± 4.87	-	18.5 ± 0.59
42	211	282 ± 17.4	29.0	77.8 ± 2.82	10.1	10.2 ± 0.35
43	257	391 ± 27.4	42.7	72.5 ± 2.53	12.5	14.8 ± 0.39
66	-	300 ± 15.5	124	58.8 ± 1.88	30.7	11.1 ± 0.92
TOR-97-06-	OL Zn	D Zn	OL Cu	D Cu	OL Ni	D Ni
E23	3.04	2.71 ± 0.31	3.33	2.21 ± 0.62	2.86	2.80 ± 0.27
D19	4.74	5.23 ± 0.50	5.51	3.49 ± 0.18	3.44	2.80 ± 0.27
C11	6.07	6.44 ± 0.28	4.70	1.52 ± 0.03	3.89	2.43 ± 0.61
C16	-	46.2 ± 0.98	13.5	30.8 ± 0.54	10.2	4.59 ± 0.28
B7	-	40.9 ± 1.30	8.08	13.7 ± 0.39	5.16	3.57 ± 0.32
B9	5.02	4.65 ± 0.40	6.38	4.04 ± 0.28	2.76	2.11 ± 0.23
G41	15.9	25.6 ± 2.05	6.17	12.6 ± 1.39	3.47	3.57 ± 0.32
TOR-98-04-			OL Cu	D Cu	OL Ni	D Ni
MZ 13			17.1	66.0 ± 0.37	-	-
MZ 14			6.0	7.81 ± 0.07	2.56	2.64 ± 0.35
MZ 15			12.1	41.7 ± 0.56	3.03	2.90 ± 0.15
MZ 16			19.0	106 ± 8.0	-	10.6 ± 0.90
MZ 17			33.7	97.7 ± 6.0	8.67	10.6 ± 1.65
MZ 18			14.1	10.5 ± 0.91	2.79	2.41 ± 0.07
MZ 19			10.8	7.54 ± 0.14	2.45	2.32 ± 0.06
MZ 20			19.0	16.2 ± 0.10	2.80	2.66 ± 0.03
MZ 21			14.0	38.3 ± 1.42	3.04	3.03 ± 0.10
MZ 22			22.7	49.3 ± 3.11	3.16	5.83 ± 0.32
MZ 23			52.1	90.7 ± 1.06	9.16	10.7 ± 0.14

5.6 Discussion

5.6.1 Analytical Performance

When comparing metal concentrations measured on-line with those measured in discrete samples (Table 5.2), differences of more than 100% occurred in some cases, while for others the values agreed within 10%. The accuracy and precision of the on-line metal monitor (Chapter 3) proved satisfactory, as did the analytical performance of voltammetric analysis in discrete samples (Chapter 2). Therefore, it is unlikely that analytical error was the reason for the observed discrepancies. Metal concentrations analysed in discrete samples were not consistently higher than values measured on-line. This excludes the contamination of discrete samples by the sampling container, ship's exhaust fumes, sampling handling or storage as a major source of error.

An alternative explanation for the observed concentration discrepancies lies in differences inherent in the sampling methods. On-line samples were pumped from a depth of 2 - 4 m from KIPPER-1 (Chapter 3), which was deployed from the side of the vessel. Discrete samples were taken with Niskin bottles mounted on a rosette from the stern of the *B/O Garcia del Cid* (TOROS 2 and 4), or with manual sampling equipment from the bows or side of small coastal vessels (TOROS 1 and 3). Differences did not only occur in the exact sampling position (ship's drift while on station), but also in sampling depth. The minimum sampling depth with the rosette was 5 - 10 m, and samples were taken manually just below the surface (ca. 0.5 m to 2 m). Depth profiles taken during the TOROS 1 survey (Table 5.2) show important concentration gradients with depth for discrete samples, especially at high concentrations within the metal plume. Therefore, the large discrepancies observed between on-line and discrete metal concentrations in coastal surveys may have been predominantly the result of the inhomogeneous nature of the water body.

5.6.2 Salinity Distribution in the Gulf of Cádiz

The salinity observed in the central and outer Gulf of Cádiz (S > 36.2) was similar for each survey and has been observed previously in this sea area (Ochoa and Bray, 1991). The excess of evaporation over precipitation in this arid region leads to high surface salinities, compared to North Atlantic waters at higher latitudes (S < 36, Brown *et al.* 1995). Low-salinity zones were observed during all four surveys, and these were associated with the river systems draining into the Gulf of Cádiz, the Guadiana (possibly combined with the Rio Piedras), the Huelva Ría and the Guadalquivir (Figure 5.1). During the surveys, the river plumes were passed at different tidal stages, which may account for the difference in the intensity and extent of the low salinity plumes between surveys. No correction was made for tidal excursion, so that low salinity zones (and metal plumes) may have been displaced from their origin at the time of sampling. Conflicting surface currents (tidal wave and prevailing current, Section 5.3) are likely to cause local circulation patterns which change throughout the tidal cycle. Such circulation may provide an explanation for the temporary dislocation of the low salinity zone associated with the Huelva system to the west of the estuary's mouth during the first three surveys (Figure 5.2 - Figure 5.4).

The low salinity signal associated with the Huelva system was less intense and covered a smaller area, compared to those of the Guadalquivir and Guadiana. This can be explained with the lower fresh water flux of the Rio Tinto and Rio Odiel (long-term combined mean annual flow 18 $m^3 s^{-1}$), compared to the Guadalquivir (164 $m^3 s^{-1}$) and Guadiana (79 $m^3 s^{-1}$) (Palanques *et al.* 1995; Borrego-Flores, 1992).

5.6.3 Dissolved Zn, Cu, Ni and Co in the Gulf of Cádiz

The distributions of dissolved Zn, Cu, Ni and Co in the Gulf of Cádiz showed the influence of riverine metal sources and the transport with the prevailing currents. Areas of elevated dissolved metal concentrations approximately overlapped with the low salinity zones in the coastal area, and this identified the Guadiana, Huelva Ría and Guadalquivir as major sources of trace metals to the coastal zone. The large tongues of elevated dissolved Zn and Cu concentrations extending from the Guadalquivir during the second and fourth surveys (Figure 5.7 and Figure 5.9) were not congruent with the observed salinity distribution. This may be explained by the different sampling depth for conductivity (water pumped from an inlet in the hull of the ship, see Chapter 3) and trace metal measurements (KIPPER-1). In this case, it is possible that the KIPPER-1 sampled the low-salinity surface plume of the Guadalquivir estuary, while the conductivity was measured in water that had undergone more intense mixing from a greater depth. In addition, the sediment in the Gulf of Cádiz is a potential diagenetic source of metals to the water column (Section 5.3), and sedimentary inputs of Zn and Cu will cause enhanced dissolved concentrations without a salinity signal.

The importance of Huelva Ría as source of metals to the Gulf of Cádiz was established in Chapter 4. The observed metal concentrations in the Huelva Ría plume area were highest in November 1996 and lowest in October 1998, with intermediate concentrations during the spring and summer surveys. Tidal cycle studies at the mouth of the estuary (Chapter 4 and Section 5.5.4) and high resolution on-line measurements in estuarine discharge areas have shown that the intensity of the metal plume is highly dependent on the state of the tide. Therefore, the inter-survey variability in metal discharge

from Huelva Ría into the Gulf of Cádiz can be more accurately assessed from estuarine surveys (Chapter 4).

Dissolved concentrations of Zn and Cu in the Huelva Ría plume reported by van Geen *et al.* (1997) were similar to those observed during TOROS surveys (Table 5.3 and Table 5.4), while the maximum Ni concentration given by van Geen was higher (factor 2) than that observed in the present work.

The concentration of dissolved Zn, Cu and Co in the Huelva Ría plume was several fold higher than levels reported in literature for the plumes of major European rivers, including the Humber, Mersey, Rhine/Scheldt and the Rhone (Table 5.4). The range of Ni concentrations encountered in Huelva Ría and Guadalquivir plume during TOROS surveys were similar to those reported for coastal regions of the North Sea and the Gulf of Lyons. The high degree of contamination of the Huelva Ría plume with Zn and Cu resulted from the high metal flux from the Tinto/Odiel rivers, compared to other major European rivers (see Chapter 4).

The transport of dissolved Zn, Cu and Ni from the mouth of the estuary in an easterly direction was evident from the results of high resolution measurements (Figure 5.6 - Figure 5.9). The influence of prevailing west-east surface currents on the metal plume was most distinct during the autumn/winter surveys (TOROS 1 and 4, second part), when inshore surveys (minimum depth 5 m and 10 m, respectively) were undertaken. Dissolved Zn, Cu and Ni were transported from Huelva Ría along the shoreline towards the Guadalquivir estuary and beyond. This confirms the previous suggestions that metal contamination from the north of the Gulf of Cádiz is transported eastward and into the Mediterranean Sea (van Geen *et al.* 1997).

Table 5.3 - Dissolved concentrations of Zn, Cu and Ni measured during quarterly surveys by the Medio Ambiente (1998) at the mouth of the Guadiana, Rio Piedras, Punto Umbria, Huelva Ría and Guadalquivir. The range of concentrations encountered at the mouth of Huelva Ría during TOROS surveys is given in the lower part of the table.

Estuary	Zn (nM)	Cu (nM)	Ni (nM)	Co (nM)
Rio Piedras	140	47	17	
Guadiana	110 - 250	32 - 47	17 - 51	
Guadalquivir	230 - 290	32 - 47	34 - 51	
Huelva Ría	400 - 9800	110 - 520	17 - 140	
Huelva Ría (TOROS)	54 - 3650	23 - 340	4 - 41	1.7 - 97

Table 5.4 - Dissolved metal concentrations in surface waters of the Gulf of Cádiz and European coastal seas reported in literature. All concentrations in nM, unless otherwise stated in the footnote.

Location	Zn	Cu	Ni	Co
Huelva Ría plume[1]	≤ 3060	≤ 290	≤ 90	
Guadalquivir plume[2]	40 - 200	≤ 21	≤ 6	
Gulf of Cádiz EM[3]	12	5.8	3.0	
North Atlantic[4]	< 0.5 - 0.8	0.85 - 1.5	1.7 - 2.5	0.037 - 0.057
Humber Bay, North Sea[5]	27	13	20	< 0.17
Central North Sea[5]	2.9 - 28	1.6 - 2.9	1.0 - 6.1	≤ 0.45
Scheldt/Rhine Bay[5 §]	5 - 30	2.5 - 10	5 - (> 10)	0.2 - 0.8
English Channel[6]	1.9 - 18	1.3 - 5.3	3.0 - 4.2	≤ 0.02 - 0.24
Liverpool Bay, Irish Sea[7]	11 - 54	8 - 18	7.0 - 16	
Gulf of Lyons[8]		2.0 - 14	1.5 - 6.5	
Outer Gulf of Cádiz (TOROS)	2.9 - 11	2.7 - 7.7	1.5 - 5.7	< 0.1 - 0.5

[1] Surface water collected 3 km south of Huelva Ría mouth, concentration in nmol kg^{-1} (van Geen *et al.* 1997).
[2] Concentration in nmol kg^{-1} (van Geen *et al.* 1997; van Geen *et al.* 1991).
[3] Shelf end-member concentration at S = 36.28 for the Gulf of Cádiz after van Geen *et al.* (1991), concentrations in nmol kg^{-1}.
[4] North Atlantic Surface Water (Morley *et al.* 1997; Landing *et al.* 1995; Morley *et al.* 1993; Kremling and Pohl, 1989; van Geen *et al.* 1988; Bruland and Franks, 1983).
[5] Coastal and central North Sea, salinity between 33.140 (Humber Bay) and 35.005 (central North Sea) (Tappin *et al.* 1995), [§]ranges estimated from graphs.
[6] Range observed in samples from the centre of the English Channel between the mid-channel and the opening to the Atlantic Ocean (Tappin *et al.* 1993).
[7] Concentration in surface water the eastern Irish Sea, including the Mersey river plume ca. 15 km off the estuary's mouth (Achterberg and van den Berg, 1996).
[8] Rhone plume in the Gulf of Lyons, Mediterranean Sea, values estimated from graph at chlorinity > 21 g l^{-1} (Elbaz-Poulichet *et al.* 1996).

The second part of the TOROS 4 survey indicated the transport of Zn and Ni from a more westerly location towards Huelva Ría. Salinity distributions and the location of dissolved Zn (TOROS 3 and 4), Cu (TOROS 1 and 3) and Ni (TOROS 1, 3 and 4) plumes to the west of Huelva Ría pointed towards the Guadiana or Rio Piedras as sources of these metals to the coastal zone. Elevated metal concentrations have been reported by the Medio Ambiente (1998) for both estuaries (Table 5.3). Because of its higher water discharge the Guadiana probably had a greater influence on the water quality in the Gulf of Cádiz, compared to the Rio Piedras. Van Geen *et al.* reported dissolved Zn concentrations of up to 100 nmol kg^{-1} in surface waters along the southern Portuguese coast. The eastward transport of metal-enriched coastal water with the Atlantic surface current may be an alternative (or additional) explanation for the elevated Zn concentrations observed in the north-western Gulf of Cádiz.

The dissolved metal plume in the eastern Gulf of Cádiz can be attributed to the Guadalquivir estuary, which contributes the greatest amount of fresh water to this coastal zone and carries elevated dissolved concentrations of Zn, Cu and Ni from industrial and mining sources (Table 5.3). Contour plots and concentrations reported for the Guadalquivir suggest that this estuary may be a greater source of dissolved Ni to the Gulf of Cádiz, compared to Huelva Ría. However, rough flux estimates based on linear metal-salinity relationships in the Gulf of Cádiz indicate that both estuaries have a Ni flux of similar magnitude (ca. 40 - 70 t a^{-1} Ni, see Chapter 4).

The Iberian Pyrite Belt is enriched in Zn and Cu (among others, see Chapter 4), for which the Huelva system appears to be the main source in the Gulf of Cádiz. Nickel is not particularly enriched in the local geology, so that urban or industrial effluents are the likely source of Ni in the Guadalquivir. Contour plots indicate that the dissolved concentrations of Cu and Ni in the Guadalquivir plume were higher in November 1996, compared to the

subsequent TOROS surveys and levels reported in literature (Table 5.4). This illustrates a high level of variability in the metal flux from this river, and further investigations are required in order to assess more accurately the importance of metal discharges from the Guadalquivir estuary, compared to the Huelva system.

The summer (TOROS 2) and autumn (TOROS 4) surveys supplied data on metal concentrations in the outer Gulf of Cádiz. The concentration range of Zn and Cu encountered south of a line drawn between 37.2° N, 7.5° W and 36.0° N, 6.2° W (Figure 5.7 and Figure 5.9) were similar during both surveys (TOROS 2: 2.9 - 9.2 nM Zn and 2.8 - 7.7 nM Cu, TOROS 4: 3.8 - 11 nM Zn and 2.7 - 6.5 nM Cu. The concentration of Ni in the outer Gulf of Cádiz was significantly lower in October 1998 (1.1 - 2.0 nM), compared to June 1997 (2.6 - 5.7 nM). This may be explained with the reduced dissolved Ni concentration in the lower Huelva Ría in October (1.8 - 4.0 nM) compared to June (8.0 - 13 nM). Concentrations in the Guadalquivir plume (Figure 5.7 and Figure 5.9) suggested a similar reduction of Ni discharge from this river. Levels of dissolved Zn, Cu and Ni estimated as shelf end-member at S = 36.28 by van Geen *et al.* (1991) (Table 5.4) were at the upper limit of the range observed for the outer part of the surveyed area during the TOROS surveys.

In the outer Gulf of Cádiz, dissolved concentrations of Cu, Ni and Co were in a similar range to those reported for other European shelf waters, for example the central North Sea and the English Channel (Table 5.4). An exception may be Zn, which had lower maximum values in the Gulf of Cádiz. Compared to typical dissolved surface water concentrations in the North Atlantic Ocean (Table 5.4, upper limit), the observed concentration ranges in the outer Gulf of Cádiz represent an enrichment by factor 3.6 - 14 for Zn and 1.8 to 5.1 for Cu. Nickel in surface waters was depleted during the October survey (factor 0.51 - 0.8) and up to 2.3 times enriched during the June survey. From the

limited amount of data available from the analysis of Co in discrete samples, the enrichment of surface water in the outer Gulf of Cádiz was estimated to be 1.8 - 8.8 times above the North Atlantic.

There was no relationship between salinity and Zn, Cu or Ni for the complete set of data in the Gulf of Cádiz during any survey. This may be partially explained with the low fresh water discharge from the Huelva system, where conservative behaviour of Zn, Cu, Ni and Co was observed in the lower estuary (Chapter 4). The salinity range in the Huelva Ría plume was small and metal concentrations were too high for an overall linear relationship to be detected in the Gulf of Cádiz. In addition, the distribution of dissolved Zn, Cu and Ni in the Gulf of Cádiz may have been influenced by factors, other than mixing. Possible processes include the removal of dissolved metals by adsorption to particles or through uptake by phytoplankton, and the addition of dissolved metals to the water column through the remobilisation from the metal-rich sediment of the Gulf of Cádiz. High levels of particulate Cu, Pb, Co, Cr, Fe, Mn and Zn concentrations in the Gulf of Cádiz were reported by Nelson and Lamothe (1993), whereby the fine character of the particles suggested an estuarine origin. The removal of Zn, Cu, Ni and Co from solution at mid-salinities and conservative behaviour at $S > 35$ in Huelva Ría, and the linear metal-salinity relationship of Cu and Ni in the Guadalquivir plume (Chapter 4) suggest that at the time of the TOROS surveys, sorption of these metals to particles was largely completed within the estuarine environment. This is supported by van Geen *et al.* (1991), who found linear salinity relationships for dissolved Cu, Ni and Cd in the Gulf of Cádiz in a data set that excluded the immediate Huelva Ría plume. However, the depletion of surface waters in the Gulf of Cádiz with Ni, compared to NASW, indicates that removal of this metal takes place within the shelf sea.

High concentrations of Fe, Zn, Cu, Ni, Co, Pb and Fe found in shelf sediment (van Geen *et al.* 1997; Palanques *et al.* 1995; Nelson and Lamothe, 1993) identify it as potential diagenetic source of metals to the water column (see Section 5.3). However, the importance of remobilisation from sediments in this coastal area has, so far, not been investigated.

5.7 Conclusions

The on-line monitoring of dissolved Zn, Cu and Ni in the Gulf of Cádiz provided data on the intensity, extent and transport of estuarine metal plumes at a high spatial resolution. The Huelva Ría metal plume was characterised by a strong variability in estuarine metal discharge during tidal cycles and between the seasons. Most intense was the contamination with Zn and Cu, followed by Co and Ni. The estuarine plume did not extend far into the Gulf of Cádiz, but was predominantly transported eastward along the shore with the prevailing current. Dissolved metal concentrations in the Guadalquivir estuary were generally lower, compared to the Huelva system. However, the higher fresh water discharge of the Guadalquivir resulted in a metal plume that, at times, projected far into the Gulf of Cádiz and that contributed noticeably to the contamination of coastal waters with dissolved Zn, Cu and Ni. The Guadiana estuary was identified as a source of metal inputs, which may be of a similar order of magnitude as the Guadalquivir. Furthermore, there was evidence that Zn contamination reported in literature may be transported into the Gulf of Cádiz from Portuguese coastal waters. The data corroborated previous reports of a circulation pattern that facilitates the transport of metal contamination along the shore from the western to the eastern boundaries of the Gulf of Cádiz and into the Mediterranean Sea. Mixing of coastal metal pollution with North Atlantic water resulted in the enrichment of the outer areas of the Gulf of Cádiz with dissolved metals

associated with the mining industry (Zn, Cu and Co up to 14, 5.1 and 8.8 times, respectively), while Ni was at times depleted (enrichment 0.51 - 2.3 times).

The exploitation of results from the high resolution measurements for transport modelling of pollutants is planned in collaboration with TOROS research partners.

5.8 REFERENCES

Achterberg, E.P. and van den Berg, C.M.G. (1996) Automated monitoring of Ni, Cu and Zn in the Irish Sea. *Mar.Poll.Bull.* **32**, 471-479.

Borrego-Flores, J. (1992) Sedimentologia del estuario del Rio Odiel (Huelva, S.O. Espana). University of Sevilla, PhD Thesis.

Borrego, J., Lopez, M., Pendon, J.G. and Morales, J.A. (1997) C/S ratios in estuarine sediments of the Odiel river mouth, S.W. Spain. *Journal of Coastal Research* **14**, 32-39.

Brown, E., Collin, A., Park, D., Phillips, J., Rothery, D. and Wright, J. (1995) *Seawater, its composition, properties and behaviour*, 2 edn. Milton Keynes: Pergamon in assoc. with Open University.

Bruland, K.W. and Franks, R.P. (1983) Mn, Ni, Cu, Zn, and Cd in the western North Atlantic. In: Wong, C.S., Boyle, E., Bruland, K.W., Burton, J.D. and Goldberg, E.D., (Eds.) *Trace Metals in Sea Water*, pp. 395-414. New York and London: NATO Scientific affairs Division & Plenum Press.

Burrough, P.A. and McDonnel, R.A. (1998) *Principles of Geographical Information Systems*, New York: Oxford University Press.

Elbaz-Poulichet, F., Garnier, J.-M., Guan, D.M., Martin, J.-M. and Thomas, A.J. (1996) The conservative behaviour of trace metals (Cd, Cu, Ni and Pb) and As in the surface plume of stratified estuaries: Example of the Rhone River (France). *Estuarine, Coastal and Shelf Science* **42**, 289-310.

Gibbs, R.J. (1986) Segregation of metals by coagulation in estuaries. *Mar.Chem.* **18**, 149-159.

Guieu, C., Chester, R., Nimmo, M., Martin, J.-M., Guerzoni, S., Nicolas, E., Mateu, J. and Keyse, S. (1997) Atmospheric input of dissolved and particulate metals to the northwestern Mediterranean. *Deep-Sea Research Part II-Topical Studies In Oceanography* **44**, 655-674.

Hydes, D.J. and Kremling, K. (1993) Patchiness in dissolved metals (Al, Cd, Co, Cu, Mn, Ni) in North Sea surface waters: Seasonal differences and influence of suspended sediment. *Cont.Shelf.Res.* **13**, 1083-1101.

Isaaks, E.H. and Srivastavia, R.M. (1989) *An Introduction to Applied Geostatistics*, New York: Oxford University Press.

Jackson, G.A. and Burger, J. (1998) Aggregation in the marine environment. *Environmental Science & Technology* **32**, 2805-2814.

Jarvie, H.P., Neal, C. and Tappin, A.D. (1997) European land-based pollutant loads to the North Sea: An analysis of the Paris Commission data and review of monitoring strategies. *Sci.Total.Environ.* **194-195**, 39-58.

Kremling, K. and Pohl, C. (1989) Studies on the spatial and seasonal variability of dissolved cadmium, copper and nickel in north-east Atlantic surface waters. *Marine Chemistry* **27**, 43-60.

Landing, W.M., Cutter, G.A., Dalziel, J.A., Flegal, A.R., Powell, R.T., Schmidt, D., Shiller, A., Statham, P., Westerlund, S. and Resing, J. (1995) Analytical intercomparison results from the 1990 Intergovernmental Oceanographic Commission open-ocean baseline survey for trace metals: Atlantic Ocean. *Marine Chemistry* **49**, 253-265.

Laslett, R.E. (1995) Concentrations of dissolved and suspended particulate Cd, Cu, Mn, Ni, Pb and Zn in surface waters around the coasts of England and Wales and in adjacent Seas. *Estuarine, Coastal and Shelf Science* **40**, 67-85.

Leblanc, M., Benothman, D., Elbaz-Poulichet, F., Luck, J.M., Carvajal, D., Gonzalez-Martinez, A.J., Grande-Gil, J.A., Ruiz de Almodovar, G. and Saez-Ramos, R. (1995) Rio Tinto (Spain), an acidic river from the oldest and most important mining areas of Western Europe: Preliminary data on metal fluxes. In: Pasava, Kribek and Zak, (Eds.) *Mineral Deposits*, 1 edn. pp. 669-670. Rotterdam: Balkema.

Martin, J.-M. and Whitfield, M. (1983) The significance of the river input of chemical elements to the ocean. In: Wong, C.S., Boyle, E., Bruland, K.W., Burton, J.D. and Goldberg, E.D., (Eds.) *Trace metals in sea water*, pp. 265-269. New York: Plenum Press, Ltd.

Medio Ambiente Seccion de Medio Ambiente, (Ed.) (1998) Ejecucion del plan de policia de aguas del litoral Andaluz. Informe del año 1997, Sevilla: E.S.I.I. de Sevilla. Dpto. Ingen. Química y Ambiental.

Morley, N.H., Burton, J.D., Tankere, S.P.C. and Martin, J.-M. (1997) Distribution and behaviour of some dissolved trace metals in the western Mediterranean Sea. *Deep-Sea Research II* **44**, 675-691.

Morley, N.H., Statham, P.J. and Burton, J.D. (1993) Dissolved trace metals in the southwestern Indian Ocean. *Deep-Sea Research I* **40**, 1043-1062.

Nelson, C.H. and Lamothe, P.J. (1993) Heavy Metal Anomalies in the Tinto and Odiel River and Estuary System, Spain. *Estuaries* **16**, 496-511.

Ochoa, J. and Bray, N.A. (1991) Water mass exchange in the Gulf of Cadiz. *Deep-Sea Research* **38**, S465-S503

Palanques, A., Diaz, J.I. and Farran, M. (1995) Contamination of heavy metals in the suspended and surface sediment of the Gulf of Cadiz (Spain): the role of sources, currents, pathways and sinks. *Oceanologica Acta* **18**, 469-477.

Salomons, W. and Förstner, U. (1983) Metals in estuaries and coastal environments. In: Salomons, W. and Foerstner, U., (Eds.) *Metals in the Hydrocycle*, pp. 216-221. Berlin: Springer Verlag.

Sanudo-Wilhelmy, S.A. and Flegal, A.R. (1996) Trace metal concentrations in the surf zone and in coastal waters off Baja California, Mexico. *Environmental Science & Technology* **30**, 1575-1580.

Tappin, A.D., Hydes, D.J., Burton, J.D. and Statham, P.J. (1993) Concentrations, distributions and seasonal variability of dissolved Cd, Co, Cu, Mn, Ni, Pb and Zn in the English Channel. *Cont.Shelf.Res.* **13**, 941-969.

Tappin, A.D., Millward, G.E., Statham, P.J., Burton, J.D. and Morris, A.W. (1995) Trace metals in the central and southern North Sea. *Estuarine, Coastal and Shelf Science* **41**, 275-323.

Turekian, K.K. (1977) The fate of metals in the ocean. *Geochimica et Cosmochimica Acta* **41**, 1139-1144.

van Geen, A., Adkins, J.F., Boyle, E.A., Nelson, C.H. and Palanques, A. (1997) A 120 yr record of widespread contamination from mining of the Iberian pyrite belt. *Geology* **25**, 291-294.

van Geen, A., Boyle, E.A. and Moore, W.S. (1991) Trace metal enrichments in waters of the Gulf of Cadiz, Spain. *Geochimica et Cosmochimica Acta* **55**, 2173-2191.

van Geen, A. and Boyle, E.A. (1990) Variability of trace-metal fluxes through the Strait of Gibraltar. *Palaeogeography, Palaeoclimaology, Palaeoecology (Global and Planetary Change Section)* **89**, 65-79.

van Geen, A., Rosener, P. and Boyle, E.A. (1988) Entrainment of trace metal-enriched Atlantic shelf-water in the inflow to the Mediterranean Sea. *Nature* **331**, 423-426.

Williams, M.R., Millward, G.E., Nimmo, M. and Fones, G. (1998) Fluxes of Cu, Pb and Mn to the north-eastern Irish Sea: the importance of sedimental and atmospheric inputs. *Mar.Poll.Bull.* **36**, 366-375.

Chapter 6

Dissolved Metal Speciation

6.1 Abstract

In order to elucidate some of the processes that lead to the observed metal distribution in the Huelva system, thermodynamic equilibrium calculations were carried out for the Rio Tinto, Rio Odiel and their estuaries. Furthermore, the dissolved speciation of Cu in Huelva Ría and the Gulf of Cádiz was studied using voltammetric methods with ligand competition, and the concentration and stability constants of Cu complexing organic ligands were determined.

Thermodynamic calculations of the inorganic speciation offered explanations for the behaviour of metals in the Rio Tinto, Rio Odiel and their estuary. The inorganic speciation of Fe and Al in the fresh water end-member was dominated by sulphate complexation, and this remained so in the estuary up to a salinity of about 20. The low pH (< 4) in this system subdued the formation of iron hydroxide species, which would explain the absence of colloidal material and the conservative behaviour of trace metals in this part of the estuary. At higher pH (8.2) and salinity (36.5) in Huelva Ría, hydroxide species dominated the inorganic speciation of Fe (100% $Fe(OH)_4^-$, $Fe(OH)_2$ aq and $Fe(OH)_2$) and Al (99.9% $Al(OH)_4^-$ and $Al(OH)_2$ aq). Under these conditions, the removal of Zn, Cu, Ni and Co was observed in the estuary, indicating co-removal with Fe and Al flocs.

Results from electrochemical speciation studies showed that the fraction of organically complexed Cu decreased from over 80% in the Gulf of Cádiz to less than 50% in Huelva Ría. Copper was predominantly labile (> 90%) in estuarine samples with a total

concentration in excess of 2 μM Cu. Organic ligand concentrations (C_L) increased with total dissolved Cu (Cu_T) from coastal to estuarine waters (C_L = 5.3 - 199 nM, Cu_T = 3.6 - 254 nM), and ligands were found to be saturated with Cu in Huelva Ría. The relationship between total and labile Cu, copper complexing organic ligand and free cupric ion concentrations indicated that subtle changes in pH value affected the toxicity of Cu in the system. Equilibrium calculations showed that the cupric ion concentration in Huelva Ría may reach levels that are toxic to some species of phytoplankton.

6.2 Introduction

The speciation of metals in natural environments is of great importance, because it is the species of a metal that determine its reactivity and toxicity. Most speciation techniques are operational in character, beginning with the filtration of the sample, during which the partitioning between particulate and dissolved fractions is achieved. The commonly used filtration pore size (0.45 μm or 0.4 μm) is convenient but arbitrary. It does not allow a distinction between truly dissolved and colloidal phases, the latter of which has a high affinity for some metals (Muller, 1996; Horowitz *et al.* 1996). On the other hand, colloid separation methods (e.g. cross-flow filtration) are more cumbersome and prohibit the processing of large numbers of samples, and the chosen method has to be appropriate to fulfil the aims of the investigation.

Analytical techniques that allow the accurate determination of individual inorganic and organic metal species in a sample are not available. For this reason thermodynamic equilibrium calculation methods have been developed to facilitate the evaluation of the inorganic speciation of metals in marine and estuarine waters (Turner *et al.* 1981; Dickson

and Whitfield, 1981). Such calculations are based on equilibrium constants, the determination of which has been an area of intense research, but still, some conflicts and uncertainties remain (Byrne and Miller, 1985). The time scales of inorganic reactions (e.g. substitution, dissociation, addition, rearrangement and electron transfer) span a wide range, from fractions of seconds to days and years (Burgess, 1992). Therefore, when using the equilibrium approach, one has to be aware of its limitations. The assumption of equilibrium is not always valid, especially in highly dynamic estuarine environments, where metals undergo important removal and remobilisation processes between dissolved, colloidal, particulate and sedimentary phases.

Dissolved metal speciation in natural water is rarely exclusively inorganic. Great disparities between the calculated inorganic equilibrium speciation and observed speciation in waters containing metal complexing ligands, have been observed. The speciation of Cu in natural waters has been studied most intensely, whereby commonly a high proportion of the dissolved Cu concentration was found complexed by strong organic ligands (van den Berg and Donat, 1992; Sunda and Huntsman, 1991; Coale and Bruland, 1990).

Copper is of primary interest in polluted aquatic systems because of its role as micro-nutrient and its toxicity to marine flora and fauna (Apte *et al.* 1990). In open ocean and coastal surface waters, total dissolved Cu concentrations are typically in the high pM to mid nM range (Achterberg *et al.* 1999; Coale and Bruland, 1988; Bruland and Franks, 1983b; Martin and Meybeck, 1979). Toxicity studies have shown that the cupric ion is the biologically available species and therefore its activity is related to toxic effects in estuarine and marine algae, cyanobacteria and macroalgae (Gledhill *et al.* 1997 and references therein; Anderson and Morel, 1978). Experiments have shown that Cu toxicity (to algae) can be ameliorated by the addition of hydrophilic metal chelators or other micro-nutrients (e.g. Mn and Fe), indicating that Cu competitively inhibits enzyme-systems

requiring other metals (Coale and Bruland, 1988 and references therein). Hereby, the reduction of Cu toxicity stems from the formation of complexes that cannot traverse the cell membranes of organisms or are too stable to dissociate at the cell membrane (Apte *et al.* 1995; Buffle, 1988).

The complexation of Cu by inorganic and organic ligands has been shown to influence not only the biological availability and toxicity of the metal but also its particle reactivity and hence its biogeochemical behaviour and dissolved distribution (Coale and Bruland, 1988; van den Berg, 1982). A variety of techniques have been used to study complexation of Cu with strong organic ligands, including ASV (Coale and Bruland, 1988; Kramer and Duinker, 1984), AdCSV (van den Berg and Donat, 1992), chemiluminescence with ligand competition (Sunda and Huntsman, 1991), equilibration with MnO_2 (van den Berg, 1982), and ligand exchange (Sunda and Hanson, 1987; Moffett and Zika, 1987; Donat *et al.* 1986). Generally, results of these studies have indicated that Cu speciation in estuarine and marine waters is dominated by strong complexation, and that Cu complexing ligands have stability constants in the region of 10^7 - $10^{16.5}$ (Moffett, 1995; Donat and van den Berg, 1992; Coale and Bruland, 1988; Sunda and Hanson, 1987).

Comparisons between speciation studies in UV-irradiated and untreated waters have shown that the Cu complexing ligands were susceptible to photo-oxidation and this confirmed their predominantly organic nature (Gledhill and van den Berg, 1994; Sunda and Hanson, 1987). The range of detected stability constants indicates the presence of different classes of organic ligands and a natural variability between samples, but also reflects the variability in detection windows of the speciation methods applied. In many studies two classes of ligands have been detected (L_1 and L_2), whereby L_1 is characterised by high conditional stability constants and low concentrations ($\log K'_{CuL1} > 12$, low nM range), while L_2 has been found at higher concentrations (low to high nM range) and forms

Cu complexes with lower stability constant ($logK'_{CuL2} < 11$) (Moffett *et al.* 1990; Coale and Bruland, 1988; Sunda and Hanson, 1987). However, the number of organic Cu ligand classes reported is most likely the result of fitting limited experimental data to a model, rather than an accurate representation of the complexation properties of natural organic matter. Nevertheless, the classification of Cu complexing ligands is useful when comparing sets of data.

The free cupric ion activity in near-surface marine and coastal waters is relatively constant (10^{-14} - 10^{-13} M) as a consequence of the complexation of dissolved Cu with strong organic ligands (Sunda and Huntsman, 1995; Coale and Bruland, 1990). The highest concentrations of strong organic ligands have been found in near-surface waters, which has led to the suggestion that the compounds are of biological origin and susceptible to photochemical decomposition (Moffett *et al.* 1990). Moffett and Brand (1996) found evidence for the production of a Cu chelator ($logK_{CuL} \approx 13$) by the cyanobacterium *Synechococcus sp.* in response to Cu stress. The suggestion was made that this compound, and possibly similar chelators produced by other algae and bacteria, may have an ecological role in regulating the biological availability of Cu in the water column.

The aims of the work presented in this chapter were to deepen our understanding of the metal biogeochemistry of the Huelva system and to find explanations for observed metal behaviour. The inorganic equilibrium speciation of Fe, Al, Mn, Zn, Cu, Ni, Co, Cd and U in the Rio Tinto, Rio Odiel and their estuaries was calculated. The dissolved speciation of Cu(II) was studied by determining the electrochemically labile Cu concentration. Ligand titrations were carried out in surface samples from the Gulf of Cádiz and Huelva Ría using adsorptive cathodic stripping voltammetry. The degree of organic complexation and the free cupric ion concentration were calculated and the results used to estimate the cupric ion concentration at high metal concentrations.

6.3 METHODS

6.3.1 REAGENTS AND EQUIPMENT

The preparation and use of reagents for voltammetric analysis of dissolved total and labile Cu has been described in Chapter 2. Reagents used for the analysis of total dissolved Fe, Al, Mn, Zn, Cu, Ni, Co, Cd and U using ICP methods have been listed in Chapter 3. Materials of equipment used for sampling, filtration and storage of water samples and the cleaning procedures applied have been described in Chapter 3.

6.3.2 INSTRUMENTATION

Field instruments used for the *in-situ* measurement of pH, Eh, temperature, dissolved oxygen and conductivity have been described in Chapter 3. The instrumentation used for the analysis of dissolved metals using voltammetry has been described in Chapter 2 and for the use of ICP-MS and ICP-AES has been described in Chapter 3.

6.3.3 SAMPLING PROTOCOL

Samples for voltammetric speciation measurements were taken during filtration as sub-samples of discrete samples from estuarine transects in Huelva Ría and the Gulf of Cádiz during all four TOROS surveys. A summary of samples in which speciation measurements were carried out is given in Table 6.1 in chronological order. The sampling stations in Huelva Ría are presented in Chapter 4, and locations in the Gulf of Cádiz are given in Chapter 5 and Section 6.4.2.3.

Table 6.1 - Discrete samples taken in Huelva Ría and the Gulf of Cádiz for voltammetric speciation measurements. Sample locations and mode of sampling are given in Chapter 4 for the estuary and in Chapter 5 and Section 6.4.2.3 for the Gulf of Cádiz. Analytical treatment: ASV - analysis of 'labile' metal concentrations using anodic stripping voltammetry, AdCSV - analysis of 'labile' metal concentrations using adsorptive cathodic stripping voltammetry, LT - titration with tropolone for the determination of Cu complexing organic ligand concentrations. TC - tidal cycle study.

TOROS 1, Nov '96	Day	Sample ID: TOR-96-11-	Analytical Sample Treatment
Transect Huelva Ría	20	13 - 17	labile Cu: AdCSV
Transect Huelva Ría	20	25 - 33	labile Cu: AdCSV
Coastal Survey	21	34 - 38	labile Cu: AdCSV
Coastal Survey	24	39 - 43	labile Cu: AdCSV
Transect Huelva Ría	25	44 - 50	labile Cu: AdCSV
Transect Huelva Ría	25	50 - 64	labile Cu: AdCSV
Coastal Survey	25	65 - 68	labile Cu: AdCSV

TOROS 2, Jun '97	Day	Sample ID: TOR-97-06-	Analytical Sample Treatment
TC, La Rábida	6	7 - 19	labile Cu: ASV
Transect Huelva Ría	15	HR1 - HR13, G47bis	labile Cu: ASV
Transect Huelva Ría	18	HR1bis - HR13bis, G47tris	labile Cu: ASV

TOROS 3, Apr '98	Day	Sample ID: TOR-98-04-	Analytical Sample Treatment
TC, Club Nautico	16	CN1 - CN13	labile Cu: ASV
TC, Mazagón	21	MZ1 - MZ12	labile Cu: AdCSV, DP, some LT
Coastal Survey	22	MZ13 - MZ17	labile Cu: AdCSV, DP, some LT
Coastal Survey	23	MZ18 - MZ23	labile Cu: AdCSV, DP, some LT
Transect Huelva Ría	24	HR1 - HR10	labile Cu: ASV

TOROS 4, Oct. '98	Day	Sample ID: TOR-98-10-	Analytical Sample Treatment
Coastal Survey	11	A1, A3, A4	labile Cu: AdCSV, some LT
Coastal Survey	12	A5, C6,	labile Cu: AdCSV
Coastal Survey	13	E5 - E7, F8 - F6	labile Cu: AdCSV, some LT
Coastal Survey	14	G6	labile Cu: AdCSV
Transect Huelva Ría	16	HR13 - HR7, HR3 - HR1	labile Cu: AdCSV, some LT
Confluence	16	G48/96, G48/97	labile Cu: AdCSV
TC, Mazagón	19/20	G47/MZ 1 - 13	labile Cu: AdCSV, some LT

6.3.4 Sample Treatment

Samples taken for speciation studies were filtered in the same way as discrete samples for total dissolved metal determination (see Chapter 4). Filtered samples for the determination of electrochemically labile fraction of dissolved Cu were stored refrigerated awaiting electrochemical speciation analysis, which was carried out within 48 hours of sample collection at a laboratory in the University of Huelva (TOROS 1 and 3), or within 24 hours in the laboratory onboard *B/O Garcia del Cid* (TOROS 2 and 4). During TOROS 3 and 4, sub-samples destined for the determination of copper complexing organic ligand concentrations from Huelva Ría and the Gulf of Cádiz were frozen immediately after filtration and were maintained frozen during transport to the UK using dry ice.

6.3.5 Analytical Methods

Theory, analytical procedures and analytical performance for the measurement of electrochemically labile Cu and the determination of Cu complexing organic ligand concentrations have been described in detail in Chapter 2. Table 6.1 summarises the analytical treatment applied to each sample. The detection window of the electrochemical speciation methods has been estimated in Chapter 2, and the results are summarised as follows:

- AdCSV labile Cu determination (0.2 mM Tropolone, HEPES pH 7.8):

  $\log\alpha'_{CuTrop} = 3.17 - 2.87$ at S = 15 - 25 and $\log\alpha'_{CuTrop} = 2.87 - 2.64$ at S = 25 - 37.

- Cu complexing ligand titrations (0.3 mM Tropolone, HEPES pH 7.8):

  $\log\alpha'_{CuTrop} = 3.0 - 2.95$ at S = 33.5 - 36.1.

- ASV labile Cu determinations (HEPES pH 7.8):

  $\log\alpha_{Cu'} = 0.55 - 1.06$ at S = 32 - 35 and $\log\alpha_{Cu'} = 1.06 - 1.20$ at S = 35 - 36.5.

It follows that AdCSV and ASV labile Cu concentrations are not directly comparable, because the analytical detection windows of the methods were different.

6.3.6 Equilibrium Speciation Modelling using MINEQL+

6.3.6.1 Dissolved Inorganic Metal Speciation

Thermodynamic equilibrium calculations were carried out in order to explore the changes in inorganic speciation of dissolved metals along the pH and salinity gradient between the fresh water and sea water end-members in the Tinto/Odiel system. Calculations were carried out using the program MINEQL+ (version 3.01a) (Schecher and McAvoy, 1994). The program calculates the thermodynamic equilibrium speciation of constituents, using the Debye-Hückel equation to calculate activity coefficients for ionic strength corrections to stability constants. Where available, the enthalpy change of reactions were used for temperature corrections made to stability constants.

In natural waters true equilibrium is often not achieved, especially when the reaction rates of redox and dissolved metal-ligand interactions are slow, compared to the rate of physical and chemical changes in the system. In addition, biological activity has an impact on the inorganic chemistry in aquatic environments. Therefore, thermodynamic calculations do not always reflect the metal speciation that would be observed if direct measurements were possible in the field. Moreover, speciation calculations are sensitive to the magnitude of the stability constants used, especially for equilibria with ligands present in high concentrations (Pan and Susak, 1991). Stability constants given in literature vary between authors by fractions of or whole log units.

The selection of equilibria and their logK values are of prime importance in determining the speciation of elements in thermodynamic calculations. Equations of the main equilibria considered are listed in Table 6.2.

The stability constants provided within the MINEQL+ software (predominantly derived from Turner *et al.* 1981) were used, except for $\log K_{CuHCO3} = 1.8$, $\log K_{Cu(CO3)2} = 10.6$ (Byrne and Miller, 1985), and $\log K_{Cu(OH)2} = -16.2$ (Stumm and Morgan, 1996).

For the calculations, the pH was fixed at values observed in the field. The major ion composition in fresh water end-members was taken from measurements in discrete samples taken during all four surveys (Table 6.3).

Thermodynamic calculations for the estuary were carried out using values obtained during the first TOROS survey (November 1996, Table 6.4). This survey was selected because the range of salinity and pH values observed in the estuary was greater, compared to the following surveys. Estuarine major ion concentrations were calculated for the appropriate ionic strength using an ion pairing model by van den Berg, except for sulphate, which was measured by Elbaz-Poulichet (see Chapter 4). Dissolved metal concentrations used in the calculations were largely analysed by the author, and some values have been provided by TOROS colleagues. Calculations for fresh water endmembers were carried out for all four surveys. Concentrations of a number of constituents for some surveys were estimated from values determined for other TOROS surveys. Details of data sources are given in Table 6.3 and Table 6.4.

Following from field observations of dissolved oxygen and redox potential, fully oxic conditions were assumed for riverine and estuarine waters and pε was not considered in the model. Iron was assumed to be present as Fe(III). The stability of individual species and oxidation states of an element under certain conditions is indicated in Eh-pH diagrams (e.g. Garrels and Christ, 1965; Stumm and Morgan, 1996). The pH values (< 4.0) and

redox potential (Eh ≈ 500 mV) observed in the Rio Tinto, Rio Odiel and their upper estuary describe boundary conditions between Fe(II) and Fe(III) (Figure 7.23, Garrels and Christ, 1965). This is consistent with the observations made by Elbaz-Poulichet *et al.* (2000), who reported the presence of both oxidation states in the fresh water end-member of the Rio Tinto with a ratio of Fe(III):Fe(II) = 10.

Under the conditions mentioned above (oxidising and acidic), species of Mn(II) are more stable in solution, compared to its higher oxidation states (Figures 7.28, Garrels and Christ, 1965). Cobalt is not stable in the trivalent form within the stability boundaries of water, unless extremely oxidising conditions prevail at alkaline pH values (Coffey and Jickells, 1995; Pan and Susak, 1991). Under oxidising conditions, uranium is stable in the U(VI) oxidation state, as soluble complexes of the uranyl ion (UO_2^{2+}, e.g. $[UO_2(CO_3)_3]^{4-}$ in sea water) (Klinkhammer and Palmer, 1991). Considering this, in the equilibrium calculations, Co and Mn were included in their bivalent form, and uranium was represented by UO_2^{2+}.

The aim of these equilibrium calculations was to model the dissolved inorganic speciation in the rivers and estuary based on the dissolved total metal concentrations found in the field. Therefore, solid species were not considered.

Table 6.2 - Equilibrium equations for the main metal species considered in thermodynamic calculations with MINEQL+. Unless stated otherwise, equilibrium constants for these reactions were used as provided with the program and their values are given with the calculation results in the following section.

Element	Equation
Ca, Cd, Co, Cu, Mg, Mn, Ni, Pb, Zn	$M^{2+} + H_2O = MOH^+ + H^+$
Cu	$M^{2+} + 2H_2O = M(OH)_2 + 2H^+$
Cd, Pb	$2M^{2+} + H_2O = M_2(OH)^{3+} + H^+$
Fe	$M^{3+} + H_2O = MOH^{2+} + H^+$
Fe	$M^{3+} + 2H_2O = M(OH)_2^+ + 2H^+$
Fe	$2M^{3+} + 2H_2O = M_2(OH)_2^{4+} + 2H^+$
Fe, Al	$M^{3+} + 3H_2O = M(OH)_3\ aq + 3H^+$
Fe, Al	$M^{3+} + 4H_2O = M(OH)_4^- + 4H^+$
Fe	$3M^{3+} + 4H_2O = M_3(OH)_4^{5+} + 4H^+$
Cd, Zn	$M^{2+} + H_2O + Cl^- = MOHCl\ aq + H^+$
Na	$M^+ + CO_3^- = MCO_3^-$
Ca, Cd, Co[#], Cu, Mg, Ni, Pb, Zn	$M^{2+} + CO_3^- = MCO_3\ aq$
Cu[1], Ni, Pb, Zn, UO_2	$M^{2+} + 2CO_3^- = M(CO_3)_2^{2-}$
Cd, UO_2	$M^{2+} + 3CO_3^- = M(CO_3)_3^{4-}$
Na	$M^+ + HCO_3^- = MHCO_3\ aq$
Ca, Cd, Co[#], Cu, Mg, Mn, Ni, Pb, Zn	$M^{2+} + HCO_3^- = MHCO_3^+$
Na	$M^+ + SO_4^{2-} = MSO_4^-$
Ca, Cd, Co, Cu, Mg, Mn, Ni, Pb, Zn, UO_2	$M^{2+} + SO_4^{2-} = MSO_4\ aq$
Cd, Ni, Pb, Zn	$M^{2+} + 2SO_4^{2-} = M(SO_4)_2^{2-}$
Fe, Al	$M^{3+} + SO_4^{2-} = MSO_4^+$
Fe, Al	$M^{3+} + 2SO_4^{2-} = M(SO_4)_2^-$
Cd	$M^{2+} + PO_4^{3-} = MPO_4^-$
Ca, Cu, Mg, Mn, Zn, UO_2	$M^{2+} + HPO_4^{2-} = MHPO_4\ aq$
UO_2	$M^{2+} + 2HPO_4^{2-} = M(HPO_4)_2^{2-}$
Cd, Co, Cu, Mn, Ni, Pb, Zn, UO_2	$M^{2+} + Cl^- = MCl^+$
Cd, Cu, Mn, Ni, Pb, Zn	$M^{2+} + 2Cl^- = MCl_2\ aq$
Cd, Cu, Mn, Pb, Zn	$M^{2+} + 3Cl^- = MCl_3^-$
Fe	$M^{3+} + Cl^- = MCl^{2+}$
Fe	$M^{3+} + 2Cl^- = MCl_2^+$
Fe	$M^{3+} + 3Cl^- = MCl_3\ aq$
Cd, Mg, Pb, Zn, UO_2	$M^{2+} + F^- = MF^+$
Cd, Mg, Pb, Zn, UO_2	$M^{2+} + 2F^- = MF_2\ aq$
Pb, Zn, UO_2	$M^{2+} + 3F^- = MF_3^-$
Fe, Al	$M^{3+} + F^- = MF^{2+}$
Fe, Al	$M^{3+} + 2F^- = MF_2^+$
Fe, Al	$M^{3+} + 3F^- = MF_3\ aq$
Fe, Al	$M^{3+} + 4F^- = MF_4^-$

[#] Added to the Mineql+ data base from (Pan and Susak, 1991), calculated from data presented in (Byrne *et al.* 1988).

Table 6.3 - TOROS 1 - 4: Metals and major ion concentrations used in equilibrium speciation calculations for fresh water end-members (N - Niebla, G - Gibraleón, T1 - T4 - TOROS 1 - 4 surveys). Anion and cation concentrations are given in mol l^{-1}.

Sample	T1 1 (N)	T1 2 (G)	T2 (N1)	T2 (G1)	T3 (N1)	T3 (G1)	T4 (N1)	T4 (G1)
pH	2.47	2.84	2.21	3.00	2.56	3.2	2.26	2.83
T (°C)	19	19	19.5	18	19	18	21	21
Cl^-	8.7E-4[1]	7.1E-4[1]	1.1E-3[1]	5.0E-4[1]	8.2E-4[1]	1.4E-4[1]	8.7E-4[1a]	7.1E-4[1a]
F^-	5.0E-5[2]	5.0E-5[2]	5.0E-5[2]	5.0E-5[2]	5.0E-5[2]	5.0E-5[2]	5.0E-5[2]	5.0E-5[2]
K^+	4.1E-5[3]	3.3E-5[3]	4.1E-5[3a]	3.3E-5[3a]	4.1E-5[3a]	3.3E-5[3a]	4.1E-5[3a]	3.3E-5[3a]
Na^+	1.3E-6[4a]	4.4E-7[4a]	1.3E-6[4]	4.4E-7[4]	1.3E-6[4a]	4.4E-7[4a]	1.3E-6[4a]	4.4E-7[4a]
Ca^{2+}	1.8E-3[3]	2.7E-3[3]	1.8E-3[3]	2.7E-3[3]	1.8E-3[3]	2.7E-3[3]	1.8E-3[3]	2.7E-3[3]
Mg^{2+}	3.4E-3[3]	3.6E-3[3]	3.4E-3[3]	3.6E-3[3]	3.4E-3[3]	3.6E-3[3]	3.4E-3[3]	3.6E-3[3]
SO_4^{2-}	2.7E-2[1]	1.2E-2[1]	8.6E-3[1]	5.5E-3[1]	2.3E-2[1]	6.1E-3[1]	2.7E-2[1]	1.2E-2[1]
PO_4^{3-}	1.4E-5[5]	7.5E-6[5]	8.4E-10[6]	1.4E-9[6]	8.4E-10[6a]	1.4E-9[6a]	1.4E-5[5a]	7.5E-6[5a]
CO_3^{2-}	1.2E-5[7]	1.2E-5[7]	1.2E-5[7]	1.2E-5[7]	1.2E-5[7]	1.2E-5[7]	1.2E-5[7]	1.2E-5[7]
Mn^{2+}	1.7E-4	2.0E-4	1.1E-4	7.2E-5	7.30E-5	1.9E-4	7.8E-4	4.0E-4
Fe^{2+}	1.1E-2	9.1E-4	1.7E-3[8]	3.9E-5[8]	1.2E-3[1]	3.9E-5[1]	1.3E-2[9]	1.11E-3[9]
Zn^{2+}	6.1E-4	3.6E-4	3.0E-4	1.4E-4	3.6E-4	1.9E-4	2.6E-3	4.2E-4
Cu^{2+}	4.6E-4	1.4E-4	1.2E-4	5.1E-5	1.7E-4	7.2E-5	8.6E-4	7.4E-5
Ni^{2+}	4.7E-6	4.6E-6	1.8E-6	1.5E-6	1.2E-6	2.0E-6	1.7E-5	3.6E-6
Co^{2+}	9.6E-6	7.6E-6	3.7E-6	2.4E-6	6.4E-6	4.7E-6	3.9E-5	8.5E-6
Cd^{2+}	1.4E-6	6.0E-7	7.8E-7	4.3E-7	7.9E-7	4.2E-7	6.0E-6	6.7E-7
Pb^{2+}	3.1E-6	2.3E-7	3.1E-6	2.8E-7	5.0E-7	1.3E-6	6.3E-7	9.3E-4
UO_2^{2+}	3.0E-8	2.5E-8	2.9E-8	1.8E-8	1.1E-8	1.8E-8	7.2E-8	2.3E-8

[1] Provided by F. Elbaz-Poulichet, University of Montpellier II.
[1a] Assumed to be similar as measured for TOROS 1 by F. Elbaz-Poulichet.
[2] Estimated from (Medio Ambiente, 1998).
[3] Provided by M. López, University of Huelva.
[3a] Assumed to be similar as measured for TOROS 1 survey by M. López.
[4] Measured by D. Henon, University of Plymouth.
[4a] Assumed to be similar as measured for TOROS 2 by D. Henon, University of Plymouth.
[5] Provided by A. Cruzado, C.S.I.C. Blanes.
[5a] Assumed to be similar as measured for TOROS 1 by A. Cruzado, C.S.I.C. Blanes.
[6] Provided by M. López, University of Huelva.
[6a] Assumed to be similar as measured for TOROS 2 by M. López, University of Huelva.
[7] Calculated from $K_{CO2} \times P_{CO2} = 10^{-1.47} \times 3.5E\text{-}04$ (atmospheric pressure); fixed solids: $P_{CO2(g)} = 21.66$.
[8] Provided by N. Morley, Southampton Oceanography Centre.
[9] Assumed to be 20% higher than in the samples of the TOROS 1 survey.

Table 6.4 - TOROS 1: Metals and major ion concentrations used in equilibrium speciation calculations for fresh water end-members (N - Niebla, G - Gibraleón) and estuarine waters (TR - Ría del Tinto , OR - Ría del Odiel, HR - Huelva Ría, S - salinity). All anion and cation concentrations are given in mol l^{-1}.

Sample	T1 1 (N)	T1 2 (G)	TR S5	OR S5	TR S20	OR S20	TR S30	HR S36.5
Salinity	0	0	5	5	20	20	30	36.5
pH	2.47	2.84	2.43	3.21	2.54	4.3	3.09	8.2
T (°C)	19	19	19	19	19	19	19	19
Cl^-	8.7E-4[1]	7.1E-4[1]	7.8E-2	7.8E-2	3.1E-1	3.1E-1	4.7E-1	5.7E-1
F^-	5.0E-5[2]	5.0E-5[2]	5.0E-5[2]	5.0E-5[2]	3.0E-4[2]	5.0E-5[2]	7.4E-4[2]	3.0E-4[2]
K^+	4.1E-5[3]	3.3E-5[3]	1.5E-3	1.5E-3	5.8E-3	5.8E-3	8.7E-3	1.1E-2
Na^+	1.3E-6[4]	4.4E-7[4]	6.7E-2	6.7E-2	2.7E-1	2.7E-1	4.0E-1	4.9E-1
Ca^{2+}	1.8E-3[3]	2.7E-3[3]	3.3E-3	4.2E-3	5.9E-3	5.9E-3	8.8E-3	1.1E-2
Mg^{2+}	3.4E-3[3]	3.6E-3[3]	1.1E-2	1.1E-2	3.0E-2	3.0E-2	4.6E-2	5.6E-2
SO_4^{2-}	2.7E-2[1]	1.2E-2[1]	5.1E-2	1.4E-2	6.2E-2	2.4E-2	5.4E-2	2.5E-2
PO_4^{3-}	1.4E-5[5]	7.5E-6[5]	2.3E-4	2.3E-6[7]	2.0E-4	3.0E-6[10]	1.3E-4	5.5E-6[10]
CO_3^{2-}	1.2E-5[6]	1.2E-5[6]	1.2E-5[6]	1.2E-5[6]	1.2E-5[6]	6.6E-5[8]	1.2E-5[6]	1.3E-3[8]
Fe^{3+}	1.1E-2	9.1E-4	1.8E-2	3.9E-4	2.8E-3	1.0E-4	1.9E-4	1.0E-7[9]
Al^{3+}	3.6E-3	2.3E-3	5.4E-3	1.7E-3	1.7E-3	6.9E-4	5.0E-4	1.3E-7
Mn^{2+}	1.7E-4	2.0E-4	3.1E-4	1.7E-4	1.0E-4	8.2E-5	8.3E-8	4.0E-6
Zn^{2+}	6.1E-4	3.6E-4	1.9E-3	2.1E-4	3.8E-4	8.8E-5	8.7E-5	1.6E-6
Cu^{2+}	4.6E-4	1.4E-4	7.7E-4	8.9E-5	2.1E-4	4.3E-5	4.6E-5	2.8E-6
Ni^{2+}	4.7E-6	4.6E-6	6.9E-6	3.2E-6	2.6E-6	1.6E-6	9.3E-7	2.1E-7
Co^{2+}	9.6E-6	7.6E-6	1.8E-5	5.5E-6	5.4E-6	2.6E-6	1.4E-6	2.8E-7
Cd^{2+}	1.4E-6	6.0E-7	3.2E-6	4.4E-7	1.0E-6	2.6E-7	3.0E-7	8.4E-8
Pb^{2+}	3.1E-6	2.3E-7	1.9E-7	2.9E-7	1.2E-7	6.0E-8	4.9E-8	1.0E-8
UO_2^{2+}	3.0E-8	2.5E-8	1.1E-8	2.2E-8	2.8E-7	7.7E-9	8.3E-8	6.0E-9

[1] Provided by F. Elbaz-Poulichet, University of Montpellier II.
[2] Estimated from (Medio Ambiente, 1998).
[3] Provided by M. López, University of Huelva.
[4] Assumed to be similar as measured for TOROS 2 by D. Henon, University of Plymouth.
[5] Provided by A. Cruzado, C.S.I.C. Blanes.
[6] Calculated from $K_{CO2} \times P_{CO2} = 10^{-1.47} \times 3.5E\text{-}04$ (atmospheric pressure); fixed solids: $P_{CO2(g)} = 21.66$.
[7] Assumed to be similar as measured for TOROS 2 by A. Cruzado, C.S.I.C. Blanes.
[8] Alkalinity measured in samples of similar pH and salinity during TOROS 2 survey by V. Herzl, University of Plymouth, expressed as $[CO_3^{2-}]$.
[9] Estimated value.
[10] Estimated from values measured during TOROS 2 and 4 surveys by A. Cruzado, C.S.I.C. Blanes.

6.3.6.2 Inorganic Metal Speciation Including Dissolved Solids

In order to assess the solubility of metals at high concentrations in the upper estuary and to test whether equilibrium calculations were an appropriate approach for the prediction of speciation in this system, the formation of dissolved solids was permitted in one set of calculations. In this case, the saturation with solids formed from dissolved species was indicated in the modelling results by the 'solids saturation index':

$$SI = \log \frac{Q}{K_s} \qquad (6.1),$$

where Q is the ion activity product and K_S is the solubility constant of the solid at the specified temperature. Hereby, SI = 0 signifies the equilibrium of solid and dissolved phases, while SI < 0 and SI > 0 indicate under- and over-saturation of the solution with the solute species, respectively.

6.3.6.3 Dissolved Cu Speciation Including Organic Ligands

In order to assess the toxicity of Cu in the waters of Huelva Ría and the Gulf of Cádiz, the cupric ion concentration was calculated, whereby data obtained from ligand titrations (see Section 6.4.3) was used in thermodynamic calculations with MINEQL+. A bivalent Cu complexing ligand (L^{2-}) was introduced into the calculations, which was characterised by the value of the conditional stability constant of the Cu-ligand complex ($\log K'_{CuL}$). For the calculations, major ion concentrations were calculated according to the salinity of the respective sample, and the pH values were used as measured in the field (pH 8.3 for T4 MZ samples).

Values for $logK'_{CuL}$ were determined at pH 7.8 and at ambient temperature (ca. 22°C) with ligand titrations. According to Byrne *et al.* (1988) the speciation of Cu is influenced by the pH and temperature of the system. Compensations for temperature are made within Mineql+, using ΔH, and as this value is not available for the CuL complex, thermodynamic calculations were carried out at 22°C (a water temperature that occurs naturally in Huelva Ría during summer months). The adjustment of $logK'_{CuL}$ to pH 8.3 was made following the procedure suggested by Gledhill and van den Berg (1994) for iron speciation and applied by Achterberg et. al. (1997) for Cu. The assumptions are made that one proton is exchanged for one Cu ion on the ligand L, that proton competition is important at the considered pH and that the effect of a single proton is predominant over the effects of major ions (e.g. Ca^{2+} and Mg^{2+}). From these assumptions it can be estimated that an increase in pH value by 0.5 will result in an increase of $logK'_{CuL}$ by 0.5. Although this estimate increases the uncertainty in the calculations, it is probably a reasonable approach when considering that Cu is not strongly hydrolysed and pH and temperature changes have a lesser effect on its speciation when compared with Fe or Al (Byrne *et al.* 1988). This is supported by a direct relationship between pH and $logK'_{CuL2}$ (the conditional stability constant of class 2 ligands) found empirically by Anderson *et al.* (1984).

6.4 Results

6.4.1 Inorganic Equilibrium Speciation of Fe, Al, Mn, Zn, Cu, Ni, Co, Cd, Pb and U

Rio Tinto and Rio Odiel

The calculated dissolved inorganic speciation of metals at Niebla and Gibraleón is presented in Table 6.5. In the Rio Tinto, free hydrated ions (M^{n+}) and aqueous metal sulphates (MSO_4 aq) dominated the inorganic speciation of Mn, Zn, Cu, Ni, Co, Cd and

Pb. The variations in metal speciation between surveys mirrored the pH values, whereby the fraction of free ions was higher at lower pH values in the water. Also present were $M(SO_4)_2^{2-}$ species for Zn, Cd and Pb, and MCl^+ for Cd and Pb. The speciation of Fe was dominated by $FeSO_4^+$ and $Fe(SO_4)_2^-$, while Fe^{3+} and hydroxide complexes constituted minor fractions. The inorganic speciation of Mn, Zn, Cu, Ni, Co, Cd and Pb in the Rio Odiel was similar to that calculated for the Rio Tinto, with high proportions of free hydrated ions and aqueous metal sulphates. The calculation results showed higher proportions of metal sulphates for surveys with higher sulphate concentrations in the water. $M(SO_4)_2^{2-}$ species for Zn, Cd and Pb, as well as $CdCl^+$ were present. Sulphate was the main species calculated for dissolved Fe, and as in the Rio Tinto $Fe(SO_4)_2^-$, hydroxide complexes and Fe^{3+} were also present.

Initially, calculations for simplified solutions had been carried out, whereby the pH, temperature, major anion and cation concentrations for the Rio Tinto and Rio Odiel were taken from the TOROS 1 survey (Table 6.4), and the speciation of Fe, Al, Mn, Zn, Cu, Ni, Co, Cd and Pb was calculated separately. Compared to the speciation calculated for the 'full' solution (Table 6.5), the speciation calculations for individual metals resulted in lower free ionic and higher metal-sulphate fractions (e.g. Zn: 18.1% Zn^{2+}, 10.7% $Zn(SO_4)_2^{2-}$ and 71.2% $ZnSO_4$ aq). This can be attributed to the reduced competition for the formation of metal-sulphate complexes in the solution containing a lower total metal concentration. Similar calculations were carried out for individual metals at S = 36.5, and the results did not show any important differences to the results of calculations that included all trace metals simultaneously. This can be explained by the dominance of sea water related species (metal complexes with hydroxide, chloride and carbonate) and the excess of these ligands with respect to the combined total dissolved metal concentration involved.

Table 6.5 - TOROS 1 - 4: Thermodynamic equilibrium calculations for river water using MINEQL+. The fraction (%) of each metal species with respect to its total dissolved metal concentration (Table 6.3) is given for four surveys in the Rio Tinto at Niebla (N) and Rio Odiel at Gibraleón (G). Empty cells: % total < 1.

		Rio Tinto				Rio Odiel			
Species	LogK	T1 N	T2 N	T3 N	T4 N	T1 G	T2 G	T3 G	T4 G
Fe^{3+}	0	1.9	6.8	1.2	16.3	2.2	4.3	3.2	2.2
$FeOH^{2+}$	-2.35	2.5	5.1	1.9	13.4	7.0	18.4	21.4	6.2
$Fe(OH)_2^+$	-5.67				1.2	2.3	9.3	17.1	2.1
$Fe_2(OH)_2^{4+}$	-3.15				5.7				
$FeSO_4^+$	3.86	80.7	83.2	75.7	61.3	77.1	63.9	54.3	77.5
$Fe(SO_4)_2^-$	5.35	14.4	4.3	20.9		11.3	4.1	4.0	12.0
Mn^{2+}	0	50.5	77.7	39.8	91.7	55.4	74.2	71.4	54.3
$MnSO_4$ aq	2.23	49.4	22.0	60.1	8.0	44.4	25.6	28.6	45.5
Zn^{2+}	0	42.3	72.4	31.7	89.5	47.5	68.1	64.8	46.2
$Zn(SO_4)_2^{2-}$	3.28	2.7		4.8		2.0			2.2
$ZnSO_4$ aq	2.35	54.9	27.1	63.4	10.4	50.4	31.3	34.5	51.5
Cu^{2+}	0	46.8	75.2	36.3	90.7	51.8	71.2	68.2	50.5
$CuSO_4$ aq	2.29	53.1	24.6	63.6	9.2	48.2	28.7	31.8	49.4
Ni^{2+}	0	48.2	76.2	37.6	91.1	53.2	72.4	69.4	52
$NiSO_4$ aq	2.27	51.7	23.6	62.2	8.7	46.7	27.5	30.5	47.9
Co^{2+}	0	35.3	65.4	26.1	85.8	39.9	60.3	56.8	38.6
$CoSO_4$	2.5	64.6	34.4	73.8	14	60.0	39.6	43.1	61.3
Cd^{2+}	0	35.7	63.4	26.2	82.4	40.7	61.3	59	39.5
$CdCl^+$	1.97	2.9	6.5	2	5.6	2.7	2.9		2.6
$Cd(SO_4)_2^{2-}$	3.5	3.8		6.6		2.9		1.1	3.2
$CdSO_4$ aq	2.44	57.6	29.5	65.1	11.9	53.7	35.1	39.1	54.8
Pb^{2+}	0	22.8	50.4	15.9	75.9	26.6	45.5	42.2	25.5
$PbCl^+$	1.53		1.9		1.9				
$PbSO_4$ aq	2.75	74.3	47.2	79.9	22.1	71	53.1	56.9	72.0
$Pb(SO_4)_2^{2-}$	3.47	2.3		3.7		1.8			1.9

Ría del Tinto

For the Ría del Tinto the equilibrium calculations were carried out with values from the November 1996 survey (TOROS 1, Table 6.4). Results for the dissolved speciation of Fe, Mn, Zn, Cu, Ni, Co, Cd, Pb and UO_2^{2+} are given in Table 6.6. The inorganic speciation of Mn, Zn, Cu, Ni, Co, Cd and Pb at S = 0 was dominated by aqueous sulphates (49 - 74%) and free hydrated ions (23 - 51%). The trivalent metals Fe and Al occurred mainly as MSO_4^+ and $M(SO_4)_2^-$, with minor free ion concentrations (1.9% Fe^{3+} and 10.9% Al^{3+}). At low salinity (S = 5), the fraction of free hydrated ions increased initially for Fe, Mn, Zn, Cu, Ni, Co and Pb. Further increases in salinity resulted in progressive complexation of these metals by chloride, forming mainly MCl^{2+} and MCl^+ and other chloro species of Fe, Ni, Cd and Pb. In the lower Ría del Tinto a large fraction of Al was complexed with fluoride (53% AlF_3 aq), and FeF^{2+} was important in the speciation of Fe (15%).

The speciation of uranyl in the Rio Tinto was dominated by sulphate (61.6% UO_2SO_4 aq and 10.3% $UO_2(SO_4)_2^{2-}$) and the free ion in solution (24.8% UO_2^{2+}). The combined proportion of these three species decreased to less than 5% in the estuary of the Rio Tinto, where between 87% (S = 5) and 98.3% (S = 30) of the total uranyl concentration was present as $UO_2(HPO_4)_2^{2-}$.

Table 6.6 - TOROS 1: Thermodynamic equilibrium calculations using MINEQL+ for the Rio Tinto (T1 1 (N)) and three points in the Ria del Tinto at S = 5 (metal maximum), S = 20 (mid estuary) and S = 30 (lower estuary). Metal concentrations are given in Table 6.4. Empty cells: % total < 1.

	T1 1 (N)		TR S5		TR S20		TR S30	
Name	LogK	%Total	LogK	%Total	LogK	%Total	LogK	%Total
Fe^{3+}	0	1.9	0	12.3	0	11.2	0	8.9
$FeOH^{2+}$	-2.35	2.5	-2.85	4.6	-2.93	4.6	-2.94	12.6
$FeOH_2^{+}$	-5.67	-		-		-	-6.56	3.7
$Fe_2(OH)_2^{4+}$	-3.15	-	-3.15	2.8		-		-
$FeCl_2^{+}$	2.13	-		-	0.68	5.2	0.64	8.7
$FeCl^{2+}$	1.4	-	0.63	4.1	0.52	11.6	0.50	13.4
FeF^{2+}	6.2	-		-		-	5.27	15.1
FeF_2^{+}	10.8	-		-		-	9.24	1.3
$FeSO_4^{+}$	3.86	80.7	2.34	61.3	2.12	51.6	2.07	29.4
$Fe(SO_4)_2^{-}$	5.35	14.4	3.32	13.5	3.02	14.7	2.97	6.3
Al^{3+}	0	10.9	0	50.3	0	41.6	0	4.4
AlF^{2+}	7.01	-		-	6.14	15.9	6.12	53.1
AlF_2^{+}	12.8	-		-		-	11.0	34.0
AlF_3 aq	17.0	-		-		-	15.2	5.4
$AlSO_4^{+}$	2.99	61.4	1.24	32.3	1.24	24.9	1.20	1.9
$Al(SO_4)_2^{-}$	4.88	27.6	2.55	17.4	2.55	17.3	2.49	1.1
Mn^{2+}	0	50.5	0	67.9	0	56.9	0	55.0
$MnCl^{+}$	0.61	-	0.10	6.6	0.03	18.8	0.01	26.5
$MnCl_2$ aq	0.04	-		-		-	-0.85	1.7
$MnSO_4$ aq	2.23	49.4	1.21	25.4	1.06	23.3	1.04	16.4
Zn^{2+}	0	42.3	0	60.8	0	52.3	0	54.5
$ZnCl_3^{-}$	0.36	-		-		-	-0.54	1.6
$ZnCl^{+}$	0.31	-		-	-0.27	8.8	-0.28	13.3
$ZnCl_2$ aq	0.32	-		-	-0.55	1.4	-0.57	3.2
$Zn(SO_4)_2^{2-}$	3.28	2.7	2.26	5.9	2.12	8.5	2.09	5.1
$ZnSO_4$ aq	2.35	54.9	1.33	30.1	1.19	28.4	1.16	21.6
Cu^{2+}	0	46.8	0	67.5	0	60.6	0	62.0
$CuCl_2$ aq	016	-		-		-	-0.89	1.8
$CuCl^{+}$	0.3		-0.21	3.2	-0.28	9.9	-0.30	14.7
$CuSO_4$ aq	2.29	53.1	1.28	29.3	1.13	28.8	1.10	21.5
Ni^{2+}	0	48.2	0	67.6	0	56.4	0	53.1
$NiCl^{+}$	0.4	-	-0.11	4.0	-0.18	11.6	-0.20	15.9
$NiCl_2$ aq	0.96	-		-	0.09	6.7	0.07	13.7
$NiSO_4$ aq	2.27	51.7	1.25	27.7	1.10	25.3	1.08	17.4
Co^{2+}	0	35.3	0	56.3	0	49.4	0	51.6
$CoCl^{+}$	0.5	-	-0.01	4.3	-0.08	12.8	-0.10	19.5
$CoSO_4$	2.5	64.6	1.48	39.4	1.34	37.9	1.31	28.9

Table 6.6 - continued.

	T1 1 (N)		TR S5		TR S20		TR S30	
Name	LogK	%Total	LogK	%Total	LogK	%Total	LogK	%Total
Cd^{2+}	0	35.7	0	22.6	0	6.5	0	3.8
$CdCl^{+}$	1.97	2.9	1.46	50.6	1.39	49.5	1.38	42.2
$CdCl_3^{-}$	2.34	-	1.58	0.0	1.47	5.8	1.45	11.0
$CdCl_2$ aq	2.58	-	1.82	8.8	1.71	32.2	1.69	40.7
$Cd(SO_4)_2^{2-}$	3.5	3.8	2.48	3.6	2.34	1.8		
$CdSO_4$ aq	2.44	57.6	1.43	13.9	1.28	4.4	1.25	1.9
Pb^{2+}	0	22.8	0	30.5	0	15.5	0	11.4
$PbCl_2$ aq	1.78	-	1.02	1.9	0.91	12.3	0.89	19.5
$PbCl^{+}$	1.53	-	1.03	24.9	0.95	43.4	0.94	46.3
$PbCl_3^{-}$	1.67	-		-	0.79	2.9	0.77	7.0
$PbCl_4^{2-}$	1.33	-		-		-	0.73	3.0
$PbSO_4$ aq	2.75	74.3	1.73	38.0	1.59	21.1	1.56	11.3
$Pb(SO_4)_2^{2-}$	3.47	2.3	2.45	4.6	2.31	3.9	2.28	1.6
UO_2^{2+}	0	24.8	0	4.3	0	3.1		-
UO_2HPO_4 aq	20.9	1.2	19.1	1.1		-		
$UO_2(HPO_4)_2^{2-}$	43.2	1.7	40.6	87.5	40.2	89.3	40.2	98.3
UO_2SO_4 aq	2.63	61.6	1.61	4.0	1.47	3.1		-
$UO_2(SO_4)_2^{-2}$	4.09	10.3	3.07	2.6	2.93	3.1		-

Ría del Odiel and Huelva Ría

For the Rio Odiel and its estuary (TOROS 1, Table 6.4), the results from thermodynamic equilibrium calculations of dissolved Fe, Al, Mn, Zn, Cu, Ni, Co, Cd, Pb and U are given in Table 6.7. The inorganic speciation of Mn, Zn, Cu, Ni, Co, Cd and Pb at S = 0 was similar to that in the Rio Tinto, dominated by aqueous sulphates (44 - 71%) and free hydrated ions (27 - 55%), while Fe occurred mainly as $FeSO_4^+$ and $Fe(SO_4)_2^-$ (77 and 11%, respectively). At low salinity (S = 5), the fraction of free hydrated ions increased initially for Fe, Al, Mn, Zn, Cu, Ni, Co and Pb. Further increases in salinity resulted in progressive complexation of metals by chloride (important for Cd, Pb and Mn), carbonate (important for Cu, Ni, Pb and Zn) and/or hydroxide (Fe and Al).

At sea water salinity, the inorganic speciation of Mn and Co was similar to that at S = 5 (M^{n+}, MCl^- and MSO_4 aq), while important transformations had taken place for Fe and Al ($M(OH)_4^-$ and $M(OH)_3$ aq), Zn (Zn^{2+}, ZnOHCl aq, $ZnCO_3$ aq, $Zn(CO_3)_2^{2-}$ and $ZnSO_4$ aq), Cu and Pb (MCO_3 aq and $M(CO_3)_2^{2-}$), Ni ($NiCO_3$ aq) and Cd ($CdCl_2$ aq, $CdCl^+$ and $CdCl_3^-$). Similar to results for the Rio Tinto the dissolved speciation of uranyl in the Rio Odiel was dominated by sulphates (57.2% UO_2SO_4 aq and 7.83% $UO_2(SO_4)_2^{2-}$) and the free ion in solution (28.1% UO_2^{2+}). At low salinity (S = 5), the free ionic fraction became more important (56.3% UO_2^{2+}), and at S = 20 uranyl was almost entirely complexed by phosphate (93.4% $UO_2(HPO_4)_2^{2-}$). Under near sea water conditions dissolved uranyl was complexed by carbonate (95.6% $UO_2(CO_3)_3^{4-}$).

Table 6.7 - TOROS 1: Thermodynamic equilibrium calculations using MINEQL+ for the Rio Odiel (T1 2 (G)) and three points in the Ría del Odiel and Huelva Ría at S = 5 (metal maximum), S = 20 (lower Ría del Odiel) and S = 36.5 (lower estuary). Metal concentrations are given in Table 6.4. Empty cells: % total < 1.

	T1 2 (G)		OR S5		OR S20		HR S36.5	
Name	LogK	%Total	LogK	%Total	LogK	%Total	LogK	%Total
Fe^{3+}	0	2.2	0	12.4		-		-
$FeOH^{2+}$	-2.35	7.0	-2.81	30.9	-2.94	16.5		-
$FeOH_2^{+}$	-5.67	2.3	-6.37	13.9	-6.56	80.0	-6.56	11.5
$Fe_2(OH)_2^{4+}$	-3.15	-	-3.15	2.2		-		
$Fe(OH)_3$ aq	-13.6	-		-		-	-14.49	21.4
$Fe(OH)_4^{-}$	-21.6	-		-		-	-22.19	67.1
$FeCl^{2+}$	1.4	-	0.69	4.8		-		-
$FeSO_4^{+}$	3.86	77.1	2.46	31.8	2.07	1.3		-
$Fe(SO_4)_2^{-}$	5.35	11.3	3.48	3.0		-		-
Al^{3+}	0	13.7	0	68.4	0	73.8		-
$AlOH^{2+}$	-10.1	-		-	-5.75	2.6		-
$Al(OH)_3$ aq	-16	-		-		-	-16.9	12.8
$Al(OH)_4^{-}$	-23.7	-		-		-	-24.2	87.1
$AlSO_4^{+}$	2.99	63.0	1.59	25.1	1.24	18.1		-
$Al(SO_4)_2^{-}$	4.88	23.2	3.01	6.3	2.55	5.1		-
Mn^{2+}	0	55.4	0	77.9	0	55.0	0	53.5
$MnCl^{+}$	0.61	-	0.14	8.4	0.01	21.8	0.02	31.6
$MnCl_2$ aq	0.04	-		-		-	-0.85	2.5
$MnSO_4$ aq	2.23	44.4	1.29	13.6	1.04	10.8	1.04	11.3
Zn^{2+}	0	47.5	0	76.5	0	69.1	0	26.0
ZnOHCl aq	-7.48	-		-		-	-8.07	19.9
$ZnOH^{+}$	-9.16	-		-		-	-9.46	1.4
$Zn(OH)_2$ aq	-16.9	-		-		-	-17.19	4.2
$ZnHCO_3^{+}$	12.4	-		-		-	11.22	1.1
$ZnCl_3^{-}$	0.36	-		-		-	-0.53	1.4
$ZnCl^{+}$	0.31	-	-0.15	4.2	-0.28	11.6	-0.28	7.8
$ZnCl_2$ aq	0.32	-		-	-0.57	1.9	-0.56	2.3
$ZnCO_3$ aq	5.3	-		-		-	4.12	14.1
$Zn(CO_3)_2^{2-}$	9.63	-		-		-	8.45	12.6
$Zn(SO_4)_2^{2-}$	3.28	2.0	2.34	1.3	2.09	1.8	2.10	1.2
$ZnSO_4$ aq	2.35	50.4	1.41	17.7	1.16	14.8	1.17	7.2
Cu^{2+}	0	51.8	0	79.6	0	73.4	0	4.6
$CuOH^{+}$	-8	-		-		-	-8.30	3.7
$Cu(OH)_2$ aq	-16.24	-		-		-	-16.54	3.4
$CuCl^{+}$	0.3	-	-0.17	4.2	-0.30	11.9	-0.29	1.4
$CuCO_3$ aq	6.73	-		-		-	5.55	68.1
$Cu(CO_3)_2^{2-}$	10.51	-		-		-	9.33	17.1
$CuSO_4$ aq	2.29	48.2	1.36	16.1	1.10	13.8	1.11	1.1

Table 6.7 - continued.

	T1 2 (G)		OR S5		OR S20		HR S36.5	
Name	LogK	%Total	LogK	%Total	LogK	%Total	LogK	%Total
Ni^{2+}	0	53.2	0	78.8	0	53.1	0	4.2
$NiCl^{+}$	0.4	-	-0.07	5.2	-0.20	15.9	-0.19	1.5
$NiCl_2$ aq	0.96	-		-	0.07	13.7	0.07	1.6
$Ni(CO_3)_2^{2-}$	10.11	-		-		-	8.93	6.2
$NiCO_3$ aq	6.87	-		-		-	5.69	85.2
$NiSO_4$ aq	2.27	46.7	1.33	15.1	1.08	17.4		-
Co^{2+}	0	39.9	0	70.8	0	51.6	0	52.3
$CoOH^{+}$	-9.2	-		-		-	-9.50	2.6
$CoCl^{+}$	0.5	-	0.03	5.9	-0.10	19.5	-0.09	24.2
$CoSO_4$ aq	2.5	60.0	1.56	23.2	1.31	28.9	1.32	20.6
Cd^{2+}	0	40.7	0	23.4	0	3.8	0	2.6
CdOHCl aq	-7.47	-		-		-	-8.06	2.1
$CdCl^{+}$	1.97	2.7	1.50	58.0	1.38	42.2	1.38	36.0
$CdCl_3^{-}$	2.34	-		-	1.45	11.0	1.45	13.9
$CdCl_2$ aq	2.58	-	1.88	10.7	1.69	40.7	1.69	42.4
$CdCO_3$ aq	5.4	-		-		-	4.22	1.8
$Cd(SO_4)_2^{2-}$	3.5	2.9		-		-		-
$CdSO_4$ aq	2.44	53.7	1.51	6.7	1.25	1.9		-
Pb^{2+}	0	26.6	0	38.5	0	11.4	0	1.5
$PbOH^{+}$	-7.71	-		-		-	-8.01	2.4
$PbCl^{2}$ aq	1.78	-	1.08	2.8	0.89	19.5	0.90	3.9
$PbCl^{+}$	1.53	-	1.07	35.0	0.94	46.3	0.94	7.6
$PbCl_3^{-}$	1.67	-		-	0.77	7.0	0.78	1.7
$PbCl_4^{2-}$	1.33	-		-	0.73	3.0		-
$PbCO_3$ aq	7.24	-		-		-	6.06	72.6
$Pb(CO_3)_2^{2-}$	10.64	-		-		-	9.46	7.6
$PbSO_4$ aq	2.75	71.0	1.81	22.5	1.56	11.3	1.57	1.1
$Pb(SO_4)_2^{2-}$	3.47	1.8	2.53	1.1	2.28	1.6		-
UO_2^{2+}	0	28.1	0	56.3	0	3.3		-
UO_2Cl^{+}	0.2	-	-0.26	2.4		-		-
$UO_2(CO_3)_3^{4-}$	21.5	-		-		-	21.5	95.6
$UO_2(CO_3)_2^{2-}$	17	-		-		-	15.8	4.2
UO_2HPO_4 aq	20.9	2.1	19.2	1.2		-		-
$UO_2(HPO_4)_2^{2-}$	43.2	4.5	40.8	5.9	40.2	93.4		-
UO_2SO_4 aq	2.63	57.2	1.7	26.7	1.47	1.3		-
$UO_2(SO_4)_2^{-2}$	4.09	7.8	3.16	7.2		-		-

6.4.2 Copper Speciation Studies

6.4.2.1 Huelva Ria Transects

Total dissolved and labile concentrations of Cu were analysed in discrete samples from Huelva Ría during all four surveys. The results are given in Table 6.8, together with the percent fraction of the labile Cu concentrations with respect to the total. The widest range of salinity and pH was covered in November (S = 14 - 36.9 and pH 6.29 - 8.61), and the lowest in October (S = 36.1 - 36.6 and pH 7.76 - 8.01). High water temperatures were observed in June (22.2 - 25.2°C, day transect) and lower ones in April (16.3 - 20.5°C, day transect) and October (18.4 - 21.0°C, night transect). The DOC concentrations in Huelva Ría were similar during the surveys (mean: 0.20, 0.29 and 0.25 mM for June, April and October, respectively), with a slightly higher maximum encountered in October (0.38 mM DOC), compared to June and April (0.30 and 0.33 mM DOC, respectively).

In November 1996, the total dissolved metal concentrations observed were 0.18 - 7.7 μM Cu. The proportion of AdCSV-labile Cu in Huelva Ría was high (64 - 100%, median 97%), with the exception of one sample in the lower estuary (36%). Overall, the labile fraction decreased with increasing pH and decreasing total Cu concentration.

In June 1997, total dissolved Cu concentrations in Huelva Ría were lower (0.19 - 3.1 μM Cu), compared to November 1996. Concentrations were lower still in April 1998 (TOROS 3, 170 - 820 nM Cu) and October 1998 (TOROS 4, 30 - 520 nM Cu). However, when comparing Cu concentrations at equal salinity or pH between the surveys, total Cu concentrations were highest in June. The ASV labile Cu fraction in was 52 - 100% (median 74%) and 46 - 92% (median 70%) of the total dissolved concentration in June and April, respectively, and AdCSV labile Cu was between 28 and 64% (median 55%) in October.

Table 6.8 - Total dissolved and ASV or AdCSV labile Cu concentrations in Huelva Ría. TOR-yy-mm: Sample label, D: distance from Mazagón, Cu_L: labile dissolved Cu concentration, Cu_T: Total dissolved concentration, Cu_L %: proportion of labile dissolved fraction in percent (values > 100% resulted from the mean numerical value of $Cu_L > Cu_T$ within the error of the measurement, and can be interpreted as fully labile). Errors: SPM and DOC ≤ 12%, metal determinations ≤ 10%. Blank cells: no reliable data. The term 'labile' was defined in Chapter 2, Section 2.4.

TOR-96-11	D km	S	pH			Cu_L µM	Cu_T µM	Cu_L %
29	19.1	35.4	6.56			6.1	6.0	101
51	18.4	14.0	6.29			6.0	6.0	100
50	17.7	26.9	6.42			6.1	6.6	93
30	17.6	35.3	6.90			5.2	6.2	84
49	16.1	30.1	6.40			5.6	5.9	96
54	14.7	32.1	6.42			7.5	7.7	97
45	12.4	16.6	6.12			6.4	6.0	107
56	12.2	31.9	6.47			3.9	3.6	107
57	11.7	33.2	6.69			3.1	2.9	106
58	10.6	33.4	6.77			2.2	2.1	101
59	9.5	33.1	6.92			1.5	1.5	100
60	8.8	32.9	7.18			0.73	0.84	87
61	7.5	34.4	7.51			0.40	0.56	72
62	5.0	34.4	7.99			0.17	0.27	64
63	4.0	34.5	8.18			0.08	0.21	36
64	1.7	35.1	8.19			0.15	0.18	86

TOR-97-06	D km	S	pH	T °C	DOC mM	Cu_L µM	Cu_T µM	Cu_L %
HR 1	20.3	34.2	6.99	25.2	0.25	1.6	3.1	52
HR 2	19.7	33.6	7.08		0.25	1.8	2.2	79
HR 3	18.5	34.8	7.08	24.3	0.30	1.9	2.3	82
HR 4	16.6	34.9	7.43	24.4	0.17	1.4	1.9	73
HR 5	15.0	34.9	7.41	22.4	0.18	1.5	2.5	61
HR 6	13.7	34.0	7.10	25.0	0.23	1.8	3.1	58
HR 7	12.7	34.9	7.22	23.8	0.20		3.1	
HR 8	11.2	35.3	7.51	22.9	0.14	1.1	1.4	77
HR 9	9.8	34.9	7.48	23.3	0.18	1.1	1.8	61
HR 10	7.6	34.9	7.40	24.8	0.22	2.3	2.2	103
HR 11	5.7	35.0	7.57	23.6	0.17	1.3	1.7	76
HR 12	4.0	34.5	7.59	24.2	0.20	1.2	1.6	72
HR 13	1.5	36.0	7.88	22.2	0.09		0.19	

Table 6.8 - continued.

TOR-98-04	D km	S	pH	T °C	DOC mM	Cu_L µM	Cu_T µM	Cu_L %
HR 10	18.5	34.0	7.93	20.5	0.24	0.49	0.68	72
HR 9	17.3	34.3	7.88	20.3	0.29	0.41	0.56	74
HR 8	15.9	34.8	7.82	19.4	0.29	0.46	0.64	71
HR 7	13.6	34.5	7.90	19.7	0.33	0.38	0.82	46
HR 6	12.4	34.6	8.02	19.4	0.30	0.39	0.63	62
HR 5	10.5	35.7	7.98	19.6	0.29	0.25	0.59	43
HR 4	8.7	34.9	8.07	18.9	0.27	0.32	0.45	71
HR 3	6.6	34.9	7.94	18.0	0.31	0.24	0.35	68
HR 2	3.9	35.1	8.11	17.6	0.29	0.19	0.44	44
HR 1	1.5	37.0	8.15	16.3	0.27	0.15	0.17	92

TOR-98-10	D km	S	pH	T °C	DOC mM	Cu_L µM	Cu_T µM	Cu_L %
HR1	20.4	36.6	7.82	20.9	0.38	0.26	0.51	50
HR2	19.7	36.6	7.84	21.0	0.35	0.24	0.52	46
HR3	18.8	36.6	7.82	20.9	0.35	0.14	0.50	28
D48-a	15.3	36.1				0.19	0.32	59
D48-b	15.2	36.2				0.19	0.31	61
HR7	12.2	36.2	7.81	19.8	0.27	0.18	0.35	53
HR8	11.3	36.2	7.79	19.2	0.24	0.19	0.36	53
HR9	9.8	36.2	7.76	18.9	0.23	0.17	0.29	60
HR10	7.8	36.1		18.5	0.20	0.09	0.16	57
HR11	5.9	36.1		18.2	0.19	0.06	0.10	64
HR12	4.1	36.1	8.01	18.4	0.17	0.03	0.05	58
HR13	1.5	36.1	7.99	18.7	0.15	0.02	0.03	53

6.4.2.2 Tidal Cycle Studies

The total and labile concentrations of Cu determined in discrete samples taken during tidal cycle studies (TCs) are presented as time series in Figure 6.1: Club Nautico at the confluence of Ría del Tinto with Huelva Ría (TOROS 3), Figure 6.2: mouth of the estuary (TOROS 3) and Figure 6.3: four kilometres outside the estuary in the Gulf of Cádiz (TOROS 4). The locations of these TCs are given in Chapter 4, Figure 4.9.

At the confluence (Club Nautico, Figure 6.1), low water was marked by distinct minima of salinity (32.7) and pH (7.35) and maxima of total and labile Cu concentrations (1.63 and 1.13 μM, respectively). The mean DOC concentration (data not shown) during the TC was 250 μM C, with a maximum of 353 μM C occurring shortly after low water and values between 200 and 260 μM C during the remainder of the survey time.

Little variation in salinity (35.02 - 36.69, Cruzado and Velasquez, 1999) and pH (8.19 - 8.33) was observed during the TC at the mouth of the estuary (Figure 6.2). DOC varied between 128 and 177 μM C, with the lowest concentration near high water. This was also the case for total and labile Cu (91.2 and 63.4 nM, respectively) concentrations. Dissolved metal peaks coincided with the lowest pH and salinity values at the beginning of the TC (Cu_T = 338 nM) and near low water (Cu_T = 229 nM).

During the coastal TC (Figure 6.3) the salinity (36.2 - 36.3) remained almost constant and little variation was observed for DOC (147 - 181 μM C). Maxima of total dissolved and labile Cu (68.5 and 50.4 nM, respectively) occurred approximately one hour ahead of low water and metal minima were observed near high water (Cu_T = 10.7 nM).

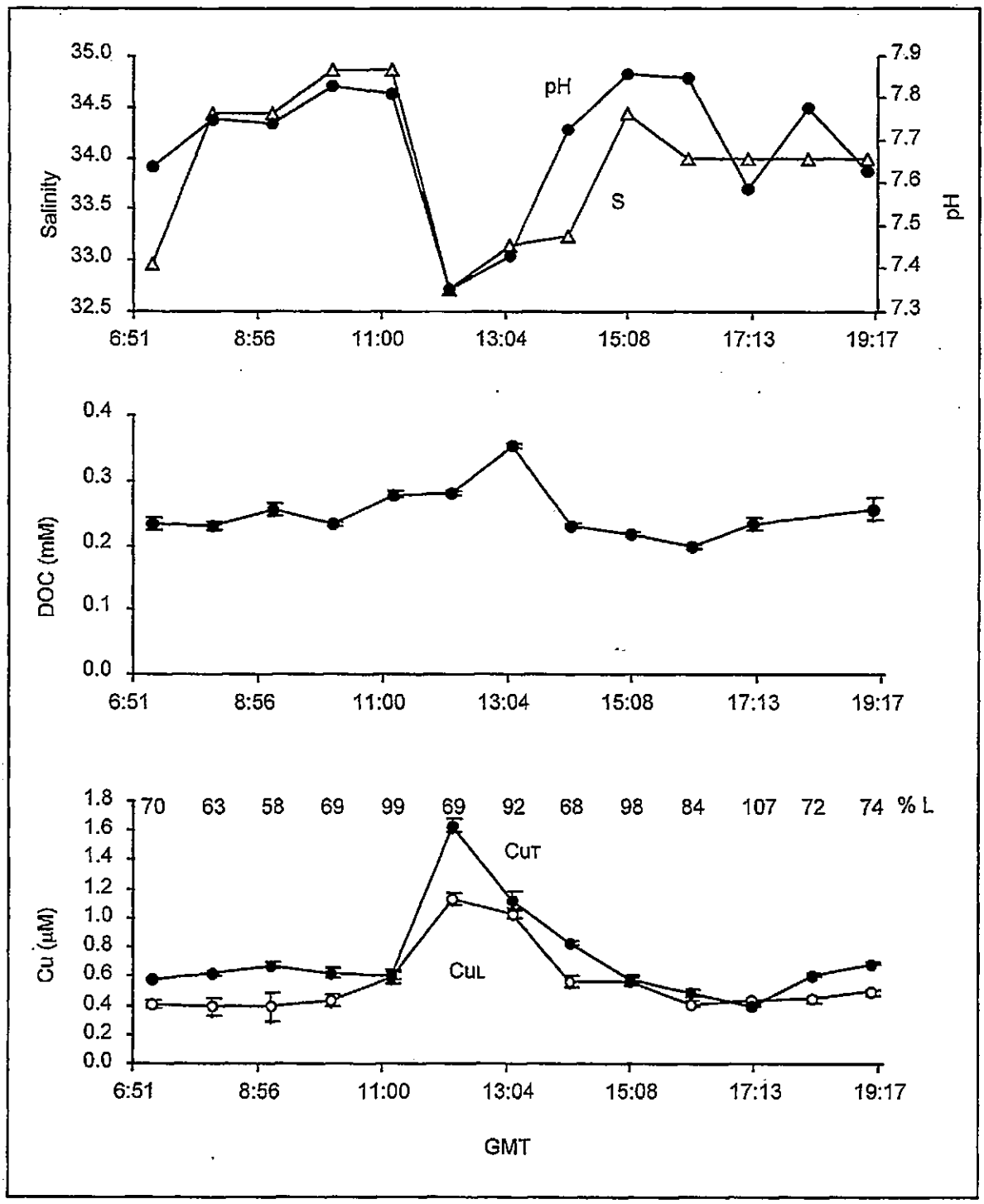

Figure 6.1 - TOROS 3: Salinity, pH, DOC and total dissolved and labile Cu concentrations in discrete samples taken during a tidal cycle study from a jetty off Club Nautico near the confluence of the two estuarine branches (location CN see Chapter 4, Figure 4.9). Cu_T and Cu_L - total dissolved and labile Cu concentration, respectively, % L - labile Cu fraction in percent of the total. Low water at Mazagón was at 11:49 h GMT and high water at 18:09h GMT.

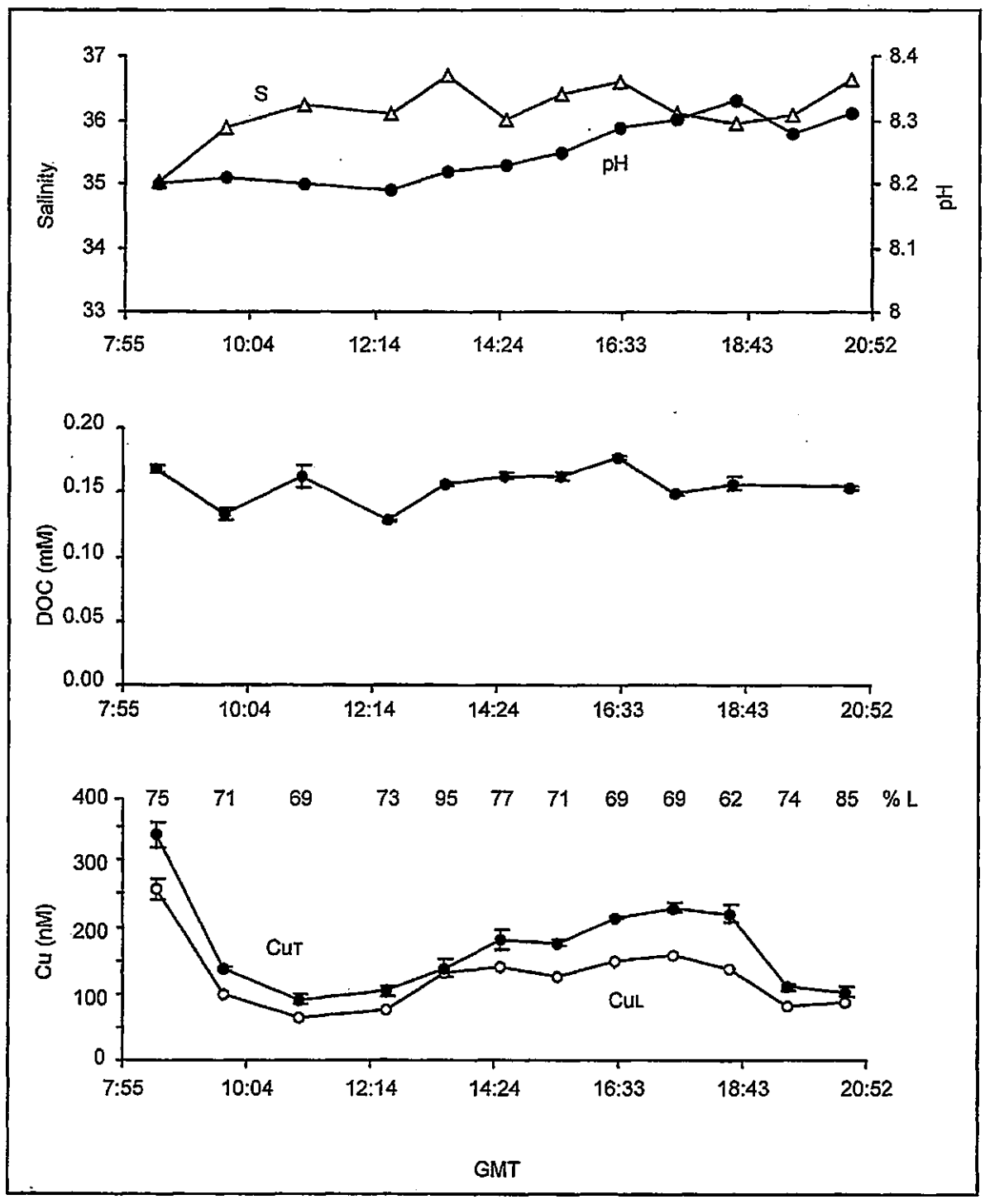

Figure 6.2 - TOROS 3: Salinity, pH, COC and total dissolved and labile Cu concentrations in discrete samples taken during a tidal cycle onboard *Cirry Tres* anchored in the mouth of the estuary (location T3 MZ see Chapter 4, Figure 4.9). Salinity from (Cruzado and Velasquez,1999). Cu_T and Cu_L - total dissolved and labile Cu concentration, respectively, % L - labile Cu fraction in percent of the total. High water at Mazagón was at 11:51 h GMT and low water at 17:58h GMT.

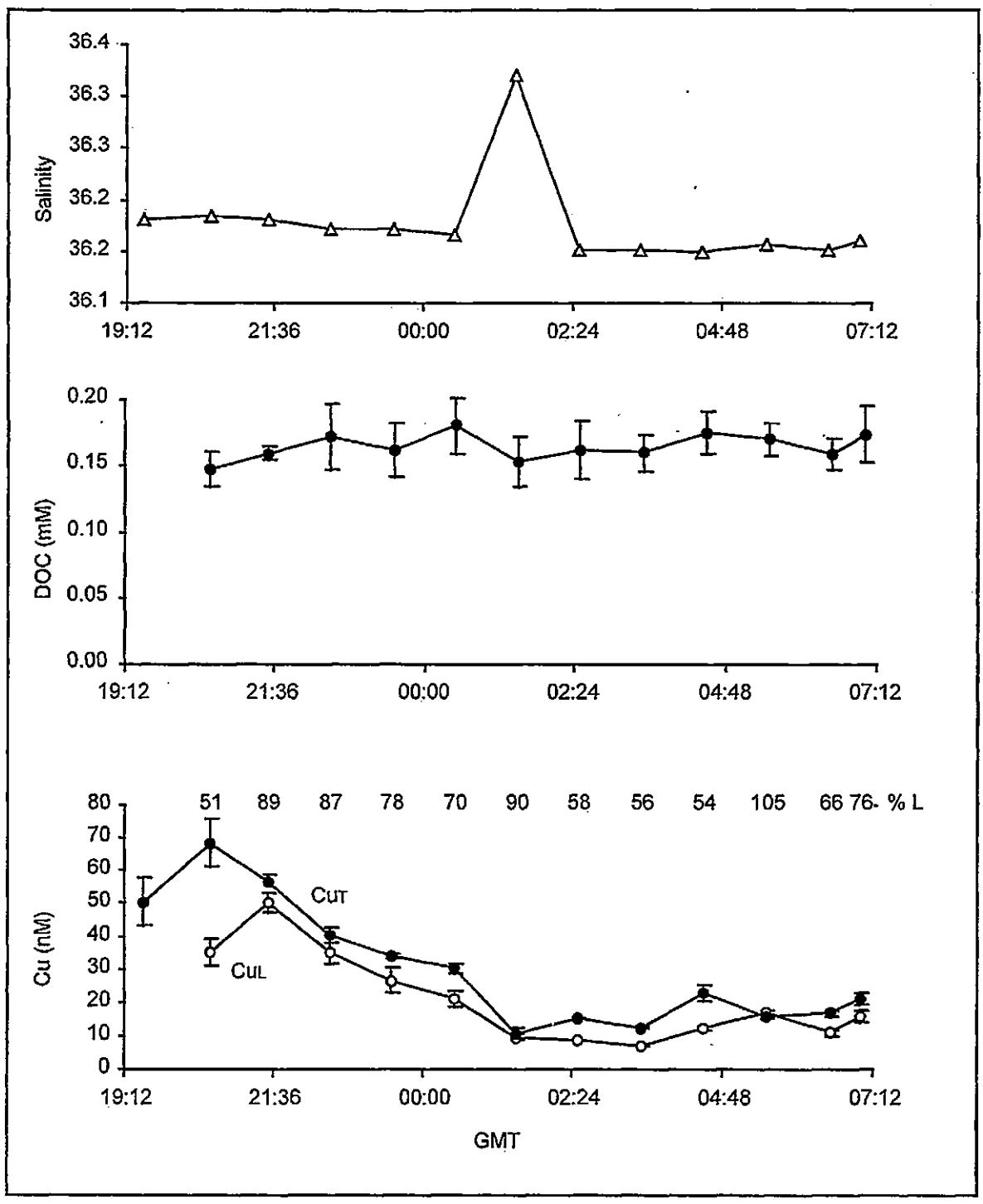

Figure 6.3 - TOROS 4: Salinity, DOC and total dissolved and labile Cu concentrations in discrete samples taken during a tidal cycle onboard *B/O Garcia del Cid* anchored in the mouth of the estuary (location T4 MZ see Chapter 4, Figure 4.9). Cu_T and Cu_L - total dissolved and labile Cu concentration, respectively, % L - labile Cu fraction in percent of the total. Low water at Mazagón was at 21:52 h GMT and high water at 3:59h GMT.

6.4.2.3 Copper Speciation in the Gulf of Cádiz

In the Gulf of Cádiz, an important fraction of dissolved Cu was present in an electrochemically non-labile form (Figure 6.4 and Figure 6.5). Total Cu concentrations decreased with increasing distance from the influence of the estuarine discharge (Chapter 5), from a maximum of 70 - 340 nM Cu at Mazagón (all surveys) to values below 4 nM Cu offshore in the Gulf of Cádiz. During surveys with vessels allowing sampling at 5 m depth (TOROS 1 and 3), elevated trace metal concentrations have been observed close inshore to the east of Mazagón (Chapter 5).

In November 1996 (TOROS 1, Figure 6.4 A), the labile Cu fraction in inshore samples was between 43 and 97%, while offshore samples had lower proportions of labile Cu (12 - 65%). The labile Cu fraction in April (12 - 79%, Figure 6.4 B) was highest at Mazagón and to the south of Huelva Ría. In October, the proportion of labile Cu (29 - 88%, Figure 6.5) exhibited no distinct pattern in the Gulf of Cádiz.

Dissolved organic carbon concentrations between 123 and 343 μM C were observed in coastal waters in April 1998.

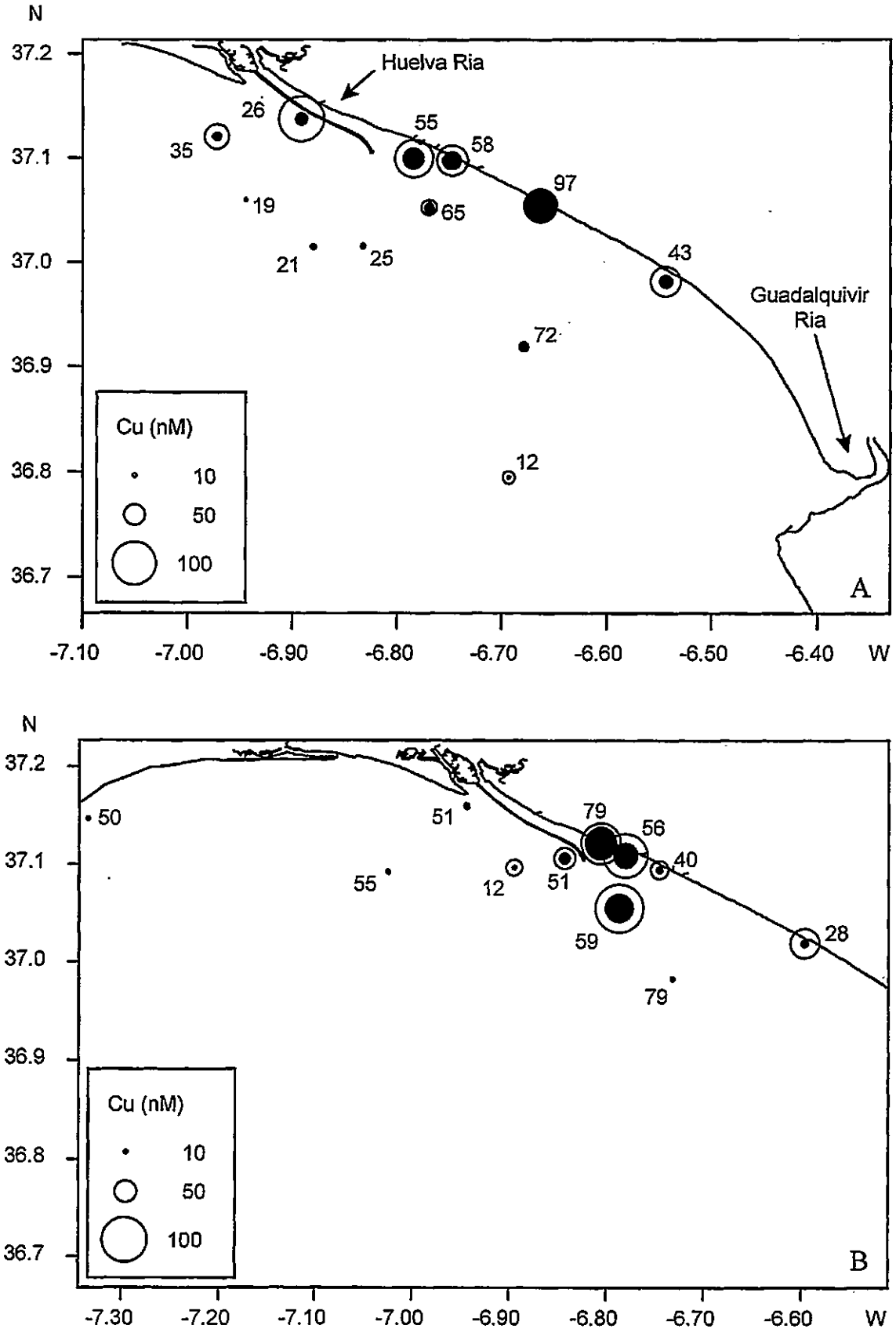

Figure 6.4 - TOROS 1 and 3: Total and AdCSV labile dissolved Cu concentration in the Gulf of Cádiz, A: November 1996, B: April 1998. The open and closed circles indicate the magnitude of the total and labile concentration, respectively (see legends). The numbers next to the sample stations show the size of the labile fraction in percent of the total.

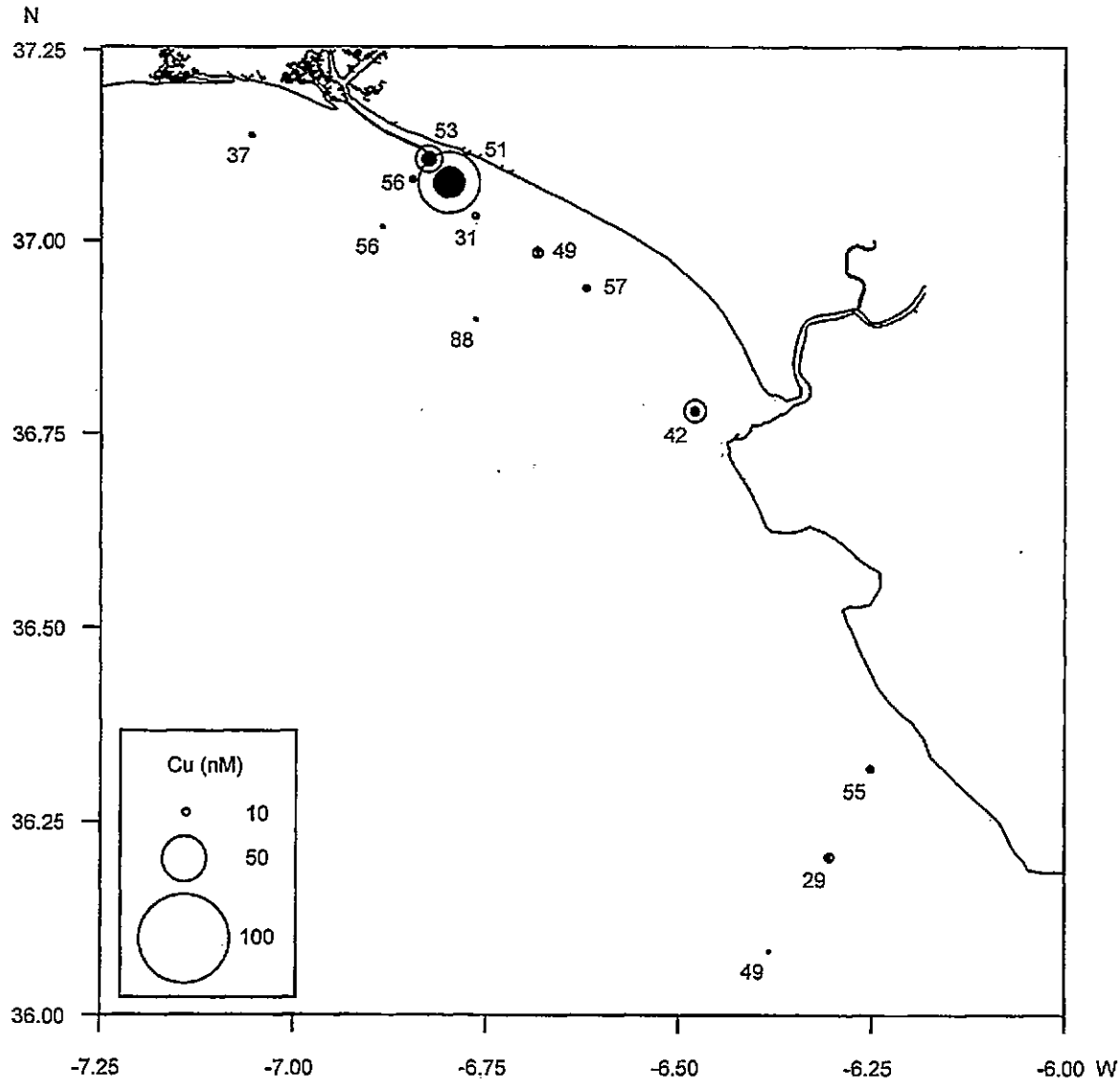

Figure 6.5 - TOROS 4: Total and AdCSV labile dissolved Cu concentrations in the Gulf of Cádiz, October 1998. The open and closed circles indicate the magnitude of the total and labile concentration, respectively (see legend). The numbers next to the sample stations show the size of the labile fraction in percent of the total.

6.4.3 LIGAND TITRATIONS

Ligand titrations carried out in samples from Huelva Ría and at the mouth of the estuary showed saturation of the titrated ligands with Cu, while samples from the Gulf of Cádiz had a buffering capacity for added Cu. Examples of the titration results and data transformation for extreme cases are illustrated in Figure 6.6. In the case of ligand saturation, the current response increased linearly with the added Cu (Figure 6.6, A). A capacity to complex Cu was indicated by a transition from a shallow slope of the current response (i_p) at the beginning of the titration to a steeper slope towards the saturation point (Figure 6.6, C). The ligands were fully titrated when the calculated (from the sensitivity) current response and the titration graph had equal slopes (Figure 6.6, A and C, dashed and solid lines, respectively), which was achieved for all samples. Data transformation (Chapter 2) yielded linear relationships of the form $Cu_L/CuL = mCu_L + b$ for all samples, indicating that only one class of Cu complexing organic ligands was detected by the method applied (Cu_L and Cu_T are the labile and total Cu concentrations, respectively, and the non-labile Cu concentration is $CuL = Cu_T - Cu_L$). The intercept (b) was small (≤ 10% of maximum Cu_L/CuL value) compared to the uncertainty of the method (Chapter 2).

Titrations were carried out to determine the concentration of Cu complexing organic ligands and their stability constants in Huelva Ría and the Gulf of Cádiz, and the results are given in Table 6.9 together with sample salinity, pH (*in-situ*), DOC, total dissolved, labile and free ionic Cu concentrations (expressed ad $pCu^{2+} = -\log[Cu^{2+}]$). Ranges of total Cu and ligand concentrations at each sample location are indicated in Figure 6.7. The samples used for ligand titrations had near to sea water salinities (35.8 - 36.3) and pH values (7.76 - 8.36). DOC concentrations were between 123 μM C in the Gulf of Cádiz and 230 μM C in the estuary.

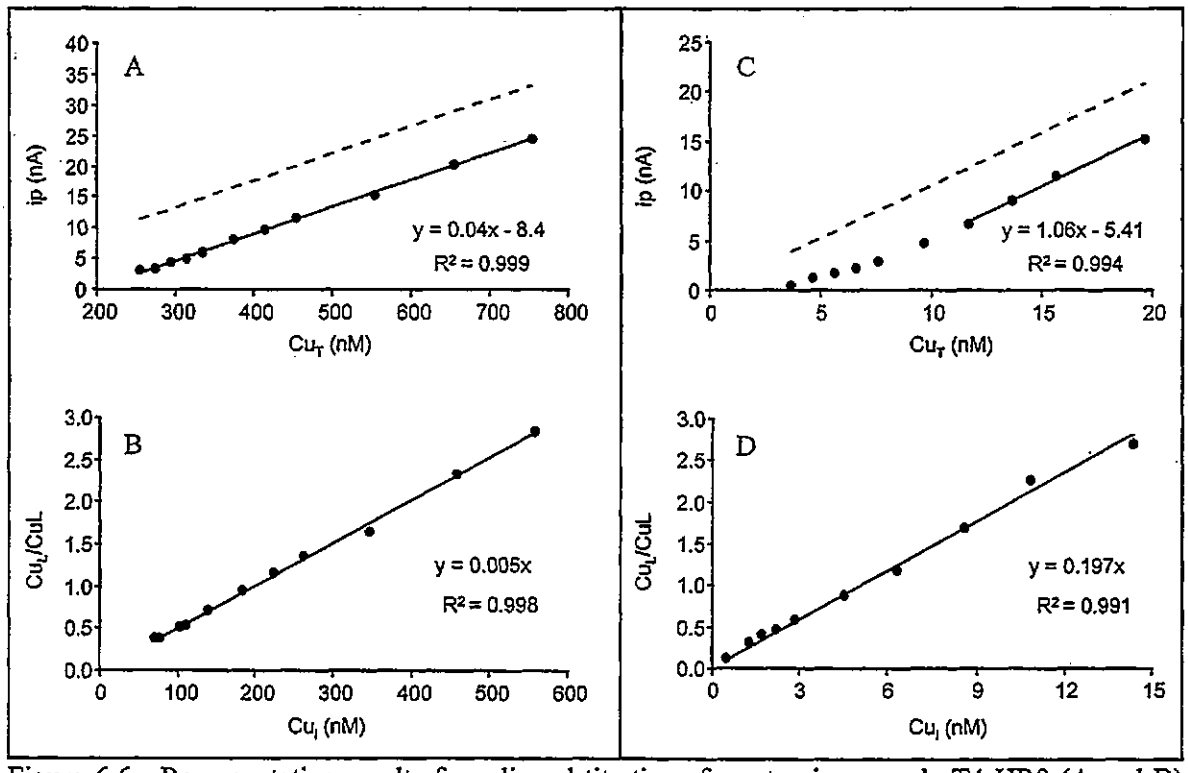

Figure 6.6 - Representative results from ligand titrations for estuarine sample T4 HR9 (A and B) and coastal sample T4 A1 (C and D). (A) shows ligand saturation with linear current response during titration, while (C) shows complexation of added Cu with curvature at the beginning of the titration. The dashed line signifies the theoretical current response calculated from the sensitivity and the total Cu concentration present. The linearity of the transformed data (B and D) indicates that only one class of ligand was detected in both samples.

Table 6.9 - Results from ligand titrations carried out with [Tropolone] = 0.3 mM and pH = 7.8. Cu_T and Cu_L - total dissolved and AdCSV labile Cu concentration; C_L - concentration of ligands forming Cu complexes with the conditional stability constant $logK'_{CuL}$; $pCu^{2+} = -log[Cu^{2+}]$, $log\alpha_{CuL}$ - alpha coefficient of the CuL complex at natural sample pH.

Location	S	pH field	DOC µM	Cu_T nM	Cu_L nM	pCu^{2+}	C_L nM	$logK'_{CuL}$	$log\alpha_{CuL}$
Estuary									
T4 HR 9	36.2	7.76	230	254	70	8.4	199	11.5	1.7
Mazagón									
T3 MZ 4	36.1	8.23	128	87	45	8.6	48	11.2	1.3
T3 MZ 7	36.4	8.21	162	152	61	8.4	95	11.5	1.4
T3 MZ 10	35.9	8.33	157	200	82	8.3	126	11.3	1.4
T4 MZ 3	36.2	-	159	46	17	9.0	32	11.6	1.5
T4 MZ 7	36.2	-	153	9.1	2.6	11.2	12	11.7	3.2
Gulf of Cádiz									
T3 MZ 16	35.8	8.36	162	93	25	9.0	80	11.6	2.0
T3 MZ 21	36.0	8.30	123	37	1.6	11.1	38	12.6	3.7
T4 A1	36.3	-	-	3.6	0.5	12.7	5.3	12.3	3.5
T4 E5	36.2	-	-	4.7	1.6	11.7	8.0	11.8	3.3
T4 F7	36.1	-	-	7.2	3.2	11.3	10	11.7	3.2

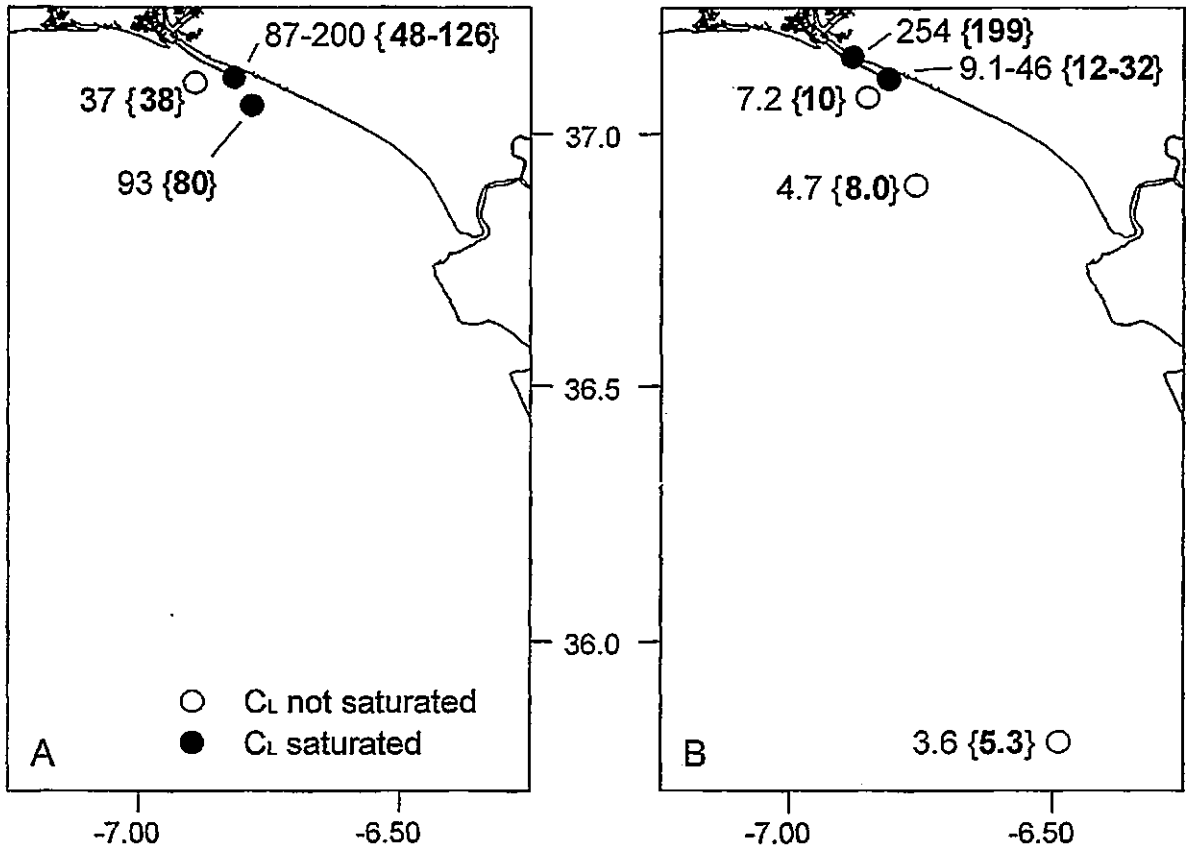

Figure 6.7 - Locations of samples taken for ligand titrations during TOROS 3 (A) and TOROS 4 (B). Numbers indicate ranges of total dissolved Cu and strong ligand concentrations {**bold**} in nM.

Dissolved Cu concentrations and the concentration of ligands that form Cu complexes with a stability constant of $\log K'_{CuL}$ = 11.2 - 12.6 (in the following called 'strong ligands' for short) were high in the estuary (T4 HR 9: Cu_T = 254 nM, C_L = 199 nM) and decreased with the Cu concentration towards the outer Gulf of Cádiz (T4 A1: Cu_T = 3.6 nM, C_L = 13 nM). The stability constants of the determined CuL complexes ranged between $\log K'_{CuL}$ = 11.3 and 12.6. The stability of the complexes of Cu with L (as expressed with the α-coefficient) ranged from $\log\alpha_{CuL}$ = 1.3 to 3.7. The free ligand concentration required for the calculation of $\log\alpha_{CuL}$ (see Chapter 2, Equation 2.14) was calculated according to the method described in (van den Berg and Donat, 1992), using mass balances for the metal and ligand concentrations. The distinction between total and free ligand concentration was important because the ligand concentrations was approximately equal or lower than Cu_T in all titrated samples. Samples in which $Cu_T > C_L$ had lower α-coefficients ($\log\alpha_{CuL} < 2$) and higher free hydrated ion concentrations ($pCu^{2+} \leq 9$), compared to samples in which $Cu_T < C_L$ ($\log\alpha_{CuL} > 3$ and $pCu^{2+} > 11$). In the latter group, 25% - 42% of the ligand L was not complexed with Cu. The concentration of the free ligand (L' in %) was calculated using MINEQL+ and also following the method suggested in (van den Berg and Donat, 1992), whereby results from both methods agreed.

6.5 Discussion

6.5.1 Dissolved Inorganic Metal Speciation

The high proportion of free hydrated ions and metal sulphates calculated for the fresh water end-members is indicative of a typical AMD system dominated by low pH and high sulphate concentrations. In the estuarine mixing zone of the Ría del Tinto, the iron speciation remained dominated by sulphate up to S = 20, although chloro complexes and Fe^{3+} gained in importance with increasing salinity (Table 6.6). Discharges from phospho-

gypsum deposits in the lower Ría del Tinto (Chapter 4) resulted in elevated fluoride concentrations (350 - 740 μM, Medio Ambiente, 1998).. As a result, Al and Fe formed complexes with F in the high salinity (S = 30), low pH (3.09), region of the lower Ría del Tinto. No such complexes were formed at near-sea water pH values in Huelva Ría. Iron hydroxide species remained below 5% of the total at $S \leq 20$, and no hydroxide species of Al were formed according to the equilibrium calculations. This may partially explain the absence of colloidal material in the Ría del Tinto mixing zone and that removal of trace metals from solution with coagulating iron flocs is not an important process in this area of the estuary (Chapter 4).

In the Ría del Odiel, the formation of Fe hydroxides (30.9% $FeOH^{2+}$ and 13.9% $FeOH_2^+$ at S = 5, 80% $FeOH_2^+$ at S = 20) may have been induced by the higher pH values and the lower sulphate concentration, compared to the Ría del Tinto. Under sea water conditions (S = 36.5, pH = 8.2), the dissolved equilibrium speciation of Fe and Al was dominated by MOH_4^- (67% and 87.1%, respectively, Table 6.7). The predominant complexation of trivalent metals by hydroxide ($M(OH)_2$, $M(OH)_3$ and $M(OH)_4$) has been shown to be typical for sea water solutions (Chapman *et al.* 1996; Turner *et al.* 1981; Dyrssen and Wedborg, 1980). Flocs formed from Fe, Al or Mn hydroxides have a high capacity for the scavenging metals and other cations. The equilibrium calculations suggested that in the Tinto/Odiel system conditions for floc formation were met only at near-sea water pH and salinity. Under such conditions the loss of Zn, Cu, Ni and Co from solution was observed in Huelva Ría (Chapter 4), indicating that the co-removal of these metals with Fe or Al hydroxide flocs may have been an important process.

The inorganic speciation of dissolved Mn, Zn, Cu, Ni, Co, Cd and Pb were similar in the Ría del Tinto at $S \leq 30$ and Ría del Odiel at $S \leq 20$ and reflected the influence of low pH and high sulphate concentrations of AMD affected waters. With increasing salinity the

fraction of aqueous metal sulphates decreased in favour of chloro complexes, which were especially important for Cd and Pb. In comparison to the fresh water, the free ionic fraction increased in the estuary for Fe, Al, Mn, Zn, Cu, Ni and Co, and in parallel the proportions of metal sulphates decreased. The reduced complexation of these metals in the estuary was caused by competition from the increasing concentrations of major sea water cations (e.g. Ca, Mg and Na), which were increasingly complexed by sulphate.

At higher pH and alkalinity (expressed as CO_3^{2-}) the complexation of dissolved Cu, Ni, Pb and Zn by carbonate became important in Huelva Ría. Cadmium remained largely complexed by chloride (> 90%) and the speciation of Mn and Co did not change greatly between the low pH/low salinity environment and sea water conditions. This behaviour was expected, because pH has a greater influence on the speciation of metals which are predominantly complexed with carbonate, compared to weakly complexed metals (e.g. Mn and Co) (Byrne *et al.* 1988). The speciation of uranyl in the estuary was characterised by the transition from the cation UO_2^{2+} and aqueous sulphate to the anion $UO_2(HPO_4)_2^{2-}$.

The calculated speciation of Fe, Al, Mn, Zn, Cu, Ni, Co, Cd, Pb and UO_2^{2+} at S = 36.5 agreed largely with the expected sea water speciation of these metals (Stumm and Morgan, 1996; Pan and Susak, 1991; Byrne *et al.* 1988; Bruland, 1983a; Turner *et al.* 1981), although metal concentrations in Huelva Ría were higher by several orders of magnitude. Discrepancies from literature values, for example the large predicted carbonate associations with Zn, Ni and Pb in Huelva Ría, have been the result of the use of different stability constants for the calculations.

Thermodynamic calculations allowing dissolved solids to form in the fresh water end-member of the Rio Tinto at Niebla for TOROS 1 concentrations (Table 6.4) resulted in the formation of dissolved haematite and jurbanite solids (100% Fe as Fe_2O_3; 39% Al as $AlOHSO_4$ at pH = 2.47). The negative saturation indices indicated that the solution had not

reached saturation with respect to these solids. There was no predicted formation of solids for Zn, Cu, Pb and Mn, and hence the dissolved speciation of these metals remained largely as those shown in Table 6.6. In subsequent calculations the salinity and major ion concentrations were adjusted to S = 5 and pH = 3.42, S = 20 and pH = 2.54, and S = 30 and pH = 3.09 (values see Table 6.4). The speciation of Fe changed from 100% haematite (S = 0) to 100% $FeOH^{2+}$ (S = 30). The speciation of Al changed from 2.7% Al^{3+}, 31% $AlSO_4^+$, 28% $Al(SO_4)_2^-$ and 39% jurbanite (S = 0) to 27% Al^{3+}, 18% $AlSO_4^+$, 14% $Al(SO_4)_2^-$ and 39% diaspore (AlO(OH) (S = 5) to 46% Al^{3+}, 31% $AlSO_4^+$ and 23% $Al(SO_4)_2^-$ at S = 30. Thus equilibrium calculations suggest the formation of dissolved Fe and Al solids in the estuary. The negative saturation indices of these solids was consistent with field observations, which did not indicate the removal of Fe and Al from solution in this salinity range (Chapter 4). For Mn, Zn, Cu, Ni, Co, Cd and Pb the consideration of dissolved solids in the equilibrium calculations did not influence the composition of the predicted dissolved speciation and no solids were formed. This leads to the conclusion that equilibrium calculations may be a reasonable approach to investigate the dissolved inorganic speciation of Mn, Zn, Cu, Ni, Co, Cd and Pb at low pH in the Tinto/Odiel system. In the case of Fe and Al, the difference between inclusion and exclusion of solids in the calculation indicates non-equilibrium in the dissolved phase (e.g. slow reaction rates and biological activity).

The equilibrium calculations of inorganic metal speciation have shown that in the absence of organic ligands a large proportion of dissolved Zn, Mn, Cu, Co and Ni will be present in their most toxic, the free ionic, form in regions of the estuary which are biologically highly productive (lower Ría del Tinto, Huelva Ría). However, the dissolved organic matter and chlorophyll observed in the estuary (Chapter 4) implied the possible presence of metal complexing organic ligands in the water. The complexation of trace metals by organic ligands reduces the concentration of free hydrated metals and weakly

complexed species (e.g. hydroxo and chloro complexes) in solution, thus reducing their biological availability and toxicity.

6.5.2 Dissolved Copper Speciation in Huelva Ría

A clear trend in the speciation of dissolved Cu was detected in Huelva Ría in November 1996, when a wide range of pH, salinity and dissolved Cu concentrations was observed in samples collected along two transects. In the upper Huelva Ría nearly all dissolved Cu was present in electrochemically labile forms, while non-labile Cu species gained in importance towards the mouth of the estuary (Table 6.8) and with increasing distance from Huelva Ría in the Gulf of Cádiz (Figure 6.4 A).

Dissolved Cu concentrations between 5.9 and 7.7 μM were observed at S = 14 - 36.9 in the upper Huelva Ría. The high proportion of labile Cu in this area of the estuary suggests that the Cu concentration in the water greatly exceeded the capacity of organic matter to form strong (non-labile to the applied method) complexes with Cu. This was supported with results from ligand titrations carried out in samples from the TOROS 3 and 4, which showed that in Huelva Ría the total Cu concentration (Cu_T) was higher than the concentration of strong ligands (C_L). Once strong Cu complexing ligands were saturated, any additional Cu resulted in the increase of electrochemically labile species only, and as a result the labile Cu concentration was largely determined by the magnitude of Cu_T. At lower Cu levels in coastal waters (Cu_T < 40 nM), C_L exceeded Cu_T and as a result an important fraction of dissolved Cu became non-labile.

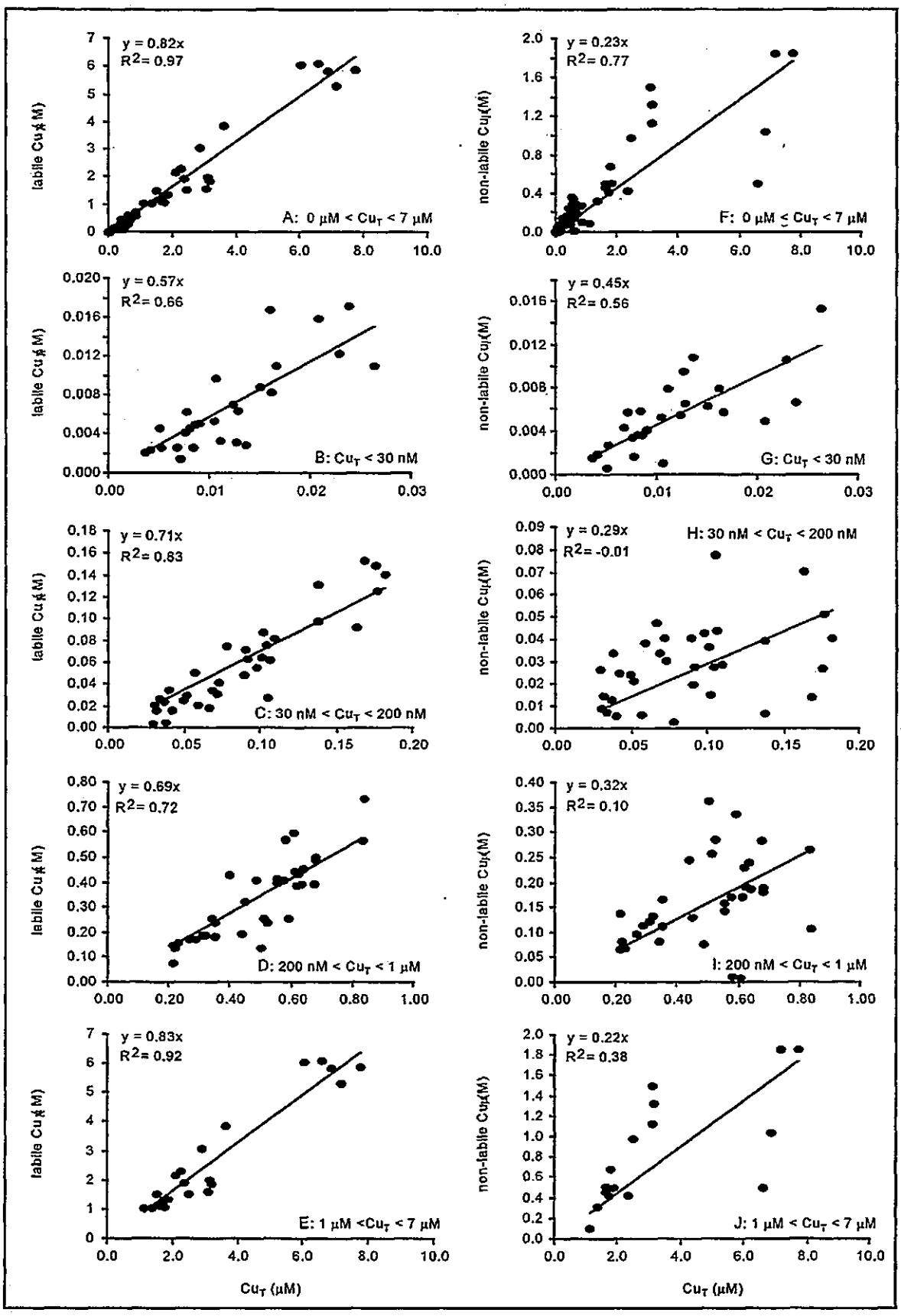

Figure 6.8 - Relationship between labile and total Cu concentrations (A - E) and non-labile and total Cu concentrations (F - G). Least squares regression was calculated for speciation data from all surveys and included estuarine transects, tidal cycles and coastal samples. (A) and (F): complete concentration range, (B) and (G): $Cu_T < 30$ nM, (C) and (H): $Cu_T = 30$ - 200 nM, (D) and (I): $Cu_T =$ 200 nM - 1 µM, (E) and (J): $Cu_T = 1$ - 7 µM. Linear relationships are statistically significant at 1% confidence level for (A) - (E) and (G). (F) is statistically significant, but this may be the result of the wide concentration range covered.

The diminishing importance of the labile Cu fraction at $Cu_T < 1$ μM in the middle reaches of Huelva Ría in November indicates that the labile Cu concentration (Cu_L) and C_L were within the same order of magnitude. This may also have been the case during the following surveys, when important non-labile Cu concentrations were observed in Huelva Ría at $Cu_T < 2$ μM (Table 6.8). Estuarine ligand concentrations determined for the surveys in April and October 1998 ($C_L \approx 100$ - 200 nM, Table 6.9), support this argument.

The transition from predominantly labile Cu in the estuary to more non-labile Cu in coastal waters is also evident in Figure 6.8. A strong linear relationship between labile and total dissolved Cu concentrations is evident in Figure 6.8 (A), whereby the full range of concentrations in all samples used for speciation studies was included. The relationship between labile and total Cu was weaker at lower than at higher Cu concentrations. This is illustrated in Figure 6.8 (B) - (E), for which the data was split into several concentration ranges. The slope of the least squares regression of Cu_L versus Cu_T shows a decrease in the average labile fraction from 83% (Cu_T = 1 - 7 μM) in Huelva Ría to 57% ($Cu_T < 30$ nM) in the Gulf of Cádiz.

A statistically significant relationship between non-labile and total dissolved Cu was found at low Cu concentrations ($Cu_T < 30$ nM, Figure 6.8, G) only. This supports the suggestion that in coastal waters the non-labile Cu concentration was partially determined by the total dissolved Cu concentration, while in the Huelva Ría Cu_L increased linearly with Cu_T above the point of ligand saturation.

6.5.3 Differences in Cu Speciation between Surveys

In comparison to the clear trend observed during the first survey (November), the speciation data was more scattered (with respect to the labile fraction, and labile and total Cu concentrations) during the following surveys. Estuaries are naturally highly dynamic

environments, in which physical and chemical parameters may change more rapidly than the time needed to establish chemical equilibrium. In Huelva Ría, riverine, industrial and municipal discharges, exchange with polluted sediments and primary productivity are additional sources of variation for pH, temperature, DOC, SPM and dissolved metal concentrations (Chapter 4). Therefore, disequilibrium at the time of sampling may have added uncertainty to the measurement of labile Cu, especially because changes in the chemical equilibrium may have taken place during the logistically necessary delay between collection and processing of discrete samples.

A higher proportion of Cu was complexed by strong ligands in Huelva Ría in June 1997, April and October 1998, compared to November 1996 (Table 6.8). As discussed previously, ASV and AdCSV labile Cu concentrations are not directly comparable and therefore the differences in the labile fraction may have been partially an artefact of the analytical methods used. Compared to the ASV method, the detection window of the AdCSV method (used in November and October) is such that Cu complexes with somewhat higher stability constants may be included in labile measurements. The different detection windows may have contributed to the lower labile fraction observed in April and June (ASV), compared to November. However, differences in the speciation results for the upper Huelva Ría were observed between November (Cu_T > 6 μM Cu) and October (Cu_T < 260 nM Cu, both AdCSV), while the speciation of Cu at concentrations below 200 nM in samples from the November and October surveys were similar. This indicates that the total concentration was a crucial factor influencing the speciation of Cu in this system.

Lower total dissolved Cu concentrations were encountered during the transects in June, April and October (maximum 2.3 μM, 490 nM and 260 nM Cu, respectively) compared to November (maximum 7.7 μM Cu). A plot of Cu_T (Figure 6.9) versus salinity (A) and pH (B) illustrates that similar Cu concentrations were encountered at equal salinity

or equal pH during all surveys. The differences in Cu_T were predominantly the result of the salinity and pH ranges covered during the surveys, rather than the magnitude of riverine metal discharge. Figure 6.9 (C - F) clarifies this by showing the autumn/winter and spring/summer surveys separately. As suggested, at $Cu_T < 1$ μM the concentrations of strong ligands and total dissolved Cu were in the same order of magnitude. As a result, the complexation of Cu with strong ligands was noticeable in the diminished labile Cu fractions measured.

In June, Cu_T and Cu_L were higher at equal salinity, compared to concentrations in April (Figure 6.9, E) and higher at equal pH, compared to concentrations in November (Figure 6.9, B) (significant difference of means in both cases at 1% confidence level). In addition, Figure 6.9 (G) shows that a lower proportion of Cu was labile at equal total concentrations in June, compared to November, although the riverine metal input to the estuary in June was the lowest of all surveys (Chapter 4).

Any seasonal influence on Cu speciation cannot be assessed from speciation results only, as these were not directly comparable (see Section 6.3.5). However, chlorophyll measurements carried out by the research partners from C.S.I.C. during all TOROS surveys (Cruzado *et al.* 1999; Cruzado and Velasquez, 1999; Cruzado *et al.* 1998) indicate a possible link between the level of primary productivity and the proportion of non-labile Cu in Huelva Ría. Chlorophyll levels in the estuary were higher in June 1997 (total chlorophyll maximum $Chl_T = 55.8$ μg l^{-1}), April 1998 ($Chl_T = 45.6$ μg l^{-1}), and October 1998 ($Chl_T = 53.8$ μg l^{-1}), when higher non-labile Cu fractions were observed, compared to November ($Chl_T = 12.4$ μg l^{-1}), when Cu was mostly labile. The chlorophyll maxima in Huelva Ría occurred in the vicinity of the fertiliser factories in the upper estuary and around the confluence with the nutrient-rich Ría del Tinto.

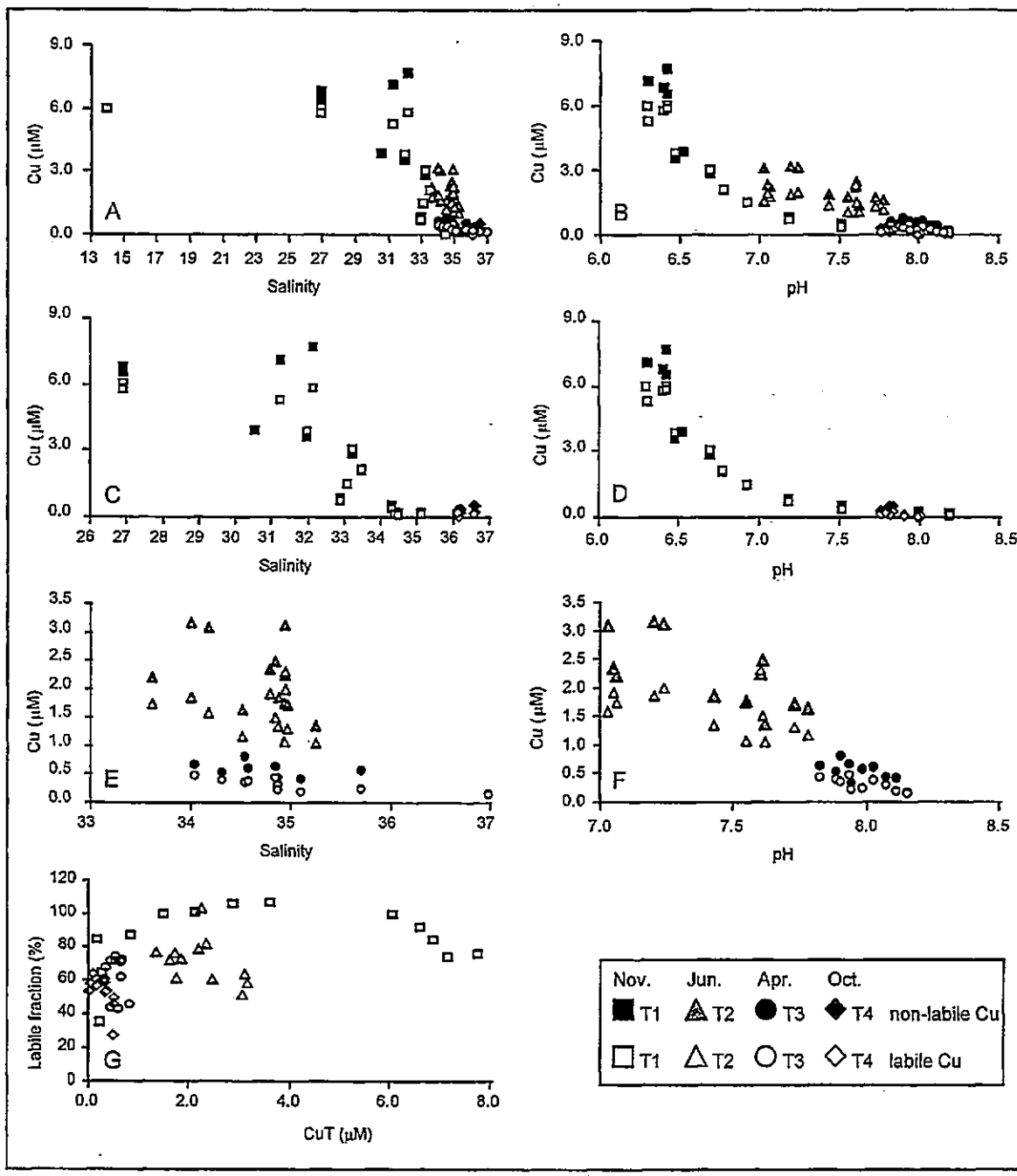

Figure 6.9 - TOROS 1 - 4: Results from Cu speciation studies for all four surveys (T1: November 1996, T2: June 1997, T3: April 1998, T4: October 1998). A and B: Total and labile dissolved Cu for all surveys plotted vs. salinity and pH, respectively; C and D: Total and labile Cu concentration during autumn/winter surveys; E and F: Total and labile Cu concentration during spring/summer surveys; G: Labile Cu fraction versus total Cu concentration for all surveys. Open symbols refer to the ASV (T2 and T3) or AdCSV (T1 and T4) labile dissolved Cu fraction, closed symbols to total dissolved Cu concentrations.

Marine algae and cyanobacteria are known to produce organic compounds capable of complexing Cu (Gledhill *et al.* 1997; Sunda and Huntsman, 1995; Sunda and Huntsman, 1991; Coale and Bruland, 1988), and therefore may contribute importantly to the pool of Cu complexing strong ligands in times of high primary productivity. Moffet *et al.* (1990) observed that the complexation of Cu in Sargasso Sea was greatest at maximum chlorophyll concentrations. Gordon *et al.* (1996) showed that the concentration of copper complexing ligands isolated from estuarine water (immobilised metal affinity chromatography) varied seasonally with picoplankton abundance. In other cases, however, no clear relationship between plankton, metal and ligand concentrations was observed (Plavsic *et al.* 1990).

The evidence suggests that the speciation of dissolved Cu in Huelva Ría was influenced by a combination of total Cu concentration, strong ligand concentration and pH. The degree of complexation and total dissolved Cu concentration may be interdependent. It has been suggested that the complexation of Cu by strong ligands reduces the rate of Cu removal from solution by competition with adsorption onto particles, and thus maintains higher dissolved Cu concentrations than in the absence of organic ligands (van den Berg *et al.* 1990 and 1987; Plavsic *et al.* 1982). Lacking data from ligand titrations for June 1997, it can only be assumed that the high total dissolved Cu concentrations observed during this survey may have been linked to a seasonally elevated concentration of Cu complexing organic ligands during the summer.

6.5.4 Comparison with Cu Speciation in Other Coastal Systems

The degree of Cu complexation with natural organic ligands was lower in the Gulf of Cádiz (< 88%, Figure 6.4 and Figure 6.5) and Huelva Ría (0 - 64%, Table 6.8), compared to results from most Cu speciation studies reported in literature for marine,

coastal and estuarine waters (> 90%). More than 99% Cu was calculated to be organically complexed using data from ligand titrations (ASV) of the north Pacific Ocean (Coale and Bruland, 1990). In estuarine and shelf waters (Cu_T = 5 - 38 nM), Sunda and Huntsman (1991) found > 99% organically complexed (chemiluminescence and ligand competition with EDTA), while in the Irish Sea, this fraction was ≥ 95% Cu (Cu_T = 7 - 27 nM, AdCSV) (Nimmo *et al.* 1989; van den Berg, 1984b). Similar observations were made by Apte *et al.* (1990) in the Humber estuary. Van den Berg and Donat (1992) carried out ligand titrations spanning a wide range of competition strengths using AdCSV. They found that Cu was fully complexed by dissolved organic material in sea water and argued that a minimum of two different competition strengths have to be used in ligand determinations to fully characterise the Cu complexation.

In apparent contradiction to this, Cu in South San Francisco Bay was found to be only to 80 - 92% organically complexed (Cu_T = 45 - 48 nM, ASV, AdCSV) (Donat *et al.* 1994). However, the given explanation is in line with van den Berg and Donat (1992), suggesting a two-ligand model for organic complexation of Cu, whereby the stronger ligand (L_1) was present at concentrations below that of Cu. As a result ca. 27% and 65% Cu was complexed by L_1 and L_2, respectively. According to the authors, the saturation of L_1 and the predominant complexation of Cu with weaker ligands L_2 resulted in a more labile organic Cu pool and an overall reduction of the degree of organic complexation. In the Tamar estuary less than 50% Cu was complexed by organic ligands (van den Berg *et al.* 1990), and this was partially attributed to the high competition strength used for the ligand titrations (AdCSV with oxine, α_{CuAL} = 8.35 at S = 34), which was similar to the determined α_{CuL} at all salinities. Only very strong CuL complexes were detected with this method, and at Cu_T = 16 - 300 nM it was likely, that a proportion of dissolved Cu was complexed by weaker ligands, which remained undetected.

Only one class of ligands was detected in the Gulf of Cádiz, but this does not preclude the existence of ligands with α-coefficients outside the detection window of the ligand titration method. Very weak ligands ($logK'_{CuL} << 11$) would not have been detected in the titrations, while during labile measurements Cu complexes with such ligands would have dissociated and the released Cu measured as labile Cu. Further experiments would be required to establish whether or not a weaker class of ligands exists at sufficient concentrations to influence the Cu speciation in this way.

In Huelva Ría and its plume, the non-labile Cu fraction (0 - 64%) was lower than outside the estuary's influence in the Gulf of Cádiz (45 - 88%). This can be explained by the complete saturation of all organic ligand classes in Huelva Ría and subsequent complexation of additional Cu by inorganic ligands. In this sense, the Huelva system differs from other metal-rich estuaries (e.g. the Tamar estuary), because the reduction of the non-labile (organic) fraction of Cu to less than 1% was caused by the extreme metal concentrations in the system, rather than artefacts of the method.

6.5.5 Copper Complexation by Strong Ligands

The results from ligand titrations have a level of uncertainty attached to them. Limitations stemming from the operational character of this speciation method and sources of errors resulting from the sample preservation have been discussed in Chapter 2 and in earlier sections of this Chapter. In addition, the saturation of L by Cu in some samples resulted in an excess of free Cu in the sample, which increased with the added Cu during the titration. Titrations were carried out at one analytical competition strength only, and only one class of ligands was detected. As the presence of at least two classes of ligands in natural estuarine and coastal waters has been commonly reported, it is possible that excess free Cu may have been complexed by undetected ligands. In this case the calculated cupric

ion concentration would be an overestimation. Further uncertainty was introduced because the α-coefficient of the CuL complex was below the lower limit of detection (detection window ≈ 10^2 - 10^4, assuming approximately one decade on either side of α_{CuAL}, van den Berg and Donat, 1992) in samples with ligand saturation.

Notwithstanding the discussed limitations, it is the extreme gradient of physical and chemical parameters, Cu and ligand concentrations between Huelva Ría and the outer Gulf of Cádiz, that allows the interpretation of results from the ligand titrations.

The conditional stability constants of the detected ligand class were $\log K'_{CuL}$ = 11.2 - 11.7 in estuarine samples and $\log K'_{CuL}$ = 11.6 - 12.6 in coastal samples. These values were intermittent between the strong and weak organic ligand classes often reported in literature ($\log K'_{CuL1} > 12$ and $\log K'_{CuL2} < 11$, respectively) (Moffett, 1995; van den Berg and Donat, 1992; Coale and Bruland, 1988; Sunda and Hanson, 1987). The relatively narrow range of stability constants and their magnitude are the result of the competition strength selected for the method, which placed the detection window at approximately $\log \alpha'_{CuTrop}$ = 3.0 ± 1.0. It may also indicate a common origin of the organic ligands detected in the system.

The range of ligand concentrations determined in the Gulf of Cádiz (C_L = 5.3 - 80 nM, Cu_T = 3.6 - 93 nM) and Huelva Ría (C_L = 87 - 254 nM, Cu_T = 48 - 200 nM) were similar to those found in other coastal and estuarine environments affected by a similar degree of metal pollution (Table 6.10).

Table 6.10 - Concentrations and stability constants of Cu complexing strong ligands determined by different methods in estuarine and marine waters. nr - not reported; na - not applicable; CL_1 - strong Cu complexing ligand; CL_2 - less strong Cu complexing ligand.

Location	log α_{CuAL}	pH	Cu_T nM	CL_1 nM	CL_2 nM	$logK'_{CuL1}$	$logK'_{CuL2}$
NE Pacific[1]	na	nr	0.582	> 1.21	6.53	> 10.7	8.58
CN1519[2]	3.12	8.35	3.2	21	-	12.2	-
CN1519[2]	4.85	8.35	3.2	4.0	-	14.2	-
CN1519[2]	6.36	8.35	3.2	1.2	-	15.6	-
Sta 2[3]	nr	7.7	1.2	3.7	-	11.9	-
Sch 9[4]	nr	7.7	10.7	16	-	13.4	-
Sch 6[4]	nr	7.7	152	203	-	13.0	-
NB[5]	na	8.0	27	50	100	12.4	10.1
Peru[5]	na	8.2	3.7	3.8	75	12.3	9.2
Tamar[6]	2.48	7.7	30 - 110	140 - 500	-	9.1 - 10.1	-
Humber[7]	see[7]	8.0	11 - 123	20 - 410	-	> 10	-

[1] Surface water in the NE Pacific, ASV (Coale and Bruland, 1988).
[2] North Sea, AdCSV ligand competition with 0.324 mM Tropolone, 0.83 µM (a) and 4.71 µM (b) Oxine (van den Berg and Donat, 1992).
[3] Pacific Ocean, AdCSV ligand competition with 0.2 mM benzoylaceton (Moffett, 1995).
[4] Scheldt estuary, AdCSV ligand competition with 0.2 mM catechol (van den Berg *et al.* 1987).
[5] Narragansett Bay (1) and Peruvian coast, SEP-PAK C-18 with cupric ion calibration (Sunda and Hanson, 1987).
[6] Tamar estuary, various salinities, AdCSV ligand competition with 25 µM catechol, $logK'_{CuL}$ estimated from graph, α_{CuAL} given for sea water salinity (van den Berg *et al.* 1986; van den Berg, 1984).
[7] Humber estuary, various salinities, AdCSV ligand competition with 1.0 - 2500 µM catechol, corresponding to log α_{CuAL} = 1.7 - 7.2 (Apte *et al.* 1990).

Ligand concentrations of several hundred nM are not uncommon in estuaries (Apte *et al.* 1990; Sunda and Hanson, 1987; van den Berg *et al.* 1987; van den Berg, 1984a), while in coastal and marine waters much lower ligand concentrations have been reported, especially for ligand class L_1 with $\log K'_{CuL1} \geq 11$ (Moffett, 1995; van den Berg and Donat, 1992; Coale and Bruland, 1988; Sunda and Hanson, 1987). A similar trend to that found in the Huelva system was observed in the Humber estuary, where the total ligand concentrations ($\log K'_{CuL} > 10$) decreased from over 250 nM ($S < 5$) to less than 50 nM ($S > 30$) (Apte *et al.* 1990).

The concentration of strong ligands in the Gulf of Cádiz was similar or just above the level of Cu in solution, and similar observations have been made for class 1 ligands in other estuarine and coastal environments (Moffett, 1995; van den Berg and Donat, 1992; Sunda and Hanson, 1987).

The highest concentrations have been reported for class 2 ligands ($\log K'_{CuL2} < 11$), which have not been found saturated with Cu (Hirose, 1994 and references therein). In Huelva Ría, where ligand concentrations were high, conditional stability constants were somewhat lower, compared to those in the Gulf of Cádiz. Saturation of class 1 ligands ($\log K'_{CuL1} > 12$) has been observed previously, however, in such cases a complexing capacity for Cu was available in class 2 ligands (Table 6.10). The complete saturation of all detected ligands in Huelva Ría appears to be a rare case, and this is because of the high level of metal pollution in this system. The presence and available complexing capacity of a weaker ligand class ($\log K'_{CuL} < 10$) would be an interesting area of further investigation.

6.5.6 Estimation of Cu complexation in Upper Huelva Ría

The concentration of strong ligands was higher in the estuary, compared to coastal waters (Figure 6.7, Table 6.9). However, the strong relationship between labile and total Cu at Cu_T > 1 μM (Figure 6.8, E) indicates that there was an upper limit to the concentration of strong Cu complexing ligands. In order to project the Cu speciation to Cu concentrations above the linear range of the analytical speciation method, equilibrium calculations that included a strong ligand L^{2+} ($logK'_{CuL}$ = 11.7, C_L = 500 nM) were carried out with Mineql+. For this, the major ion concentrations were taken for S = 36.5 (Table 6.4), the pH was fixed at 8.3 and the Cu concentration was altered between Cu_T = 200nM and 6.0 μM in 50 steps. The value of $logK'_{CuL}$ was corrected to pH 8.3 as described in Section 6.3.6.3 ($logK'_{CuL}$ = 12.2 at pH 8.3). The results of the calculations (Figure 6.10, A) show that at $Cu_T < C_L$ additional Cu was predominantly complexed by the ligand L. Beyond the saturation point of L (at $Cu_T \geq C_L$) additional Cu was complexed by inorganic ligands, whereby the electrochemically labile $Cu(OH)_2$ aq ($logK'_{CuOH2} \approx -17.6$ at pH = 8.3 and S = 36.5) became the dominant species. Donat *et al.* (1994) came to similar conclusions when modelling the Cu speciation for water from South San Francisco Bay. For Huelva Ría, the concentrations of $Cu(OH)_2$ aq, $CuCO_3$ and Cu^{2+} were predicted to be 5.3 μM, 130 nM and 13 nM, respectively, at the end of the titration (Cu_T = 6 μM).

Specific to the November survey were mildly acid pH values in samples of high salinity (Table 6.8). Figure 6.10 (B) shows the results of thermodynamic calculations carried out as described for Figure 6.10 (A), but with additional titration of pH (changed from 8.3 to 6.0) and according change of $logK'_{CuL}$ (changed from 12.2 - 9.9, see above) in 50 steps.

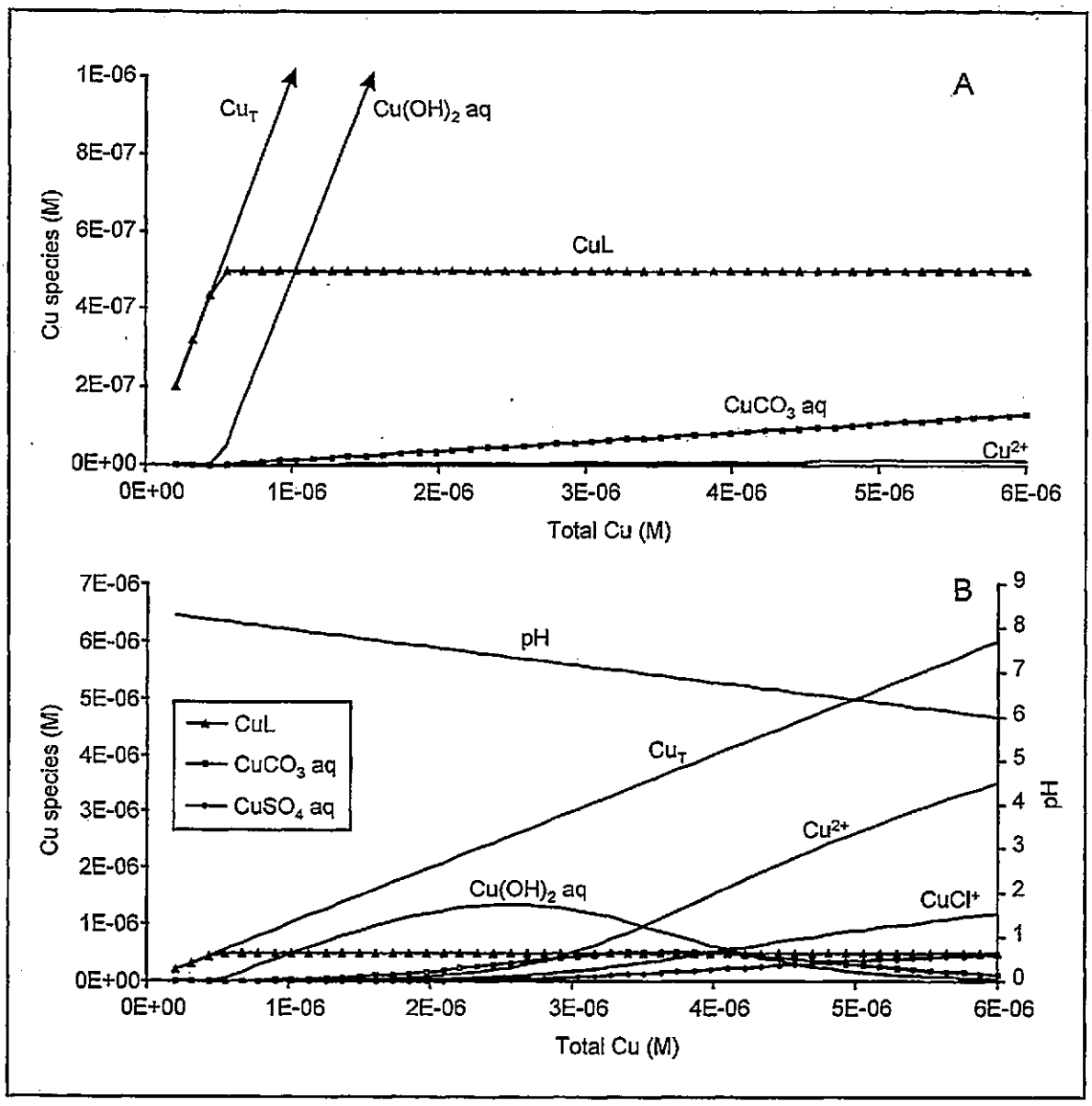

Figure 6.10 - Equilibrium calculation (Mineql+) of the Cu speciation in Huelva Ría under incorporation of a Cu complexing divalent ligand (L^{2-}, C_L = 500 nM, log K_{CuL} = 11.7 at pH 7.8). (A) - Cu titration with Cu_T = 200 nM - 6.0 µM (50 steps), the y-axis was expanded and $Cu(OH)_2$ aq continued to a concentration of 5.3 µM in linear relationship with Cu_T; (B) - Cu titration as for (A) and additional pH titration with pH = 8.3 - 6.0 and logK'CuL = 12.2 - 9.9 in 50 steps (see text). Species with concentrations below 10^{-8} M are not shown.

As a result of the decreasing pH value, ligand saturation occurred at Cu_T = 792 nM (pH 8.01), compared to Cu_T = 555 nM (pH 8.3) in example (A). The concentration of $Cu(OH)_2$ aq increased initially and after ligand saturation reached a peak at around pH 7.4. Further decreases in pH values resulted in a decline of $Cu(OH)_2$ aq concentrations, whereby Cu^{2+}, $CuCl^+$ and $CuSO_4$ aq reached 3.5 µM, 1.2 µM and 480 nM, respectively. A maximum in $CuCO_3$ was attained at pH 7 (520 nM), which declined to 114 nM at the end of the modelled titration.

The comparison of the two scenarios illustrates the importance of pH for the speciation of Cu. At pH values below 7 and extreme ligand saturation, parallels to the Cu speciation in the absence of L can be found (Section 6.5.1, c.f. results for S = 30 in Ría del Tinto). Thermodynamic calculations showed that below ligand saturation the complexation of Cu by the ligand L maintains low cupric ion concentrations ($pCu^{2+} \geq 12$) at pH 8.3. With slightly lower pH values (8.01) in scenario B, values of $pCu^{2+} \leq 9$ were reached below ligand saturation. The implications for the toxicity of Cu in the system are discussed in Section 6.5.7.

6.5.7 Biological Link with Cu Speciation

Following from the close relationship between the concentrations of dissolved Cu and Cu complexing organic ligands in sea water, Moffett (1995) suggested a regulatory dependence between Cu_T and C_L. Phytoplankton and cyanobacteria take up cupric ions as essential nutrient, and produce and release Cu complexing chelators with high stability constants ($\log K'_{CuL} \approx 13$, Moffett and Brand, 1996; Moffett *et al.* 1990). Upon photo-degradation and decay of the chelates the cupric ions are released back into solution. Experiments have shown that in this way, some estuarine and marine plankton species may partake in the regulation of free cupric ion concentrations in near-surface waters (Gledhill

et al. 1997 and references therein; Moffett, 1995; Sunda and Huntsman, 1995; Coale and Bruland, 1988). Other potential sources of organic ligands in estuarine systems include decaying organisms, influx of humic material, sewage effluent and industrial discharges.

In the absence of organic ligands the speciation of Cu would be solely inorganic, resulting in an equilibrium concentration of free Cu^{2+} in the region of 0.1 - 2 nM (pCu^{2+} = 10 - 8.7) in coastal waters (Moffett *et al.* 1997). Such concentrations would be toxic to a variety of aquatic organisms, however, to different degrees (Table 6.11). For example, the reproductive rates of most cyanobacteria are reduced at $pCu^{2+} < 12$, while eucaryotic algae show generally normal growth at $pCu^{2+} \geq 11$ (Brand *et al.* 1986, reported in Coale and Bruland, 1988). As a result, eucaryotic algae may have a competitive advantage over cyanobacteria in waters with high cupric ion concentrations.

The complexation of Cu with natural organic ligands reduces the cupric ion concentration to fairly constant levels of around $pCu^{2+} \approx 14 - 13$ in near-surface marine waters (Sunda and Huntsman, 1995; Coale and Bruland, 1990). It has been suggested that the ubiquitous marine cyanobacterium *Synechococcus* produces extracellular chelators in response to Cu stress as a detoxification mechanism (Moffett and Brand, 1996), thus decreasing the toxic species of Cu to a tolerable level. Other species of picoplankton have been shown to produce Cu chelators with lower stability constants (by 2 - 3 log units), compared to class 1 ligands (Moffett *et al.* 1990 and references therein; Gledhill *et al.* 1997 and references therein).

The cupric ion concentration determined from ligand titrations ranged between pCu^{2+} = 12.7 - 11.3 in the Gulf of Cádiz, pCu^{2+} = 11.2 - 9.0 in the Huelva Ría plume and up to pCu^{2+} = 8.3 in Huelva Ría.

Table 6.11 - Effect of cupric ion activity on marine algae. No effect - above this pCu^{2+} no effect was observed, sub-lethal - below this pCu^{2+} sub-lethal effects were observed ($pCu^{2+} = -\log[Cu^{2+}]$).

Organism	Effects studied	No effect pCu^{2+}	Sub-lethal pCu^{2+}
Gonyaulax tamarensis[1]	motility, carbon uptake	> 11	< 9.7
Nannochloris atomus[2]	50% growth inhibition		< 9.3
Thalassiosira pseudonana[3]	100% growth inhibition		< 8.4
T. pseudonana[4]	50% growth inhibition		< 9.3
Skeletonema costatum[5]	growth inhibition	> 8.5	
Synechococcus[6]	growth inhibition		< 11.4

[1] Dinoflagellate (Anderson and Morel, 1978).
[2] Green algae, data from Sunda and Guillard (1976) reported in Anderson and Morel (1978).
[3] Diatom, estuarine strain, data from Sunda and Guillard (1976) reported in Anderson and Morel (1978).
[4] Diatom, open ocean strain (Anderson and Morel, 1978).
[5] Diatom, data from Morel *et al.* (1978) reported in Anderson and Morel (1978).
[6] Cyanobacterium , data from Brand *et al.* (1986) reported in Moffett (1995).

A shift in the phytoplankton community structure in the Huelva system, compared to other estuarine environments was evident from work carried out by Velasquez (Cruzado *et al.* 1998). In June 1997, no marine or estuarine diatoms species were identified in the upper Ría del Tinto, and in the mid- and lower Ría del Tinto, only tolerant species were found (e.g. *Skeletonema costatum*, cf. Table 6.11). This species became more abundant in Huelva Ría. Less tolerant species (*Thalassiosira sp.*) were identified in the lower part of the estuary, possibly washed in from coastal regions. Most abundant were chlorophyceae, cryptophyceae and nanoflagellates in the most polluted part of the upper estuary. The diversity of plankton species and their abundance increased with diminishing metal concentrations in the lower Huelva Ría.

The existence of *Skeletonema costatum* in waters containing cupric concentrations with reported sub-lethal effects (Table 6.11) suggests that a process of adaptation has increased the tolerance of some organisms to the contamination in the Huelva system. The bioaccumulation and development of tolerance to otherwise toxic levels of Zn, Cu and Pb in halophytes (e.g. *Zostera noltii*, *Spartina ssp.*) of the Odiel salt marshes (Luque, *et al.* 1999) shows that this process is not restricted to planktonic primary producers.

Adverse effects on plankton species and community structure have been observed in other systems with elevated Cu concentrations. Coinciding with a 1000-fold increase in the cupric ion concentration, the cell density of cyanobacteria decreased 20-fold and growth ceased in Eel Pond and Falmouth Inner Harbour (Cape Cod), compared to coastal concentrations (Moffett *et al.* 1997). The sharp increase in cupric ion concentration was attributed to the saturation of class 1 ligands by anthropogenic Cu (≈ 30 - 55 nM). Changes in ecosystem diversity and development of tolerance to increased levels of Cu have been observed in higher plants (e.g. macroalgae) and animals (e.g. crustaceans) in other metal

contaminated systems (He *et al.* 1998; Bryan and Langston, 1992; Bryan and Gibbs, 1983; Bryan *et al.* 1980).

No detailed ecological study has been published for the Huelva system. However, from the limited Cu speciation data available from the presented work, it can be concluded that the long-term contamination of the estuary with AMD-related trace metals had a profound impact on the species diversity and community structure in this system. The development of tolerance to Cu and other metals present at elevated concentrations in the local biota has important implications for the accumulation of metals in the food chain, which could pose a health risk to the human population.

6.6 Conclusions

Thermodynamic calculations have shown that the inorganic speciation of Fe, Al, Mn, Zn, Cu, Ni, Co, Cd and U in the Rio Tinto and Rio Odiel was strongly influenced by the sulphate-dominated, low pH environment typical for AMD affected waters. During estuarine mixing, the pH value remained low in the Ría del Tinto and was gradually neutralised in the Ría del Odiel and Huelva Ría (Chapter 4). The calculations showed that hardly any Fe and Al hydroxides were formed at pH < 4. This partially accounted for the absence of colloids and the conservative behaviour of metals up to high salinities and near-neutral pH values. The similarity in the inorganic speciation of Fe, Al, Mn, Zn, Cu, Ni, Co and Cd at low pH explained their congruent behaviour observed in the Ría del Tinto and Ría del Odiel. The strength of the AMD signal in the rivers, combined with acid industrial discharges in the estuary determined the speciation of metals and hence their geochemical behaviour in this estuarine system.

Huelva Ría has a high nutrient status and is a productive estuary. As observed in other estuarine systems, the concentration of Cu complexing organic ligands was higher within Huelva Ría than in adjacent coastal waters. Speciation studies and ligand titrations suggested that ligand concentrations in the high nM range occurred in Huelva Ría, whereby these ligand are fully saturated with Cu. Speciation calculations showed that slight (downward) shifts of pH values would result in a large proportion of excess Cu to be present as cupric ion. The four surveys showed that the Rio Tinto and Rio Odiel are a variable source of metals and acidity, and therefore toxicity levels may change dramatically between seasons. In the Gulf of Cádiz dissolved Cu concentrations were below the ligand concentrations. Copper was strongly complexed to more than 80%, which reduced the cupric ion concentration to sub-toxic levels.

Free cupric ions are the most toxic form of this metal and comparisons with literature indicated that concentrations causing sub-lethal effects were reached in Huelva Ría. The presence of a small selection of primary producers in this estuarine environment shows a high level of adaptation to long-term metal contamination, which is not uncommon. However, tolerance to high levels of Cu - and other metals at toxic levels - metal may induce biological accumulation in the food chain, which is an important consideration for the health of local population.

6.7 REFERENCES

Achterberg, E.P., Colombo, C. and van den Berg, C.M.G. (1999) The distribution of dissolved Cu, Zn, Ni, Co and Cr in English coastal surface waters. *Cont.Shelf.Res.* **19**, 537-558.

Achterberg, E.P., van den Berg, C.M.G., Boussemart, M. and Davison, W. (1997) Speciation and cycling of trace metals in Esthwaite Water: a productive English

lake with seasonal deep-water anoxia. *Geochimica et Cosmochimica Acta* **61**, 5233-5253.

Anderson, D.M., Lively, J.S. and Vaccaro, R.F. (1984) Copper complexation during spring phytoplankton blooms in coastal waters. *Journal of Marine Research* **42**, 677-695.

Anderson, D.M. and Morel, F.M. (1978) Copper sensitivity of Gonyaulax tamarensis. *Limnology and Oceanography* **23**, 283-295.

Apte, S.C., Benko, W.I. and Day, G.M. (1995) Partitioning and complexation of copper in the Fly River, Papua New Guinea. *Journal of Geochemical Exploration* **52**, 67-79.

Apte, S.C., Gardner, M.J., Ravenscroft, J.E. and Turrell, J.A. (1990) Examination of the range of copper complexing ligands in natural waters using a combination of cathodic stripping voltammetry and computer simulation. *Anal.Chim.Acta* **235**, 287-297.

Brand, L.E., Sunda, W.G. and Guillard, R.R.L. (1986) Reduction of marine phytoplankton reproduction rates by copper and cadmium. *Journal of Exploration, Marine Biology and Ecology* **96**, 225-250.

Bruland, K.W. (1983a) Trace elements in sea water. In: Riley, J.P. and Chester, R., (Eds.) *Chemical Oceanography*, 8 edn. pp. 162-165, 196-207. London: Academic Press.

Bruland, K.W. and Franks, R.P. (1983b) Mn, Ni, Cu, Zn, and Cd in the Western North Atlantic. In: Wong, C.S., Boyle, E., Bruland, K.W., Burton, J.D. and Goldberg, E.D., (Eds.) *Trace Metals in Sea Water*, pp. 395-414. New York and London: NATO Scientific affairs Division & Plenum Press.

Bryan, G.W. and Gibbs, P.E. (1983) Heavy metals in the Fal estuary. *Marine Biological Association of the United Kingdom, Occasional Publication* **Number 2.**

Bryan, G.W. and Langston, W.J. (1992) Bioavailability, accumulation and effects of heavy metals in sediments with special reference to United Kingdom estuaries: a review. *Environmental Pollution* **76**, 89-131.

Bryan, G.W., Langston, W.J. and Hummerstone, L.G. (1980) The use of biological indicators of heavy metal contamination in estuaries. *Marine Biological Association of the United Kingdom, Occasional Publication* **Number 1.**

Buffle, J. (1988) *Complexation Reactions in Aquatic Systems*, Chichester: Ellis Horwood Ltd.

Burgess, J. (1992) Kinetic aspects of chemical speciation. *Analyst* **117**, 605-611.

Byrne, R.H., Kump, L.R. and Cantrell, K.J. (1988) The influence of temperature and pH on trace metal speciation in seawater. *Mar.Chem.* **25**, 163-181.

Byrne, R.H. and Miller, W.L. (1985) Copper(II) carbonate complexation in seawater. *Geochimica et Cosmochimica Acta* **49**, 1837-1844.

Chapman, B.M., Jones, D.R. and Jung, R.F. (1996) Processes controlling metal ion attenuation in acid mine drainage streams. *Pure and Applied Chemistry* **68**, 1639-1656.

Coale, K.H. and Bruland, K.W. (1988) Copper complexation in the Norteast Pacific. *Limnology and Oceanography* **33**, 1084-1101.

Coale, K.H. and Bruland, K.W. (1990) Spatial and temporal variability in copper complexation in the North Pacific. *Deep-Sea Res.* **47**, 317-336.

Coffey, M.F. and Jickells, T.D. (1995) Ion chromatography-inductively coupled plasma-atomic emission spectrometry (IC-ICP-AES) as a method for determining trace metals in estuarine water. *Estuarine, Coastal and Shelf Science* **40**, 379-386.

Cruzado, A. and Velasquez, Z. Cruise reports and data from TOROS field experiments. 1999. Internet Communication.

Cruzado, A., Velasquez, Z., Garcia, H.E., Bahamon, N., Perez, M.d.C., Grimaldo, N.S., Pla, S. and Simic, L. (1998) TOROS, 2nd Field Experiment, 10 - 21 June 1997. TOROS II, Blanes, Spain: CEAB, Centro de Estudios Avanzados de Blanes.

Cruzado, A., Velasquez, Z., Ridolfi, F., Bahamon, N., Grimaldo, N.S., Simic, L. and Pla, S. (1999) TOROS, 4nd Field Experiment, 1 - 20 October 1998. TOROS IV, Blanes, Spain: CEAB, Centro de Estudios Avanzados de Blanes.

Dickson, A.G. and Whitfield, M. (1981) An ion-association model for estimating acidity constants (at 25°C and 1 atm total pressure) in electrolyte mixtures related to seawater (ionic strength <1 mol kg^{-1} H2O). *Mar.Chem.* **10**, 315-333.

Donat, J.R., Lao, K.A. and Bruland, K.W. (1994) Speciation of dissolved copper and nickel in South San Francisco Bay: a multi-method approach. *Anal.Chim.Acta* **284**, 547-571.

Donat, J.R., Statham, P. and Bruland, K.W. (1986) An evaluation of a C-18 solid-phase extraction technique for isolating metal organic-complexes from central north Pacific-Ocean waters. *Mar.Chem.* **18**, 85-99.

Donat, J.R. and van den Berg, C.M.G. (1992) A new cathodic stripping voltammetric method for determining organic copper complexation in seawater. *Mar.Chem.* **38**, 69-90.

Dyrssen, D. and Wedborg, M. (1980) Major and minor elements, chemcal speciation in estuarine waters. In: Olausson, E. and Cato, I., (Eds.) *Chemistry and biogeochemistry of estuaries*, pp. 71-120. Chichester: John Wiley & Sons.

Elbaz-Poulichet, F., Dupuy, C., Cruzado, A., Velasquez, Z., Achterberg, E.P. and Braungardt, C.B. (2000) Influence of sorption processes by Fe oxides and algal uptake on arsenic and phosphate cycle in an acidic estuary (Tinto river, Spain). *Water Research* **in press.**

Filella, M., Buffle, J. and Van Leeuwen, H.P. (1990) Effect of physico-chemical heterogeneity of natural complexants. Part I. Voltammetry of labile metal-fulvic complexes. *Anal.Chim.Acta* **232**, 209-223.

Garrels, R.M. and Christ, C.L. (1965) *Solutions, Minerals and Equilibria*, Harper & Row, New York.

Gledhill, M., Nimmo, M., Hill, S. and Brown, M. (1997) The toxicity of copper (II) species to marine algae, with particular reference to macroalgae. *Journal of Phycology* **33**, 2-11.

Gledhill, M. and van den Berg, C.M.G. (1994) Determination of complexation of iron(III) with natural organic complexing ligands in seawater using cathodic stripping voltammetry. *Mar.Chem.* **47**, 41-54.

Gordon, A.S., Dyer, B.J., Kango, R.A. and Donat, J.R. (1996) Copper ligands isolated from estuarine water by immobilized metal affinity chromatography: Temporal variability and partial characterization. *Mar.Chem.* **53**, 163-172.

He, M., Wang, Z. and Tang, H. (1998) The chemical, toxicological and ecological studies in assessing the heavy metal pollution in Le An river, China. *Wat.Res.* **32**, 510-518.

Hering, J.G. and Morel, F.M.M. (1990) Kinetics of trace metal complexation: ligand-exchange reactions. *Environmental Science & Technology* **24**, 242-252.

Hirose, K. (1994) Conditional stabiliy constants of metal complexes of organic ligands in seawater: past and present, and a simple coordination chemistry model. *Anal.Chim.Acta* **284**, 621-634.

Horowitz, A.J., Lum, K.R., Garbarino, J.R., Hall, G.E.M., Lemieux, C. and Demas, C.R. (1996) Problems associated with using filtration to define dissolved trace element concentrations in natural water samples. *Environmental Science & Technology* **30**, 954-963.

Keil, R.G., Mayer, L.M., Quay, P.D., Richey, J.E. and Hedges, J.I. (1997) Loss of organic matter from riverine particles in deltas. *Geochimica et Cosmochimica Acta* **61**, 1507-1511.

Klinkhammer, G.P. and Palmer, M.R. (1991) Uranium in the oceans, Where it goes and why. *Geochimica et Cosmochimica Acta* **55**, 1799-1806.

Kramer, C.J.M. and Duinker, J.C. (1984) Complexation capacity and conditional stability constants for copper of sea and estuarine waters, sediment extracts and colloids. In: Kramer, C.J.M. and Duinker, J.C., (Eds.) *Complexation of trace metals in natural waters*, pp. 217-228. The Hague: Nijhof/Junk.

Luque,C.J., Castellanos,E.M., Castillo,J.M., Gonzalez,M., Gonzales-Vilches,C. and Figueroa,M.E. (1999) Metals in Halophytes of a Contaminated Estuary (Odiel Saltmarshes, SW Spain). *Marine Pollution Bulletin* **38**, 49-51.

Mackey, D.J. and Zirino, A. (1994) Comments on trace metal speciation in seawater or do "onions" grow in the sea? *Anal.Chim.Acta* **284**, 635-647.

Martin, J.-M. and Meybeck, M. (1979) Elemental Mass-Balance of Material Carried by Major World Rivers. *Mar.Chem.* **7**, 173-206.

Medio Ambiente Seccion de Medio Ambiente, (Ed.) (1998) Ejecucion del plan de policia de aguas del litoral Andaluz. Informe del año 1997, Sevilla: E.S.I.I. de Sevilla. Dpto. Ingen. Química y Ambiental.

Moffett, J.W. (1995) Temporal and spatial variability of copper complexation by strong chelators in the Sargasso Sea. *Deep-Sea Research I* **42**, 1273-1373.

Moffett, J.W. and Brand, L.E. (1996) Production of strong, extracellular Cu chelators by marine cyanobacteria in response to Cu stress. *Limnology and Oceanography* **41**, 388-395.

Moffett, J.W., Brand, L.E., Croot, P.L. and Barbeau, K.A. (1997) Cu speciation and cyanobacterial distribution in harbors subject to anthropogenic Cu inputs. *Limnology and Oceanography* **42**, 789-799.

Moffett, J.W. and Zika, R.G. (1987) Solvent extraction of copper acetylacetonate in studies of copper(II) speciation in seawater. *Mar.Chem.* **21**, 301-313.

Moffett, J.W., Zika, R.G. and Brand, L.E. (1990) Distribution and potential sources and sinks of copper chelators in the Sargasso Sea. *Deep-Sea Res.* **37**, 27-36.

Morel, N.M., Reuter, J.E. and Morel, F.M. (1978) Copper toxicity to *Skeletonema costatum*. *Journal of Phycology* **14**, 43-51.

Muller, F.L.L. (1996) Interactions of copper, lead and cadmium with the dissolved, colloidal and particulate components of estuarine and coastal waters. *Mar.Chem.* **52**, 245-268.

Nimmo, M., van den Berg, C.M.G. and Brown, J. (1989) The chemical speciation of dissolved Nickel, Copper, Vanadium and Iron in Liverpool Bay, Irish Sea. *Estuarine, Coastal and Shelf Science* **29**, 57-74.

Pan, P. and Susak, N.J. (1991) The speciation of cobalt in seawater and fresh waters at 25C. *Geochemical Journal* **25**, 411-420.

Plavsic, M., Krznaric, D. and Branica, M. (1982) Determination of the apparent copper complexing capacity of seawater by anodic stripping voltammetry. *Mar.Chem.* **11**, 17-31.

Plavsic, M., Vojvodic, V. and Cosovic, B. (1990) Characterization of surface-active substances during a semi-field experiment on a phytoplankton bloom. *Anal.Chim.Acta* **232**, 131-140.

Schecher, W.D. and McAvoy, D.C. (1994) *MINEQL+, user's manual*, Hallowell, ME: Environmental Software.

Schoemann, V. and de Jong, J.T.M. (1998) Effects of phytoplankton blooms on the cycling of manganese and iron in coastal waters. *Limnology and Oceanography* 1427-1441.

Stumm, W. and Morgan, J.J. (1996) *Aquatic Chemistry-Chemical equilibria and rates in natural waters*, 3 edn. New York: John Wiley & Sons.

Sunda, W.G. and Guillard, R.R. (1976) Relationship between the cupric ion activity and the toxicity of copper to phytoplankton. *J.Mar.Res.* **34**, 511-529.

Sunda, W.G. and Hanson, A.K. (1987) Measurement of free cupric ion concentration in seawater by a ligand competition technique involving copper sorption onto C18 SEP-PAK cartridges. *Limnology and Oceanography* **32**, 537-551.

Sunda, W.G. and Huntsman, S.A. (1991) The use of chemiluminescence and ligand competition with EDTA to measure copper concentration and speciation in seawater. *Mar.Chem.* **36**, 137-163.

Sunda, W.G. and Huntsman, S.A. (1995) Regulation of copper concentration in the oceanic nutricline by phytoplankton uptake and regeneration cycles. *Limnology and Oceanography* **40**, 132-137.

Turner, D.R., Whitfield, M. and Dickson, A.G. (1981) The equilibrium speciation of dissolved components in freshwater and seawater at 25°C and 1 atm pressure. *Geochimica et Cosmochimica Acta* **45**, 855-881.

van den Berg, C.M.G. (1982) Determination of copper complexation with natural organic ligands in seawater by equilibrium with MnO_2. *Mar.Chem.* **11**, 307-342.

van den Berg, C.M.G. (1984a) Determination of the complexing capacity and conditional stability constants of complexes of copper(II) with natural organic ligands in seawater by cathodic stripping voltammetry of copper-catechol complex ions. *Mar.Chem.* **15**, 1-18.

van den Berg, C.M.G. (1984b) Organic and inorganic speciation of copper in the Irish Sea. *Mar.Chem.* **14**, 201-212.

van den Berg, C.M.G., Buckley, P.J.M., Huan, Z.Q. and Nimmo, M. (1986) An electrochemical study of the speciation of copper, zinc and iron in two estuaries in England. *Estuarine, Coastal and Shelf Science* **22**, 478-486.

van den Berg, C.M.G. and Donat, J.R. (1992) Determination and data evaluation of Cu complexation by organic ligands in sea water using CSV at varying detection windows. *Anal.Chim.Acta* **257**, 281-291.

van den Berg, C.M.G., Merks, A.G.A. and Duursma, E.K. (1987) Organic complexation and its control of the dissolved concentrations of copper and zinc in the Scheldt Estuary. *Estuarine, Coastal and Shelf Science* **24**, 785-797.

van den Berg, C.M.G., Nimmo, M., Daly, P. and Turner, D.R. (1990) Effects of the detection window on the determination of organic copper speciation in estuarine waters. *Anal.Chim.Acta* **232**, 149-159.

Chapter 7

Conclusions and Future Work

7.1 Conclusions

The spatially compact Tinto/Odiel system presented a unique opportunity to study the biogeochemistry of dissolved trace metals from their origin in the metalliferous mining district of the Iberian Pyrite Belt to their entrainment by Atlantic surface currents in the Gulf of Cádiz. A multidisciplinary approach to estuarine and marine science was of particular importance in order to understand the behaviour of metals in this complex system. The participation within the TOROS project allowed the author to benefit from the expertise of colleagues working in many disciplines, including geology, hydrology, sedimentology, biology, chemistry, geochemistry and oceanography, as well as remote sensing, modelling and data management. Several questions remain unanswered, most importantly the interaction of metals between the dissolved and particulate phase. The author is awaiting the completion of studies on suspended particulate matter carried out by a colleague, working in parallel with TOROS, with anticipation.

The geology and geography of their catchment have determined the character of the Rio Tinto and Rio Odiel since historic times, and especially throughout the last several thousand years, when the massive metal sulphide deposits in the Iberian Pyrite Belt have been exploited by mining. The cycle of dry summers and flash floods during autumn and winter was identified as the most likely cause for the strong seasonal character of the variations in river water quality. Physical, chemical and microbiological weathering of natural deposits and mine tailings generated a metal-rich and acidic leachate (acid mine drainage, AMD), which entered the headwaters of the two rivers. The rate of weathering

and erosion, and the transport of leachate and mineral grains depend on the availability of moisture, and the kinetics of redox reactions and biological activity is partially determined by temperature. Seasonal investigations of river systems affected by AMD are still rare. Although only four surveys were carried out and no flood-event was sampled directly, the presented work improved our understanding of the cyclical nature of AMD geochemistry in arid climates.

The level of contamination with dissolved Fe, Al, Mn, Zn, Cu, Ni, Co, Cd, Pb and U observed in the Rio Tinto and Rio Odiel was comparable with the most polluted water courses on a global scale. Discharge-weighted dissolved metals fluxes calculated for the riverine end-members were important not only locally, but also in comparison with the world's major rivers. Annual metal fluxes to the estuary were 9900 t Zn, 4500 t Mn, 3400 t Cu, 180 t Co, 77 t Ni, 67 t Pb, 34 t Cd and 1.9 t U, whereby the contribution was higher during the wet, compared to the dry seasons.

Thousands of years of contamination resulted in the development of a specialised ecosystem, in which acidophilic micro-organisms and yeasts thrive. Although equilibrium calculations showed that the free cupric ion are likely to exceed concentrations that are toxic to many marine organisms, a number of algae and marginal plants have adapted to the stress of pH and high metal concentrations.

The catchment geology provides little buffering capacity, and as a consequence the pH in the rivers was maintained at values below three. Although dissolved metal concentrations were very high, thermodynamic equilibrium calculations indicated that none of the formed inorganic species reached saturation. The high solubility of inorganic metal species in AMD (mainly free hydrated ions and metal sulphates) implied that abiotic processes cannot account for the observed loss of Fe, Al, Mn, Zn, Cu, Ni, Co, Cd and Pb from solution along the length of the Rio Tinto and Rio Odiel. This led to the suggestion

that the precipitation of solid Fe and Mn phases was mediated by acidophile micro-organisms. Further removal of metals from solution may have been facilitated through scavenging by fresh precipitates and concretion onto existing solids.

The metal geochemistry in the estuary was determined by seasonally variable riverine inputs, industrial discharges, and the changes of salinity, pH and water movement throughout the tidal cycle. The neutralisation of pH was slow in the Ría del Tinto and Ría del Odiel. While effluent from phosphogypsum deposits remained unrestricted, very low pH values were maintained throughout the Ría del Tinto ($pH < 3$ up to $S \doteq 30$).

In the upper Ría del Tinto mixing zone, the increase in the dissolved concentrations of Fe, Al, Mn, Zn, Cu, Ni, Co and Cd was attributed to the tidal re-suspension of particles, dissolution from reducing sediments and leaching from particles at the prevailing low pH. The input of organic-rich industrial effluent in this part of the estuary may have caused local anoxia, thus favouring reducing conditions. An exception was Pb, which was removed rapidly from solution at low salinity due to its high particle affinity. Effluent from the phosphogypsum deposits introduced U and phosphate into the lower Ría del Tinto, where maxima of both were observed. Phosphate was also released from the fertiliser industry into the upper parts of Huelva Ría, and as a result, the estuary was highly productive and phytoplankton blooms were observed during the summer survey.

Dissolved metals behaved largely conservatively in the mid- and lower Ría del Tinto and in the Ría del Odiel. Removal of Zn, Cu, Ni and Co from solution was observed in waters where the pH value exceeded five at salinities ≥ 30. This study highlighted the importance of pH for the partitioning of trace metals between the solid and dissolved phase in estuaries receiving large quantities of AMD.

Results from speciation studies indicated the presence of a seasonal signal to the removal of Cu in Huelva Ría. Although the metal flux from the rivers was lowest in June,

dissolved metal concentrations observed in the lower Huelva Ría at equal salinity were higher during summer, compared to the other seasons. Concentrations of Cu complexing organic ligands in the estuary reached high values (up to 200 nM) in the lower Huelva Ría, and Cu speciation studies showed that a higher proportion of Cu was strongly complexed in June (median: 26%), compared to the winter survey (median: 3%). The available data indicated that the removal of Cu from solution was reduced by complexation with organic ligands, and although direct evidence is lacking, the concentration of these organic ligands may have been enhanced during and after seasonal phytoplankton blooms.

The hypothesis in published work of a toxicity-regulating aspect to the release of Cu complexing organic ligands by some phytoplankton species was supported by the strong linear relationship between the concentrations of total dissolved Cu and strong Cu complexing ligands observed in samples from the Gulf of Cádiz and Huelva Ría. In coastal water with total Cu concentrations below ca. 35 nM, the ligand concentration exceeded that of Cu, and equilibrium calculations showed that the level of free Cu in solution remained below toxic concentrations. At higher total Cu concentrations in Huelva Ría, the complexing capacity of strong ligands was exceeded, although the concentration of strong ligands was higher in the estuary than in coastal waters. Thermodynamic speciation calculations incorporating an organic ligand showed the preferential complexation of Cu by the organic ligand. Beyond the point of ligand saturation the cupric ion concentration increased rapidly with the total dissolved Cu concentration. The resulting toxic cupric ion concentrations imply that plankton and marsh plants growing in the Ría del Tinto and Ría del Odiel underwent a high level of adaptation. Published work on AMD systems commonly focussed on inorganic metal speciation. The inclusion of organic complexation offered valuable insights into the biogeochemical behaviour of Cu and its potential toxicity in this highly contaminated and highly productive estuarine system, and provided the basis for more detailed future research.

The removal of Zn, Cu, Ni and Co from solution was essentially complete at pH values above 7.5, so that the net dissolved metal flux from the estuary could be estimated using extrapolation to a virtual riverine end-member. The calculations indicated the removal of 63% Zn, 75% Cu, 22% Ni and 49% Co from solution within the estuary. The annual export of dissolved metals from Huelva Ría was calculated to be 3700 t Zn, 850 t Cu, 68 t Ni and 86 t Co, which identified this estuary as the main contributor of dissolved Zn and Cu to the Gulf of Cádiz, and an important metal source to European coastal waters. However, a large error was involved in all flux calculations for this system.

In the Gulf of Cádiz, on-line measurements of dissolved Zn, Cu and Ni showed metal plumes associated with the Tinto/Odiel system, and with the two major rivers (in terms of water discharge) in the area, the Guadiana and Guadalquivir. The intensity, extent and transport of metal plumes were strongly dependent on tidal movement. The near-real time measurement of metal concentration proved an invaluable tool for the detailed and interactive examination of the plume development, and the on-line work carried out in the Huelva system has contributed to publications (see Appendix).

Surveys in shallow waters allowed the tracking of metal plumes from the northern shore of the Gulf of Cádiz to the east and south-east and towards the Strait of Gibraltar. This long-shore movement was the result of the well-documented entrainment of Gulf of Cádiz water with the Atlantic surface current that flows into the western Mediterranean Sea. Because of this surface circulation pattern, the highest concentrations of dissolved Zn, Cu and Ni were observed along the shore. Concentrations decreased towards the outer regions of the Gulf of Cádiz, where the enrichment with respect to dissolved concentrations in North Atlantic surface waters was factor 3.6 - 14 for Zn, 2.5 - 6.5 for Cu and 1.8 - 8.8 for Co. Although less restricted by land than the Irish Sea or North Sea, the

circulation pattern and high input of metals from riverine sources makes the Gulf of Cádiz one of the most metal contaminated sea areas in Europe.

7.2 Future Work

This study has provided the base for a better understanding of metal behaviour in AMD affected coastal systems. Several areas of research have been addressed by partners in the TOROS project and researchers working in parallel with it. This included a detailed study of nutrient and chlorophyll distribution, metal concentrations in suspended particulate matter (including kinetic mixing experiments), metal concentrations in dissolved and particulate matter throughout the water column in the Gulf of Cádiz and the modelling of contaminant transport. Joint publications are planned for the near future.

Further research is needed in order to calculate dissolved and particulate metal fluxes from the Huelva system in a more accurate manner. Hereby, the study of dissolved and particulate metal discharge during major flood-events is of particular importance. A long-term approach in co-operation with local authorities could elucidate patterns in seasonal and annual variability. Such a set of data could be used for predictive modelling and would provide the base line for future remediation programmes.

The specific role of acidophile micro-organisms in the cycling of metals in this system is of interest to a more detailed study of seasonal variability, and the possible utilisation of micro-organisms for remediation purposes.

The adaptation of flora and fauna to high levels of metal contamination and low pH values demands further investigation. Adapted organisms may accumulate high levels of metals, thus introducing them into the food chain. The reaction of algae to metal stresses and the role of algal exudates are still poorly understood. The extreme nature of the Huelva

system may provide an opportunity to study highly adapted organisms in order to improve our knowledge about the rate of metal uptake, the level of metal storage and the detoxification mechanisms in biota.

The effect of pH on the inorganic and organic speciation of metals was evident from the observations made. Further research is needed in order to elucidate the effect of pH variations on the organic complexation of Cu and other metals. In this context the effect on the conditional stability constant for metal-ligand complexes are of particular interest. The separation of different classes of ligands, if present, by using several detection windows could provide information about differences in the sources of ligands between the estuary and coastal sea. The characterisation of organic ligands would be desirable, but may not be achieved in the near future.

Appendices

8.1 Appendix 1: Published Materials

Reprints of photocopies of Author's copies of the following publications are included:

Achterberg, E.P., Braungardt, C. and Whitworth, D.J. Electrochemical monitor for near real-time determination of dissolved trace metals in marine waters. *Chemical sensors in oceanography*, pp. 227-247, **in press.**

Achterberg, E.P. and Braungardt, C. (1999a) Stripping voltammetry for the determination of trace metal speciation and in-situ measurements of trace metal distributions in marine waters. *Anal.Chim.Acta* **400**, 381-397.

Achterberg, E.P., Braungardt, C., Morley, N.H., Elbaz-Poulichet, F. and Leblanc, M. (1999b) Impact of Los Frailes mine spill on riverine, estuarine and coastal waters in southern Spain. *Water Research* **33**, 3387-3394.

Braungardt, C., Achterberg, E.P. and Nimmo, M. (1998) On-line voltammetric monitoring of dissolved Cu and Ni in the Gulf of Cádiz, south-west Spain. *Anal.Chim.Acta* **377**, 205-215.

Elbaz-Poulichet, F., Dupuy, C., Cruzado, A., Velasquez, Z., Achterberg, E.P. and Braungardt, C.B. (2000) Influence of sorption processes by Fe oxides and algal uptake on arsenic and phosphate cycle in an acidic estuary (Tinto river, Spain). *Water Research,* **in press.**

Elbaz-Poulichet, F., Morley, N.H., Cruzado, A., Velasquez, Z., Green, D., Achterberg, E.P. and Braungardt, C.B. (1999) Trace metal and nutrient distribution in an extremely low pH (2.5) river-estuarine system, the Ria of Huelva (south-west Spain). *The Science of the Total Environment* **227**, 73-83.

8.2 Appendix 2: Data

A CD-ROM is attached to this thesis, containing the raw data used in this thesis. The names of files are largely self-explanatory, and their contents are described in a MS Word 97 file, 'read me.doc'.

a copy of this CD-ROM is accessible via the Author:

Charlotte Braungardt (cbraungardt@plymouth.ac.uk)

and via the director of studies:

Eric P. Achterberg (eachterberg@plymouth.ac.uk)

current address:

University of Plymouth

Department of Environmental Sciences

Drake Circus

Plymouth PL4 8AA

UK

10. ELECTROCHEMICAL MONITOR FOR NEAR REAL-TIME DETERMINATION OF DISSOLVED TRACE METALS IN MARINE WATERS

ERIC P. ACHTERBERG, CHARLOTTE BRAUNGARDT and DAVID J. WHITWORTH

Department of Environmental Sciences, University of Plymouth, Plymouth PL4 8AA, UK

10.1 INTRODUCTION

Measurements of chemical constituents in marine waters present many challenges as a result of the distinctive composition of seawater, the large temporal and spatial variabilities in marine systems and the problematic accessibility of study areas. With an increasing global environmental awareness, there is now a greater demand for instrumentation that can be used for chemical marine monitoring. The most used chemical marine sensor systems today are based upon electrochemical principles and are for the determination of oxygen and pH. However, electrochemical methods have also been developed for the determination of trace metals in seawater. Monitoring of trace metals in marine systems is important for overseeing the health of our seas. For example, monitoring programmes for trace metals and other chemical constituents in the North Atlantic and Arctic Oceans (including the North Sea) have been internationally agreed in the Oslo-Paris conventions (Ospar). Ospar represents 15 European countries which have coastlines on or rivers discharging into the north-east Atlantic.

The concentrations of dissolved metals in unpolluted oceanic waters are generally very low, typically at nanomolar (10^{-9} mol l^{-1}) levels or less. Copper, Zn and Ni, for example, occur at levels of between 0.5 and 5×10^{-9} moles l^{-1} in waters of the Atlantic Ocean (Bruland and Franks, 1983; Buckley and van den Berg, 1986; Jickells and Burton, 1988; Kremling and Pohl, 1989), whilst the concentrations of these metals are approximately ten times higher in coastal waters of the Irish sea and North Sea (Tappin *et al.*, 1995; Achterberg and van den Berg, 1996). Levels of dissolved Cu, Zn and Ni in some mine polluted estuarine systems in southern Spain (Huelva) and south-west England (Restronguet Creek) can however reach levels of 10^{-6} to 10^{-5} mol l^{-1} (Leblanc *et al.*, 1995; Bryan and Langston, 1992; Rijstenbil *et al.*, 1991). Different approaches are taken to monitor metals in the marine environment. The US Mussel Watch programme utilises mussels which are collected in coastal areas (Lauenstein *et al.*, 1990; Larsen, 1992; Stephenson and Leonard, 1994). The programme has been successful in highlighting pollution hot-spots, by

determining metals (and other pollutants) in the mussel tissue. As mussels are filter feeders, the pollutant levels in mussels largely reflect the levels in suspended particulate matter and not in the dissolved phase (by definition the dissolved phase passes through a 0.4–0.45 μm membrane filter and the particulate phase is retained). The pollutant levels in mussels provide a picture about perturbation in their environment over a longer period, and can therefore be used to check the health of that environment. A picture of historical pollution levels in marine systems can also be obtained from determinations of pollutants in sediments. Metal levels at different depth in the sediments can be related to historical time periods, but care must be taken that processes like bioturbation and metal mobility through redox processes have not disturbed the vertical metal profiles. A great deal of progress has been made in recent years in using behavioural and functional responses of organisms to pollutants (including metals and xenobiotic organic compounds) in natural waters (Baldwin and Kramer, 1994). The use of such bio-indicators provide a near-instantaneous feed-back on toxic pollutant levels in the water. However, more work will need to be done with respect to the selectivity and sensitivity of these methods.

The most reliable methods for monitoring dissolved trace metal concentrations in the marine environment still involve chemical determinations. These analyses provide information on the dissolved form of metals which, for example, may affect the level of growth of phytoplankton and bacteria in the sea. Dissolved metal monitoring can also identify metal containing waste discharges into marine waters. Traditionally, sea water samples are collected in a discrete manner. From a survey vessel discrete surface water samples can be obtained using a pump with a bottom-weighted hose, and in deeper waters with the use of samplers (e.g. Go-Flo or Niskin bottles) which are attached to a hydrowire and lowered in the sea with the use of a winch. The samples are usually filtered on-board ship and subsequently analysed in a land-based laboratory. Commonly used laboratory techniques for dissolved trace metal analysis in sea water include Graphite Furnace Atomic Absorption Spectrometry (GFAAS) and Inductively Coupled Plasma Mass Spectrometry (ICP-MS) (after solid-phase extraction for trace metal preconcentration and matrix removal), chronopotentiometry, colorimetry, chemiluminescence and stripping voltammetry. This approach of laboratory based analyses of discrete samples is time-consuming and therefore expensive. Only a limited number of samples can be collected using discrete sampling techniques and as a result important changes in water quality may be missed. Trace metal levels in estuarine, coastal and oceanic waters are often low. Inadequate sampling and sample treatment techniques have for a long time prevented the uncontaminated collection and analysis of sea water samples. Sample contamination may arise from components of the sampling gear and from sample handling operations. Concentrations of elements like Ni, Cu, Zn and Fe which were determined in sea water samples collected prior to the mid-seventies and sometimes early eighties were therefore in many cases affected by sample contamination. Nowadays, the use of PTFE coated samplers, free of internal metal components, and with as few external metal components as possible, greatly

improves contamination-free sample collection. Improved understanding of post-sampling contamination has resulted in the introduction of ultra-trace working practices (Morley *et al.*, 1988). Sample bottles (preferably High Density Polyethylene; HDPE), filters and filtration equipment are acid cleaned prior to use, and all sample handling is performed in a clean environment (class-100 laminar flow hood in a clean room) (Howard and Statham, 1993). These precautions against sample contamination are essential in order to obtain high quality trace metal data, but greatly reduce the number of samples that can be processed by a research worker.

10.2 ELECTROCHEMICAL TECHNIQUES: POTENTIOMETRY

pH is the most commonly measured chemical parameter in natural waters and knowledge of pH is necessary for the understanding of speciation of trace elements in these waters. The determination of pH is most often performed using potentiometry, whereby the potential over an electrode pair is measured without current flow. A reference electrode (Ag/AgCl or calomel) and ion-selective electrode (glass electrode) are used for this purpose. Potentiometry is also used for the determination of trace metals in natural waters using metal-selective solid state electrodes. Such electrodes are available for Cu, Ag, Pb and Cd and determine the activity of the metals in solution. The metal-selective electrodes incorporate membranes fabricated from insoluble crystalline materials and these contain the metal ion for which the electrode is selective. The application of the electrodes is hampered by poor sensitivity and accuracy: metal-selective electrodes usually exhibit a non-Nernstian behaviour at analyte concentrations below 10^{-7} mol l^{-1}. Another major drawback for application of metal-selective electrodes to oceanography is that serious interferences are often produced by the major ions in seawater.

10.3 ELECTROCHEMICAL TECHNIQUES: STRIPPING VOLTAMMETRY

The most suitable electrochemical methods for the determination of low levels of trace metals in sea water make use of stripping techniques: anodic and adsorptive cathodic stripping voltammetry (ASV and ACSV, respectively). Important advances have been made during the past 20 years in the application of stripping voltammetry to marine trace metal measurements. The strength of stripping voltammetry is in its extremely low detection limits (10^{-10}–10^{-11} mol l^{-1}). Analytical developments have resulted in our ability to determine a wide range of trace metals in seawater (over 20 metals including: Co, Cu, V, U, Fe, etc.; van den Berg, 1989; 1991), and the instrumentation has been computerised and made portable.

The basic voltammetric equipment for marine applications consists of a voltammetric analyser, a three-electrode cell (working electrode, reference electrode

and counter electrode) and a computer for automated measurements and data acquisition. Modern voltammetric analysers are simple, low-cost and able to perform a range of scan forms. The reference electrode is often a Ag/AgCl electrode and the counter electrode may be a platinum wire or a carbon rod. The most popular working electrode for environmental trace metal analysis is a hanging mercury drop working electrode (HMDE), but glassy carbon and carbon fibre electrodes on which a mercury film is plated are also used in stripping voltammetry. The advantage of an HMDE is that with the formation of each new drop, a new electrode surface is produced, which is important for unattended trace metal monitoring activities. The drops generated by modern mercury drop electrodes are very small (e.g. VA Stand 663 from Metrohm (Switzerland) produces drops with an area of 0.52 mm^2), and safe storage and recycling of the used mercury will ensure minimal environmental and health risks.

Anodic stripping voltammetry has been applied successfully for trace measurements of Cu, Cd, Pb and Zn in seawater. Other elements can be determined using this technique, but their seawater concentrations are too low for ASV, or the analysis is hampered by interferences. A deposition, or pre-concentration, step is carried out under conditions of forced convection (e.g. solution stirring or flow). The deposition potential should be ca. 0.3–0.4 V more negative than the reduction potential of the metal. During the deposition step of an ASV analysis, metal ions are collected in the mercury drop by reduction (to metallic state) and amalgamation with the mercury (see equation 10.1).

$$M^{n+} + ne^- + Hg \leftrightarrow M(Hg) \qquad (10.1)$$

Only a small fraction of the metal is actually being deposited during the deposition step. The sensitivity of ASV is improved by using a mercury film rather than a mercury drop electrode because the smaller volume of the mercury film results in a greater concentration factor of the metals collected into the mercury. The deposition is followed by a voltammetric scan towards more positive potentials during which the metal in the mercury is oxidised and the current produced is determined. The resultant current potential stripping voltammogram provides quantitative information: the height of the peak is proportional to the metal concentration; and also qualitative information: the potential of the peak is an indication for the metal analysed. Different scan forms are being applied during the measurement of trace metals in seawater to improve the sensitivity of the methods. The most basic scan form is linear sweep, but pulse-voltammetric waveforms (e.g. differential pulse and square wave) are more useful as they effectively correct for background current contributions. The limit of detection for ASV analysis of Cu and Cd in seawater is typically 10^{-11} and 10^{-10} mol l^{-1}, respectively. Depending on the encountered trace metal levels in a marine system, ASV allows for simultaneous determination of more than one metal.

Adsorptive cathodic stripping voltammetry makes use of a specific ligand (L), which is added to the water sample and forms an adsorptive complex with the trace metal(s) under investigation (equation 10.2).

$$Mn^{+} + zL \rightarrow ML \tag{10.2}$$

$$ML \rightarrow ML\ (\text{adsorbed}) \tag{10.3}$$

$$ML\ (\text{adsorbed}) + e^{-} \rightarrow M(n-1)^{+} + zL \tag{10.4}$$

A pH buffer is used to control the pH of the sample as the formation of the metal-ACSV ligand is pH dependent. Generally, ACSV is carried out at a hanging mercury drop electrode. A minute fraction of the metal-ligand complex is adsorbed on the surface of the mercury drop (equation 10.3) and a potential scan is carried out. The adsorption step is carried out at a carefully controlled potential as it determines the adsorption efficiency. In most cases, an adsorption potential is chosen which is slightly more positive (ca. 0.1 V or more) than the reduction potential of the metal-ligand complex. The scan direction is towards more negative potentials and the resulting current is determined (see Figure 10.1).

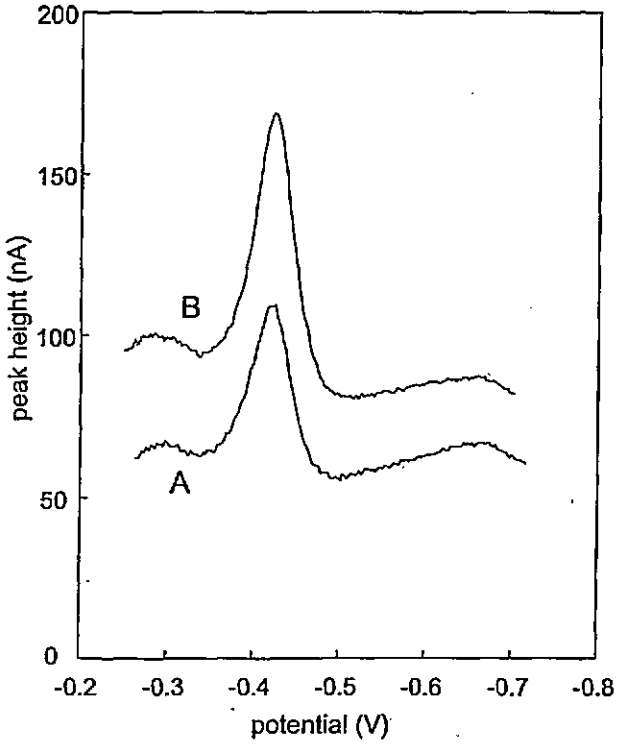

Figure 10.1 Voltammetric scan of dissolved Cu in seawater. Oxine (0.15 mM) was used as the ACSV ligand, Hepes (10 mM) was used as pH buffer (pH 7.7). Voltammetric conditions were: 20 s deposition at −1 V, 8 s equilibration at −0.25 V and 200 Hz square wave scan towards more negative potentials. Scan A is for sample, and scan B is for sample plus standard addition (5×10^{-9} mol l^{-1} final concentration).

The reduction current is the result of the reduction of a reducible group on the ligand or of the metal itself in the adsorbed complex (equation 10.4). The scan forms applied during ACSV include linear sweep, but fast pulse-voltammetric waveforms (e.g. differential pulse and square wave) are also used if the reduction of the metal-ligand complex is electrochemically reversible. The limit of detection of ACSV for metals is typically on the order of 10^{-9}–10^{-11} mol l^{-1}. Even lower metal concentrations (down to 10^{-12} mol l^{-1} for Pt, Ti, Co) can be determined by using a catalyst in order to enhance the reduction current. Multi-elemental ACSV methods have been developed recently (Colombo and van den Berg, 1997), whereby with the use of mixed ACSV ligands up to 6 trace metals (Cu, Pb, Cd, Ni, Co and Zn) can be determined simultaneously in coastal and estuarine waters. Voltammetric trace metal analysis commonly makes use of the standard addition method for the quantification of metal concentrations in water samples.

Voltammetric techniques have the advantage that they allow determination of trace metals directly in sea water, without a separate pre-concentration step. Alkali metals in seawater do not interfere with trace metal determinations, but actually increase the sensitivity. In addition, the high sensitivity and selectivity allow the determination of trace metal speciation (Achterberg and van den Berg, 1994a). Speciation analysis involves the determination of different physico-chemical forms of trace metals. In the case of ACSV, ligand competition is used for speciation measurements whereby the added ACSV ligand competes for trace metals with naturally occurring ligands (Figure 10.2). The competition conditions

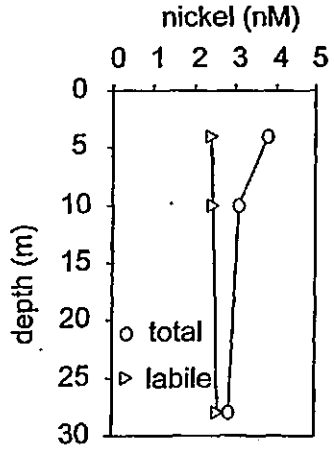

Figure 10.2 Depth profile of dissolved Ni speciation in the Gulf of Cadiz (November 1996), determined using ACSV. Labile and total Ni were determined using DMG (dimethylglyoxime, ACSV ligand) concentrations of 2×10^{-5} and 2×10^{-4} mol l^{-1}, respectively. Labile Ni was determined at sea, whereas total Ni (after UV-digestion of the samples) was analysed in the laboratory. Largest difference between total and labile Ni was observed in the surface waters and can probably be attributed to presence of enhanced Ni complexing organic matter, produced by primary producers.

can be carefully manipulated by choosing a suitable ACSV ligand (with known conditional stability constants for the metal under investigation) and an appropriate ACSV ligand concentration. For example, ACSV ligands used for speciation measurements of Cu in seawater include Tropolone, Salicylaldoxime and Oxine, with Tropolone being the weakest Cu complexing ACSV ligand and Oxine the strongest. Metal speciation is becoming more important because of the recognition that data on total dissolved metal concentrations does not yield sufficient information about the toxicity, bioavailability and geochemical behaviour of trace metals in natural waters. For many metals (including Cu, Zn, Cd and Ni) the free aqueous form is reported to be the most bioavailable and toxic (Tessier and Turner, 1995), but only a few analytical techniques (including stripping voltammetry and chemiluminescence) are sensitive enough to determine labile/free aqueous metal fractions in sea water. It is important for metal speciation measurements to be performed as soon as possible upon sampling, as chemical equilibria are readily disturbed during sample storage. The application of *in-situ* (including ship-board) techniques is therefore required.

10.4 SHIP-BOARD VOLTAMMETRIC TECHNIQUES

In recent years there has been a move towards trace metal analysis on-board ship. This approach not only reduces the risk of sample contamination, but often also results in a higher sample through-put and hence an increased amount of environmental data. Analytical instrumentation for ship-board use will preferably need to have a limited weight and size, in other words be portable. This precludes the use of GFAAS and ICP-MS techniques, because the instrumentation is bulky. In addition, instrumentation for GFAAS and ICP-MS is very sensitive to the constant vibrations caused by the ship's engines. Electrochemical techniques often make use of portable instrumentation. The purchase and running costs of such instrumentation are much lower than for GFAAS and ICP-MS, and make the electrochemical techniques very suitable for field monitoring of dissolved trace metals. Most methods for dissolved trace metal analysis using voltammetry can be operated in an automated batch or flow-analysis mode. In this case sample and reagent transport and metal standard additions are performed using pumps. The application of computers in such systems allows fully automated sample and reagent transport, standard additions, metal analysis, data acquisition and treatment (Achterberg and van den Berg, 1994a). The automated batch or flow-analysis approach not only reduces the risk of sample contamination and increases the sample through-put, it also enhances the quality of the data by the fully computerised operation. As pointed out before, mercury drop electrodes are commonly used and have the advantage over other types of electrodes that a fresh electrode surface is formed each time a new drop is made. It is our experience that this type of electrode behaves very well at sea. Even during force 10 storms on the Beaufort scale, or on ships with strong engine vibrations, the mercury drops do not dislodge during the collection or scanning steps. With the

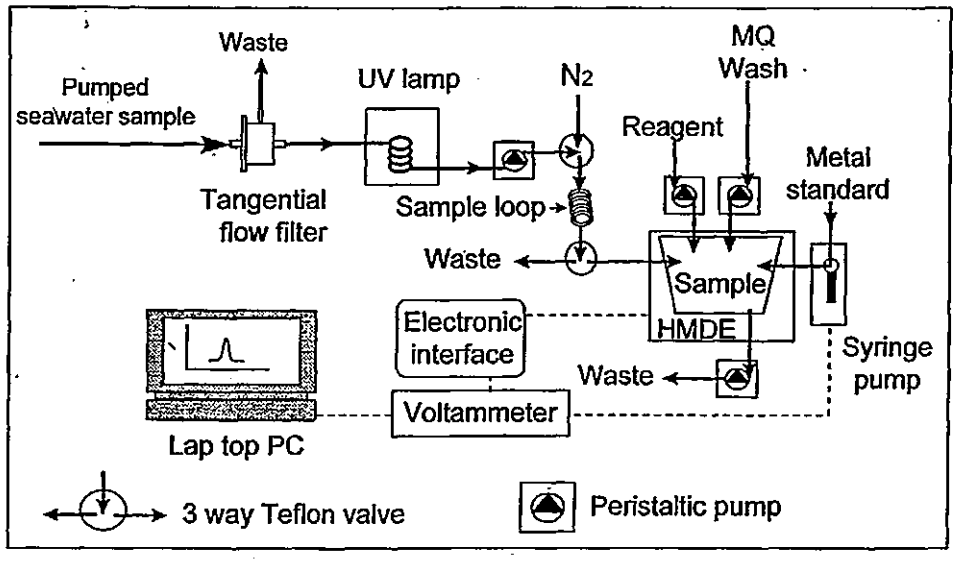

Figure 10.3 Diagram of automated voltammetric system with dotted lines representing electrical connections and solid lines representing sample and reagent flows. HMDE: hanging drop mercury electrode.

use of fast scan forms (e.g. square wave at 300 Hz) any movement of the vessel goes unnoticed during the voltammetric scan and high quality scans are obtained.

An example of an automated voltammetric metal monitor which is used for both land-based laboratory and near real-time *in-situ* analysis of trace metals is shown in Figure 10.3. The monitor comprises of an μAutolab voltammetric analyser (EcoChemie, The Netherlands) and a Metrohm hanging mercury drop electrode (VA Stand 663, Switzerland). The sample and reagent transport is performed using peristaltic pumps and metal standard additions are made to the voltammetric cell using a syringe pump (Cavro). Three-way inert Teflon® valves (Cole-Parmer) are used to fill and empty a sample loop (ca. 10 ml). The voltammeter and peripheral instruments are controlled using a portable PC. All tubing used in the voltammetric system is made of Teflon®, with the exception of pump tubing, which is Santoprene®. On-line filtration of the seawater is performed using a tangential flow filtration system (Figure 10.4). A membrane filter (0.45 μm pore size, 47 mm diameter) is placed in the filter holder and sample is obtained at a rate of a few ml min^{-1}. A filter can be used for a prolonged period of time, even in turbid estuaries, because the filtration system is self-cleansing. Particulate material is constantly removed from the filter by a pronounced cross-filter sea water flow (up to ca. 2–3 l min^{-1}). An on-line UV-digestion unit (Figure 10.4) is used for the break-down of surfactants and natural metal-complexing organic ligands (Achterberg and van den Berg, 1994b). The surfactants need to

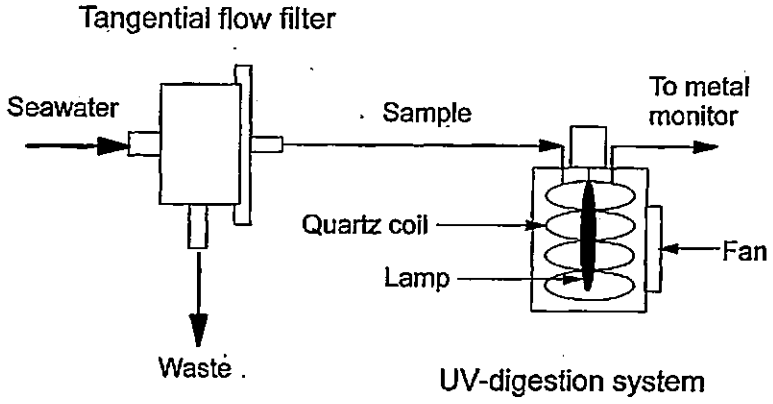

Figure 10.4 Diagram of on-line tangential flow filtration system and on-line UV-digestion system.

be removed because they may interfere with the voltammetric analysis by fouling the working electrode surface. Metal-complexing ligands occur naturally in sea water and are thought to be released by phytoplankton (algal exudates), bacteria (e.g. siderophores), but also include breakdown products of marine organisms (e.g. porphyrins) and humic substances from land-run off. The complexation of metals by the natural ligands reduces the electrochemically labile metal concentration and hence the voltammetric signal, and their destruction releases the metals and results in the determination of total dissolved metal concentrations. The UV-digestion unit contains a medium pressure mercury vapour lamp (100 to 400 W lamps are used) and a quartz glass coil (inner diameter 1 mm, length 3–4 m) and is cooled using a fan (Figure 10.4). The optimal temperature for UV-digestion of organic compounds is ca. 70–80 °C.

The voltammetric system presented in Figure 10.3 operates in an automated batch-mode, with the analysis of 10 ml aliquots at a rate of one complete measurement every ca. 10–20 min. Each sample is fully calibrated, resulting in high quality data required for biogeochemical and pollution studies. The use of a lower calibration frequency would increase the sample through-put, but may pose problems in coastal and estuarine waters where important variations in the sample matrix would result in pronounced changes in the sensitivity of the voltammetric analysis. Dedicated soft-ware was produced for the voltammetric system for data acquisition, treatment and storage. The soft-ware is self-decisive and intelligent: it is able to reject failed scans, to perform additional scans when required and to make additional metal standard addition in case the initial peak increase was insufficient. The software capabilities have resulted in stand-alone monitoring system, allowing unattended 24 h operation. Table 10.1 shows the sequence of operation for an automated trace metal analysis using the system outlined above.

Table 10.1 Operational sequence for automated voltammetric metal measurements. Valve 1 and 2 are positioned before and after the sample loop, respectively (see Figure 10.3).

10.5 UNDERWAY PUMPING

A very recent development in marine trace metal studies is the application of analytical monitoring equipment on-board ship for near real-time measurements of surface waters using voltammetry (Achterberg and van den Berg, 1996). This new methodology uses underway pumping as a means of sample collection and thereby obviates the need for the vessel to halt for the collection of discrete samples. Near real-time dissolved trace metal determinations may be performed using on-line voltammetry. Sample contamination is prevented by eliminating contact of the sea water with metal components by using inert materials (e.g. Teflon®, Polyvinyl Chloride, Polyethylene). An effective underway pumping system can be designed using a peristaltic or Teflon®-bellows pump and a long (20–60 m) and strong Polyethylene or Polyvinyl Chloride hose. The hose is hung overboard and attached to a "fish" (torpedo-like structure, KIPPER-1) which is towed from a strong cable attached to a winch (Figure 10.5). The design and weight (ca. 40 kg) ensures that KIPPER-1 stays at a constant depth (ca. 3–4 m) even at speeds over 10 knots. KIPPER-1 is made of solid carbon steel with an inlet at the front and a hole through the middle for the sampling hose. The fish is coated with a non-metallic epoxy-based paint. All the tubing used is rapidly equilibrated with the sea water as it is automatically and continuously rinsed

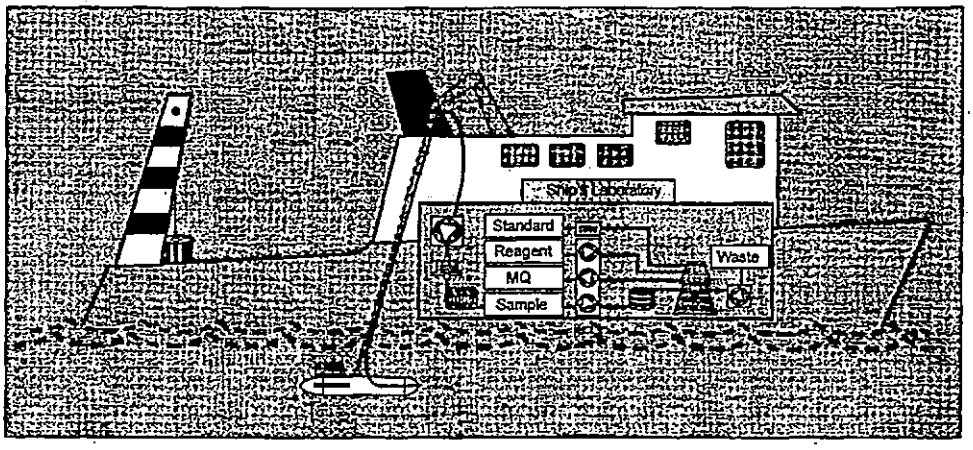

Figure 10.5 Schematic drawing showing the underway pumping system with KIPPER-1, the path of the sample through on-line filtration, on-line UV-digestion and to the metal monitor in the ship's laboratory.

during sample collection. This underway method of sampling is therefore largely self-cleansing. The fish should be positioned away, below and forward of the ship, so that the water is collected without contact with the ship's hull. Ship's hulls are known to release trace metals, especially after treatment with metal based paints to reduce attachment of barnacles and plankton.

Advantages of this method of underway sampling include a minimization of changes in chemical speciation of trace metals in sea water due to rapid analysis upon sampling, and a reduced risk of sample contamination. This monitoring approach results in enhanced sampling frequencies and is therefore an important tool for biogeochemical and pollution studies in marine systems which require high-resolution measurements. The data can, for example, be used in numerical computer models for modelling metal distributions and behaviour in marine systems. The near real-time analysis also provides the opportunity for an interactive sampling campaign, because the results of the measurements are directly available and can be evaluated on-board ship whilst the vessel is steaming.

10.6 OPEN OCEAN APPLICATION OF THE AUTOMATED VOLTAMMETRIC METAL MONITOR; NI IN THE ATLANTIC OCEAN

The low concentrations of trace metals in open ocean waters require very sensitive monitoring instrumentation. For dissolved Ni, the lowest levels (nanomolar or subnanomolar) occur in the surface waters, as a result of biological removal. The low inputs of trace metals to the open ocean and the effectiveness of the removal mechanisms result in rather uniform surface ocean concentrations for

Ni (and also for e.g. Cu, Cd and Zn). As a result of these processes, the variation in concentrations of Ni and many other trace metals is therefore not as large in surface waters of the open ocean, compared with coastal waters. Figure 10.6 shows results of near real-time determinations of Ni in the Atlantic Ocean. The automated voltammetric instrumentation was used on-board *RRS Discovery* during an OMEX (Ocean Margin Exchange) cruise in the Atlantic shelf and Channel region in August/September 1995. OMEX investigates fluxes of trace metals, nutrients an organic compounds over the Atlantic shelf waters. The automated metal monitor used during the OMEX cruise is similar to the system displayed in Figure 10.3. Surface sea water was pumped up with the use of a Teflon®-bellows pump from the fish which was positioned at a depth of 3–4 m. The seawater was not subjected to on-line filtration and UV-digestion and therefore "electrochemically-labile" Ni was determined. However, because the added chelating ligand (DMG) that was used forms a very strong complex with Ni and the organic matter and suspended particle concentrations were low in these waters, the observed labile concentrations were most likely close to the total dissolved Ni concentrations.

Each data point in Figure 10.6 is individually calibrated, resulting in high quality data. A simultaneous determination of Ni and Cu was performed on the Atlantic Ocean (Cu data not presented here). Only a fraction of the measurements performed during the 3 week cruise are presented here. The results show low Ni concentrations (between 1.2 and 2.5×10^{-9} mol l^{-1}) in the Atlantic Ocean, with oscillating Ni levels due to the vessel repeatedly crossing the shelf break towards open Atlantic waters (decease in Ni) or towards shelf waters (increase in Ni).

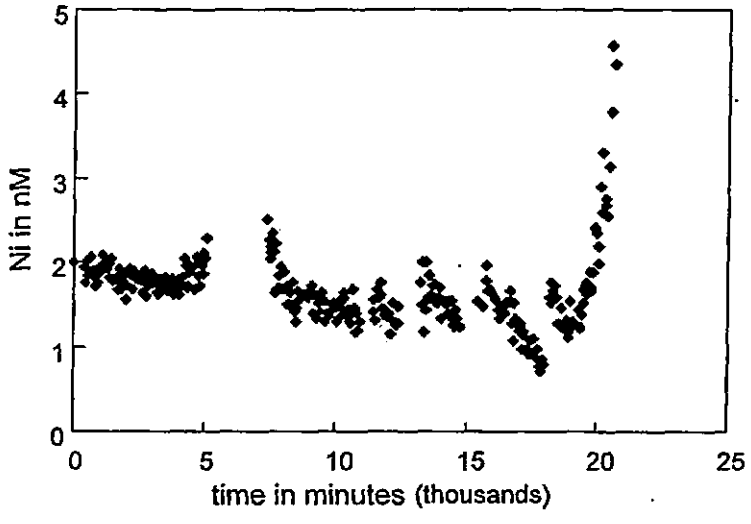

Figure 10.6 Labile Ni concentrations versus time in surface waters of the Atlantic shelf region between southern Ireland and western France (OMEX cruise, September 1995).

A further increase in Ni concentration was observed (to ca. 4.5×10^{-9} mol l^{-1}) as the vessel steamed into the English Channel towards Southampton. This increase in the concentration of Ni can be attributed to mixing of clean Atlantic waters with waters from the North Sea and riverine and atmospheric inputs into coastal waters in the vicinity of the British mainland. The gap in the graph (between ca. 5000 and 7000 min) is caused by a break in monitoring activities due to a hurricane.

10.7 COASTAL WATER APPLICATION OF THE AUTOMATED VOLTAMMETRIC METAL MONITOR; CU IN THE GULF OF CADIZ

High population density and industrialization in coastal areas have generated demand on marine resources, and have resulted in pollutant inputs into coastal waters. Sources of metals to coastal environments include effluents from industry, mining and ore processing activities, as well as the dumping of sewage sludge and industrial wastes at sea. Metal concentrations in coastal waters are variable as a result of the changing strength of point and diffuse sources, and seasonal variations in metal removal mechanisms. Tidal movement and currents influence local as well as long-range metal distributions at sea.

The strong variability in coastal waters requires a high spatial and temporal resolution in the design of sampling strategies. The movement of currents and tides has to be considered in order to avoid sampling a moving parcel of water repeatedly at adjacent sampling stations. Seasonal variations may affect not only biological and geochemical processes but also the direction and strength of prevailing and wind-induced currents. Data sets acquired during separate cruises can only be compared with each other if tidal movement and salinity distributions are taken into account.

Traditionally, a large number of discrete samples are taken and processed during coastal surveys, but such studies are expensive and time-consuming and can be viewed as "snap-shot" exercises. Ship-time and other economic considerations frequently limit the number of discrete samples that can be taken. The application to coastal monitoring of automated, near real-time ship-board monitors for metal analysis in surface waters addresses some of the challenges encountered in coastal sampling: (a) high spatial resolution can be achieved at slow steaming speeds, (b) calibrated measurements can span a wide concentration range, (c) precious steaming time between sampling stations is utilised, and (d) the scientist on duty has the opportunity to perform other tasks while overseeing the correct functioning of the metal monitor. The use of the automated voltammetric instrumentation is illustrated by its application in coastal waters of the Gulf of Cadiz, south-west Spain. The research is part of the TOROS project, which is an European Union funded ELOISE project and investigates metal fluxes in the Gulf of Cadiz. The shelf waters of the Gulf of Cadiz are enriched in dissolved metals, especially Cu, Zn, Pb and Cd. Studies conducted in the small, but strongly polluted Tinto and Odiel rivers have indicated that these rivers are important sources of metals to the coastal waters (Van Geen *et al.*, 1991; 1997; Leblanc *et al.*, 1995). The Tinto and Odiel rivers are characterised by low and

seasonal variable water discharge (combined annual average $15\,m^3\,s^{-1}$), and fresh water metal loads of up to 11×10^{-3} mol l^{-1} Fe, 6.1×10^{-4} mol l^{-1} Zn, 4.6×10^{-4} mol l^{-1} Cu and low pH values (pH 2.5–3) (data from November '96).

Figure 10.7 illustrates the advantages of high-resolution monitoring for this coastal system. Discrete samples (denoted by stars) were taken in the Gulf of Cadiz between the coast and the 500 m isobath on a grid of approximately 10–15 km. Discrete sampling was performed using a modified Niskin samplers on a CTD rosette. The continuous underway sampling approach resulted in a much better coverage of the coastal area compared with discrete sampling. The underway pumping system operated almost continuously during steaming and station time for 10 days. The ship's speed was 8 knots, and the resolution of the automated on-line metal analyses of surface samples was between 3.3 and 4.5 km. The distribution of dissolved Cu in Figure 10.8 shows enhanced metal levels in the coastal region between the mouths of the Huelva (15×10^{-9} mol l^{-1} Cu) and the Guadalquivir (20×10^{-9} mol l^{-1} Cu) estuaries. The data used in this plot were obtained during the first 4 days of the cruise in June 1997, and have not been corrected for tidal movement. A decrease in Cu concentrations with increasing distance from the coast was observed. This can be explained by the mixing of metal-polluted estuarine with cleaner Atlantic waters.

In Figure 10.9, four separate surveys on successive days in June 1997 are shown, and the size of the station markers is proportional to the dissolved Cu

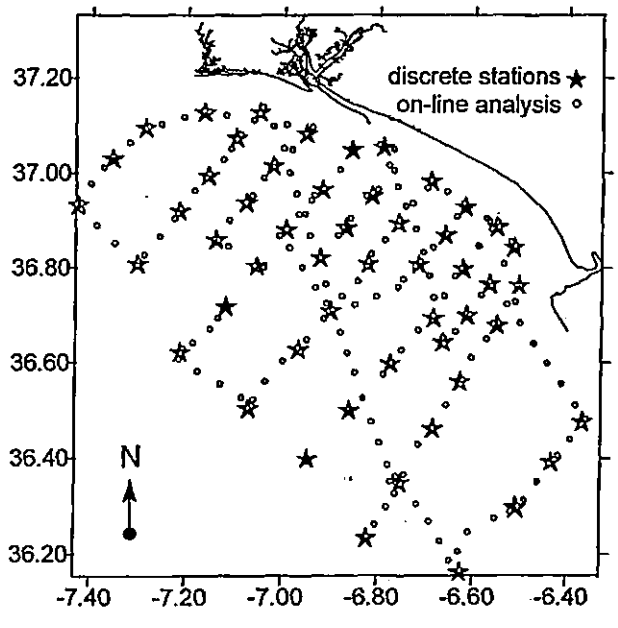

Figure 10.7 Discrete and on-line sampling during a four day survey in the Gulf of Cadiz, Spain (June 1997).

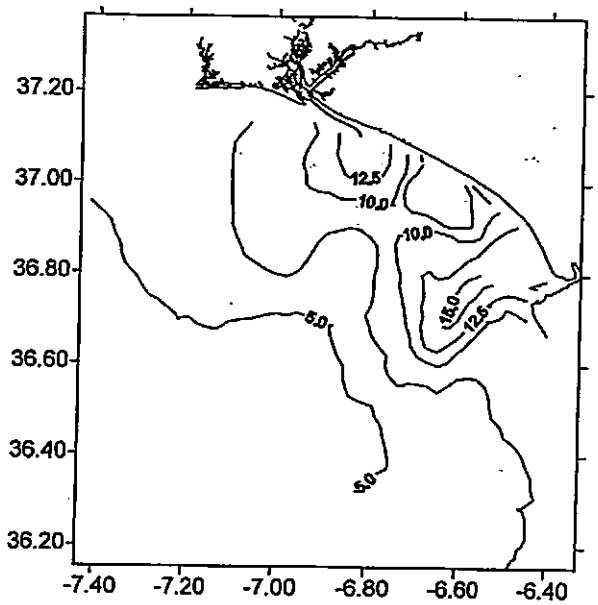

Figure 10.8 Contour plot of dissolved Cu in surface waters of the Gulf of Cadiz; automated on-line analysis during four day survey (June 1997).

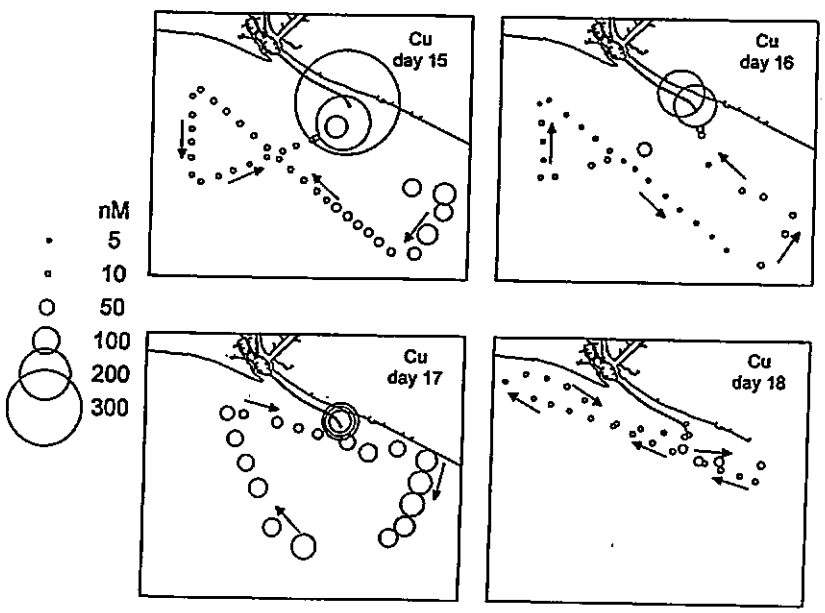

Figure 10.9 Dissolved Cu in coastal waters at the mouth of the Huelva estuary at different tidal stages (June 1997).

concentration measured. During the 4 days the ship's motion was not interrupted for discrete sampling exercises and sampling and analysis were carried out continuously at a speed of 4 knots. This resulted in high resolution data with a distance between sampling points of ca. 1.5–2.5 km, clearly showing the tidally dependent development of the Huelva estuarine plume. On day 15, elevated dissolved Cu concentrations ($60–76 \times 10^{-9}$ mol l^{-1}) were measured two to three hours after low water (LW) in an area to the south-east of the Huelva estuary. One day later (day 16), around the time of high water (HW), Cu concentrations between 13 and 14×10^{-9} mol l^{-1} were observed in this area. A steep increase in dissolved Cu concentrations to levels above 200×10^{-9} mol l^{-1} was observed during both days upon returning to the estuary about one hour ahead of LW. On day 17, the research vessel remained anchored at the mouth of the estuary for a 2.5 hour period, and left this position at the time of LW. Dissolved Cu levels increased during this period from 79 to 139×10^{-9} mol l^{-1}. On the subsequent semicircle around the estuary's mouth (radius approximately 10–12 km), elevated Cu levels were observed to the south-east ($68–85 \times 10^{-9}$ mol l^{-1} Cu) and south (90×10^{-9} mol l^{-1} Cu), with a decreasing trend to the west of the estuary. The three short surveys show the variability in the development of the metal plume in the Gulf of Cadiz and therefore, the data illustrates the value of high-resolution ship-board metal monitoring in tidally influenced waters.

10.8 APPLICATION OF AN AUTOMATED METAL MONITOR TO AN ESTUARINE ENVIRONMENT; NI IN THE TAMAR

Estuaries are highly reactive zones, where fluvial discharges mix with sea water and dissolved elements interact with organic material and particles in the water column. Thus constituents in river water undergo chemical and physical transformations during tidal mixing, and as a consequence only a limited proportion of trace metals carried by river water reach the open ocean. Enhanced concentrations of dissolved trace metals occur in many estuaries and are attributed to inputs from natural and anthropogenic sources. The concentration of dissolved trace metals is subject to large temporal and spatial variations as a result of variability in the extent of run-off, biological activity, tidal movement and anthropogenic discharges. An understanding of the fate of trace metals in estuaries is important for an evaluation of their impact on estuarine organisms, and fluxes into the oceans.

The study of trace metals in estuaries is complicated by the strong physico-chemical gradients (salinity, major ions, pH and turbidity) and high variability in trace metal concentration noticed in these systems. Large changes in water matrix chemistry present challenges which impair the performance of most analytical techniques. A typical style of surveying in estuaries involves sampling along an axial transect of an estuary. This is undertaken using a vessel which travels along the centre of an estuary from one water end-member to another e.g. from coastal marine water past the tidal limit to fresh river water (or vice versa). Discrete samples are collected by manually submerging sample bottles for

obtaining surface water, by using a peristaltic pump with a bottom weighted hose or Go-Flo or Niskin samplers for deeper samples. Salinity is generally accepted as the main index of mixing of sea water with river waters. A higher sampling frequency is usually adopted in the upper estuary where large salinity gradients occur and where variations in trace metal concentrations are more pronounced. Measurements of estuarine master variables (salinity, pH, dissolved oxygen and temperature) are usually carried out at the time of sampling using portable meters and probes, this procedure allows an interactive sampling campaign. Analysis of the samples is then undertaken upon return to a laboratory, the time between sampling and analysis could be in the order of days which may compromise the integrity of the water samples.

A very suitable approach for trace metal studies in estuarine environments involves the application of automated metal monitors, yielding high temporal resolution measurements of trace metals. Figure 10.10 shows the instrumental set-up utilised for automated analysis of total dissolved Ni by ACSV during a tidal cycle study carried out on the Tamar estuary, south-west England. The voltammetric metal monitor was transported in and operated from a regular medium sized town van, and powered by a 5 kW, 220–240 V portable generator. Surface water samples were collected using a float deployed in the estuarine channel. The float was attached to an anchor by a two metre nylon rope and a PVC hose was attached to the float and submerged to a depth of ca. 50 cm. Water was continuously pumped using a peristaltic pump (flow ca. 0.5–2 l min^{-1}) and on-line tangential filtration and UV-digestion was applied as described previously. A tidal cycle study describes a sampling style where samples are collected from a single geographical location on the estuary, and the changes in physicochemical conditions observed over the tidal cycle (ca. 13 hours) are particular to water mixing driven by tidal behaviour. This type of study may yield valuable information on biogeochemical processes occurring in the estuary, especially in estuaries with large salinity gradients. The main advantages of this approach include the ease of transportation and deployment of instrumentation and the relatively low costs of the studies compared with ship-board sampling exercises.

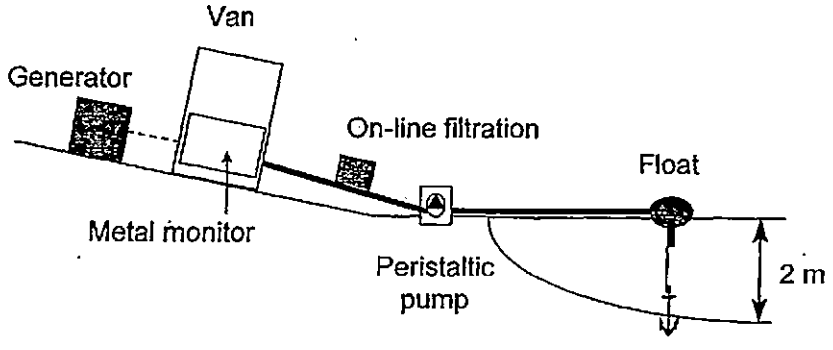

Figure 10.10 Monitoring set-up employed during tidal cycle study in the Tamar estuary.

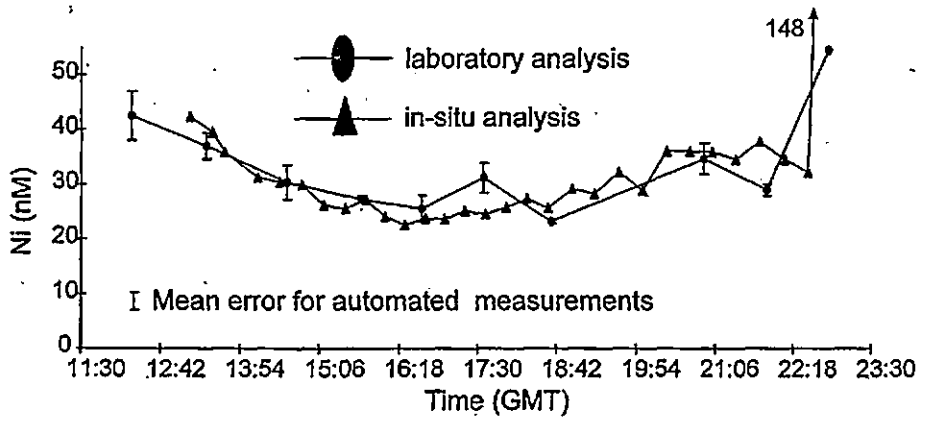

Figure 10.11 Results of tidal cycle study in the Tamar (July 1997), showing dissolved Ni concentrations from *in-situ* and laboratory analysis.

Figure 10.11 shows the results of automated total dissolved Ni measurements obtained from the *in-situ* application of the metal monitor on a bank of the Tamar Estuary July 1997). Figure 10.11 also shows values for total dissolved Ni obtained in discrete water samples collected from the estuary during the same study and analysed in the University laboratory. Quality of trace metal analysis in the laboratory was verified using certified reference materials. The *in-situ* and laboratory obtained data are within analytical uncertainty of each other, which demonstrates the high quality of the *in-situ* measurements. An important advantage of the *in-situ* monitoring approach includes the larger number of data points obtained during the automated study: 32 automated measurements compared with 10 discrete measurements. This allows a more thorough geochemical interpretation of the data. The trace metal measurements are presented in Figure 10.12, with complementary salinity and suspended particulate material (SPM) data. Salinity was obtained from conductivity measurements and SPM concentrations were obtained from weight of material collected on pre-weighed 0.45 µm membrane filters. Enhanced total dissolved Ni and SPM concentrations were observed at low salinities (up to 148 nM of Ni at a salinity of ~1) and low Ni and SPM concentrations were found at high salinities (23 nM of Ni at a salinity of ~24). Dilution of river water with enhanced Ni concentrations, with Ni depleted seawater therefore seems to be an important process determining the Ni behaviour in this estuarine system.

10.9 CONCLUSIONS AND FUTURE OF AUTOMATED MONITORING

The extremely low detection limits, coupled with its multi-element and speciation capabilities, high accuracy, modest cost and suitability to ship-board and flow analysis, have made stripping voltammetry an important technique for marine

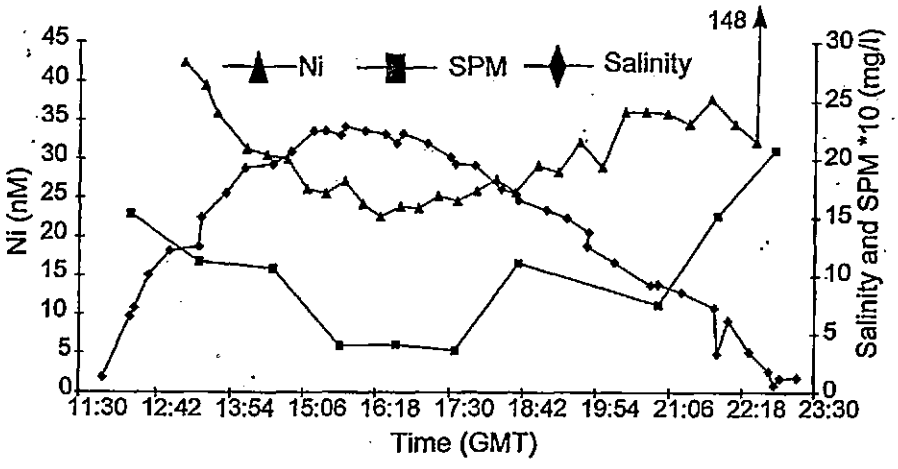

Figure 10.12 Results of tidal cycle study in the Tamar (July 1997), showing *in-situ* measured dissolved Ni concentrations with salinity and SPM (suspended particulate matter) data.

trace metal monitoring. The voltammetric trace metal monitor as described in this chapter, has been applied to different marine systems, ranging from unpolluted open ocean waters to metal polluted estuarine systems. The high resolution, high quality data obtained using the monitor are valuable for pollution control purposes, but also for biogeochemical modelling exercises. The automated voltammetric system, with on-line filtration and UV-digestion has recently been improved by incorporation of an on-line CTpH meter, for automated conductivity, temperature and pH measurements, complimenting the trace metal data. This low-cost approach of simultaneous automated data collection results in high quality data-sets which allow better interpretation of the chemical speciation in marine systems. The fully automated systems used on the Atlantic shelf, Tamar and Gulf of Cadiz perform ca. 3–6 fully calibrated metal determinations per hour. This number can be increased by using a flow cell fitted to an hanging mercury drop electrode. Up to 50–60 trace metal determinations per hour can then be performed, with calibration by switching to reagent with added metal standard at regular intervals (typically after 300 metal determinations) (Colombo and van den Berg, 1997). This approach is however less suitable for estuarine and near-coastal waters, where strong variations in salinity and dissolved organic matter concentrations will result in large changes in the sensitivity of the metal determination.

The trend in automated trace metal determinations is towards *in-situ* deployment of analytical instrumentation, with underwater application of sensors. This approach not only further reduces the risk of sample contamination, but also potentially leads to an improved way of trace metal speciation measurements as the *in-situ* analysis results in a minimal disturbance of the chemical equilibria.

The *in-situ* application of a hanging mercury drop electrode in a Swiss lake has been reported recently (de Vitre *et al.*, 1991; Tercier and Buffle, 1993). These workers used differential pulse ASV for the automated determination of Cu, Pb and Cd in Swiss lakes. A novel *in-situ* voltammetric profiling system reported by Belmont *et al.* (1996) makes use of a agarose membrane covered mercury plated Iridium-based micro-electrode for the determination of "ASV labile" Cu, Cd, Pb and Zn in fresh and marine waters. This system employs a coating on the electrode surface, and the diffusion of trace metals through this coating forms the time limiting step of the analysis, resulting in a measurement frequency of $2\,h^{-1}$. Wang *et al.* (1995) have reported the remote analysis of labile Cu in an estuarine system (San Diego Bay) using stripping potentiometry with a gold fibre electrode. This method has a reported limit of detection of ca. 5 nM, and is therefore suitable for estuarine and coastal waters with enhanced metal levels, but not for unpolluted ocean waters.

Acknowledgements

We would like to thank Dr. P.J. Statham (University of Southampton) for enabling EPA to participate in the OMEX cruise (D216). We thank the European Union for funding the TOROS project (Environment & Climate Programme ENV4-CT96–0217) and the University of Plymouth for funding DJW's studentship.

References

Achterberg, E.P. and van den Berg, C.M.G. (1994a). Automated voltammetric system for shipboard determination of metal speciation in sea water, *Anal. Chim. Acta*, 284, 463–471.

Achterberg, E.P. and van den Berg, C.M.G. (1994b). In-line ultra-violet digestion of natural water samples for trace metal determination using an automated voltammetric system, *Anal. Chim. Acta*, 291, 213–232.

Achterberg, E.P. and van den Berg, C.M.G. (1996). Automated monitoring of Ni, Cu and Zn in the Irish Sea, *Mar. Poll. Bull.*, 32, 471–479.

Baldwin, I.G. and Kramer, K.J.M. (1994). Biological Early Warning Systems. In *Biomonitoring of coastal waters and estuaries*, edited by Kramer, K.J.M. pp. 1–23. CRC Press.

Belmont, C., Tercier, M.L., Buffle, J., Fiaccabrino, G.C., Koudelka-Hep, M. (1996). Mercury-plated Iridium based microelectrode arrays for trace metals detection by voltammetry – optimum conditions and reliability, *Anal. Chim. Acta*, 329, 203–214.

Bruland, K. and Franks, R.P. (1983). Mn, Ni, Cu, Zn and Cd in the Western North Atlantic. In *Trace Metals in Seawater*, edited by Wong, C.S., Boyle, E.A., Bruland, K.W., Burton, J.D. and Goldberg, E.D. pp. 395–414. Plenum Press.

Bryan, G.W. and Langston, W.J. (1992). Bioavailability, accumulation and effects of heavy metals in sediments with special reference to United Kingdom estuaries: a review, *Envir. Poll.*, 76, 89–131.

Buckley, P.J.M. and van den Berg, C.M.G. (1986). Copper complexation profiles in the Atlantic Ocean, *Mar. Chem.*, 19, 281–296.

Colombo, C. and van den Berg, C.M.G. (1997). Simultaneous determination of several trace metals in seawater using cathodic stripping voltammetry with mixed ligands, *Anal. Chim. Acta*, 337, 29–40.

de Vitre, R.R., Tercier, M.-L. and Buffle, J. (1991). *In situ* voltammetric measurements in natural waters: the advantages of microelectrodes, *Anal. Proceedings*, 28, 74–75.

Howard, A.G. and Statham, P.J. (1993). *Inorganic trace analysis: philosophy and practice*, Wiley, p. 182.

Jickells, T.D. and Burton, J.D. (1988). Cobalt, copper, manganese and nickel in the Sargasso Sea, *Mar. Chem.*, 23, 131–144.

Kremling, K. and Pohl, C. (1989). Studies on the spatial and seasonal variability of dissolved cadmium, copper and nickel in North-East Atlantic surface waters, *Mar. Chem.*, 27, 43–60.

Larsen, P.F. (1992). Marine environmental quality in the Gulf of Maine, *Rev. Aquat. Sci.*, 6, 67.

Lauenstein, G.G., Robertson, A. and O'Connor, T.P. (1990). Comparison of trace metal data in mussels and oysters from a Mussel Watch Programme of the 1970s with those from a 1980s programme, *Mar. Poll. Bull.*, 21, 440–447.

Leblanc, M., Benothman, D., Elbaz-Poulichet, F. and Luck, J.M. (1995). Rio Tinto (Spain), an acidic river from the oldest and most important mining areas of Western Europe: Preliminary data on metal fluxes. In *Mineral deposits: From their origins to their environmental impacts, Proceedings of the third biennial SGA meeting, Prague*, edited by Pasava, J., Kribek, B. and Zak, K. pp. 669–670, A.A. Balkema.

Morley, N.H., Fay, C.W. and Statham, P.J. (1988). Design and use of a clean shipboard handling system for seawater samples, *Advances in Underwat. Technol.*, 16, 283–289.

Rijstenbil, J.W., Merks, A.G.A., Peene, J., Poortvliet, T.C.W. and Wijnholds, J.A. (1991). Phytoplankton composition and spatial distribution of copper and zinc in the Fal estuary (Cornwall, UK), *Hydrobio. Bull.*, 25, 37–44.

Stephenson, M.D. and Leonard, G.H. (1994). Evidence for the decline of silver and lead and the increase of copper from 1977 to 1990 in the coastal marine waters of California, *Mar. Pollut. Bull.*, 28, 148–153.

Tappin, A.D., Millward, G.E., Statham, P.J., Burton, J.D. and Morris, A.W. (1995). Trace metals in the Central and Southern North Sea, *Estuar. Coastal Shelf Sci.*, 41, 275–323.

Tercier, M.L. and Buffle, J. (1993). *In situ* voltammetric measurements in natural waters: future prospects and challenges, *Electroanalysis*, 5, 187–200.

Tessier, A. and Turner, D.R. (1995). *IUPC Series on Analytical and Physical Chemistry of Environmental Systems, Metal speciation and bioavailability in aquatic systems*, Vol. 3, Wiley, p. 679.

Van den Berg, C.M.G. (1989). Adsorptive cathodic stripping voltammetry of trace elements in sea water, *Analyst*, 114, 1527–1530.

Van den Berg, C.M.G. (1991). Potentials and potentialities of cathodic stripping voltammetry of trace elements in natural waters, *Anal. Chim. Acta*, 250, 165–276.

Van Geen, A., Boyle, E.A. and Moore, W.S. (1991). Trace metal enrichments in waters of the Gulf of Cadiz, Spain, *Geochim. Cosmochim. Acta*, 55, 2173–2191.

Van Geen, A., Adkins, J.F., Boyle, E.A., Nelson, C.H. and Palanques, A. (1997). A 120 yr record of widespread contamination from mining of the Iberian pyrite belt, *Geology*, 25, 291–294.

Wang, J., Foster, N., Armalis, S., Larson, D., Zirino, A. and Olsen, K. (1995). Remote stripping electrode for *in situ* monitoring of labile copper in the marine environment, *Anal. Chim. Acta*, 310, 223–231.

ELSEVIER

Analytica Chimica Acta 400 (1999) 381–397

ANALYTICA CHIMICA ACTA

www.elsevier.com/locate/aca

Stripping voltammetry for the determination of trace metal speciation and in-situ measurements of trace metal distributions in marine waters

Eric P. Achterberg *, Charlotte Braungardt

Department of Environmental Sciences, Plymouth Environmental Research Centre, University of Plymouth, Plymouth PL4 8AA, UK

Received 15 April 1999; accepted 21 July 1999

Abstract

Progress in marine chemistry has been driven by improved sampling and sample handling techniques, and developments in analytical chemistry. Consequently, during the last 20 years our understanding of marine trace metal biogeochemistry has improved a great deal. Stripping voltammetric techniques (anodic stripping voltammetry and adsorptive cathodic stripping voltammetry) have made an important contribution to this understanding. The selectivity and extremely low detection limits have made stripping voltammetry a widely used technique for trace metal speciation and trace metal distribution measurements in seawater. Stripping voltammetry is very suitable for ship-board and in-situ applications because of the portability, low cost and capability for automation of the voltammetric instrumentation. Future developments in stripping voltammetry can be expected in the field of stand-alone submersible voltammetric analysers, capable of continuous trace metal measurements. Future applications of stripping voltammetry can be found in the interactions between trace metal speciation and growth and the functioning of organisms in pristine and metal polluted marine waters.

Keywords: In-situ measurements; Trace metals; Voltammetry; Anodic stripping voltammetry; Adsorptive cathodic stripping voltammetry; Seawater; Monitor; Metal speciation

1. Introduction

Electrochemical techniques typically used by marine chemists for seawater analyses include potentiometry (pH) and amperometry (dissolved oxygen). Electrochemical techniques are also suitable for the determination of trace metals in seawater and voltammetry is the most common method. In seawater, trace metals often occur at low concentrations ($<10^{-8}$ M) and in case these concentrations are below the detection limit of the technique used, a preconcentration step is required prior to analysis. Moreover, the preconcentration step isolates the metal from the matrix and thereby enhances the selectivity of the analysis. Voltammetry is based on the measurement of a current response as a function of the potential applied to an electrochemical cell. In stripping voltammetry a preconcentration step is combined with a stripping step, thereby enhancing sensitivity and selectivity. During the preconcentration step, the trace metal of interest is collected onto or in a working electrode and during the stripping step the collected metal is oxidised or reduced back into solution [1]. The stripping voltammetric techniques suitable for the determination of ultra-low levels of trace

* Corresponding author. Tel.: +44-1752-233036; fax: +44-1752-233035

E-mail address: eachterberg@plym.ac.uk (E.P. Achterberg)

0003-2670/99/$ – see front matter
PII: S0003-2670(99)00619-4

metals in seawater include anodic stripping voltammetry (ASV) and adsorptive cathodic stripping voltammetry (AdCSV).

Important advances have been made during the past 25 years in the application of stripping voltammetry to marine trace metal measurements. The strength of stripping voltammetry is in its extremely low detection limits (10^{-10}–10^{-12} M), its multi-element and speciation capabilities and its suitability for on-line, ship-board and in-situ applications [1]. Analytical developments have resulted in our ability to determine a wide range of trace metals in seawater (over 20 metals) [2,3], and the instrumentation has been computerised, automated and become portable.

2. Voltammetric instrumentation

The basic voltammetric instrumentation for seawater analysis consists of a voltammetric analyser, a three-electrode cell (working electrode, reference electrode and counter electrode) and a computer for automated measurements and data acquisition. Modern voltammetric analysers are simple, low-cost and able to perform a range of scan forms. The Ag/AgCl/KCl reference electrode is commonly used and the counter electrode may be a platinum wire or a carbon rod. The most popular working electrodes for environmental trace metal analysis are the hanging mercury drop electrode (HMDE) and the mercury film electrode (MFE). The automatic HMDE and the rotating Hg coated electrodes are particularly suitable for stripping voltammetry.

The advantage of an HMDE is its reliability. With the formation of each new drop, a new electrode surface is produced, which is important for unattended trace metal monitoring activities. The drops generated by modern Hg drop electrodes are very small (e.g. VA Stand 663 from Metrohm (Switzerland) produces drops with an area of 0.52 mm^2), and safe storage and recycling of the used Hg will ensure minimal environmental risks.

The MFE may be formed by in-situ plating of Hg on glassy carbon [4], or by preliminary deposition. The MFE is robust and has an excellent sensitivity due to a high surface area to volume ratio [4]. Hg is commonly plated on glassy carbon electrodes, but gold [5], iridium [6,7], graphite pencil [8] and carbon fibre [9] have also been used. The application of semi-permeable protective membranes to cover the MFE in order to prevent diffusion of interfering compounds (e.g. surfactants) towards the electrode surface has been reported. Cellulose acetate [10], agarose [11] and Nafion [12] have been used as membranes on MFE and work by size-exclusion and/or electric repulsion.

Non-Hg electrodes, for example made from gold [13] or various carbon substrates have also been used for electrochemical measurements in natural waters. Such solid electrodes are suitable for the determination of Cu, Hg and Pb, and elements which have oxidation potentials more positive than Hg (e.g. Ag, Au, Se and Te) [1]. The surface of these electrodes is often poorly defined and the capacitance current [14] is higher than for Hg electrodes. Consequently, the voltammetric analysis of trace metals with solid electrodes is less sensitive and reproducible compared with HMDE or MFE. However, the attractions of Hg-free electrodes for electrochemical trace metal measurements have resulted in research efforts in this field. Recent developments include circuit-board printed gold electrodes for Pb analysis [15] and the application of gold fibre microelectrodes for the determination of Cu, Hg, Pb and Se in water [13].

In recent years much progress has been made in the field of microelectrodes. Such electrodes have a size $< 10\,\mu m$ and may have a bare or Hg coated surface. Microelectrodes have a reduced capacitance current and an excellent signal to noise ratio and these characteristics allow subnanomolar trace metal analysis [6,16]. Furthermore, they offer enhanced deposition efficiency because of increased mass transport, which is the result of diffusion. Measurements using microelectrodes can therefore be performed in quiescent solutions, which is attractive for in-situ deployments in natural waters. Successful applications of trace metal determinations in natural waters have been reported for gold microelectrodes [13], Hg plated carbon fibre microelectrodes [17] and Hg plated iridium microelectrodes [6,18,19].

3. Anodic stripping voltammetry

ASV is an established and widely used voltammetric technique. Most applications of ASV have been reported with the use of HMDE or MFE, and the

technique has been applied successfully for trace measurements of Cu, Cd, Pb and Zn in seawater [20]. ASV is suitable for the determination of other elements (e.g. In, Tl), however, their seawater concentrations are commonly too low, or the analysis is hampered by interferences.

During ASV analysis, a deposition, or preconcentration, step is carried out under conditions of forced convection, which may include solution stirring or flow (microelectrodes need no forced convection). The deposition potential should be ca. 0.3–0.4 V more negative than the reduction potential of the metal. During the deposition step metal ions are collected in the Hg by reduction (to a metallic state) and amalgamation with the Hg (see Eq. (1)). Only a small fraction of the metal is actually being deposited during the deposition step.

$$M^{n+} + ne^- + Hg \leftrightarrow M(Hg) \quad (1)$$

The sensitivity of ASV is improved by using a Hg film rather than a Hg drop electrode because the smaller volume of the Hg film results in a greater concentration factor of the metals collected into the Hg. The deposition is followed by a voltammetric scan towards more positive potentials during which the metal in the Hg is oxidised and the current produced is determined. The resultant current-potential stripping voltammogram provides (a) quantitative information: the height of the peak is proportional to the metal concentration; and (b) qualitative information: the potential of the peak is an indication for the metal analysed. Quantification of metal concentrations in samples during voltammetric analysis (both ASV and AdCSV) is commonly by use of the standard addition method. This is the preferred method as the sensitivity of the stripping voltammetric analysis may vary between samples of different ionic strength and containing different concentrations of surfactants and natural trace metal complexing organic ligands.

Different scan forms have been applied during the ASV measurement of trace metals in seawater to improve the sensitivity of the methods. The most basic scan form for a MFE is linear sweep, but pulse-voltammetric waveforms (e.g. differential pulse and square wave) are commonly used for HMDE and are more useful as they effectively correct for background current contributions. The limit of detection for ASV analysis of Cu and Cd in seawater is typically 10^{-11} and 10^{-10} M, respectively. Depending on the encountered trace metal levels in a marine system, ASV allows for simultaneous determination of more than one metal.

4. Adsorptive cathodic stripping voltammetry

AdCSV is a very sensitive technique for the analysis of numerous trace metals which cannot be determined in seawater using conventional electrolytic stripping procedures. AdCSV makes use of a specific added ligand (AL), which is added to the water sample and forms an adsorptive complex with the trace metal(s) under investigation (Eq. (2)).

$$yM^{n+} + zAL^{m-} \leftrightarrow M_y(AL)_z^{(yn-zm)} \quad (2)$$

$$M_y(AL)_z^{(yn-zm)} \leftrightarrow M_y(AL)_z^{(yn-zm)} \text{ adsorbed} \quad (3)$$

$$M_y(AL)_z^{(yn-zm)}\text{adsorbed} + e^- \leftrightarrow yM^{(n-1)+} + zAL^{m-} \quad (4)$$

A pH buffer is used to control the pH of the sample, as the formation of the metal–AdCSV ligand complex is pH dependent. Generally, AdCSV is carried out using a HMDE. A minute fraction of the metal–ligand complex is adsorbed on the surface of the Hg drop (Eq. (3)) and a potential scan is carried out. The adsorption step is carried out at a carefully controlled potential as it determines the adsorption efficiency. In most cases, an adsorption potential is chosen which is slightly more positive (ca. 0.1 V or more) than the reduction potential of the metal–ligand complex. The scan direction is towards more negative potentials and the resulting current is measured (see Fig. 1). The current produced is the result of the reduction of a reducible group on the ligand or of the metal itself in the adsorbed complex (Eq. (4)). The scan forms applied during AdCSV include linear sweep, but fast pulse-voltammetric waveforms (e.g. differential pulse and square wave) are also used if the reduction of the metal–ligand complex is electrochemically reversible. The advantages of fast scan forms include compensation against the capacitance current contribution, a reduction of interferences from dissolved oxygen and an improved speed of analysis.

Table 1
AdCSV methods for direct determination of trace elements in seawater

Element	Complexing ligand	Detection limit (nM)	Reference
Al	1,2-Dihydroxyantraquinone-3-sulfonic acid (DASA)	1	[106]
As	Pyrrolidine Dithiocarbamate (PDC)	3	[62]
Co	Dimethylglyoxime (DMG); Nioxime with nitrite as catalyst	0.1; 0.003	[21,107]
Cr	Diethylenetriaminepentaacetic acid (DTPA) with nitrate as catalyst	0.05	[41]
Cu	8-Hydroxyquinoline (oxine); Salicylaldoxime (SA)	0.2; 0.1	[65,66]
Fe	Catechol; 1-Nitroso-2-Naphthol (N-N)	0.2;.0.1	[108,109]
Mo	2,5-dichloro-3,6-dihydroxy-1,4-benzoquinone; Mandelic acid with chlorate as catalyst	0.2; 0.002	[23,110]
Ni	DMG	0.1	[107]
Pt	Formazone	0.0004	[22]
Sb	Catechol	0.6	[111]
Se	$Cu(I)_2Se$	0.01	[112]
Sn	Tropolone	0.05	[113]
Ti	Mandelic acid with chlorate as catalyst	0.007	[23]
U	Mordant Blue; oxine in presence of EDTA	1; 0.2	[114,115]
V	Catechol with bromate as catalyst	0.07	[116]
Zn	Ammonium Pyrrolidine Dithiocarbamate (APDC)	0.07	[117]

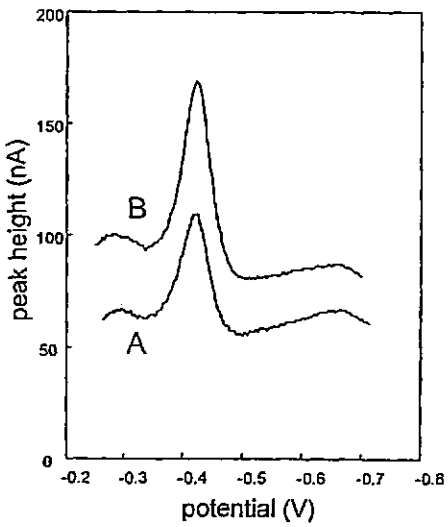

Fig. 1. Voltammetric scan of dissolved Cu in seawater. Oxine (0.15 mM) was used as the AdCSV ligand and HEPES (10 mM) as pH buffer (pH 7.8). Voltammetric conditions were: 20 s deposition at — 1 V, 8 s equilibration at — 0.25 V and 200 Hz square wave scan towards more negative potentials. Scan A is for a seawater sample, and scan B is for the sample plus standard addition (5×10^{-9} M, final concentration).

The adsorptive accumulation approach results in a very effective preconcentration with short adsorption times, allowing fast and extremely sensitive trace metal measurements. The limit of detection of AdCSV for trace metals is typically on the order of 10^{-9}–10^{-11} M. Even lower metal concentrations can be determined by enhancing the reduction current catalytically (10^{-12} M for Co [21], Pt [22] and Ti [23]). AdCSV methods have been developed and applied during the last 20 years for a wide range of trace metals in seawater. Table 1 lists AdCSV methods for direct determination of trace metals in seawater, together with their limit of detection. Table 1 is not intended as a complete list, neither does it cover all elements for which AdCSV methods are available, nor does it include all reported AdCSV ligands. The organic ligands in Table 1 contain N and O donor groups (e.g. DMG and oxine), in addition to S donors (e.g. APDC). To be suitable for AdCSV, ligands are required to have two properties: (a) the ability to form a complex with the element of interest, and (b) electroactivity (i.e. capability to adsorb onto the surface of the HMDE). Many of the ligands shown in Table 1 have aromatic ring structures. DMG is an exception, but forms a ring structure on chelation with Ni^{2+} [2]. The adsorption of the ligands is affected by the deposition potential and it therefore appears that the presence of electrostatic and π–electron interactions are significant for the adsorption process [2].

In many cases, AdCSV has been utilised as a single-element method. However, multi-element AdCSV methods for HMDE have been developed recently [24], whereby with the use of mixed AdCSV ligands up to 6 trace metals (Cu, Pb, Cd, Ni, Co and Zn) can be determined simultaneously in coastal and estuarine waters.

5. Measurements of total dissolved trace metals in seawater

The largest problem associated with trace metal studies in the marine environment is the contamination of samples during the stages of sampling, filtration, storage, sample preparation and analysis. This contamination problem has long hampered marine trace metal studies, and consequently dissolved trace metal data published before the end of the 1970s can be regarded as suspect. The introduction of strict clean working practices [25,26] gave rise to high quality trace metal data, and resulted in an improved understanding of oceanic trace metal distributions and processes. Clean working practices at sea include the use of acid cleaned samplers for contamination-free collection of discrete seawater samples. The samplers (Go-Flo or Niskin) typically have a volume of 10–20 l and are made from PVC with a Teflon inner lining and a PTFE tap and silicone seals (instead of rubber). Upon sampling, the seawater is filtered using acid-cleaned membrane filters (typical 0.4 μm polycarbonate, 47 mm diameter) fitted into acid-cleaned filtration units (made from FEP, polysulfone or polyethylene), and subsequently stored in acid-cleaned high density polyethylene (HDPE) sample bottles. Acid cleaning of HDPE sample bottles can be performed by overnight cleaning with hot detergent, followed by a 1-week soak in 6 M HCl (AnalaR grade, Merck) and subsequently a 1-week soak in 2 M HNO_3 (AnalaR grade, Merck). In between the soaks, the bottles are rinsed with copious amounts of de-ionised water. Prior to use, the bottles are filled with de-ionised water, acidified to pH 2 with quartz-distilled acid and stored in two re-sealable polyethylene bags. Filtered discrete seawater samples are acidified with ultra-clean quartz-distilled acid [27], prior to ship-board or land-based analysis (typically samples are acidified to pH 2 in case of subsequent voltammetric analysis). All sample handling should take place in a class-100 laminar flow hood, which is ideally situated in a clean container (supplied with particle-free clean air).

A widely used analytical technique for the analysis of trace metals in seawater is graphite furnace atomic absorption spectrometry (GFAAS) after solvent extraction (e.g. [28]). The extraction procedure may involve the use of metal complexation using DDDC/APCD . (Dipyrrolidine Dithiocarbamate/Ammonium Pyrrolidine Dithiocarbamate) and extraction of the metal complex into chloroform, often followed by back extraction into nitric acid. This process not only removes compounds from the seawater matrix which interfere with the analysis (e.g. Ca, Mg, Cl, Na), but also results in preconcentration of the analyte under investigation. The use of solid-phase preconcentration techniques (e.g. Chelex column [29]) prior to GFAAS analysis has also been reported, and allows automation of the analytical method using a flow analysis approach. Multi-element techniques, such as ICP-AES and ICP-MS (inductively coupled plasma atomic emission and mass spectrometry, respectively) have a high potential for total dissolved trace metal analysis in seawater. In recent publications, the developments of ICP-AES [30] and ICP-MS [31,32] methods have been reported for analysis of trace metals in seawater after solid phase extraction. Application of such methods by the marine chemistry research community is, however, not yet common.

Stripping voltammetric techniques do not have the multi-element capabilities of ICP-AES/ICP-MS, but have the advantage of allowing determinations directly in seawater, as preconcentration is performed in the voltammetric cell itself. Alkali metals present in seawater do not interfere with trace metal determinations, but in many cases actually increase the sensitivity of the voltammetric methods because of their role as electrolyte. The reduction in the sample handling minimises the risk of sample contamination and allows automation of the instrumentation. A common treatment of acidified samples is the application of UV-digestion prior to total dissolved trace metal analysis by stripping voltammetry [33]. The UV light breaks down surfactants, which could interfere with the analysis by adsorbing onto the HMDE or MFE during the preconcentration step and therefore, hinder the passage to the electrode of metal cations (ASV) or of metal–AdCSV ligand complexes. In addition, the UV-digestion breaks down metal-complexing organic ligands, which occur naturally in seawater. Fig. 2 shows a home-built UV-digestion unit with a 400 W medium pressure Hg vapour lamp (Photochemical Reactors). The UV-digestion is performed on discrete samples (ca. 30 ml) placed in quartz tubes with a Teflon screw cap. A UV-digestion period of 3 h is sufficient [33] to achieve the breakdown of interfering

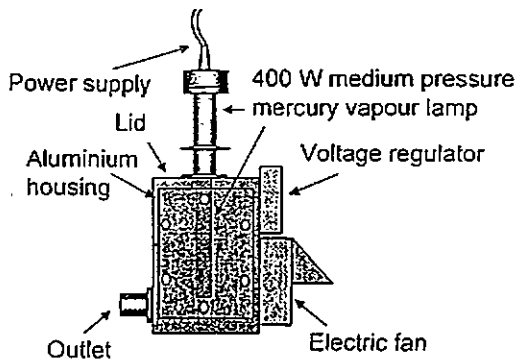

Fig. 2. Drawing of an UV-digestion system for breakdown of dissolved organic compounds in natural waters.

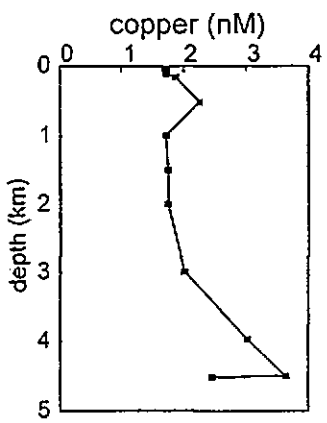

Fig. 3. Depth profile of total dissolved Cu in the Northeast Atlantic Ocean (*RRS Challenger* cruise 1991).

organic substances in acidified samples. In order to aid the breakdown, 10 mM H_2O_2 (final concentration) is added to the sample prior to UV-digestion. The UV unit is air-cooled using a fan, resulting in a sample temperature during digestion of ca. 70°C.

Fig. 3 shows a depth profile of total dissolved Cu in the Northeast Atlantic Ocean (station 11; position: 45 25.44 N and 20 0.31 W) collected during the *RRS Challenger* cruise CH76/91. The sample collection, filtration, storage and analysis were undertaken using ultra-clean working practices. Total dissolved Cu in the oceanic samples was determined after UV-digestion, using AdCSV with Tropolone (0.4 mM, final concentration) as complexing ligand and HEPES (*N*-hydroxyethylpiperazine-*N*′-2′-ethanesulphonic acid) as pH buffer (0.01 M final concentration;

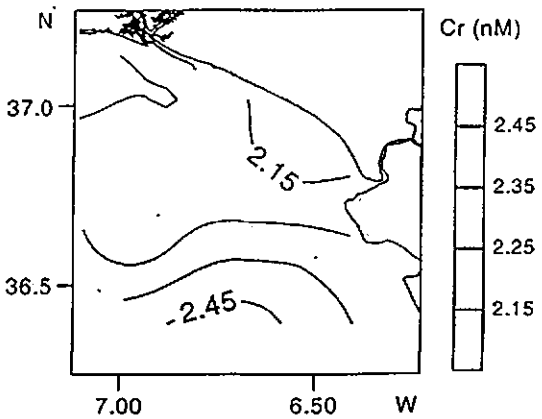

Fig. 4. Contour plot of total dissolved Cr in the Gulf of Cadiz.

pH 7.77) [34]. Certified reference material (CRM; NASS-2 open ocean seawater) was analysed to verify the accuracy of the AdCSV method. Dissolved Cu at station 11 showed lowest concentrations (ca. 1.6 nM) in the surface ocean, and an increase in concentration (to ca. 3.5 nM) with depth [35]. This behaviour is typical for Cu in the open ocean, as it is taken up as a micro-nutrient by phytoplankton in the surface waters and released in deeper waters upon sinking and degradation of the phytoplankton cells [36].

AdCSV has shown advantages over GFAAS methods for the analysis of Cr, U and V in seawater. These metals occur in oxygenated seawater mainly as negatively charged metal oxides and carbonates (CrO_4^{2-}, $[UO_2(CO_3)_3]^{4-}$, $VO_2(OH)_3^{2-}$). Commonly used preconcentration/matrix removal methods for these trace metals are often cumbersome (e.g. Co-APDC coprecipitation of Cr and V [37]) and the GFAAS methods for U and V are not very sensitive. Consequently, few studies have been reported on the behaviour of these metals in seawater. Sensitive AdCSV methods for Cr, U and V in seawater are available (see Table 1). Applications of these methods include a study of dissolved Cr distribution in English coastal waters [38], U in the Tamar estuary [39] and V in the Mediterranean [40]. Fig. 4 shows a surface contour plot of the distribution of total dissolved Cr in the Gulf of Cadiz (southwest Spain). Discrete samples were obtained from a depth of ca. 5 m using modified Niskins and filtered on-board ship (B/O *Garcia del Cid*; TOROS IV survey, October 1998). Total dissolved Cr was analysed in the laboratory in Plymouth, using DTPA as AdCSV ligand,

acetate as the pH buffer (pH 5.2) and nitrate as redox catalyst (final concentrations 2.5, 50, and 500 mM, respectively) [41]. Prior to analysis, samples were subjected to UV-digestion (3 h) to break down interfering surfactants and convert any Cr(III) present to Cr(VI) [33]. Total dissolved Cr concentrations in the surface waters Gulf of Cadiz ranged between 1.6 and 2.9 nM and were lower than in Western Mediterranean surface waters (between ca. 2.5 and 4 nM [42]), but comparable to levels observed in the surface waters around England (between ca. 1 and 2.5 nM) [38]). As a result of the higher suspended particulate matter concentrations in coastal waters compared with open ocean waters, the particle scavenging of dissolved Cr is probably more effective at reducing Cr concentrations in the coastal seas [38].

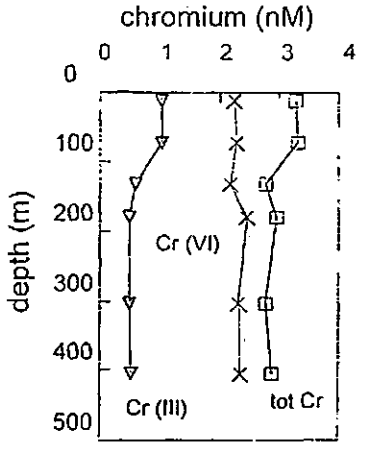

Fig. 5. Depth profiles of total dissolved Cr, Cr(VI) and Cr(III) at station 7 in the Western Mediterranean (37.5°N, 10°E) analysed on-board ship within 24 h upon sampling (*FS Valdivia* cruise, 1992).

6. Trace metal speciation studies

The high sensitivity and selectivity of stripping voltammetry make this technique very suitable for trace metal speciation studies. Speciation analysis involves the determination of different physico-chemical forms of trace metals. Metal speciation studies have become important because of the recognition that total dissolved metal concentrations do not yield sufficient information about the toxicity, bioavailability and geochemical behaviour of trace metals in natural waters. Many metals are essential for growth and metabolism of organisms, and these are termed micro-nutrients (e.g. Co, Cu, Fe and Zn). Growth limitation may occur when concentrations of micro-nutrients become too low (e.g. in the case of the dinoflagellate Gonyaulax tamarensis $[Cu^{2+}]<3\times10^{-13}$ M) [43]. On the other hand, enhanced concentrations of metals may cause toxic effects (G. tamarensis at $[Cu^{2+}]>2.5\times10^{-10}$ M) [44]. For many metals (including Cu, Zn, Cd and Ni) the free aqueous ions have been reported to be the most bioavailable and toxic, because of their ability to pass through the cell membrane of phytoplankton and macro algae [45,46]. In contrast, metals complexed by organic ligands (e.g. humic acids, fulvic acids, EDTA and NTA) are not able to pass cell membranes, and the presence of such ligands in natural waters reduces the availability of metals to organisms.

Only a few analytical techniques (including stripping voltammetry and chemiluminescence [47]) are sensitive enough to determine labile/free aqueous metal fractions in natural waters. Trace metal speciation measurements need to be performed as soon as possible upon sampling, as the chemical equilibria in natural waters are readily disturbed during sample storage. The application of in-situ (including ship-board) techniques is therefore, preferred.

A great number of trace metal speciation studies in marine waters utilising stripping voltammetry have been reported during the last decade [39,42,48–61]. Stripping voltammetry has been used to investigate (A) redox speciation, (B) the fraction of organically complexed metal, and (C) concentration of naturally present metal complexing organic ligands.

(A) AdCSV has been used to determine the different redox species of As [62], Fe [63] and Cr [42] in marine waters. The thermodynamically stable form of Cr in oxygenated seawater is Cr(VI) (as CrO_4^{2-}). However, significant amounts of Cr(III) have been found in natural oxygenated waters. Fig. 5 shows depth profiles of dissolved Cr species in the Western Mediterranean [42]. Total dissolved Cr (comprising of Cr(III) and Cr(VI)) was determined after UV-digestion of the seawater, and dissolved Cr(VI) after selective removal of Cr(III) from seawater using Lichrosorb Si 60 silica (Merck) [42]. Dissolved Cr(III) was determined as the difference between total dissolved Cr and Cr(VI). Total dissolved Cr concentrations ranged between 3 and

4 nM, with somewhat lower Cr(VI) concentrations. Dissolved Cr(III) concentrations ranged between 0.5 and 1.5 nM, with maximum concentrations in the surface layer, this maximum has been attributed to photochemical reduction of Cr(VI) to Cr(III) [42].

(B) Dissolved inorganic/organic speciation measurements in seawater may be performed using ASV and AdCSV. The ASV method measures the equilibrium concentrations of free metal ions and labile metal complexes that dissociate to free metal ions during the analytical timescale of the measurement. ASV therefore, determines inorganic trace metals (i.e. free metal ions and inorganic complexes) and may include a fraction of relatively labile organic complexes. Ligand competition is used for speciation measurements by AdCSV, whereby the added ligand competes for trace metals with naturally occurring metal-complexing ligands. This method determines inorganic and weakly complexed trace metals. The competition conditions, or detection windows [64], can be carefully controlled by choosing a suitable AdCSV ligand (with known conditional stability constants for the metal under investigation) at an appropriate concentration. For example, AdCSV ligands used for speciation measurements of Cu in natural waters include Tropolone [34], Salicylaldoxime [65] and oxine [66], with Tropolone being the weakest Cu complexing AdCSV ligand and oxine the strongest. The ligand competition approach is used to determine labile trace metal fractions, and also to determine the concentration of natural metal complexing ligands with their conditional stability constants (see (C)). An example of the former approach is presented in Fig. 6, which shows depth profiles of labile and total dissolved Ni in the Gulf of Cadiz (TOROS I survey, November 1996). Dissolved labile Ni was determined within 48 h upon sampling in a land-based laboratory. The filtered seawater samples were allowed to equilibrate (in FEP bottles, 30 ml) for a period of 12 h after addition of DMG (final concentration 20 μM) and HEPES buffer (final concentration 10 mM, pH 7.77). Total dissolved Ni was determined in Plymouth after UV-digestion of acidified samples. The largest difference between total and labile Ni was observed in the surface waters, where the non-labile Ni fraction ranged between 37% and 72% of the total. The high proportion of non-labile Ni in the surface waters can most likely be attributed to presence of enhanced concentrations of Ni complexing organic matter. Little is known about the nature of metal complexing organic matter, but it is thought to include algal exudates and breakdown products of phytoplankton cells.

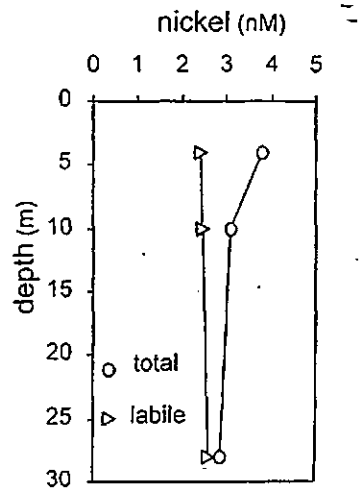

Fig. 6. Depth profiles of labile and total dissolved Ni in the Gulf of Cadiz. Dissolved labile Ni was determined within 48 h upon sampling. Total dissolved Ni was determined in the laboratory in Plymouth, after UV-digestion of acidified samples.

(C) Metal titrations are used to determine the concentration of natural metal complexing ligands (L) and their conditional stability constants (K'_{ML}). For this purpose, a seawater sample is divided into typically 10 sub-samples (in polystyrene or FEP vials), to which increasing amounts of metal are added. After addition of the AdCSV ligand and a pH buffer, an equilibration period of typically 12 h is applied. Subsequently, the labile metal concentrations are measured in the sub-samples. Linear [67,68] or non-linear [69] data transformation allow the determination of L and K'_{ML}, in addition to the free aqueous metal concentration. The natural ligand concentration (L) and K'_{ML} provide information about the capacity of natural waters to buffer additional inputs of metals, and the binding strength of L for the metal under investigation, respectively. The free aqueous metal concentration, which is calculated from L and K'_{ML}, provides information about the possible biological effects of the metal.

The natural ligands determined using the AdCSV method with ligand competition are operationally defined. The detection window for titrations is described using the α coefficient of the complex formed between

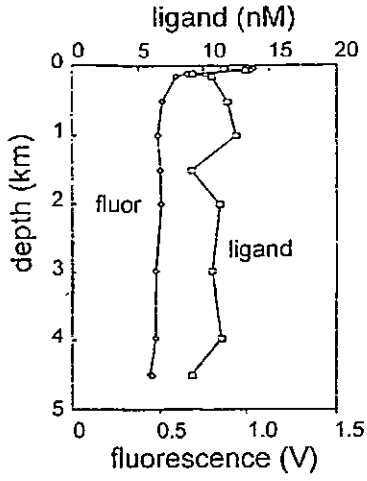

Fig. 7. Depth profile of the concentration of natural Cu complexing ligands and fluorescence in the Northeast Atlantic Ocean (48°N, 20°W). Seawater samples were equilibrated in FEP bottles (30 ml) after addition of Cu in the presence of Tropolone and borate buffer (final concentrations 0.4 and 10 mM, respectively).

the added AdCSV ligand and the metal under the specific experimental conditions [64]. The α coefficient is the ratio between the metal concentration which is complexed by a particular ligand or group of ligands over the free metal concentration [70] and can be defined by

$$\alpha'_{M(AL)_n} = \sum K'_{M(AL)_n}[AL]^n \quad (5)$$

where $K'_{M(AL)_n}$ is the conditional stability constant for the nth complex between the metal and added ligand and [AL] is the added ligand concentration. Ligand competition techniques optimally detect natural ligands that are within plus or minus one-order of magnitude of the detection window [71]. If the metal–natural ligand complexes have α coefficients that are outside this range of detection, errors in the determination of the conditional stability constant are encountered.

Fig. 7 shows a depth profile of concentrations of natural Cu complexing ligands in the Northeast Atlantic Ocean determined using automated AdCSV [72] on-board ship [35]. The depth profile of natural Cu complexing ligands showed a close similarity with in-situ determined fluorescence, which is a measurement of the chlorophyll and phaeopigment concentrations. The maximum ligand concentration coincided with a maximum in fluorescence, indicating that the ligands observed in the Atlantic were derived from primary producers. The conditional stability constants of the Cu complexing natural ligands ranged between 12 and 13 (log values), at the detection window used ($\log \alpha_{CuTrop} = 3.29$). The calculated free cupric ion concentrations [Cu^{2+}] ranged between 7×10^{-14} and 2.5×10^{-13} M, indicating that [Cu^{2+}] was neither bio-limiting nor toxic.

The AdCSV method has also been used to determine the organic complexation of Fe in seawater. In some cases, nearly the whole (99%) dissolved Fe pool in seawater has been reported to be bound by strong Fe complexing organic ligands (L) ($K'_{FeL} > 10^{18}$) [73–75]. The strong complexation significantly reduces the concentration of free iron ions [74], which are thought to be available for uptake by phytoplankton in seawater. The interest in dissolved Fe and its speciation in oceanic waters has been caused by the proposed hypothesis that Fe is limiting primary productivity in certain remote parts of the worlds' ocean which exhibit high concentrations of macro-nutrients (N, P), but low chlorophyll levels [76]. The sensitivity and speciation capabilities make AdCSV a suitable technique to investigate the concentration and conditional stability constants of the Fe complexing natural ligands.

7. Ship-board trace metal measurements

The need for monitoring of metals in marine environments is well established. In the case of the UK, the requirements have been specified by the Paris convention and European Union Directives. Although existing laboratory-based techniques are powerful, the sample handling/processing stages prior to analysis are time consuming and carry a risk of sample contamination. There is a need for rapid and automated ship-board trace metal monitors which produce high quality data at a high resolution. The use of analytical instrumentation at sea places special demands on the instrumentation with respect to automation, portability and robustness.

Suitable techniques for ship-board dissolved trace metal analysis include colorimetry, chemiluminescence and stripping voltammetry. These techniques can be operated in a flow-analysis mode, whereby sample and reagent transport (including any sample

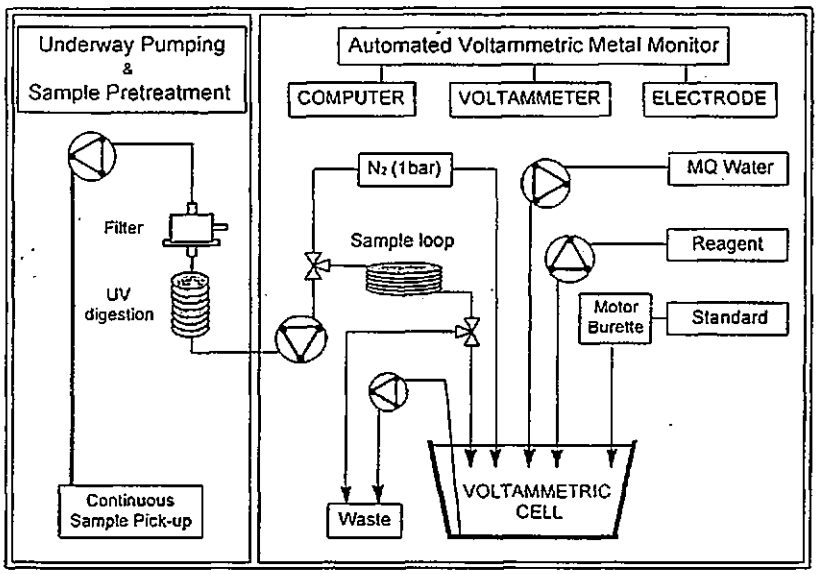

Fig. 8. Manifold of an automated voltammetric system for ship-board analysis of trace metals. Sample pick-up could be from sample changer, or pumped seawater supply.

preconcentration, interference and matrix removal) and analysis of the trace metals is performed on-line with a minimum risk of sample contamination. The on-line approach allows ready automation of the analysis with computerised sample and reagent transport, and computer-controlled data acquisition. Ship-board application of colorimetric methods includes the determination of Mn in hydrothermal plume samples [77] and in Atlantic shelf waters [78]. Reported ship-board application of chemiluminescence includes the analysis of dissolved Cu in the Pacific Ocean [79], Mn in the Pacific Ocean [80], Fe in the East China Sea [81], the Atlantic Ocean [82] and the Southern Ocean [83]. The colorimetric and chemiluminescence flow-analysis methods commonly make use of solid state preconcentration/matrix removal procedures. By contrast, stripping voltammetry does not require a matrix removal step and allows for the determination of a wider range of metals. Fig. 8 presents a manifold of a voltammetric system which has been used on-board ships in an automated batch-mode. Aliquots of 10 ml can be analysed at a rate of one complete measurement every ca. 10–20 min [72]. Each sample is fully calibrated, resulting in high quality data required for biogeochemical and pollution studies.

8. Near real-time trace metal analysis

A recent development in marine trace metal studies is the application of analytical monitoring instrumentation on-board ship for near real-time measurements of surface waters using AdCSV with a HMDE [38,84,85]. This approach uses underway pumping as a means of sample collection and thereby obviates the need for the vessel to halt for the collection of discrete samples. Sample contamination is prevented by eliminating contact of the seawater with metal components by using inert materials (e.g. Teflon®, Polyvinyl Chloride, Polyethylene). An effective underway pumping system can be designed using a peristaltic or Teflon®-bellows pump and a long (20–60 m) and strong Polyethylene or Polyvinyl Chloride hose. The hose is hung overboard and attached to a 'fish' (torpedo-like structure, KIPPER-1) which is towed from a strong cable attached to a winch (Fig. 9). The design and weight (ca. 40 kg) ensures that KIPPER-1 stays at a constant depth (ca. 3–4 m) even at speeds over 10 knots. KIPPER-1 is made from solid carbon steel with an inlet at the front and a hole through the centre for the sampling hose. The fish is coated with a non-metallic epoxy-based paint. All tubing used is rapidly equilibrated with the seawater as it is

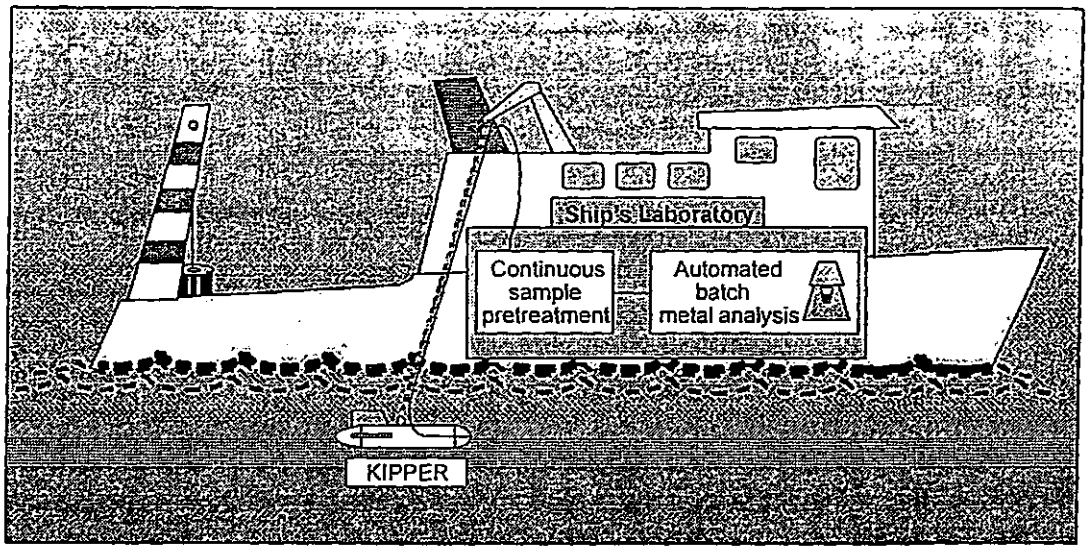

Fig. 9. Drawing of ship-board continuous underway sampling and analysis system.

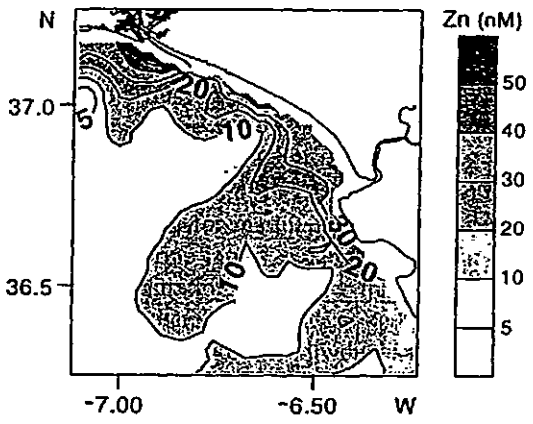

Fig. 10. Contour plot of total dissolved Zn in the Gulf of Cadiz, determined on-board ship using automated AdCSV with continuous underway sampling.

automatically and continuously rinsed during sample collection. Equally, on-line filtration and UV-digestion is carried out continuously prior to analysis. A tangential filtration unit is used, and the UV-digestion unit has a 400 W medium pressure Hg vapour lamp surrounded by a ca. 3.5 m long quartz coil (1 mm i.d.) [85].

Fig. 10 illustrates, with the example of Zn, the advantages of high-resolution monitoring in the coastal waters of the Gulf of Cadiz (TOROS IV survey, October 1998, B/O *Garcia del Cid*). The continuous underway sampling and analysis approach resulted in an extensive coverage of the coastal area. The automated voltammetric instrumentation operated largely unattended and almost continuously on-board ship during steaming and station time. Dissolved Zn and Cu concentrations were analysed simultaneously, using a mixed reagent of ligand and buffer (oxine, 0.02 mM; HEPES, 0.01 M, final concentrations). At a ship's speed of 8 knots, and a rate of 4–5 measurements per hour, the spatial resolution between samples during automated on-line metal analyses was between 3.3 and 4.5 km. The distribution of dissolved Zn in Fig. 10 shows enhanced metal levels in the coastal region in the form of plumes extending from the polluted Huelva estuary (northwest in Fig. 10, 50–65 nM Zn) and the Guadalquivir estuary (east in Fig. 10, 30–40 nM Zn). Elevated concentrations between these estuaries indicate the transport of water along the shore in a south-easterly direction. The decrease in Zn concentrations with increasing distance from the coast can be explained by the mixing of metal-polluted estuarine water with cleaner Atlantic waters.

Field applications of automated voltammetric monitors have also been reported for estuarine studies [86]. Estuaries are highly reactive zones, where fluvial discharges mix with seawater and dissolved elements interact with organic material and particles in the water

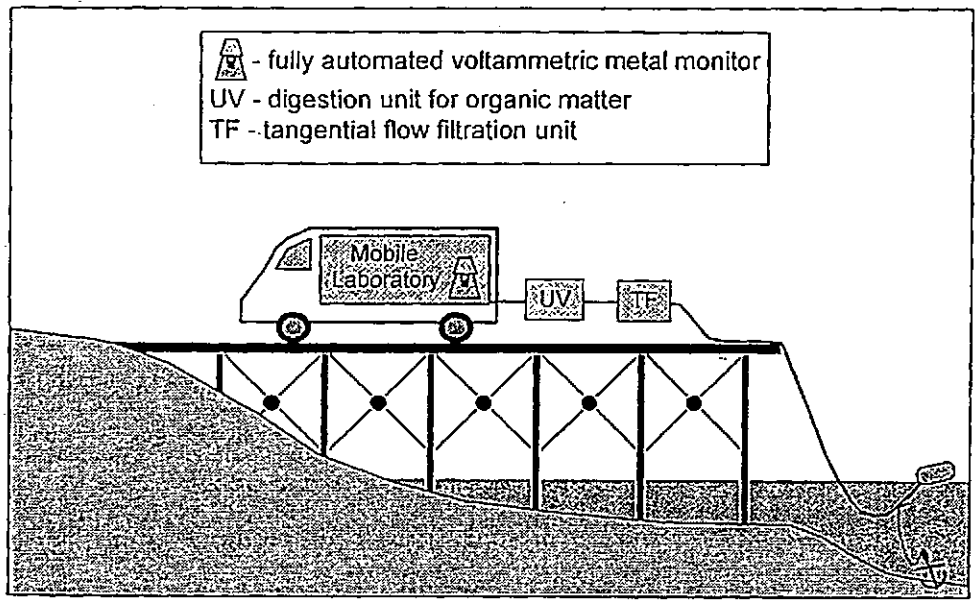

Fig. 11. Set-up for estuarine trace metal monitoring with continuous sample collection and automated AdCSV trace metal analysis.

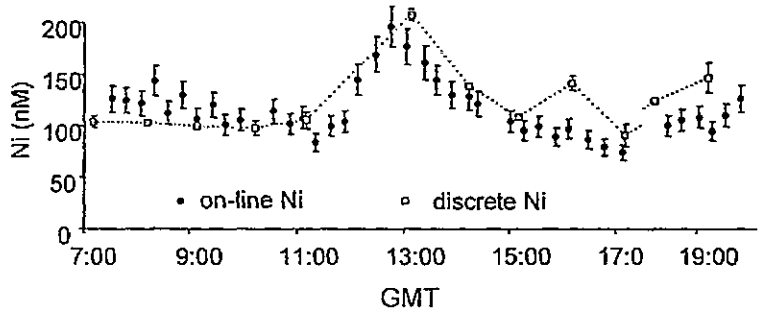

Fig. 12. On-line continuous dissolved total Ni measurements in the Huelva estuary during a tidal cycle (April 1998). Discrete measurements were performed in the laboratory in Plymouth by AdCSV (after UV-digestion).

column. Fig. 11 shows the instrumental set-up utilised for automated analysis of total dissolved Ni by AdCSV during a tidal cycle study carried out in the lower Huelva estuary, (TOROS III survey, April 1998). The voltammetric metal monitor was operated from a van, and powered by a portable generator. Surface water samples were collected in the estuarine channel using a braided PVC sampling hose which was submerged at a depth of ca. 0.5 m below the surface by a float and an anchor. Fig. 12 shows the results of a tidal cycle study, during which total dissolved Ni measurements were obtained with the automated metal monitor. At high salinity ($S=37$), total dissolved Ni concentrations ranged between 75 and 145 nM, while at low water ($S=34$), total dissolved Ni peaked at around 200 nM. Therefore, dilution of river water with enhanced Ni concentrations, by seawater depleted in Ni, was an important process determining the Ni behaviour in this estuarine system. Important advantages of the in-situ monitoring approach include the reduced risk of sample contamination, consistency in sample position, and the larger number of data points obtained during the automated study: 41 automated measurements compared with 13 discrete measurements.

The strong variability in coastal and estuarine waters requires high spatial and temporal resolution in the design of sampling strategies. This monitoring approach results in enhanced sampling frequencies and is therefore, an important tool for biogeochemical and pollution studies. The data can, for example, be used in numerical computer models for modelling of metal distributions and behaviour in estuaries and coastal waters. The near real-time analysis also provides the opportunity for an interactive sampling campaign, because the results of the measurements are directly available and can be evaluated on-board ship whilst the vessel is steaming.

Recent developments in HMDE design include a flow-cell, which has been incorporated into an automated voltammetric system, and resulted in a measurement frequency of 60 h^{-1} for total dissolved Co with a limit of detection of 5.4 pM [87,88]. This voltammetric monitor utilises on-line de-oxygenation with nitrogen or sulphite and semi-permeable tubing to remove interfering oxygen, and calibration of the analysis is performed at ca. 4 h intervals [89]. Application of the design for total dissolved Cu and Co monitoring of surface waters in the Western North Sea resulted in ca. 15 000 data points for each metal over a 2-week period [90]. Calibration of the AdCSV method at 4 h intervals is suitable for marine waters which are removed from riverine inputs. Changes in salinity and surfactant concentrations may alter the sensitivity of the method and therefore, estuarine and near-coastal studies require calibration of individual samples using the standard addition method.

9. Conclusions and future developments

The selectivity, extremely low detection limits for more than 20 elements, high accuracy, modest cost and suitability to flow analysis, have made stripping voltammetry an important technique for total dissolved trace metal studies and trace metal speciation analysis. The future importance of stripping voltammetry will most likely be found in trace metal monitoring and metal speciation studies.

Still little is known about the interaction between metal ions and organisms, and current knowledge is largely based on laboratory experiments. The capability of stripping voltammetry to determine concentrations of metal complexing ligands, their conditional stability constants and the free aqueous metal ion concentrations is important for growth limitation studies in open ocean waters where micro-nutrients (e.g. Fe, Co, Zn and Cu) may be deficient [91], and for toxicity studies in metal polluted waters [92]. Much effort is currently devoted to Fe redox speciation studies in seawater [63,93] and investigations into Fe complexing natural ligands in Fe deficient oceanic waters [55,75,94,95]. The very low concentrations of Fe and its chemical speciation in these remote oceanic regions are of significance for phytoplankton growth and consequently atmosphere–ocean CO_2 exchange. Recently attention has also turned towards the role of Zn with respect to oceanic phytoplankton growth [96], and stripping voltammetry has been used to establish a link between phytoplankton growth and free aqueous Zn ions.

Further applications of stripping voltammetry can be expected in metal polluted marine waters. Algae in such environments have been reported to produce metal-chelating compounds, phytochelatins [97,98]. Phytochelatins are polypeptides with thiol groups and are thought to reduce metal toxicity inside algal cells. These compounds can be determined using HPLC [99]. An investigation in a coastal water reported that phytochelatin concentrations showed a positive relationship with the free cupric ion concentration (as determined with AdCSV), and not with total dissolved Cu [100]. The combination of HPLC and AdCSV therefore, forms a powerful tool for investigations into biochemical effects of trace metals on organisms.

Trace metal speciation studies in natural waters provide an important insight into the geochemical behaviour of trace metals. Total dissolved metal measurements give an overall picture of metal removal or supply in natural waters, but speciation measurements can aid our understanding of the processes involved. Studies (using AdCSV) in the authors' laboratory into trace metal sorption kinetics involving dissolved and particulate phases in estuarine waters have shown that organically bound Cu species were more particle reactive than organically bound Ni species [101]. Furthermore, the implications of trace metal complexation by colloidal fractions in seawater have become apparent with the emergence of novel filtration techniques. For example, stripping voltammetry (ASV using a MFE) used in conjunction with cross-flow

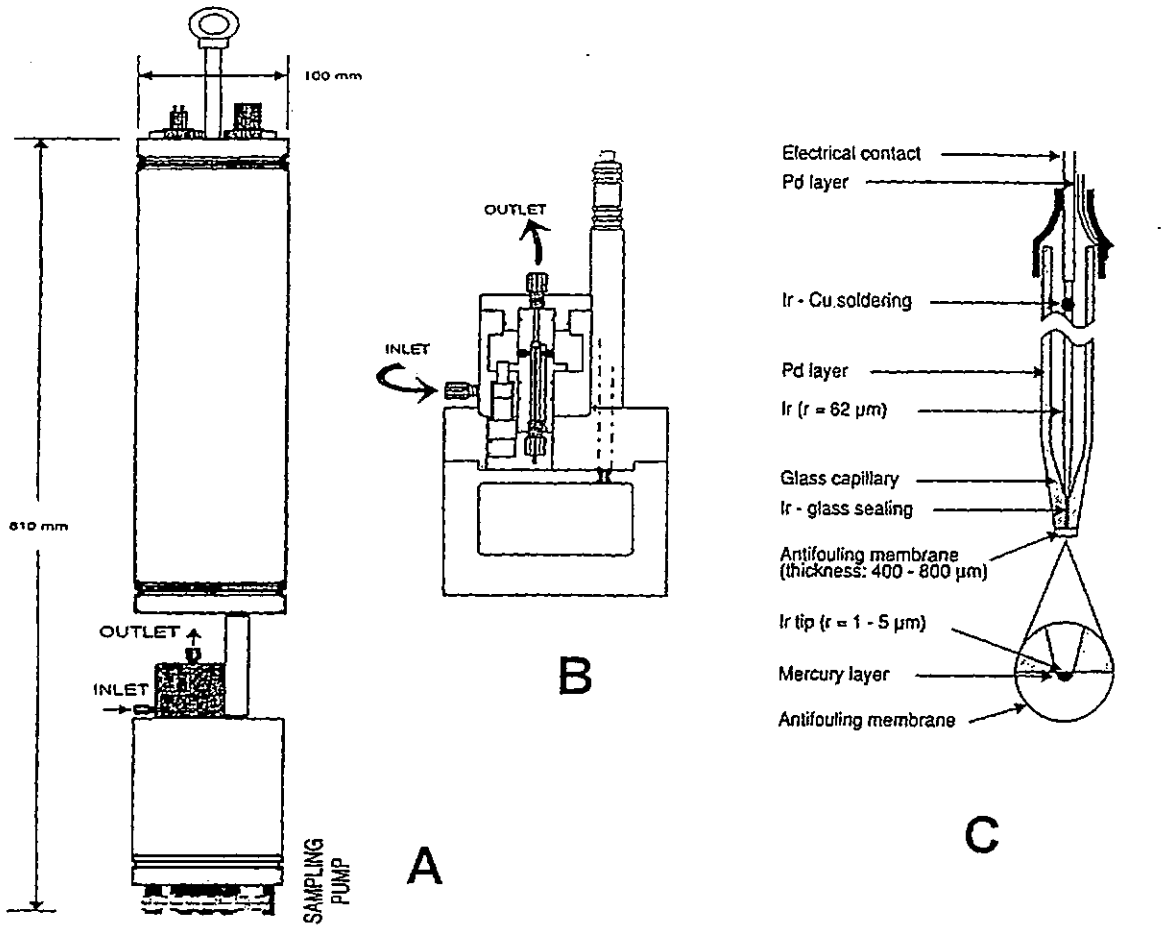

Fig. 13. (a) Drawing of the VIP system, consisting of a voltammetric probe (bottom part), an Ocean seven 301 probe for measurements of chemical and physical parameters (top part) and a sampling pump; (b) drawing of the flow-through voltammetric cell; (c) drawing of the gel coated and Hg plated Ir microelectrode (with permission from Idronaut).

ultrafiltration, have shown that Zn and Cd were associated with much smaller organic compounds (<1 kDa) than Cu (1–8 kDa) [60]. Such observations have significant implications for estuarine pollutant transport processes and can be used to improve estuarine contaminant models.

This paper has illustrated the usefulness of near-real time ship-board voltammetric monitoring of trace metals in surface waters. The trend in automated trace metal measurements is towards in-situ deployment of miniaturised analytical instrumentation, with submersible continuous application of sensors. This approach not only further reduces the risk of sample contamination, but also potentially leads to an improved way of trace metal speciation measurements as the in-situ analysis results in a minimal disturbance of the chemical equilibria. The limited availability of reliable commercially available voltammetric sensors and problems caused by fouling of the sensor-surface has hampered long-term submersible applications. However, in recent years important progress has been made and different designs of submersible voltammetric systems have been reported. A submersible probe using a sessile Hg drop electrode and allowing in-situ ASV measurements of trace elements in the water column of lake Bret has been described [102,103]. The submersible application of solid electrodes is however, preferable because of their

robustness. Fig. 13 shows the voltammetric in-situ profiling (VIP) system, which has been successfully applied in freshwater and seawater for the ASV determination of Cu, Pb, Cd, Zn and Mn [104,105]. The VIP uses a flow-cell with a Hg-plated Ir microelectrode (single or array) [18,19]. The microelectrode is covered with an agarose gel to prevent fouling of its surface [11]. The probe can be used for measurements down to 500 m in seawater and is able to determine trace metals with sub-nanomolar detection limits in the presence of oxygen. The time limiting step of the analysis is the diffusion of trace metal species through the protective gel, and the measurement frequency is ca. 3–4 h^{-1}. Only 'truly dissolved' (i.e. mobile species smaller than a few nanometers) trace metal species pass through the agarose membrane. Consequently, speciation studies can be conducted by additional sampling and analysis of total dissolved trace metals in discrete samples. One of the few other applications of a submersible electrochemical sensor in seawater has been reported by Wang et al. [13]. These workers successfully applied a sensor with a bare Au fibre electrode in contaminated coastal waters for the determination of Cu and Pb utilising stripping potentiometry. The remote sensor has a reported limit of detection of ca. 5 nM for labile Cu, and is therefore suitable for estuarine and coastal waters with enhanced metal levels, but not for unpolluted ocean waters.

Submersible electrochemical sensors are very suitable for automated real-time analysis of trace metals in natural waters. Unattended high resolution measurements will allow the monitors to be used for detailed biogeochemical studies and as early warning systems for metal pollution events. The submersible sensors have to be rugged and reliable and therefore, make use of solid electrodes. Bare Au and Hg plated Ir fibre microelectrodes have shown to work successfully, but further developments in electrode technology will be required to improve the sensitivity of the non-Hg electrodes and to widen the range of trace metals that can be determined using microelectrodes in seawater at the required low concentrations.

Acknowledgements

We would like to thank Elsevier for the invitation to participate in the Measurements for the next Millennium symposium. We thank the European Union for funding the TOROS project (Environment & Climate Programme ENV4-CT96-0217). We would like to thank Dr. M. Gledhill for her valuable comments on the manuscript.

References

[1] J. Wang, in: P.T. Kissinger, W.R. Heineman (Eds.), Laboratory Techniques in Electroanalytical Chemistry, Marcel Dekker, New York, 1996, pp. 719–738.
[2] C.M.G. van den Berg, Analyst 114 (1989) 1527.
[3] M.G. Paneli, A. Voulgaropoulos, Electroanalysis 5 (1993) 355.
[4] M. Florence, J. Electroanal. Chem. 27 (1970) 273.
[5] G.W. Luther III, P.J. Brendel, B.L. Lewis, B. Sundby, L. Lefrancois, N. Silverberg, D.B. Nuzzio, Limnol. Oceanogr. 43 (1998) 325.
[6] R.R. de Vitre, M.M. Tsacopoulos, J. Buffle, M.-L. Tercier, Anal. Chim. Acta 249 (1991) 419.
[7] J. Herdan, R. Feeney, S.P. Kounaves, A.F. Flannery, C.W. Storment, G.T.A. Kovacs, R.B. Darling, Environ. Sci. Technol. 32 (1998) 131.
[8] A.M. Bond, P.J. Mahon, J. Schiewe, V. Vicente-Beckett, Anal. Chim. Acta 345 (1997) 67.
[9] A.M. Bond, W.A. Czerwinski, M. Llorente, Analyst 123 (1998) 1333.
[10] J. Wang, M. Bonakdar, M.M. Pack, Anal. Chim. Acta 192 (1987) 215.
[11] M.L. Tercier, J. Buffle, Anal. Chem. 68 (1996) 3670.
[12] A. Economou, P. Fielden, Analyst 118 (1993) 1399.
[13] J. Wang, N. Foster, S. Armalis, D. Larson, A. Zirino, K. Olsen, Anal. Chim. Acta 310 (1995) 223.
[14] P.T. Kissinger, in: P.T. Kissinger, W.R. Heineman (Eds.), Laboratory Techniques in Electroanalytical Chemistry, Marcel Dekker, New York, 1996, pp. 20–40.
[15] C. Colombo, P.C. Hauser, Analyst (1999).
[16] J. Wang, J.M. Zadeii, J. Electroanal. Chem. Interfacial Electrochem. 246(2)) (1988) 297–305.
[17] J. Amez del Pozo, A. Costa-Garcia, P. Tuñón-Blanco, Anal. Chim. Acta 289 (1994) 169.
[18] C. Belmont, M.L. Tercier, J. Buffle, G.C. Fiaccabrino, M. Koudelka-Hep, Anal. Chim. Acta 329 (1996) 203.
[19] M.L. Tercier, N. Parthasarathy, J. Buffle, Electroanalysis 7 (1995) 55.
[20] A. Zirino, S.H. Leiberman, M.L. Healy, in: B.J. Berkowitz, R. Horne, M. Banus, P.L. Howard, M.J. Pryor, G.C. Whitnack, H.V. Weiss (Eds.), Marine Electrochemistry, Electrochemical Soc., Princeton, NJ, pp. 319–332.
[21] M. Vega, C.M.G. van den Berg, Anal. Chem. 69 (1997) 874.
[22] C.M.G. van den Berg, G.S. Jacinto, Anal. Chim. Acta 211 (1988) 129.
[23] K. Yokoi, C.M.G. van den Berg, Anal. Chim. Acta 257 (1992) 293.
[24] C. Colombo, C.M.G. van den Berg, Anal. Chim. Acta 337 (1997) 29.

[25] K.W. Bruland, R.P. Franks, Anal. Chim. Acta 105 (1979) 233.
[26] N.H. Morley, C.W. Fay, P.J. Statham, Advances in Underwater Technology, Ocean Science and Offshore Engineering, Graham & Trotman, 1988, pp. 283–289.
[27] A.G. Howard, P.J. Statham, Inorganic Trace Analysis: Philosophy and Practice, Wiley, Chichester, 1993.
[28] P.J. Statham, Anal. Chim. Acta 169 (1985) 149.
[29] W.G. Sunda, Mar. Chem. 14 (1984) 365.
[30] C.R. Lan, M.H. Yand, Anal. Chim. Acta 287 (1994) 111.
[31] M.J. Bloxham, S.J. Hill, P.J. Worsfold, J. Anal. Atomic Spectrom. 9 (1994) 935.
[32] W. Sirinawin, D. Turner, S. Westerlund, P. Kanatharana, Mar. Chem. 62 (1998) 175.
[33] E.P. Achterberg, C.M.G. van den Berg, Anal. Chim. Acta 291 (1994) 213.
[34] J.R. Donat, C.M.G. van den Berg, Mar. Chem. 38 (1992) 69.
[35] E.P. Achterberg, Ph.D. Thesis, University of Liverpool, 1993.
[36] K.W. Bruland, in: J.P. Riley (Ed.), Chemical Oceanography, Academic Press, London, pp. 157–220.
[37] R.M. Sherrell, E.A. Boyle, Deep-Sea Res. 35 (1988) 1319.
[38] E.P. Achterberg, C. Colombo, C.M.G. van den Berg, Cont. Shelf Res. 19 (1999) 537.
[39] C.M.G. van den Berg, S.H. Khan, P.J. Daly, J.P. Riley, D.R. Turner, Estuarine, Coastal and Shelf Sci. 33 (1991) 309.
[40] E.P. Achterberg, C.M.G. van den Berg, in: J.M. Martin, H. Barth (Eds.), EROS 2000 (European River Ocean System) Project Workshop, Commission of the European Communities, Brussels, 1995, pp. 251–257.
[41] M. Boussemart, C.M.G. van den Berg, M. Ghaddaf, Anal. Chim. Acta 262 (1992) 103.
[42] E.P. Achterberg, C.M.G. van den Berg, Deep-Sea Res. II 44 (1997) 693.
[43] R.C. Schenck, Mar. Biol. Lett. 5 (1984) 13.
[44] D.M. Anderson, F.M. Morel, Limnol. Oceangr. 23 (1978) 283.
[45] P.G.C. Campbell, in: A. Tessier, D.R. Turner (Eds.), Metal Speciation and Bioavavailibility in Aquatic Systems, Wiley, Chichester, pp. 45–103.
[46] M. Gledhill, M. Nimmo, S.J. Hill, M.T. Brown, J. Phycol. 33 (1997) 2.
[47] W.G. Sunda, S.A. Huntsman, Mar. Chem. 36 (1991) 137.
[48] C.M.G. van den Berg, A.G.A. Merks, E.K. Duursma, Estuarine Coastal Shelf Sci. 24 (1987) 785.
[49] O. Abollini, E. Mentasti, C. Sarzanini, V. Porta, C.M.G. van den Berg, Anal. Proc. 28 (1991) 72.
[50] G. Capodaglio, G. Scarponi, P. Cescon, Anal. Proc. 28 (1991) 76.
[51] E. Deaver, J.H. Rodgers, Environ. Toxicol. Chem. 15 (1996) 1925.
[52] L.J.A. Gerringa, T.C.W. Poortvliet, H. Hummel, Estuarine, Coastal Shelf Sci. 42 (1996) 629.
[53] P.B. Kozelka, S. SanudoWilhelmy, A.R. Flegal, K.W. Bruland, Estuarine Coastal Shelf Sci. 44 (1997) 649.
[54] F.L.L. Muller, Mar. Chem. 52 (1996) 245.
[55] E.L. Rue, K.W. Bruland, Mar. Chem. 50 (1995) 117.
[56] H.B. Xue, W.G. Sunda, Environ. Sci. Technol. 31 (1997) 1902.
[57] H. Zhang, C.M.G. van den Berg, R. Wollast, Mar. Chem. 28 (1990) 285.
[58] F.L. Muller, Mar. Chem. 52(1996) (1996) 245.
[59] P.B. Kozelka, K.W. Bruland, Mar. Chem. 60 (1998) 267.
[60] M.L. Wells, P.B. Kozelka, K.W. Bruland, Mar. Chem. 62 (1998) 203.
[61] L.A. Miller, K.W. Bruland, Anal. Chim. Acta 343 (1997) 161.
[62] J. Zima, C.M.G. van den Berg, Anal. Chim. Acta 289 (1994) 291.
[63] M. Gledhill, C.M. van den Berg, Mar. Chem. 50 (1995) 51.
[64] C.M.G. van den Berg, J.R. Donat, Anal. Chim. Acta 257 (1992) 281.
[65] M.L.A.M. Campos, C.M.G. van den Berg, Anal. Chim. Acta 284 (1994) 481.
[66] C.M.G. van den Berg, J. Electroanal. Chem. 215 (1986) 111.
[67] I. Ruzic, Anal. Chim. Acta 140 (1982) 99.
[68] C.M.G. van den Berg, Mar. Chem. 11 (1982) 307.
[69] L.J.A. Gerringa, P.M.J. Herman, T.C.W. Poortvliet, Mar. Chem. 48 (1995) 131.
[70] A. Ringbom, E. Still, Anal. Chim. Acta 59 (1972) 143.
[71] S.C. Apte, M.J. Gardner, J.E. Ravenscroft, Anal. Chim. Acta 212 (1988) 1.
[72] E.P. Achterberg, C.M.G. van den Berg, Anal. Chim. Acta 284 (1994) 463.
[73] M. Gledhill, C.M.G. van den Berg, Mar. Chem. 47 (1994) 41.
[74] C.M.G. van den Berg, Mar. Chem. 50 (1995) 139.
[75] E.L. Rue, K.W. Bruland, Limnol. Oceanogr. (1997) 42.
[76] J.H. Martin, R.M. Gordon, Deep-Sea Res. 35 (1988) 177.
[77] I.Y. Kolotyrkina, L.K. Shpigun, Y.A. Zolotov, G.I. Tsysin, Analyst 116 (1991) 707.
[78] J. Olafsson, Sci. Total Environ. 49 (1986) 101.
[79] K.H. Coale, K.S. Johnson, P.M. Stout, C.M. Sakamoto, Anal. Chim. Acta 266 (1992) 345.
[80] E. Nakayama, K. Isshiki, Y. Sohtin, H. Karatani, Anal. Chem. 61 (1989) 1392.
[81] H. Obata, H. Karatani, M. Matsui, E. Nakayama, Mar. Chem. 56 (1997) 97.
[82] A.R. Bowie, E.P. Achterberg, R.F.C. Mantoura, P.J. Worsfold, Anal. Chim. Acta 361 (1998) 189.
[83] J.T. de Jong, J. den Das, U. Bahtmann, M.H. Stoll, G. Kattner, R.F. Nolting, H.J. de Baar, Anal. Chim. Acta 377 (1998) 113.
[84] E.P. Achterberg, C.M.G. van den Berg, Mar. Pollut. Bull. 32 (1996) 471.
[85] C. Braungardt, E.P. Achterberg, M. Nimmo, Anal. Chim. Acta (1998).
[86] D.-J. Whitworth, E.P. Achterberg, M. Nimmo, P.J. Worsfold, Anal. Chim. Acta 371 (1998) 235.
[87] C. Colombo, C.M.G. vandenBerg, A. Daniel, Anal. Chim. Acta 346 (1997) 101.
[88] A. Daniel, A.R. Baker, C.M.G. vandenBerg, Fresenius' J. Anal. Chem. 358 (1997) 703.
[89] C. Colombo, C.M. van den Berg, Anal. Chim. Acta 377 (1998) 229.
[90] C. Colombo, E.P. Achterberg, C.M.G. van den Berg, Estuarine Coastal Shelf Sci., submitted for publication, 1999.
[91] K.W. Bruland, J.R. Donat, D.A. Hutchins, Limnol. Oceanogr. 36 (1991) 1555.
[92] F. Elbaz-Poulichet, N.H. Morley, A. Cruzado, Z. Velasquez, D. Green, E.P. Achterberg, C.B. Braungardt, Sci. Total Environ., in press, 1999.

[93] J. Albaiges, J. Algaba, P. Arambarri, F. Carrera, G. Baluja, L.M. Hernandez, J. Castroviejo, Sci. Total Environ. 63 (1987) 13.
[94] R.F. Nolting, L.J.A. Gerringa, M.J.W. Swagerman, K.R. Timmermans, H.J.W. de Barr, Mar. Chem. 62 (1998) 335.
[95] A.E. Witter, G.W. Luther III, Mar. Chem. 62 (1998) 241.
[96] F.M.M. Morel, J.R. Reinfelder, S.B. Roberts, C.P. Chamberlain, J.G. Lee, D. Yee, Nature 369 (1994) 740.
[97] B.A. Ahner, S. Kong, F.M. Morel, Limnol. Oceanogr. 40 (1995) 649.
[98] B.A. Ahner, F.M. Morel, Limnol. Oceanogr. 40 (1995) 658.
[99] J.W. Rijstenbil, J.A. Wijnholds, Mar. Biol. 127 (1996) 45.
[100] B.A. Ahner, F.M. Morel, J.W. Moffett, Limnol. Oceanogr. 42 (1997) 601.
[101] V.M.C. Herzl, G.E. Millward, R. Wollast, E.P. Achterberg, Limnol. Oceanogr., submitted for publication, 1999.
[102] M.-L. Tercier, M.J. Buffle, A. Zirino, R.R. de Vitre, Anal. Chim. Acta 237 (1990) 429.
[103] M.L. Tercier, J. Buffle, Electroanalysis 5 (1993) 187.
[104] M.L. Tercier, J. Buffle, F. Graziottin, Electroanalysis 10 (1998) 355.
[105] M.-L. Tercier-Waeber, M.C. Belmont-Hebert, J. Buffle, Environ. Sci. Technol. 32 (1998) 1515.
[106] C.M.G. van den Berg, K. Murphy, J.P. Riley, Anal. Chim. Acta 188 (1986) 177.
[107] B. Pihlar, P. Valenta, H.W. Nurnberg, Frensius' Z. Anal. Chem. 307 (1981) 337.
[108] C.M.G. van den Berg, Z.Q. Huang, J. Electroanal. Chem. 177 (1984) 269.
[109] K. Yokoi, C.M.G. van den Berg, Electroanalysis 4 (1992) 65.
[110] M. Karakaplan, S. Gucer, Frensius' J. Anal. Chem. 342 (1992) 186.
[111] G. Capodaglio, C.M.G. van den Berg, G. Scarponi, J. Electroanal. Chem. 235 (1987) 275.
[112] C.M.G. van den Berg, S.H. Khan, Anal. Chim. Acta 231 (1990) 221.
[113] C.M.G. van den Berg, S.H. Khan, J.P. Riley, Anal. Chim. Acta 222 (1989) 43.
[114] J. Wang, J.M. Zadeii, Talanta 34 (1987) 247.
[115] C.M.G. van den Berg, M. Nimmo, Anal. Chem. 59 (1987) 924.
[116] M. Vega, C.M.G. van den Berg, Anal. Chim. Acta 293 (1994) 19.
[117] C.M.G. van den Berg, Mar. Chem. 16 (1985) 121.

PERGAMON
www.elsevier.com/locate watres

PII: S0043-1354(99)00282-1

Wat. Res. Vol. 33, No. 16, pp. 3387–3394, 1999

Printed in Great Britain
0043-1354/99/$ - see front matter

IMPACT OF LOS FRAILES MINE SPILL ON RIVERINE, ESTUARINE AND COASTAL WATERS IN SOUTHERN SPAIN

ERIC P. ACHTERBERG[1]*, CHARLOTTE BRAUNGARDT[1], NICK H. MORLEY[2], FRANCOISE ELBAZ-POULICHET[3] and MARC LEBLANC[3]

[1]Department of Environmental Sciences, University of Plymouth, Plymouth PL4 8AA, UK; [2]Department of Oceanography, University of Southampton, Southampton Oceanography Centre, Southampton SO14 3ZH, UK and [3]Laboratory Hydrosciences, UMR 5569, CNRS-ORSTOM-University of Montpellier II, CC057, 34095 Montpellier Cedex 5, France

(First received 1 May 1999; accepted in revised form 1 June 1999)

Abstract—On April 25, 1998, a spill at the Los Frailes mine in southern Spain resulted in a very high input of metals (including Ag, As, Cd, Cu, Fe, Pb, Tl and Zn) into the river Guadiamar. Calculations indicate that the discharges into the Guadiamar of Cu (5100 t), Pb (24,700 t), Zn (26,200 t) and Ag (138 t, based on mud only) were higher than the annual production by the Los Frailes mine for Ag and Pb, and *ca.* two times less for Cu and Zn. For many metals, the increase in concentration in the affected river (Guadiamar), 2 days after the initial discharge, was by several orders of magnitude. However, 6 months after the incident, no evidence of the spill could be observed in the plume of the river (Guadalquivir) which discharged the mine waters into the coastal waters of the Gulf of Cadiz. This observation can possibly be explained by low rainfall, natural metal removal processes in the river and estuarine environments and by human interventions. © 1999 Elsevier Science Ltd. All rights reserved

Key words—mine spill, metal pollution, Los Frailes, Guadiamar, Guadalquivir, Gulf of Cadiz

INTRODUCTION

The retaining dam of a tailing reservoir at the Los Frailes mine in Andalucia (southern Spain; Fig. 1) collapsed on April 25, 1998, resulting in a 60 m breach in the reservoir wall. The failure released 5–7 × 10^6 m^3 of acid sludge and water (pH 2) into the river Guadiamar (van Geen and Chase, 1998). During the 18 days following the spill, an estimated 26 t of dead fish was removed from the rivers (Pain *et al.*, 1998). The released sulphide sludge formed a layer up to *ca.* 1.5 m thick covering 4000–5000 ha of the river bed and flood plains, including agricultural land, of the Guadiamar up to 40 km downstream (Medio Ambiente, 1998†). Contamination of the Doñana Park ("worlds' biosphere reserve" of UNESCO, 45 km south of the mine) was prevented by diverting the acidic waters.

The Los Frailes mine (owned by Boliden Apirsa S.L.) has an annual production of approximately 65 t Ag (1 t = 1000 kg), 13,800 t Cu, 18,000 t Pb and 47,800 t Zn. The average grade of the massive polymetallic sulphide ore at Los Frailes is 62 g t^{-1} Ag (Leistel *et al.*, 1998b), 0.1–4 g t^{-1} Au (Leistel *et al.*, 1998a), 0.34% Cu (Leistel *et al.*, 1998b), 2.25% Pb (Leistel *et al.*, 1998b) and 3.92% Zn (Leistel *et al.*, 1998b). The ores also contain important amounts of As, Hg and Tl (Almodovar *et al.*, 1998). The mine has been worked since 1997 with waste material collected in a tailing reservoir retained by an earth/rock dam. The failure of the dam resulted in a loss of *ca.* 20% of tailings from the reservoir. We visited the area affected by the incident before (April 20, 1998) and after (April 27 and October 15, 1998) the dam failure, and performed extensive trace metal monitoring surveys in the Gulf of Cadiz in June 1997 and October 1998.

METHODS

River sampling was performed using clean methods (plastic gloves were worn) either from the banks or from bridges. Samples were initially taken into acid-cleaned high density polyethylene (HDPE) bottles. The samples were filtered (polycarbonate filters, Nuclepore 0.4-μm porosity) within 4 h of sampling, and were then acidified to pH 1.5 using nitric acid. Marine surface water samples were obtained either by discrete sampling using modified Niskin bottles attached to a CTD rosette (Morley *et al.*, 1988) (As and Mn; with analysis using discrete laboratory

*Author to whom all correspondence should be addressed. [Tel.: +44-1752-233-036; fax: +44-1752-233035]; e-mail: eachterberg@plym.ac.uk.

†Medio Ambiente (1998) Aznalcollar mining spill. Internet Communication. http://www.cma.junta-andalucia.es/aznalcollar/idxaznalcollar.htm.

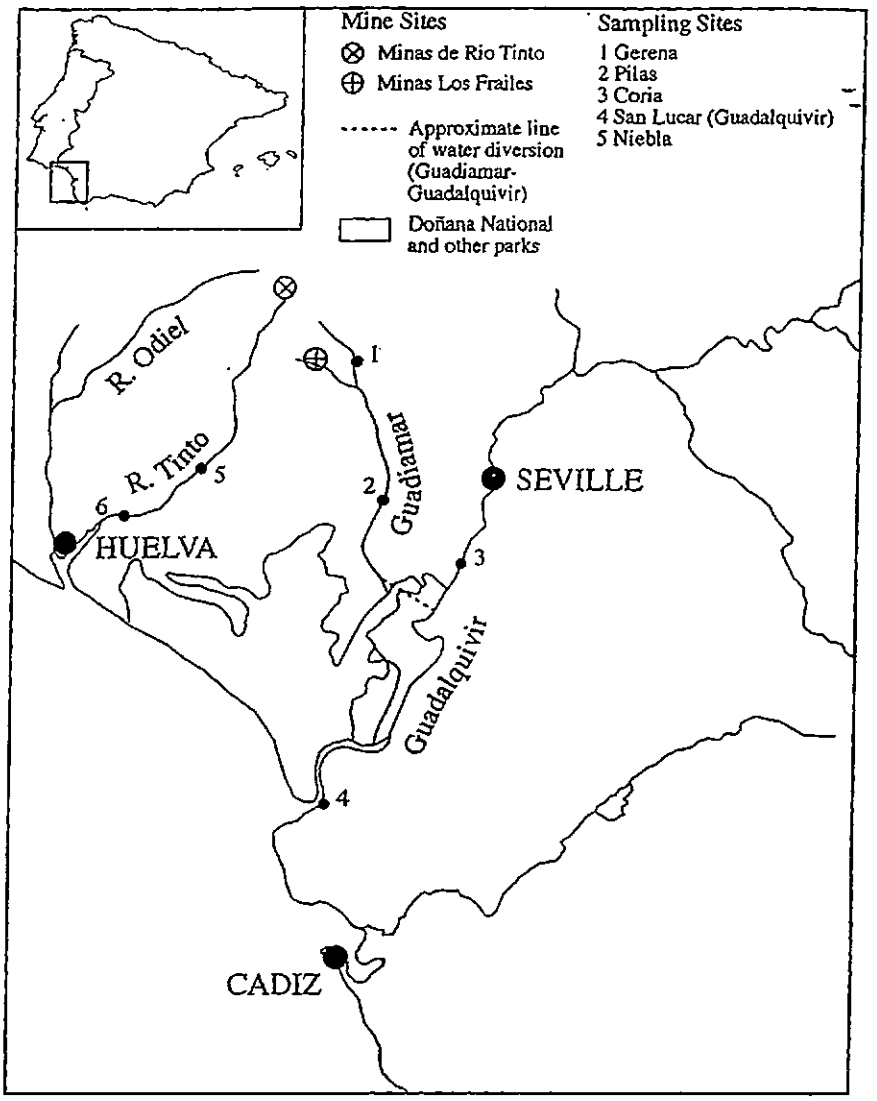

Fig. 1. Map showing Doñana Park, rivers, mines and sampling locations in southern Spain. The diversion of the Guadiamar waters into the Guadalquivir following the mine spill is indicated on the map.

methods, see below) with similar filtration and sample preservation to the above, or by continuous underway sampling from a depth of *ca.* 3–4 m below the sea-surface (Cu and Zn; with analysis using high resolution on-line ship-board methods, see below). Mud samples were obtained from the Guadiamar on April 27. The mud was subjected to a total digestion using Aqua Regia [mixture of concentrated HNO_3 (three parts) and HCl (one part)] and HF (Rantala and Loring, 1985) or concentrated HNO_3. In addition, an extraction using 1 M HCl was performed in order to release weakly bound, non-detrital, trace metals (Millward *et al.*, 1996) from the sludge. This digest provides an estimation of the availability of metals to organisms by mimicking their digestive conditions (Bryan and Langston, 1992), and yields results which correlate well with the biologically availability of particulate trace metals (Luoma, 1983).

Conductivity and pH of the river water were determined using field instrumentation (HANNA model HI-9635 conductivity meter; HANNA model HI 9025 pH meter). Anions were determined using capillary ion analysis (Waters, USA), according to Waters (1996). Dissolved Mn in discrete seawater samples was determined using GFAAS [graphite furnace atomic absorption spectrometry (Perkin Elmer 1100b), after solvent extraction using APDC/DDDC; Morley *et al.*, 1997]. Total dissolved inorganic As in discrete seawater samples was determined after a prereduction involving potassium iodide in the presence of ascorbic acid. Arsenic was determined using a hydride generation system coupled to an ICP-MS (inductively coupled plasma mass spectrometry; VG-Plasmaquad). This method is similar to that described by Andreae (1977), but has been modified according to Branch *et al.* (1991). Total dissolved Cu and Zn concentrations in the continuous underway samples were determined on-board ship using automated adsorptive cathodic stripping voltammetry (ACSV). The analysis was performed using square wave ACSV in the presence of 8-hydroxyquinoline (2×10^{-5} M) and HEPES pH buffer (*N*-hydroxyethylpiperazine-*N*′-2′-ethanesulphonic acid, pH 7.78; 0.01 M), employing an automated voltammetric trace metal monitor with an μAutolab voltammeter (Ecochemie) and hanging mercury drop electrode (VA 663 Stand, Metrohm), according to Braungardt *et al.* (1998). This approach provides near-real

time continuous high-resolution dissolved trace metal measurements (Achterberg *et al.*, 1999).

Metal concentrations in discrete fresh water samples and in digested mud were determined using a range of analytical techniques, including ICP-MS (PlasmaQuad PQ2+ Turbo, VG Elemental), ACSV, Flame AAS (atomic absorption spectrometry, with Deuterium background correction; Pye Unicam) and ICP-AES (inductively coupled plasma atomic emission spectrometry; Varian Liberty 200). All trace metal determinations were verified by analyses of certified reference materials and by duplication of analyses between laboratories where possible (Elbaz-Poulichet *et al.*, 1999).

RESULTS AND DISCUSSION

The sulphide mud discharged by the Los Frailes mine (sampled from the Guadiamar approximately 10 km downstream of the mine) had a high Fe concentration (36%; see Table 1) and consisted mainly of very fined grained pyrite (*ca.* 80%). The elements present in the highest concentrations in the mud (Fe, Zn, Pb and Cu) were those which also have the highest content in the sulphide ores mined in the region (Table 1); accessory metals born by pyrite (As and Tl) or Zn sulphides (Cd, Hg and Tl) were also abundant. The remaining elements belong to gangue minerals such as quartz, sericite (Al–Si–K) or barite ($BaSO_4$). Metals in the mud (Table 1) were enriched by one to three orders of magnitude compared to averaged crustal rocks as indicated by the enrichment factor (except Al, Ba, Cr, Mg, Mn, Ni, Sr and V). The quantity of the metal released by 1 M HCl was less than *ca.* 45% of the total, except for Pb (95%) and U (75%), indicating that a significant portion of metals were contained in the refractory fractions of the mud. However, because of the high metal concentrations in the mud, ingestion would most likely have caused adverse effects to organisms.

Dissolved trace metal concentrations and pH in samples taken from the Guadalquivir at site 3, prior to the incident (April 20, 1998) and in the Guadiamar (April 27, 1998) at site 1 upstream of the Los Frailes mine showed no signature of acid mine drainage (AMD) contamination. In particular, the Guadiamar at site 1 can be classed as a relatively pristine river (Table 2) when compared with other systems (Martin *et al.*, 1993). Metal levels in the Guadiamar increased dramatically following the failure of the tailings dam. For many metals, the increase was by several orders of magnitude at site 2, when compared to the upstream sampling site 1 (e.g. Co 1.5×10^4 times, Tl 900 times, Zn 1.5×10^5 times). In addition, the dissolved concentrations for most elements observed at site 2 (April 27, 1998) were similar (Fe, Mn and Pb) or higher than those found in the Rio Tinto (site 5). The Rio Tinto drains the Iberian Pyrite Belt (IPB) and is strongly affected by AMD (Van Geen *et al.*, 1997; Elbaz-Poulichet *et al.*, 1999). The plug of acidic mine tailings was prevented from entering the Doñana park by closure of water inlets between the Guadiamar and the park, and was diverted into the Guadalquivir at 20 km from its mouth. An increase in metal concentrations, particularly Cu and Zn, was observed upstream of the input in the Guadalquivir at site 3 (April 27, 1998), and suggests that the tidal movement of the Guadalquivir had transported metals upstream towards Seville.

Table 1. Total digest performed using Aqua Regia/HF, or concentrated HNO_3. Enrichment factors have been calculated for sludge (total digest) compared with average crustal rock (from Martin and Whitfield, 1983). Data for Los Frailes sulphide ore from Leistel *et al.* (1998b). nd means not determined and na not available

Element	Sludge (μg g^{-1}) (total)	Enrichment factor	Sludge (μg g^{-1}) (1 M HCl)	Los Frailes sulphide ore (μg g^{-1})
Ag	50†	715	nd	62
Al	9720	0.14	1210	30000§
As	6100†	772	nd	4000
Au	0.1†	10	nd	0.1–4¶
Ba	123	0.28	29	na
Cd	55.7	279	15	6.9
Co	47.7	3.7	5.2	100
Cr	30.7	0.71	13	8§
Cu	1850	58	685	3400
Fe	358000	10.2	14400	420000
Hg	15†	750‡	nd	na
Mg	2480	0.15	590	na
Mn	645	0.90	285	400
Ni	25.4	0.52	3	12
Pb	8963	560	8500	22500
Rb	6144†	768‡	nd	na
Sn	22†	11	nd	na
Sr	5.7†	0.015‡	nd	na
Tl	103†	206‡	nd	na
U	79	26.3	59.7	na
V	26.2	0.27	3.2	60§
Zn	7623	60	3190	39200

†HNO_3 used.
§Data from La Zarza ore (Borrego, 1992).
¶Data from Leistel *et al.* (1998a).
‡Data from Wedepohl (1991).

Table 2. Concentrations of dissolved metals in water samples. nd means not determined

Site	Guadiamar Site 1 April 27	Guadiamar Site 2 April 27	Guadiamar Site 2 Oct 16	Guadalquivir Site 3 April 20	Guadalquivir Site 3 April 27	Guadalquivir Site 3 Oct 16	Guadalquivir Site 4 April 20	Guadalquivir Site 4 Oct 16	Rio Tinto Site 5 June 1997
pH	7.77	6.07	7.65	7.37	7.37	7.69	7.89	7.85	2.21
Cond (mS cm^{-1})	1.7	4	1.3	17	19	1.2	210	366	8
SO_4^{2-} (mM)	0.1	31	4.9	1.6	0.3	2.4	nd	21	8.6
As (nM)	29	402	158	nd	27	47	nd	53	203
Ba (nM)	nd	253	nd	nd	nd	nd	nd	nd	151
Cd (nM)	< 1	6392	< 1	< 1	3.8	< 1	2.9	< 1	782
Co (nM)	1.3	18.8 × 10^3	79	9.5	27	7.7	3.1	1.6	3710
Cu (nM)	15	1385	45	27	253	86	41	27	121 × 10^3
Fe (μM)	2	400	0.73	nd	1.1	0.3	nd	0.90	1.2 × 10^3
Mn (μM)	0.23	307	4.8	0.14	0.18	< 0.05	0.13	0.42	112
Ni (nM)	5.1	16.3 × 10^3	77	40	47	35	37	20	1780
Pb (nM)	nd	777	7.3	nd	0.5	nd	nd	nd	3058
Rb (nM)	2.67	134	nd	nd	22	nd	nd	nd	38
Sr (μM)	2.0	4.5	nd	nd	21	nd	nd	nd	2.0
Tl (nM)	0.38	338	nd	< 0.1	0.48	0.30	nd	nd	45
U (Nm)	2.2	4.5	nd	7.6	9.6	7.7	8.9	12	28.7
Zn (μM)	0.03	4.0 × 10^3	2.28	0.02	3.21	0.41	0.04	0.18	295

Following the tailings release, the sulphate concentration at site 2 (31 mM) was *ca.* 300 times higher than upstream (site 1). The very high sulphate concentrations were however not accompanied by a low pH (6.07, site 2), despite the reported low acidity of the tailings (pH 2). The acidity of the tailings was buffered by the alkaline Guadiamar river water. The rivers in the area under investigation flow through regions of carbonate geology (Albaiges *et al.*, 1987) and are slightly alkaline (pH *ca.* 7–8). This influenced the pH of the Guadiamar downstream of the tailing discharges, and also had pronounced effects on the metal speciation. Both of these properties influence the bioavailability and toxicity of the metals (Campbell, 1995). Speciation calculations using MINEQL+ 3.01a (Schecher and McAvoy, 1994) indicated that Ba, Cd, Tl, Pb and Rb were present in their free ionic form (100%) in the Guadiamar water at site 2 (April 27, 1998). Free ionic forms were also important for Co, Cu, Ni and Zn (Table 3). The free ionic forms of many metals are assumed to be the toxic species, because of their ability to transfer through cell membranes of organisms and affect cell functioning (Campbell, 1995).

Upon oxidation of the pyrite in the mud, S becomes very mobile and can be used to index the relative mobility of the metals (van Geen *et al.*, 1997). The ratios of mud to river water (site 2, April 27) composition normalised to sulphur show clusters of metals in four categories (Table 4): (a) Cd, Co and Zn were enriched in the mud and possibly more mobile than S (index > 5); (b) Ba and Tl were enriched in the mud and of comparable mobility to S (index range 0.1–5); (c) As, Cu, Fe, Pb, Rb and U were enriched in the mud, but highly im-

Table 3. Results of thermodynamic speciation calculations for the Guadiamar at site 2 (April 27). Calculations were performed using MINEQL+ 3.01a, pH 6.07, and assuming typical major ion and alkalinity values for the region (total carbonate alkalinity 4.6 mM at site 1, October 1998). Metal species denoted with asterix (*) are solid phases because their solubility constants have been exceeded

Metal species	Fractions (%)
Zn^{2+}	39
$ZnHCO_3^+$	2.9
$Zn(SO_4)_2^{2-}$	8.1
$ZnSO_4$ Aq	37.1
*$ZnCO_3$, 1 H_2O	11.8
Cu^{2+}	42.6
$CuHCO_3^+$	12.8
$CuCO_3$ Aq	8.1
$CuSO_4$ Aq	35.4
Ni^{2+}	46.7
$NiHCO_3^+$	4.1
$NiCO_3$ Aq	12.2
$NiSO_4$ Aq	36.8
Co^{2+}	23.7
$CoSO_4$ Aq	31.6
*$CoCO_3$	44.6

Table 4. Mobilisation of metals relative to S; S content of mud of 46% was assumed. Estimation of the total amount of metals discharged by the Los Frailes spill into the Guadiamar watershed. It was assumed that the Los Frailes mud had a density of 2.5×10^4 g l^{-1}. Also presented is the estimated total annual amount metals discharged by Rio Tinto into its estuary (an annual mean water flow of 3 $m^3 s^{-1}$ was assumed for Rio Tinto (Elbaz-Poulichet *et al.*, 1999). nd means not determined

	Mobilisation relative to S	Total estimated discharge (t)	Total estimated discharge (t a^{-1}) Rio Tinto
SO_4^{2-}	1		
Ag	–	138	nd
As	0.002	16,800	1.4
Ba	0.11	339	nd
Cd	5.2	168	8.3
Co	9.4	153	21
Cu	0.02	5100	728
Fe	0.025	985,000	6500
Mn	10.5	2100	570
Ni	15.2	89	10
Pb	0.007	24,700	60
Rb	0.001	16,900	0.3
Sr	27.6	23.5	16
Tl	0.27	285	0.9
U	0.005	217	0.6
Zn	13.8	26,200	1800

mobile (index < 0.1); (d) Mn, Ni and Sr were not enriched in the mud but enriched in the river (index > 5). These results agree well with similar calculations for the Tinto river (van Geen *et al.*, 1997), with the exception of As, Cu and Fe. These elements were all enriched in the sulphide ores found in the Tinto watershed, but As and Fe showed a mobility similar to S (index 0.46 and 0.61, respectively) and Cu was more mobile than S (index 3.6) (van Geen *et al.*, 1997). These differences indicate that the oxidation of the sulphides in the Los Frailes tailings mud in the Guadiamar system was not as advanced when compared with the Tinto watershed. It can be inferred that further oxidation of the Los Frailes muds will have resulted in the release of As, Fe and Cu to the overlying waters.

In absence of direct measurements, an estimate of the total amount of metal discharged by the spill into the Guadiamar watershed can only be made subject to a number of assumptions. The mining company reported‡ that the amount of material in the discharged mine tailings was *ca.* 4×10^6 and 1.1×10^6 m^3, for the dissolved and particulate phases, respectively. The contribution of the acidic tailing waters to the Guadiamar can be estimated using the alkaline character of the river. The total carbonate alkalinity for a typical sample upstream of the Los Frailes mine (site 1) was 4.6 mM (pH 7.77), and at that pH we can assume that bicarbonate is the dominant species. The pH observed at site 2 on April 27 (pH 6.07) would suggest that the system was very close to the pK_1 value of the carbonate system ($pK_1 = 6.14$, 20°C, $I = 10^{-3}$) (Stumm and Morgan, 1996), indicating that half of the total carbonate had been titrated to carbonic acid by the acidic mine waters (confirmed by MINEQL+ calculations). Assuming the pH of the tailing water was 2, then *ca.* 20% of the Guadiamar consisted of water from the tailing dam. Table 4 shows the estimated metal discharges from the Los Frailes tailing dam. The calculations indicate that the discharges into the watershed of the Guadiamar of Cu (5,100 t), Pb (24,700 t), Zn (26,200 t) and Ag (138 t, based on mud only) were higher than the annual production by the Los Frailes mine for Ag and Pb and *ca.* two times less for Cu and Zn. The estimated metal discharges were considerably higher than the annual flux of dissolved metals delivered by the Rio Tinto to its estuary (Table 4).

In October 1998, we observed a decrease in dissolved concentration of several orders of magnitude for most metals at site 2, when compared with April 27, 1998 (Table 2). Although most of the mud had been removed from agricultural fields and floodplains with the use of bulldozers, the higher metal levels at site 2 in October compared with site 1 (April 27) were most likely due to supply by the contaminated river sediments. At the mouth of the Guadalquivir (site 4) Mn and Zn levels were somewhat higher in October, compared with April (prior to dam failure) despite a possible higher dilution of the river water with seawater as indicated by the higher conductivity. The enhanced metal levels at sites 2 and 4 in October indicate that the legacy of the mining spill was affecting the rivers and estuarine waters.

Results from surface water trace metal monitoring exercises for dissolved As, Cu, Mn and Zn in the coastal waters of the Gulf of Cadiz did not show enhanced metal concentrations in the plume of the Guadalquivir in the aftermath of the Los Frailes spill (June 1997 compared with October 1998; Fig. 2a–d). Dissolved As, Cu, Mn and Zn in the plume showed concentrations of *ca.* 20, 15, 35 and 30 nM, respectively, in both June 1997 and October 1998. A lack of obviously enhanced metal concentrations in the Guadalquivir plume (Fig. 2) suggests that the land-based run-off of metals from

‡Boliden reports second quarter results (1998). Internet communication. http://www.newswire.ca/releases/august1998/12/c1846.html.

Los Frailes was of little importance for the near coastal waters in October 1998. It is possible that this is in part the result of near drought conditions in the summer–autumn of 1998, which are likely to have prevented the physical mobilisation of the sediments and to have slowed down chemical weathering of the sulphide rich muds.

The monitoring exercise showed higher dissolved Zn concentrations (Fig. 2d) in the Gulf of Cadiz away from the Guadalquivir plume in October 1998 compared with June 1997. This enrichment may be due to release of Zn from sediments deposited in this coastal area following the mine spill. However, the net residual currents in the Gulf of Cadiz are in an easterly direction (van Geen *et al.*, 1991). Therefore, a sedimentary source directly linked to the Los Frailes spill can only be used to explain enhanced Zn levels in the eastern part of the Gulf of Cadiz and does not explain enhanced Zn concentrations in areas to the west and south-west of the Guadalquivir plume in October 1998. Further investigations will be required to study the importance of trace metal release by sediments and seasonal changes in metal concentrations in the Gulf of Cadiz.

Although no obvious trace metal enrichment in the coastal waters was observed as a result of the mine spill, the waters of the Gulf of Cadiz have higher trace metal levels than those reported for other coastal areas, e.g. British Isles (Achterberg *et al.*, 1999). This trace metal enrichment can be explained by the high inputs from the rivers draining the IPB. The main core of the metal enriched water extends out as far as about the 50 m depth contour throughout the water column, with some evidence of recycling from the sediments. The Rio Odiel and Tinto have been implicated as major metal sources for the Gulf of Cadiz (van Geen *et al.*, 1991; van Geen *et al.*, 1997). Moreover, Fig. 2 shows that the Guadalquivir also forms an important source of trace metals for the Gulf of Cadiz.

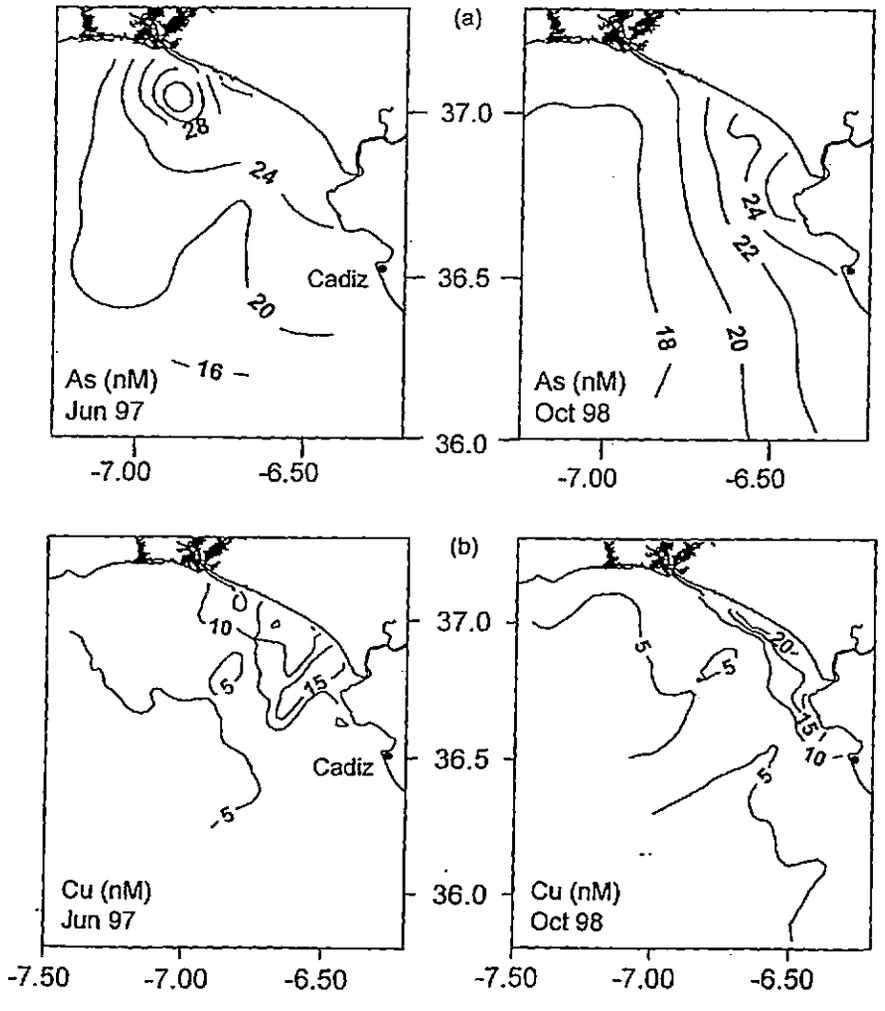

Fig. 2(a) and (b).

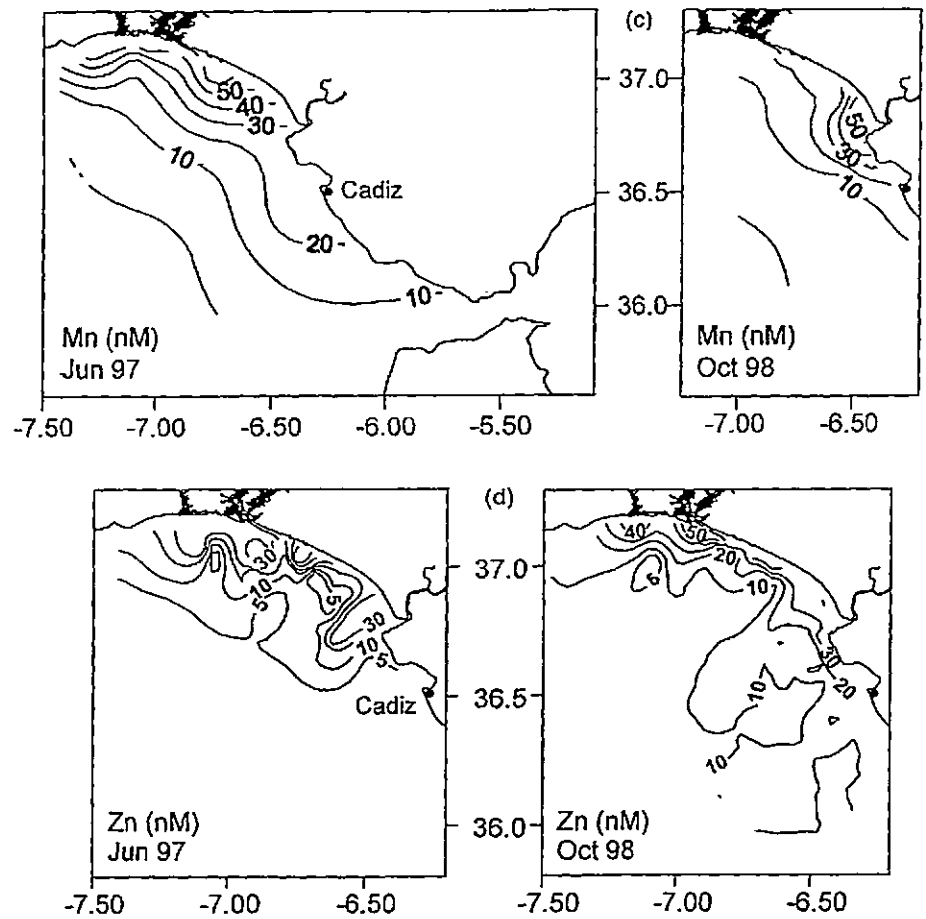

Fig. 2. Contour plots showing results from total dissolved trace metal measurements in the Gulf of Cadiz. As and Mn data (in nM) were obtained from samples collected using discrete sampling methods. Cu and Zn measurements (in nM) were performed on-board ship using continuous underway sampling with high-resolution trace metal monitoring techniques. Water depth in the coastal region varied from 1–2 m depth in-shore, to *ca.* 500 m off-shore.

CONCLUSIONS

The rivers which drain the mines of the Iberian Pyrite Belt have discharged large amounts of metals into the Gulf of Cadiz over an extremely long period. This study reveals that the collapse of the tailing reservoir at Los Frailes has not impacted, up to October 1998, the chemistry of As, Cu, Mn and Zn [also Cr, Fe, Ni and V (not presented)] in the coastal waters. The metals did not show obviously enhanced concentrations in the plume of the Guadalquivir in October 1998 compared with June 1997. This lack of significant impact on the coastal waters is probably in part the result of human intervention and natural removal processes, but is also likely to be related to climatic conditions in the region. The mechanical removal of the mud was apparently efficient in preventing contamination reaching the coastal region; the metal precipitation processes due to alkaline character of the water were important for Co and Zn (Table 3) and have been enhanced by the addition of lime to the AMD from Los Frailes; finally estuarine processes involving Fe flocculation and metal-co-precipitation (Johnson, 1986; Featherstone and O'Grady, 1997) have acted to trap metals in the sediments. Nevertheless the Guadiamar and Guadalquivir remain contaminated rivers as a result the failure of the tailings dam and the potential effects on the Doñana park necessitate continuous monitoring and complementary investigations.

Acknowledgements—We would like to thank the crew of the B/O *Garcia del Cid* for their assistance during sampling in the Gulf of Cadiz. This work is a contribution to the European Union ELOISE Programme (ELOISE No. 105) and was supported by the European Commission (DGXII) under contract TOROS (ENV4-CT96-0217), Environment and Climate Programme and BBSRC Grant 67/5 10058 European Community EC CT96-1461.

REFERENCES

Achterberg E. P., Colombo C. and van den Berg C. M. G. (1999) The distribution of dissolved Cu, Zn, Ni, Co and

Cr in English coastal surface waters. *Cont. Shelf Res.* 19, 537–558.

Albaiges J., Algaba J., Arambarri P., Carrera F., Baluja G., Hernandez L. M. and Castroviejo J. (1987) Budget of organic and inorganic pollutants in the Donana National Park (Spain). *Sci. Total Environ.* 63, 13–28.

Almodovar G. R., Saez R., Pons J. M., Maestre A., Toscano M. and Pascual E. (1998) Geology and genesis of the Aznalcollar massive sulphide deposits, Iberian Pyrite Belt, Spain. *Miner. Deposita* 33, 111–136.

Andreae M. O. (1977) Determination of As species in natural waters. *Anal. Chem.* 49, 820–823.

Borrego J. (1992) Sedimentologia del estuario del Rio Odiel (Huelva, S.O. Espana). Ph.D. thesis, University of Seville, Spain (315 pp.).

Branch S., Corns W., Ebdon L., Hill S. and O'Neill P. (1991) Determination of As by hydride generation inductively coupled plasma mass spectrometry using a tubular membrane gas–liquid separator. *J. Anal. Atom. Spectrom.* 6, 155–158.

Braungardt C., Achterberg E. P. and Nimmo M. (1998) On-line voltammetric monitoring of dissolved Cu and Ni in the Gulf of Cadiz, south-west Spain. *Anal. Chim. Acta* 377, 208–215.

Bryan G. W. and Langston W. J. (1992) Bioavailability, accumulation and effects of heavy metals in sediments with special reference to United Kingdom estuaries: a review. *Environ. Pollut.* 76, 89–131.

Campbell P. G. C. (1995) Interactions between trace metals and aquatic organisms: a critique of the free ion activity model. In *Metal Speciation and Bioavailibility in Aquatic Systems*, eds. A. Tessier and D. R. Turner, p. 45. John Wiley & Sons, Chichester.

Elbaz-Poulichet F., Morley N. H., Cruzado A., Velasquez Z., Green D., Achterberg E. P. and Braungardt C. B. (1999) Preliminary assessment of trace metal and nutrient concentrations (including metal speciation) in an extremely low pH (2.5) river–estuarine system, the Ria of Huelva (south-west Spain). *Sci. Total Environ.* 227, 73–83.

Featherstone A. M. and O'Grady B. V. (1997) Removal of dissolved copper and iron at the freshwater–saltwater interface of an acid mine stream. *Mar. Poll. Bull.* 34, 332–337.

Johnson C. A. (1986) The regulation of trace element concentrations in rivers and estuarine waters contaminated with acid mine drainage: the adsorption of Cu and Zn on amorphous Fe oxyhydroxides. *Geochim. Cosmochim. Acta* 50, 2433–2438.

Leistel J. M., Marcoux E., Deschamps Y. and Joubert M. (1998a) Antithetic behaviour of gold in the volcanogenic massive sulphide deposits of the Iberian pyrite belt. *Miner. Deposita* 33, 82–97.

Leistel J. M., Marcoux E., Thieblemont D., Quesada C., Sanchez A., Almodovar G. R., Pascual E. and Saez R. (1998b) The volcanic-hosted massive sulphide deposits of the Iberian pyrite belt. *Miner. Deposita* 33, 2–30.

Luoma S. N. (1983) Bioavailability of trace metals to aquatic organisms: a review. *Sci. Total Environ.* 28, 1–22.

Martin J. M. and Whitfield M. (1983) The significance of the river input of chemical elements to the ocean. In *Trace Metals in Seawater*, eds. C. S. Wong, E. Goldberg, K. Bruland and E. Boyle, pp. 265–296. Plenum Press, New York.

Martin J. M., Guan D. M., Elbaz-Poulichet F., Thomas A. J. and Gordeev V. V. (1993) Preliminary assessment of the distributions of some trace elements (As, Cd, Cu, Fe, Ni, Pb and Zn) in a pristine aquatic environment: the Lena River estuary (Russia). *Mar. Chem.* 43, 185–199.

Millward G. E., Allen J. I., Morris A. W. and Turner A. (1996) Distributions and fluxes of non-detrital particulate Fe, Mn, Cu, Zn in the Humber coastal zone, UK. *Continental Shelf Res.* 16, 967–993.

Morley N. H., Burton J. D., Tankere S. P. C. and Martin J.-M. (1997) Distribution and behaviour of some dissolved trace metals in the western Mediterranean Sea. *Deep-Sea Res. II* 44, 675–691.

Morley N. H., Fay C. W. and Statham P. J. (1988) Design and use of a clean shipboard handling system for seawater samples. In *Advances in Underwater Technology, Ocean Science and Offshore Engineering*, Graham & Trotman, pp. 283–289.

Pain G. N., Sanchez A. L. and Mehlhorn T. L. (1998) The Donana ecological disaster: contamination of a world heritage estuarine marsh ecosystem with acidified pyrite mine waste. *Sci. Total Environ.* 222, 45–54.

Rantala R. T. T. and Loring D. H. (1985) Cadmium, copper, lead and zinc in particlute material. *Int. J. Anal. Chem.* 19, 166–170.

Schecher W. D., McAvoy D. C. (1994) MINEQL+, user's manual. Environmental Software, Hallowell, ME.

Stumm W. and Morgan J. J. (1996) *Aquatic Chemistry: Chemical Equilibria and Rates in Natural Waters*. John Wiley & Sons, New York.

van Geen A., Adkins J. F., Boyle E. A., Nelson C. H. and Palanques A. (1997) A 120 yr record of widespread contamination from mining of the Iberian pyrite belt. *Geology* 25, 291–294.

van Geen A., Boyle E. A. and Moore W. S. (1991) Trace metal enrichments in waters of the Gulf of Cadiz, Spain. *Geochim. Cosmochim. Acta* 55, 2173–2191.

van Geen A. and Chase Z. (1998) Recent mine spill adds to contamination of southern Spain. *Eos* 79, 449–450.

Waters (1996). Operator's manual. Water Capillary Anion Analysis. Analysis of common anions (N-601a). Revised version 3. Waters, USA, p. 6.1–6.7.

Wedepohl K. H. (1991) The composition of the upper earth's crust and the natural cycles of selected metals. In *Metals and Their Compounds in the Environment: Occurrence, Analysis and Biological Relevance*, ed. E. Merian, p. 3. VHC, Weinheim.

ELSEVIER

Analytica Chimica Acta 377 (1998) 205–215

ANALYTICA CHIMICA ACTA

On-line voltammetric monitoring of dissolved Cu and Ni in the Gulf of Cadiz, south-west Spain

Charlotte Braungardt, Eric P. Achterberg*, Malcolm Nimmo

Department of Environmental Sciences, University of Plymouth, PL4 8AA Plymouth, UK

Received 30 January 1998; received in revised form 11 June 1998; accepted 24 June 1998

Abstract

Geochemical processes in estuarine and coastal waters often occur on temporally and spatially small scales, resulting in variability of metal speciation and dissolved concentrations. Thus, surveys, which are aimed to improve our understanding of metal behaviour in such systems, benefit from high-resolution, interactive sampling campaigns. The present paper discusses a high-resolution approach to coastal monitoring, with the application of an automated voltammetric metal analyser for on-line measurements of dissolved trace metals in the Gulf of Cadiz, south-west Spain. This coastal sea receives metal-rich inputs from a metalliferous mining area, mainly via the Huelva estuary. On-line measurements of dissolved Cu, Zn, Ni and Co were carried out on-board ship during an eight-day sampling campaign in the study area in June 1997. A pumping system operated continuously underway and provided sampled water from a depth of ca. 4 m. Total dissolved metal concentrations measured on-line in the Gulf of Cadiz ranged between <5 nM Cu (<3 nM Ni) ca. 50 km off-shore and 60–90 nM Cu (5–13 nM Ni) in the vicinity of the Huelva estuary. The survey revealed steep gradients and strong tidal variability in the dissolved metal plume extending from the Huelva estuary into the Gulf of Cadiz. Further on-line measurements were carried out with the automatic metal monitor from the bank of the Odiel estuary over a full tidal cycle, at dissolved metal concentrations in the μM range. The application confirmed the suitability of the automated metal monitor for coastal sampling, and demonstrated its adaptability to a wide range of environmental conditions in the dynamic waters of estuaries and coastal seas. The near-real time acquisition of dissolved metal concentrations at high resolution enabled an interactive sampling campaign and therefore the close investigation of tidal variability in the development of the Huelva estuary metal plume.

Keywords: Trace metal monitoring; Voltametry; Dissolved Cu; Dissolved Ni; In-situ analysis; Coastal waters

1. Introduction

In many parts of the world, estuaries and coastal seas are under strong environmental pressure, especially when situated in densely populated and industrialised regions. As a result of a growing global environmental awareness and the introduction of new environmental laws, a better understanding of biogeochemical processes affecting aquatic pollutant behaviour is required. For this reason, an increased effort is made to monitor physical and chemical parameters in marine systems. Coastal waters are highly dynamic and complex systems which are

*Corresponding author. Tel.: +44-1752-233000; fax: +44-1752-233035; e-mail: eachterberg@plym.ac.uk

0003-2670/98/$ – see front matter
PII: S0003-2670(98)00426-7

characterised by steep physical and chemical gradients, both on temporal and spatial scales. A series of processes act upon the chemical speciation of pollutants, and hence, their relative associations with dissolved, colloidal and particulate phases in the water column. For example, important factors influencing dissolved trace metal concentrations in estuarine and coastal waters include fresh water inputs, pH, redox conditions, tidal mixing and re-suspension, formation of colloids, precipitation, sorption, biological cycling and organic complexation [1–3].

The dynamic nature of coastal waters requires high resolution monitoring, if small scale processes are to be understood. In the marine analytical field, the application of in situ automated monitoring techniques is becoming more common, as such methods allow the analysis of closely spaced samples at a higher frequency than traditional discrete sampling strategies (e.g. [4,5]). Electrochemical methods are well established and commonly used for the monitoring of pH (potentiometry) and dissolved oxygen (amperometry) in natural waters. Adsorptive stripping voltammetry is an electrochemical technique which has been developed during the last decades for the analysis of trace metals in natural waters. One of the earliest voltammetric ship-board trace metal analysers was constructed by Clavell and Zirino [6] in 1977. Since then, robust, reliable and relatively cheap on-line automated voltammetric metal monitoring systems with good accuracy and precision have been developed and applied [7–12].

The current paper discusses the advantages of an on-line high-resolution monitoring approach for the determination of dissolved metals in the Gulf of Cadiz, south-west Spain. This coastal system receives metal-rich waters from rivers which rise in an important mining area and flow through industrialised zones. As a consequence of the enhanced metal inputs and tidal water movements, high spatial and temporal variability of dissolved metal concentrations occurs in the estuarine and coastal waters. In order to gain a better understanding of the complex biogeochemical processes affecting the metal behaviour and the variability in dissolved metal concentrations, a high resolution in situ on-line monitoring strategy was the preferred option over discrete sample collection followed by land-based laboratory analysis of the trace metals.

In order to meet the analytical challenges of on-line dissolved metal analysis in samples with changing salinity and metal concentrations (nM to μM), adsorptive cathodic stripping voltammetric (ACSV) methods were chosen. This approach proved valuable in the study area, which receives high inputs of organic compounds, acids and metals, and, as a result, has complex and constantly changing sample matrices. A modification of the fully automated on-line voltammetric metal monitoring system described by Achterberg and Van den Berg [7,8] was used for the near real-time high-resolution analysis of surface waters from the river bank and on-board ship. The system provided measurements of total dissolved Cu, Zn, Ni and Co with a sampling frequency of about 15–20 min. This approach reduced the risk of sample contamination and facilitated an interactive sampling campaign. Sample was obtained directly from the sea or estuary using a continuous pumping system. On-line sample pre-treatment was performed whereby the sample was filtered and UV-digested to supply the metal monitor with particle-free and organic-free surface seawater sample. Subsequently, the treated sample was analysed automatically in an ACSV batch mode. Hence, ACSV methods allowed the direct determination of dissolved trace metals in aqueous samples, without laboratory-based pre-concentration or matrix removal steps, as are required prior to analysis of saline samples using ICP-MS (inductively coupled plasma-mass spectroscopy) or GFAAS (graphite furnace atomic absorption spectroscopy) methods.

2. Study area

Spanish shelf waters and sediments in the Gulf of Cadiz (Fig. 1) have been reported to be enriched with trace metals, especially Cu, Zn and Cd [13,14]. Several papers have recently suggested the Tinto and Odiel rivers as a possible source for metals to the Gulf of Cadiz [14–17]. Water from this sea area is entrained by the flow of Atlantic water through the Straits of Gibraltar. This has raised some concern with respect to a possible enrichment of the Western Mediterranean Sea with trace metals originating in the Gulf of Cadiz [13,18]. The research presented in this paper forms part of the Tinto Odiel River Ocean Study (TOROS), which investigates biogeochemical fluxes

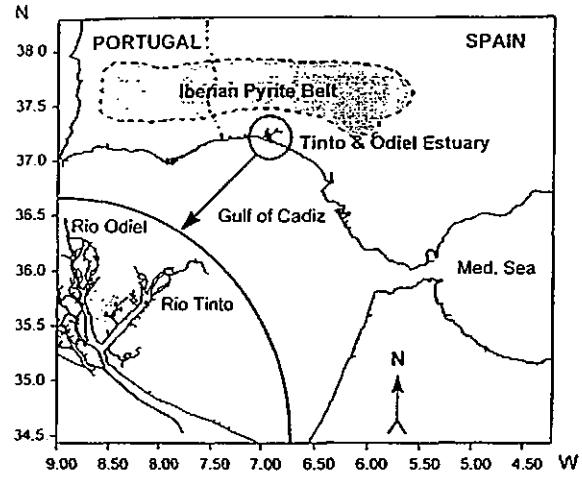

Fig. 1. Location of the Iberian Pyrite Belt and the Tinto/Odiel rivers in the south-west of Spain. The inset shows the confluence of the two estuaries at the city of Huelva (hatched).

of metal pollution in the Tinto/Odiel estuarine system and the Gulf of Cadiz.

The Rio Tinto and Rio Odiel are two small rivers (83 and 128 km in length, respectively), which drain a combined catchment area of about 3400 km^2 in one of the most important metal sulphide mineralisation regions in the world, the Iberian Pyrite Belt [16] (Fig. 1). The massive sulphide ore bodies in the Pyrite Belt are rich in metals, especially Zn, Pb and Cu, with traces of Cd, Ag and Au. This area has been mined for Cu and precious metals since Phoenician times [19], leaving a legacy of large quantities of slag and processed ore. Today, sulphide ores are extracted mainly for the production of sulphuric acid.

The Tinto and Odiel rivers have low average discharge volumes (annual mean 3 and 15 $m^3 s^{-1}$, respectively), with a large seasonal variation [20]. As a result of weathering and anthropogenic inputs, the fresh water of the Tinto and Odiel rivers is extremely low in pH (pH 2–3.5) and high in metal concentrations (e.g. 340–460 μM Cu, 1.6–6.9 μM Ni and 1.7–10.9 mM Fe, unpublished data from November 1996 and June 1997). The two rivers join in a common estuary at the city of Huelva, which is an important industrial centre in the south-west of Spain (inset in Fig. 1). Among the industries which discharge effluents into the estuary are paper and fertiliser plants, ore roasting facilities, titanium dioxide and copper production plants, oil refineries and sewage works.

3. Methods

3.1. Reagents and analytical methods

De-ionised water was obtained from a Milli-Q system (MQ, ≥18 MΩ, Millipore). Hydrochloric acid (HCl), ammonia (NH_3) and ethanol of Analar grade (Merck) were purified by distillation in a sub-boiling quartz still. An aqueous HEPES pH buffer stock solution (1 M pH 7.8) was prepared from *N*-hydroxyethylpiperazine-*N*-2-ethanesulphonic acid (Merck) in MQ. Oxine stock solution (0.1 M) was prepared from 8-hydroxyquinoline (Merck) in MQ. DMG solution (0.1 M) was prepared from dimethylglyoxime (Merck) in ethanol. Mixed reagents for the on-line voltammetric analysis were prepared on a daily basis from the stock solutions of HEPES and the appropriate ACSV ligand. Total dissolved Cu and Zn were determined simultaneously in the presence of oxine (2×10^{-5} M) and HEPES (0.01 M), and the mixed reagent for Ni and Co analysis contained DMG (2×10^{-4} M) and HEPES (0.01 M) (all final concentrations in voltammetric cell). Addition of 250 μl of mixed reagent to 10 ml samples in the voltammetric cell gave the required ACSV ligand concentrations and pH 7.8 (method adapted from [9]). Mixed standards for Cu/Zn and Ni/Co (Spectrosol, Merck) were prepared in a range of concentrations (10^{-4}, 10^{-5}, 10^{-6} M) and acidified with HCl (0.1%, v/v). The standard with the appropriate metal concentration was used according to the dissolved metal levels encountered in the sampling area.

On-line trace metal analysis was carried out using square wave ACSV. A full description of the principles of ACSV is given elsewhere [21–23]. Prior to analysis, the sample was purged for 200 s with oxygen-free nitrogen (Air Liquide) to avoid electrochemical interference from dissolved oxygen. In-between cathodic scans, the purge was repeated for a short time (15 s). The wide range of dissolved metal concentrations in the Huelva estuary and Gulf of Cadiz required the adaptation of analytical parameters to the encountered waters. Typical instrumental parameters for the analysis of relatively pristine water in the outer Gulf of

Table 1
Typical parameters for square wave cathodic stripping voltammetry during ship-board analysis of total dissolved Cu and Ni in surface waters of the Gulf of Cadiz (nM range) and in the mid-Odiel estuary (μM range) (values in brackets refer to the simultaneously analysed metal (i.e. Zn with Cu, and Co with Ni))

Voltammetric parameter concentration range	Cu (Zn) (<20 nM)	Ni (Co) (<20 nM)	Cu (Zn) (1–4 (7) μM)	Ni (Co) (0.5–1 (2) μM)
Deposition potential (V)	−0.5	−0.8	−0.5	−0.97
Deposition time (s)	40	40	0	2
Stirrer setting (max. 6)	5	5	0	1
Scan frequency (Hz)	100	100	50	50
Initial potential (V)	−0.2	−0.8	−0.2	−0.8
Final potential (V)	−1.3	−1.2	−1.3	−1.2
Step potential (mV)	2.4	2.4	4.9	4.9
Modulation amplitude (mV)	25	25	10	10
Reduction potential (V)	−0.45 (−1.02)	−0.97 (−1.04)	−0.45 (−1.02)	−0.97 (−1.04)
Limit of detection (LOD)	0.48 nM	0.21 nM	–	–
Linear range	25 nM	20 nM	4 (7) μM	1 (2) μM
R^2 for linear range	0.99	0.99	0.99	0.99

Cadiz and highly polluted estuarine water are given in Table 1.

Discrete estuarine samples, taken in parallel with on-line analysis, were acidified (HCl, 0.1% v/v) in Spain, and analysed in the laboratory in Plymouth by ICP-MS (PlasmaQuad PQ^{2+} Turbo, VG Elemental, Winsford, Cheshire). The samples were 50 times diluted using MQ prior to analysis, and acidified with HNO_3 (Aristar, Merck). Indium was used as internal standard to compensate for instrumental fluctuations.

3.2. *In situ monitoring instrumentation*

A schematic diagram of the automated metal monitoring system is shown in Fig. 2. Continuous sampling was carried out underway using a torpedo-

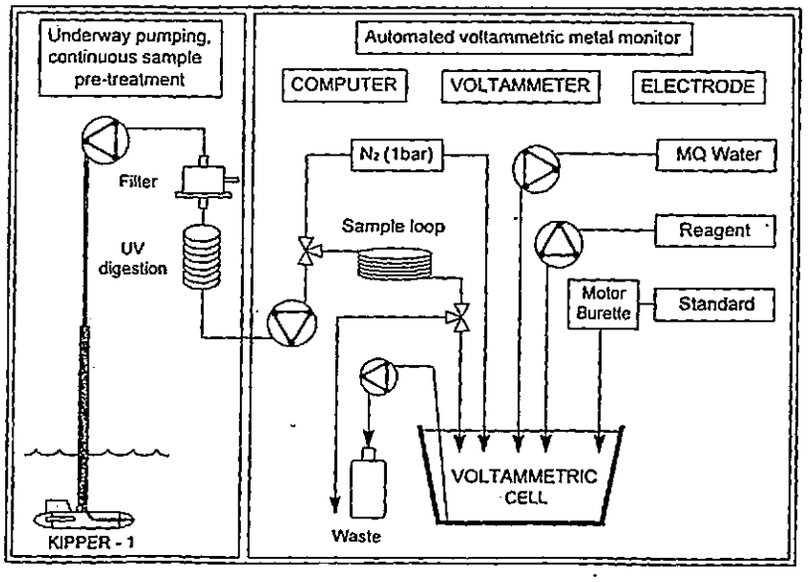

Fig. 2. Detailed diagram of the continuous underway pumping system and sample pre-treatment (left box), linked to the computer controlled, automated voltammetric metal monitor operating in batch mode (right box).

shaped fish (KIPPER-1), which was designed and constructed from mild steel at the University of Plymouth. A braided tube (PVC) was inserted into a bore that lead from the front of KIPPER-1, through its centre and out at the holding ring. The braided tube contained the sample pick-up tube (i.d. 8 mm, PVC), leading to the peristaltic sample pump which was positioned in the ship's laboratory. The design and weight (ca. 40 kg) of KIPPER-1 ensured that the sampling hose pointed forward and was kept at a constant depth (ca. 3–4 m) at speeds between 1 and 12 knots. KIPPER-1 was coated with metal-free epoxy-based paint (International Paint) and was deployed from a winch, away from the ship's hull to avoid the sampling of water which had been in contact with the hull. The braided tubing was attached to the lower part of the winch cable, which was taped in order to prevent contamination. Continuous pumping of large volumes of seawater (1–2 l min^{-1}) flushed the pick-up tubing and allowed equilibration of the material (PVC) with the metal levels in the sampled water [10]. From the peristaltic sampling pump a Teflon® tube (i.d. 0.6 mm) lead to the continuous two-step on-line sample pre-treatment (filtration and UV-digestion) and further to the automated metal monitor (Fig. 2).

The on-line filtration was carried out with a cross-flow filtration unit made from an adapted Swinnex filter holder (47 mm diameter cellulose nitrate membrane filter, 0.45 μm pore size, Whatman, USA). Filtration was followed by the on-line UV-digestion of dissolved organic matter. This step was necessary for the breakdown of surfactants and natural metal-complexing organic ligands, which may interfere with the voltammetric analysis of total dissolved metals [9]. The UV-digestion unit contained a medium pressure mercury vapour lamp (400 W, Photochemical Reactors) surrounded by a quartz glass coil (i.d. 1.0 mm, length ca. 3.5 m), and the system was cooled by a fan to ca. 70°C. The sample cooled to ambient temperature during its transfer from the UV-digestion unit to the voltammetric cell.

The pre-treated sample was conveyed to a sample loop (9.90 ml) by a peristaltic pump, which formed part of a custom-built automated sample and reagent transport system. This unit also delivered reagents to the voltammetric cell and rinsed it with MQ after a measuring cycle was completed. The sample loop was enclosed by two inert three-way valves (Teflon®, Cole-Parmer), which were set in a position that allowed flushing and filling of the loop with sample water before analysis. The valves were actuated to empty the contents of the sample loop into the voltammetric cell by means of nitrogen gas (oxygen free N_2, 1 bar). Teflon® tubing was used throughout the monitor, with the exception of the pump tubing, which was Santoprene®.

The voltammetric system comprised of a Metrohm hanging mercury drop electrode (VA Stand 663, Switzerland), which was connected to a μAutolab voltammetric analyser (EcoChemie, Netherlands). Metal standard additions for the internal calibration of each measurement were made to the voltammetric cell using a syringe pump (Cavro). The voltammeter and all peripheral components of the metal monitor were controlled using a portable PC (Compaq 386SX). Dedicated software carried out peak evaluation, data acquisition and storage. The software was self-decisive, thus rejected sub-quality scans with a standard deviation above a pre-set value of eight percent, and initiated additional scans. The software also initiated further standard additions, if the increase in peak height as a consequence of the first standard addition was insufficient (i.e. less than 100%).

The risk of contamination during on-line analysis was reduced by acid-cleaning of all sample tubing (pumping of ca. 5 l 5% HCl (Analar, Merck), followed by MQ) and the sample transport system in the metal monitor (pumping of 500 ml 1% HCl, followed by MQ) before and between individual parts of the survey. Cross-contamination between samples was minimised by careful planning of the cruise track. Reagents were handled on a clean bench under a laminar flow hood in the ship's laboratory. The analysis of each sample batch was individually calibrated by means of internal standard additions. This approach took account of changing sample matrices (e.g. as a result of salinity variations) which may result in changes in the method sensitivity.

3.3. Sampling

In June 1997, two fully automated metal monitors were almost continuously in operation for a period of eight days on board the Spanish research vessel *Garcia del Cid*. On-line high resolution measurements of

dissolved metals were performed during estuarine transects and coastal surveys. During the surveys, two automated voltammetric metal monitors were used for the simultaneous analysis of Zn and Cu (system 1), and Ni and Co (system 2). However, only Cu and Ni data from the cruise in the coastal waters of the Gulf of Cadiz in June 1997 will be presented in this paper. Samples were analysed in batches of ca. 10 ml, at a rate of one measuring cycle every 15–20 min.

In addition to the ship-board measurements, on-line metal analyses at one point in the Odiel estuary (near Huelva bridge) were carried out to record a time-series of metal concentrations over a full tidal cycle (duration 13 h). This study was carried out from a mobile laboratory positioned on the bank of the estuary, using a 240 V petrol generator for the supply of power. The continuous sample pick-up was anchored some distance from the shore. Parallel to the on-line monitoring, discrete samples were taken from the shore at lower resolution (hourly intervals), and these were used, among other purposes, for inter-comparison with results from the automated on-line analysis.

4. Results and discussion

4.1. Analytical performance

The analysis of a reagent blank in MQ batches gave concentrations of 0.46±0.16 nM Cu (n=5) and 0.04±0.02 nM Ni (n=4). For the determination of the limits of detection (LOD), seawater (Gulf of Cadiz) was analysed in batches, using ACSV with the voltammetric parameters for the concentration range <20 nM, as listed in Table 1. The seawater concentrations were 2.61±0.16 nM (LOD=0.48 nM) for Cu (n=5) and 2.88±0.07 nM (LOD=0.21 nM) for Ni (n=4) (Table 1), where the LOD was calculated as three times the standard deviation. Further reduction of the LOD can be achieved, when required, by increasing the deposition time. The maximum dissolved metal concentrations that could be analysed with ACSV without sample dilution, were determined using the parameters listed in Table 1 for the µM concentration range. By lowering the stirring rate during deposition, decreasing the deposition time, and altering the scanning parameters and deposition potential in order to lower the sensitivity, the linear range was extended to 4 and 1 µM for Cu and Ni respectively. The linear ranges were verified in laboratory experiments, resulting in regression coefficients (least square) of R^2=0.99 for Cu and R^2=0.99 for Ni. In the field, parameters were changed interactively according to the metal concentrations encountered. The accuracy of the applied analytical methodology was verified by the analysis of certified reference materials (SLEW-2 and CASS-3). Good recoveries (>87%) during discrete batch analysis were evident (Table 2). The reproducibility of on-line analysis with the automated metal monitor was determined in filtered, UV-irradiated and acidified (HCl, pH 2) seawater, which was sampled in the vicinity of Plymouth and contained Cu and Ni at concentrations similar to levels observed in the coastal waters of the Gulf of Cadiz. Several aliquots of this water were analysed in automated on-line mode for Cu and Ni. In order to adjust the pH of the acidified aliquots, NH_3 was added to the voltammetric cell with the mixed reagent. The relative standard deviation in this experiment was 5.9% for Cu (23.2±1.38 nM, n=16) and 7.4% for Ni (10.4±0.77 nM, n=13).

Table 2
Analysis of UV-irradiated reference materials (CASS-3 and SLEW-2) by ACSV in batches of 10 ml (confidence intervals refer to ± SD of the sample mean)

	n	ACSV result (nM)	Certified (nM)	Recovery (%)
CASS-3				
Cu	4	8.17±1.05	8.14±0.98	100
Ni	6	6.48±0.40	6.58±1.06	99
SLEW-2				
Cu	4	22.2±2.54	25.49±1.73	87
Ni	3	12.7±1.05	12.07±0.92	105

4.2. Environmental data

Results from automated on-line analysis for total dissolved Cu during the estuarine tidal cycle study in the Odiel compared well with concentrations determined in discrete samples collected in parallel from the bank of the Odiel estuary (June 1997). The extreme conditions with respect to metal concentrations and sample matrices, encountered during the tidal cycle study, made the manual dilution of samples

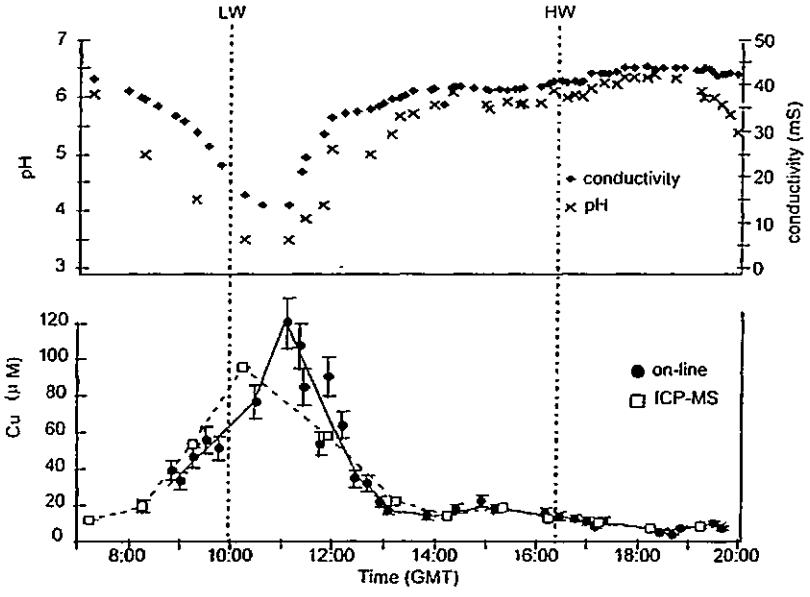

Fig. 3. Time series of conductivity, pH and dissolved Cu over a tidal cycle in the mid-Odiel estuary at Huelva bridge. The lower part shows on-line voltammetric measurements of Cu from the river bank and results from ICP-MS analysis of discrete samples, taken parallel at hourly intervals. Error bars refer to a typical error of ±8% between repeated scans during on-line analysis (ACSV), and to standard deviation of sample replicates during discrete analysis (ICP-MS). LW and HW: low and high water at Mazagon harbour (situated at the mouth of Huelva estuary).

during parts of the automated on-line analysis necessary. Results from automated tidal cycle study are presented in Fig. 3 and show that total dissolved Cu concentrations increased steeply during ebb tide and reached a maximum of 121 μM, coinciding with a minimum conductivity and low pH (pH 3.5).

By comparing the two sets of data in Fig. 3, it is apparent that on-line high resolution monitoring provided the position (time) and concentration of the Cu maximum, while the discrete sample analysis failed to fully resolve the tidal variability during the monitored period. From the close agreement between discrete and on-line data, it follows that contamination from carry-over between samples during on-line measurements was minimal. Because the two sets of data resulted from the analysis of different samples, and not sub-samples of one another, the results are not directly statistically comparable. However, this intercomparison showed that the on-line monitoring produced good quality data in extreme sampling matrices and over a wide range of metal concentrations.

During the first part of the coastal survey, the *Garcia del Cid* cruised for a period of four days between the coast line and the 500 m depth contour in the Gulf of Cadiz. During this period, a total of 52 separate discrete depth profiles were obtained, for which the vessel had to halt at each sampling station. Also during this period, continuous underway sampling was carried out and the voltammetric metal monitor operated almost continuously on-board ship. About 250 measurements of dissolved Cu and Ni in the surface waters were performed during steaming and while the vessel was on station. Fig. 4 compares the high resolution achieved with on-line monitoring (3.5–4.5 km between measurements along the cruise track), with the spacing of discrete sampling stations (ca. 10–15 km). This graph shows the much higher sampling frequency obtained using the automated monitoring approach, resulting in a better spatial resolution.

The total dissolved Cu and Ni concentrations in surface waters of the Gulf of Cadiz are shown in Figs. 5 and 6, in the form of contour plots. The metal distribution data have not been corrected for tidal movement, as, at present, no detailed information on currents is available for the study area. Enhanced metal levels were observed around the mouths of the

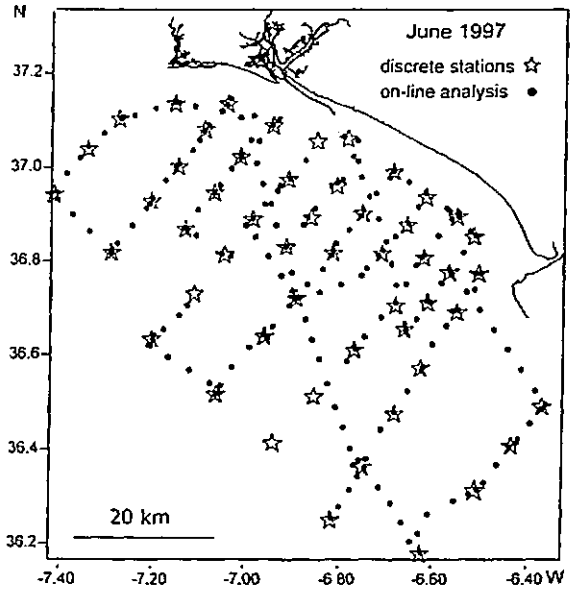

Fig. 4. Comparison between the resolution of discrete sampling stations (stars) and on-line automated measurements (circles) of Cu in the Gulf of Cadiz, June 1997.

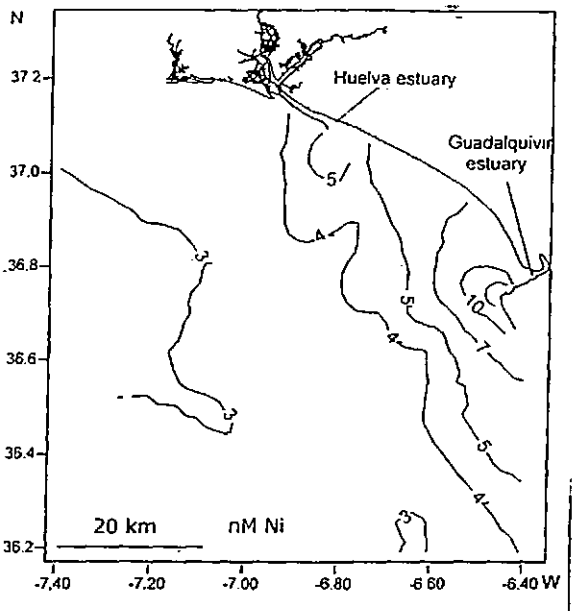

Fig. 6. Total dissolved Ni (nM) distribution in the Gulf of Cadiz, June 1997. The contour plots were created from ca. 250 on-line measurements, performed on-line during four days of steaming with the *Garcia del Cid*.

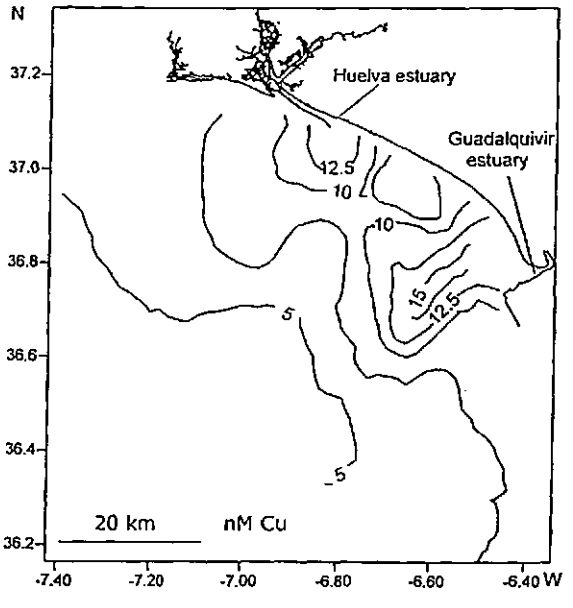

Fig. 5. Total dissolved Cu (nM) distribution in the Gulf of Cadiz, June 1997. The contour plots were created from ca. 250 on-line measurements, performed on-line during four days of steaming with the *Garcia del Cid* (see Fig. 4).

Huelva (15 nM Cu, 5 nM Ni) and the Guadalquivir (20 nM Cu, 15 nM Ni) estuaries. Metal concentrations decreased with increasing distance from the coast to levels below 5 nM Cu and 3 nM Ni at the sea-ward limit of the sampling area. This decrease can be explained by the mixing of metal-polluted estuarine with more pristine North Atlantic waters, which typically has concentrations of 1–1.5 nM Cu and 1.8–2.5 nM Ni in surface waters [24–27]. The difference between the enrichment of Cu (ca. 3–5 times) and Ni (ca. 1–2 times) in the outer Gulf of Cadiz, calculated with respect to typical off-shore concentrations for the Atlantic Ocean may be related to the strong enrichment of Cu, and the absence of Ni enrichment in the geology of the Iberian Pyrite Belt. Dissolved metal concentrations measured during this survey are comparable to those published by Van Geen et al. [13], who reported typical dissolved metal concentrations over the Spanish shelf in the region of 6.6 nmol kg^{-1} Cu and 3.4 nmol kg^{-1} Ni, and levels of 8–21 nmol kg^{-1} Cu and 3–6 nmol kg^{-1} Ni some 40 km to the south-west of the Guadalquivir estuary.

The waters of the Guadalquivir river and estuary have been reported to carry a lower metal load

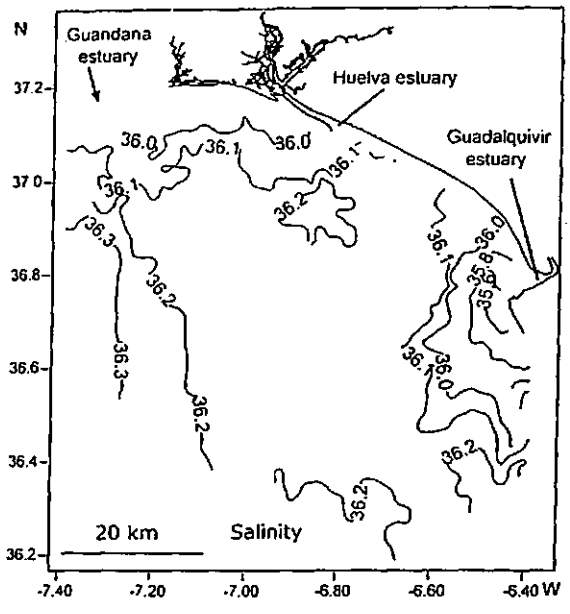

Fig. 7. Salinity distribution in the Gulf of Cadiz, June 1997. Measurements were undertaken with ship-board instrumentation operating in parallel with the on-line metal monitor.

(9.5–16 nmol kg^{-1} Cu and 21–79 nmol kg^{-1} Ni, [13]), than the concentrations found at the mouth of the Huelva estuary (50–600 nM Cu and 7.5–290 nM Ni, unpublished data from November 1996 and June 1997). However, the metal signal from the Guadalquivir river at the time of sampling extended farther into the Gulf of Cadiz than the Huelva river plume (Figs. 5 and 6). This compares well with the salinity distribution for the same period (Fig. 7), which shows an extended area of low salinity off the Guadalquivir estuary, while the fresh water discharge from the Huelva river had only a minor influence on the surface salinity in the Gulf of Cadiz. Therefore, the more distinct Guadalquivir metal plume, compared with that from the Huelva, can most likely be explained by the higher discharge volume of the Guadalquivir (annual mean: Guadalquivir 79 $m^3 s^{-1}$, Huelva 18 $m^3 s^{-1}$ [14,20]).

The second part of the coastal survey in June 1997 was dedicated to the investigation of the development and the tidal variability of the Huelva estuary metal plume. During this part of the survey, a spatial resolution of 1.5–2 km for the on-line metal measurements was achieved by lowering the cruise speed from eight to four knots, and the ship steamed continuously without stopping for discrete sampling.

Fig. 8 shows dissolved Cu concentrations along a similar cruise track, followed during two consecutive days. On day 15, 2.5 h after low water (LW), concentrations of 60–80 nM Cu were measured to the south-east of the Huelva estuary. One day later, concentrations were considerably lower (13–14 nM Cu) when the same area was sampled around the time of high water (HW). On both days, Cu concentrations increased steeply upon returning to the estuary, whereby Cu levels were higher on day 15 at LW

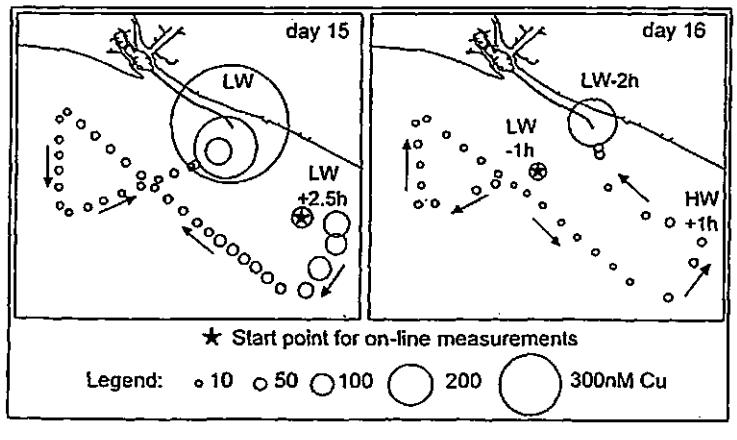

Fig. 8. On-line ship-board measurements of total dissolved Cu in the plume of the Huelva estuary during two consecutive days. The size of circles relates to the concentration; direction of the cruise track is indicated by arrows. The star denotes the first measurement of each day. On day 15 (16) the survey began 2.5 h after LW (1 h before LW) and took 10 h (12.5 h). LW, HW–low and high water at Mazagon harbour.

(>500 nM), than on day 16, when the vessel returned 2 h ahead of LW (>200 nM).

The observed variations in metal concentrations illustrate the importance of tidal movement for the timing of near-shore coastal surveys, and the value of on-line high-resolution monitoring. Observed metal concentrations close to the Huelva river mouth at the beginning of the survey (Figs. 5 and 6) and on day 16 suggested this estuary to be a minor contributor of Cu and Ni to the Gulf of Cadiz. However, the analysis during day 15 (and day 18, data not presented here) showed that highly contaminated water enters the Gulf of Cadiz from the Huelva river around the time of low water. The combination of low riverine water discharges with high metal concentrations caused small salinity changes in the vicinity of the Huelva estuary to be accompanied by marked gradients in dissolved metals, which were highly variable with tidal movement. Monitoring exercises performed over a period of several days and during different states of the tide are therefore required for the investigation of estuarine plumes, especially in coastal areas receiving low volume discharges, which contain high contaminant concentrations. During a survey in April 1998, high resolution on-line monitoring of Cu, Ni, Zn and Co was carried out on-board ship, while anchored in the mouth of the Huelva estuary over a full tidal cycle. Results from this study provided important data for the calculation of metal fluxes from this estuarine system to the coastal sea, and will be reported elsewhere.

Reported metal anomalies in fine sediment around the Huelva estuary suggested that metals were removed from solution within the estuarine mixing zone and were settled rapidly in the form of metal bearing flocs around the mouth of the Huelva estuary [14]. This process may also contribute to the limited spatial reach of the Huelva dissolved metal plume.

5. Conclusions

On-line analysis of total dissolved Cu and Ni was performed with a fully automated voltammetric metal monitor in the Gulf of Cadiz. The survey provided high resolution data, which revealed areas of elevated dissolved metal concentration associated with discharges from the Huelva and Guadalquivir estuaries. The application of the underway pumping system in combination with near-real time metal analysis enabled the close investigation of tidal variations in the Huelva estuary plume. The data collected during on-line analysis highlighted the importance of a high-resolution approach to contaminant monitoring at different states of the tide. Especially in highly dynamic coastal systems, the undertaking of a single survey would only provide a snap-shot of the state of the coastal environment and may therefore result in erroneous conclusions to be drawn.

In coastal and estuarine waters, the ACSV analysis proved to be highly suited for the changing sample matrix and the wide concentration range encountered during the survey. Comparisons between on-line and discrete samples showed the high quality of the acquired data, with no important carry-over between samples during the tidal cycle study, which was performed in a strongly contaminated part of the Odiel estuary. Careful planning of the sampling succession and intermediate acid-cleaning of the underway sampling system was important in order to reduce the risk of cross-contamination and enable the move from areas of high to those of low dissolved metal concentrations. The near-real time acquisition of data facilitated an interactive sampling campaign, which was of particular value in this complex system with small salinity changes and strong metal concentration gradients. Further advantages of the on-line measurement of dissolved metals in coastal areas with the automated voltammetric metal monitor over discrete sampling include the virtually effortless acquisition of high-resolution data, while contamination during sample handling is avoided, and the need for discrete analysis can be reduced to a few control samples. Moreover, dissolved metal speciation measurements can be performed with ACSV methods [8,21,28,29], because the technique allows the determination of different physico-chemical forms of dissolved trace metals. Trace metal speciation studies were carried out on seawater and samples from the lower estuary, and a series of experiments with suspended particulate matter was carried out by fellow researchers. These results will be reported elsewhere.

Future analytical developments will involve the interfacing of on-line conductivity, temperature and salinity measurements to the metal monitor, which will aid the interpretation of the contaminant studies. In addition, the connection of a GPS (global position-

ing system) is in process, which will allow the environmental data to be linked in real-time mode to the position of the vessel.

Acknowledgements

This work is a contribution to the European Union ELOISE Programme (ELOISE no. 011) in the framework of the TOROS project carried out under contract ENV4-CT96-0217.

We thank the crew and scientists on the *Garcia del Cid* and our colleagues from the University of Huelva for their assistance in the field.

References

[1] F.L.L. Muller, Mar. Chem. 52 (1996) 245.
[2] A.W. Morris, A.J. Bale, R.J.M. Howland, G.E. Millward, D.R. Ackroyd, D.H. Loring, R.T.T. Rantala, Water Sci. Technol. 18 (1986) 111.
[3] C.R. Olsen, N.H. Cutshall, I.L. Larsen, Mar. Chem. 11 (1982) 501.
[4] K.S. Johnson, R.L. Petty, J. Thomsen, in: A. Zirino (Ed.), Mapping Strategies in Chemical Oceanography, Am. Chem. Soc. (1985) 7.
[5] K.N. Andrew, N.J. Blundell, D. Price, P.J. Worsfold, Anal. Chem. 66 (1994) 916A.
[6] C. Clavell, A. Zirino, in: A. Zirino (Ed.), Mapping Strategies in Chemical Oceanography, Am. Chem. Soc. (1985) 139.
[7] E.P. Achterberg, C.M.G. Van Den Berg, Mar. Pollut. Bull. 32 (1996) 471.
[8] E.P. Achterberg, C.M.G. Van Den Berg, Anal. Chim. Acta 284 (1994) 463.
[9] E.P. Achterberg, C.M.G. Van Den Berg, Anal. Chim. Acta 291 (1994) 213.
[10] C.M.G. Van Den Berg, E.P. Achterberg, Trends in Anal. Chem. 13 (1994) 348.
[11] C. Collado-Sanchez, J. Perez-Pena, M.D. Gelado-Caballero, J.A. Herrera-Melian, J.J. Hernandez-Brito, Anal. Chim. Acta 320 (1996) 19.
[12] M.-L. Tercier, J. Buffle, Electroanalysis 5 (1993) 187.
[13] A. Van Geen, E.A. Boyle, W.S. Moore, Geochim. Cosmochim. Acta 55 (1991) 2173.
[14] A. Palanques, J.I. Diaz, M. Farran, Oceanol. Acta 18 (1995) 469.
[15] A. Van Geen, J.F. Adkins, E.A. Boyle, C.H. Nelson, A. Palanques, Geology 25 (1997) 291.
[16] M. Leblanc, D. Benothman, F. Elbaz-Poulichet, J.M. Luck, D. Carvajal, A.J. Gonzalez-Martinez, J.A. Grande-Gil, G. Ruiz de Almodovar, R. Saez-Ramos, in: Pasava, Kribek, and Zak Mineral Deposits, Balkema, 1995, p. 669.
[17] C.H. Nelson, P.J. Lamothe, Estuaries 16 (1993) 496.
[18] A. Van Geen, P. Rosener, E.A. Boyle, Nature 331 (1988) 423.
[19] J.A. Thornburn, Bull. Peak Dist. Mines Hist. Soc. 11 (1990) 97.
[20] J. Borrego-Flores, Thesis, Sedimentologia del estuario del Rio Odiel, University of Sevilla, Huelva, SO, Espana, 1992.
[21] M. Nimmo, C.M.G. Van den Berg, J. Brown, Estuarine, Coastal and Shelf Science 29 (1989) 57.
[22] G. Henze, in: J.A.C. Broekaert, S. Güçer (Eds.), Metal Speciation in the Environment, Springer, Berlin, 1990, p. 391.
[23] C.M.G. Van den Berg, in: J.P. Riley, R. Chester (Eds.), Chemical Oceanography, Academic Press, New York, 1988, p. 197.
[24] N.H. Morley, P.J. Statham, J.D. Burton, Deep Sea Res. I 40 (1993) 1043.
[25] W.M. Landing, G.A. Cutter, J.A. Dalziel, A.R. Flegal, R.T. Powell, D. Schmidt, A. Shiller, P. Statham, S. Westerlund, J. Resing, Mar. Chem. 49 (1995) 253.
[26] K.W. Bruland, R.P. Franks, in: C.S. Wong, E. Boyle, K.W. Bruland, J.D. Burton, E.D. Goldberg (Eds.), Trace Metals in Sea Water, NATO Scientific Affairs Division and Plenum Press, New York, 1983, p. 395.
[27] K. Kremling, C. Pohl, Mar. Chem. 27 (1989) 43.
[28] J.R. Donat, C.M.G. Van den Berg, Mar. Chem. 38 (1992) 69.
[29] J.R. Donat, Proceedings of the 37th Conference of the International Association for Great Lakes Research and Estuarine Research Federation, International Association for Great Lakes Research, Buffalo, USA, 1994, p. 166.

WR 2703[B] (00/0) [AUTO 9/2/00]—V4-(NS)—pp 1-9

PII: S0043-1354(00)00073-7

Wat. Res. Vol. 00, No. 0, pp. 1–9, 2000

Printed in Great Britain
0043-1354/00/$ - see front matter

PERGAMON
www.elsevier.com/locate/watres

INFLUENCE OF SORPTION PROCESSES BY IRON OXIDES AND ALGAE FIXATION ON ARSENIC AND PHOSPHATE CYCLE IN AN ACIDIC ESTUARY (TINTO RIVER, SPAIN)

FRANCOISE ELBAZ-POULICHET[1]*, CLAUDE DUPUY[1], ANTONIO CRUZADO[2], ZOILA VELASQUEZ[2], ERIC P. ACHTERBERG[3] and CHARLOTTE B. BRAUNGARDT[3]

[1]CNRS-Universite Montpellier II, Laboratory of Hydrosciences-ISTEEM CC57, F-34095, Montpellier cedex, France; [2]CSIC/CEAB, Cami de Santa Barbara S/N, 17300, Blanes, Spain and [3]Department of Environmental Sciences, University of Plymouth, Plymouth PL4 8AA, UK

(First received 1 February 1999; accepted in revised form 1 October 1999)

Abstract—Inorganic arsenic and phosphate distributions have been studied in the acidic mixing zone of the Tinto river in November 1996, June 1997, and April 1998. This mixing zone receives high inputs of As, PO_4^{3-} and Fe in relation with acid mine drainage and run-off from phosphogypsum waste. In the early stage of mixing the dissolution of detritic Fe phases (pyrite and oxides) releases Fe and As to water. This process is counterbalanced by removal due to precipitation of Fe-oxides and Fe-organic complexes and algae fixation. In autumn, the amount of algae is negligible and a release of As, Fe and PO_4^{3-} to the dissolved phase was observed. As a consequence, high As and PO_4^{3-} concentrations are registered in the water (up to 43 nM for As and 330 μM for PO_4^{3-}). In spring, the removal dominates in relation with high algae productivity. As a result As and PO_4^{3-} are depleted in the dissolved phase in spring compared to autumn and high concentrations of As (up to 1530 $\mu g\ g^{-1}$ and 700 $\mu g\ g^{-1}$ in June and in April, respectively) were observed in the suspended particulate matter. In autumn dissolved As is correlated with Fe whilst in spring As behaves in a similar way as PO_4^{3-}. © 2000 Elsevier Science Ltd. All rights reserved

Key words—arsenic, phosphate, iron, biogeochemistry, acidic estuary, algae

INTRODUCTION

Arsenic and phosphorus are both group VA elements and are therefore chemically similar. Phosphate (PO_4^{3-}) is an essential nutrient for organisms and the uptake of arsenate (AsO_4^{3-}) as a substitute for phosphate has been observed for phytoplankton. However, the P/As ratio in phytoplankton is about 10-fold higher than the ratio in their ambient environment, demonstrating that these organisms take up P preferentially (Morris *et al.*, 1984). This process, well documented for the open ocean (Andreae, 1979), has been also reported for P-enriched estuaries (Froelich *et al.*, 1985). The removal of As in such estuaries is balanced by a release of this element following biomethylation and the estuarine profile of As remains near conservative, as is the case in unpolluted estuaries (Carpenter *et al.*, 1978). In contrast, anthropogenically perturbed estuaries often display high As concentrations at points in the estuarine profile (Andreae *et al.*, 1983), resulting in a deviation from conservative As behavior. Removal of As and PO_4^{3-} from the water column also takes place by scavenging involving Fe on surface active suspended matter (Kitts *et al.*, 1994). As and PO_4^{3-} are therefore involved in a multiplicity of reaction pathways, the respective importance of each depends on several factors, which all would require an environment case study to elucidate.

This paper describes the distribution of inorganic As and PO_4^{3-} concentrations along the salinity gradient of the Tinto estuary (southern Spain). This estuary is marked by extremely high As and PO_4^{3-} concentrations and a high biological productivity. Seasonal variations of As and PO_4^{3-} concentrations are discussed with regards to biological and physicochemical parameters.

STUDY AREA

The Tinto estuary (Fig. 1) is a partial to well mixed estuary with a maximum tidal amplitude of about 3 m. The upper limit of saline intrusion

*Author to whom all correspondence should be addressed. Fax: +33-4-67-146774; e-mail: elbaz@dstu.univ-montp2.fr

WR 2703[B] (00/0) [AUTO 9/2/00]—V4-(NS)—pp 1-9

is located between the stations SR and TR10 in the Tinto river (Fig. 1).

The Tinto estuary is a site of major industrial activities. The fertilizer industry treats imported phosphate ore and generates large amounts of phosphogypsum wastes which are dumped on the northern bank of the estuary. The phosphogypsum wastes (about 10^{10} kg) cover an area of approximately 4.10^6 m^2 (Travesi *et al.*, 1997). The wastes contain high quantities of As (personal communication, R.M. Canto) and contributes to the input of dissolved and particulate material to the estuary (Elbaz-Poulichet *et al.*, 1999).

The Tinto river drains the Tinto mining district situated in the Iberian Pyrite Belt, one of the largest massive sulfide deposits in the world (Leistel *et al.*, 1998). In addition to Zn, Cu and Pb, the deposit contains significant amount of As and traces of Au and Ag. Former mining activities of the gossan (the upper oxidized part of the deposit) and present day mining of the sulfidic zone has left enormous quantities of As-rich Fe-hydroxides and pyrite slag. As a result of erosion processes, detrital pyrite and Fe-hydroxides are abundant in the sediments throughout the Tinto estuary. The drainage of pyrite wastes releases large amounts of metals and sulfuric acid into the river (Elbaz-Poulichet and Leblanc, 1996; Nelson and Lamothe, 1993; Van Geen *et al.*, 1997; Van Geen and Chase, 1998).

The mean water discharges of Tinto river is 3 m^3 s^{-1}. However important variations are observed (Borrego-Flores, 1992), with low discharges generally during summer and high river discharges in winter (December–February) after important but aleatory rain events.

MATERIALS AND METHODS

Sampling

Three surveys were carried out for this study: November 1996, June 1997 and April 1998. They correspond with periods of contrasting primary productivity: low in November, high in June and moderate in April. The position of sampling stations is reported in Fig. 1. Samples were taken by hand, using clean sampling procedures, from a small boat with reference to salinity.

Sample pretreatment and analyses

Eh and pH were measured in the field laboratory (Huelva) immediately upon sampling. Chloride concentrations were calculated from Na^+ concentrations assuming $Na^+/Cl^- = 0.56$ in seawater with a salinity of 35‰ (Riley and Chester, 1971) or determined directly using Capillary Ion Analysis.

Samples for nutrients (PO_4^{3-}, NO_3^-, NO_2^-) were immediately deep-frozen after filtration using Millipore filters (0.45 μm: Teflon). Analytical determinations were carried out by automatic segmented flow techniques according to Whitledge *et al.* (1981).

Samples for chlorophyll a, b, c determinations, were filtered through 47-mm GF/F filters and chilled between collection and analysis. The phytoplankton pigments were determined using a spectrometric technique, following extraction with 5 ml acetone during 24 h. The resulting suspension was centrifuged and the absorbance of the supernatant was obtained at 750, 664, 667 and 630 nm.

Samples for dissolved organic carbon (DOC) were filtered on GFF glass fiber filters and analyzed using a high temperature oxidation technique.

Water samples for total dissolved Fe and As analysis

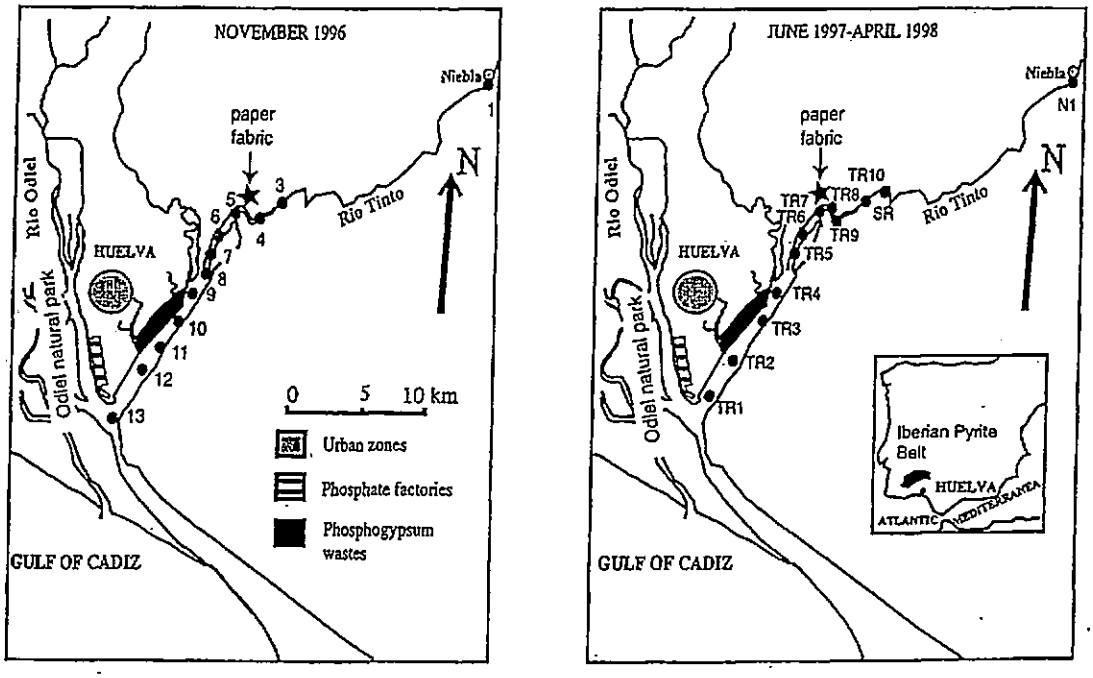

Fig. 1. Sketch map of the Tinto estuary showing the location of samples for each of the three surveys.

Table 1. Dissolved nutrients, arsenic, iron, dissolved organic carbon (DOC) and supporting parameters in Tinto estuary

	Stations[a]	Cl^- (g l^{-1})	pH	Eh (V)	SO_4^{2-} (mM)	PO_4^{3-} (μM)	Total Fe (mM)	FeII (μM)	FeIII (mM)	total As (μM)	AsIII (nM)	AsV (nM)	NO_2^- (μM)	NO_3^- (μM)	DOC (mg l^{-1})	Total chlorophyll (μg l^{-1})	Chlorophyll-a (μg l^{-1})
November 1996	1	0.03	2.47		27.1	14	13			29.2						0.43	0.15
	3	1.90	2.43		51.0	233	20			42.7						2.39	2.12
	4	6.59	2.46		65.4		10			22.6						10.06	6.93
	5	9.58	2.45		71.7	328	6			13.8						8.32	5.81
	6	10.39	2.47		64.3	278	3			12						8.98	6.10
	7	13.08	2.50		61.4	177				8.56						7.97	5.70
	8	13.76	2.66		62.2	66	0.36			4.89						6.75	4.11
	9	15.53	2.59		59.9	184	0.32			8.40						4.71	4.11
	10	16.44	2.86		50.9	112	0.19			4.19						8.86	4.11
	11	16.33	3.09		54.0	127				4.25						14.00	4.11
	12	17.71	2.68		57.4	90				3.84						10.41	4.11
June 1997	TR0[b]		2.55			45											
	N1	0.04	2.55	0.58	8.6		1.69			0.20			0.010	0.646		1.5	4.11
	SR	0.50	2.60	0.54	9.6		2.23			0.23							
	TR10	4.26	2.40	0.50	22.6		2.37			0.75			0.030	3.85	10	3.73	
	TR9	6.09	2.40	0.45	19.4	26	1.96			0.62			0.033	3.96	16.85	6.86	
	TR7	9.37	2.50	0.48	33.0	23	1.27			0.64			0.035	3.67	24.60	286	209
	TR6	13.23	2.55	0.46	35.5	147	0.39			0.24			0.023	5.60	15.70	465	342
	TR5	13.51	2.55	0.46	36.2	120	0.40			0.20			0.017	3.95	19.59	384	275
	TR4	14.65	2.65	0.41	35.9	278	0.27			0.37			0.023	3.59	8.83	387	279
	TR3	16.32	3.00	0.40	36.0	274	0.12			0.32			0.023	3.42	8.41	328	235
	TR2	16.91	3.40	0.44	36.5	243	0.02			1.19			0.026	4.62	9.50	323	241
	TR1	17.80	5.40	0.54	37.0	11	0.0001			1.11			0.022	2.84	3.82	348	255
	TR8[c]	5.97	5.20	0.22	27.9	11	1.01			0.54			0.030	3.46	80.00	247	186
April 1998	N1	0.03	2.56	0.55	23		1.23	110	1.12	1.76	2.24	1.75				188	139
	TR10	0.68	2.61	0.54	17	6.85	1.26	242	1.01	0.15	0.86	0.15	2.49	99.8	3.28	3.31	2.40
	TR9	1.70	2.65	0.54	16	10.22	1.27	217	1.05	0.12	1.06	0.12	1.88	98.8	4.46	10.59	6.79
	TR8	4.45	2.78	0.53	17	5.80	1.17	193	0.98	0.61	0.39	0.061		94.4	4.69	9.06	5.77
	TR7	6.36	2.85	0.52	19	3.07	0.93	189	0.74	0.07	1.90	0.068	1.84	82.2	4.22	32.65	22
	TR6	8.43	3.04	0.50	20	8.01	0.41	171	0.25	0.03	1.17	0.033	0.56	90.7	4.31	63.32	41
	TR5	8.68	3.80	0.49		2.45	0.43	183	0.25	6.4E-05	1.06	0.063	0.40	76.8	4.47	46.09	32
	TR4	18.73	6.27	0.25	28	74.74				6.0E-04	6.15	0.592	1.04	19.3	3.56	55.88	39
	TR3	15.58	5.72	0.33	27	0.95				3.1E-05	2.56	0.028	0.06	58.3	4.19	132.78	90
	TR2	15.75	6.37	0.37	26	1.14				2.6E-05	2.51	0.023	0.72	58.6	3.64	61.62	44
	TR1	19.04	6.55	0.36	25	38.45				3.5E-04	3.03	0.347	1.08	12.9	4.62	47.54	32

[a]Station numbers correspond to locations in Fig. 1.
[b]Sample taken in the mining area.
[c]Sample taken in the effluent of the paper fabric.

were filtered through 0.2 μm PVDF filters (Millipore), and acidified to 1‰ with concentrated HNO_3 (Merk Suprapur). Samples for dissolved As(III) determinations were not acidified, but deep-frozen and analyzed within less than one week after sampling. This procedure yields good results for this speciation analysis (Seyler and Martin, 1989).

For dissolved Fe(II) determinations, filtered samples were buffered to pH 4.5 with an ammonium acetate/acetic acid buffer in the field, and Fe(II) complexed by adding 2.5 ml of a 0.5% (w/w) phenantroline solution to 25 ml of samples (Rodier *et al.*, 1996). Analyses were undertaken in the laboratory by colorimetry. Total dissolved Fe was determined by Flame Atomic Absorption Spectrometry. Dissolved Fe(III) was calculated as the difference between total dissolved Fe and Fe(II).

Total dissolved inorganic As was measured after a pre-reduction involving potassium iodide in the presence of ascorbic acid. For dissolved As(III) determinations, the pH was adjusted to 4.8 using an acetic acid–sodium acetate buffer. Arsenic was determined using a hydride generation system coupled to an ICP-MS (VG-Plasmaquad). This method is similar to that described by Andreae (1977), but has been modified according to Branch *et al.* (1991).

The suspended particulate matter (SPM) collected on the 0.2 μm PVDF filters was dried at 105°C and digested in sealed Teflon PFA vials with concentrated, hot (105°C) HNO_3. The analysis of Fe and inorganic As for the digested samples were carried out as just described for water.

The Reference Materials for Trace Metals, National Research Council of Canada: NASS-4 (seawater) and SLRS-3 (river water) were used to evaluate precision and accuracy of the methods. For total dissolved As, measured values on 10 replicate analyses (15.3 ± 1.5 nM for NASS-4 and 9.1 ± 0.1 nM for SLRS-3) agreed well with the recommended values (16.6 ± 1.2 nM for NASS-4 and 9.6 ± 0.7 nM for SLRS-3). Detection limits were 1 nM for As(III) and 1.5 nM for total As.

Mixing experiments

The mixing experiments were carried out during June survey. They were performed as comparison with processes taking place in the water column of the Tinto mixing zone. Unfiltered river water from station SR and seawater from a near shore station in the Gulf of Cadiz were mixed in different proportions. After 1 h, the samples were filtered, acidified and analyzed for Fe and As in a similar way as the field samples.

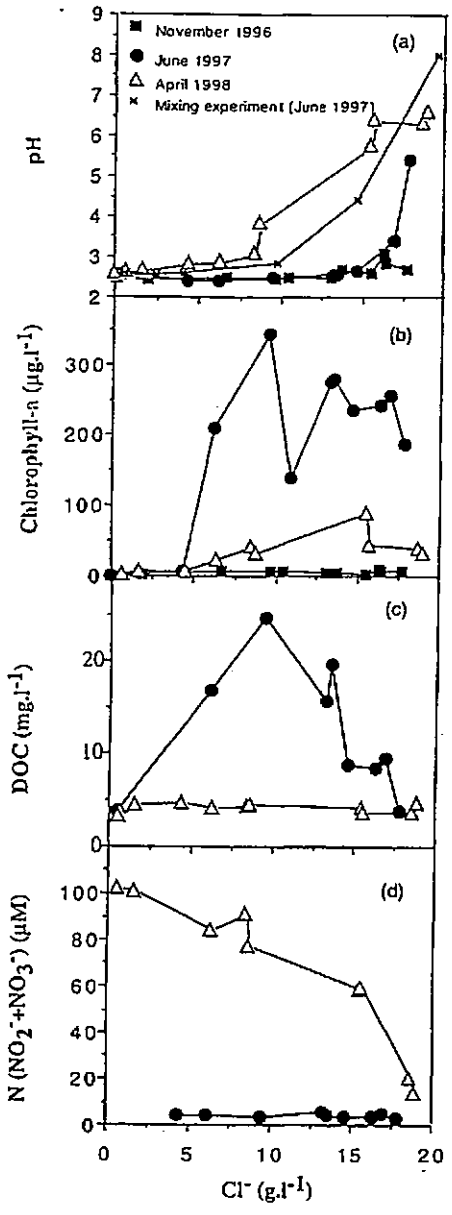

Fig. 2. pH, chlorophyll-a, Dissolved Organic Carbon (DOC) and Nitrate+Nitrite as a function of Cl^-.

PRESENTATION OF THE DATA

Main chemical and biological characteristics (Table 1)

The pH remains rather constant (pH≅2.5) in the river end-member during the three surveys, but shows a seasonal variation in the estuary (Fig. 2a). In April, the increase of pH in the mixing zone coincides with an increase in Cl^- content from 8.43 to 19 g l^{-1} (Fig. 2). In November and June, subtle variations were observed: the first stage of mixing between river and seawater (Cl^- < 6.1 g l^{-1}) was marked by a slight pH decrease (Table 1) followed by a slight increase.

The seasonal differences in pH with distance along the river–estuary transect was mainly due to variable input of acidic phosphogypsum effluents (pH 1.5). This input, which occurs in the vicinity of station TR4 (Fig. 1b), was important enough at times to keep the pH down in the lower mixing zone. This effect was observed in November, when the pH did not exceed the value of 3 in this part of the estuary. In April the pH profile, similar to that obtained from the mixing experiments (Fig. 2a), suggested a negligible input of acidic effluents.

Eh data, available only for June and April, range between 0.400–0.450 V and 0.248–0.554 V, respectively, indicating oxic conditions in the water column. The chlorophyll-a concentrations (Fig. 2b) show the highest values (maximum: 342 μg l^{-1}) in June and the lowest (<9.86 μg l^{-1}) in November.

In April, intermediate values (maximum: 90 $\mu g\ l^{-1}$) are observed in the mixing zone. The seasonal differences show that algae productivity is especially important during late spring and summer periods. Main algae species, observed in the Tinto mixing zone, are chlorophyceae. However a few diatoms and chryptophyceae are also present (Table 2).

Dissolved organic carbon displays seasonal variations (Fig. 2c) with enhanced concentrations in June (3.7 mg l^{-1} < DOC < 24.6 mg l^{-1}) and comparatively low concentrations in April (DOC < 4.69 mg l^{-1}). In June, DOC was correlated with chlorophyll, suggesting a contribution to DOC from algae exudates or breakdown products during high primary productivity. Dissolved oxidized nitrogen (DON: $NO_3^- + NO_2^-$) was depleted in June (Fig. 2d). This is probably related to the important algae production.

Dissolved Fe concentrations exhibit seasonal variation (Fig. 3a–c), with a maximum value of 18 mM and 13 mM in November and April, respectively. The water discharges were relatively constant during the three sampling exercises and therefore cannot account for the observed variations in Fe concentrations. When plotted against chlorinity, an increase in dissolved Fe can be observed in the early stages of mixing (Cl^- < 4.26 g l^{-1}); a similar behavior was found for several other metals (Elbaz-Poulichet *et al.*, 1999). This increase reflects a release of Fe to water. At higher chlorinity ~~(concentrations)~~, Fe concentrations decrease in a rather conservative manner as a result of simple dilution of river water with sea water, and do not exhibit the extensive removal observed in many other estuaries (e.g. Boyle *et al.*, 1977).

Arsenic and phosphate in the dissolved phase

Highest concentrations of As were registered during November (ca 45 μM; Fig. 3a), and a strong positive correlation between dissolved As and Fe appears ($r = 0.999$, $P = 0.01$).

In June and April, concentrations of dissolved As were lower than in November, and no correlation with Fe was observed. The trends (Fig. 3e and f) was marked by a maximum at station TR4 near the confluence of the Tinto and a small tributary draining the phosphogypsum wastes. A removal of As was clearly apparent in the chlorinity range defined by the As maximum and the river reference station.

PO_4^{3-} is introduced mainly in the mixing zone by phosphogypsum waste and its concentration remains relatively low (45 μM). In June and April, a maximum PO_4^{3-} concentration was observed in the vicinity of TR4 (Fig. 3e and f). Compared to the Redfield ratio (N/P = 16), the value of N/P was lower than 0.25 throughout the mixing zone in June, reflecting N-limiting conditions. In April, the N/P ratio reached a value of 60, and potential N-limitation was occuring only downstream of station TR3. In June and April, dissolved PO_4^{3-} and As showed a similar behavior (Fig. 3e and f). In open oceanic waters, a strong correlation has been observed between P and As (e.g. Andreae, 1979; Cutter and Cutter, 1995) and ~~have~~ has been attributed to a nutrient-like behavior of As which is taken up by algae in a similar manner as PO_4^{3-}. The distri-

Table 2. SPM, Particulate Fe, As concentrations and phytoplankton in the Tinto estuary

	Stations	SPM (mg l^{-1})	Fe (mg g^{-1})	As ($\mu g\ g^{-1}$)	Chlorophyceae (cells/ml)	Cryptophyceae (cell/ml)	Diatomophyceae (cell/ml)
June 1997	TRO[a]				9200		3.0
	N1	15	212	165			
	SR	39	160	320			
	TR10	199	283	1470			
	TR9	253	260	1530	211,000	130	64.0
	TR7	209	236	1320	41,600		
	TR6	186	31	90	485,000		
	TR5	172	61	190	605,000		
	TR4	138	29	135	337,000	65	
	TR3	81	62	275	401,000		
	TR2	64			486,000	110	
	TR1	62	26	215	377,000		220
	TR8[b]		46		404,000		30
April 1998	N1	4	555	2			
	TR10	155	101	135			
	TR9	163	142	225			
	TR8	239	150	260			
	TR7	68	164	305			
	TR6	147	182	455			
	TR5	18	105	370			
	TR4	55	74	500			
	TR3	120	145	700			
	TR2	128	98	555			
	TR1	36	46	325			

[a]Sample taken in the mining area.
[b]Sample taken in the effluent of the paper fabric.

bution of PO_4^{3-} in November was different from June and April, with the presence of two maximums (Fig. 3d): the highest maximum in concentration upstream and the smallest one near the phosphogypsum waste effluents.

Distribution of Fe and As in the suspended particulate matter (Table 2)

In June and April, the decrease of particulate Fe during the early stages of mixing (Fig. 4a and Table 2), corresponded with the on-set of dissolved Fe mobilization (Fig. 3). At somewhat higher chlorinity values (1–5 g l^{-1} Cl^-) an increase in particulate Fe is observed, especially in June, reflecting iron precipitation. In high salinity zone (Cl^- > 10 g l^{-1}), the relative depletion of particulate Fe (Fig. 4a) can best be explained by dilution of the SPM because of the abundance of algae.

In June, particulate As concentrations increased during the first stage of mixing (Fig. 4a) and displayed maximum concentrations (1532) at chlorinities between 4.26 and 9.37 g l^{-1}, before decreasing to 90–275 μg g^{-1} dry weight at Cl^- > 13 g l^{-1}. The distribution of particulate As in the mixing zone therefore coincided strongly with Fe. This has been previously observed in the Humber Plume and attributed to As adsorption on Fe-hydroxides (Millward *et al.*, 1997).

In April, particulate As concentrations showed increasing concentrations with chlorinity, until 700 μg g^{-1} dry weight for Cl^- = 15.58 g l^{-1}, followed by a rapid decrease. This behavior differs from that of Fe but coincides strongly with that of chlorophyll (Fig. 4b).

DISCUSSION

In the Tinto mixing zone, the distribution of As, Fe and PO_4^{3-} is affected by the presence of two different sources: acid mine drainage generating Fe and As forms a primary source, whereas run-off

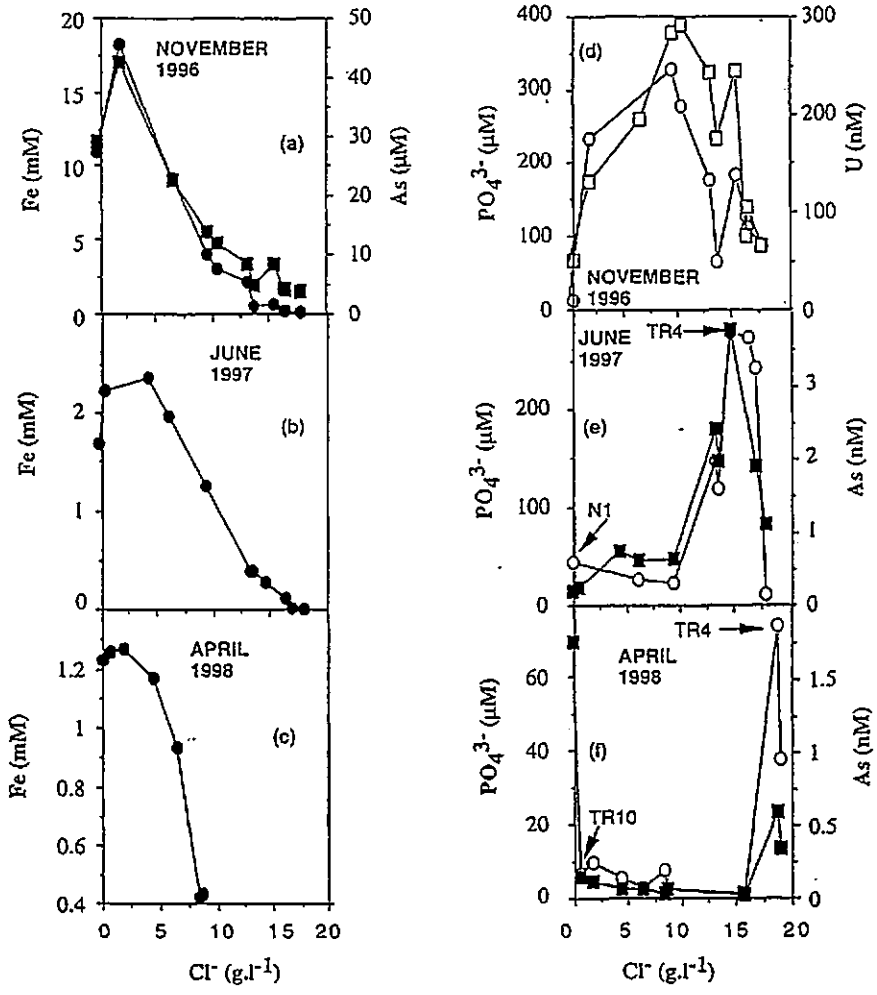

Fig. 3. Dissolved Fe (●), dissolved As (■), dissolved Phosphate (○) as a function of Cl^-. Uranium (□) reported on Fig. 3d are from Elbaz-Poulichet *et al.* (1999).

from phosphogypsum waste introducing PO_4^{3-} and As to the Tinto constitutes a secondary source.

The relationships between dissolved As and Fe in November (Fig. 3a) and that between particulate As and particulate Fe in June (Fig. 4a) outline the importance of Fe in interpreting the behavior of As in the Tinto system. Fe solid phases are important geochemical carriers of As and may contribute to the removal of dissolved As (Kitts *et al.*, 1994). According to Eh and pH data the dominant Fe species in the river end-member should be Fe(II). However, Fe(II) and Fe(III) determinations (Table 1) demonstrate that the two species co-exist in the dissolved phase with Fe(III) being the dominant species (Fe(III)/Fe(II) = 10 at the station N1). This result is corroborated by the orange–yellow color of the Tinto river, and implies that thermodynamic equilibrium is not achieved because of spatial, temporal and kinetic effects that continually perturb the local environment as demonstrated elsewhere in acidic sulfate waters (Bigham *et al.*, 1996). The Fe(III) formation starts in the tailing waters through bacterial oxidation of Fe(II) by T. Ferrooxidans at pH close to 2.5 (Salomons, 1995).

The data reported in Fig. 3 and 4 suggest that dissolved and particulate Fe are subjected to both release and removal processes. At $Cl^- < 10$ g l^{-1}, a release of Fe is apparent from the Fig. 3a–c. The two Fe species (Fe(II) and Fe(III)) are involved in the processes (Table 1), as well as Mn, Cu, Ni, Zn (Elbaz-Poulichet *et al.*, 1999). The release of these metals to the water phase and the presence of abundant corroded detrital pyrite in the sediments of the river bed and tidal marshes suggests an origin from pyrite dissolution according to the classical reaction:

$$8H_2O + FeS_{2(s)} + 14Fe^{3+} = 2SO_4^{2-} + 15Fe^{2+} + 16H^+ \quad (1)$$

This reaction results in an increase of $[H^+]$, and may explain the slight decrease of pH during the early steps of mixing in November and June (Table 1). In April, the relatively low amount of Fe in the river indicates a limited release of Fe from the sediments and the decrease of pH is not detectable. An additional release of dissolved Fe may be attributed to the dissolution of detrital Fe-oxides in the vicinity of the paper factory; the effluent input into the river results in a reduction in the dissolved oxygen concentration (Elbaz-Poulichet *et al.*, 1999), probably due to the oxydation of the organic matter which is important (DOC = 80 mg l^{-1}) in the effluent (sample TR8, Table 1).

Removal of Fe with increasing salinity has been reported for many estuaries (Boyle *et al.*, 1977), and is also observed in our mixing experiments (Fig. 5). But in the Tinto mixing zone, the removal of Fe is swamped by a release process operating in the low chlorinity region and the balance is in favor of dissolution even in June where high DOC concentrations may enhance, in low pH waters (pH 2.5), the Fe precipitation as humic complexes (Luther *et al.*, 1996).

In April and June, As and PO_4^{3-} showed a similar behavior (Fig. 3e and f), suggesting that the same removal processes control their distributions.

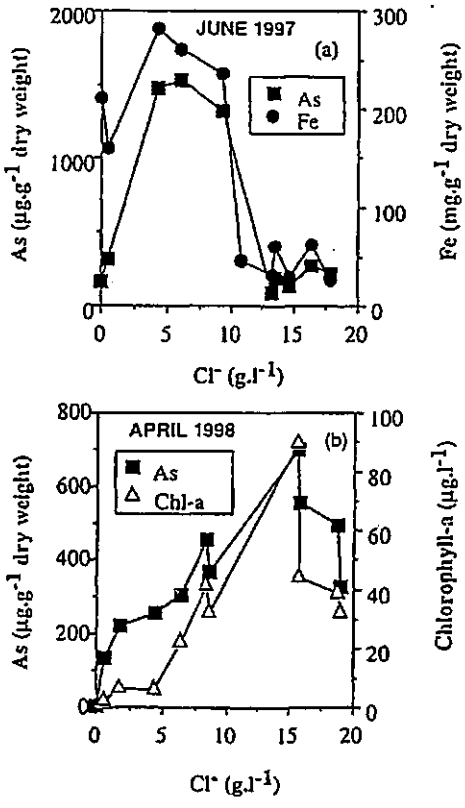

Fig. 4. (a) Arsenic and iron as a function of Cl^- in suspended particulate matter. (June 1997 survey); (b) Arsenic in suspended particulate matter and chlorophyll-a as a function of Cl^- (April 1998 survey).

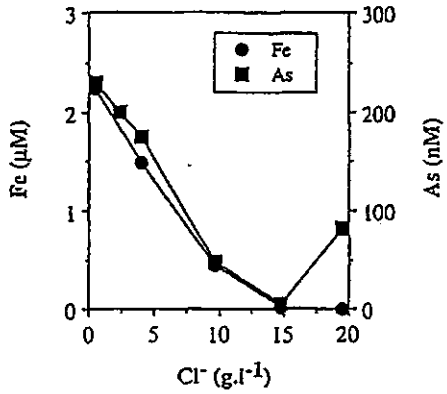

Fig. 5. Iron and arsenic as a function of Cl^- in riverwater/seawater mixing experiments (June 1997 survey).

The concentration of As(III) was negligible (Table 1) during that period and the stable As species, as predicted from Eh-pH data, was the hydrolyzed form of As ($HAsO_4^{2-}$), which shares with the hydrolyzed form of P (HPO_4^{2-}) similar chemical behavior. In April, the correlation between particulate As and chlorophyll (Fig. 4b) suggests uptake of arsenate by algae or adsorption on cell walls. The uptake process, has been reported for PO_4^{3-} in acidic mine drainage (Tate *et al.*, 1995), and has been also proposed for As in the P-rich Charlotte estuary (Froelich *et al.*, 1985) and in the Humber Plume (Millward *et al.*, 1997). In the Tinto mixing zone, the P/As ratio in water (100) is similar (Fig. 6) to the removal ratio $(Ct-Co)_{PO_4^{3-}}/(Ct-Co)_{As}$ (see caption of Fig. 6 for explanation). This suggests that algae do not discriminate between As and P. If the process is uptake and not sorption on wall cells, the difference with other estuaries where discrimination is observed may possibly be explained by differences in algae species as proposed by Sanders (1985).

In June, a positive correlation was apparent between chlorophyll and dissolved As disappearance from the dissolved phase but no correlation was observed between chlorophyll and particulate As. This suggests that fixation (uptake or adsorption on wall cells) by algae is not the only process determining As behavior. The correlation between As and Fe in SPM, clearly indicates a co-precipitation of As with Fe. Compared to April, the co-precipitation process was enhanced by the high Fe concentrations (Fig. 3b) and probably by the enhanced DOC concentrations (Fig. 2c) which generally increases the floculation of Fe colloids (Sholkovitz, 1978).

The removal processes explain why the As concentrations in the nearshore waters of the Gulf of Cadiz remain fairly low (21–24 nM, Morley *et al.*, 1999) compared to metals which are not taken up in the Tinto mixing zone (Elbaz-Poulichet *et al.*, 1998).

In November, dissolved As behaves in a similar way as Fe (Fig. 3a), and is subjected to release at low chlorinity and probably co-precipitation further down the estuary. During this period, the release is probably enhanced by the abundance of Fe (see Eq. 1) in the river end-member but algae fixation is not involved. The balance is in favor of the release (Fig. 3a) which is important enough to mask the phosphogypsum source. Inversely, in June and April, the balance for As is in favor of removal as it is also the case for PO_4^{3-}. However the PO_4^{3-} concentrations in November (Fig. 3d) remained high throughout the estuary and deserved special attention. The REE distribution (Elbaz-Poulichet and Dupuy, 1999) reveals that inputs from phosphogypsum wastes occur both under dissolved and particulate phase. This observation may explain the PO_4^{3-} distribution: the first peak concentration at $Cl^- = 15$ g l^{-1} is possibly related to the release of soluble PO_4^{3-}, whereas the second peak at $Cl^- = 8$ g l^{-1} reflects a subsequent dissolution of PO_4^{3-} from phosphogypsum SPM. Uranium which has its source only in phosphogypsum, displays a similar distribution (Fig. 3d), with two maximum in concentrations (Elbaz-Poulichet *et al.*, 1999). PO_4^{3-} is subjected to co-precipitation with Fe-oxides, but this removal process is probably of less importance than the source inputs.

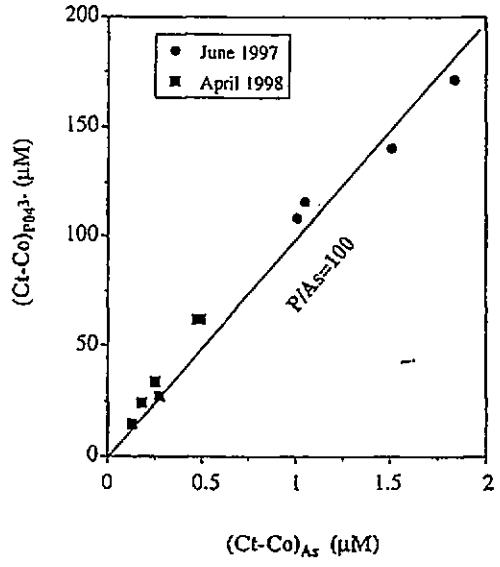

Fig. 6. $(Ct-Co)_{PO_4^{3-}}$ vs $(Ct-Co)_{As}$. Ct is the theoretical dissolved concentration of As or PO_4^{3-} established from the theoretical mixing line between N1 and TR4 in June (Fig. 3e) and TR10 and TR4 in April (Fig. 3f). Co is the observed concentration.

CONCLUSION

This study demonstrates that As and PO_4^{3-} distributions are seasonally variable in the acidic water of the Tinto mixing zone. The differences are related to a transfer from dissolved to particulate phase operating in this system. During spring 1997 and 1998, the fixation by algae complemented the co-precipitation with Fe. During late autumn 1996, the removal was negligible and was balanced by the release of As and PO_4^{3-} from detrital pyrite and phosphogypsum, respectively. In spring, when the removal was the dominant process, As showed a similar behavior compared with PO_4^{3-}; otherwise, it behaved as Fe in autumn.

Finally, the dissolved inorganic As, transported in the estuary was about three times more important in autumn compared to spring. The discrepancy is mainly due to the phytoplankton production which largely contributes to As and PO_4^{3-} removal in spring. During this season, the As content of SPM can reach 1530 µg g^{-1} dry weight.

These removal processes limit As concentrations

to 21–24 nM in the Gulf of Cadiz but the sedimentary stock which is continuously dredged and disposed on the edge of the Odiel natural park is highly toxic and could constitute an important secondary As source.

Acknowledgements—This research was supported by the European Commission (DGXII) under contract TOROS (ENV4-CT96-0217), Environment and Climate Program (ELOISE). We thank our colleagues of the University of Huelva, especially Jose Borrego, Juan Antonio Morales and Mercedes Lopez-Guillen, for their assistance on site and Liliane Savoyant and Simone Pourtales for their assistance in ICP–MS analyses. Nicholas Morley is thanked for Fe analyses.

REFERENCES

Andreae M. O. (1977) Determination of As species in natural waters. *Anal. Chem.* 49, 820–823.

Andreae M. O. (1979) Arsenic speciation in seawater and interstitial waters: the influence of biological–chemical interactions on the chemistry of a trace element. *Limnol. Oceanogr.* 24, 440–452.

Andreae M. O., Barnard W. R. and Ammons J. M. (1983) The biological production of dimethylsulfide in the ocean and its role in the global atmospheric sulfur budget. *Ecolog. Bull.* 35, 167–177.

Borrego-Flores J. (1992) Sedimentologia del estuario del Rio Odiel (Huelva, S.O. Espana). PhD thesis, University of Sevilla. 315pp.

Boyle E. A., Edmond J. M. and Sholkovitz E. R. (1977) The mechanism of iron removal in estuaries. *Geochim. Cosmochim. Acta* 41, 1313–1324.

Branch S., Corns W., Ebdon L., Hill S. and O'Neill P. (1991) Determination of As by hydride generation inductively coupled plasma mass spectrometry using a tubular membrane gas–liquid separator. *J. Anal. At. Spectr.* 6, 155–158.

Carpenter R., Peterson M. L. and Jahne R. A. (1978) Sources, sinks, and cycling of Arsenic in the Puget Sound region. In *Estuarine Interactions*, ed. M. L. Wiley, pp. 4589–4800. Academic Press, New York.

Cutter G. A. and Cutter L. A. (1995) Behaviour of dissolved antimony, arsenic and selenium in the Atlantic Ocean. *Mar. Chem.* 49, 295–306.

Elbaz-Poulichet F. and Dupuy C. (1999) Behaviour of Rare Earth Elements at the freshwater-seawater interface of two acid mine rivers: the Tinto and Odiel (Andalucia, Spain). *Appl. Geochem.* (in press).

Elbaz-Poulichet F. and Leblanc M. (1996) Transfert de metaux d'une province miniere a l'ocean par les fleuves acides (Rio Tinto, Espagne). *C.R. Acad. Sci. Paris* 322(IIa), 1047–1052.

Elbaz-Poulichet F. and the participants of TOROS project (1998) Fate and impact of acid mine drainage and industrial effluents discharges on the Ria de Huelva, the Gulf of Cadiz and the Mediterranean inflowing waters at Gibraltar. In *Proceedings of the 2nd Annual ELOISE Conference, Huelva, Spain, 30 September–3 October.*

Elbaz-Poulichet F., Morley N. H., Cruzado A., Velasquez Z., Achterberg E. and Braungardt C. (1999) Trace metal and nutrient distribution in an extremely low pH (2.5) river–estuarine system, the Ria de Huelva (south–west Spain). *Sci. Tot. Env.* 227, 73–83.

Froelich P. N., Kaul L. W., Byrd J. T., Andreae M. O. and Roe K. K. (1985) Arsenic, barium, germanium, tin, dimethylsulfide and nutrient biogeochemistry in Charlotte Harbor, Florida, a phosphate-enriched estuary. *Est. Coast. Shelf Sci.* 20, 239–254.

Kitts H. T., Millward G. E., Ebdon L. and Morris A. W. (1994) Arsenic biogeochemistry in the Humber estuary, UK. *Est. Coast. Shelf Sci.* 39, 157–172.

Leistel J. M., Marcoux E., Thieblemont D., Quesada C., Sanchez A., Almodavar G. R., Pascual G. R. and Saez R. (1998) The volcanic-hosted massive sulphide deposits of the Iberian Pyrite Belt. *Mineralium Deposita* 33, 2–30.

Luther G. W., Shellenbarger A. and Brendel P. (1996) Dissolved organic Fe(III) and Fe(II) complexes in salt marsh porewaters. *Geochim. Cosmochim. Acta* 60, 951–960.

Millward G. E., Kittsh J., Ebdon L., Allen J. I. and Morris A. W. (1997) Arsenic species in the Humber Plume, UK. *Cont. Shelf Res.* 17, 435–454.

Morley N. H., Elbaz-Poulichet F. and Nomerange P. (1999) Trace metals in the waters of the Straits of Gibraltar. Oral presentation. 24th General Assembly of the European Geophysical Society in The Hague, 19–23 April 1999. *J. Geophys. Res. Abstracts* 1, (in press).

Morris R. J., McCartney M. J., Howard A. G., Arbab-Zavar M. H. and Davis J. S. (1984) The ability of a field population of diatoms to discriminate between phosphate and arsenate. *Mar. Chem.* 14, 259–265.

Nelson C. H. and Lamothe P. J. (1993) Heavy metal anomalies in the Tinto and Odiel river and estuary system, Spain. *Estuaries* 16, 495–511.

Riley J. P. and Chester R. C. (1971) *Introduction to Marine Chemistry*. Academic Press, London and New York, 465 pp.

Rodier J., Broutin J. P., Chambon P., Champsaur H. and Rodi L. (1996) *L'Analyse des Eaux*. Dunod, Paris, 1383 pp.

Salomons W. (1995) Heavy metal aspects of mining pollution and its remediation. *J. Geochem. Explor.* 52, 5–23.

Sanders J. G. (1985) Arsenic geochemistry in Chesapeake Bay: dependence upon anthropogenic inputs and phytoplankton species composition. *Mar. Chem.* 17, 329–340.

Seyler P. and Martin J. M. (1989) Biogeochemical processes affecting arsenic species in a permanently stratified lake. *Env. Sci. Technol.* 28, 1258–1263.

Sholkovitz E. R. (1978) The flocculation of dissolved Fe, Mn, Al, Cu, Ni, Co and Cd during estuarine mixing. *Earth Planet. Sci. Let.* 41, 77–86.

Tate C., Broshears R. and McKnight D. (1995) Phosphate dynamics in an acidic mountain stream; interactions involving algal uptake, sorption by iron oxide, and photoreduction. *Limnol. Oceanogr.* 50, 938–946.

Travesi A., Gasco C., Pozuelo M., Palomares J., Garcia M. R. and Perez del Villar L. (1997) Distribution of natural radioactivity within an estuary affected by release from phosphate industry. In *Freshwater and Estuarine Radioecology*, eds G. Desmet, *et al.*, pp. 267–279. Elsevier.

Van Geen A. and Chase Z. (1998) Recent mine spill adds to contamination of southern Spain. *EOS 79* 38, 445–449.

Van Geen A., Adkins J. F., Boyle E. A., Nelson C. H. and Palanques A. (1997) A 120-yr record of widespread contamination from mining of the Iberian pyrite belt. *Geology* 25, 291–294.

Whitledge T. E., Malloy S. C., Patton C. J. and Wirick C. D. (1981) *Automated Nutrient Analyses in Seawater*. Brookhaven National Laboratory, US Department of Energy and Environment, Upton, NY, 216 pp.

ELSEVIER

The Science of the Total Environment 227 (1999) 73–83

the Science of the Total Environment

Trace metal and nutrient distribution in an extremely low pH (2.5) river–estuarine system, the Ria of Huelva (South–West Spain)

Françoise Elbaz-Poulichet[a,*], Nicholas H. Morley[b], Antonio Cruzado[c], Zoila Velasquez[c], Eric P. Achterberg[d], Charlotte B. Braungardt[d]

[a] *Laboratoire Géofluides–Bassins–Eau, UMR 5569, CNRS–ORSTOM–University of Montpellier II, CC057, 34095 Montpellier cedex 5, France*

[b] *Department of Oceanography, University of Southampton, Southampton Oceanography Centre, Waterside Campus, European Way, SO14 3ZH Southampton, UK*

[c] *Center d'Estudis Avancats de Blanes, Cami de Sta. Barbara, 17300 Blanes, Spain*

[d] *University of Plymouth, Department of Environmental Sciences, Plymouth PL4 8AA, UK*

Received 7 May 1998; accepted 23 December 1998

Abstract

Nutrient (nitrate, phosphate, silica) and dissolved metal (Al, Cu, As, Cd, Ni, Zn, Fe, U) distributions were studied in the mixing zones of the Tinto and Odiel rivers which drain the South Iberian pyrite belt. Phosphate distribution is strongly influenced by discharges from the fertiliser industry, especially in the Tinto mixing zone. The increase of silica content in this zone is related to a release of biogenic silica from diatoms. Nitrate concentrations which are influenced by urban and industrial effluents showed an important maximum in the early stages of mixing in the Tinto (as do the metals). Compared to the Odiel river, the metal concentrations in the Tinto river reached higher values in relation to more intensive mining activities. Dissolved Fe, Mn, Al, Cu, Cd and Zn concentrations were correlated in the mixing zones of both rivers. This suggests that they have the same source and are subjected to the same controlling processes in the estuary. A maximum concentration for these metals was observed in the early stage of mixing in the Tinto and reflects a decrease of redox in a low pH (< 3) environment. Downstream in the Odiel system, metals showed a slight removal. Dissolved uranium, present at a low level (0.05 μmol l^{-1}) in the rivers, is introduced by the phosphate fertiliser industry in the estuary and trapped in sedimentation areas. As a consequence, waters of the Gulf of Cadiz have a U content similar to that of the open seawater.

Keywords: Metals; Nutrients; Acidic estuary; Geochemistry

* Corresponding author. Laboratoire Géofluides–Bassins–Eau, UMR 5569, CNRS–ORSTOM–University of Montpellier II, CC057, 34095 Montpellier cedex 5, France. E-mail: elbaz@dstu.univ-montp2.fr

0048-9697/99/$ - see front matter
PII: S0048-9697(99)00006-6

1. Introduction

The Tinto and Odiel rivers (South Western, Spain) drain the Iberian Pyrite Belt, which is one of the largest sulphide deposits in the world and contains more than 1700 Mt of sulphides (Leistel et al., 1998). This predominantly Zn–Cu–Pb mineralisation, has been worked continuously since the Phoenician and Roman eras (Rothenberg and Blanco Freijero, 1980), leaving enormous quantities of pyrite wastes and slags. As a consequence of the production of sulfuric acid by drainage of those wastes, the pH of the two rivers remains low and relatively constant pH (approx. 2.5 in the Tinto and 3 in the Odiel) throughout the year over a distance of 100 km from the mining area down to the estuary (Nelson and Lamothe, 1993; Elbaz-Poulichet and Leblanc, 1996; van Geen et al., 1997).

High metal concentrations have been reported in the riverine end-member (Elbaz-Poulichet and Leblanc, 1996; van Geen et al., 1997), in the sediments of their common estuary (Perez et al., 1991; Nelson and Lamothe, 1993) and in the coastal shelf sediments of the Gulf of Cadiz (van Geen et al., 1997). Although knowledge of dissolved metal distribution in the estuarine zone is needed to estimate the impact that those rivers will have on the highly productive region of the Gulf of Cadiz, scarce U data (Martinez-Aguirre et al., 1994) have been reported.

Moreover, the Gulf of Cadiz where important metal enrichments in waters have been reported (van Geen et al., 1988, 1991), provides up to 20% of the Atlantic inflow into the Gibraltar Strait and thus contributes significantly to the contamination of the Western Mediterranean sea in general and to the Alboran sea, in particular, which is also a region of intensive fishing activity.

In order to evaluate budgets for the trace metal transfer from the mineralisation zone to the Gulf of Cadiz, the present study investigates the processes that control metal behaviours in the Tinto and Odiel mixing zones and in their common estuary: the Ria of Huelva. This system is characterized by extreme pH conditions (< 3) also provides an unique opportunity to improve our understanding of metal cycling in this particular case.

Data on sulphate, silicate, nitrate and phosphate and dissolved trace elements (Fe, Mn, Al, Cu, Cd, Zn and U) are presented.

2. Study area

The Tinto and Odiel (83 and 128 km in length, respectively), have similar drainage basin areas (approx. 1680 km^2). The mean water discharges of the Odiel and the Tinto rivers are 15 $m^3\ s^{-1}$ and 3 $m^3\ s^{-1}$, respectively. However, important variations are observed (Borrego-Flores, 1992) with low discharges generally during summer and high river discharges in winter (December, January and February) after important rain events. Mining activity is still active in the Tinto catchment. Less intensive mining occurs in the Odiel catchment (Nelson and Lamothe, 1993) where, in addition, a dam has been built, trapping sediments and acid mine wastes from ore processing plants.

The estuary can be described as a well to partially mixed estuary with a maximum tidal amplitude of approximately 3 m. The upstream limit of saline intrusion is located at the east of San Juan Del Puerto on the Tinto river and upstream of Station 18 on the river Odiel (Fig. 1). The turbidity maximum occurs between Stations 3 and 11 in the Tinto and between Station 23 and 29 in the Odiel. The tidal zones include salt–marsh areas, which are particularly well developed on the right bank of the Odiel river. The two rivers meet at the town of Huelva and form a ria (outer estuary) extending over approximately 15 km, the western bank of the ria being partly a natural spit.

The estuarine zones of the two rivers are sites of major industrial activities. On the east bank of the Odiel, phosphate-based fertiliser, pyrite roasting and copper smelting plants are present between Stations 29 and the confluence (Fig. 1). Approximately 8 million m^3 of liquid effluents are discharged into the Odiel each year, containing approximately 4.10^8 kg of phosphogypsum

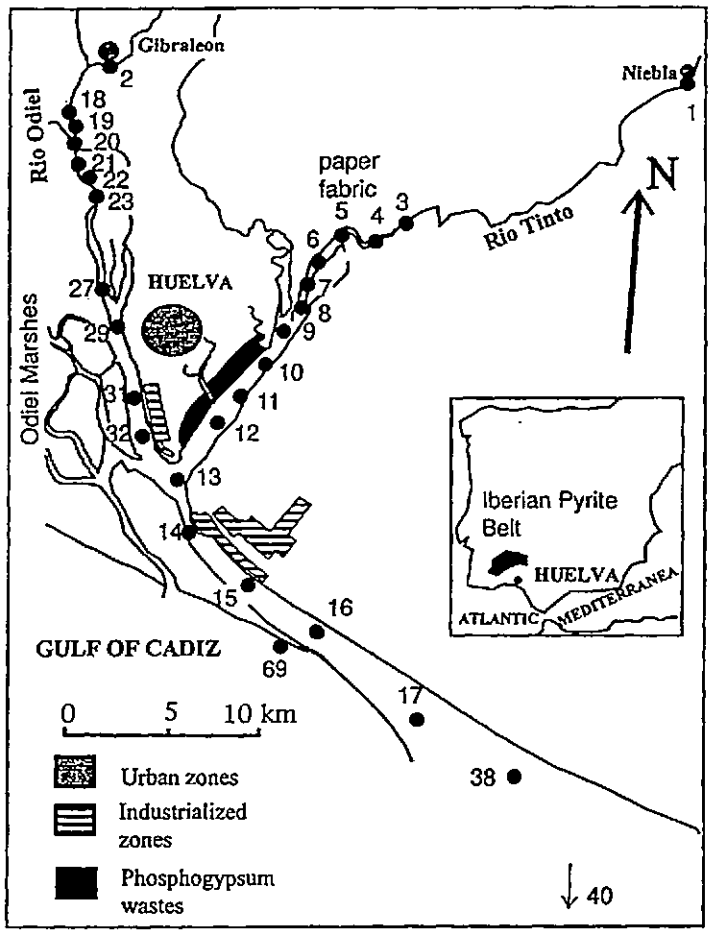

Fig. 1. Sketch map of Huelva Ria. The Tinto and Odiel river meet in a common estuary at Huelva (outer estuary).

(Travesi et al., 1997). On the Rio Tinto, there is a paper mill at Moguer (Station 5), which processes eucalyptus wood from local sources. Large waste deposits of phosphogypsum exist on the northern bank of the Tinto near the junction of the two rivers (Stations 9–12). The thickness of the deposits is 4–6 m and their total surface covers approximatively 4.10^6 m^2. It is estimated that 10^{10} kg of phosphogypsum have been deposited (Travesi et al., 1997). These wastes are drained by a small tributary which also carries the effluents from the sewage treatment plant of the town of Huelva. Pyrite deposits are found at the junction of the two rivers. Furthermore, on the eastern bank of the outer estuary the industrial area includes an oil refinery downstream.

3. Material and methods

3.1. Sampling

The location of the sampling stations are reported in Fig. 1. Water samples were collected in November 1996 during normal low water discharge. Samples were taken by hand from the river banks and from a small boat in the estuary. In the coastal area, a bottom-weighted polyethylene hose was lowered into the water column and samples were drawn into large polyethylene Nalgene containers (10l) using a vacuum hand pump.

For metals, bottles were previously acid cleaned according to the procedure currently used in the different laboratories involved.

3.2. Determinations of nutrients and major physicochemical parameters

For phosphate and silica determinations, the samples were filtered through Millipore Teflon filters and immediately deep-frozen. Analysis was carried out in the C.E.A.-Blanes by automatic segmented flow techniques according to Whitledge et al. (1981).

Sulphate was carried out, after filtration through PVDF (0.2 μm) Millipore filters, by Capillary Ion Analysis (CIA) at Laboratoire Geofluides–Bassins–Eaux (GBE). Na^+ was determined, after passing through 0.4 μm Nuclepore filters, by Flame Atomic Absorption Spectrophotometry at Southampton Oceanography Center (SOC). Chloride concentrations were calculated from Na^+ concentrations assuming $Na^+/Cl^- = 0.56$ in seawater having a salinity of 35 ppt (Riley and Chester, 1971). Determinations of pH were undertaken in the field laboratory (Huelva) immediately after sampling. The salinity at Stations 38 and 40 (Fig. 1) in the Gulf of Cadiz, was calculated from conductivity measurements.

3.3. Metal determinations

Analyses of dissolved metals after filtration on 0.4 μm Nuclepore filters were carried out at SOC and at GBE according to the scheme presented in Table 1. In order to prevent contamination risks, two sets of filtration units were used: one for the highly contaminated rivers and estuarine samples, the other for the coastal waters. When Cathodic Stripping Voltammetry (CSV) was used for Cu and Ni determinations, the analytical instrumentation was thoroughly cleaned using diluted HCl after analysis of the highly contaminated waters. Determinations of instrumental and reagent blanks were performed to check the effectiveness of the cleaning routine. Blank values were below 2 nM for Cu and 1 nM for Ni.

The analyses by different techniques in the three laboratories, show a good agreement as indicated by the values obtained on the certified river (CASS-2, CASS-3, SLRS-2) and seawater (NASS-4) reference materials from Canadian National Research Center (Table 1).

4. Results and Discussion

4.1. Variations of pH, sulphate, nitrate, phosphate and silica (Fig. 2)

The low pH registered all along the Tinto ($\cong$ 2.5) and Odiel ($\cong$ 2.8) rivers overlap with those reported by Nelson and Lamothe (1993), Elbaz-Poulichet and Leblanc (1996) and van Geen et al. (1997). These low values which remain fairly constant at all times of the year, result from acid mine drainage and are due to the oxidation of pyrite (FeS_2), with a consequent production of sulphuric acid. While neutralisation occurs rapidly in the Odiel mixing zone (Fig. 2), pH values remained low in the mixing zone of the Tinto in relation with the runoff from phosphogypsum wastes which release hydrofluordric and phosphoric acid. The F content, low in the river (< 1 mg l^{-1}), increases up to 7–15 mg l^{-1} in the vicinity of the phosphogypsum wastes (Medio Ambiente, 1998).

In relation to salinity (Fig. 2), nutrients behave differently according to the rivers and display generally non-linear relationships with chloride. Such an evolution cannot result simply from dilution and/or absorption effects due to seawater input and it clearly implies additional sources. Some of them may be easily recognised: this is true for sulphate and phosphate which are released in the Odiel river by phosphate fertiliser factories and in the Tinto river by the wastes generated by these factories.

In both rivers the maximum of dissolved silica occurs at chlorinity between 12 and 19 g l^{-1}. This silica maximum could be due to inputs from phosphogypsum wastes or associated with the presence of diatoms which are abundant (Perez et al., 1997) in the outer estuary. In the Tinto and in the Odiel mixing zone, a few living diatoms are still observed but scanning electron microscopy observations show an increasing number of broken

Table 1
Analysis of dissolved metal concentrations

Laboratory	Filtration	Metals	Location of samples analysed	Method material	Certified reference	Measured value (mean ± 1σ)	Recommended value (mean ± 1σ)
SOC (Southampton Oceanography Center)	0.4 μm Nuclepore Polycarbonate filters	Cu, Cd, Zn, Mn, Fe, Al	River and mixing zone	FAAS [a], GFAAS [b]			
UP (University of Plymouth)	0.45 μm Whatman Cellulose nitrate filters	Cu, Ni, Cd, Zn, Al, U, As	River mixing zone, outer estuary, Gulf of Cadiz	ICP-AES [c] ICP-MS [d] CSV [e]	CASS-3	Cu: 8.17 ± 0.55 nM Ni: 6.68 ± 0.53 nM	Cu: 8.14 ± 0.98 nM Ni: 6.58 ± 1.06 nM
GBE (Geofluides, Bassins, Eau)	0.4 PVDF Millipore filters	Mn, As, U	River, mixing zone, outer estuary, Gulf of Cadiz	ICP-MS [d]	SLRS-2 NASS-4	U(SLRS2): 0.187 ± 0.016 nM U(NASS-4): 12.02 ± 0.18 nM	U(SLRS2): 0.205 ± 0.008 nM U(NASS4): 11.3 ± 0.50 nM As(NASS-4): 16.8 ± 1.3 nM

[a]FASS: Flame Atomic Absorption Spectrometry was used at SOC for the analysis of Cu, Cd, Zn and high Fe samples.
[b]GFAAS: Graphite Furnace Atomic Absorption Spectrometry (with matrix modification and standard additions) was used at SOC for Al and low Fe samples in the river and mixing zone.
[c]ICP-AES: Inductively–Coupled Plasma Atomic Emission Spectrometry was used at the UP for the analysis of Fe, Cu, As, Zn in river and mixing zone.
[d]ICP-MS: Inductively Coupled Plasma–Mass Spectrometry was used in the UPl to analyse Mn, U, Cu, Cd, U, Zn and Al in river and mixing zone.
In the GBE laboratory Cu, Mn analysis in river and mixing zone and U analysis throughout the study area were also performed by ICP-MS. For dissolved As, an hydride generation system was coupled to the ICP-MS (method similar to that of Branch et al., 1991). This technique involves a pre-reduction step with KI in order to obtain total dissolved As concentrations.
[e]CSV (Cathodic Stripping Voltammetry) was used by UP for the determination of total dissolved Ni and Cu and for speciation measurements. The voltammetric determinations were performed, using a micro-Autrolab voltammeter (Ecochimie) with a Hanging Mercury Drop Electrode (Metrohm, 663 VA Stand). The buffer used throughout was 0.01 M HEPES (pH 7.7)
In order to destroy naturally occurring metal complexing organic ligands, samples for total dissolved Cu and Ni determination were subject to UV digestion after acidification to pH 2. Total metals were determined, in the presence of Hepes buffer, in separate aliquots with 2×10^{-5} M oxine (Cu) or 2×10^{-4} M dimethyl glyoxime (DMG) (Ni), as described by Philar et al. (1981) and van den Berg (1986).

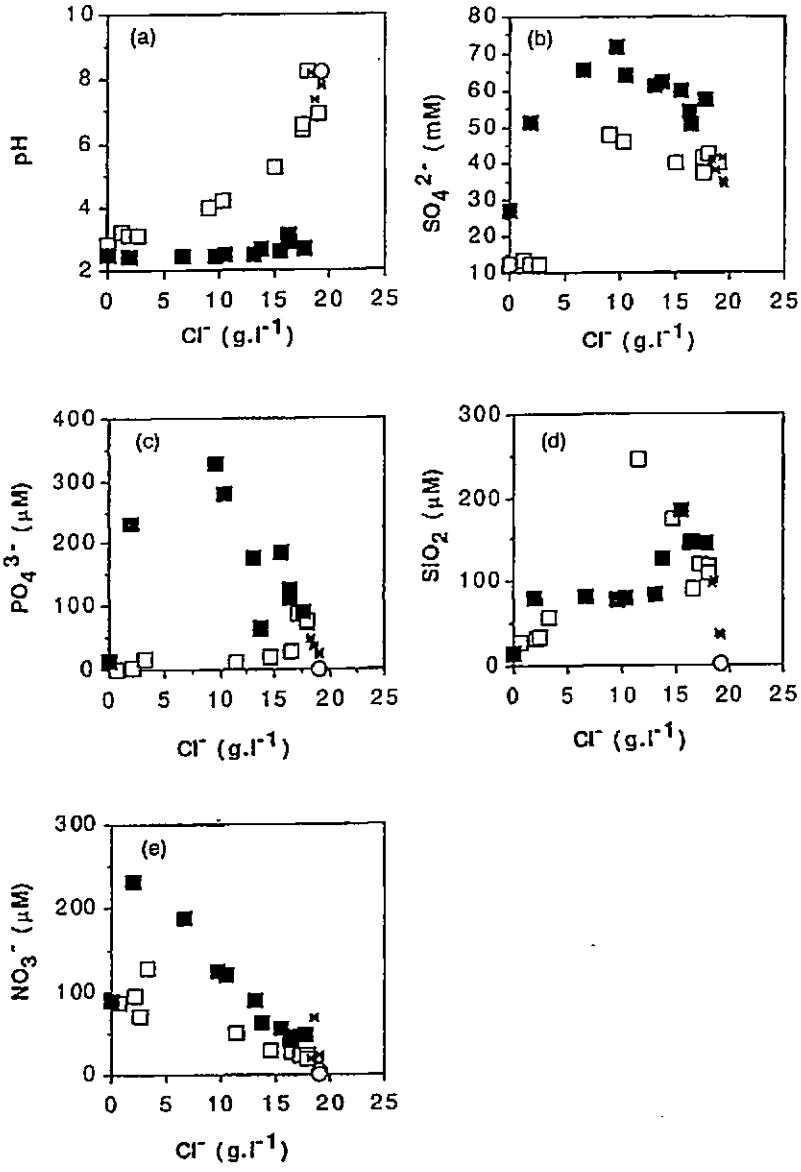

Fig. 2. Variations of pH, sulfate and major nutrients as a function of chloride content. Symbols: □ Odiel mixing zone; ■ Tinto mixing zone; ○ Outer estuary; and × Gulf of Cadiz.

diatom tests which totally disappear at Station 6. The subsequent decomposition of biogenic silica may explain the observed maxima.

In the Odiel river, nitrate (Fig. 2) can be considered as almost conservative. Its distribution is more complex in the Tinto river: this anion increases in the early stage of mixing with the highest value encountered at Station 3, where the effluent discharges from a paper factory occur. In this station, Total Organic Carbon increases from 3 to 42 mg l^{-1}, and probably undergoes a remineralisation, inducing an increase of nitrate in solution. This mineralisation is favoured by the abundant presence of bacteria (C. Courties, per-

sonal communication). Under normal pH conditions, a similar mechanism has been suggested by Windom et al. (1988) to explain maxima of nitrate concentration in organic rich tropical estuaries.

4.2. Metal distribution (Table 2a, b).

4.2.1. Rivers

In the Tinto river, dissolved metals have high concentrations (Table 2a, Station 1) with values similar to those previously reported (Nelson and Lamothe, 1993; Elbaz-Poulichet and Leblanc, 1996 and van Geen et al., 1997); they are also representative of the whole system. In the Odiel river, where less intensive mining occurs (Nelson and Lamothe, 1993), dissolved metals (excepted Mn and Ni) have lower concentrations (Table 2b, Station 2). The similarity of Mn and Ni content in the two rivers, may indicate that these elements are influenced by the dissolution by low pH waters of rock minerals containing them all along the rivers rather than by the mining activities.

4.2.2. Mixing zone

Similar to nitrate, Fe, Mn, Al, Cu, Cd and Zn contents also increase between the Stations 1 and 3 in the Tinto river (Figs. 2 and 3). The increase is unlikely to be an artefact as it has been observed

Table 2
pH, chlorinity and dissolved metals in river water and mixing zone (November 1996)

Station	Cl^- ($g\,l^{-1}$)	pH	Fe (μM)	Mn (μM)	Cu (μM)	Cd (nM)	As (nM)	U (nM)	Zn (μM)	Al (mM)	Ni (nM)
(a) pH, chlorinity and dissolved metals in the Tinto river and mixing zone											
1	0.031	2.47	10.89	186	448	1382	29253	50	669	3.55	4697
3	1.9	2.43	18.28	347	745	3216	42747	131	1776	5.44	6915
4	6.59	2.46	9.17	193	430	1895	22653	195	1049	3.59	4421
5	9.58	2.45	4.09	140	291	1205	13867	283	596	2.27	2978
6	10.39	2.47	3.05	123	255	1041	12009	292	500	1.97	2655
7	13.08	2.5	2.23	72	139	907	8561	242	406	1.66	2349
8	13.76	2.66	0.59	49	82	557	4892	176	217	0.96	1496
9	15.53	2.59	0.64	54	94	609	8375	245	240	1.05	1654
10	16.44	2.86	0.23	33	52	368	4195	104	132	0.62	1121
11	16.33	3.09	0.19	24	37	306	4252	75	109	0.50	925
12	17.71	2.68	0.12	23	34	256	3844	65	86	0.39	696
(b) pH, chlorinity and dissolved metal concentrations in the Odiel river, mixing zone, the surface samples of the outer estuary											
2	0.03	2.84	910	215	136.7	868	369	30.9	356	2.637	4646
18	1.96	3.09	477	179	98.4	671	51	21.3	242	1.655	3796
19	2.69	3.13	457	174	94.8	702	67	19.0	229	1.637	3535
20	1.28	3.21	393	161	89.9	632	52	18.8	212		3217
21	9.06	3.96	190	73	41.7	300	0	11.6	124		2112
22	10.23	4.2	120	63	32.6	255	47	7.7	92	0.768	1664
23	15.09	5.28	55	38	15.3	191	34	1.9	60	0.256	1147
27	17.49	6.43		19	6.3	161	522	1.3	34	0.058	369
29	17.49	6.56		17	5.4	201	911	3.1	27	0.071	311
31	19.04	6.92		10	3.9	163	1355	4.0	19	0.156	208
32	18.11	8.26		11	4.6	171	1396	4.8	18	0.076	390
13	18.42	8.2		8	3.0	146	1285	6.1	16	0.012	210
14	18.73	7.34		5	1.57	122	1161	9.4	7	0.065	140
15	19.35	7.8			0.223		671	12.4	2	0.005	61
16	19.51	8.1			0.103		146	13.1	1	0.003	17.01
17	19.35	8.04			0.071		86	13.4		0.002	7.52
69	19.35	8.26					147	11.6			
38	19.35	8.26					148	12.5			
40	19.35	8.26			0.298		34	11.9			8.29

by each laboratory team which have collected their own samples at the same stations. The input of organic-rich effluents from the paper factory favours oxygen consumption and thus a decrease of pH. Even if this decrease remains small, because of the low pH of the river water, dissolution of iron oxyhydroxydes still present in the sediments occurs and hence an increase of soluble Fe content. The Fe-oxide phases, which result from erosion of the upper oxidized horizon in the mineralisation zone are transported downstream during flood events. The simultaneous increase of other metals, including Mn, results from the dissolution of the iron phase where they are trapped as suggested by the significant correlation between Fe and the following metals Mn, Al, Cu, Cd and Zn (Fig. 4). Downstream Station 3 in the Tinto, the decrease of metal concentrations results from dilution by seawater. In the Odiel mixing zone, metals (e.g. Fe and Mn, Fig. 3) are removed from

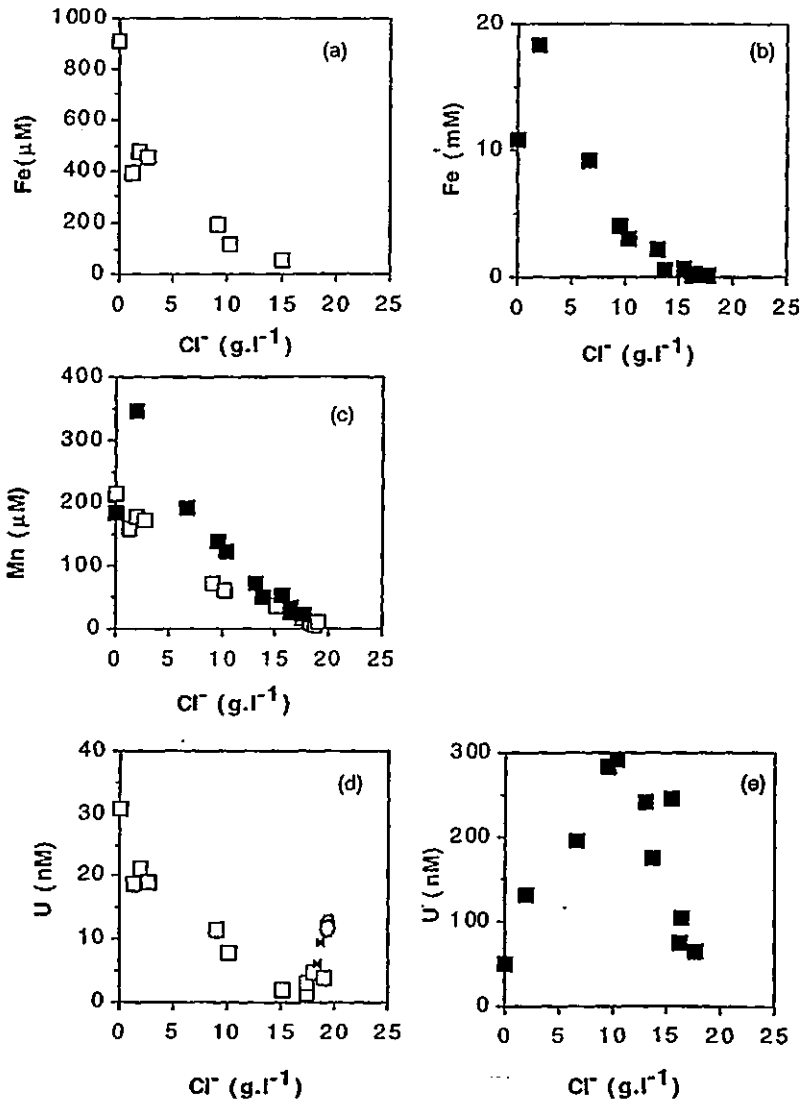

Fig. 3. Relationship between dissolved metal concentrations and Mn in the mixing zone.

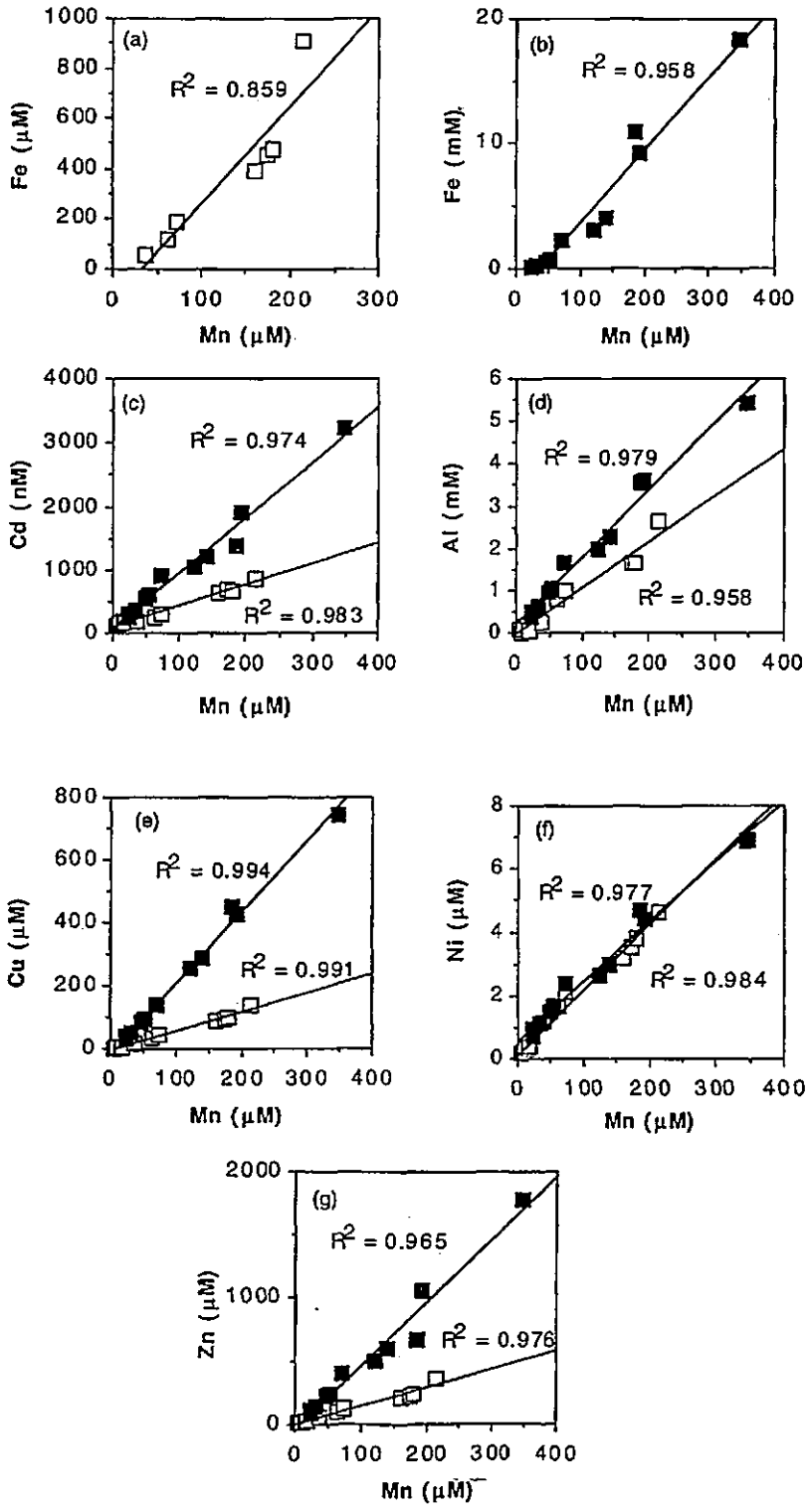

Fig. 4. Dissolved metal concentrations as function of chloride content. Variations of pH, sulfate and major nutrients as a function of chloride content. Symbols: □ Odiel mixing zone; ■ Tinto mixing zone; ○ Outer estuary; and × Gulf of Cadiz.

the river water in relation to higher pH, but the removal process is relatively inhibited compared to normal estuaries (e.g. Boyle and Edmond, 1977; Sanudo-Wilhelmy et al., 1996). This is due to the high solubility of Fe hydroxides in low pH waters.

Dissolved U shows a concentration maximum in the Tinto estuary (Fig. 3), with a distribution similar to that of phosphate which reflects the high U content (11 $\mu g\ g^{-1}$ dry wt.) of the phosphogypsum. In the Odiel river, U concentrations show a minimum value (1.3 nM) at a chlorinity $Cl = 17.5\ g\ l^{-1}$, then increase to reach 13.4 nM in the Ria, a value which is slightly higher than the value observed in the Gulf of Cadiz at Station 40 (11.9 nM), typical of normal oceanic waters (Martin and Whitfield, 1983). This distribution indicates a removal of dissolved U. This dissolved U is trapped by the organic-rich sediments during the tidal transport of Odiel river water through the neutral pH marshes of the Odiel regional park. The same mechanism has been suggested by Martinez-Aguirre and Garcia-Leon (1997) to explain the high activity of ^{210}Po, ^{210}Pb and ^{226}Ra which are derived from phosphate ore processing and phosphogypsum deposits in the sediments of the marshes. Thus most of the U introduced in the estuary is retained in the marsh system as suggested by Church et al. (1996) — it is not exported to the Gulf of Cadiz.

5. Conclusion

This study confirms high metal contents in the Tinto and Odiel rivers and indicates an additionnal inputs of sulphate, phosphate and U due to the industrial activities. Moreover the industrial activities modify the physicochemical conditions in the Tinto and favour the release in solution of metals and nitrate which were previously immobilized in the sediments. Silica increases in the acidic mixing zone probably in relation with dissolution of biogenic silica from diatoms. In the mixing zone removal processes are inefficient in the Tinto and are relatively weak in Odiel resulting in export of dissolved metal to the Gulf of Cadiz, the exception is U which is trapped in the marshes.

In this context the industrial activity drastically contributes to enhance the pollution generated by mining activity.

Acknowledgements

This research was supported by the European Commission (DGXII) under contract TOROS (ENV4-CT96-0217), Environment and Climate Program (ELOISE). We thank our colleagues of the University of Huelva, especially Jose Borrego, Juan Antonio Morales and Mercedes Lopez-Guillen, for their assistance in the field and Lilianne Savoyant and Simone Pourtales for their assistance in ICP-MS analyses. We are grateful to Claude Dupuy who help us considerably to improve this manuscript.

References

Borrego-Flores J. Sedimentologia del estuario del Rio Odiel. PhD thesis, University of Sevilla. S.O. Espana: Huelva, 1992:315.

Boyle EA, Edmond JM. The mechanism of iron removal in estuaries. Geochim Cosmochim Acta 1977;41:1313–1324.

Church TM, Sarin MM, Fleisher MQ, Ferdelman TJ. Salt marshes: an important coastal sink for dissoved Uranium. Geochim Cosmochim Acta 1996;60:3879–3887.

Elbaz-Poulichet F, Leblanc M. Transfert de metaux d'une province miniere a l'ocean par les fleuves acides (Rio Tinto, Espagne). C R Acad Sci Paris 1996;t.322 (sÈrie IIa):1047–1052.

Leistel JM, Marcoux E, Thieblemont D et al. The volcanic-hosted massive sulphide deposits of the Iberian Pyrite Belt. Mineral Deposita 1998;33:2–30.

Martin JM, Whitfield M. The significance of the river input of chemical elements to the ocean. In: Wong CS et al, editors. Trace metals in seawater. New York: Plenum Press, 1983: 265–296.

Martinez-Aguirre A, Garcia-Leon M. Radioactive impact of phosphate ore processing in a wet marshland in Southwester Spain. J Environ Radioact 1997;34:45–47.

Martinez-Aguirre A, Garcia-Leon M, Ivanovitch M. U and Th in solution and suspended matter from rivers affected by phosphate rock processing in southwestern Spain. Nucl Instrum Meth Phys Res 1994;A 339:287–293.

Medio Ambiente. Report E.S.I.I. de Sevilla; dpto; Ingen; Quimicay Ambiente; Seccion de Medio Ambiente. 1998: 140–168.

Nelson CH, Lamothe PJ. Heavy metal anomalies in the Tinto and Odiel river and estuary system, Spain. Estuaries 1993; 16:495–511.

Perez M, Usero J, Gracia I. Trace metals in sediments from the Ria de Huelva. Toxicol Environ Chem 1991;31/32:275–283.

Perez MC, Velasquez ZR, Ridolfi F, Cruzado A. Phytoplankton of the Rio Tinto, an acidic river from SW Spain, Presented to VI International Phycological Congress, Leyden, The Netherlands, 9–16 August, 1997.

Philar B, Valenta P, Nurnberg HW. New high-performance analytical procedure for the voltametric determination of nickel in routine analysis of waters, biological materials and food. Fres Z Anal Chem 1981;307:337–346.

Riley JP, Chester RC. Introduction to marine chemistry. London and New York: Academic Press, 1971:465.

Rothenberg B, Blanco Freijero A. Scientific studies in early mining and extractive metallurgy. In: Craddock P, editor. British Museum Occasion, 1980:20.

Sanudo-Wilhelmy J, Riviera-Duarte I, Flegal AR. Distribution of colloidal trace metals in the San Francisco Bay estuary. Geochim Cosmochim Acta 1996;60:4933–4944.

Travesi A, Gasco C, Pozuelo M, Palomares J, Garcia MR, Perez de Villar L. Distribution of natural radioactivity within an estuary affected by releases from the phosphate industry. In: Desmet et al. (Eds.), Freshwater and Estuarine Radioecology, Elsevier, 1997, pp. 267–279.

van den Berg CMG. The determination of trace metals in sea-water using cathodic stripping voltammetry. Sci Total Environ 1986;49:89–99.

van Geen A, Rosener P, Boyle EA. Entrainment of trace metal-enriched Atlantic Shelf water in the inflow to the Mediterranean Sea. Nature 1988;331:423–426.

van Geen A, Boyle EA, Moore WS. Trace metal enrichments in waters of the Gulf of Cadiz, Spain. Geochim Cosmochim Acta 1991;55:2173–2191.

van Geen A, Adkins JF, Boyle EA, Nelson CH, Palanques A. A 120-year record of widespread contamination from mining of the Iberian pyrite belt. Geology 1997;25:291–294.

Whitledge TT et al. Automated analysis of seawater. Nat Tech Inf Service. Springfield, USA, 1981.

Windom H, Smith RG, Rawlinson R, Hungspreugs M, Dharmvanij S, Wattayakorn G. Trace metal transport in a tropical estuary. Mar Chem 1988;24:293–305.